

Towards Selective Inhibitors of  
FGFR Kinases using a *De Novo*  
Design Approach

Lewis Daniel Turner

Submitted in accordance with the requirements for the degree  
of Doctor of Philosophy

**The University of Leeds**  
**School of Chemistry**

**April 2018**

The candidate confirms that the work submitted is their own, except where work which has formed part of jointly authored publications has been included. The contribution of the candidate and the other authors to this work has been explicitly indicated below. The candidate confirms that appropriate credit has been given within the thesis where reference has been made to the work of others.

The work in Chapter Two of the thesis has appeared in the publication as follows:

Identification of an Indazole-Based Pharmacophore for the Inhibition of FGFR Kinases Using Fragment-Led *De Novo* Design, 2017, Turner, L. D.; Summers, A. J.; Johnson, L. J.; Knowles, M. A.; Fishwick, C. W. G. *ACS Med. Chem. Lett.* **2017**, 1264-1268.

Lewis Turner was responsible for all aspects of the work carried out in Chapter Two including: design principle, synthesis and characterisation of compounds, and manuscript preparation.

Abbey Summers and Laura Johnson synthesised fragments based on the guidance and support from the candidate. Margaret Knowles and Colin Fishwick provided supervisory support and editorial feedback for preparation of the manuscript.

This copy has been supplied on the understanding that it is copyright material and that no quotation from the thesis may be published without proper acknowledgement.

© 2018 The University of Leeds and Lewis Daniel Turner

The right of Lewis Daniel Turner to be identified as Author of this work has been asserted by him in accordance with the Copyright, Designs and Patents Act 1988.

## Acknowledgements

---

Firstly, I would like to thank Professor Colin Fishwick for all his advice and supervision over the past few years. Working on this multi-disciplinary project has allowed me to expand my scientific knowledge in other areas of science which has directly influenced my future career path. Without Colin, this wouldn't have been possible. I would also like to thank Professor Margaret Knowles and Dr Julie Burns for their help with all things cell biology.

I would also like to thank all members of the Fishwick group, past and present, for their support and advice. In particular, I would like to thank Dr Martin McPhillie for his input at the very start of the project which proved pivotal. I would also like to thank James Gordon and Ryan Gonciarz who started their PhDs at the same time as me who together with myself form the 'three musketeers'. We've shared a lot of laughs over the years and maybe a few pints...

Thanks must also go to all members of the Astbury group that have helped me with all things biochemical. This includes Professor Alexander Breeze and Professor John Ladbury who helped organise the collaborations, and Dr Simon Skinner and Dr Chi-Chuan Lin who taught me the ropes in terms of protein expression. Huge thanks must go to Dr Chi Trinh! Chi has helped me so much in terms of protein expression and in particular, the dark art that is protein crystallography. He is without doubt the busiest person I have ever come across but still managed to find time for me when I needed it.

Thanks must go to the MRC for funding this project and also to Life Technologies Ltd for their high quality service and fast turnaround.

Finally, I would like to thank my family for their support over the years, in particular my grandparents. They have been very supportive throughout my whole academic life and knowing they have always been there for me has been a huge help. I must also thank my grandad personally for his genuine interest in what I do, albeit even if he doesn't understand any of it (kidding). His regular inquisitive 'check-ins' were a nice reminder of the importance of this work and drug discovery in general, for which I must thank him.

## Abstract

---

The discovery of anti-cancer therapeutics remains at the forefront of modern medical science with the most recent forecast estimating that one in two people in the UK will be diagnosed with some form of cancer within their lifetime. The advancement of healthcare and overall better quality of life of the public over the past 50 years has seen a gradual increase in life expectancy. People are living longer, and with this comes new complications, outlining the need for novel anti-cancer therapeutics.

FGFR kinases are a sub-family of receptor tyrosine kinases that are involved in many cellular processes and aberrant signalling within this class is implicated in many cancers. Currently, several anti-cancer therapeutics are in clinical use for FGFR-related cancers with some acting as selective FGFR inhibitors. There are currently no examples of molecules that exhibit sub-type selectivity for the FGFRs, an attribute that may be clinically relevant for FGFR-related cancers exhibiting toxic side-effects upon treatment.

This thesis describes an attempt to identify a new series of sub-type selective FGFR kinase inhibitors. *De novo* design was carried out on the ATP binding site of an existing FGFR1 crystal structure and a small molecular scaffold based upon an indazole nucleus was identified. Subsequent enhancement using structure-based drug design led to two fragment-based lead series that exhibited single digit micromolar potency against FGFR1-3. Further rounds of *de novo* design, synthesis and biological evaluation led to one series showing preferential inhibition of FGFR2 over FGFR1/3, exhibiting potencies in the nanomolar range. This selectivity preference could not be rationalised through docking studies and therefore work was conducted in order to crystallise the inhibitors in both FGFR1/2. Analysis of the binding poses of the inhibitors bound within FGFR1/2 outlined key structural differences that may provide insight into the observed selectivity preference for FGFR2. These crystal structures have allowed the design of selective inhibitors of FGFR2 of which work is ongoing. Finally, inhibitors were evaluated for efficacy in a cellular environment. A general drop in potency of inhibitors was observed when compared to the potency of the compounds against the enzymes which may be attributed to the poor cellular uptake of the compounds.



# Table of Contents

---

Acknowledgements .....	iii
Abstract .....	iv
Table of Contents .....	v
Abbreviations .....	xii
1 Chapter One – Introduction.....	1
1.1 Cancer.....	1
1.1.1 The Origin of Cancer .....	2
1.1.1.1 The Cell Cycle.....	2
1.1.1.2 Genetic Control of Cell Division.....	3
1.2 Kinases .....	4
1.2.1 Mechanism of Action.....	5
1.3 Fibroblast Growth Factor Receptors .....	6
1.3.1 Angiogenesis .....	6
1.3.2 FGFR Structure .....	7
1.3.2.1 Domain Roles .....	8
1.3.3 Kinase Domain.....	9
1.3.4 Cell Signalling Cascade .....	10
1.3.4.1 FGFR Isoforms.....	12
1.3.5 FGFR Ligands.....	13
1.3.6 Role in Bladder Cancer .....	14
1.3.7 FGFR2 Implicated Breast Cancer .....	17
1.4 Current Treatments for Cancer.....	18
1.4.1 Surgery .....	18
1.4.2 Radiotherapy .....	18
1.4.3 Chemotherapy .....	18
1.5 Inhibition of FGFRs .....	19
1.5.1 Development of Selective Inhibitors.....	19
1.5.1.1 ATP Binding Site .....	20
1.5.1.2 Inhibitor Binding Modes .....	22
1.5.2 FGFR Inhibitors .....	23
1.5.2.1 Type I .....	23

1.5.2.2	Type II .....	25
1.5.2.3	Type III .....	26
1.6	Structure-Based Drug Design .....	27
1.6.1	Maestro .....	28
1.6.2	eHiTS .....	28
1.6.3	PyMOL .....	29
1.6.4	<i>De Novo</i> Design .....	29
1.6.5	SPROUT .....	29
1.7	Project Aims .....	31
1.7.1	Overall Aim .....	31
1.7.2	Specific Objectives .....	31
2	Chapter Two – <i>De Novo</i> Fragment-Based Design .....	32
2.1	Hit Identification .....	32
2.1.1	Binding Pose of Compound 14 .....	34
2.2	‘First Generation’ Library Synthesis .....	37
2.2.1	Retrosynthetic Analysis .....	37
2.2.2	Suzuki Mechanism .....	37
2.2.3	Pd-Catalysed Suzuki Couplings .....	38
2.2.4	Biological Evaluation of ‘First Generation’ Fragments .....	39
2.3	Library Expansion .....	41
2.3.1	‘Second Generation’ Library Synthesis .....	42
2.3.2	Five-Membered Ring Systems .....	43
2.3.3	Retrosynthetic Analysis of Structure 41 .....	45
2.3.4	Synthesis of Compound 44 .....	46
2.3.5	Biological Evaluation of ‘Second Generation’ Fragments .....	48
2.3.6	Docking of Compounds 31 and 34 .....	49
2.4	SAR Exploration .....	50
2.4.1	Amine Library .....	50
2.4.1.1	Retrosynthetic Analysis of Structures 52-58 .....	51
2.4.1.2	Synthesis of Compounds 52-58 .....	51
2.4.1.3	Biological Evaluation of Compounds 52-59 and 61-63 .....	53
2.4.1.4	Docking of Compounds 52, 55 and 59 .....	55
2.4.2	Occupation of the H1 Sub-pocket .....	56
2.4.3	Biological Evaluation of Compounds 64 and 65 .....	58

2.5	Optimisation of Lead Fragments .....	58
2.5.1	SAR Expansion of Compound 31 .....	58
2.5.1.1	Synthesis of Compounds 66-74.....	60
2.5.1.2	Biological Evaluation of Compounds 66-74.....	60
2.5.2	SAR Validation and Expansion of Compound 34 .....	62
2.5.2.1	Synthesis of Compounds 75-80.....	63
2.5.2.2	Biological Evaluation of Compounds 75-80.....	64
2.6	Chapter Two Summary .....	66
3	Chapter Three – <i>De Novo</i> Fragment Growth .....	67
3.1	Application of SPROUT to Compound 31.....	67
3.1.1	Target Library .....	68
3.1.2	Retrosynthetic Analysis of Structure 85 .....	69
3.1.3	Synthesis of the Extended Ethoxy Series.....	69
3.1.4	Biological Evaluation of the Extended Ethoxy Series .....	71
3.2	Investigation into the Potency Decrease of Compound 85 .....	74
3.2.1	Solvation at the 3-Position of the Indazole Core .....	74
3.2.2	Synthesis of Compound 106 <i>via</i> the use of Cross Coupling.....	74
3.2.3	Synthesis of Compound 106 <i>via</i> S <sub>N</sub> Ar.....	75
3.2.4	Current Inhibitors Bearing an Indazole Scaffold .....	77
3.2.4.1	Amide Target Library.....	78
3.2.4.2	Retrosynthetic Analysis of Structures 115-118.....	79
3.2.4.3	Synthesis of Compounds 115-118.....	80
3.2.4.4	Biological Evaluation of Compounds 115-118 and 133 .....	82
3.3	SAR Exploration of the Amide Series .....	84
3.3.1	Synthesis of Compounds 135-137 .....	84
3.3.2	Biological Evaluation of Compounds 135-137.....	86
3.3.3	Inverse Amide Series .....	87
3.3.3.1	Retrosynthetic Analysis of Structures 143-145.....	87
3.3.3.2	Synthesis of Compounds 143-145.....	87
3.3.3.3	Biological Evaluation of Compounds 143 and 144.....	89
3.4	Revisit of the SPROUT Extended Scaffold 85.....	90
3.4.1	Synthesis of Compounds 149-151 .....	90
3.4.2	Biological Evaluation of Compounds 149-151 and 158.....	91
3.4.3	FGFR2 Selectivity Investigation.....	93
3.4.3.1	Synthesis of Compounds 160 and 161 .....	93

3.4.3.2	Biological Evaluation of Compounds 160 and 161.....	94
3.5	Chapter Three Summary .....	95
4	Chapter Four – Expansion of FGFR2 Selectivity .....	96
4.1	Lead Design.....	96
4.1.1	Retrosynthetic Analysis of Structure 164 .....	96
4.1.2	Synthesis of Compound 164 .....	97
4.1.3	Biological Evaluation of Compounds 164 and 170 .....	99
4.2	SAR Expansion .....	100
4.2.1	Synthesis of Compounds 171 and 172.....	100
4.2.2	Synthesis of Compound 173 .....	101
4.2.3	Biological Evaluation of Compounds 171-173 and 182.....	103
4.3	SAR Expansion of the Amide Series.....	104
4.3.1	Synthesis of the Extended Amide Series .....	104
4.3.1.1	Alternative Syntheses of Amide Containing Compounds.....	107
4.4	FGFR2 Selectivity Rationalisation.....	111
4.4.1	Expression and Crystallisation of FGFR1.....	111
4.4.2	FGFR1/Ligand Co-crystal Structures .....	112
4.4.2.1	FGFR1/Compound 115 Co-crystal Structure.....	112
4.4.2.2	Alternative Loop Conformation .....	113
4.4.2.3	FGFR1/Compound 160 Co-crystal Structure.....	114
4.4.2.4	FGFR1/Compound 164 Co-crystal Structure.....	116
4.4.3	Expression and Crystallisation of FGFR2 Variants.....	117
4.4.4	FGFR2/Ligand Co-crystal Structures .....	118
4.4.4.1	FGFR2/Compound 164 Co-crystal Structure.....	118
4.4.5	Comparison of the FGFR1/FGFR2 Binding Sites .....	119
4.4.5.1	Factors Affecting Sub-Type Selectivity .....	120
4.4.6	Crystal Structure Summary .....	121
4.5	Utilisation of FGFR1/2 Crystal Structures .....	121
4.5.1	Docking of Compound 170.....	121
4.6	Cellular Efficacy.....	123
4.6.1	Cell Viability Assay .....	124
4.6.1.1	Dose Response Curves-Compound 164.....	125
4.6.1.2	Cell Viability Results for Compounds 164, 171, 172 and 6.....	127
4.7	Chapter Four Summary .....	129

5 Chapter Five – Conclusions and Future Work .....	130
5.1 Conclusion – Project Milestones .....	130
5.2 Future Work .....	132
5.2.1 Design of Selective FGFR2 Inhibitors .....	132
5.2.1.1 Proposed Synthesis of Compounds 201-204 .....	133
5.2.2 Synthesis of Amide Series .....	134
5.2.3 Optimisation of ‘Drug-Like’ Properties .....	135
6 Chapter Six – Experimental .....	136
6.1 Chemistry Experimental .....	136
6.1.1 General Procedures and Instrumentation .....	136
6.1.2 General Experimental Methods .....	137
6.1.2.1 Method A: Suzuki Reactions .....	137
6.1.2.2 Method B: Reductive Aminations .....	137
6.1.2.3 Method C: BOC Deprotections .....	138
6.1.2.4 Method D: Methoxy Deprotections .....	138
6.1.2.5 Method E: Acid Chloride Couplings .....	138
6.1.2.6 Method F: Piperazine Cyclisations .....	138
6.1.3 Compound Numbering .....	138
6.1.4 Compounds .....	139
6.1.4.1 Chapter Two Compounds .....	139
6.1.4.2 Chapter Three Compounds .....	172
6.1.4.3 Chapter Four Compounds .....	221
6.2 Biochemical Experimental .....	240
6.2.1 General Methods and Equipment .....	240
6.2.2 Media and Buffers .....	240
6.2.2.1 Growth Media .....	241
6.2.2.2 General Buffers for Protein Purification and Analysis .....	241
6.2.3 Standard Protocol .....	242
6.2.3.1 Transformation of Competent <i>E.coli</i> Cells .....	242
6.2.3.2 Inoculation of LB Agar Plates .....	242
6.2.3.3 Mini Culture .....	242
6.2.3.4 Overexpression of FGFR1 .....	243
6.2.3.5 Overexpression of FGFR2 Variants .....	243
6.2.4 Purification of FGFR1 .....	243
6.2.4.1 Ni-NTA His <sub>6</sub> -tag Chromatography .....	243

6.2.4.2	Cleavage of His <sub>6</sub> -tag and IEX Chromatography .....	244
6.2.4.3	SEC.....	244
6.2.5	Purification of FGFR2 Variants .....	244
6.2.5.1	Cobalt Resin His <sub>6</sub> -tag Chromatography .....	244
6.2.5.2	SEC.....	245
6.2.5.3	Cleavage of His <sub>6</sub> -tag.....	245
6.2.6	SDS-PAGE.....	246
6.2.6.1	Preparation of Gels .....	246
6.2.6.2	Running Procedure .....	246
6.2.6.3	Visualisation and Imaging.....	246
6.2.6.4	Protein Concentration Determination.....	247
6.2.7	Crystallisation Trials .....	248
6.2.7.1	Equipment and Protocol .....	248
6.2.7.2	Preparation of Ligands .....	248
6.2.7.3	Crystallisation of FGFR1 .....	249
6.2.7.3.1	Tray Setup and Screening Conditions .....	249
6.2.7.4	Crystallisation of FGFR2 1Y .....	250
6.2.7.5	Crystallisation of FGFR2 WT .....	250
6.2.7.5.1	Tray Setup and Screening Conditions .....	250
6.3	Biological Experimental.....	252
6.3.1	Equipment and Materials .....	252
6.3.2	Tissue Culture .....	252
6.3.2.1	Cell Lines .....	252
6.3.2.2	Inhibitors .....	252
6.3.2.3	Cell Culture .....	252
6.3.2.4	Cell Passage.....	252
6.3.2.5	Cell Counting .....	253
6.3.2.6	CellTiter-Blue® Viability Assay.....	253
7	References.....	255
8	Appendices.....	267
8.1	Appendix 1.0 – FRET-Based Z'-Lyte Assay® .....	267
8.1.1	FGFR1 Assay Conditions .....	268
8.1.2	FGFR2 Assay Conditions .....	268
8.1.3	FGFR3 Assay Conditions .....	268
8.1.4	IC <sub>50</sub> Curves.....	269

8.2	Appendix 2.0 – Protein Expression and Crystallisation.....	278
8.2.1	FGFR1-SDS-PAGE .....	278
8.2.2	FGFR1-MS.....	279
8.2.3	FGFR2-SDS-PAGE .....	280
8.2.3.1	FGFR2 1Y .....	280
8.2.3.2	FGFR2 WT.....	281
8.2.4	FGFR2-Mass Spectrometry .....	282
8.2.5	FGFR1 Sequence .....	284
8.2.6	FGFR2 1Y Sequence .....	284
8.2.7	FGFR2 WT Sequence .....	285
8.2.8	Crystallographic Statistics.....	286
8.3	Appendix 3.0 – Cell Viability Graphs.....	287
8.3.1	Duplicate Measurement Graphs.....	287
8.3.1.1	SUM52 .....	287
8.3.1.2	JMSU1.....	287
8.3.1.3	VMCUB3 .....	288
8.3.2	Dose Response Inhibitor Curves.....	288
8.3.2.1	Compound 171 .....	288
8.3.2.2	Compound 172 .....	289
8.3.2.3	Compound 6 (PD173074) .....	289
8.4	Appendix 4.0 – Amino Acid Abbreviations.....	290
8.5	Appendices References .....	290

# Abbreviations

---

<b>Abbreviation</b>	<b>Definition</b>
2D-COSY	Two-Dimensional Correlation Spectroscopy
AB	Acidic Box
ABL	Abelson Murine Leukaemia Viral Oncogene Homolog 1
ACC	Automated Column Chromatography
ADP	Adenosine Diphosphate
AGC	Containing PKA, PKG, PKC families
ALL	Acute Lymphoblastic Leukaemia
APS	Ammonium Persulfate
Ar-q	Aromatic Quaternary Carbon
ATP	Adenosine Triphosphate
ATR	Attenuated Total Reflectance
BCR	Breakpoint Cluster Region Protein
BINAP	2,2'-bis(diphenylphosphino)-1,1'-binaphthyl
BLAST	Basic Local Alignment Search Tool
BME	2-Mercaptoethanol
BOC	<i>Tert</i> -Butyloxycarbonyl
CAMK	Calcium/calmodulin-dependant protein kinase
CBL	Casitas B-Lineage Lymphoma
CDK	Cyclin Dependant Kinase
CIP	Calf-Intestinal Alkaline Phosphatase
CK1	Casein Kinase 1
CMGC	Containing CDK, MAPK, GSK3, CLK families
CML	Chronic Myeloid Leukaemia
CRKL	Crk-Like
CVs	Column Volumes
D1	Immunoglobulin-Like Domain I
D2	Immunoglobulin-Like Domain II
D3	Immunoglobulin-Like Domain III
Da	Dalton
DABCO	1,4-Diazabicyclo[2.2.2]octane
DAG	Diacylglycerol
dba	Dibenzylideneacetone
DCE	1,2-Dichloroethane
DCM	Dichloromethane
DIBAL	Diisobutylaluminium Hydride
DIPEA	<i>N,N</i> -Diisopropylethylamine



DLSF	Diamond Light Source Facility
DMF	Dimethylformamide
DMG	Dimethylglycine
DMPK	Drug Metabolism and Pharmacokinetic
DMSO	Dimethylsulphoxide
DNA	Deoxyribose Nucleic Acid
DOM	Direct <i>Ortho</i> Metalation
dppf	1,1'-Ferrocenediyl-bis(diphenylphosphine)
DTT	Dithiothreitol
DUSP6	Dual-Specificity Phosphatase 6
EDC	1-Ethyl-3-(3-dimethylaminopropyl)-carbodiimide
EDTA	Ethylenediaminetetraacetic Acid
EGTA	Ethylene Glycol-bis( $\beta$ -aminoethyl ether)-N,N,N',N'-tetraacetic
eHiTS	Electronic High-Throughput Screening
ERK	Extracellular Signal-Regulated Kinase
ES	Electro Spray Ionisation
ESR	Oestrogen Receptor
ESRF	European Synchrotron Radiation Facility
ETS	E26 Transformation-Specific
ETV	ETS Translocation Variant
EWG	Electron Withdrawing Group
FCS	Foetal Calf Serum
FDA	Food and Drug Administration
FGF	Fibroblast Growth Factor
FGFR	Fibroblast Growth Factor Receptor
FGFRL1	Fibroblast Growth Factor Receptor Like-1
FGI	Functional Group Interconversion
FLT3	Fms-like Tyrosine Kinase 3
FOXO1	Forkhead Box Class Transcription Factor
FRET	Fluorescence Resonance Energy Transfer
FRS2 $\alpha$	FGFR Substrate 2 $\alpha$
FTIR	Fourier Transform Infrared Spectroscopy
GAB	GRB2-Associated Binder
Glide	Grid-Based Ligand Docking with Energetics
GRB	Growth Factor Receptor Bound Protein
HBS	Heparin Binding Site
HEPES	4-(2-Hydroxyethyl)-1-piperazineethanesulfonic acid
HMBC	Heteronuclear Multiple Bond Correlation Spectroscopy
HOBT	Hydroxybenzotriazole
HPLC	High-Performance Liquid Chromatography
HRMS	High Resolution Mass Spectrometry

HS	Heparin Sulphate
HSPG	Heparan Sulphate Proteoglycan
HSQC	Heteronuclear Single Quantum Coherence Spectroscopy
HTS	High-Throughput Screening
IB2	Islet Brain-2
IEX	Ion Exchange
IGFR	Insulin-Growth Factor Receptor
IP <sub>3</sub>	Inositol Triphosphate
IPTG	Isopropyl $\beta$ -D-1-thiogalactopyranoside
IR	Infrared Spectroscopy
JMD	Juxtamembrane Domain
KD	Kinase Domain
KIT	Tyrosine-Protein Kinase Kit
LB	Lysogeny Broth
LC-MS	Liquid Chromatography-Mass Spectrometry
LE	Ligand Efficiency
LogD	Distribution-Coefficient
LogP	Partition-Coefficient
MAPK	Mitogen-Activated Protein Kinase
MEK	Mitogen-Activated Protein Kinase Kinase
MEM	Modified Eagle Medium
MS	Mass Spectrometry
mTOR	Mammalian Target of Rapamycin
MWCO	Molecular Weight Cut-Off
NBS	N-Bromosuccinimide
NCS	N-Chlorosuccinimide
NMR	Nuclear Magnetic Resonance
NSCLC	Non-Small-Cell Lung Carcinoma
NTA	Nitrilotriacetic Acid
OD <sub>600</sub>	Optical Density at 600 nm
PBS	Phosphate-Buffered Saline
PDB	Protein Data Bank
PDGF	Platelet Derived Growth Factor
PEG	Polyethylene Glycol
Ph*	Philadelphia Chromosome Positive
PI3K	Phosphoinositide 3-Kinase
PIP <sub>2</sub>	Phosphatidylinositol 4,5-biphosphate
PKB	Protein Kinase B
PKC	Protein Kinase C
PLC $\gamma$	Phospholipase C Gamma
PPI	Protein-Protein Interaction

PTP-1B	Protein Tyrosine Phosphatase 1B
PUNLMP	Papillary Urothelial Neoplasm of Low-Malignant Potential
RACK	Receptor for Activated C Kinase
RGC	Receptor Guanylate Cyclases
RNA	Ribose Nucleic Acid
rpm	Revolutions per Minute
RPMI	Roswell Park Memorial Institute
RTK	Receptor Tyrosine Kinase
SAR	Structure-Activity Relationship
SBDD	Structure-Based Drug Design
SD	Standard Deviation
SDS-PAGE	Sodium Dodecyl Sulphate-Polyacrylamide Gel Electrophoresis
SEC	Size Exclusion Chromatography
SEF	Similar Expression to FGF
SH2	Src Homology 2
SHB	SH2 Domain-Containing Adapter Protein B
SHP	Src Homology Phosphatase
S <sub>N</sub> Ar	Nucleophilic Aromatic Substitution
SNP	Single Nucleotide Polymorphisms
SOS	Son of Sevenless Guanine Nucleotide Exchange Factor
SP	Signal Peptide
SPR	Surface Plasmon Resonance
SPRY	Sprouty
STAB	Sodium Triacetoxyborohydride
STAT	Signal Transducer and Activator of Transcription Protein
STE	Homologs of Yeast Sterile 7, Sterile 11, Sterile 20 Kinases
TB	Terrific Broth
TCEP	Tris(2-carboxyethyl)phosphone
TEMED	Tetramethylethylenediamine
TEV	Tobacco Etch Virus
TFA	Trifluoroacetic Acid
THF	Tetrahydrofuran
TK	Tyrosine Kinase
TKL	Tyrosine Kinase-Like
TLC	Thin Layer Chromatography
TMD	Transmembrane Domain
TMP	2,2,6,6-Tetramethylpiperidine
TNM	Tumour Node Metastasis
TOF	Time of Flight
Tris	Tris(hydroxymethyl)aminomethane
TSC	Cytosolic Tuberous Sclerosis Complex

TSG	Tumour Suppressor Gene
U	Enzyme Units
UC	Urothelial Carcinoma
UniprotKB	Uniprot Knowledge Database
UPLC	Ultra-Performance Liquid Chromatography
VEGF	Vascular Endothelial Growth Factor
WHO	World Health Organisation
X-Phos	2-Dicyclohexylphosphino-2',4',6'-triisopropylbiphenyl

## Chapter One – Introduction

### 1.1 Cancer

Cancer can be defined as a class of diseases which are characterised by uncontrolled cell proliferation, survival, or migration into nearby tissues. Genes involved in cellular replication, maintenance, and repair, become mutated resulting in the formation of a tumour which can be life threatening.<sup>1</sup> In 2012, according to the world health organisation (WHO), there were 14.1 million new cases of cancer, 8.1 million deaths from cancer, and 32.6 million people living with cancer worldwide.<sup>2</sup> The vast number of people who suffer from this debilitating disease makes cancer a crucial target for drug discovery and therapeutic intervention.

In order for a cell to become cancerous it has to acquire certain properties known as the hallmarks of cancer (Figure 1.1). It is understood that at least one, if not all, of these hallmarks are required in order for a tumour to arise.<sup>1</sup>

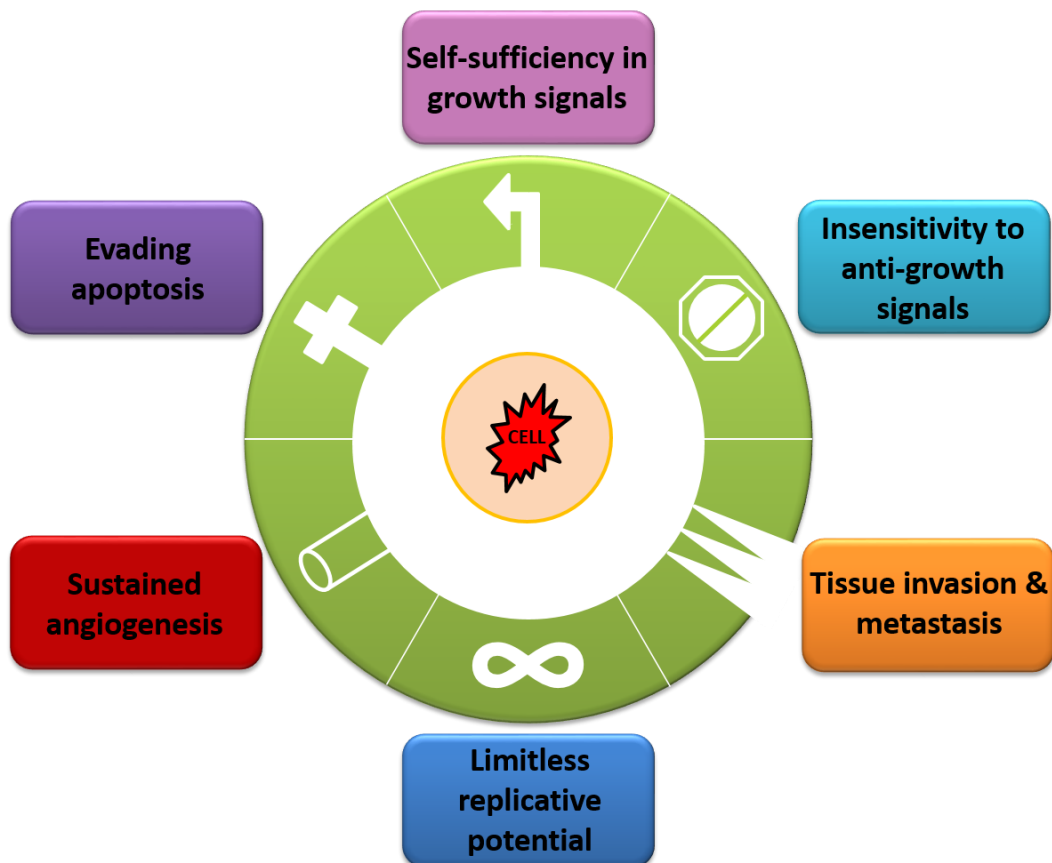


**Figure 1.1:** The hallmarks of cancer. Adapted from reference 1.

In addition to the six hallmarks, two emerging hallmarks and two enabling characteristics have been identified and defined respectively as: deregulation of

cellular energetics, avoiding immune destruction, genome instability and mutation, and tumour-promoting inflammation.<sup>3</sup> Continuous cell growth and proliferation requires major reprogramming of a cancerous cells metabolic energy pathways, and this is distinct from normal cellular energetics. Cancerous cells also proliferate through actively evading attack and elimination from immune cells. The antagonism of cancer cells by immune cells results in local inflammation of nearby tissue and has been shown to be characteristic of a cancerous phenotype.<sup>3</sup>

## 1.1.1 The Origin of Cancer

### 1.1.1.1 The Cell Cycle

Cell division is controlled by a series of events known as the cell cycle.<sup>4</sup> The cell cycle involves various cellular transformations such as: deoxyribose nucleic acid (DNA) replication, cell growth, and cell division. The process of normal cellular division ensures the replacement of old cells with new ones, maintaining the cycle in a healthy manner. There are five key stages during the life cycle of a cell;  $G_0$ ,  $G_1$ , S,  $G_2$  and M (Figure 1.2).

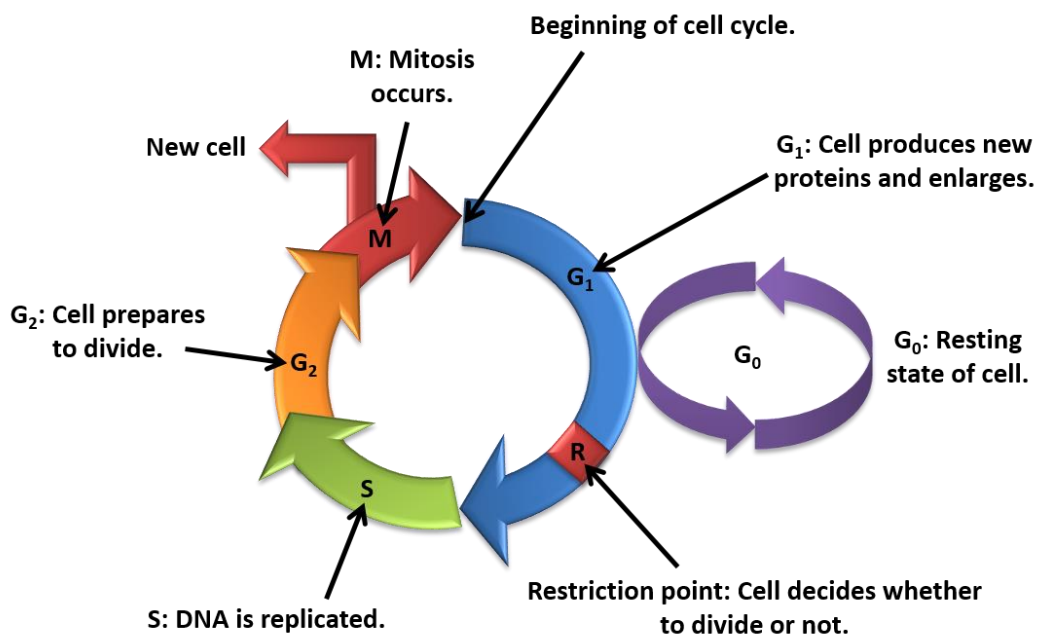


Figure 1.2: The cell cycle. Adapted from reference 4.

At the beginning of the cell cycle, the cell is in the cell growth phase  $G_1$ . In this phase extracellular signalling activates metabolic activity involving ribonucleic acid (RNA) and protein synthesis.<sup>5</sup> The cycle then reaches a restriction point; a decision is made to either proceed to cell division or to return to the resting state  $G_0$ , known as quiescence. Quiescence occurs due to a lack of response from external growth factors.<sup>5</sup>

Progression into the S phase occurs when growth-dependant cyclin-dependant kinase (CDK) activity promotes DNA replication.<sup>6</sup> Activation of CDKs induces a positive feedback loop which in turn further increases the activity of CDKs, promoting further DNA replication.<sup>6</sup> The cell then enters the G<sub>2</sub> phase in which it enlarges and prepares for division. Finally, mitosis occurs producing two daughter cells and the cycle then returns to the beginning.<sup>5</sup> Along with the restriction point between the G<sub>1</sub>/S phases there are two other known checkpoints; the G<sub>2</sub>/M checkpoint and the metaphase checkpoint.<sup>7</sup> All these checkpoints ensure that the cell cycle process is proceeding as normal. If a problem is detected then the cycle is temporarily interrupted until the problem is repaired, or if the problem is irreversible the cycle is abandoned leading to apoptosis.<sup>8</sup>

#### **1.1.1.2 Genetic Control of Cell Division**

Gene transcription is the driving force for all protein production within nature. Certain genes, known as proto-oncogenes, are responsible for causing cell proliferation, inhibition of cell differentiation, and inhibition of apoptosis.<sup>9</sup> Such genes are precursors to what are known as oncogenes. Oncogenes are responsible for uncontrolled cell proliferation, excessive cell differentiation, and increased inhibition of apoptosis that is associated with cancers.<sup>9</sup> In addition to oncogenes, cancer can arise by the inactivation of tumour suppressor genes (TSGs). TSGs code for proteins that have a damping or repressive effect on cell cycle regulation and promote apoptosis.<sup>10</sup> The mechanisms by which a proto-oncogene becomes an oncogene can be simplified into underlying genetic mutations and chromosomal translocations. Cancer phenotypes can be caused by the following genetic alterations:<sup>9</sup>

- Point mutations, deletions, or insertions that lead to hyperactive proteins or inactivate tumour suppressor genes.
- Point mutations, deletions, or insertions within the promoter region. This can lead to altered transcription factor binding and increased transcription.
- Amplification of DNA that generates extra chromosomal copies of a proto-oncogene.
- Relocation of a proto-oncogene downstream of a potent promoter through chromosomal translocation leading to higher expression of the protein.

The mechanisms by which genetic alterations can occur are numerous, ranging from heredity aspects to lifestyle choices such as smoking, diet, and exercise. Recent data

suggests that only 5-10% of all cancer cases are caused by underlying genetic defects.<sup>11</sup> The majority of cancer cases (90-95%) have been attributed to external factors such as the environment and lifestyle, meaning that to a certain extent cancer could be preventable if the right lifestyle changes were implemented.<sup>11</sup>

## 1.2 Kinases

The phosphorylation of proteins in regulating protein function has long been a study of interest and today remains a strong area of research within the scientific community. A multitude of genes code for proteins that are responsible for phosphorylating other proteins and are known as kinases. Protein kinases are crucial for numerous cellular processes within eukaryotic cells some of which include cell transcription, apoptosis, and differentiation.<sup>12</sup> The completion of the human genome project in 2003 allowed scientists to identify almost all human protein kinases (518), accounting for about 1.7% of all human genes.<sup>12</sup> Kinases can be ordered into a phylogenetic hierarchy, based primarily on sequence comparison of their catalytic domains, known as the kinome, and is represented as a dendrogram (Figure 1.3).

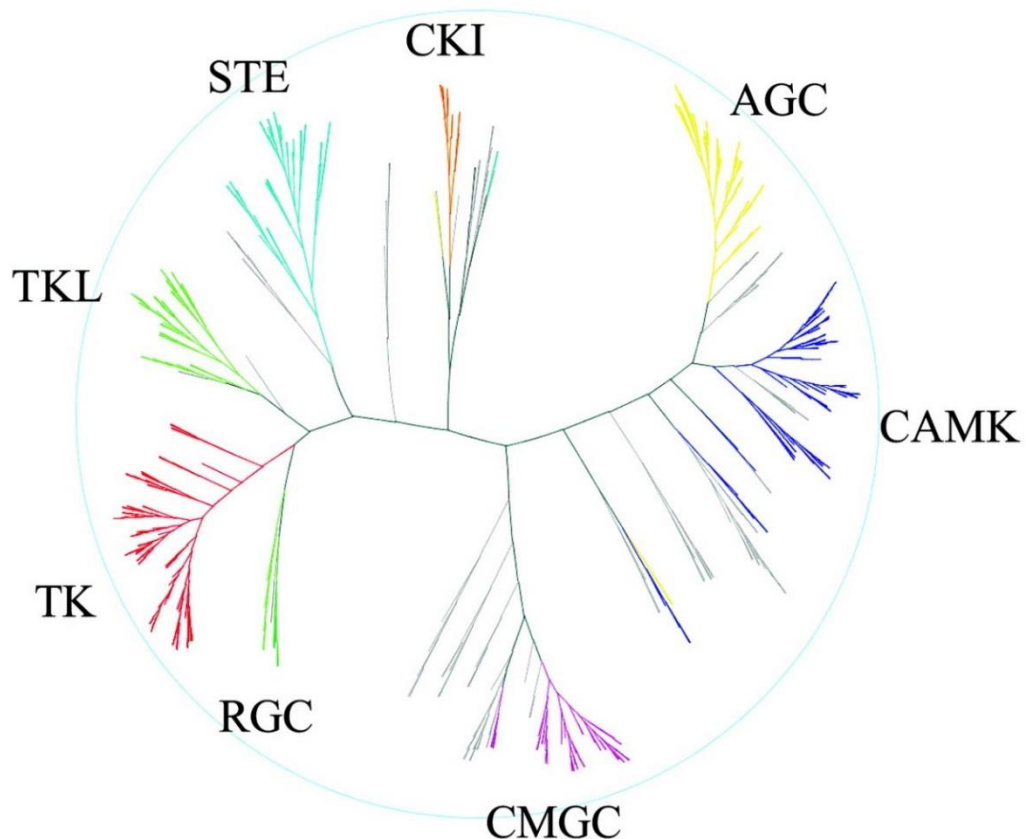


**Figure 1.3:** A simplified dendrogram of the human kinome. All eight major groups are outlined in bold. Atypical protein kinases are not outlined. Reproduced from reference 12, permission granted to use image.



The kinome consists of nine parent groups which contain a total of 134 families and 196 subfamilies.<sup>12</sup> It is apparent that both the structural differences and functional roles of protein kinases can vary vastly but all share the same basic mechanism of action.

### 1.2.1 Mechanism of Action

Protein kinases modify and regulate the activity of enzymes within eukaryotic cells by catalysing the transfer of a phosphate group from adenosine triphosphate (ATP) to hydroxy containing amino acids within the substrate protein, namely serine, threonine, and tyrosine. However, phosphorylation has also been found to occur on histidine.<sup>13</sup> The additional electrostatic functionality that the phosphate group provides allows interactions to occur with nearby residues which can be either attractive or repulsive.<sup>14</sup> These interactions induce 3D structural changes throughout the substrate protein leading to a catalytically active enzyme (Figure 1.4). This often results in a cascade of protein-protein interactions (PPIs) and eventually leads to signal transduction and gene expression.<sup>14</sup>

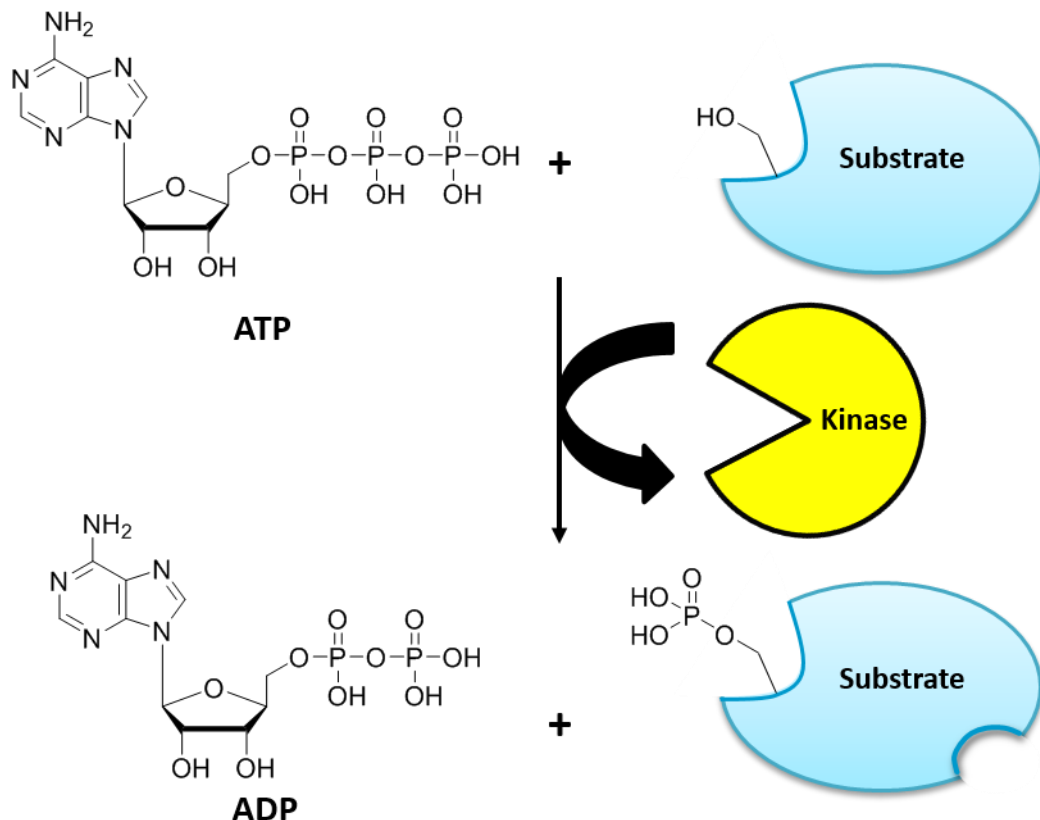


**Figure 1.4:** General mechanism of action of kinases.

Kinases help facilitate this process by localising both the substrate and ATP within the active site. Charged amino acid residues within the kinase coordinate to the negatively

charged phosphate group which help stabilise the transition state.<sup>15</sup> Additionally, some kinases have bound metal co-factors that also help coordinate phosphate groups, for example adenylate kinase.<sup>16</sup> The extra stabilisation received in both cases helps compensate for the high level of energy that is produced from cleavage of the phosphoanhydride bond present in ATP.<sup>17</sup> Adenosine diphosphate (ADP) is converted back into ATP with the aid of ATP synthase *via* the proton-motive force.<sup>14</sup> One such family that adopt this mechanism for phosphorylation are the fibroblast growth factor receptors (FGFRs).

### **1.3 Fibroblast Growth Factor Receptors**

The FGFRs are transmembrane receptor tyrosine kinases (RTKs) and transmit cellular signalling by binding fibroblast growth factors (FGFs). There are four known FGFRs, FGFR1-4.<sup>18</sup> A fifth FGFR exists, known as FGFR5 or FGFR like-1 (FGFRL1), but does not come under the category of an RTK. It has no tyrosine kinase (TK) domain and only shares a sequence homology of approximately 30% with its related receptors.<sup>19</sup>

They are crucial enzymes involved in various processes such as: control of the nervous system, tissue repair, and wound healing and have been shown to play an important role in cancer.<sup>20,21,22</sup> They also play an important role in angiogenesis, one of the hallmarks of cancer (Figure 1.1).

#### **1.3.1 Angiogenesis**

The development of a tumour, known as tumorigenesis, is a process that requires constant nutrition in order to facilitate tumour growth and development. As the tumour increases in size the existing blood supply is insufficient to maintain the current rate of growth. The lack of blood supply triggers the growth of new blood vessels from pre-existing ones, known as angiogenesis.<sup>21</sup>

Angiogenesis is a multi-step process which begins with the release of pro-angiogenic growth factors such as vascular endothelial growth factors (VEGFs), FGFs and angiopoietins.<sup>21</sup> These factors bind to receptors leading to the degradation of the basement membrane allowing endothelial cells to migrate, proliferate and differentiate forming solid endothelial cell sprouts within the surrounding matrix.<sup>21</sup> Vascular loops form and capillary tubes develop creating tight junctions, leading to the deposition of

a new basement membrane.<sup>21</sup> The new endothelial cells secrete growth factors such as platelet-derived growth factors (PDGFs) which recruit pericytes to help ensure the stability of the new blood vessel.<sup>22</sup> Inhibition of this process would thereby halt the growth of a tumour and make treatment of the cancer more manageable.

### 1.3.2 FGFR Structure

The general structure of FGFRs is uniform amongst all of them and consists of an extracellular binding domain, a single transmembrane domain, and an intracellular domain (Figure 1.5).<sup>18</sup>

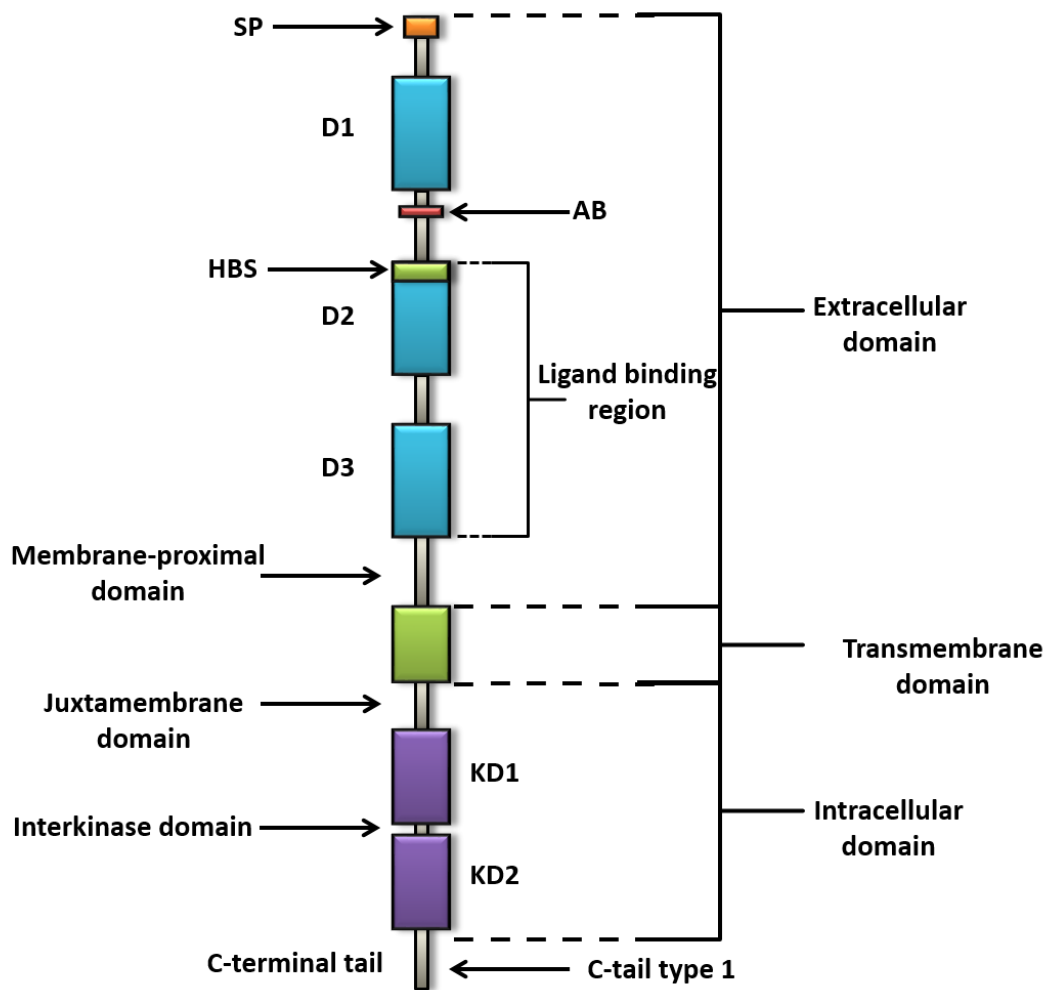


**Figure 1.5:** A simplified structure of *FGFR1*. Adapted from reference 18.

The extracellular domain contains a signal peptide (SP) and three immunoglobulin-like domains (D1, D2 and D3) connected by short flexible linkers.<sup>23</sup> The linker between D1 and D2 contains the acidic box (AB); a short amino acid sequence containing eight consecutive acidic residues including glutamate and aspartate.<sup>24</sup> The region in which ligands bind spans both D2 and D3. The N-terminal

of D2 contains a heparin binding site (HBS), a stretch of 18 amino acids that plays an important role in the recruitment of heparan sulphate (HS) and HS proteoglycans (HSPGs), which are important co-factors for FGF binding.<sup>18</sup> D3 is connected to the transmembrane domain (TMD) *via* the membrane-proximal domain. Downstream from the TMD is the intracellular domain. The intracellular domain contains two kinase domains (KD1 and KD2) which are the catalytic segments of the protein. The KDs are linked to the TMD *via* the juxtamembrane domain (JMD). The KDs are linked together *via* a fourteen amino acid long chain, known as the interkinase domain, with the C-terminal tail joined to KD2.<sup>18</sup>

### 1.3.2.1 Domain Roles

Each domain within the FGFR has specific roles within signal transduction. Several studies have shown an autoinhibitory role for D1 and the AB. Exclusion of exon one leads to the loss of D1 and AB resulting in isoforms that have a higher affinity to FGFs and HS, leading to upregulation of FGFR signalling.<sup>25,26,27</sup> Nuclear magnetic resonance (NMR) and surface plasmon resonance (SPR) spectroscopy show that the negatively charged AB interacts with the HBS on D2, thus suppressing the binding of HS. This interaction is also thought to place D1 in closer proximity to D2/D3 which blocks ligand binding leading to autoinhibition of the FGFRs.<sup>28</sup>

The region spanning D2-D3 is known as the ligand binding region. FGFs bind to this region with the help of HSPGs. HSPGs are thought to help FGF binding in three ways: i) protect FGFs from proteolytic, thermal, and pH-dependant degradation, ii) act as a storage reservoir whereby FGF can readily be liberated, or iii) help FGF-FGFR interaction by limiting the movement and orientation of the FGF ligand.<sup>29</sup>

The TMD is believed to stabilise and maintain the formation of dimers of FGFRs, a crucial event in signal transduction.<sup>30</sup> The JMD, a segment of around 40-80 amino acids, is believed to play a diverse role in the activity of RTKs. Amino acids within this region can be phosphorylated and also act as binding sites for several downstream signalling molecules.<sup>30</sup> Several studies have shown that mutations, deletions, and/or insertions within the JMD can lead to cancer, outlining the importance of the JMD in signal transduction.<sup>31,32</sup>

### 1.3.3 Kinase Domain

The kinase domains are responsible for the phosphorylation of several downstream signalling proteins.<sup>33</sup> Upon dimerisation of monomers, eight tyrosine residues are phosphorylated, six of which are phosphorylated in a specific order (Figure 1.6).<sup>34,35</sup>

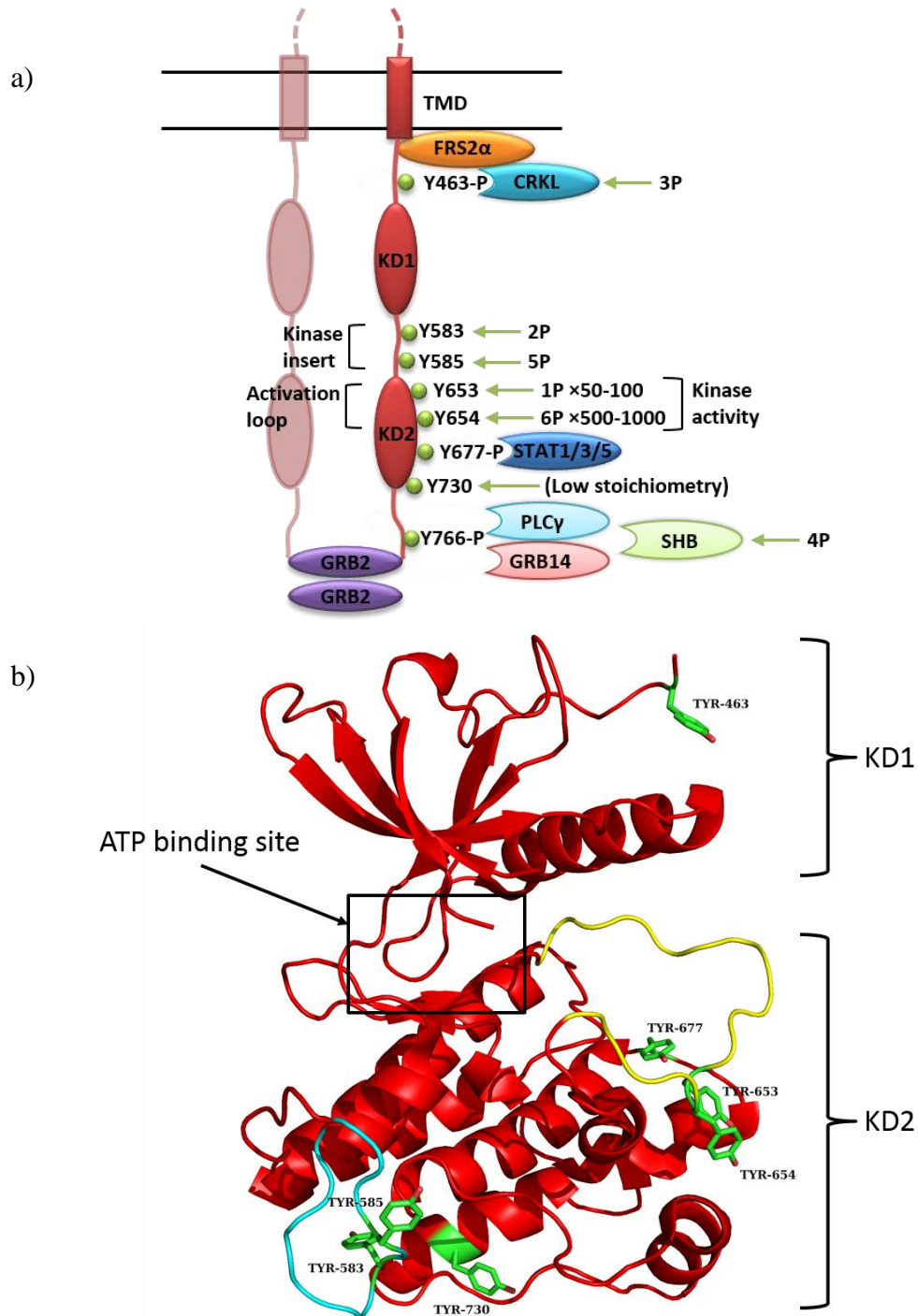


**Figure 1.6:** a) Intracellular region of *FGFR1* showing both *KD1* and *KD2*. Specific tyrosine residues that are phosphorylated are outlined with six tyrosines in order of specific phosphorylation (1P-6P). Specific signalling partners are also outlined. Adapted from reference 33. b) Apo crystal structure of the *FGFR1* kinase domains (PDB:4UWY) with the ATP binding site outlined. The kinase insert, activation loop, and tyrosine residues that are phosphorylated are outlined in cyan, yellow and green respectively. Y766 not present in crystal structure due to flexible C-tail.

During the first phase of activation, Y653 is phosphorylated which leads to a 50-100-fold increase in kinase activity. In the second phase of activation Y583, Y463, Y766 and Y585 are phosphorylated sequentially. The final phase sees the phosphorylation of Y654 leading to an overall increase in kinase activity of 500-1000-fold.<sup>33</sup> Phosphorylation of Y463 and Y677 leads to activation of Crk-like (CRKL) and signal transducer and activator of transcription proteins (STAT) respectively. Phosphorylation of Y766 can lead to the activation of either phospholipase C gamma (PLC $\gamma$ ), growth factor receptor bound protein (GRB) 14 or SH2 (Src Homology 2) domain-containing adapter protein B (SHB).<sup>33</sup> GRB2 is also phosphorylated leading to its dissociation from the receptor. FGFR substrate 2 $\alpha$  (FRS2 $\alpha$ ) is an adaptor protein that is bound to the JMD and also gets phosphorylated by Y463. This leads to the activation of numerous cytosolic pathways such as the mitogen-activated protein kinase (MAPK) pathway.<sup>33</sup>

### 1.3.4 Cell Signalling Cascade

Synergistic binding of HS and an FGF, with the help of HSPGs, causes dimerisation between receptors resulting in homodimers or heterodimers.<sup>33</sup> This results in conformational changes within the intracellular domain causing each monomer to phosphorylate the adjacent one on specific tyrosine residues, termed autophosphorylation.<sup>33</sup> The  $\gamma$ -phosphate of ATP acts as the phosphate source.<sup>36</sup> Four principal signalling cascades are triggered when the FGFR is activated; phosphoinositide 3-kinase (PI3K)-protein kinase B (PKB), RAS-MAPK, PLC $\gamma$  and STAT pathways (Figure 1.7). The PI3K-PKB and RAS-MAPK pathways are activated through the phosphorylation of FRS2 $\alpha$ . Along with FRS2 $\alpha$ , extracellular signal-regulated kinase (ERK) one/two are activated through phosphorylation of Y463 which itself directly interacts with CRKL (Figure 1.6).<sup>37</sup> FRS2 $\alpha$  interacts with numerous downstream signalling partners. GRB2 is an adapter protein that is anchored to the membrane of the cell and activation of this protein leads to the activation of the RAS-MAPK and the PI3K-PKB pathways through son of sevenless guanine nucleotide exchange factor (SOS) and GRB2-associated binder (GAB) 1 respectively.<sup>38,39</sup> The RAS-MAPK pathway leads to activation of E26 transformation-specific (ETS) transcription factors with this group of proteins regulating expression for a range of target genes such as ETS translocation variant (ETV) four/five.<sup>40</sup> Interaction of these proteins with MAPK leads to gene expression.

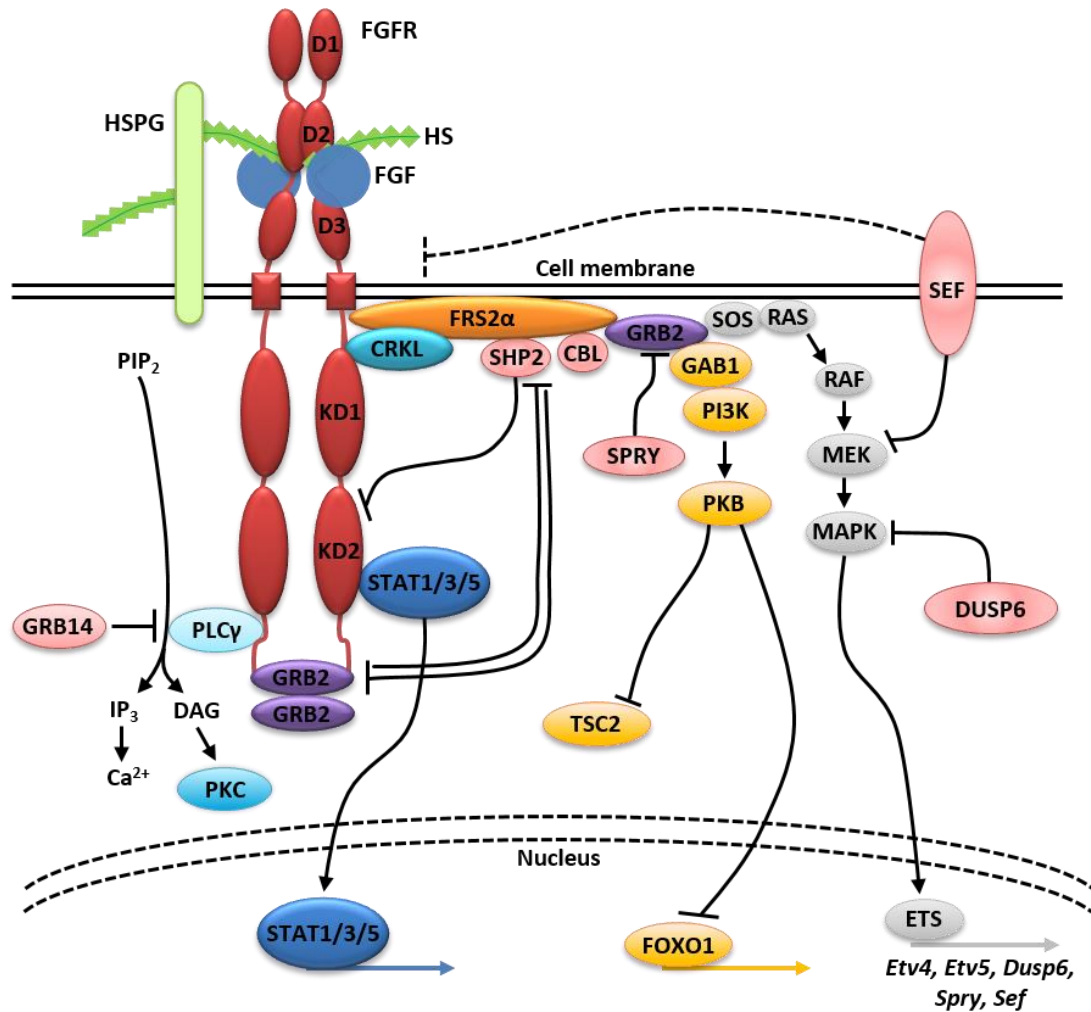


**Figure 1.7:** The FGFR signalling cascade. Adapted from reference 33.

The PI3K-PKB pathway is different to the RAS-MAPK pathway in that it functions to suppress the activity of downstream signalling partners. Two such proteins that are activated through the PI3K-PKB pathway are the fork-head box class transcription factor (FOXO1) and the cytosolic tuberous sclerosis complex (TSC) 2.<sup>41</sup> FOXO1 is a pro-apoptotic effector and becomes inactive when phosphorylated by PKB, causing it to leave the cell nucleus, promoting cell survival.<sup>41</sup> PKB can also activate the mammalian target of rapamycin (mTOR) complex 1 *via* inhibition of TSC2, this eventually leads to cell proliferation.<sup>41</sup>

The PLC $\gamma$  pathway is activated through phosphorylation of Y766 within the C-terminal tail of FGFR (Figure 1.6). This leads to hydrolysis of phosphatidylinositol 4,5-bisphosphate (PIP<sub>2</sub>) to produce diacylglycerol (DAG) and inositol triphosphate (IP<sub>3</sub>).<sup>33</sup> DAG leads to activation of protein kinase C (PKC) and IP<sub>3</sub> increases the levels of Ca<sup>2+</sup> within the cell. PKC is translocated to the plasma membrane by receptor for activated C kinase (RACK) and along with the increase in Ca<sup>2+</sup>, this process has been

shown to be important in the healthy development of egg cells during fertilisation.<sup>42</sup> Y766-P can also bind GRB14, a process which inhibits the PLC $\gamma$  pathway.<sup>43</sup> SHB also interacts with Y766 which enhances FRS2 $\alpha$  phosphorylation, regulating the RAS-MAPK pathway.<sup>44</sup> STAT1, 3 and 5 are activated through the phosphorylation of Y677 and these have been shown to play important roles in diseases in which FGFR3 is mutated or overexpressed.<sup>45,46</sup>

Several proteins negatively regulate FGFR signalling; sprouty (SPRY), similar expression to FGF (SEF), dual-specificity phosphatase 6 (DUSP6), casitas B-lineage lymphoma (CBL) and src homology phosphatase (SHP) 2. SPRY is present within all TK signalling pathways and interacts with GRB2 to suppress the RAS-MAPK and regulate the PI3K-PKB pathways respectively. Mouse knockout studies suggest SPRY is essential for growth and development, and deregulation of this protein has implications in some human cancers and autoimmune disease.<sup>47,48</sup> SEF is a membrane-bound protein and is an antagonist of FGF signalling. SEF binds to mitogen-activated protein kinase kinase (MEK) preventing MAPK dissociation from the MEK-MAPK complex, thus halting signal transduction.<sup>49</sup> SEFs extracellular domain can also inhibit FGFR signalling by directly interacting with the extracellular domains of FGFR.<sup>50</sup> DUSP6 is a specific ERK1/2 phosphatase that dephosphorylates tyrosine and threonine residues and acts as a negative feedback regulator of FGFR signalling.<sup>51</sup> CBL is an E3 ubiquitin ligase and interacts with both FRS2 $\alpha$  and GRB2. This forms a ternary complex which results in ubiquitination and degradation of FRS2 $\alpha$  and the FGFR.<sup>52</sup> SHP2 also binds to FRS2 $\alpha$  and dephosphorylates GRB2 and FGFR2, leading to a halt in the cell signalling pathway.<sup>53</sup>

Intracellular signalling is very complex and individual pathways are rarely exclusively activated, in fact, there is cross-talk in almost all intracellular signal transduction pathways leading to a vast array of gene expression possibilities.<sup>54</sup>

#### 1.3.4.1 FGFR Isoforms

Each subfamily of FGFR can exist as a variety of isoforms due to alternate splicing during transcription of the genes. Several types of isoform exist and are listed below.<sup>55</sup>

- Use of alternate exons – Exon eight/nine within D3 can both be expressed resulting in D3b or D3c isoforms. These isoforms are expressed differentially depending on tissue type and have differing affinities to FGF ligands.<sup>56</sup>



- Inclusions or exclusions of exons in the extracellular domain – Loss of exon one results in the truncation of D1 and the AB.
- C-terminal truncations – Shortening of the C-terminal tail results in disordered phosphorylation of target proteins.
- Soluble receptors – Lack of TMD results in a soluble form of the receptor. Several types exist and one of their functions is believed to act as a competitor for ligand binding.
- Specific amino acids – Inclusion of a valine/threonine motif in exon ten can result in activation of the MAPK signalling pathway *via* an interaction with FRS2 $\alpha$ . Exclusion of this motif does not initiate the MAPK signalling pathway.

Each FGFR can exist as any of these isoforms all of which have different affinities to FGF ligands.

### 1.3.5 FGFR Ligands

FGFR signalling is initiated when an FGF molecule binds to the extracellular domain. FGF molecules are small polypeptides that contain a partially conserved core (120-130 amino acids) that have a high binding affinity to HS. There are 22 known FGFs within mammals and these are characterised into seven subfamilies using phylogenetic alignments (Table 1.1).<sup>57</sup>

**Table 1.1:** Summary of all mammalian FGFs with their subfamilies and receptor preference. Adapted from reference 57.

<b>FGF Subfamily</b>	<b>Ligands</b>	<b>Receptor Preference</b>
FGF1	FGF1, FGF2	FGF1 activates all FGFRs; FGF2 prefers FGFR1c/FGFR2c
FGF4	FGF4, FGF5, FGF6	FGFR1c, FGFR2c
FGF7	FGF3, FGF7, FGF10, FGF22	FGFR1b, FGFR2b
FGF8	FGF8, FGF17, FGF18	FGFR1c, FGFR3c, FGFR4
FGF9	FGF9, FGF16, FGF20	FGFR2c, FGFR3c
FGF11	FGF11, FGF12, FGF13, FGF14	No activation of FGFRs
FGF19	FGF19, FGF21, FGF23	Hormone class, weak activation of FGFR1c, FGFR2c

The first five subfamilies of FGF ligands, FGF1, FGF4, FGF7, FGF8 and FGF 9, are paracrine signalling molecules that bind with both HS and FGFRs to form a tripartite complex.<sup>57</sup> Families FGF11 and FGF19 are different. FGF11-14, also known as FGF homologous factors, have high sequence homology to that of other FGFs but have been found not to activate FGFRs. They act intracellularly with other targets such as kinase scaffold protein, islet brain-2 (IB2), and voltage-gated sodium channels.<sup>58</sup> FGF19, 21, and 23 are weak activators of FGFRs and function as an endocrine hormone class impacting on adult metabolism and homeostasis.<sup>59</sup>

### **1.3.6 Role in Bladder Cancer**

Aberrant signalling in FGFRs has been shown to play an important role in the development of several cancers, including bladder cancer.

In 2012, bladder cancer was the 11<sup>th</sup> most common cancer worldwide accounting for 3.1% of all cancer cases, with an estimated death toll of 165,000 people.<sup>2</sup> Bladder cancer, like all cancers, is a progressive disease and has various grades and stages. Tumours are classified using the Tumour Node Metastasis (TNM) staging system.<sup>60</sup> This system classifies tumours based on their invasiveness (Ta: confined to the urothelium; T1: invasion to the lamina propria; T2: invasion into the muscular layer; T3: invasion into the submuscular layer; T4: spreading to other organs) and what state of differentiation they are in.<sup>61</sup> The differentiation state can be determined using the 2004 WHO grading system, for the non-invasive tumours this includes: papillary urothelial neoplasm of low-malignant potential (PUNLMP), non-invasive low-grade papillary urothelial carcinoma, and non-invasive high-grade papillary urothelial carcinoma.<sup>62</sup> A low grade tumour has well differentiated cells and structure whereas a high grade tumour has poorly differentiated cells and structure.

Around 70% of urothelial carcinomas (UCs) are considered as low-grade superficial papillary tumours with a relatively benign prognosis.<sup>61</sup> Treatment includes surgery and/or local chemo/immunotherapy. A major problem concerning these tumours is their propensity to recur which requires frequent surveillance in order to monitor disease progression. A good prognosis coupled with constant disease monitoring makes this type of cancer one of the most expensive and time consuming cancers to treat.<sup>61</sup> Around 15% of superficial tumours will become invasive. Treatment of these tumours is more challenging than for non-invasive tumours which results in a five-year survival rate of <40%. In recent years, studies have suggested that aberrant FGF

signalling is a common theme in UCs. Activating mutations and overexpression have been identified as causes of uncontrolled cell proliferation. In particular, numerous mutant forms of FGFR3 have been detected in a vast number of UCs (Figure 1.8).<sup>61</sup> Around 50% of both lower and upper urinary tract tumours contain mutations in FGFR3. A sample group containing 1898 bladder tumours showed mutations in three distinct exons; 7, 10 and 15 and are known as hot-spot regions.<sup>63</sup> The most common mutations within exon seven are S249C (~61%) and R248C (~8%). Both mutations here express cysteine residues within the extracellular domain.

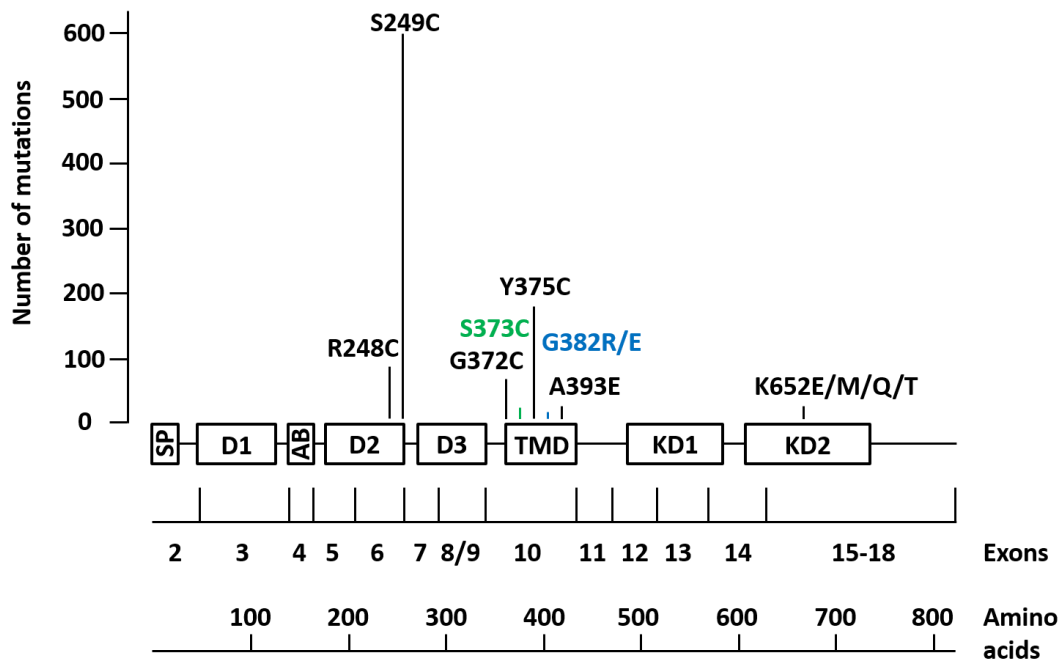


**Figure 1.8:** Structure of FGFR3 showing areas of common mutations using a sample group of 1898 bladder tumours. Adapted from reference 61.

The cysteine allows disulfide bonds to form between adjacent monomer receptors which favours ligand-independent dimerisation and therefore ligand-independent signal transduction.<sup>64</sup> The most common mutations within exon ten are Y375C (~19%) and G372C (~6%). Again, both mutations express a cysteine. Other mutations within exons seven/ten express glutamic acid residues which form intricate hydrogen bonding networks between monomers, and again, induces ligand-independent dimerisation.<sup>64</sup> Roughly 2% of bladder tumours show mutations in exon 15 which is present in the TK region of the intracellular domain.<sup>65</sup> All mutations here involve the change of the Lys-652 residue to either glutamic acid, glutamine, threonine, or methionine. All are thought to cause a conformational change within the TK domain resulting in ligand-independent receptor activation and signalling (Figure 1.9).<sup>65</sup> Dimerisation of

monomers is not observed and therefore the exact mechanism of signal transduction *via* intracellular TK mutations remains unclear.

Along with mutation, FGFR3 has also been found to be overexpressed in a high proportion of low-grade and low-stage tumours. Correlation studies show that up to 85% of mutated tumours also show higher expression of the protein.<sup>66</sup> FGFR3 overexpression was also detected in ~40% of wild-type (WT) tumours with the majority being invasive cancers. Overall, ~80% of non-invasive and ~54% of invasive UCs contain dysregulated FGFR3 signalling occurring through mutation and/or overexpression (Figure 1.9).<sup>66</sup> Another way in which excessive cell proliferation occurs is through increased sensitivity to FGFs.<sup>67</sup> Each isoform has different specificities in terms of what FGF binds (Table 1.1). In certain cancers it has been found that an isoform switch from FGFR3b to FGFR3c leads to increased cell proliferation (Figure 1.9).<sup>67</sup>

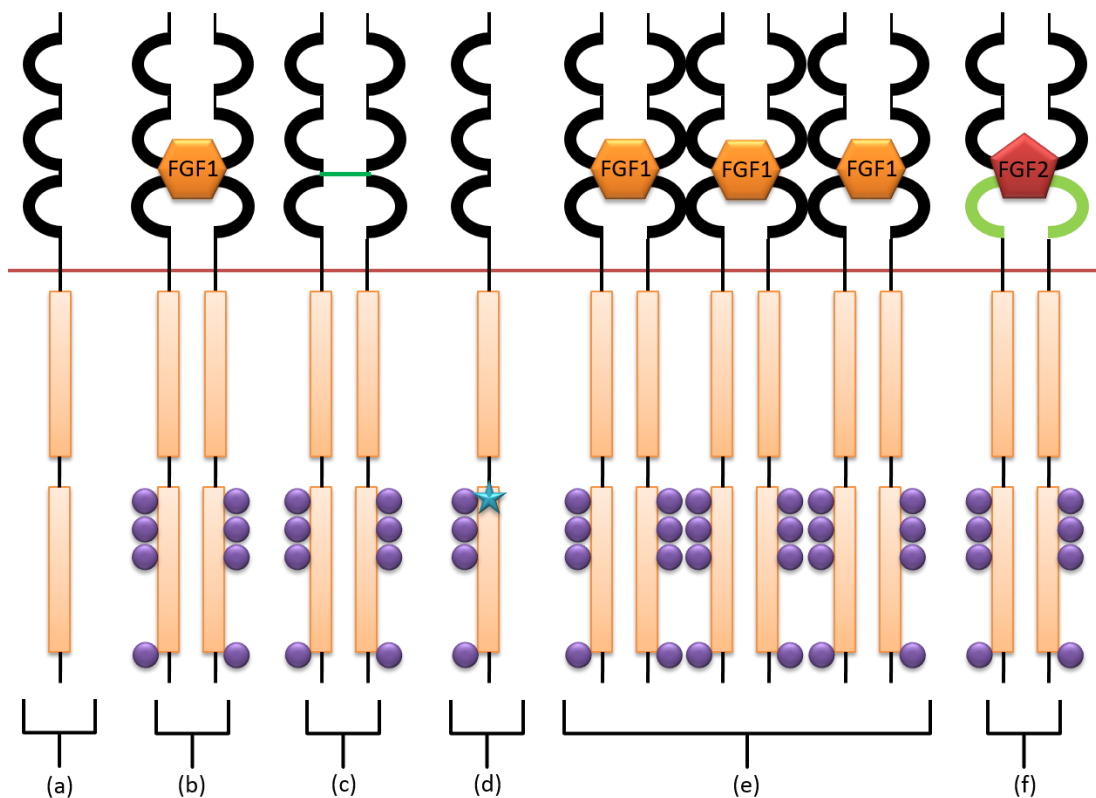


**Figure 1.9:** Mechanisms of activation of FGFR3. (a) Inactive monomer; (b) Ligand-dependant dimerization; (c) Ligand-independent dimerization due to extracellular mutations; (d) Ligand-independent activation due to mutations in the TK domain; (e) Overexpression of WT; (f) Isoform switching due to alternative splicing. Adapted from reference 61.

In contrast to FGFR3, little is known about the relevance and roles of other FGFRs in bladder cancer. However, recently a study has shown that FGFR1 has been overexpressed in various cancer cell lines and stimulation of FGFR1 led to increased

proliferation and reduced apoptosis.<sup>68</sup> There is some evidence that FGFR2 has an opposing role to FGFR1 and FGFR3. Expression within UC is downregulated and a low level of the receptor is associated with a worse prognosis.<sup>69</sup> Additionally, FGFR2 re-expression within a UC cell line led to lower proliferation *in vitro* and stunted tumour growth within nude mice, implying a tumour suppressor role for FGFR2.<sup>70</sup> The roles of FGFR4 and FGFR5 in bladder cancer remained undetermined.<sup>61</sup>

### **1.3.7 FGFR2 Implicated Breast Cancer**

In contrast to the tumour suppressor role of FGFR2 in UC, FGFR2 has been shown to be amplified in 5-10% of breast cancer patients.<sup>71</sup> A genome-wide association study of breast cancer looking at >500,000 single nucleotide polymorphisms (SNPs) in >1000 invasive breast cancer cases has identified a small set of four SNPs in intron two of FGFR2. Association testing and ancestral recombination graph analysis showed that haplotypes of FGFR2 were associated with risk of breast cancer.<sup>72</sup> A specific example of this is outlined by Campbell *et al.* where FGFR2 risk-SNPs confer breast cancer risk by augmenting oestrogen responsiveness.<sup>73</sup> It is well known that the risk of breast cancer increases with increased exposure to oestrogen through over stimulation of the oestrogen receptor (ESR)1. FGFR2 has been shown to reverse the activity of the ESR1. This is seen across multiple cell lines and has been found to be dependent on the presence of FGFR2. The presence of risk variant SNPs within FGFR2 results in lower expression and conversely an increased oestrogen response outlining a clinical need for FGFR2 inhibition in these cancer types.<sup>73</sup>

## **1.4 Current Treatments for Cancer**

### **1.4.1 Surgery**

Surgery involves the excision of a solid tumour by means of physical intervention. It is the earliest and most widely available form of treatment for cancers, however, complete removal of cancerous tissue is hard to achieve using this method, especially if the tumour has metastasised.<sup>74</sup>

### **1.4.2 Radiotherapy**

Radiotherapy is the second most important curative treatment for cancer after surgery. It works by using high energy gamma rays, or X-rays, which interact with DNA. The absorption of gamma rays, or X-rays, leads to the formation of high energy ions which consequently form short-lived free radicals.<sup>75</sup> These radicals interact with DNA which causes single-strand and double-strand DNA breaks. The damaged DNA is repaired to some extent which results in the termination of cell division and eventually apoptosis. Radiotherapy is most effective on localised tumours especially when used in conjunction with chemotherapy.<sup>75</sup>

### **1.4.3 Chemotherapy**

Chemotherapy is used in conjunction with radiotherapy and as an alternative form of treatment for cancer. Drugs are used to kill or inhibit growth of cancerous cells. Most chemotherapeutic drugs work by causing damage to DNA or preventing chromosomal replication, leading to apoptosis.<sup>76</sup> Chemotherapy offers advantages over surgery and radiotherapy. Drugs are administered either orally or intravenously, meaning that the drug can reach all disease sites through the circulatory system, an obvious benefit for metastasised cancers.<sup>76</sup> A disadvantage to chemotherapy is the propensity of drugs to target healthy cells as well as cancerous cells. The undesired toxicity of these agents often results in unpleasant side-effects such as nausea and vomiting, although, not all chemotherapies have associated toxic side effects. A drug which only kills or inhibits cell growth of cancerous cells is known as a targeted therapy and is generally considered to be distinct from chemotherapy. These drugs normally target mutant proteins that are much more abundant within the cancerous cells, thereby not affecting the WT forms found in healthy cells.<sup>76</sup>

## 1.5 Inhibition of FGFRs

The development of inhibitors for diseases harbouring FGFR aberrations is important in improving the quality of life for patients suffering from such abnormalities. Targeted treatment for the specific disease may reduce the need for more drastic methods of treatment such as surgery and/or chemotherapy. There are several aspects that need to be considered when inhibiting FGFRs.

### 1.5.1 Development of Selective Inhibitors

Kinases are well known for their high degree of similarity in terms of their amino acid sequences. In particular, families that are close together in the kinome show high sequence homology. To demonstrate this the full length amino acid sequences for FGFR1-4 were obtained from the UniProt knowledge base (UniprotKB) and then subjected to sequence alignment using the basic local alignment search tool (BLAST) (Table 1.2).<sup>77,78</sup>

**Table 1.2:** Percentage similarities of FGFR1-4 using BLAST.

FGFR	1	2	3	4
1	100			
2	72	100		
3	65	69	100	
4	60	59	64	100

The highest sequence similarity observed is between FGFR1/2 at 72% with the lowest between FGFR2/4 at 59%. The decreasing trend in percentage similarity through FGFR1-4 is to be expected due to the phylogenetic hierarchy that was established when developing the kinome (Figure 1.3).

The amino acid sequence for the kinase domains of FGFR1-4 were obtained from UniprotKB and then subjected to sequence alignment using Clustal Omega (Table 1.3).<sup>79</sup>

**Table 1.3:** Percentage similarities of the kinase domains in FGFR1-4 using Clustal Omega.

FGFR	1	2	3	4
1	100			
2	88	100		
3	84	88	100	
4	76	77	80	100

The sequence similarity within the kinase domains is higher than that of the overall sequence homology. FGFR1/2 and FGFR2/3 have the highest sequence similarity at 88%. FGFR4 shows the lowest sequence similarities to that of its counterparts at 76, 77 and 80% for FGFR1-3 respectively.

#### 1.5.1.1 ATP Binding Site

The majority of current inhibitors for FGFRs are known to occupy the ATP-binding site. One such inhibitor, CH5183284 (**1**), is a potent, selective inhibitor of FGFR1-3 exhibiting IC<sub>50</sub> values of 9.3, 7.6 and 22 nM respectively and is currently under clinical investigation for the treatment of patients that harbour FGFR genetic alterations.<sup>80</sup> The crystal structure of **1** bound within FGFR1 (Protein Data Bank (PDB) code: 3WJ6) was used as a template to display the different characteristics of the ATP-binding site (Figure 1.10).



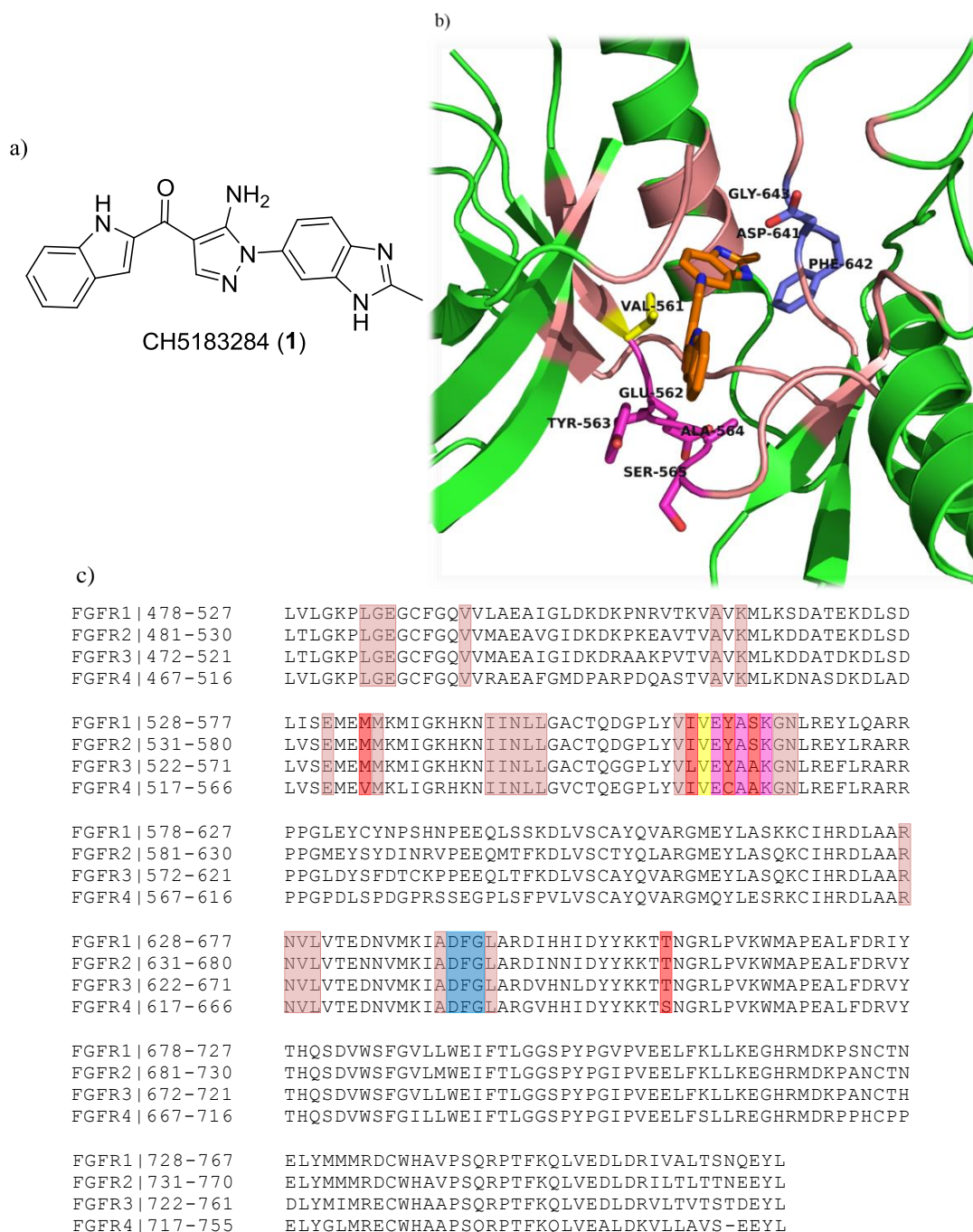


**Figure 1.10:** a) Structure of CH5183284 (1). b) Crystal structure of 1 bound within FGFR1 (PDB code: 3WJ6). 1 is outlined in orange. The gatekeeper residue Val 561, the hinge region and the DFG motif are outlined in yellow, purple and blue respectively. Residues that form the surface of the active site and the remainder of the kinase domain are outlined in pink and green respectively. c) Alignments of the kinase domains of FGFR1-4. The same colour coding applies as described in b; residues that show differences are outlined in red.

The structure of the ATP-binding site is highly conserved amongst FGFR1-4 with only five discrepancies in the residues that form the surface of the active site. The ‘gatekeeper’ residue, so called as this residue can modulate inhibitor binding, exists as a valine throughout FGFR1-4. Point mutations at this position to other amino acids

such as methionine have shown differential changes in the binding of several inhibitors.<sup>81</sup> The hinge region of the FGFRs is also highly conserved showing only two discrepancies; two residues closer to the N-terminus from the gatekeeper lies a tyrosine in FGFR1-3 but exists as a cysteine in FGFR4 and two residues along from that show serine residues in FGFR1/2 but alanine residues in FGFR3/4. Three consecutive residues in FGFR1, Asp-641, Phe-642 and Gly-643, form what is known as the DFG motif. The DFG motif is present within the activation loop and is conserved throughout FGFR1-4. It plays an important role in the regulation of kinase activity and can exist as two states; DFG-in or DFG-out.<sup>82</sup> This refers to the aspartate residue facing into or out of the binding pocket respectively. These states are interchangeable as it has the propensity to undergo rearrangements and this can be modulated by what type of inhibitor is bound.<sup>83</sup>

### 1.5.1.2 Inhibitor Binding Modes

Inhibitors of FGFRs can be broadly defined into three categories: types I, II, and III. (Figure 1.11).

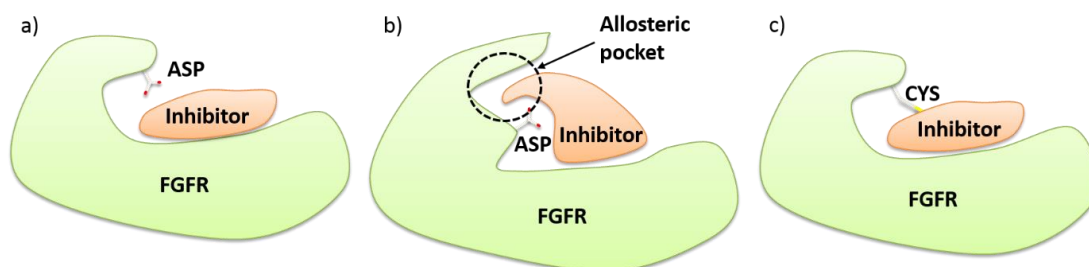


**Figure 1.11:** a) DFG-in binding mode (Type I). b) DFG-out binding mode (Type II). c) Covalent inhibitor binding mode (Type III).

Type I are competitive inhibitors of the ATP-binding site and target the active DFG-in conformation. Type II are non-competitive inhibitors of the ATP-binding site targeting the inactive DFG-out conformation. The DFG-out conformation results in the appearance of a new hydrophobic binding pocket adjacent to the ATP-binding site and provides potential for further inhibitor binding.<sup>82</sup> Type III inhibitors are irreversible covalent inhibitors. Site of the covalent bond is usually a reactive cysteine residue close to or within the ATP-binding site. This covalent modification means ATP can no longer bind and therefore results in irreversible inhibition.<sup>82</sup>

## 1.5.2 FGFR Inhibitors

### 1.5.2.1 Type I

Currently, several type I FGFR inhibitors are in clinical use, with some acting as selective FGFR inhibitors and some as pan-kinase inhibitors (Figure 1.12).

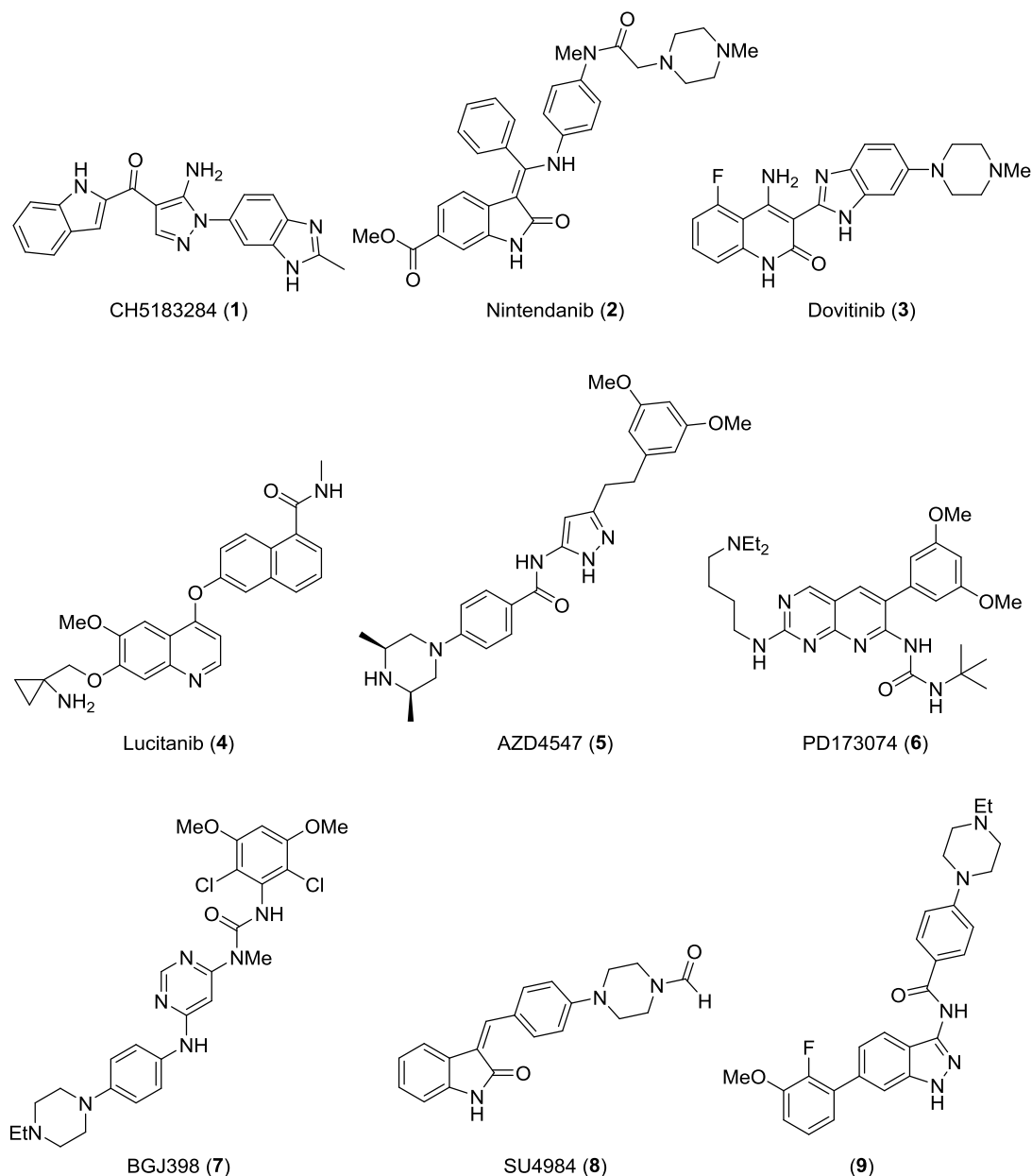


**Figure 1.12:** Current FGFR inhibitors that exhibit DFG-in binding conformations.

Compound **1** is a potent inhibitor of the FGFR kinases (Section 1.5.1.1) exhibiting  $IC_{50}$  values of 9.3, 7.6 and 22 nM respectively. Compound **1** was found to display anti-tumour activity against a panel of 327 cell lines that harbour FGFR genetic alterations with xenografts models also reflecting this. Compound **1** was discovered

using high-throughput screening (HTS) followed by structure-based drug design (SBDD) taking advantage of X-ray crystal data.<sup>80</sup>

Nintedanib (**2**) is a triple angiokinase inhibitor targeting proangiogenic pathways that are mediated by TKs such as FGFR, VEGFR, and PDGFR. *In vitro* studies outline potent IC<sub>50</sub> values ranging from 13-108 nM for the targeted TKs, however, **2** lacks selectivity amongst the different sub-types of each of these TKs. Compound **2** is currently in phase III clinical trials and has shown significant efficacy in the treatment of non-small-cell lung carcinomas (NSCLCs) and ovarian cancer.<sup>84</sup>

Dovitinib (**3**) is a multi-targeted TK inhibitor that is currently being investigated in phase II clinical trials for a wide range of FGFR related cancers.<sup>85</sup> It has been found to have activity against FGFR, VEGFR, PDGFR, Fms-like tyrosine kinase 3 (FLT3) and tyrosine-protein kinase Kit (KIT) with IC<sub>50</sub> values in the range of 1-50 nM.<sup>86</sup> Recently this molecule has been shown to have anti-tumour activity in FGFR-amplified breast cancer cell lines but not in FGFR-normal cell lines indicating a selective preference for cancerous cells.<sup>87</sup>

Lucitanib (**4**) is a dual inhibitor of VEGFR1-3 and FGFR1-2 exhibiting IC<sub>50</sub> values in the range of 7-83 nM. *In vitro* studies looking at ligand-dependant signal transduction showed that compound **4** inhibited this process. *In vivo* studies using mice showed that compound **4** completely inhibited FGF-induced angiogenesis as well as a reduction in tumour vessel density and increased tumour necrosis. Compound **4** is currently in phase II clinical trials for the treatment of VEGFR and FGFR related diseases.<sup>88</sup>

AZD4547 (**5**) is a potent and selective inhibitor of FGFR1-3 exhibiting *in vitro* IC<sub>50</sub> values of 0.2, 2.5 and 1.8 for FGFR1-3 respectively. A selectivity screen indicated that compound **5** is selective for FGFR1-3 against other kinases such as CDK2, PI3K and PKB.<sup>89</sup> *In vivo* studies on mice treated with compound **5** show 99% tumour growth inhibition. AZD4547 is now in phase II clinical trials for the treatment of gastroesophageal cancer.<sup>90</sup>

PD173074 (**6**) is a potent and selective inhibitor of FGFR1/3 with *in vitro* efficacies of 21.5 and 5 nM respectively.<sup>91,92</sup> *In vitro* studies on related kinases such as VEGFR, PDGFR and insulin growth factor receptor (IGFR) show a 1000-fold decrease in potency.<sup>91</sup> A study has shown that compound **6** suppresses cell proliferation in cell lines that harbour FGFR3 mutations when compared to WT FGFR3.<sup>92</sup>

BGJ398 (**7**) is a potent pan-FGFR inhibitor that is currently in phase I clinical trials for FGFR1-2 amplified cancers and FGFR3 mutated cancers.<sup>85</sup> In biochemical assays,

compound **7** was found to give  $IC_{50}$  values of 0.9, 1.4 and 1.0 nM for FGFR1-3 respectively. Over fifteen other RTKs were tested but were found to be unaffected by compound **7** revealing this molecule to be a selective FGFR inhibitor.<sup>93</sup>

SU4984 (**8**) was the first inhibitor to inhibit TKs that possessed an oxindole core. It inhibits FGFR1 with a moderate activity between 10-20  $\mu$ M and was also shown to inhibit autophosphorylation of FGFR1. Compound **8** also inhibited related kinases such as PDGFR and IGFR with similar potencies to that observed against the FGFRs, which demonstrates the use of an oxindole core as a general TK pharmacophore.<sup>94</sup>

Compound **9** is a potent FGFR1 inhibitor exhibiting an  $IC_{50}$  of 2.9 nM and comparable single concentration inhibition against FGFR2. Cellular assays also outline this compound to have an activity of 40.5 nM against SNU-16 cell lines. The construction of this compound was based on both compounds **5** and **7** using a scaffold hop and molecular hybridisation strategy respectively.<sup>95</sup>

### 1.5.2.2 Type II

There are two examples of type II inhibitors in the literature at present; ARQ069 (**10**) and ponatinib (**11**) (Figure 1.13). Compound **10** is a moderately potent inhibitor of FGFR1/2 with a potency of 0.84 and 1.23  $\mu$ M activity against the inactive (unphosphorylated) form. *In vitro* assays looking at inhibition of the phosphorylated forms of both FGFR1/2 show a complete loss of activity and a drop to 24.8  $\mu$ M respectively. This outlines that compound **10** prefers to target the DFG-out binding mode. These results have also been reflected in a cellular environment.<sup>96</sup>

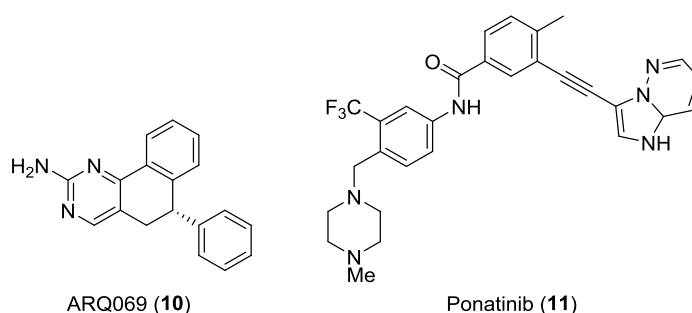


**Figure 1.13:** Current FGFR inhibitors that exhibit DFG-out binding conformations.

Currently, compound **11** is the only food and drug administration (FDA) approved type II inhibitor and is used for the treatment of chronic myeloid leukaemia (CML) and Philadelphia chromosome positive (Ph<sup>\*</sup>) acute lymphoblastic leukemia (ALL).<sup>97</sup> Compound **11** is a pan-kinase inhibitor that targets Abelson murine leukaemia viral oncogene homolog 1 (ABL), Lyn, VEGFR2 and FGFR1 with potencies of 0.37, 0.24,

1.5 and 2.2 nM respectively. Compound **11** is used as a first-line treatment for patients who suffer from cancers that have the breakpoint cluster region protein (BCR)-ABL<sup>T315I</sup> mutation as other drugs such as imatinib fail to be effective against this particular mutant.<sup>97</sup>

### 1.5.2.3 Type III

Irreversible inhibitors are often seen as a last resort due to their propensity for receptor promiscuity, however, a couple of examples do exist (Figure 1.14).

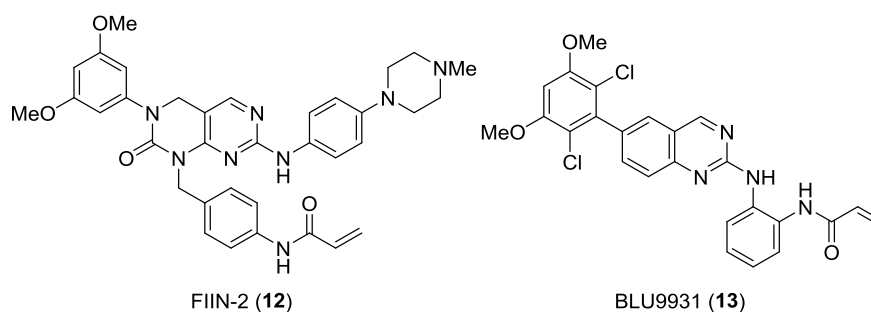


**Figure 1.14:** Current FGFR inhibitors that exhibit covalent binding interactions.

FIIN-2 (**12**) is an irreversible inhibitor of FGFR1-4 with EC<sub>50</sub> activities of 1, 4, 93 and 32 nM respectively.<sup>98</sup> Compound **12** is a derivative of compound **6** where an acryl-amido-benzyl substituent has been substituted on the N of the cyclic urea. It was tested against a panel of 456 kinases and showed good overall selectivity. X-ray crystal data of compound **12** bound with FGFR4 (PDB-4QQC) shows that the covalent bond is formed between Cys-477, a residue conserved between FGFR1-4, deep within the ATP-binding pocket.<sup>98</sup>

BLU9931 (**13**) is an irreversible, potent, and selective inhibitor of FGFR4 with an IC<sub>50</sub> value of 3 nM and IC<sub>50</sub> values of 591, 493 and 150 nM for FGFR1-3 respectively. Compound **13** differs to that of compound **12** in that it reacts with Cys552.<sup>99</sup> This explains the difference in selectivity as the residue at this position in FGFR1-3 exists as a tyrosine (Figure 1.10). Further validation into the importance of this covalent bond in selectivity targeting FGFR4 is demonstrated with a non-covalent analogue of compound **13** which shows a much lower potency of 938 nM against FGFR4.<sup>44</sup>

## 1.6 Structure-Based Drug Design

There are numerous ways in which a drug discovery programme can be initiated. Conventional methods of drug discovery such as HTS have certain disadvantages and in particular, for a typical library containing ~1 million compounds the hit rate is usually <1%.<sup>100</sup> The application of SBDD first began in the mid-80s when genomic, proteomic and structural information became available within the drug discovery scene.<sup>101</sup> X-ray crystallographic data allowed medicinal chemists to take a more rational approach to hit identification and lead optimisation. SBDD can be used iteratively (Figure 1.15).<sup>101</sup>

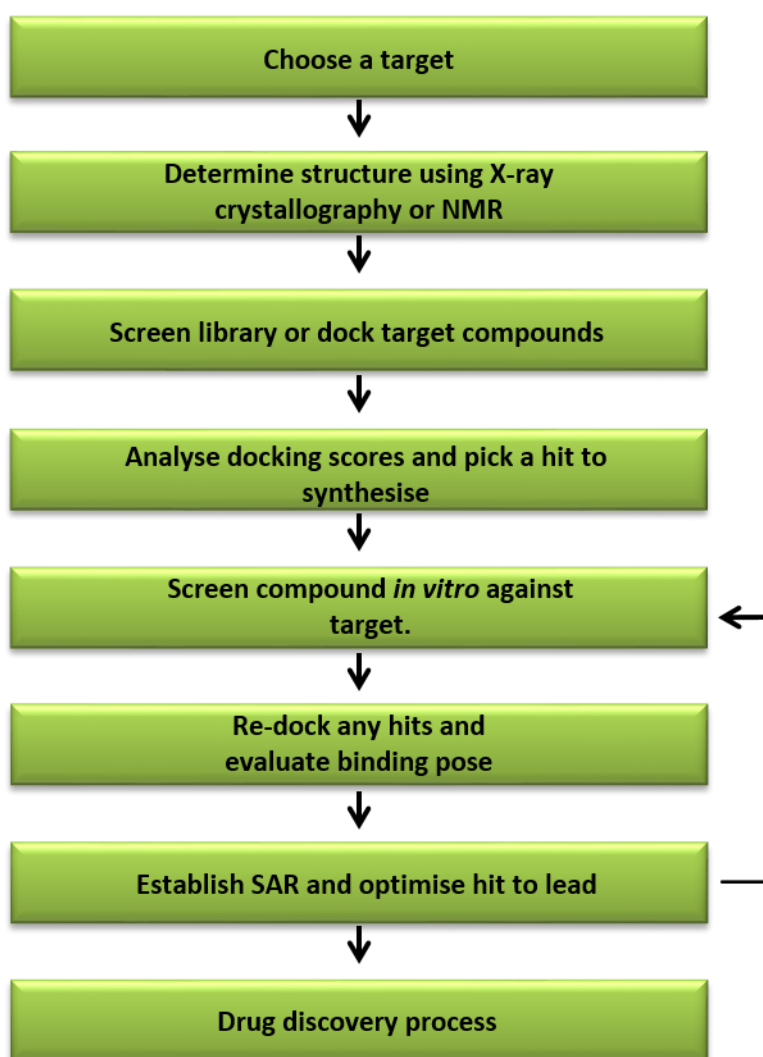


**Figure 1.15:** The process of SBDD. Adapted from reference 101.

The majority of drug discovery programmes start with target identification. Normally, this is a target that is known to play a significant role in a disease. The structure of the target is needed in order for rational SBDD to commence. Structures can be obtained

by X-ray crystallography, NMR, and homology modelling. Homology modelling involves taking the amino acid sequence of a closely related structure that has a known X-ray crystal structure. The sequences are aligned and modified to produce a crystal structure that can be used as a model. Usually, an acceptable sequence identity between the proteins needs to be >40% in order to create a reliable homology model.<sup>102</sup> The crystal structure is then analysed for binding sites/pockets in which a small molecule inhibitor could bind, often the binding site of endogenous ligands.<sup>100</sup> A target compound or compound library is then virtually screened against the target and the binding pose(s) evaluated for the compounds predicted to bind most tightly. A molecule or series of molecules are then chosen for synthesis followed by subsequent biological evaluation. Any hits are then re-docked and the binding pose(s) analysed to help rationalise structure-activity relationships (SARs). The hit can then be optimised in an iterative cycle until a reasonable candidate is identified to progress into pre-clinical studies. If at any point a candidate can no longer be optimised or fails to inhibit the target then the process is repeated from the beginning.<sup>101</sup>

### 1.6.1 Maestro

Maestro is a piece of software developed by Schrödinger Inc<sup>103</sup> that allows users to build and visualise 3D structures of ligands. X-ray crystal structures of proteins can also be visualised allowing the user to see the 3D interaction between the ligand and the receptor. An in-built tool known as Glide (grid-based ligand docking with energetics) can be used to dock ligands within the active site of receptors. A series of hierarchical filters help narrow down possible locations of where the ligand can bind within the active site.<sup>104</sup> The filtration process is based on several ligand parameters such as; position and orientation to the receptor, core conformation and rotamer-group conformations. Generated ligand conformations are then energy minimised to produce a series of predicted binding poses which the user can inspect and evaluate accordingly.<sup>104</sup>

### 1.6.2 eHiTS

A computational docking program known as electronic high-throughput screen (eHiTS) takes ligands and divides them into small rigid fragments and flexible connecting chains.<sup>100</sup> Each fragment is then docked into every site within a protein



cavity, so called ‘flood’ docking. A fast graph-matching algorithm connects all the fragments to reconstruct the original ligand which is followed by energy minimisation within the receptor. The binding poses are then scored and ranked.<sup>100</sup> Scoring is based on the complementarities of ‘surface points’ between the ligand and receptor, and the geometries of the ligand. Favourable interactions receive a positive score and unfavourable interactions receive a negative score.<sup>100</sup>

### 1.6.3 PyMOL

PyMOL is a molecular visualisation software tool that was created by Schrödinger Inc.<sup>105</sup> It can be used for various applications some of which include: predicting H-bonding interactions, analysis of 3D structure of proteins and most usefully, creating high quality images that can be used for publication. Most 3D structures found in this thesis use this software.

### 1.6.4 *De Novo* Design

Chemical space is extremely large and the estimated number of drug-like molecules is in the order of  $10^{60}$ - $10^{100}$ . Typical HTS libraries contain ~1-3 million molecules and therefore the majority of chemical space remains unexplored.<sup>106</sup> *De novo* design of molecules was first developed in the early 90s and in theory allows access to all of chemical space, no longer being confined to known chemical space. It involves the design of bioactive molecules by step-wise construction of a ligand within a receptor. Various areas within the receptor are outlined as potential binding sites which could interact with certain chemical moieties. In this approach novel ligands can be constructed that are predicted to bind to the target.<sup>106</sup>

### 1.6.5 SPROUT

The design of novel drug-like molecules can be carried out using *de novo* design software such as SPROUT. This software uses a similar approach to that of eHiTS in that it uses fragment-linking techniques to produce ligands that fit the steric and electronic constraints of the receptor.<sup>100</sup> Unlike eHiTS, atoms and fragments of molecules are matched with ‘target sites’ in such a way that a favourable interaction would occur. When fragments and target sites are satisfied the fragments are then linked together using ‘spacer templates’.<sup>100</sup> The resulting solutions can then be

clustered using a range of parameters such as estimated binding affinity or molecular complexity. These parameters can be fine-tuned by the user discarding any unwanted solutions.<sup>100</sup> SPROUT carries out this process using several modules:<sup>107</sup>

1. **CANGAROO** – This module stands for **Cleft ANalysis by Geometry-based Algorithm Regardless Of the Orientation**. In this module the receptor site and cavity (ligand) are defined.
2. **HIPPO** – This module stands for **Hydrogen-bonding Interaction site Prediction as Positions with Orientations**. In this module potential binding sites are outlined. Such sites are amino acids that can provide hydrogen bonding capability with complementary chemical functionality. Hydrophobic binding regions and metal interactions can also be defined.
3. **ELEFANT** – This module stands for **ELEction of Functional groups and Anchoring them to Target sites**. In this module small fragments that contain H-bonding functionality are chosen and assigned to complementary target sites.
4. **SPIDER** – This module stands for **Structure Production with Interactive Design of Results**. In this module spacer templates are chosen to link the fragments selected in **ELEFANT**. Structures are then generated following the constraints of the target site and boundary surface.
5. **ALLIGATOR** – This module stands for **Analyse Lots of LIGANDs, Test and Order Results**. This module clusters groups of molecules based on parameters set by the user. Such parameters include: hydrogen bonding interactions, rotatable bonds, and hydrophobic interactions.

## **1.7 Project Aims**

### **1.7.1 Overall Aim**

- To identify new types of selective inhibitors of FGFR1-3 respectively which have potential to be used in the treatment of cancer.
- To understand the specific structural requirements of small molecule tools that are needed to elicit sub-type selectivity between FGFR1-3.

### **1.7.2 Specific Objectives**

- Use computational software including SPROUT, eHiTS and Glide to identify potential molecular scaffolds to act as starting points.
- Develop efficient synthetic routes to compounds which incorporate these scaffolds and identify hits.
- Construct targeted libraries based on these hits and use docking strategies to rationalise and develop SARs.
- Elucidate the key structural differences between FGFR1-3 and utilise this knowledge to design novel, potent and selective inhibitors.

## Chapter Two – *De Novo* Fragment-Based Design

### 2.1 Hit Identification

To begin, a literature search on pre-existing crystal data for FGFRs was carried out. A recent crystal structure (PDB code: 3WJ6 – 2.15 Å) of human FGFR1 co-crystallised with CH5183284 (**1**) was identified.<sup>80</sup> The PDB file was loaded into SPROUT (Figure 2.1).

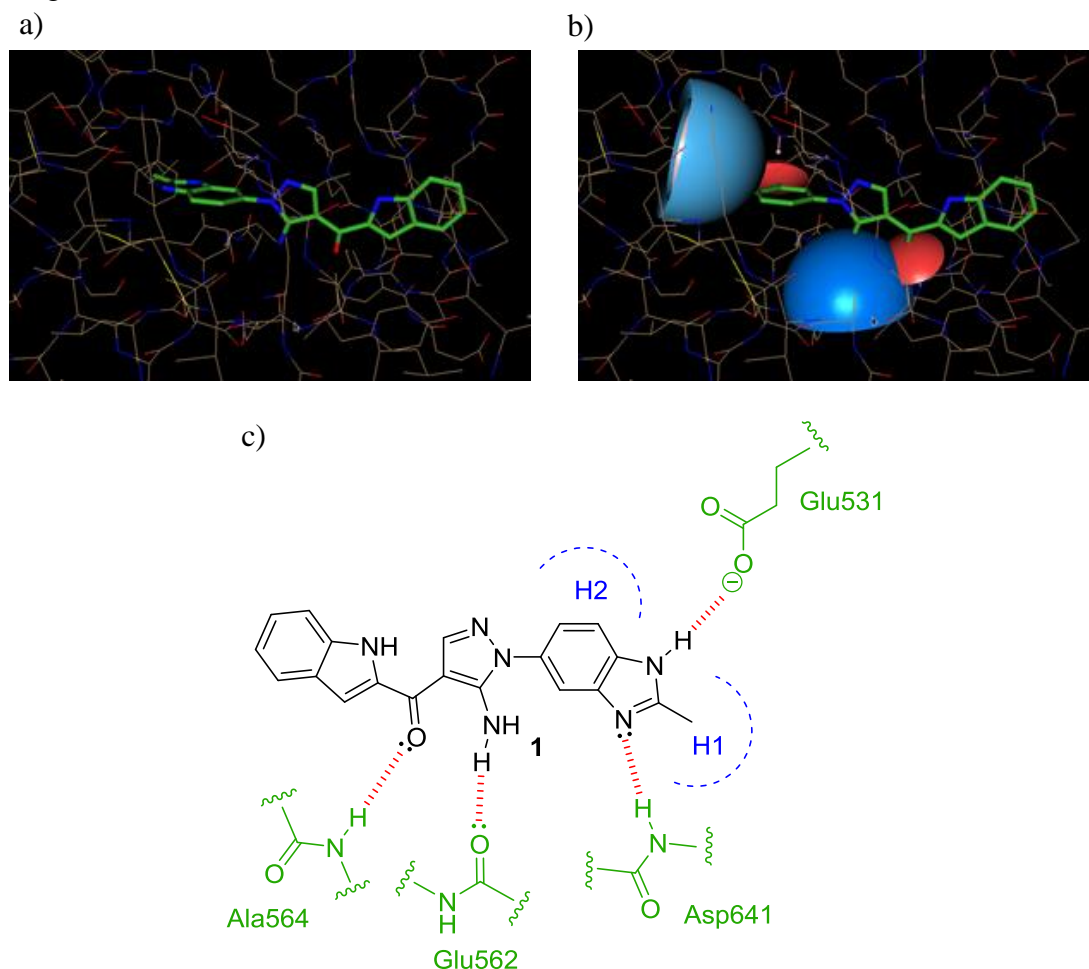


**Figure 2.1:** a) SPROUT image of co-crystal structure of **1** within ATP binding site of FGFR1. b) Co-crystal structure of **1** within FGFR1 showing predicted H-bonding interactions. Acceptor and donor sites present within the FGFR1 active site are shown in blue and red respectively. c) 2D representation of binding pose of **1** within FGFR1 showing intermolecular interactions. Amino acids, H-bonds and hydrophobic pockets are shown in green, red, and blue respectively.

Compound **1** is observed to occupy the ATP binding pocket within FGFR1 and several interactions between the inhibitor and the protein are apparent (Figure 2.2). Two H-bonds form with the benzimidazole moiety; one with the backbone nitrogen of Asp641 and the other with a side chain carboxy oxygen of Glu531. Another H-bond forms between the pyrazole NH<sub>2</sub> and the backbone carbonyl of Glu562. An H-bond is

also present between the ketone moiety and the backbone NH of Ala564. The benzimidazole methyl group occupies a small hydrophobic pocket, known as H1. Occupation of this pocket by the methyl group has been shown to increase the selectivity of compound **1** for FGFR kinases over structurally similar kinases such as VEGFRs. This raises significant implications for designing selective inhibitors of FGFR kinases.<sup>80</sup>

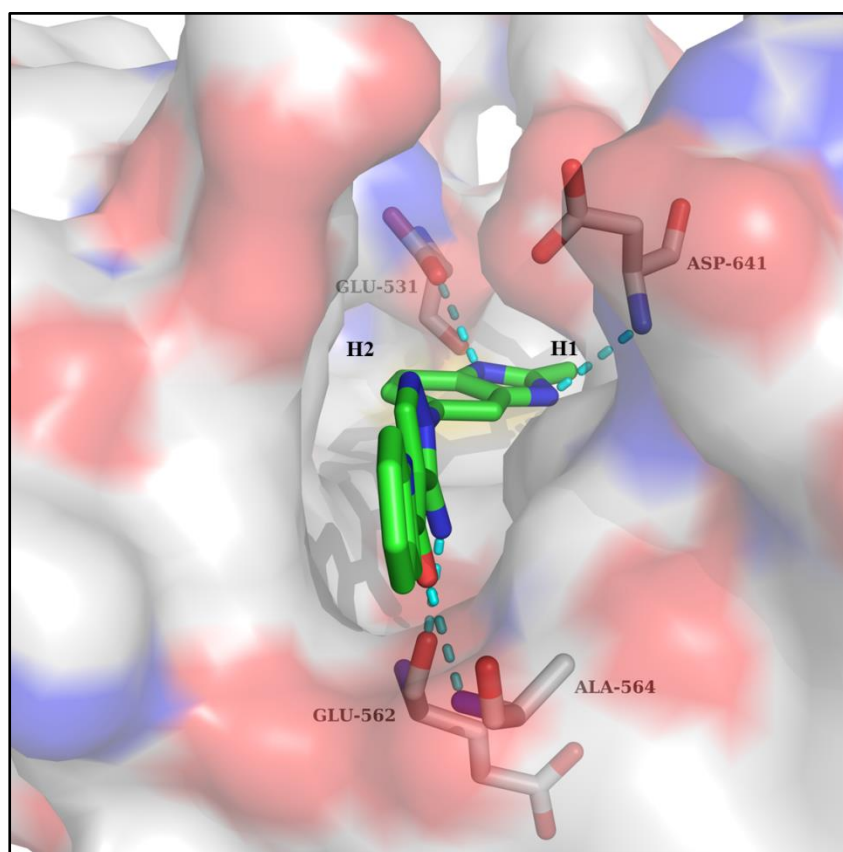
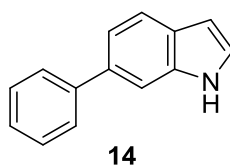


**Figure 2.2:** 'End-on' view of compound **1** occupying the ATP binding site within FGFR1. H-bonding interactions are indicated using cyan dashes and hydrophobic pockets are indicated by H1 and H2.

*De novo* design of novel FGFR inhibitor scaffolds applied to this crystal structure was carried out using SPROUT, with compound **1** acting as a template to guide the design process. Three of the four interaction sites (Glu531, Glu562 and Asp641) were selected in **HIPPO** (Section 1.6.5). Appropriate target and spacer templates were then chosen to generate 6-phenylindole (**14**) as a fragment predicted to bind to FGFR1.



### 2.1.1 Binding Pose of Compound 14

Compound **14** is predicted to bind in a similar way to that of compound **1** with the indole NH forming an H-bond with the backbone carbonyl of Glu562 (Figure 2.3). In order to strengthen the predicted SPROUT pose, compound **14** was subjected to consensus docking whereby multiple docking programs (Glide and eHiTS) were used in conjunction with each other to validate the predicted binding pose. Both docking solutions were visualised using PyMOL and showed good overlap with each other and the binding pose of compound **1** (Figure 2.3).

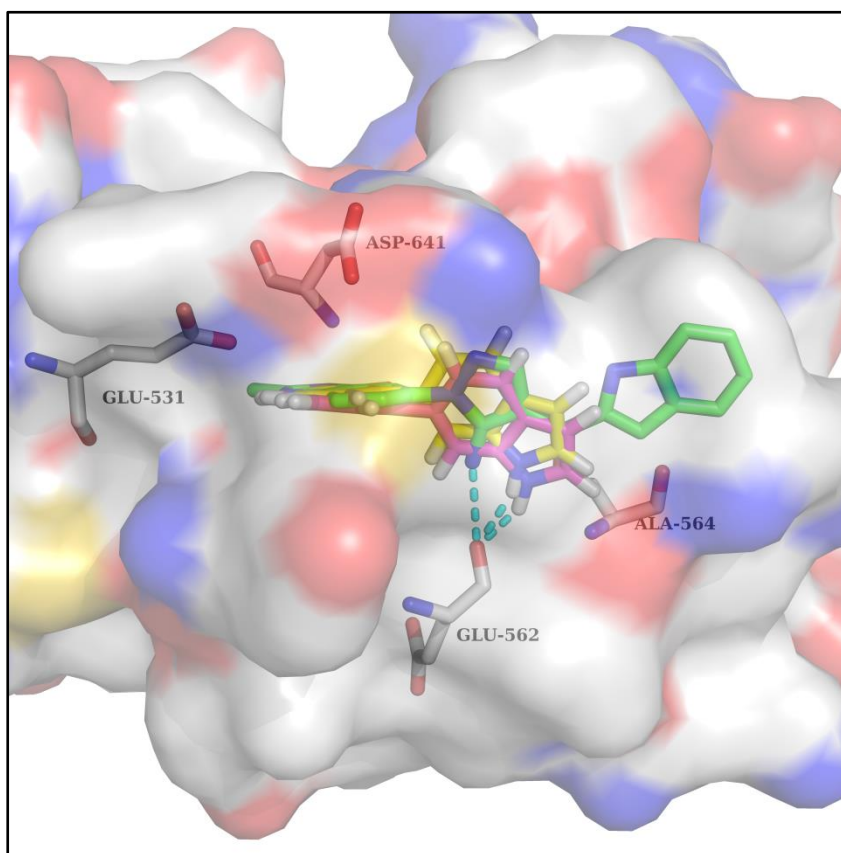


**Figure 2.3:** *Overlay of compound 1 and docking poses of compound 14 using eHiTS and Glide. Compound 1 is shown in green and the eHiTS and Glide poses for compound 14 are shown in purple and yellow respectively.*

Consensus docking was carried out for all future compounds with Glide being the chosen docking software; with results visualised in PyMOL. Upon inspection of the docking pose of compound **14** (Figure 2.4), it was determined that several modifications could be made in order to increase the number of intermolecular bonding interactions between FGFR1 and compound **14**. Substitution from an indole to an indazole would open up the opportunity for an H-bond to form between the indazole 2-position nitrogen and the backbone NH of Ala564. Substitution of the 6-

phenyl ring to a 6-pyridyl derivative could also induce an H-bond with the pyridine nitrogen and the backbone NH of Asp641.

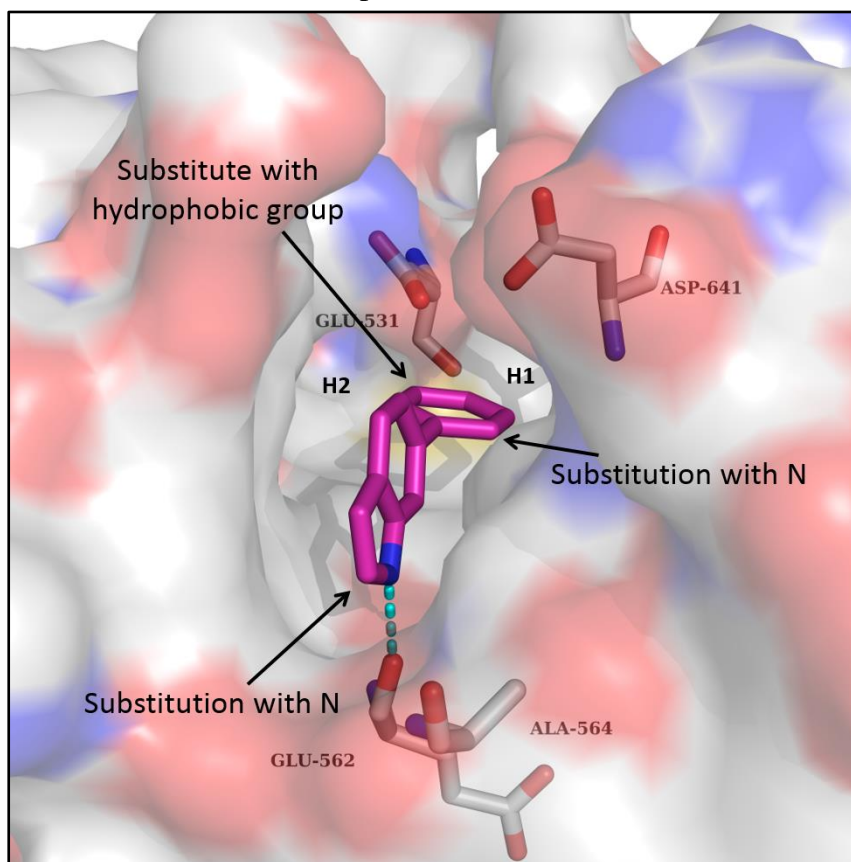


**Figure 2.4:** *De novo* designed ligand **14** docked within the ATP binding site of FGFR1 using Glide. An H-bond is predicted to form between the indole NH and the backbone carbonyl of Glu562. Modifications that could be made to increase potency of compound **14** against FGFR1 are outlined.

Furthermore, placement of a small hydrophobic group in the 3-position of the 6-phenyl ring could also allow H2 to be occupied. Manual manipulation of the docked pose of compound **14** was carried out to test what substituents could be tolerated in the H2 pocket. Halogenated compounds such as the iodo, bromo, and chloro derivatives were chosen due to their small size. The iodo and bromo derivatives were found to be too large and overlap with the boundary surface and therefore the chloro derivative was chosen, leading to target compound **15** (Figure 2.5).

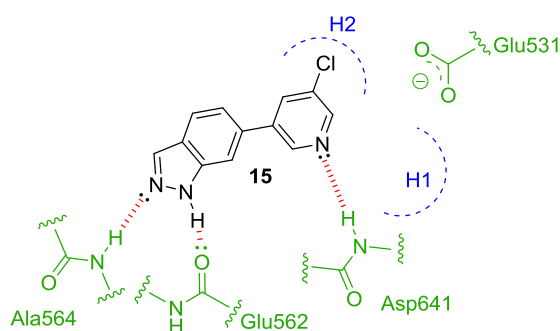


**Figure 2.5:** 2D representation of proposed binding mode of compound **15** bound within FGFR1.



Compound **15** was then subjected to docking to see whether the proposed binding mode matched the docked binding mode; the docked solution is outlined (Figure 2.6).

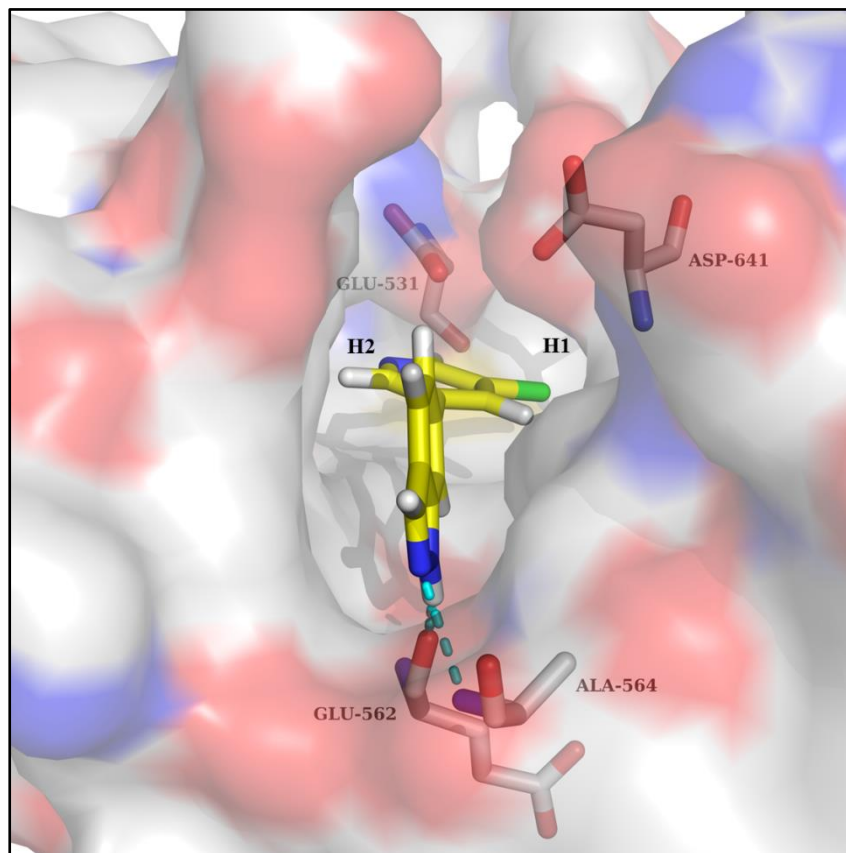
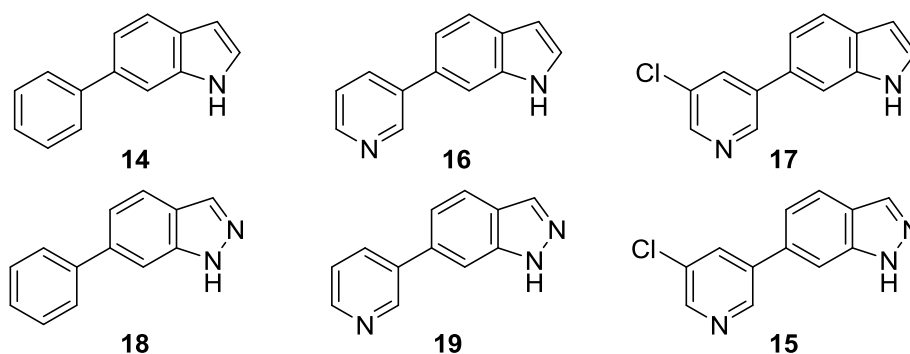


**Figure 2.6:** *Glide docking model of compound 15 bound within FGFR1. H-bonds are indicated using cyan dashes.*

As predicted by the proposed binding mode of compound **15** (Figure 2.5), a new H-bond is predicted to be possible between the indazole 2-position nitrogen and the backbone NH of Ala564. In contrast to the proposed binding mode of compound **15**, docking has resulted in the 6-position ring becoming ‘inverted’ relative to that proposed originally. This places the Cl atom orientated towards the H1 pocket instead of the H2 pocket. The Cl atom may be too large to occupy the H2 pocket and therefore is predicted to bind more favourably in the H1 pocket; this places the pyridine nitrogen away from the Asp641 residue and instead is orientated towards a hydrophobic wall, and is therefore unfavourable. To validate these hypotheses, a small library of compounds was targeted for synthesis and is outlined below.



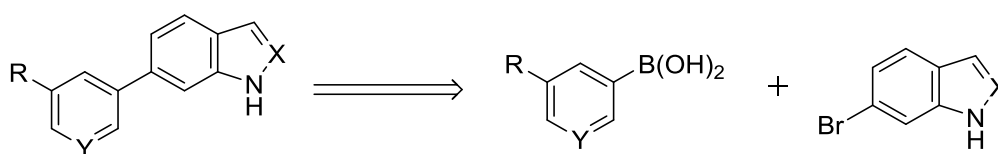


As well as compounds **14** and **15**, compounds **16-19** were also included to give a thorough SAR study for this small library.

## 2.2 ‘First Generation’ Library Synthesis

### 2.2.1 Retrosynthetic Analysis

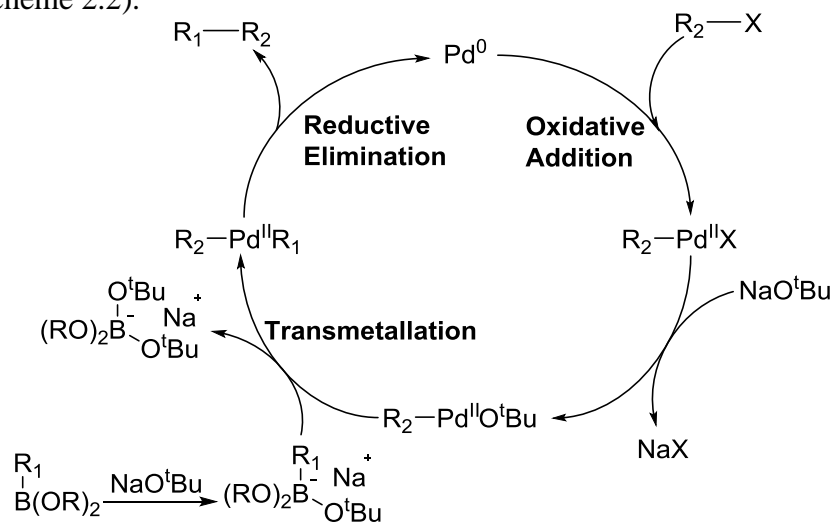
Retrosynthetic analysis of structures **14-19** indicated that the desired compounds could be made very simply from Pd-catalysed Suzuki couplings (Scheme 2.1).



**Scheme 2.1:** Retrosynthetic analysis of indole-based structures.

### 2.2.2 Suzuki Mechanism

Suzuki chemistry has become a very useful approach for forming carbon-carbon bonds in the medicinal chemist’s toolbox. A general mechanism for the process is outlined below (Scheme 2.2).<sup>108</sup>

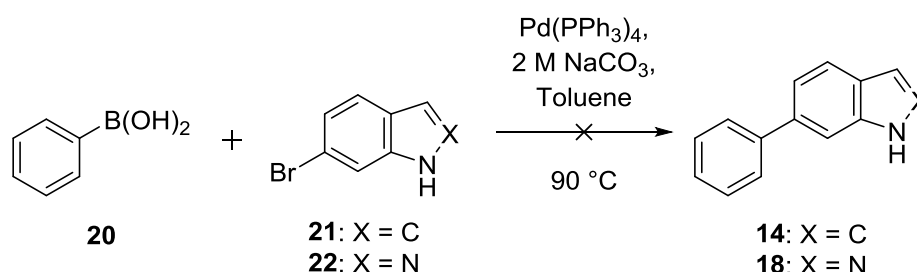


**Scheme 2.2:** General mechanism for Pd-catalysed Suzuki chemistry. Adapted from reference 108.

In the initial step Pd(0) undergoes oxidative addition with a halogenated aryl species. The Pd inserts into the carbon-halogen bond which results in oxidation of the palladium to give a Pd(II) species. Substitution of the halogen with base gives an intermediate that can then undergo transmetallation with a base-activated boronic acid/ester species, forming the penultimate intermediate. This intermediate can then undergo reductive elimination giving the desired product and the Pd(0) species which can then take part in the catalytic cycle again.

### 2.2.3 Pd-Catalysed Suzuki Couplings

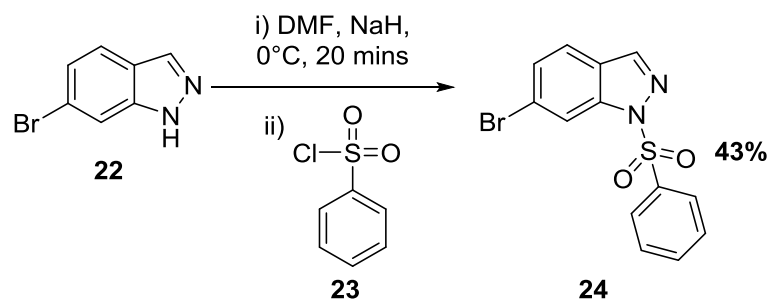
Attempts at synthesising compounds **14** and **18** *via* Suzuki couplings using an adaptation of a method outlined by Liu *et al* are summarised below (Scheme 2.3).<sup>109</sup>



**Scheme 2.3:** Attempted Suzuki coupling using thermal conditions.

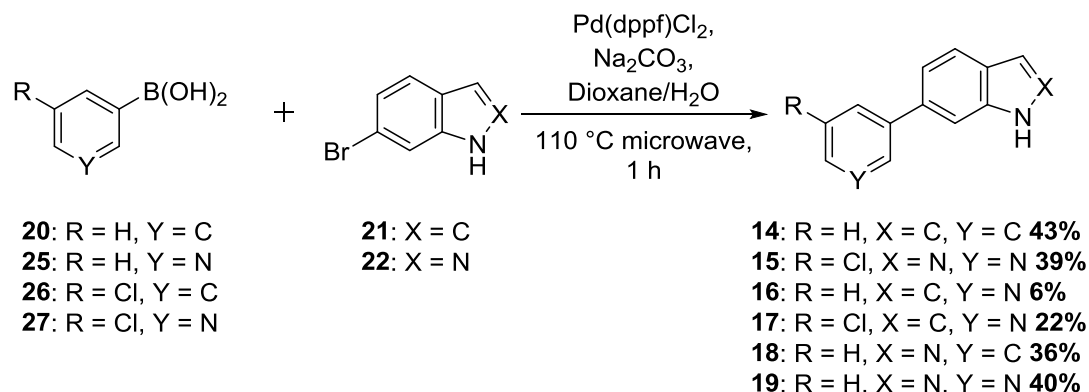
The syntheses of compounds **14** and **18** were unsuccessful; there are several possible reasons why this was the case. Some nitrogen-containing heterocycles have been known to interfere with Pd-catalysed Suzuki chemistry through their inherent ability to donate lone pairs to the metal centre, rendering the catalyst inefficient, which could be the case for compound **22**.<sup>110</sup> The unprotected free NH in compounds **21** and **22** may have the capability to participate in unwanted Buchwald coupling, leading to the failure of the reaction. Another reason could be due to the electron rich nature of the halogenated heterocyclic ring; oxidative insertion will be hindered allowing other competing pathways to take place.

To avoid the unwanted Buchwald side products, compound **22** was protected as the benzenesulfonyl derivative using an adaptation of a method outlined by Baldwin *et al* as summarised below (Scheme 2.4).<sup>111</sup>



**Scheme 2.4:** Indazole protection using a benzenesulfonyl protecting group.

Deprotonation of the indazole **22** using NaH initiates nucleophilic displacement of the chlorine atom in **23** resulting in sulfonamide **24** in a yield of 43%. Prior to subjecting **24** to Suzuki coupling, a literature search outlined the use of microwave energy to facilitate the reaction without the need of protecting groups. Therefore, compounds **14-19** were synthesised using an adaptation of a method outlined by Baldwin *et al* as summarised below (Scheme 2.5).<sup>112</sup>



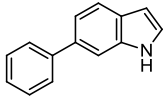
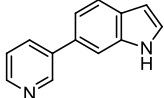
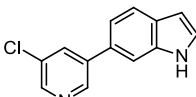
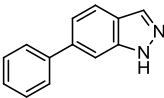
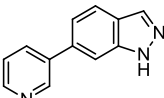
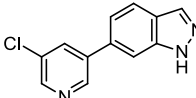
**Scheme 2.5:** Pd-catalysed microwave Suzuki couplings.

One common issue with this synthetic procedure is the appearance of an impurity that was assumed to be polymeric material. Removal of this material was difficult which may account for the low yields. Sonication of the purified solid in pentane was found to be the best way to significantly reduce the impurity to acceptable levels of <5% (<sup>1</sup>H NMR) for biological evaluation.

## 2.2.4 Biological Evaluation of ‘First Generation’ Fragments

The biological evaluation of compounds **14-19** was carried out by Life Technologies, Paisley, Scotland. Compounds **14-19** were screened against FGFR1 at an initial concentration of 500 μM using a fluorescence resonance energy transfer (FRET)-based assay (Section 8.1). The results are outlined below (Table 2.1).

**Table 2.1:** Biological results for ‘first generation’ fragments when screened against FGFR1.

Compound No.	Structure	% Inhibition <sup>a</sup> (500 $\mu$ M)	IC <sub>50</sub> <sup>a</sup> ( $\mu$ M)	LE
14		1 $\pm$ 0.0 <sup>b</sup>	NT <sup>c</sup>	N/A
16		16 $\pm$ 0.5	NT	N/A
17		21 $\pm$ 3.5	>500	N/A
18		53 $\pm$ 0.0 <sup>b</sup>	77 $\pm$ 0.9	0.38
19		66 $\pm$ 1.5	90 $\pm$ 0.9	0.38
15		73 $\pm$ 1.0	36 $\pm$ 0.9	0.39

<sup>a</sup> % Inhibition and IC<sub>50</sub> values are given as the mean  $\pm$  standard deviation (SD) of all data points,  $n = 2$ .

<sup>b</sup> No difference in measured data points. <sup>c</sup> NT = not tested.

The initial *de novo* designed fragment **14** was found to be inactive at 500  $\mu$ M. The other two indole-based compounds **16** and **17** were marginally more active but still low considering the high screening concentration. An IC<sub>50</sub> value of >500  $\mu$ M for compound **17** confirmed that the indole compounds were indeed inactive against FGFR1. Interestingly, all the indazole derivatives showed >50% increase in activity than their corresponding indole counterparts. IC<sub>50</sub> measurements confirmed that compounds **15**, **18** and **19** have modest double-digit  $\mu$ M activity against FGFR1. This outlines that the 2-position nitrogen present in the indazole compounds is crucial for inhibition of FGFR1. The ligand efficiency (LE) is a measurement of the binding energy per atom of a ligand to its binding partner and can be calculated using the equation outlined below (Equation 2.1).<sup>113</sup>

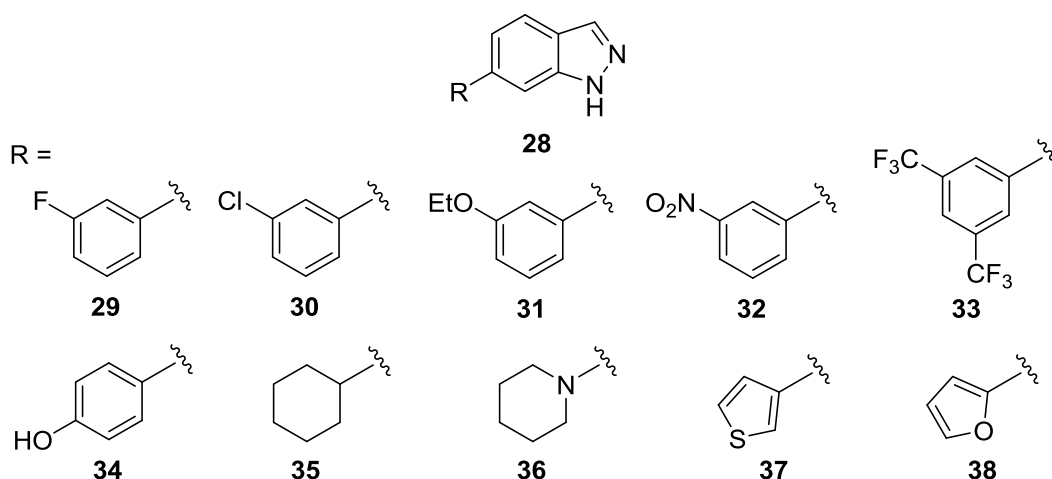
$$\text{LE} = 1.4(-\log\text{IC}_{50})/N$$

**Equation 2.1:** Formula for ligand efficiency. IC<sub>50</sub> is in mol/dm<sup>3</sup>,  $N$ =No. of non-hydrogen atoms.

The LE for compounds **15**, **18** and **19** has been calculated. A reasonable LE starting point is considered to be  $>0.3^{114}$  and therefore compounds **15**, **18** and **19** satisfy this. Compound **15** is the most active fragment against FGFR1 at  $36 \mu\text{M}$ . This could be due to the Cl atom occupying the H1 pocket as predicted from the Glide docking of compound **15** (Figure 2.6). Compound **18** is more active than compound **19**. This outlines the detrimental effect that the pyridine nitrogen has upon the binding of compound **19** to FGFR1, an aspect that can be rationalised from the docking of compound **15** (Figure 2.6).

### 2.3 Library Expansion

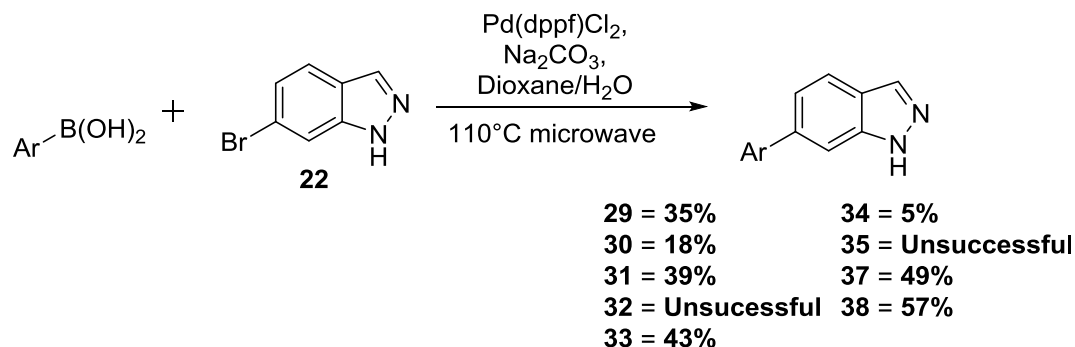
In order to expand the SARs for the active indazole pharmacophore **28**, a small library of target compounds was developed based upon readily available boronic acids and is outlined below.



Compounds **29-32** will further probe the tolerance of substituents in the 3-position of the 6-phenyl ring, compound **33** will test the effect of a di-substituted phenyl system. The docking of compound **14** (Figure 2.4) shows there may be some potential for an H-bonding interaction in the 4-position of the phenyl ring with Glu531; compound **34** will probe this hypothesis. Compounds **35-38** will outline the importance of the nature of the 6-position ring, testing saturated and five-membered rings systems.

### 2.3.1 'Second Generation' Library Synthesis

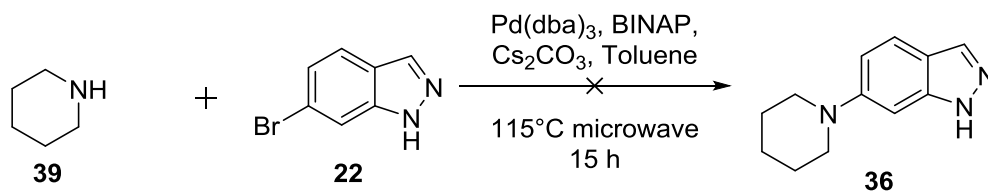
Compounds **29-38** were synthesised using Suzuki chemistry outlined previously (Scheme 2.5) and is summarised below (Scheme 2.6).



**Scheme 2.6:** Pd-catalysed microwave Suzuki couplings.

The syntheses of compounds **32** and **35** were unsuccessful under these conditions. The boronic acid species is seen as the nucleophilic component in Suzuki couplings and therefore the boronic acids used in the coupling for compounds **32** and **35** may be too electron deficient to undergo transmetallation.<sup>115</sup> Analysis of the crude reaction mixture for compound **32** by liquid chromatography-mass spectrometry (LC-MS) outlined the presence of nitrobenzene. Literature precedent indicated that boronic acid species that have strong electron withdrawing groups (EWGs) present tend to protodeboronate.<sup>115</sup> The poor yield for compound **34** cannot be attributed to the electronics of the boronic acid species as it is electron rich in nature. A search in the literature has outlined that *ortho* and/or *para* phenol boronic acids have a fast rate of protodeboronation.<sup>116</sup>

The synthesis of compound **36** was attempted using an adaptation of a method outlined by Duquenne *et al* as summarised below (Scheme 2.7).<sup>117</sup>



**Scheme 2.7:** Unsuccessful Pd-catalysed microwave Buchwald coupling.

Several reasons can explain the failure of the above reaction. Buchwald reactions are very sensitive towards the choice of solvent and base used and therefore, the conditions outlined above may have not be ideal for the starting materials used.<sup>118</sup> Due to the nature of the preparation of microwave reactions, small traces of oxygen may have been introduced into the reaction vessel leading to the poisoning of the

catalyst.<sup>118</sup> Synthesis of compounds **32** and **35** was not carried out and efforts focussed elsewhere.

### 2.3.2 Five-Membered Ring Systems

Compound **38** was docked into the FGFR1 crystal structure using Glide (Figure 2.7).

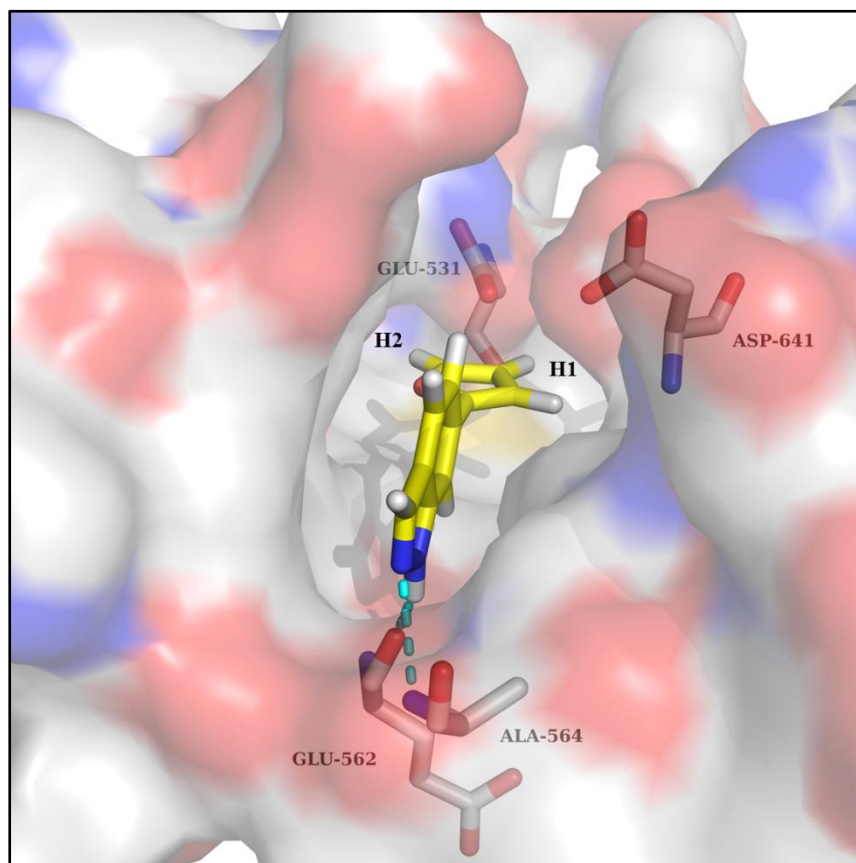


**Figure 2.7:** Glide docking model of compound **38** bound within FGFR1. Substitution at the 4/5-position of the furan ring could allow for the H1 and H2 pockets to be occupied respectively.

Compound **38** is predicted to bind to FGFR1 in a similar way to that predicted for compound **15** (Figure 2.6). Inspection of the docking model of compound **38** reveals interesting areas for potential modification. It is apparent that occupation of H1 or H2 can be achieved with substitution at the 4/5-position of the furan ring respectively. The H1 pocket is larger than the H2 pocket and therefore occupation of this particular sub-pocket by small hydrophobic groups was prioritised. A variety of small compounds were docked to find suitable candidates for synthesis, some of which are outlined below (Figure 2.8).

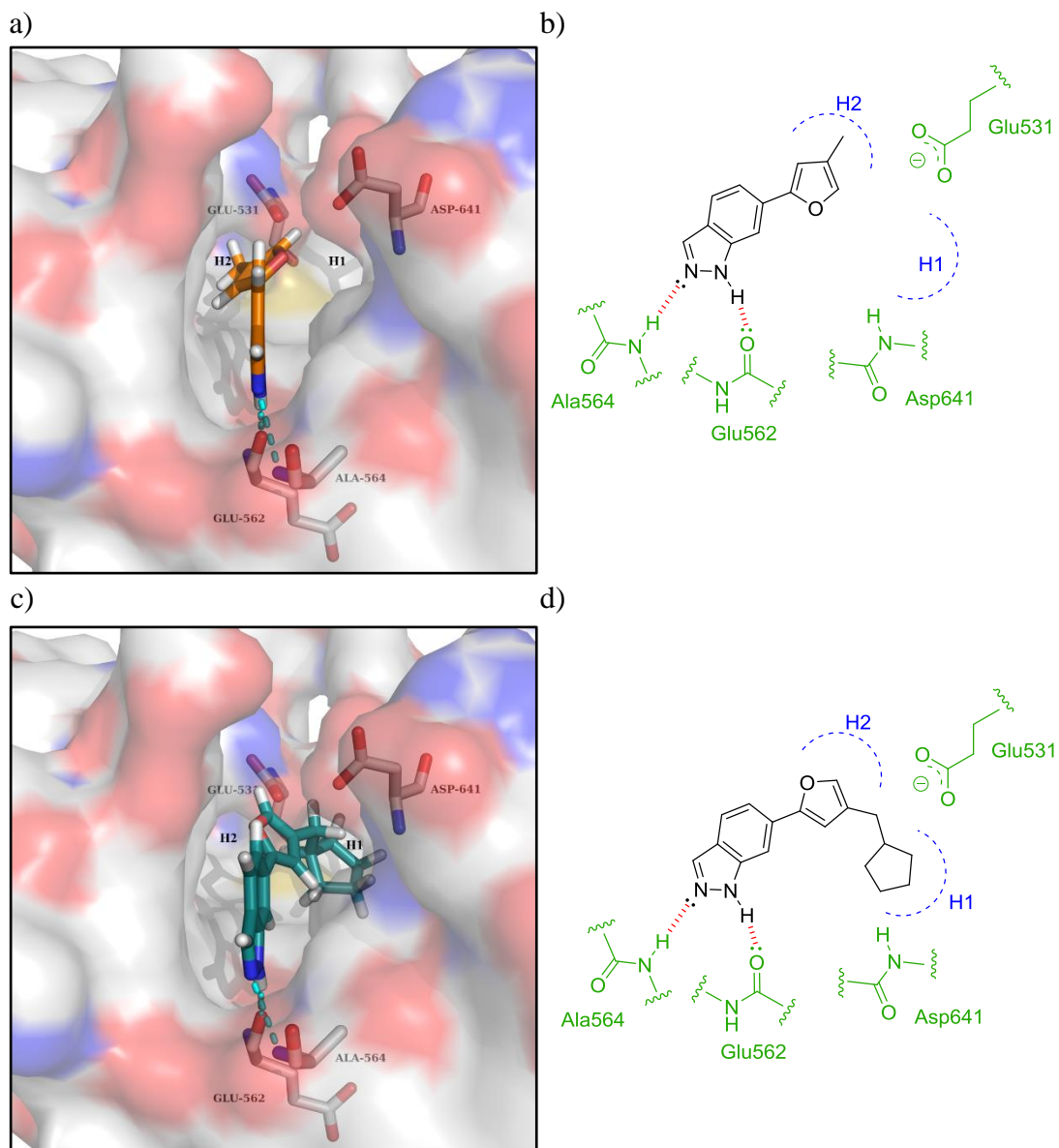
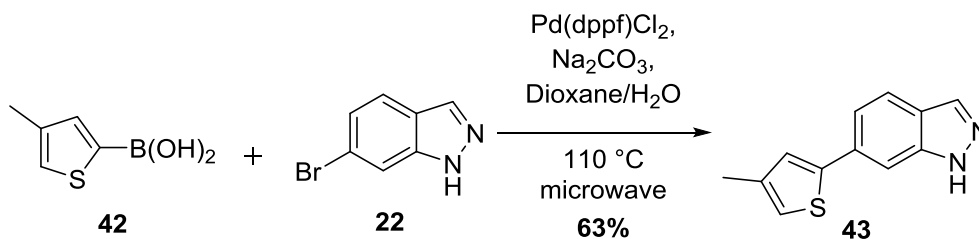


**Figure 2.8:** a) Glide docking model of compound **40** bound within FGFR1; b) 2D representation of predicted binding pose of compound **40**. The methyl moiety is predicted to occupy the H2 pocket; c) Glide docking model of compound **41** bound within FGFR1; d) 2D representation of predicted binding pose of compound **41**. The cyclopentane ring is predicted to occupy the H1 pocket.

Compound **40** is predicted to bind to FGFR1 in a similar way to that predicted for compound **38** (Figure 2.7). The furfuryl methyl group is predicted to occupy the H2 pocket. In contrast to this, the docking of compound **41** has resulted in placing the larger methylene cyclopentane moiety in the H1 pocket. This gives strength to the hypothesis that the H1 pocket is larger and therefore more accommodating for larger hydrophobic groups. Due to the accessibility of starting materials, target compound **40**



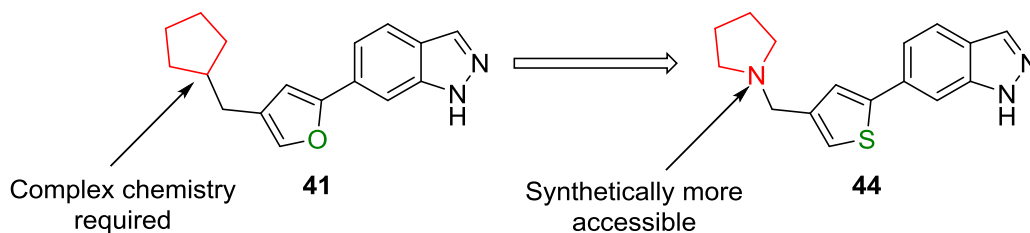
was changed to compound **43** and synthesised using Suzuki chemistry as summarised below (Scheme 2.8).



Scheme 2.8: Synthetic route to compound **43**.

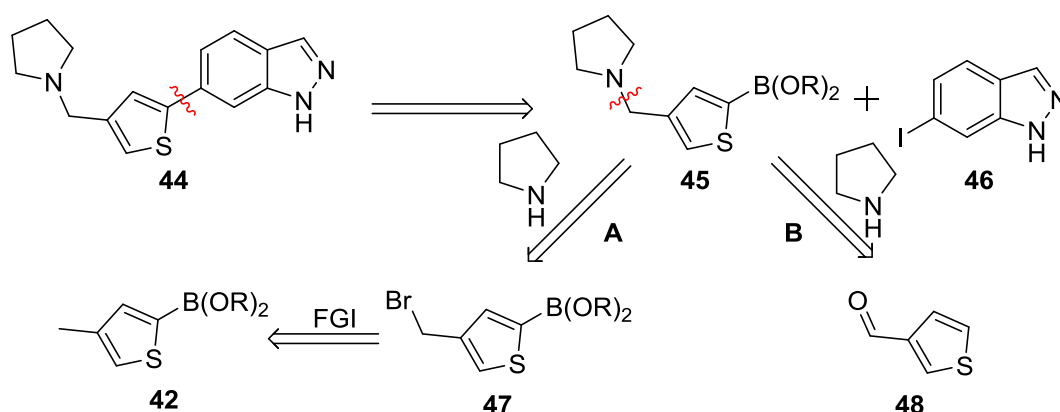
### 2.3.3 Retrosynthetic Analysis of Structure **41**

Retrosynthetic analysis of structure **41** indicated that the chemistry required to connect the cyclopentane ring to the furan ring would not be trivial and therefore a structural replacement of cyclopentane to pyrrolidine was carried out. As the docking of compound **41** (Figure 2.8) suggests, only the substitution pattern of the aromatic five-membered ring matters and therefore furan was changed to thiophene to give compound **44** (Scheme 2.9).



Scheme 2.9: Manipulation of compound **41** to the more synthetically accessible compound **44**. Structural replacement and heteroatom substitution are shown in red and green respectively.

Retrosynthetic analysis of structure **44** was carried out (Scheme 2.10).



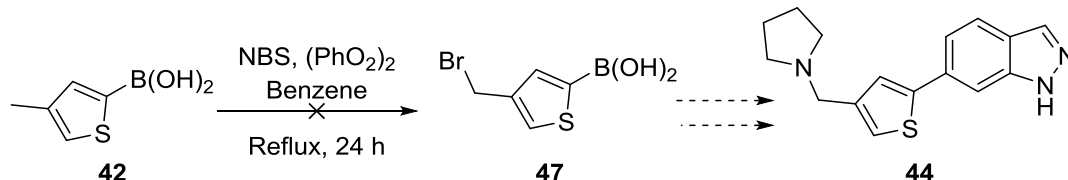
Scheme 2.10: Retrosynthetic analysis of structure **44**.

Structure **44** can first be disconnected at the 6-position of the indazole ring to give structures **45** and **46**. Structure **45** can then be disconnected between the pyrrolidine

nitrogen and the bridging methylene group *via* two routes; route **A** gives pyrrolidine and structure **47** which can then undergo a functional group interconversion (FGI) to structure **42**, route **B** gives pyrrolidine and compound **48**.

### 2.3.4 Synthesis of Compound 44

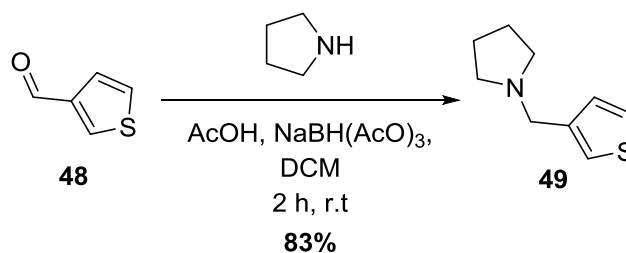
The synthesis of compound **44** was attempted using an adaptation of a method outlined by Ngwendson *et al* and is summarised below (Scheme 2.11).<sup>119</sup>



**Scheme 2.11:** Attempted route to compound **44**.

Compound **42** was subjected to radical bromination with the hope of selectively brominating the methyl group. Unfortunately the reaction was unsuccessful. There are several possible reasons why this reaction failed. Thiophene is very electron rich and N-bromosuccinimide (NBS) is a good source of electrophilic bromine and therefore over-bromination is likely. A more likely reason for the failure of this reaction is due to the presence of the boronic acid moiety. Inspection of the literature indicated that boronic acids interact with radical species to form the *ipso*-carbon radical which can be used in carbon-carbon bond formation reactions.<sup>120</sup>

It was apparent that route **B** was more plausible than route **A**. The synthesis of compound **49** was carried out using an adaptation of a method outlined by Bogenstaetter *et al* and is summarised below (Scheme 2.12).<sup>121</sup>

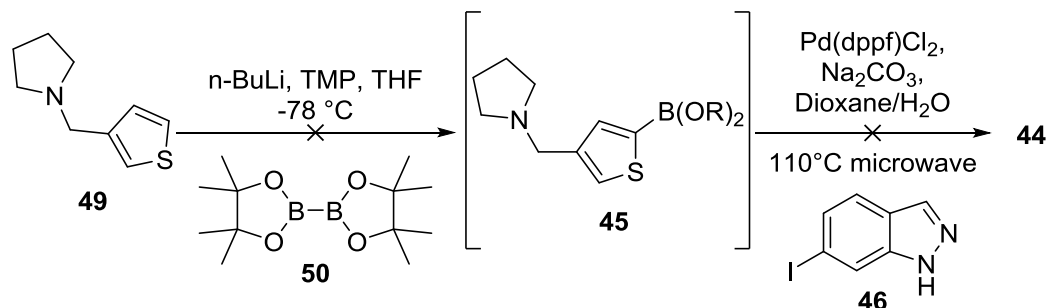


**Scheme 2.12:** Synthesis of compound **49** from compound **48** using reductive amination.

Compound **49** was synthesised from compound **48** and pyrrolidine in a yield of 83% using sodium triacetoxyborohydride (STAB) as the reducing agent in a simple acid-catalysed reductive amination reaction. Purification of this material using column chromatography would be difficult owing to the polar nature of the pyrrolidine moiety.

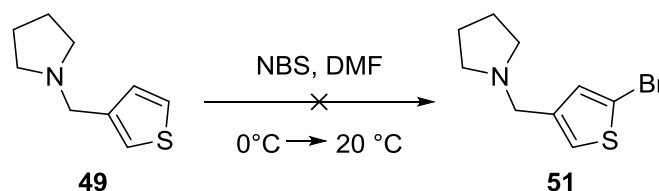
In order to bypass this issue, compound **49** was purified using Kugelrohr distillation which proved to be very successful.

The synthesis of compound **44** was attempted using an adaptation of a method outlined by Zeng *et al* and is summarised below (Scheme 2.13).<sup>122</sup>



**Scheme 2.13:** Synthetic route to compound **44** via an *in situ* borylation.

Compound **49** was subjected to lithiation followed by borylation with compound **50** to generate compound **45** as an intermediate. 2,2,6,6-Tetramethylpiperidine (TMP) reacts with <sup>n</sup>BuLi to form the sterically bulky base LiTMP. This choice of base was employed to increase the chance of selective lithiation at the 4-position of the thiophene ring as this position is less sterically hindered than that of the 2-position. Compound **45** was then cross coupled under Suzuki conditions with compound **46** to give compound **44**. Attempts at isolation of the intermediate **45** were unsuccessful. Upon <sup>1</sup>H NMR analysis of the isolated purified product, it was apparent that the undesired regioisomer had formed during the lithiation step, placing the boronate species in the 2-position of the thiophene ring. The most likely reason for this is due to the direct *ortho* metalation (DOM) effect of the pyrrolidine group. The pyrrolidine nitrogen lone pair can stabilise lithiation at the 2-position and therefore directs the borylation process. In order to overcome this problem, an attempt was made using bromination conditions, developed in-house, to synthesise compound **51** (Scheme 2.14).



**Scheme 2.14:** Attempted bromination of compound **49**.

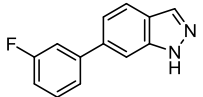
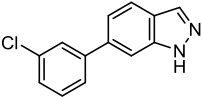
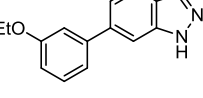
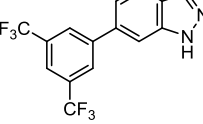
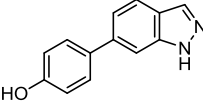
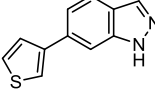
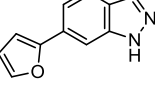
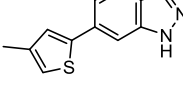
Mono-bromination of compound **49** was unsuccessful using the above conditions. Analysis of the reaction mixture using LC-MS indicated that di/tri substituted

bromination was occurring and therefore the reaction was abandoned. Further attempts at synthesising compound **44** were abandoned and efforts focussed elsewhere.

### 2.3.5 Biological Evaluation of ‘Second Generation’ Fragments

Compounds **29-31**, **33**, **34**, **37**, **38** and **43** were screened against FGFR1 at an initial concentration of 100  $\mu\text{M}$  using the FRET-based assay. The results are outlined below (Table 2.2).

**Table 2.2:** Biological results for ‘second generation’ fragments when screened against FGFR1.

Compound No.	Structure	% Inhibition <sup>a</sup> (100 $\mu\text{M}$ )	IC <sub>50</sub> <sup>a</sup> ( $\mu\text{M}$ )	LE
<b>29</b>		19 $\pm$ 1.5	NT	N/A
<b>30</b>		32 $\pm$ 0.5	NT <sup>c</sup>	N/A
<b>31</b>		85 $\pm$ 0.0 <sup>b</sup>	2.0 $\pm$ 0.4	0.44
<b>33</b>		-5 $\pm$ 0.5	NT	N/A
<b>34</b>		83 $\pm$ 3.5	12 $\pm$ 1.6	0.43
<b>37</b>		20 $\pm$ 3.0	NT	N/A
<b>38</b>		29 $\pm$ 0.5	NT	N/A
<b>43</b>		19 $\pm$ 0.5	NT	N/A

<sup>a</sup> % Inhibition and IC<sub>50</sub> values are given as the mean  $\pm$  SD of all data points,  $n = 2$ . <sup>b</sup> No difference in measured data points. <sup>c</sup> NT = not tested.

Compounds **29-31** were synthesised to probe the potential to form favourable interactions in the 3-position of the phenyl ring. Compound **31** is active with an IC<sub>50</sub> value of 2  $\mu\text{M}$  and a LE of 0.44 and is more active than both compounds **29** and **30**.

This suggests that the larger ethoxy group forms more favourable interactions within FGFR1 than the smaller halogen substituents. The increase in potency could be due to the ethoxy group lying deeper in the H1 pocket having a greater hydrophobic effect. In contrast, compound **33** is completely inactive. This suggests that there may be a limit to the size of the space that can be occupied by substituents around the 6-phenyl ring. Compound **34** is also active with an  $IC_{50}$  value of 12  $\mu M$  and a LE of 0.43. This suggests that substitution in the 4-position of the phenyl ring may offer potential to form favourable interactions. Compounds **37**, **38** and **43** all show diminished activity when compared to compounds containing six-membered ring systems in the 6-position of the indazole ring. This outlines the importance of the 6-position phenyl ring for effective inhibition of FGFR1.

### 2.3.6 Docking of Compounds **31** and **34**

Compound **31** was docked into the FGFR1 crystal structure in order to rationalise the observed activity and is outlined below (Figure 2.9).

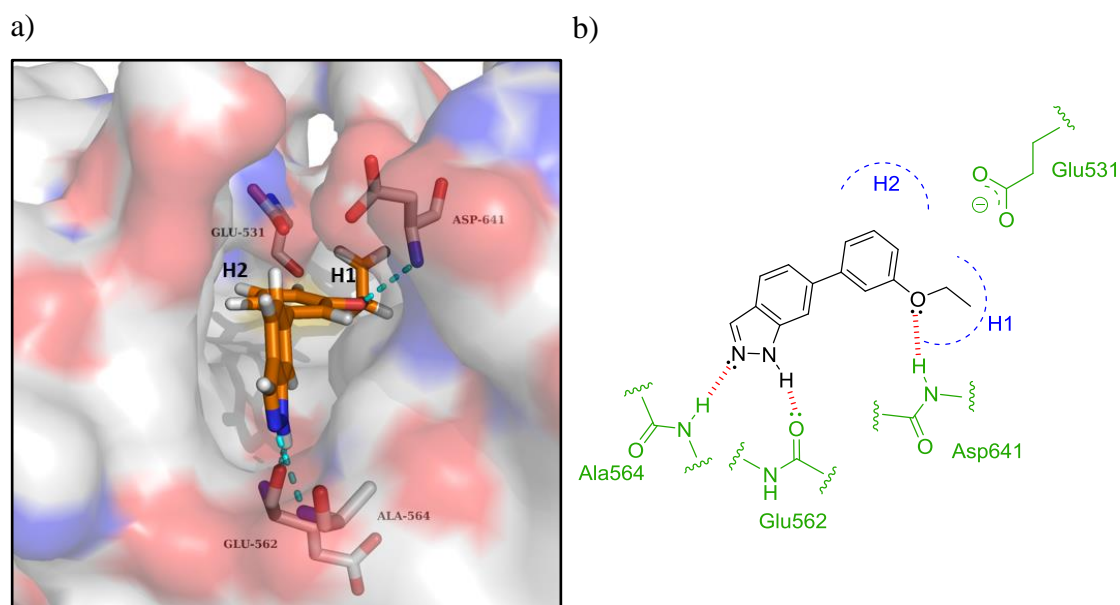


**Figure 2.9:** a) Glide docking model of compound **31** bound within FGFR1; b) 2D representation of predicted binding pose of compound **31**. The ethoxy group is predicted to occupy the H1 pocket and also form an H-bond with the backbone NH of Asp641.

Compound **31** is predicted to bind to FGFR1 in a similar way to that predicted for compound **15** (Figure 2.6). The ethoxy moiety of compound **31** is predicted to occupy the H1 pocket with the oxygen atom forming an H-bond with the backbone NH of Asp641. Comparison with the docking of compound **15** (Figure 2.6) shows that the ethyl group is placed further into the H1 pocket than that of the Cl atom, and can

therefore explain the increase in potency from compounds **31** to **15**. Compound **34** was also docked into the FGFR1 crystal structure and is outlined below (Figure 2.10).

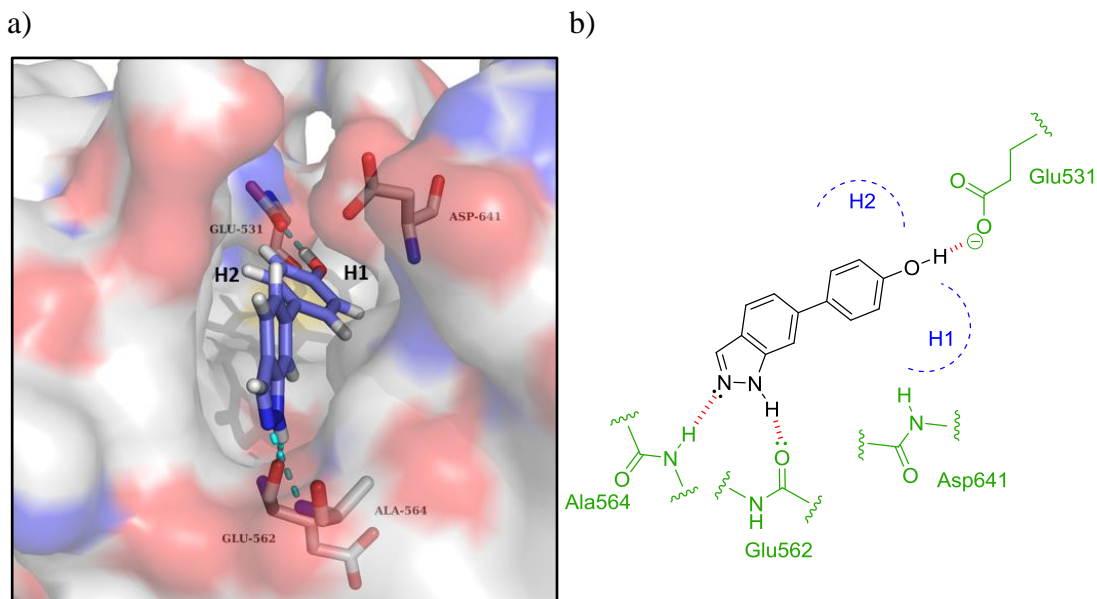


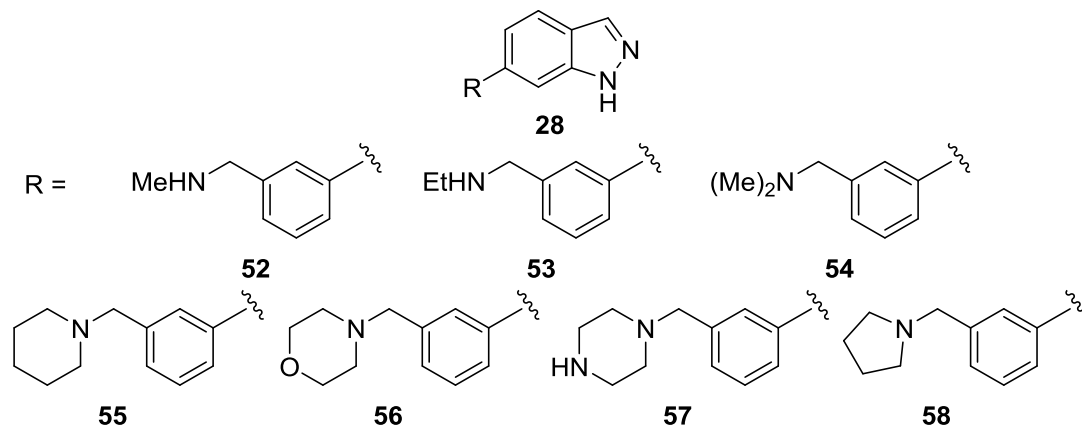
**Figure 2.10:** a) Glide docking model of compound **34** bound within FGFR1; b) 2D representation of predicted binding pose of compound **34**. The hydroxy group is predicted to form an H-bond with a side chain carboxy oxygen of Glu531.

Compound **34** is predicted to bind to FGFR1 in a similar way to that predicted for compound **31** (Figure 2.9). The 4-position hydroxy group of the phenyl ring is predicted to be an H-bond donor forming an H-bond with a side chain carboxy oxygen of Glu531. In contrast to the docking model of compound **31**, the dihedral angle between the phenyl and indazole ring has decreased, placing the 3/5-position vectors of the phenyl ring away from the H1/H2 sub-pockets. This suggests that occupation of either of these sub-pockets with small hydrophobic groups may not be possible when the phenol moiety is present.

## 2.4 SAR Exploration

### 2.4.1 Amine Library

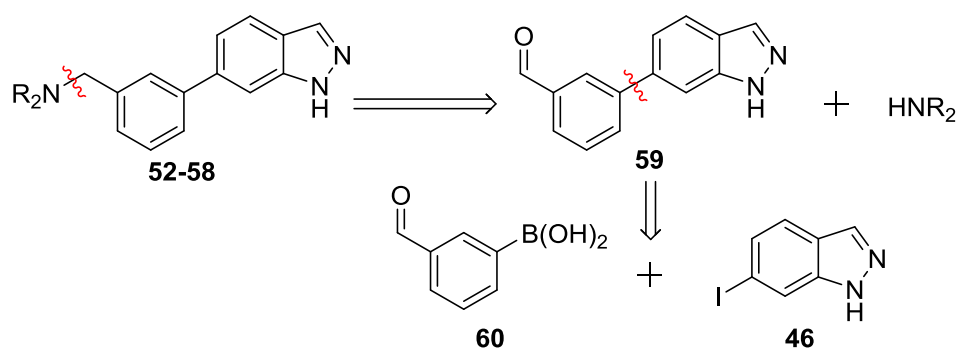
In order to further expand the SARs for the indazole pharmacophore **28**, a small library of compounds was targeted for synthesis, focusing primarily on optimisation of the 3-position substituent on the phenyl ring and is outlined below.



This library would allow rapid access to a large number of fragments *via* divergent reductive amination chemistry. Compound **52** will act as a comparison to compound **31** as the 3-position substituent has the same chain length, varying only in the position of the heteroatom. Compounds **53-58** will help establish the effect of varying the size of the 3-position substituent, looking at aliphatic and saturated heterocycles substituents.

#### 2.4.1.1 Retrosynthetic Analysis of Structures 52-58

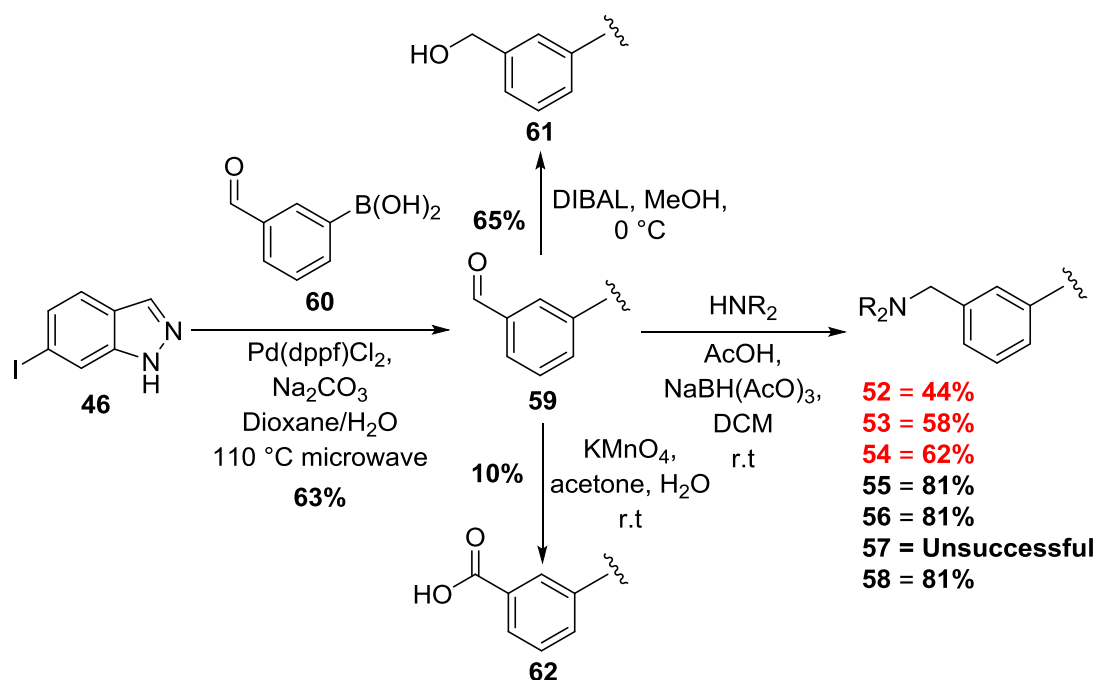
Retrosynthetic analysis of structures **52-58** indicated that the desired compounds could be made in two simple steps; Pd-catalysed Suzuki couplings followed by reductive aminations and is summarised below (Scheme 2.15).



Scheme 2.15: Retrosynthetic analysis of structures 52-58.

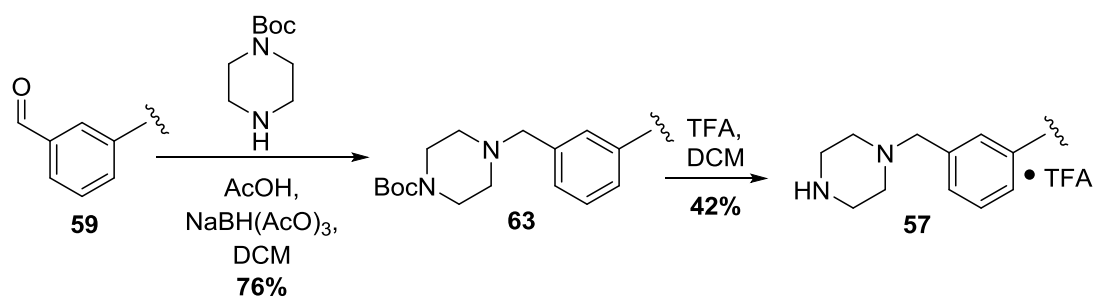
#### 2.4.1.2 Synthesis of Compounds 52-58

Compounds **52-58** were synthesised using a combination of Suzuki chemistry and reductive amination chemistry (Scheme 2.16). Compound **59** was subjected to oxidative and reductive conditions using adaptations of methods outlined by Kelly *et al* and is summarised below (Scheme 2.16).<sup>123</sup>



**Scheme 2.16:** Divergent synthesis to compounds **52-58** utilising compound **59**.<sup>1</sup>

Compounds **61** and **62** were synthesised from compound **59** to provide additional SARs. Compound **61** was formed in a modest yield of 65%, however, compound **62** proceeded in a poor yield of 10%. This was due to purification issues mostly attributed to the polar nature of the compound. The reductive aminations proceeded with modest yields apart from the case of compound **57** which was unsuccessful. Upon purification it was apparent that compound **57** was extremely insoluble and could not be isolated. To overcome this issue, compound **57** was synthesised using chemistry as summarised below (Scheme 2.17).



**Scheme 2.17:** Alternative synthesis of compound **57**.

Compound **57** was synthesised *via* the protected intermediate **63**. Purification was carried out on this intermediate followed by deprotection using trifluoroacetic acid (TFA) yielding compound **57** as the TFA salt.

<sup>1</sup>Compounds outlined in red were synthesised by Abbey Summers (MChem) under the supervision of the Author.



### 2.4.1.3 Biological Evaluation of Compounds 52-59 and 61-63

Compounds **52-59** and **61-63** were screened against FGFR1 at an initial concentration of 100  $\mu\text{M}$  using the FRET-based assay. The results are outlined below (Table 2.3).

**Table 2.3:** Biological results for compounds **52-59** and **61-63** when screened against FGFR1.

Compound No.	Structure	% Inhibition <sup>a</sup> (100 $\mu\text{M}$ )
52		54 $\pm$ 0.5
53		45 $\pm$ 0.5
54		55 $\pm$ 3.5
55		49 $\pm$ 0.5
56		24 $\pm$ 1.0
57		52 $\pm$ 4.5
63		19 $\pm$ 1.5
58		48 $\pm$ 2.5
59		77 $\pm$ 0.5
61		54 $\pm$ 0.0 <sup>b</sup>
62		35 $\pm$ 0.5

<sup>a</sup> % Inhibition values are given as the mean  $\pm$  SD of all data points,  $n = 2$ . <sup>b</sup> No difference in measured data points.

Compounds **52-59** all show lower activity against FGFR1 at 100  $\mu\text{M}$  than for the case compound **31** (Table 2.2). The size of the 3-position phenyl substituent for compound **52** is the same as the substituent in compound **31**, this suggests that the loss in potency is due to the change of the positioning and nature of the heteroatom present. Compounds **53** and **54** both show a loss in potency against FGFR1 when compared to compound **31**, possibly due to the larger 3-position phenyl substituents. Compounds **55-58** and **63** all contain saturated heterocycles and all show less activity against FGFR1 at 100  $\mu\text{M}$  than compound **31**. This could be due to the saturated ring systems being too large to fit into the H1 pocket. Additionally, the tertiary amine centres are protonated at physiological pH, potentially resulting in a repulsive interaction with hydrophobic residues within the H1 or H2 sub-pockets. Interestingly, compound **59** shows comparable inhibition at 100  $\mu\text{M}$  to that of compound **31**. This could be due to an H-bond forming between the aldehyde oxygen and the backbone NH of Asp641, as was predicted for the ether oxygen in the docking of compound **31** (Figure 2.9). Care must be taken when drawing conclusions from compounds with aldehydes present. The reactive nature of this species poses complications that may result in false positives, such as covalent inhibition. In contrast, compound **61** shows less inhibition against FGFR1 than compound **59**. This could be due to the weaker H-bonding acceptor potential of the oxygen lone pair in compound **61**. Compound **62** also shows less inhibition against FGFR1 than compound **59**. The carboxy group is negatively charged at physiological pH and therefore may experience repulsion with the nearby negatively charged residues, such as Glu531 or Asp641.

#### 2.4.1.4 Docking of Compounds 52, 55 and 59

Compound **52** was docked into the FGFR1 crystal structure in order to rationalise the observed activity and is outlined below (Figure 2.11).

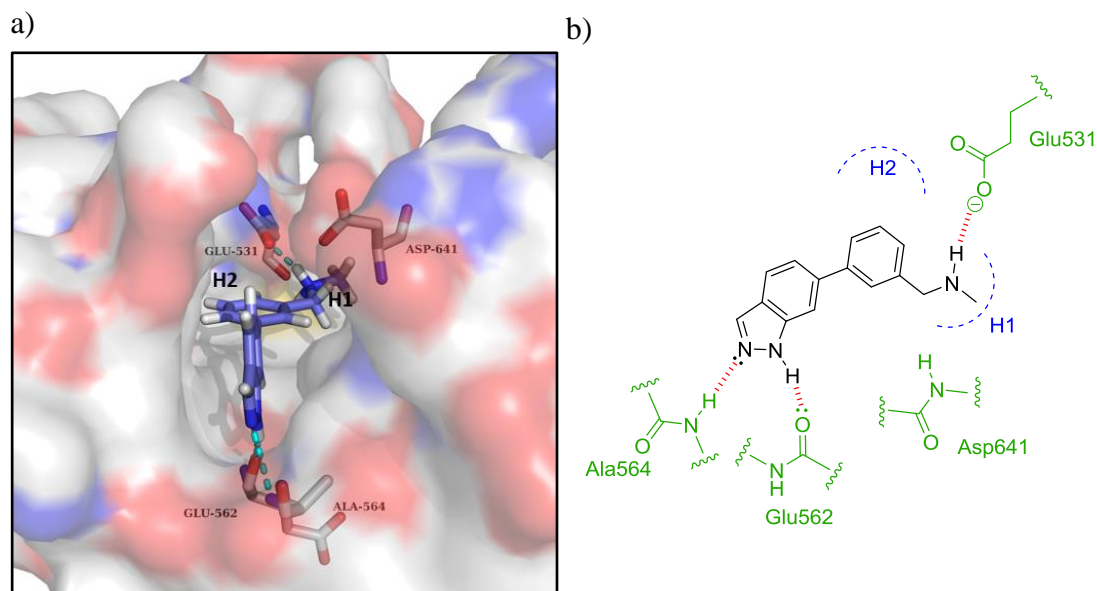


**Figure 2.11:** a) Glide docking model of compound **52** bound within FGFR1; b) 2D representation of predicted binding pose of compound **52**.

Compound **52** is predicted to bind in a similar way to that predicted by compound **31** (Figure 2.9). The 3-position substituent is predicted to occupy the H1 pocket as well as form an H-bond between the NH and a side chain carboxy oxygen of Glu531. However, the potency of this compound is lower than that observed for compound **31** which appears to be at-odds with the proposed favourable docking binding pose.

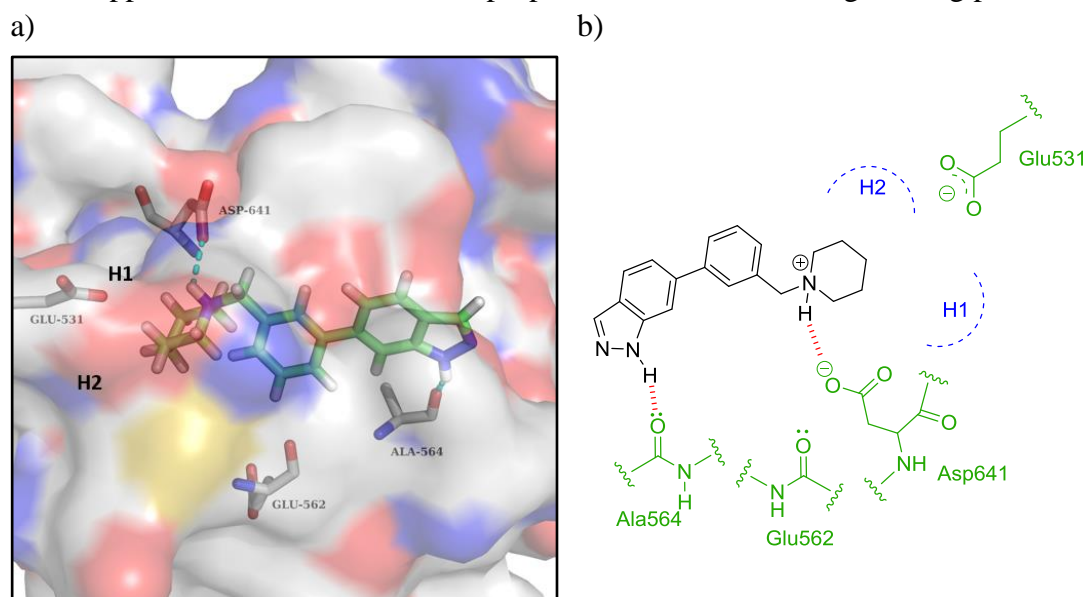


**Figure 2.12:** a) Glide docking model of compound **55** bound within FGFR1; b) 2D representation of predicted binding pose of compound **55**.

Compound **55** is predicted to bind in a different way to compound **52**. The presence of the bulky piperidine ring in compound **55** has resulted in the compound being displaced out, towards solvent, of the active site. This disrupts the crucial H-bonding interaction between the indazole nitrogens and the amino acid residues Glu562 and Ala564. This interaction has been conserved throughout all docking models of compounds containing the indazole core and therefore offers an explanation for the drop in potency for compound **55**. The protonated piperidine group is predicted to form an H-bond with a side chain carboxy oxygen of Asp641. Compounds **56-58** and **63** were docked and were also predicted to bind in a similar fashion to compound **55**. Compound **59** was also docked into the FGFR1 crystal structure in order to rationalise the observed activity and is outlined below (Figure 2.13).

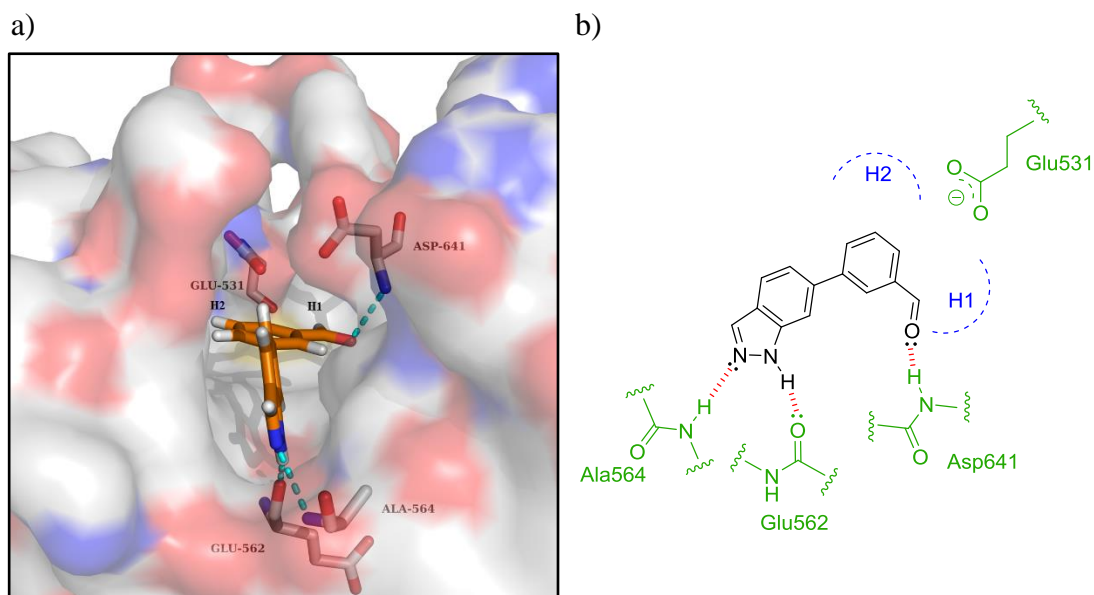


**Figure 2.13:** a) Glide docking model of compound **59** bound within FGFR1; b) 2D representation of predicted binding pose of compound **59**.

Compound **59** is predicted to bind in a similar way to that predicted for compound **52** (Figure 2.11). The aldehyde group is predicted to form an H-bond with the backbone NH of the Asp641 residue. Interestingly, the formyl hydrogen points into the H1 pocket, this suggests that small amide or ester linkages may be tolerated in this position.

## 2.4.2 Occupation of the H1 Sub-pocket

The docking of compound **59** suggests substitution at the aldehyde may lead to occupation of the H1 sub-pocket. Several derivatives prepared utilising amide

chemistry were docked into the FGFR1 crystal structure, the one with the best predicted fit is outlined below (Figure 2.14).

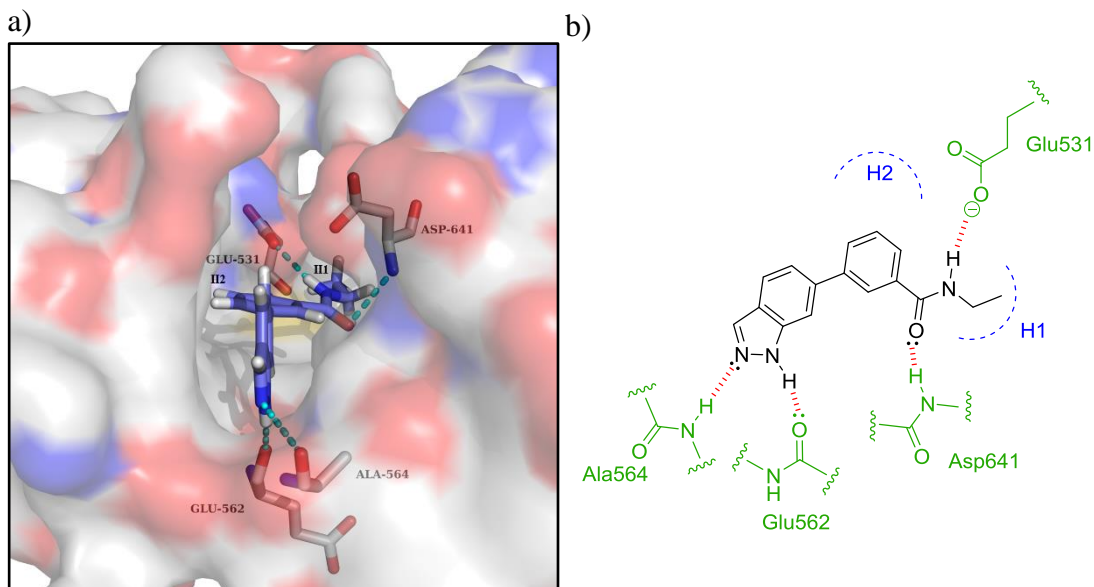
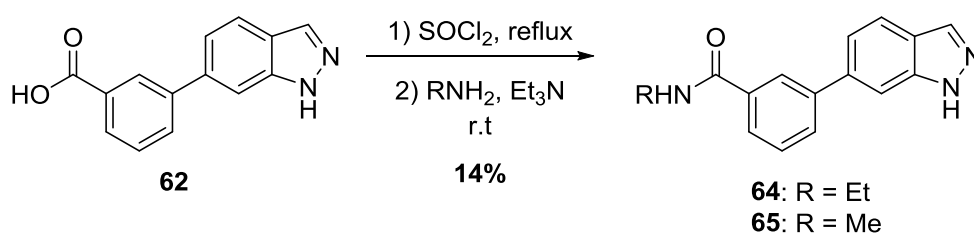


**Figure 2.14:** a) Glide docking model of compound **64** bound within FGFR1; b) 2D representation of predicted binding pose of compound **64**.

Compound **64** is predicted to bind in a similar way to that predicted for compound **52** (Figure 2.11). The ethyl amide group is predicted to occupy the H1 pocket and make two H-bonding interactions. The amide carbonyl is predicted to form an H-bond with the backbone NH of Asp641, and the amide NH is predicted to form an H-bond with a side chain carboxy oxygen of Glu531. The methyl amide (**65**) was also targeted to act as a direct comparison to compound **64**. Both were synthesised according to an adaptation of a procedure outlined by Brady *et al* as summarised below (Scheme 2.18).<sup>124</sup>



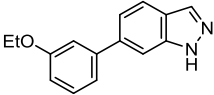
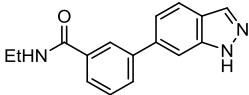
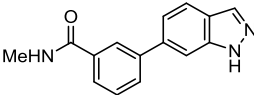
**Scheme 2.18:** Amide coupling conditions using *in situ* acyl chloride formation.

Compound **62** was chlorinated using SOCl<sub>2</sub> and the chlorine atom displaced by *in situ* nucleophilic attack of a primary amine to form the amide. Both reaction yields were low at 14%. Analysis of the crude reaction mixture by LC-MS outlined the formation of various side products and can therefore explain the poor yield.

### 2.4.3 Biological Evaluation of Compounds 64 and 65

Compounds **31**, **64** and **65** were screened against FGFR1-3 at an initial concentration of 100  $\mu\text{M}$  using the FRET-based assay. The results are outlined below (Table 2.4).

**Table 2.4:** Biological results for compounds **31**, **71** and **72** when screened against FGFR1-3.

Compound No.	Structure	IC <sub>50</sub> <sup>a</sup> ( $\mu\text{M}$ )		
		1	2	3
<b>31</b>		2.0 $\pm$ 0.4	0.8 $\pm$ 0.4	4.5 $\pm$ 1.6
<b>64</b>		>100	>100	>100
<b>65</b>		>100	>100	>100

<sup>a</sup> % IC<sub>50</sub> values are given as the mean  $\pm$  standard deviation (SD) of all data points,  $n = 2$ .

Compound **31** was tested against FGFR2/3 to determine whether there was any selective inhibition for the individual FGFR sub-types. As these compounds are fragments the selectivity difference was expected to be small. Minor differences in selectivity were observed, most noticeably between FGFR2 and FGFR3 with compound **31** being  $\sim$ 5-fold more selective for FGFR2. The docking model of compound **64** (Figure 2.14) was promising, however, compounds **64** and **65** were inactive against FGFR1-3. The reasons for the complete loss of activity for compounds **64** and **65** were unclear and further work regarding this motif was abandoned.

## 2.5 Optimisation of Lead Fragments

### 2.5.1 SAR Expansion of Compound 31

Compound **31** was subjected to further modification focusing on substitution around the indazole 6-position phenyl ring in addition to the 3-ethoxy group. Docking models outlined that occupation of both the H1/H2 sub-pockets may be achieved by substitution of small hydrophobic groups in the 5-position of the phenyl ring, as compound **66** shows (Figure 2.15).

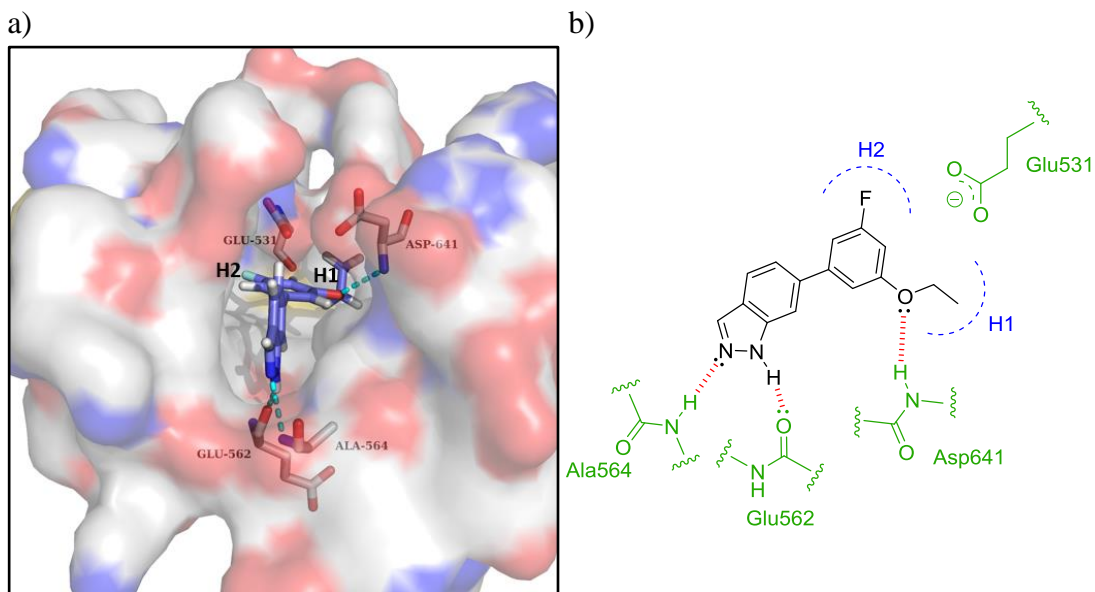
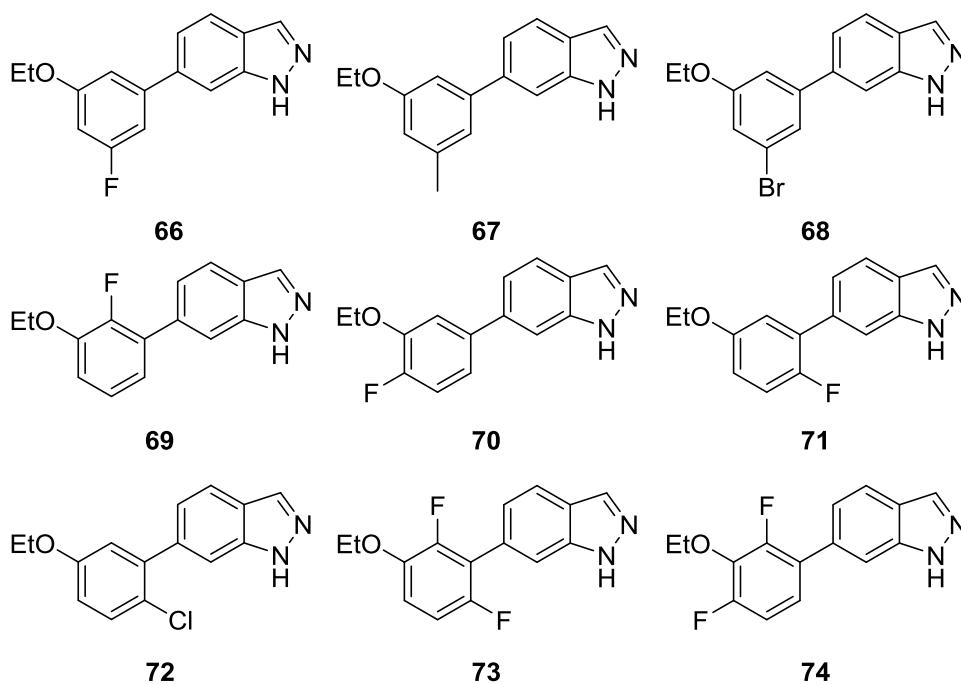


**Figure 2.15:** a) Glide docking model of compound **66** bound within FGFR1; b) 2D representation of predicted binding pose of compound **66**.

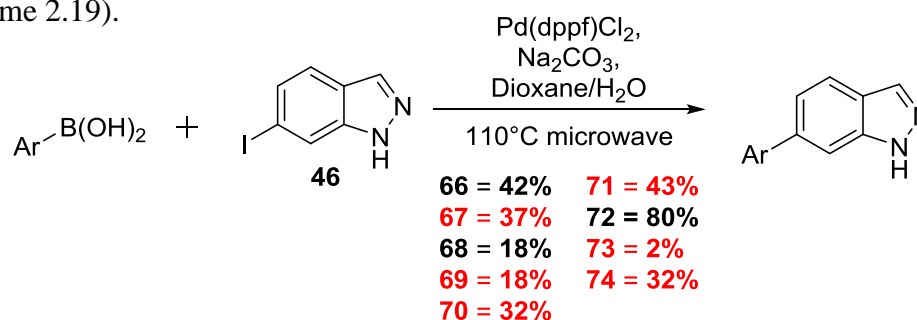
Compound **66** is predicted to bind in a similar fashion to that of compound **31** (Figure 2.9). In addition the F atom is predicted to occupy the H2 sub-pocket.

Using the docking model as a guide, a small focussed library looking at incorporating small hydrophobic groups, in addition to the 3-position ethoxy group, was developed and is outlined below.



### 2.5.1.1 Synthesis of Compounds 66-74

Compounds **66-74** were synthesised using Suzuki chemistry as summarised below (Scheme 2.19).



**Scheme 2.19:** Suzuki chemistry to 6-substituted indazoles.<sup>2</sup>

The yields for each coupling step vary quite significantly. The low yield for compound **73** can be explained by the sterically bulky, and electron poor, boronic acid making the rate of transmetallation slower.

### 2.5.1.2 Biological Evaluation of Compounds 66-74

Compounds **66-74** were screened against FGFR1-3 at an initial concentration of 100  $\mu\text{M}$  using the FRET-based assay. The results are outlined below (Table 2.5).

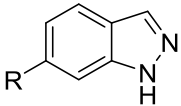
In general, further substitution on the phenyl ring results in a loss of activity. Compound **66-68** are significantly less active than compound **31** against all FGFRs. In addition to the 3-ethoxy group, compounds **66-68** show an increase in the size of the 5-position substituent which results in a decrease in potency when compared to compound **31**. This suggests that the compounds are too large to bind favourably to the FGFR. Compound **66** completely loses activity against FGFR3 and is less active against FGFR1/2 when compared to compound **31**. Interestingly, compound **66** is ~7-fold more active against FGFR2 than FGFR1, an increase from what is observed for compound **31** (~2.5-fold). This suggests that it may be possible to develop a selective FGFR2 inhibitor with precise substitution around the 6-position phenyl ring. In addition to the ethoxy group, compounds **69-71** possess mono-substituted fluorines in various substitution patterns around the 6-position ring. Compound **69** is the most active of the mono-fluorinated compounds but still weaker than compound **31**; it has also lost activity against FGFR3. This complete loss of activity against FGFR3 is reflected throughout compounds **66-74**, suggesting that the requirements for inhibition of FGFR3 are more stringent than that of FGFR1/2. Compound **70** is completely

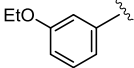
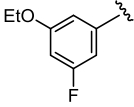
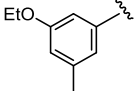
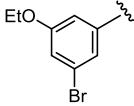
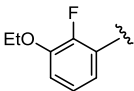
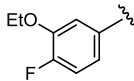
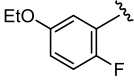
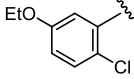
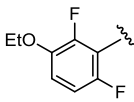
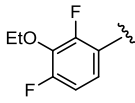
<sup>2</sup>Compounds outlined in red were synthesised by Abbey Summers (MChem) under the supervision of the Author.



inactive outlining that substitution in the 4-position of the phenyl ring is not tolerated. Compounds **71** and **72** are both inactive. This outlines that, in addition to the 3-ethoxy group, further substitution in the 6-position of the phenyl ring is not tolerated. Compounds **73** and **74** possess di-fluorinated systems and both show diminished activity against the FGFRs, reflecting the conclusions made for compounds **71** and **72**.

**Table 2.5:** Biological results for compounds **31** and **66-74** when screened against FGFR1-3.



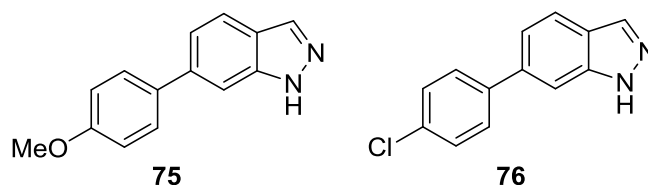
No.	Structure	% Inhibition <sup>a</sup> (100 μM)			IC <sub>50</sub> <sup>a</sup> (μM)		
		1	2	3	1	2	3
<b>31</b>		85 ± 0.0 <sup>b</sup>	NT <sup>c</sup>	NT	2.0 ± 0.4	0.8 ± 0.4	4.5 ± 1.6
<b>66</b>		63 ± 5.5	88 ± 1.0	52 ± 3.5	83 ± 0.9	12 ± 0.9	>100
<b>67</b>		24 ± 0.5	49 ± 4.0	24 ± 0.5	>100	>100	>100
<b>68</b>		14 ± 2.0	44 ± 1.0	11 ± 12	NT	NT	NT
<b>69</b>		71 ± 1.5	89 ± 1.0	56 ± 0.0	9.7 ± 1.1	6.4 ± 0.8	>100
<b>70</b>		8 ± 7.5	NT	NT	NT	NT	NT
<b>71</b>		43 ± 6.5	NT	NT	NT	NT	NT
<b>72</b>		38 ± 1.0	NT	NT	NT	NT	NT
<b>73</b>		57 ± 3.5	75 ± 1.5	46 ± 2.0	>100	52 ± 0.9	>100
<b>74</b>		31 ± 6.5	51 ± 3.0	13 ± 12	NT	NT	NT

<sup>a</sup> % Inhibition and IC<sub>50</sub> values are given as the mean ± SD of all data points, n = 2. <sup>b</sup> No difference in measured data points. <sup>c</sup> NT = not tested

In summary, additional substitution on the 6-position phenyl ring results in a less active compound but as compound **66** shows, it may be possible to utilise precise substitution patterns to obtain selectivity between the different FGFR sub-types.

### 2.5.2 SAR Validation and Expansion of Compound **34**

Compound **34** is predicted to form an H-bond between the 4-position OH and the Glu531 residue of FGFR1 (Figure 2.10). In order to validate this prediction compounds **75** and **76** were targeted for synthesis and are outlined below. The methoxy group in compound **75** lacks the ability to be an H-bond donor but is able to accept an H-bond. This will help establish what type of H-bond is occurring with Glu531. The Cl atom in compound **76** cannot be a H-bond donor and provides additional SAR in this position.



Compound **34** was also subjected to further modification focusing on substitution around the 6-position phenyl ring in addition to the 4-hydroxy group. Docking models outlined that occupation of the H2 pocket may be achieved by substitution of a small hydrophobic group at the 3-position of the phenyl ring, as compound **77** shows (Figure 2.16).

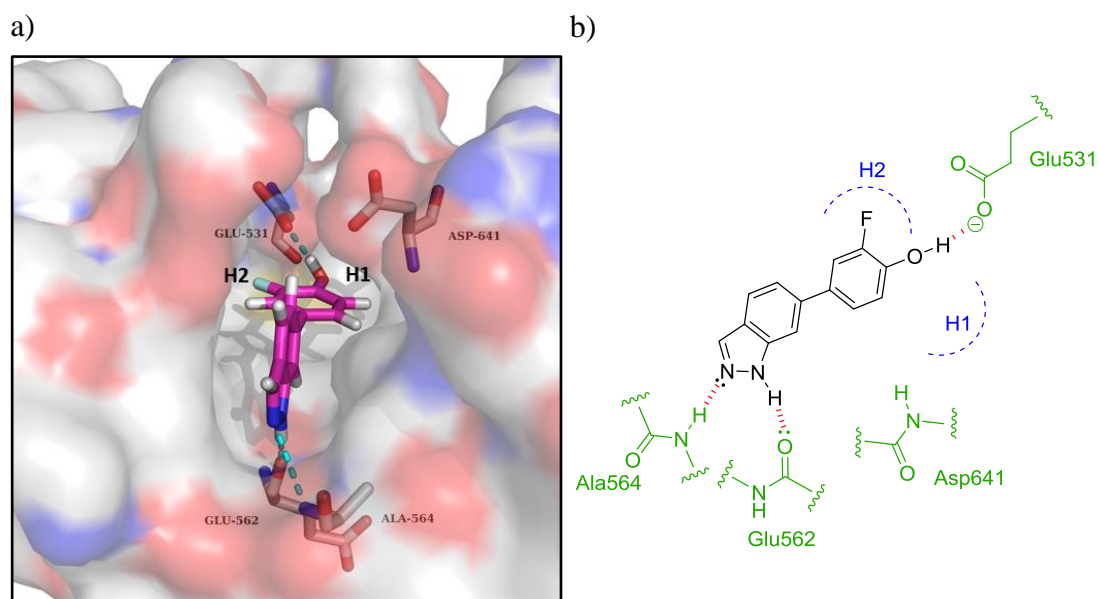
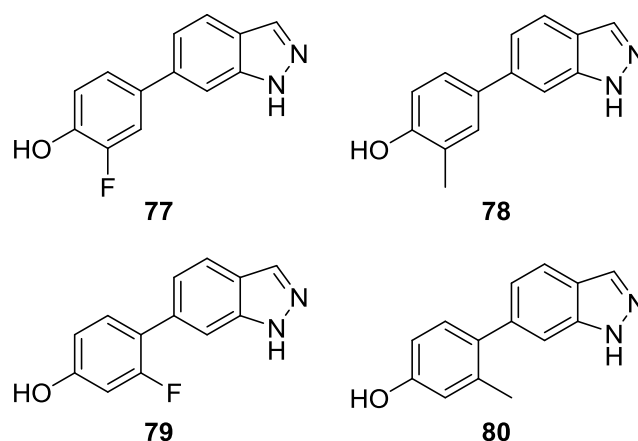


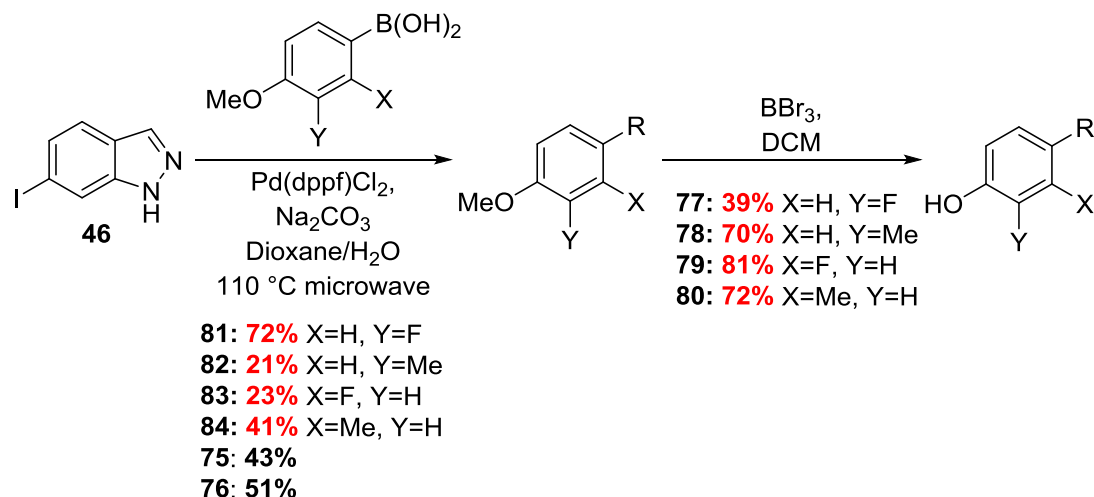
**Figure 2.16:** a) Glide docking model of compound **77** bound within FGFR1; b) 2D representation of predicted binding pose of compound **77**.

Compound **77** docks in a similar fashion to that of compound **34** (Figure 2.10) and is predicted to maintain the H-bond between the hydroxy group and the Glu531 residue. In addition to the predicted H-bonds, the fluorine atom is predicted to occupy the H2 pocket. Using the docking model as a guide, a small focussed library based on incorporation of small hydrophobic groups in addition to the 4-position hydroxy group was developed and is outlined below.



### 2.5.2.1 Synthesis of Compounds 75-80

Due to the poor yielding Suzuki step observed when using 4-hydroxyphenylboronic acids (Scheme 2.6), an alternative synthesis of compounds **77-80** was carried out using a procedure developed in-house as summarised below (Scheme 2.20). Compounds **75** and **76** were synthesised using Suzuki chemistry with the corresponding boronic acid.



Scheme 2.20: Alternative synthesis to compounds **84-89**.<sup>3</sup>

The low yielding Suzuki step for compounds **82** and **83** can be attributed to their poor solubility and subsequent difficult purification and isolation. In general, the methoxy

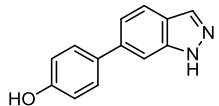
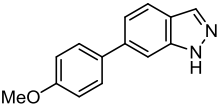
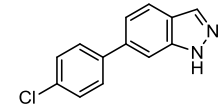
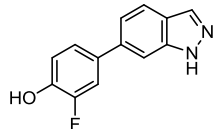
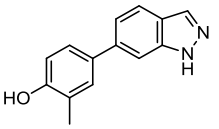
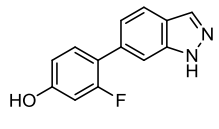
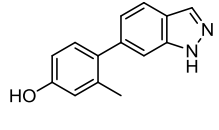
<sup>3</sup>Compounds outlined in red were synthesised by Laura Johnson (MChem) under the supervision of the Author.

deprotection step proceeds in good yields. The low yield of compound **77** was attributed to a loss of material during extraction due its inherent aqueous solubility.

### 2.5.2.2 Biological Evaluation of Compounds 75-80

Compounds **34** and **75-80** were screened against FGFR1-3 at an initial concentration of 100  $\mu\text{M}$  using the FRET-based assay. The results are outlined below (Table 2.6).

**Table 2.6:** Biological results for compounds **34** and **75-80** when screened against FGFR1-3.

Compound No.	Structure	% Inhibition <sup>a</sup>		IC <sub>50</sub> <sup>a</sup> ( $\mu\text{M}$ )	
		1	1	2	3
<b>34</b>		83 $\pm$ 3.5	12 $\pm$ 0.2	3.0 $\pm$ 0.1	51 $\pm$ 0.6
<b>75</b>		11 $\pm$ 2.0	NT <sup>b</sup>	NT	NT
<b>76</b>		12 $\pm$ 4.0	NT	NT	NT
<b>77</b>		81 $\pm$ 2.5	14 $\pm$ 0.1	7.3 $\pm$ 0.1	NT
<b>78</b>		78 $\pm$ 1.5	8.8 $\pm$ 0.1	NT	NT
<b>79</b>		76 $\pm$ 0.5	9.9 $\pm$ 0.1	5.4 $\pm$ 0.1	>100
<b>80</b>		83 $\pm$ 2.5	6.4 $\pm$ 0.1	NT	NT

<sup>a</sup> % Inhibition and IC<sub>50</sub> values are given as the mean  $\pm$  SD of all data points,  $n = 2$ . <sup>b</sup> NT = not tested.

The 4-position phenyl substituents in compounds **75** and **76** lack the ability to be H-bond donors to Glu531; this change is reflected in their activity as both compounds are inactive against FGFR1. This strengthens the hypothesis that the OH moiety in compound **34** is indeed an H-bond donor (Figure 2.10). In general, addition of small hydrophobic groups onto the 6-position phenyl ring in compound **34** results in an increase in potency against FGFR1-3, with the exception of compound **77** that exhibits a drop in potency against FGFR1. When comparing to compound **34** an increase in

potency is observed when increasing the size of the hydrophobic substituent from a fluorine (compounds **77** and **79**) to a methyl group (compounds **78** and **80**) in both substitution patterns. This suggests the decrease in potency from compound **34** to **77** is unlikely to be due to an increased steric clash between the inhibitor and the enzyme (unless an alternative binding pose has been adopted). A likely explanation could be due to the 3-position fluorine; the fluorine is electron withdrawing and reduces the H-bond donor potential of the 4-hydroxy group. The 3-position fluorine also has the potential to be an H-bond acceptor and could partake in an intramolecular H-bond with the 4-hydroxy moiety, again, reducing the H-bond donor potential of the OH group to Glu531. Compounds **79** and **80** outline that substitution in the 2-position is more preferable than that of the 3-position which as compounds **77** and **78** show less inhibition against the FGFRs. All compounds are more active against FGFR2 than FGFR1/3. Interestingly, compound **79** shows an increase in potency against FGFR1/2 but a loss of activity against FGFR3 when compared with compound **34**. This highlights the stricter constraints for FGFR3 inhibition of which was previously outlined for the ethoxy-containing compound series (Section 2.5.1.2).

## 2.6 Chapter Two Summary

*De novo* design identified compound **14** as a potential hit fragment against FGFR1. Using SBDD, two main inhibitor series were identified and the SARs for these systems are outlined below (Figure 2.17).

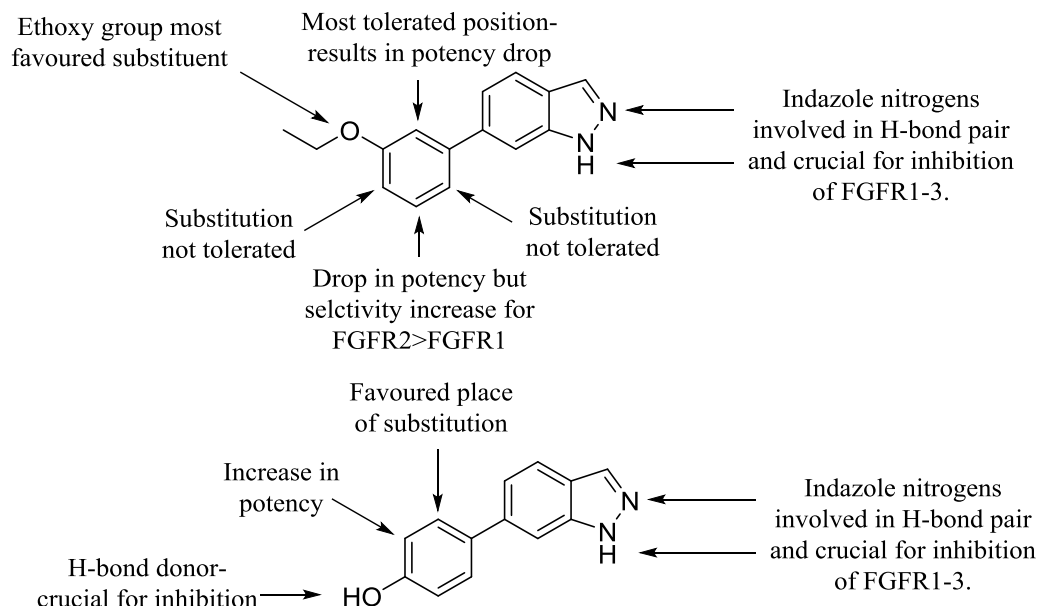


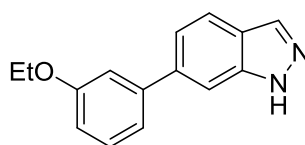
**Figure 2.17:** SARs for lead fragments **31** and **34**.

Both fragment series exhibit low micromolar activity against FGFR1-3 with some derivatives showing small signs of selectivity preference for FGFR2 over FGFR1/3. Both series can undergo fragment growth to improve the potency against FGFR1-3 with the aim of elucidating the specific structural requirements of small molecules that are needed to achieve FGFR sub-type selectivity.

## Chapter Three – *De Novo* Fragment Growth

### 3.1 Application of SPROUT to Compound 31

In order to increase the potency of the FGFR inhibitor fragments, SPROUT was used to extend the structures of the fragments giving rise to larger compounds predicted to inhibit FGFR1. Lead fragment **31** was chosen as the representative compound to extend. The modelled fragment/FGFR complex was loaded into SPROUT.



**31**

Previous literature reports suggest that substitution at the 3-position of the indazole ring would lead to more favourable binding.<sup>84,95,125</sup> Inspection of the residues extending out of the active site was carried out. The adjacent residue to Ala564, Ser565, was chosen as the next amino acid in which additional H-bonding contacts could be made *via* suitable extension of the indazole fragment structure. Appropriate target and spacer templates were chosen and several solutions found. These were analysed for ease of synthesis; the docking pose of the top-ranked solution (**85**) is outlined below (Figure 3.1).

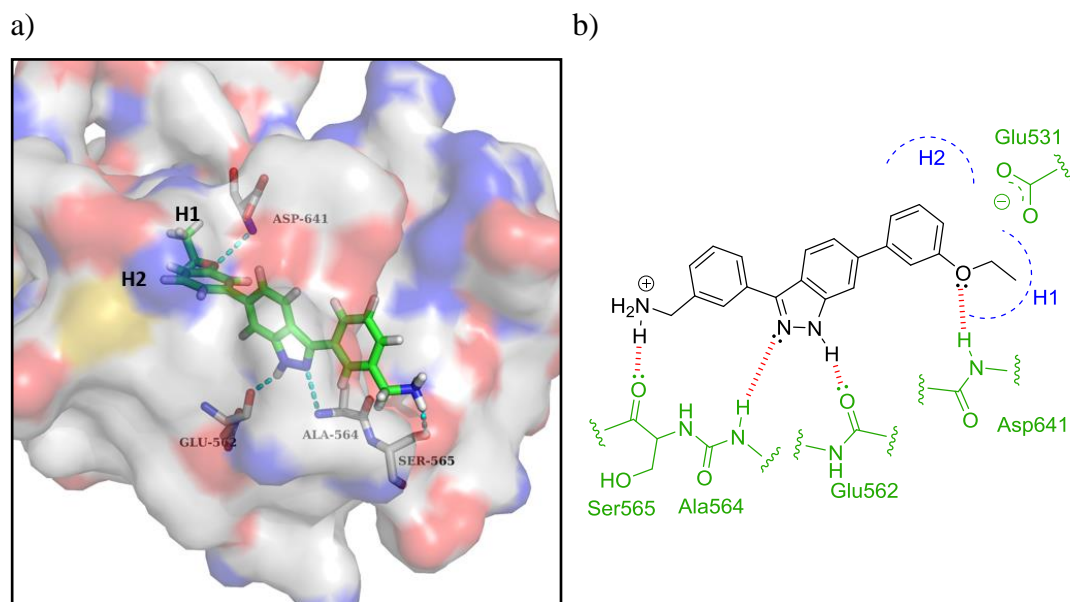


**Figure 3.1:** a) Glide docking model of compound **85** bound within FGFR1; b) 2D representation of predicted binding pose of compound **85**.

In order to independently check the validity of the SPROUT-designed inhibitor-protein complex, molecular scaffold **85** was docked using Glide. The

resulting pose of compound **85** corresponded very well to that generated using SPROUT. The indazole nitrogens of compound **85** are predicted to bind in the same way as compound **31** (Figure 2.9). The benzylamine moiety located at the indazole 3-position is predicted to be located at the entrance of the active site. The protonated amine moiety is predicted to make an H-bond with the backbone carbonyl of Ser565.

### 3.1.1 Target Library

Based on the new predicted H-bond between compound **85** and Ser565, an extended library looking to exploit this interaction was developed and is outlined below (Figure 3.2).

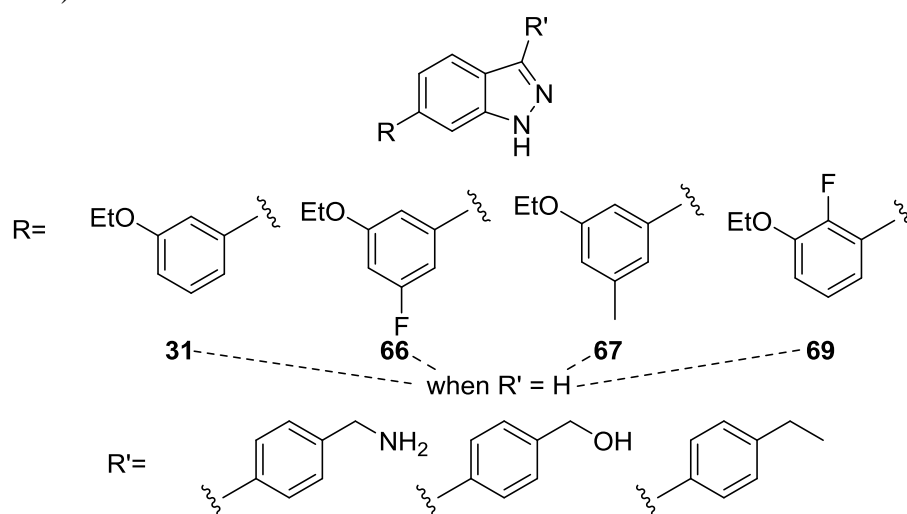


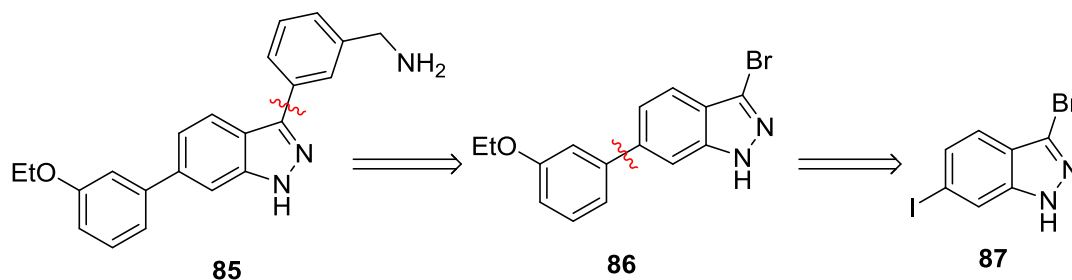
**Figure 3.2:** Focus library showing all the chosen extended variants of the ethoxy series.

In addition to inclusion of the benzylamine moiety within the extended inhibitor structure, the hydroxymethyl and ethyl analogues were also identified as targets for synthesis. It was reasoned that comparison of the binding of these derivatives to the FGFRs with that shown by the aminomethyl-based molecule **85**; would prove the existence of the predicted H-bond between the benzylamine amino group and the Ser565 backbone carbonyl (Figure 3.1). The extended versions of compound **66** were also targeted for synthesis as this fragment showed promise in achieving selectivity for FGFR2 over FGFR1/3. It was also planned to prepare the extended versions of compound **67** in order for these systems to act as a control series; as fragment **67** was inactive it is hypothesised that the larger systems should also be inactive. The extended versions of compound **69** were also targeted for synthesis as this was the second most potent fragment.



### 3.1.2 Retrosynthetic Analysis of Structure 85

Structure **85** was subjected to retrosynthetic analysis (Scheme 3.1).

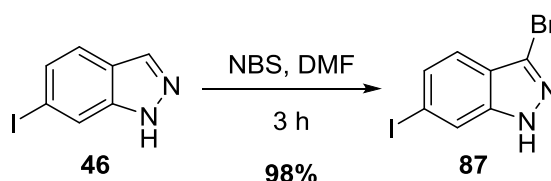


**Scheme 3.1:** Retrosynthetic analysis of structure **85**.

It was reasoned that the extended versions of compounds **31**, **66**, **67** and **69** could be made very simply by two consecutive Suzuki coupling reactions starting from compound **87**.

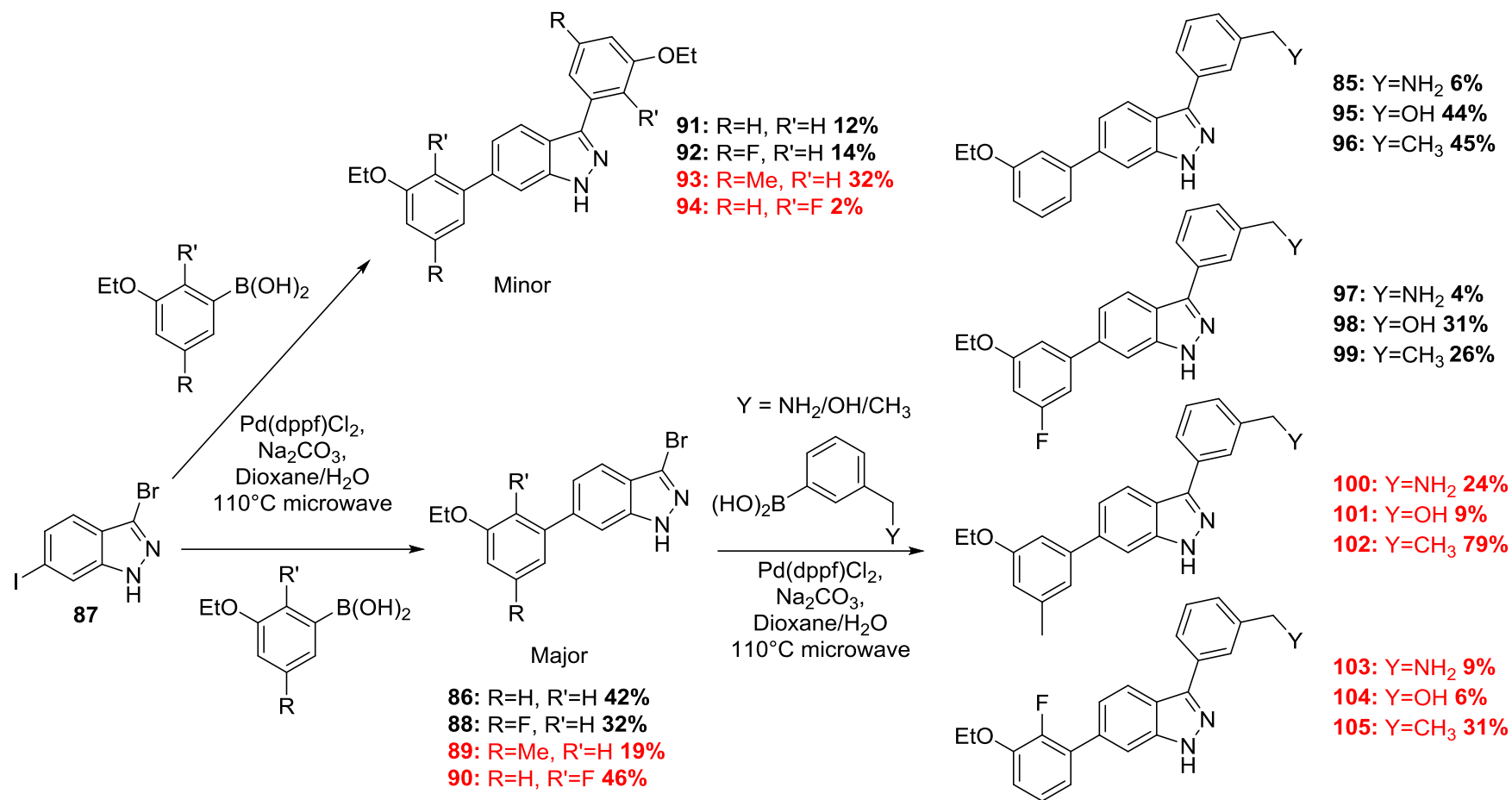
### 3.1.3 Synthesis of the Extended Ethoxy Series

In order to gain access to the extended variants, iodide **87** was identified as a key intermediate. Compound **87** was synthesised using a procedure developed in-house and is summarised below (Scheme 3.2).



**Scheme 3.2:** Selective bromination of compound **46** to make compound **87**.

Compound **46** can be brominated selectively at the 3-position of the indazole ring using NBS. The reaction is very high yielding and no over-bromination or undesired regiomers are observed. Compound **87** was then subjected to a selective Suzuki coupling using the conditions outlined previously (Scheme 2.4) as summarised below (Scheme 3.3). The presence of two different halogens in compound **87** allowed selective substitution of each halogen, yielding compounds **86** and **88-90** in the initial step. In all cases, formation of the bis-arylated compounds (**91-94**) was observed as the minor product with the exception of compound **93** which forms as the major product. Compounds **86** and **88-90** were then further reacted under Suzuki conditions using the desired boronic acids. The yields for the second Suzuki steps were found to be somewhat variable but in general, the yields of the methyl amino-based compounds (**85**, **97**, **100** and **103**) were low as purification of these proved troublesome. A total of sixteen final compounds were synthesised.

Scheme 3.3: Synthesis of extended ethoxy series using selective Suzuki couplings.<sup>4</sup><sup>4</sup>Compounds outlined in red were synthesised by Abbey Summers (MChem) under the supervision of the Author.

### 3.1.4 Biological Evaluation of the Extended Ethoxy Series

Compounds **85** and **91-105** were screened against FGFR1-3 at a concentration of 10  $\mu$ M using the FRET-based assay. The results are outlined (Table 3.1a/b).

**Table 3.1a:** Biological results for compounds **85** and **91-105** when screened against FGFR1-3.

Entry No.	Structure		% Inhibition <sup>a</sup> (10 $\mu$ M)		
	R	R'	1	2	3
1 ( <b>91</b> )			4.0 $\pm$ 2.5	5.0 $\pm$ 11	6.0 $\pm$ 5.0
2 ( <b>85</b> )			52 $\pm$ 2.0	71 $\pm$ 4.0	48 $\pm$ 0.5
3 ( <b>95</b> )			30 $\pm$ 0.5	59 $\pm$ 1.5	13 $\pm$ 4.0
4 ( <b>96</b> )			-9.0 $\pm$ 1.0	7.0 $\pm$ 5.5	-8.0 $\pm$ 4.5
5 ( <b>92</b> )			-4.0 $\pm$ 2.0	8.0 $\pm$ 1.5	19 $\pm$ 3.0
6 ( <b>97</b> )			59 $\pm$ 1.5	47 $\pm$ 4.0	56 $\pm$ 4.0
7 ( <b>98</b> )			27 $\pm$ 1.0	31 $\pm$ 3.0	22 $\pm$ 2.5
8 ( <b>99</b> )			1.0 $\pm$ 3.0	-10 $\pm$ 0.0 <sup>b</sup>	2.0 $\pm$ 2.5

<sup>a</sup> % Inhibition values are given as the mean  $\pm$  SD of all data points,  $n = 2$ . <sup>b</sup> No difference in measured data points.

**Table 3.1b:** Biological results for compounds **85** and **91-105** when screened against FGFR1-3.

Entry No.	Structure		% Inhibition <sup>a</sup> (10 μM)		
	R	R'	1	2	3
9 (93)			-4.0 ± 1.5	2.0 ± 1.0	-12 ± 6.5
10 (100)			23 ± 4.0	28 ± 1.5	-3.0 ± 1.5
11 (101)			7.0 ± 0.5	13 ± 1.0	4.0 ± 12
12 (102)			-15 ± 0.5	2.0 ± 1.5	-4.0 ± 1.5
13 (94)			-9.0 ± 0.5	2.0 ± 0.5	4.0 ± 4.5
14 (103)			73 ± 0.0	82 ± 2.0	70 ± 4.5
15 (104)			37 ± 0.0	61 ± 2.0	21 ± 6.5
16 (105)			-3.0 ± 0.0	4.0 ± 0.5	6.0 ± 5.0

<sup>a</sup> % Inhibition values are given as the mean ± SD of all data points,  $n = 2$ . <sup>b</sup> No difference in measured data points.

Analysis of the above results show that addition of the substituted aromatic ring in the 3-position of the indazole ring is generally unfavourable for binding to the FGFR enzymes, with compounds **91-94** (entries **1**, **5**, **9** and **13**) being inactive, possibly because the R' groups are too large. Compounds **96**, **99**, **102** and **105** (entries **4**, **8**, **12** and **16**) all contain the ethyl moiety and are also inactive. Interestingly, the hydroxymethyl and the aminomethyl derivatives for all compounds show better inhibition against FGFR1-3 than the corresponding ethyl derivatives. This is consistent with the predicted H-bond that forms between the amine in compound **85**

and Ser565 (Figure 3.1).  $IC_{50}$  measurements were conducted and are outlined below (Table 3.2).

**Table 3.2:** Biological results for compounds **31**, **85**, **91**, **95**, **96**, **97** and **103** when screened against FGFR1-3.

Compound No.	Structure		$IC_{50}^a$ (10 $\mu$ M)		
	R	R'	1	2	3
<b>31</b>		H	$2.0 \pm 0.4$	$0.8 \pm 0.4$	$4.5 \pm 1.6$
<b>91</b>			>10	NT <sup>b</sup>	NT
<b>95</b>			>10	>10	>10
<b>96</b>			>10	NT	NT
<b>85</b>			>10	$2.1 \pm 0.9$	$2.6 \pm 1.1$
<b>97</b>			$8.4 \pm 1.4$	$3.7 \pm 1.0$	$5.8 \pm 0.7$
<b>103</b>			$3.7 \pm 0.6$	$2.4 \pm 0.9$	$5.2 \pm 0.9$

<sup>a</sup>  $IC_{50}$  values are given as the mean  $\pm$  SD of all data points,  $n = 2$ . <sup>b</sup> NT = not tested.

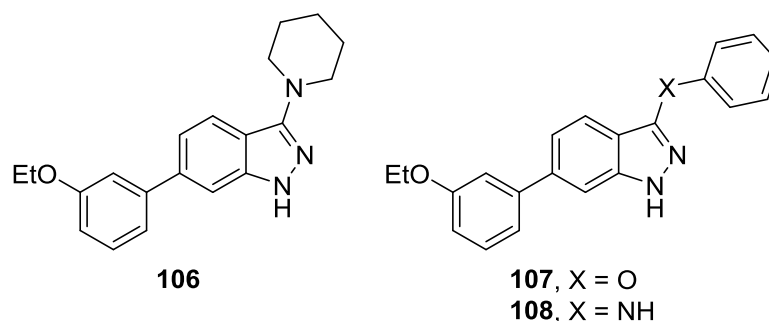
$IC_{50}$  measurements confirmed that compounds **91**, **95**, and **96** are inactive against FGFR1 suggesting the other bis-arylated, ethyl, and hydroxymethyl derivatives are also inactive. Compounds **85**, **97**, and **103** are active against most of the FGFRs but do not show an improvement in potency when compared to lead fragment **31**. Therefore, it is very unlikely that the benzylamine amino group in compounds **85**, **97** and **103** is forming an H-bond with Ser565, a predicted H-bond from the docking of compound **85** within FGFR1 (Figure 3.1). A potential reason for the retained activity of compounds **85**, **97** and **103** could be due to better solvation within the active site of

the compound. The 3-position substituent, in particular the aminomethyl moiety, is predicted to protrude out of the active site towards solvent (Figure 3.1). The aminomethyl group (compounds **85**, **97** and **103**) will be charged at physiological pH and will therefore help solvate the compound in a water-filled environment, which won't be reflected for the hydroxymethyl or ethyl variants (compounds **95** and **96**).

## 3.2 Investigation into the Potency Decrease of Compound **85**

### 3.2.1 Solvation at the 3-Position of the Indazole Core

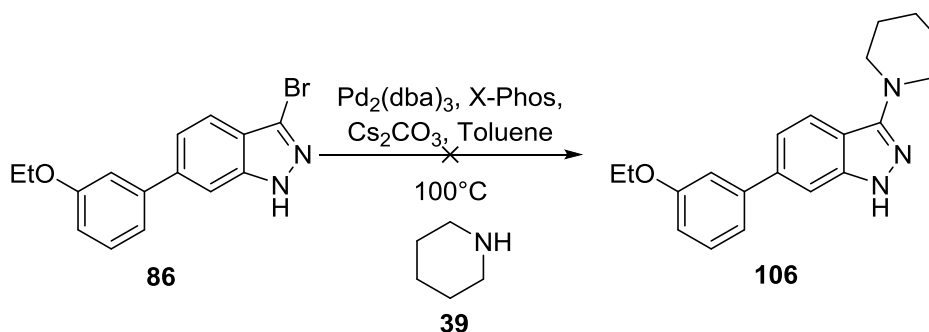
In order to further explore whether solvation at the 3-position of the indazole-based inhibitors is important, compound **106** was targeted for synthesis.



Compound **106** has a saturated ring substituted at the 3-position which will help solubilise the compound in an aqueous environment. Compounds **107** and **108** both contain single atom linkers connected to an aromatic ring; it was reasoned that these will allow comparisons to be made with the saturated system of compound **106**. They will also establish the effect of what a single atom linker has upon the potency of these compounds against the FGFRs.

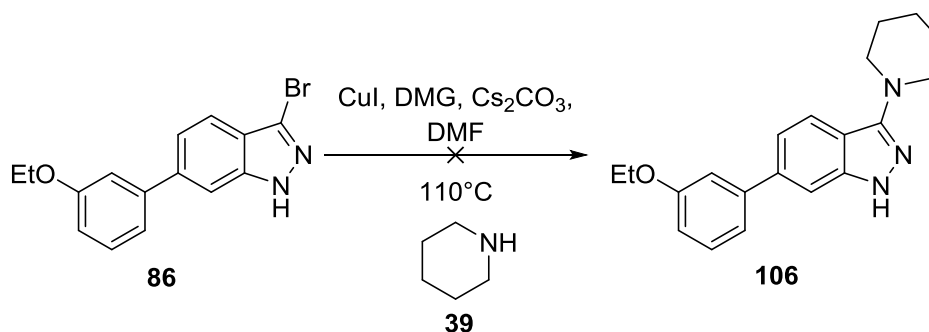
### 3.2.2 Synthesis of Compound **106** via the use of Cross Coupling

Attempts at synthesising compound **106** were carried out using Buchwald chemistry using an adaptation of a method outlined by Akatsuka *et al* and is summarised below (Scheme 3.4).<sup>126</sup>



**Scheme 3.4:** *Unsuccessful Buchwald chemistry.*

Unfortunately, the synthesis of compound **106** using the above conditions was unsuccessful. Analysis of the crude reaction mixture using LC-MS showed no conversion to the desired product. An interesting observation was the formation of the debrominated product of **86** (**31**), which suggests the catalytic cycle does not go to completion. Reaction conditions were varied, including changing the catalyst, ligand and base, none of which yielded the desired product. Attempts at synthesising compound **106** using Ullmann chemistry were carried out using a method developed in-house and are summarised below (Scheme 3.5).



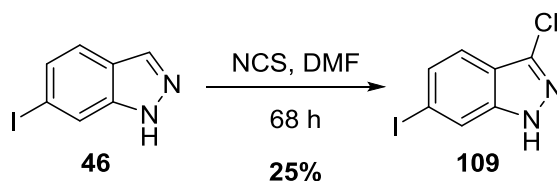
**Scheme 3.5:** *Synthetic route to compound 106 using copper-catalysed Ullmann Chemistry.*

The above conditions also failed to yield compound **106**. Analysis of the crude reaction mixture using LC-MS showed only the presence of starting material. It is possible that these reactions failed because of small traces of either oxygen and/or water present within the reaction vessel, rendering the catalyst ineffective. Another reason could be the presence of an indazole NH. Inspection of the literature revealed that in general, the indazole NH was protected when present as a component in such cross-couplings. Therefore alternative routes to compound **106** were considered.

### 3.2.3 Synthesis of Compound **106** via $\text{S}_{\text{N}}\text{Ar}$

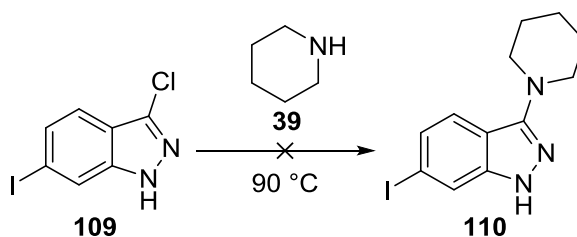
Literature precedent outlined the potential use of nucleophilic aromatic substitution ( $\text{S}_{\text{N}}\text{Ar}$ ) chemistry in order to synthesise compound **106**.<sup>127</sup> A suitable halogen would

need to be installed in order to satisfy the requirements for  $S_NAr$  and therefore compound **46** was subjected to in-house chlorination conditions as summarised below (Scheme 3.6).



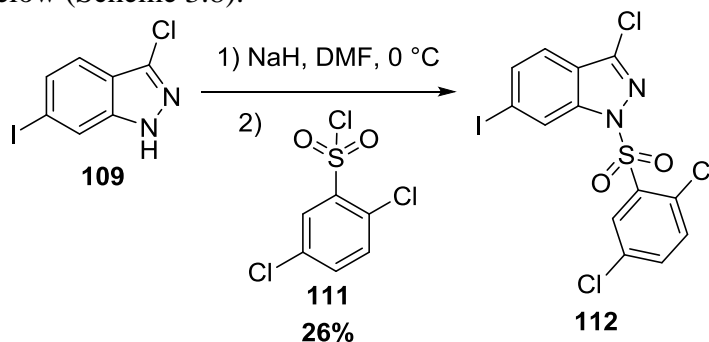
**Scheme 3.6:** Chlorination of compound **46**.

Chlorination of compound **46** using N-chlorosuccinimide (NCS) was slow compared to the analogous bromination of the indazole ring using NBS (Scheme 3.2). The yield of the reaction was also lower as other regioisomers were formed as well as bis-chlorinated compounds, making purification troublesome. Compound **109** was then subjected to  $S_NAr$  chemistry outlined by Allen *et al* and is summarised below (Scheme 3.7).<sup>127</sup>



**Scheme 3.7:** Unsuccessful  $S_NAr$  conditions.

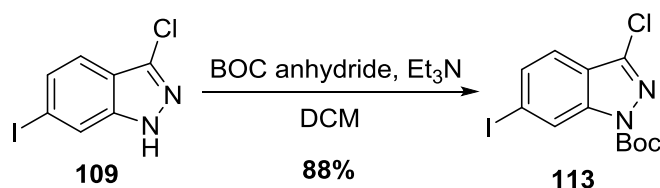
In order to obtain compound **110**, compound **109** was refluxed in neat piperidine but unfortunately the desired product was not obtained. This may imply that the indazole is too electron rich for a successful  $S_NAr$  reaction. This is consistent with literature reports which describe the need for EWGs to be present on the indazole ring in similar  $S_NAr$  processes.<sup>128</sup> A way to render the indazole ring electron deficient would be to protect the indazole NH with a suitable EWG. Protection using a sulfonyl group was carried out using similar conditions outlined previously (Scheme 2.3) and is summarised below (Scheme 3.8).



**Scheme 3.8:** Protection of the indazole NH using compound **111**.



Compound **109** was deprotonated using NaH to form an anion which, in turn, proceeds to attack the sulfonyl group of compound **111** displacing the Cl atom affording compound **112**. The protecting group was found to be base-labile and therefore an optimisation study into the amount of NaH added was carried out. It was determined that 1.2 eq was the optimum amount of NaH. However, the reaction only proceeded to give the product in 26% yield. Compound **112** was subjected to  $S_NAr$  conditions as seen in Scheme 3.7 but in this case, the reaction was unsuccessful. Analysis of the crude reaction mixture using LC-MS confirmed the presence of compound **109** indicating the removal of the protecting group. Another compound was also detected that corresponded to the piperidine-sulfonyl conjugate, indicating that the protecting group was susceptible to nucleophilic attack. It was therefore decided that this protecting group was unsuitable. A base-resistant protecting group appeared attractive, and the *N-tert*-butyloxycarbonyl (BOC) derivative was synthesised according to an adaptation of a procedure outlined by Blunt *et al* as summarised below (Scheme 3.9).<sup>129</sup>



**Scheme 3.9:** Protection of the indazole NH using a BOC group.

The formation of compound **113** proceeded in a similar manner to that of compound **112** in a yield of 88%. As seen in Scheme 3.7, compound **113** was subjected to reflux in neat piperidine but unfortunately, the reaction was unsuccessful. It was determined that piperidine was acting as a nucleophile for the BOC group in a similar manner as seen in the case of the sulphonyl variant (Scheme 3.8). It was concluded that an *N*-acyl protecting group was susceptible to nucleophilic attack and therefore was unsuitable for  $S_NAr$ -based chemistry. Further work on this area was terminated and efforts focussed elsewhere.

### 3.2.4 Current Inhibitors Bearing an Indazole Scaffold

During the course of the present research, a study carried out by Liu *et al* was published which outlined the discovery of very similar indazole-based compounds for the inhibition of FGFR kinases.<sup>95</sup> A co-crystal structure (PDB code: 4ZSA) of compound **114** bound within FGFR1 was solved (Figure 3.3).

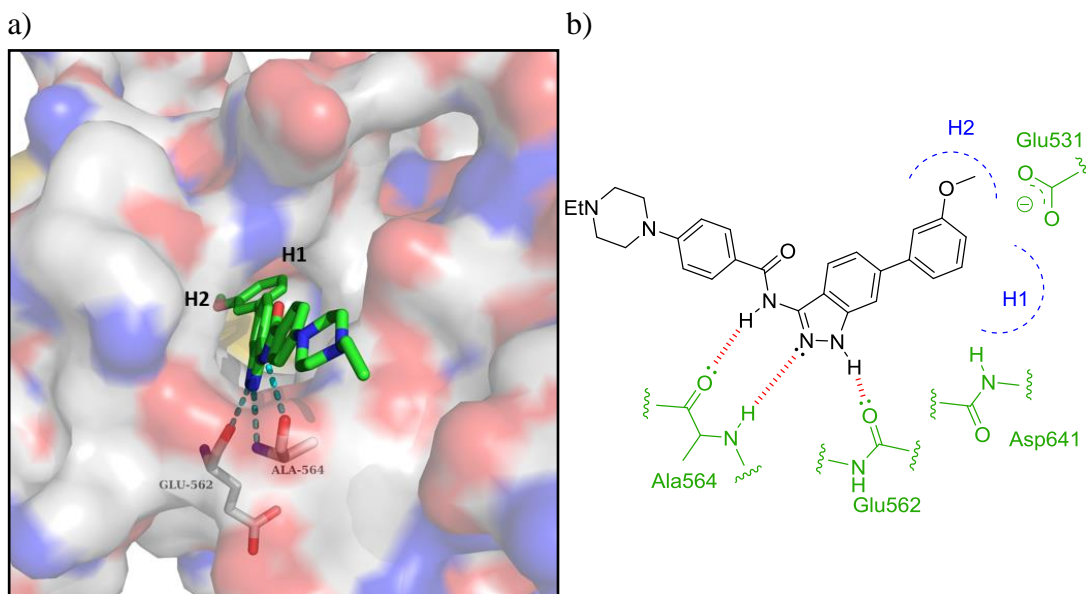


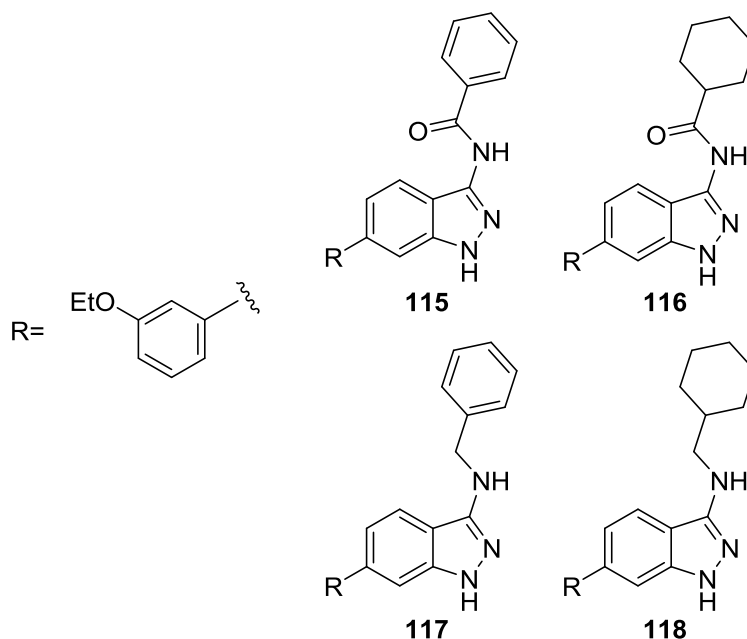
**Figure 3.3:** a) Co-crystal structure of compound **114** (PDB: 4ZSA) bound within the active site of FGFR1; b) 2D representation of binding pose of compound **114**.

Compound **114** has an  $IC_{50}$  value of 15 nM against FGFR1. Interestingly, the core of the inhibitor described in this study is almost identical to that of compound **85** (Section 3.1) with the only major difference being the indazole 3-position substituent. As discussed previously, the data in Tables 3.1a/b reveal that direct substitution of an aromatic ring in the 3-position of the indazole is unfavourable, and therefore, the presence of the amide moiety in compound **114** appears to be very important for inhibition of FGFR1. Two possibilities as to why the amide moiety may be important for binding of these inhibitors are: i) in the published co-crystal structure of compound **114**, an H-bond can be seen between the backbone carbonyl of Ala564 and the amide NH and, ii) the more variable positioning of the indazole 3-position decoration. Having an aromatic ring directly attached to the 3-position means the trajectory of that part of the molecule is linear. The indazole 3-position/amide C-N bond is free to rotate allowing the 3-position appendage to occupy more varied trajectories when compared to the linear trajectory that compound **85** would experience, and, it is hypothesised that this could be key for inhibition for the FGFRs.

### 3.2.4.1 Amide Target Library

Based on the literature outlined above, a focussed library of compounds incorporating the amide functionality into the 3-position was developed. This would help validate

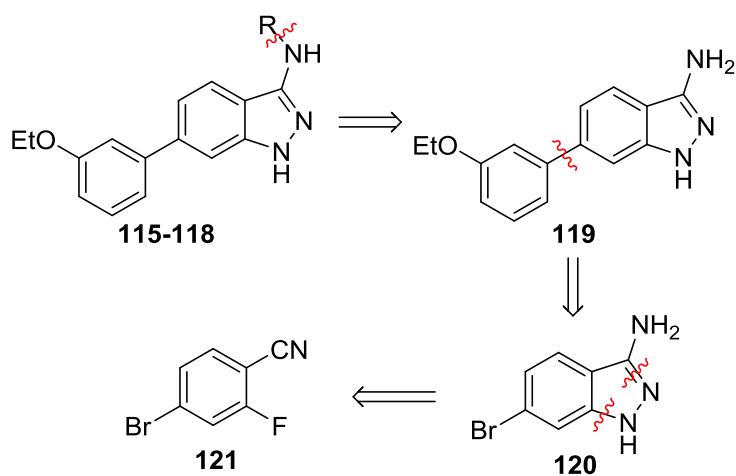
the hypothesis that compounds containing the amide functionality will regain activity against the FGFRs.



It was reasoned that exploring the binding of compound **115** to the FGFRs will help establish the importance of the amide linker between the two aromatic systems. Compound **116** will establish how changing the phenyl ring to a cyclohexyl ring affects binding to the FGFRs. Compounds **117** and **118** will help establish the importance of the carbonyl functionality in the 3-position linker.

### 3.2.4.2 Retrosynthetic Analysis of Structures 115-118

Structures **115-118** were subjected to retrosynthetic analysis as summarised below (Scheme 3.10).

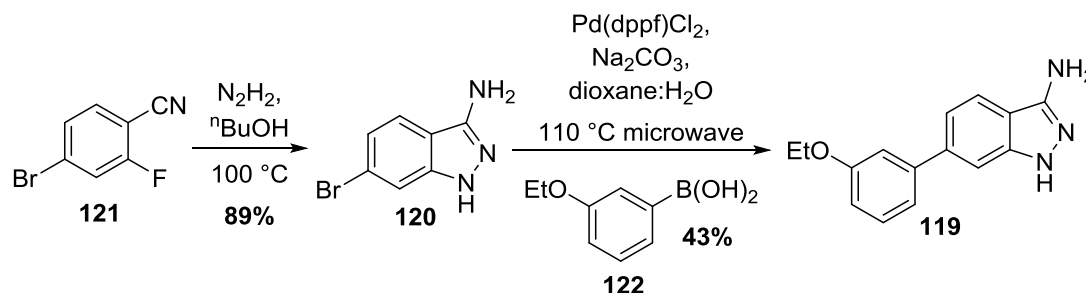


**Scheme 3.10:** Retrosynthetic analysis of amides and amines.

The first disconnection can be made at the N-R bond giving structure **119**. The second disconnection can be made at the indazole 6-position affording structure **120**. Finally the five-membered ring can be disconnected to give structure **121**.

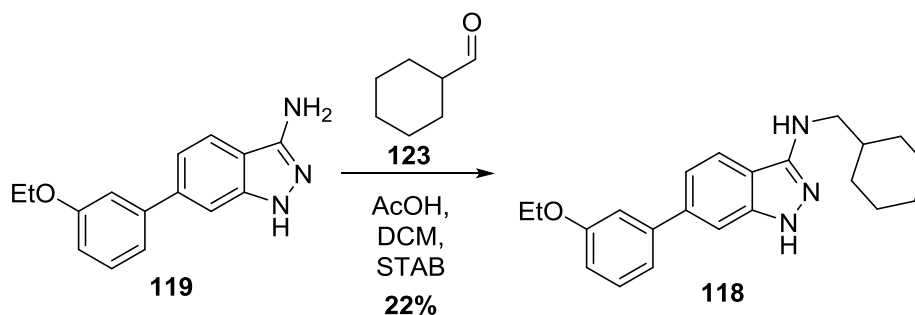
### 3.2.4.3 Synthesis of Compounds 115-118

In order to gain access to compounds **115-118**, compound **119** would need to be obtained and was synthesised using the procedure outlined below (Scheme 3.11).



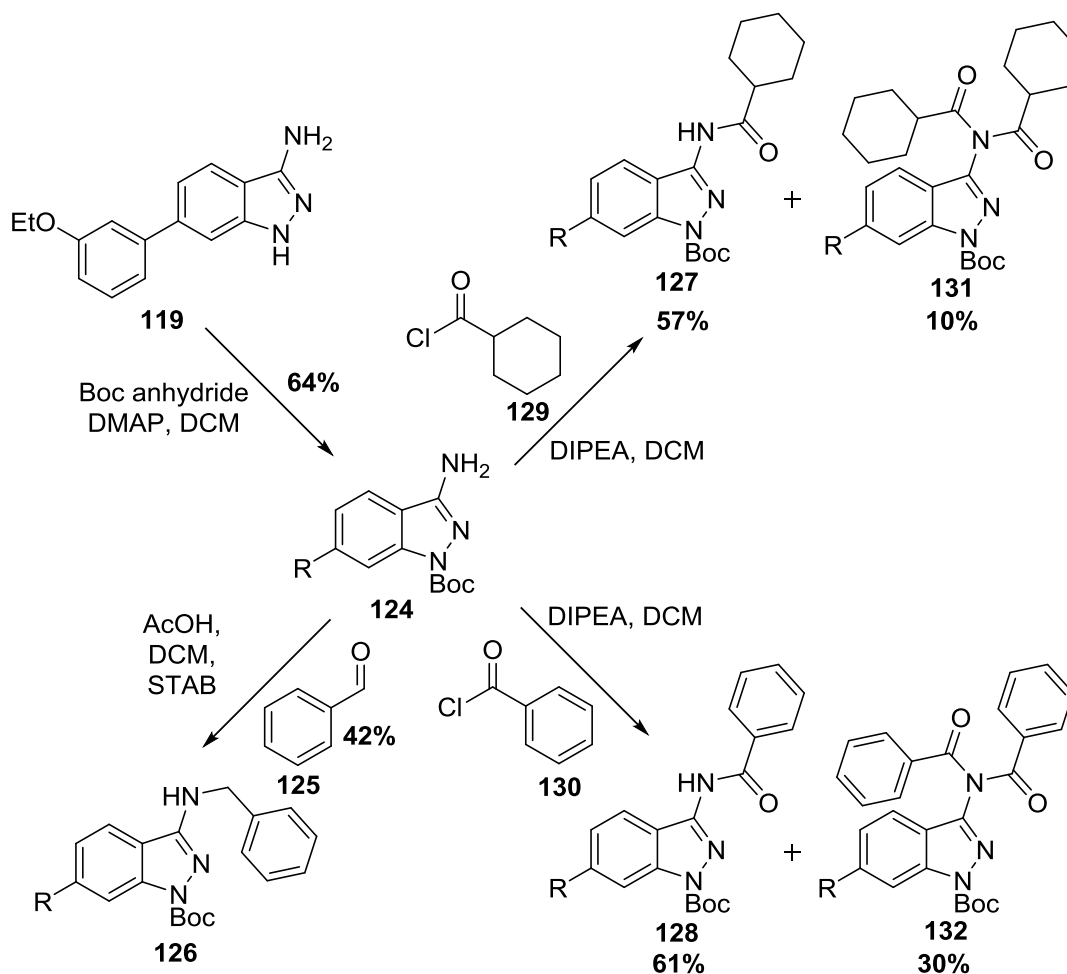
Scheme 3.11: Synthetic route to compound **119**.

Compound **120** was first synthesised using a procedure outlined by Bahmanyar *et al.*<sup>130</sup> Compound **121** was subjected to  $S_NAr$  with hydrazine followed by an intramolecular ring closing condensation to give compound **120** in a yield of 89%. Compound **120** was then subjected to Suzuki conditions with compound **122** to afford compound **119**. Compound **119** was then subjected to reductive amination conditions as summarised below (Scheme 3.12).



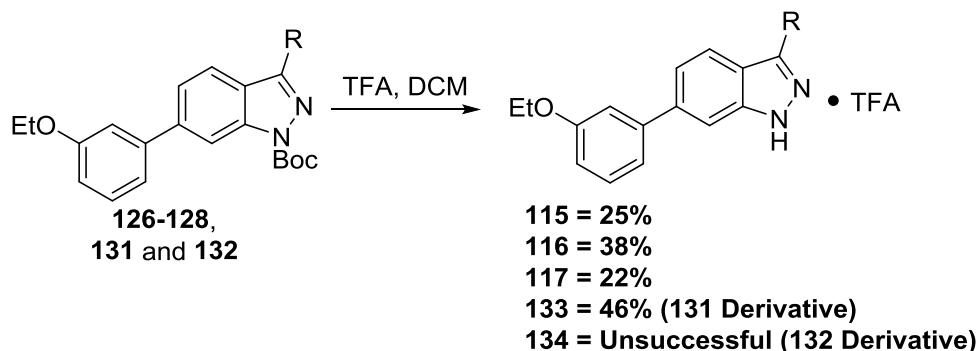
Scheme 3.12: Synthesis of compound **118** using reductive amination.

Compound **119** was reacted with compound **123** under reductive amination conditions resulting in compound **118** in a yield of 22%. It was thought that the low yield was attributed to the 1-position indazole NH competing with the 3-position  $NH_2$  in the initial attack of the aldehyde moiety, and so, compound **119** was subjected to BOC protection (Scheme 3.13). The N-protected molecule **124** was reacted in both acyl chloride coupling and reductive amination conditions (Scheme 3.13).



**Scheme 3.13:** Divergent use of compound **124**.

Compound **124** was reacted with compound **125** under reductive amination conditions to afford compound **126** in a yield of 42%. Using conditions outlined by Gao *et al*<sup>131</sup>, compound **124** was reacted with acyl chlorides **129** and **130** to afford compounds **127** and **128** respectively in moderate yields. Interestingly in both cases, over-reaction was observed, affording compounds **131** and **132**. Classically, the formation of these compounds would not be expected due to the weaker nucleophilicity of an amide versus the amine precursor. However, it is possible that due to the extended delocalised system between the indazole and the amide, the pKa of the amide NH was now low enough to enable deprotonation by *N,N*-diisopropylethylamine (DIPEA). This would create a delocalised anion, reaction of which may explain the formation of the N-substituted products **131** and **132**. Compounds **126-128**, **131** and **132** were then deprotected using a method developed in-house as summarised below (Scheme 3.14).



**Scheme 3.14:** BOC deprotections using TFA.

Yields for the deprotection of the BOC group for each case were lower than expected. This was due to the poor solubility of the compounds, resulting in troublesome purification. The deprotection of compound **132** was unsuccessful, the reasons as to why this was the case were unclear and as compound **132** was collected as a by-product, attempts to resynthesize compound **134** were not carried out.

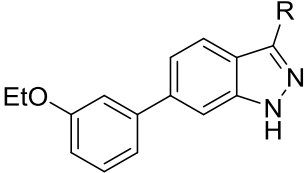
#### 3.2.4.4 Biological Evaluation of Compounds 115-118 and 133

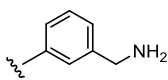
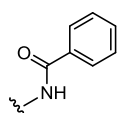
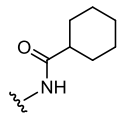
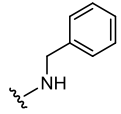
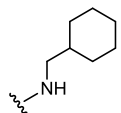
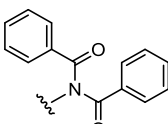
Compounds **115-118** and **133** were screened against FGFR1-3 using the FRET-based assay. The results are outlined below (Table 3.3).

Analysis of the data in Table 3.3 reveal that compound **115** is active against FGFR1 with an  $IC_{50}$  value of 0.46  $\mu$ M; a dramatic increase in potency when compared to compound **85**. Compound **115** also shows an increase in potency against FGFR2 exhibiting an  $IC_{50}$  of 0.14  $\mu$ M whereas compound **85** only shows an  $IC_{50}$  value of 2.1  $\mu$ M against FGFR2. This >10-fold increase in potency is not observed for FGFR3. These results show that the amide present in compound **115** is crucial for binding to FGFR1/2. Compound **116** is completely inactive suggesting the sterically bulkier cyclohexane ring is not desirable for effective inhibition against the FGFRs. Both compounds **117** and **118** show a drop in activity against FGFR1. As both compounds are still able to form the predicted H-bond between the indazole 3-position amine and the backbone carbonyl of Ala564 (Figure 3.3), the activity drop is more likely to be down to the conformation of the 3-position appendage. An amide bond is conformationally restricted whereas the corresponding methylene amine has a much higher degree of flexibility. Compounds **117** and **118** have flexible linkers between the indazole and 3-position phenyl ring and therefore in order to adopt the most favourable conformation, of which the amide in compound **115** appears to adopt, there will be an entropic penalty upon binding compounds **117** and **118**, resulting in a drop

in potency. Compound **133** is inactive as it is almost certainly too large to fit the steric constraints of the ATP binding pocket.

**Table 3.3:** Biological results for compounds **85**, **115-118** and **133** when screened against FGFR1-3.

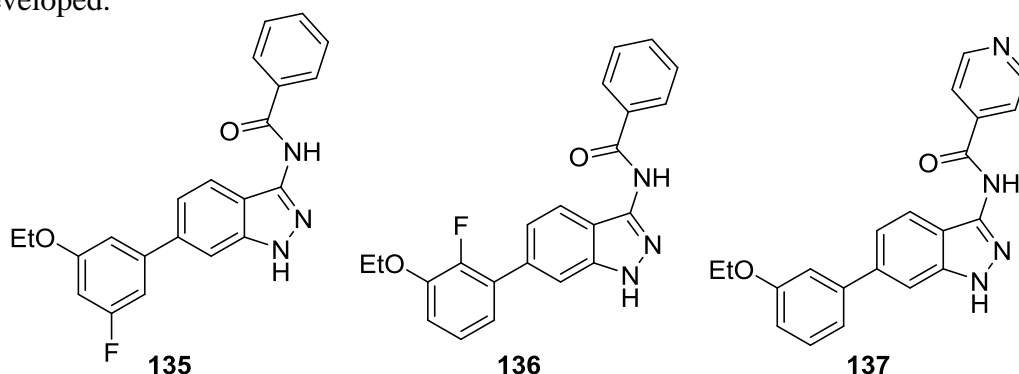


Compound No.	Structure R	IC <sub>50</sub> <sup>a</sup> (μM)		
		1	2	3
85		>10	2.1 ± 0.9	2.6 ± 1.1
115		0.46 ± 0.01	0.14 ± 0.01	2.2 ± 0.02
116		>10	NT <sup>b</sup>	NT
117		3.2 ± 0.1	NT	NT
118		>10	NT	NT
133		>10	NT	NT

<sup>a</sup> IC<sub>50</sub> values are given as the mean ± SD of all data points, n = 2. <sup>b</sup> NT = not tested.

### 3.3 SAR Exploration of the Amide Series

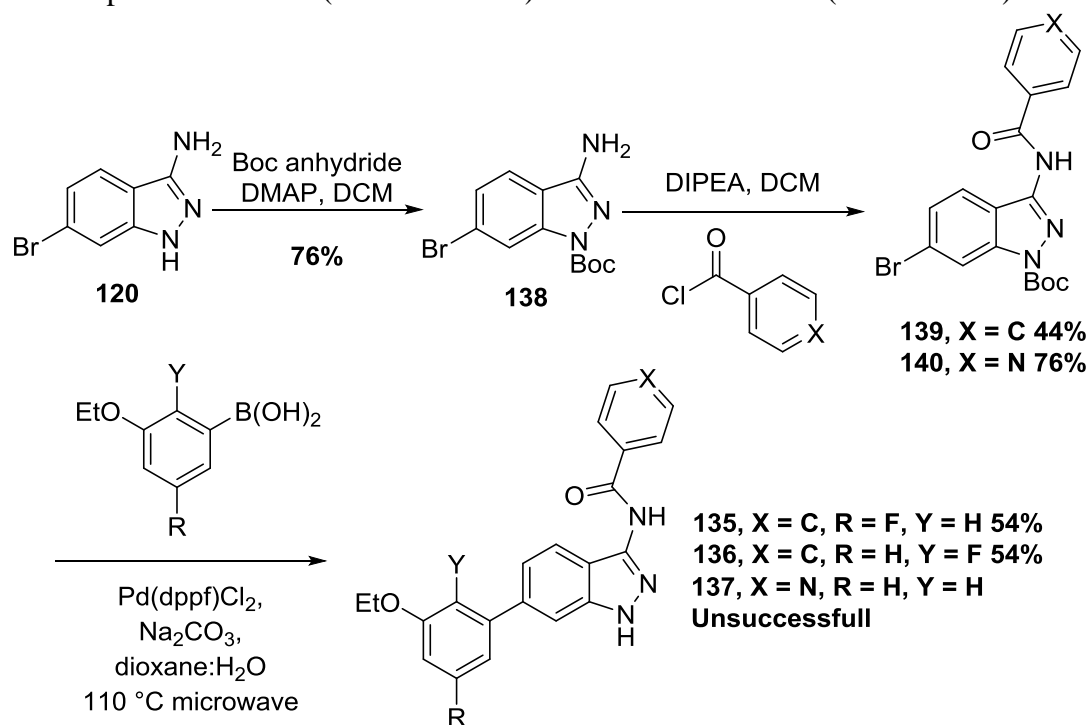
In order to expand the SARs for the amide series, the following target library was developed.



It was reasoned that compounds **135** and **136** will help establish whether the minor differences observed in FGFR1-3 selectivity for fragments **66** and **69** (Section 2.5.1) will be reflected for the larger variants (compounds **135** and **136**) upon an increase in potency. Compound **137** will look to probe the importance of solvation at the 3-position, a hypothesis mentioned previously (Section 3.2.1), as pyridine can help solubilise the compound in an aqueous environment.

#### 3.3.1 Synthesis of Compounds 135-137

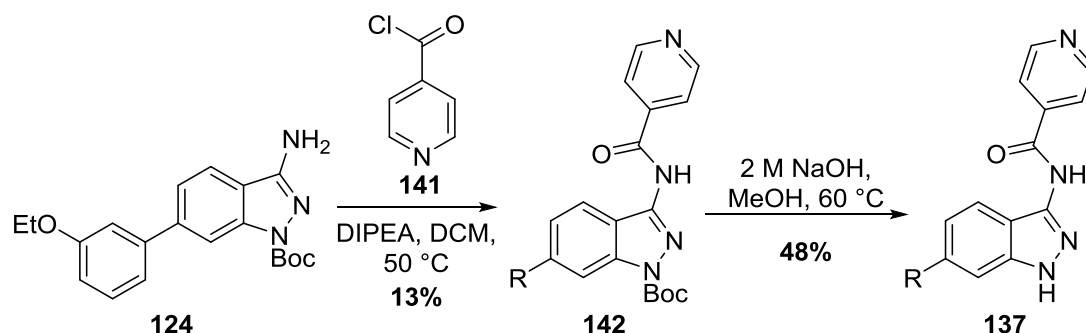
Compounds **135-137** were synthesised in a similar fashion to that described previously for compounds **115-118** (Section 3.2.4.3) and is outlined below (Scheme 3.15).



Scheme 3.15: Synthetic route to compounds **135-137**.



The 1-position NH in compound **120** was protected to give compound **138** in a yield of 76%. Compound **138** was coupled with the desired acyl chloride to give the corresponding amides **139** and **140**. The formation of compound **140** was higher yielding than the corresponding benzene derivative **139**. This was probably due to the pyridine nitrogen present in compound **140** increasing the reactivity of the acyl chloride towards nucleophilic substitution. Compounds **139** and **140** were then subjected to Suzuki coupling to afford compounds **135** and **136** in moderate yields. Synthesis of compound **137** was unsuccessful. Analysis of the crude reaction mixture using LC-MS confirmed the presence of compound **119** and **120** (Section 3.2.4.3). It was apparent that the Suzuki coupling was successful but unfortunately the amide bond was labile in the Suzuki conditions, a phenomenon probably caused by the electron withdrawing potential of the pyridine nitrogen. Compound **137** was synthesised by rearrangement of the synthetic steps as summarised below (Scheme 3.16).



**Scheme 3.16:** *Alternative synthesis of compound 137.*

Compound **124** was coupled with compound **141** to afford compound **142** in a poor yield. The reaction required heating which was unexpected; the previous acyl chloride coupling example (Scheme 3.15) using compound **141** proceeded in good yield at room temperature. In light of the observation that the BOC protecting group in these compounds was base labile, compound **137** was synthesised from compound **142** in a moderate yield using in-house conditions. The conditions were mild enough as to not affect the amide bond that had been shown to be base labile previously (Scheme 3.15).

### 3.3.2 Biological Evaluation of Compounds 135-137

Compounds **135-137** were screened against FGFR1-3 using the FRET-based assay. The results are outlined below (Table 3.4).

**Table 3.4:** Biological results for compounds **115** and **135-137** when screened against FGFR1-3.

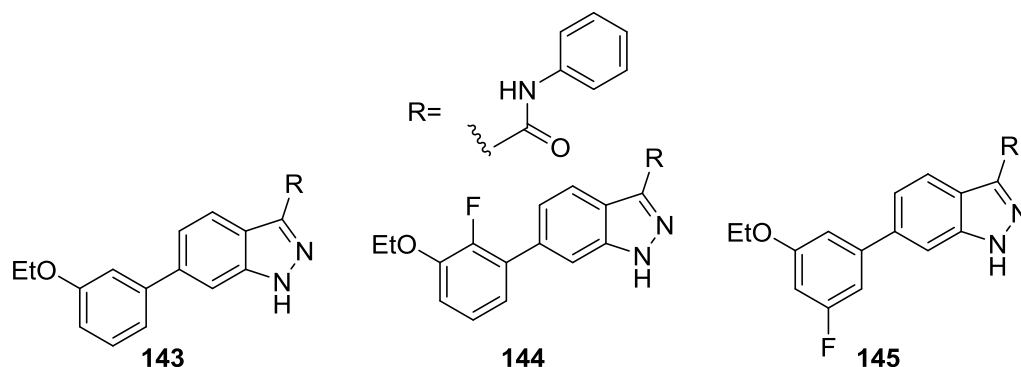
Compound No.	Structure		IC <sub>50</sub> <sup>a</sup> (μM)		
	R	R'	1	2	3
<b>115</b>			0.46 ± 0.01	0.14 ± 0.01	2.2 ± 0.02
<b>135</b>			0.30 ± 0.01	0.20 ± 0.01	>10
<b>136</b>			0.30 ± 0.01	0.18 ± 0.01	>10
<b>137</b>			0.59 ± 0.01	0.26 ± 0.01	6.8 ± 0.04

<sup>a</sup> IC<sub>50</sub> values are given as the mean ± SD of all data points, n = 2.

Compounds **135** and **136** both show a slight increase in potency against FGFR1 when compared to compound **115**. This is in contrast to the trend observed for the corresponding fragments (Section 2.5.1.2) as the unsubstituted ethoxy fragment (**31**) shows the best inhibition against FGFR1-3. However, the selectivity difference seen for fragment **66** (Section 2.5.1.2) has not been reflected in the larger compound **135**, as the selectivity between FGFR1/2 is now negligible. Compound **137** shows a decrease in potency against FGFR1-3 when compared to compound **115**. This suggests that the pyridine nitrogen is not aiding solvation at the entrance of the active site which was previously hypothesised (Section 3.3).

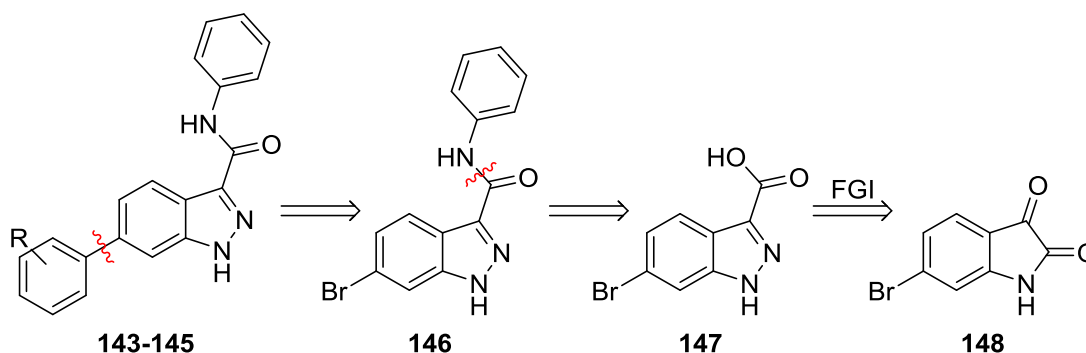
### 3.3.3 Inverse Amide Series

The crystal structure of compound **114** bound within FGFR1 (Figure 3.3) shows the amide NH forming an H-bond to the backbone carbonyl of Ala564. In order to test the importance of this H-bond the following small library was targeted for synthesis.



#### 3.3.3.1 Retrosynthetic Analysis of Structures 143-145

Structures **143-145** were subjected to retrosynthetic analysis as summarised below (Scheme 3.17).

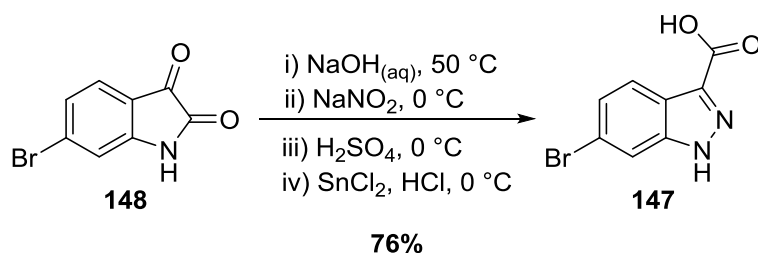


Scheme 3.17: Retrosynthetic analysis of compounds **143-145**.

The first two disconnections, Suzuki and amide couplings, led to compound **147**. This compound is functionalised with a carboxylic acid at the 3-position of the indazole ring. An FGI was then carried out to give the isatin **148**.

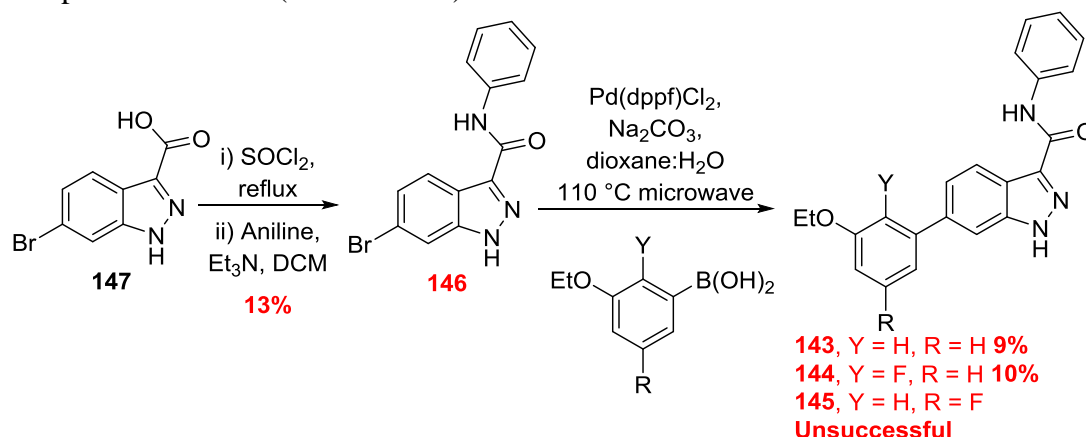
#### 3.3.3.2 Synthesis of Compounds 143-145

In order to gain access to compounds **143-145**, compound **147** was synthesised using a procedure outlined by Gauss *et al* and is summarised below (Scheme 3.18).<sup>132</sup>



**Scheme 3.18:** Synthesis of compound **147**.

Compound **148** was subjected to basic conditions leading to ring opening of the isatin. This unmasked the aniline moiety then underwent diazotisation followed by reduction with  $\text{SnCl}_2$  leading to the formation of the hydrazine intermediate. This then takes part in a ring-closing condensation reaction to give compound **147** in a yield of 76%. Purification of compound **147** was troublesome due to the highly insoluble nature of the compound. However, the reaction proceeded cleanly enough to use the product without purification. Compound **147** was subjected to *in situ* acyl chloride formation conditions outlined previously (Scheme 2.17), followed by Suzuki couplings to afford compounds **143-145** (Scheme 3.19).



**Scheme 3.19:** Synthetic route to compounds **151-153**.<sup>5</sup>

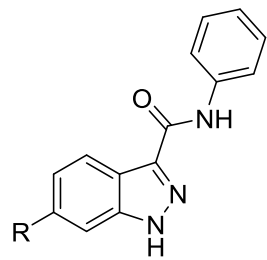
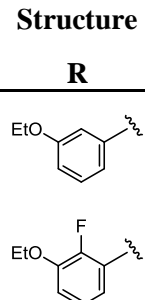
Compound **147** was subjected to *in situ* acyl chloride formation followed by substitution with aniline to afford compound **146** in a yield of 13%. The low yield can be attributed to the poor solubility of the compound and therefore troublesome purification. Compound **146** was then Suzuki coupled to afford compounds **143** and **144** in poor yields. Synthesis of compound **145** was unsuccessful. Analysis of the crude reaction mixture using LC-MS indicated that the corresponding boronic acid had degraded. Synthesis of compound **145** was not carried out due to time constraints of the project.

<sup>5</sup>Compounds outlined in red were synthesised by Laura Johnson (MChem) under the supervision of the Author.

### 3.3.3.3 Biological Evaluation of Compounds 143 and 144

Compounds **143** and **144** were screened against FGFR1-3 using the FRET-based assay. The results are outlined below (Table 3.5).

**Table 3.5:** Biological results for compounds **143** and **144** when screened against FGFR1-3.

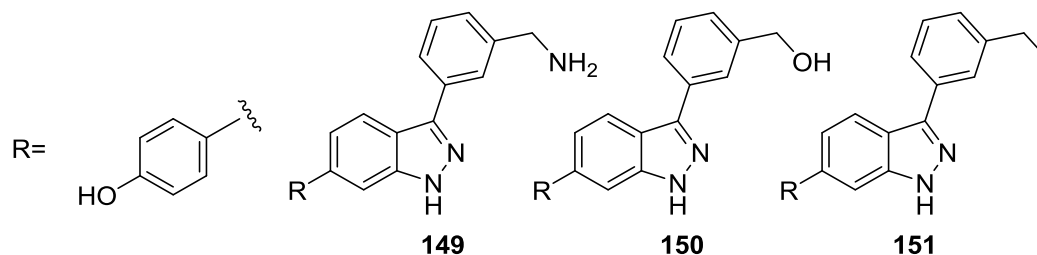
Compound No.	Structure R	IC <sub>50</sub> <sup>a</sup> (μM)		
		1	2	3
<b>143</b>		>10	NT <sup>b</sup>	NT
<b>144</b>		>10	NT	NT

<sup>a</sup> % IC<sub>50</sub> values are given as the mean ± SD of all data points, n = 2. <sup>b</sup> NT = not tested.

Both compounds **143** and **144** are completely inactive against FGFR1. This indicates that SARs around the 3-position of the indazole are very subtle. The amide NH is positioned one atom away from that observed in compound **115** (Section 3.2.4.1). This could indicate that the amide NH in compounds **143** and **144** is not within range of forming an H-bond with the backbone carbonyl of Ala564, hence offering an explanation for the observed drop in potency. The drop in the activity could also be due to the change in electron delocalisation around the amide bond. The amide nitrogen lone pair is no longer conjugated with the indazole ring, instead, the amide carbonyl will have an electron withdrawing effect on the indazole ring. This will weaken the H-bonding acceptor potential of the 2-position indazole nitrogen, which has been shown to be a crucial aspect for FGFR inhibition. The reversal of the amide bond may also effect the stereoelectronics of the system resulting in an unfavourable conformation, this could affect the binding of the compound and explain the drop in potency.

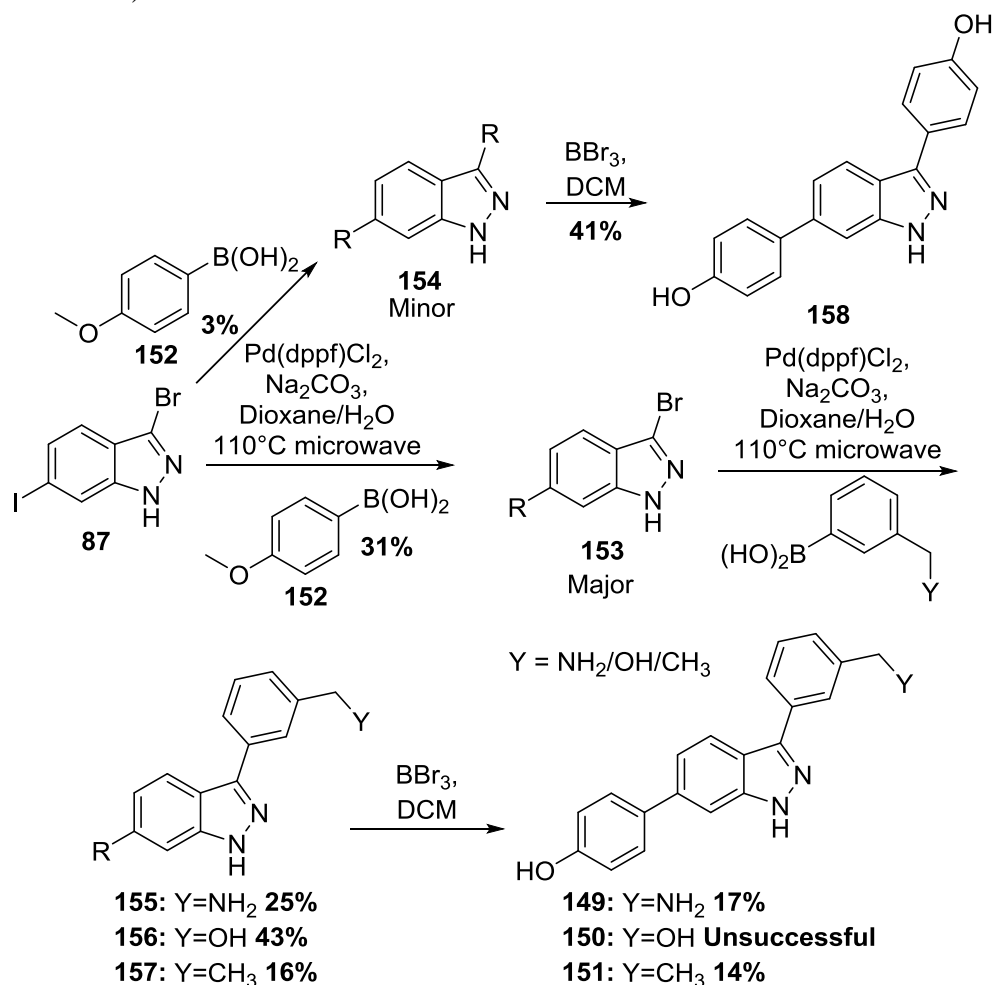
### 3.4 Revisit of the SPROUT Extended Scaffold 85

The SPROUT compound **85** (Section 3.1) was originally designed using the ethoxy-based fragment **31** (Section 2.3) as a starting point. In order to verify this design approach, the extended derivatives of phenol-based fragment **34** (Section 2.3) were targeted for synthesis and are outlined below.



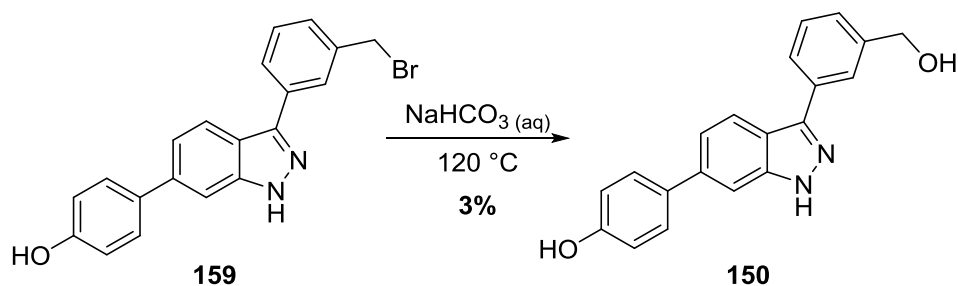
#### 3.4.1 Synthesis of Compounds 149-151

Compounds **149-151** were synthesised using Suzuki chemistry as summarised below (Scheme 3.20).



Scheme 3.20: Synthetic route to compounds **149-151**.

A selective Suzuki coupling was carried out by reacting compound **87** with boronic acid **152** to afford compound **153** as a major product, and compound **154** as a minor product. Compound **153** was subjected to further Suzuki chemistry to gain access to the protected phenol compounds **155-157**. Methoxy deprotection using  $\text{BBr}_3$  was then carried out to afford compounds **149** and **150** proceeding in variable yields. Compound **154** was also subjected to methoxy deprotection in order to obtain compound **158**. The synthesis of compound **150** was unsuccessful. Analysis of the crude reaction mixture using LC-MS had determined that an ‘Appel-like’ reaction had occurred whereby a Lewis-acid-activated oxygen species is displaced in an  $\text{S}_{\text{N}}2$  like fashion by a halogen.<sup>133</sup> The hydroxymethyl OH had interacted with the  $\text{BBr}_3$  forming a borate complex which was then displaced with a bromide anion affording compound **159**, an intermediate not isolated. Compound **150** was synthesised from compound **159** using a procedure developed in-house as summarised below (Scheme 3.21).



**Scheme 3.21:** Synthetic route to compound **150**.

The synthesis of compound **150** proceeded in a poor yield. This can be explained by the poor nucleophilicity of  $\text{OH}^-$ , however, sufficient material was obtained for biological evaluation.

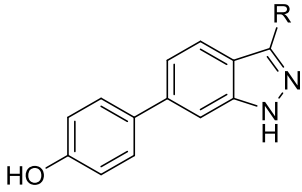
### 3.4.2 Biological Evaluation of Compounds **149-151** and **158**

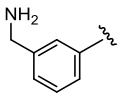
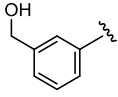
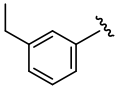
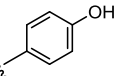
Compounds **149-151** and **158** were screened against FGFR1-3 using the FRET-based assay. The results are outlined below (Table 3.6).

Compounds **149-151** and **158** all showed an increase in potency against FGFR1-3 when compared to lead fragment **34**. However, the increase was only marginal and therefore the addition of the aromatic ring has resulted in a substantial decrease in LE. Interestingly compound **158**, synthesised as a by-product, showed the best inhibition against FGFR1-3. It also showed preferential binding to FGFR2 with an  $\text{IC}_{50}$  value of  $0.25 \mu\text{M}$ , which is  $\sim 8$ -fold selective for FGFR2 over FGFR1/3. This compound demonstrates the first significant selectivity difference between the different FGFR

sub-types. As compound **149-151** were less active than compound **158**, this may suggest substitution in the *meta*-position of the 3-position phenyl ring is unfavourable.

**Table 3.6:** Biological results for compounds **34**, **149-151** and **158** when screened against FGFR1-3.



Compound No.	Structure R	IC <sub>50</sub> <sup>a</sup> (μM)			LE		
		1	2	3	1	2	3
<b>34</b>	H	12 ± 0.2	3.0 ± 0.03	51 ± 0.6	0.43	0.48	0.38
<b>149</b>		3.5 ± 0.03	0.8 ± 0.01	9.0 ± 0.1	0.32	0.36	0.29
<b>150</b>		3.0 ± 0.03	NT <sup>b</sup>	NT	0.32	N/A	N/A
<b>151</b>		5.9 ± 0.06	NT	NT	0.31	N/A	N/A
<b>158</b>		2.1 ± 0.03	0.25 ± 0.01	2.7 ± 0.02	0.35	0.40	0.34

<sup>a</sup> IC<sub>50</sub> values are given as the mean ± SD of all data points, n = 2. <sup>b</sup> NT = not tested.

Compound **115** (Section 3.2.4.4) shows ~4-fold selectivity for FGFR2 over FGFR1 whereas compound **158** shows ~8-fold selectivity for FGFR2 over FGFR1. There are two major differences between these compounds; the substituent on the 6-position phenyl ring and the nature of the 3-position substituent (Figure 3.4). It is apparent that the selectivity preference for FGFR2 observed for compound **158** is arising from either the phenol and/or the aryl-aryl bond.

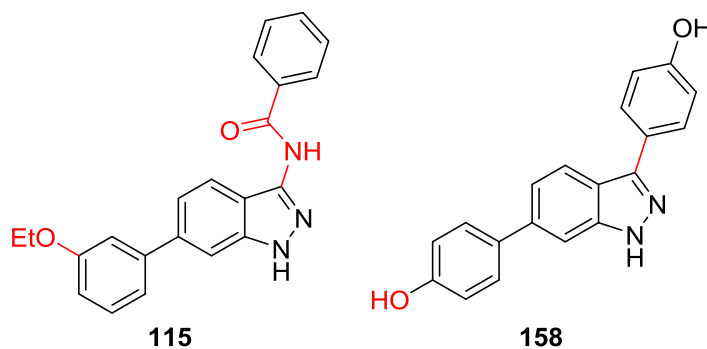
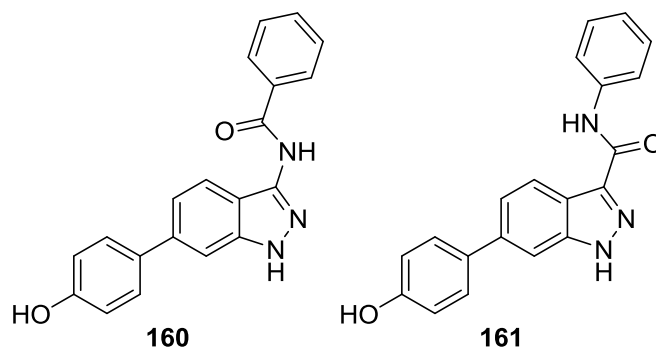


**Figure 3.4:** Compounds **115** and **158**. Areas of difference resulting in FGFR1/2 selectivity are outlined in red.



### 3.4.3 FGFR2 Selectivity Investigation

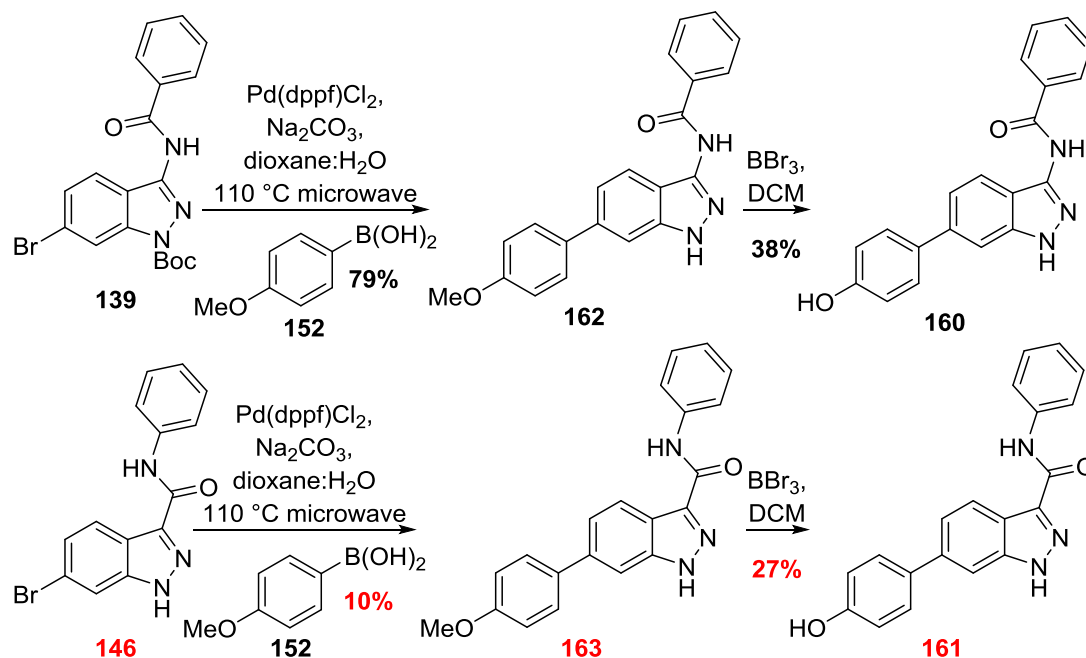
In order to determine the precise aspects that govern the FGFR2 selectivity preference of compound **158**, a compound (**160**) incorporating an amide bond into the 3-position indazole/phenyl bond of compound **158** was targeted for synthesis and is outlined below.



Compound **161** was also targeted for synthesis to give a complete SAR study for the inverse amide series (Section 3.3.3).

#### 3.4.3.1 Synthesis of Compounds 160 and 161

Compounds **160** and **161** were synthesised using conditions as summarised below (Scheme 3.22).



Scheme 3.22: Synthetic routes to compounds **160** and **161**.<sup>6</sup>

Compounds **139** and **146** were subjected to Suzuki couplings with compound **152** to afford compound **162** and **163** respectively in variable yields. Synthesis of compound

<sup>6</sup>Compounds outlined in red were synthesised by Laura Johnson (MChem) under the supervision of the Author.

**163** proceeded in a poor yield due to insolubility of the compound leading to troublesome purification. Compounds **162** and **163** were then subjected to deprotection using  $\text{BBR}_3$  to afford final compounds **160** and **161** respectively in poor yields.

### 3.4.3.2 Biological Evaluation of Compounds 160 and 161

Compounds **160** and **161** were screened against FGFR1-3 using the FRET-based assay. The results are outlined below (Table 3.7).

**Table 3.7:** Biological results for compounds **158**, **160** and **161** when screened against FGFR1-3.

Compound No.	Structure R	IC <sub>50</sub> <sup>a</sup> (μM)		
		1	2	3
<b>158</b>		2.1 ± 0.03	0.25 ± 0.01	2.2 ± 0.02
<b>160</b>		0.40 ± 0.01	0.11 ± 0.01	3.5 ± 0.03
<b>161</b>		>10	NT <sup>b</sup>	NT

<sup>a</sup> IC<sub>50</sub> values are given as the mean ± SD of all data points, n = 2. <sup>b</sup> NT = not tested.

Compound **160** shows an increase in potency against FGFR1/2 but not against FGFR3 when comparing to the results of compound **158**. The potency has dramatically increased against FGFR1 but only marginally for FGFR2 resulting in a selectivity drop of ~8-fold to ~4-fold when comparing compounds **158** and **160** respectively. This demonstrates that the most influential aspect to FGFR2 selectivity for compound **158** is the aryl-aryl bond at the indazole 3-position. It is important to note that this selectivity is only observed when the phenolic species is present and so it is a combination of both aspects that governs selectivity. Compound **161** is inactive which reflects the results for the other compounds (**143** and **144**) in the inverse amide series (Section 3.3.3.3).

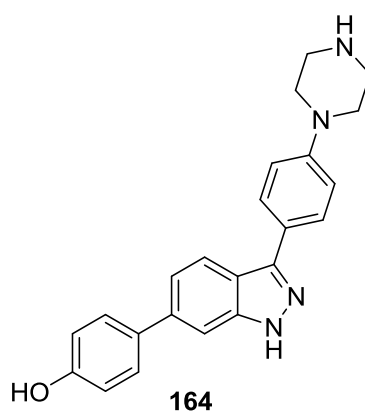
### 3.5 Chapter Three Summary

Fragment leads **31** and **34** were expanded upon using *de novo* design to identify compound **85** as a larger compound predicted to inhibit FGFR1. Subsequent synthesis of several ethoxy-containing analogues outlined that this compound motif was unsuccessful in inhibiting FGFR1. However, one such phenol-containing analogue (**158**) showed preferential inhibition for FGFR2 over FGFR1 exhibiting ~8-fold selectivity. Literature precedent outlined the use of an amide functionality at the 3-position of the indazole ring. Incorporation of the amide motif into the indazole core, outlined by compounds **115**, **135**, **136**, **137** and **160**, found that activity against the FGFRs was regained when compared to the results exhibited by compound **85**. However, selectivity for FGFR2 over FGFR1 was diminished. Exploitation of the selectivity preference for FGFR2 was made a priority which involved further development of compound **158**.

## Chapter Four – Expansion of FGFR2 Selectivity

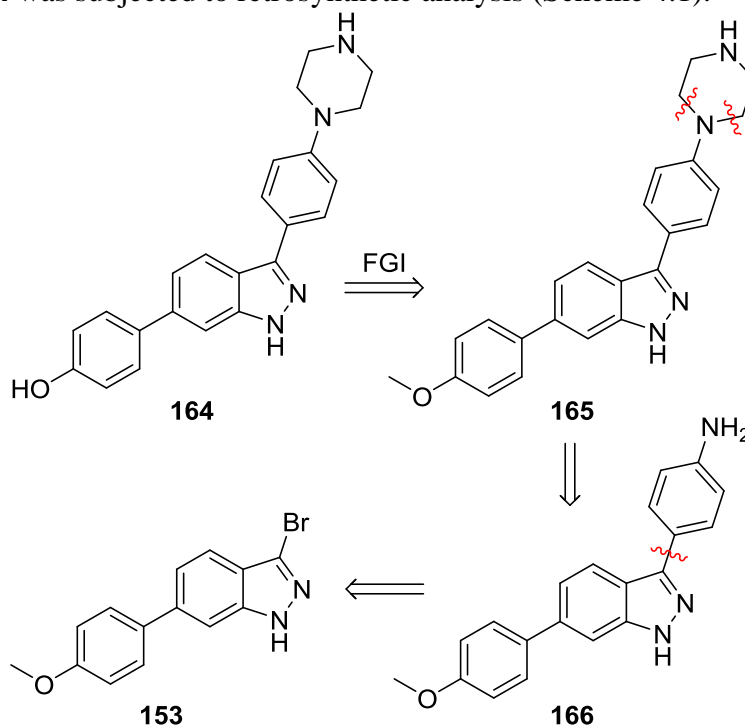
### 4.1 Lead Design

Section 3.2.4 outlines the use of compound **114**, which bears an indazole scaffold, as a potent inhibitor of FGFR kinases.<sup>95</sup> This compound also contains a phenyl piperazine moiety connected *via* an amide to the indazole 3-position. Literature reports have outlined the use of piperazine as a useful group to improve the pharmacokinetic profile of FGFR inhibitors.<sup>84,125</sup> Therefore, the phenyl piperazine moiety was seen as an appropriate group to append to the indazole 3-position, leading to compound **164**.



#### 4.1.1 Retrosynthetic Analysis of Structure 164

Structure **164** was subjected to retrosynthetic analysis (Scheme 4.1).

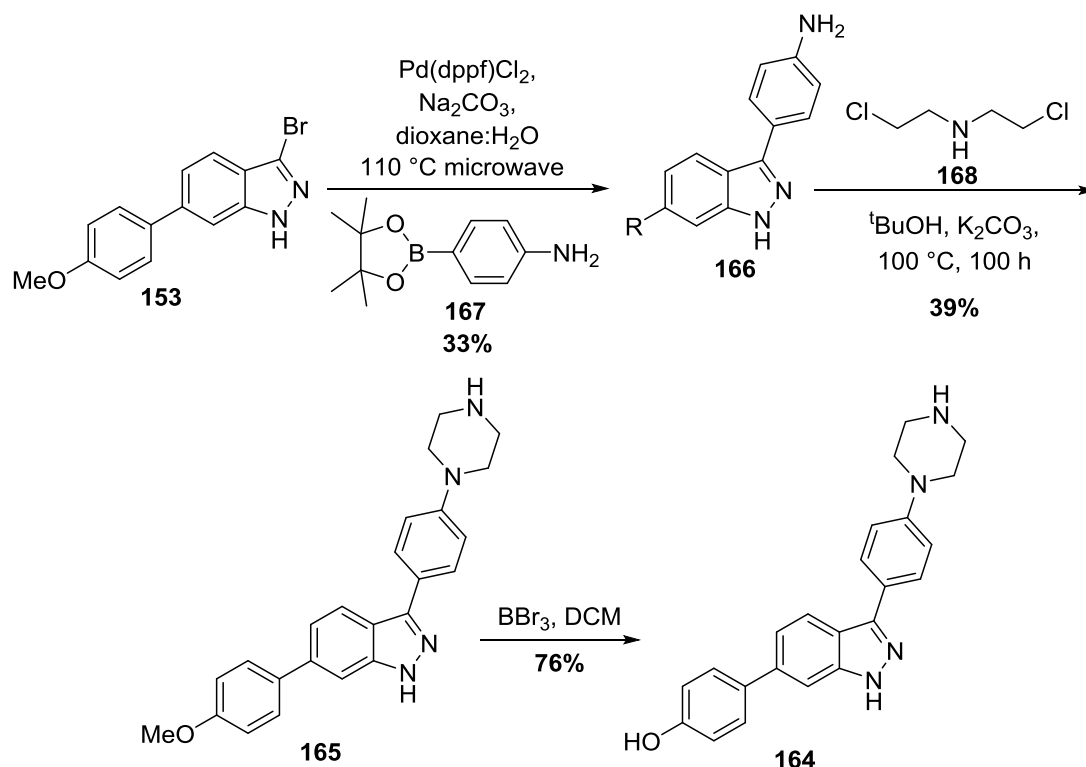


**Scheme 4.1:** Retrosynthetic analysis of compound **164** leading to compound **153**.

FGI on structure **164** gives structure **165**. The use of a methoxy protecting group has been shown to be necessary as explained previously (Section 2.5.2.1). Structure **165** can then be disconnected at the piperazinyl N-C bonds to afford the aniline **166**. This can undergo another disconnection at the indazole 3-position to give structure **153**, a compound synthesised previously (Section 3.4.1).

#### 4.1.2 Synthesis of Compound 164

Compound **164** was synthesised according to conditions summarised below (Scheme 4.2).

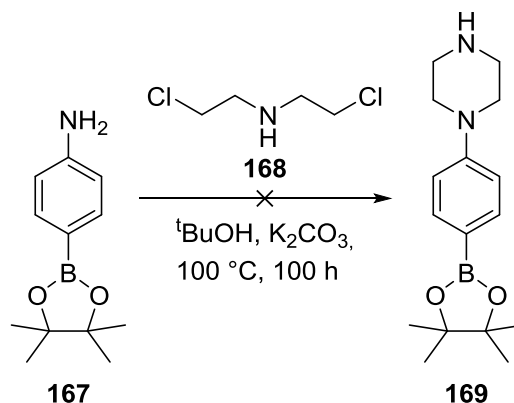


Scheme 4.2: Synthetic route to compound **164**.<sup>7</sup>

Compound **166** was synthesised from compounds **153** and **167** using Suzuki chemistry and proceeded in a low yield of 33%. A likely explanation for the low yield would be the significant loss of product during purification; isolation of pure product required both normal and reverse-phase chromatography. Compound **165** was synthesised from compound **166** according to a procedure outlined by Zhibo *et al.*<sup>134</sup> Compound **166** reacts with compound **168** displacing both chlorines in a double S<sub>N</sub>2 reaction affording compound **165** in a yield of 39%. The reaction conditions were very harsh, requiring temperatures higher than that of the solvent boiling point, and long periods of time to

<sup>7</sup> Caution - Specific risk assessment incorporated for use of compound **168** (nitrogen mustard precursor).

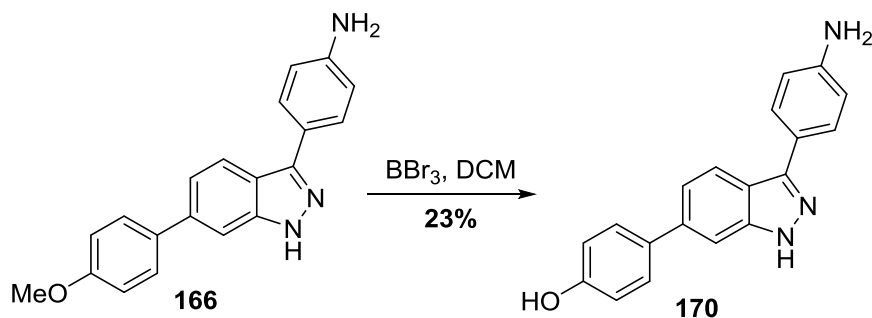
go to completion. The poor reactivity of the aniline in compound **166** is a likely reason for the ineffective coupling with compound **168**. The nucleophilicity of the aniline is reduced as a result of the electron withdrawing effect of the indazole. In addition to this, the long reaction times could be attributed to the insolubility of compound **166** in <sup>t</sup>BuOH. In order to overcome the poor nucleophilicity of the aniline, formation of the piperazine ring was attempted prior to Suzuki coupling as summarised below (Scheme 4.3).



**Scheme 4.3:** Re-ordering of steps to give compound **169**.

The synthesis of compound **169** was unsuccessful. Analysis of the crude reaction mixture using LC-MS indicated the hydrolysis of the boronic ester to give the boronic acid. This was seen as inconsequential as Suzuki chemistry was still feasible, however, isolation of the purified compound **169** by chromatography was unsuccessful. Analysis of the eluent using LC-MS had confirmed degradation of the product. It was concluded that compound **169** was unstable in solution and therefore this synthetic route was abandoned.

In order to overcome the poor solubility of compound **166** in <sup>t</sup>BuOH, attempts at using different solvents such as DMF were carried out. However, these resulted in the formation of many side-products and therefore it was decided to proceed with <sup>t</sup>BuOH as the solvent. Compound **165** was then deprotected with BBr<sub>3</sub> to afford compound **164** in a yield of 76%. For further SARs, compound **166** was also subjected to deprotection as summarised below (Scheme 4.4).



**Scheme 4.4:** Demethylation of compound **166** to give compound **170**.

The demethylation of compound **166** proceeded in a low yield of 23%. This can be attributed to the aqueous solubility of compound **170**. Upon extraction, analysis of the aqueous layer using LC-MS outlined the presence of compound **170**, leading to troublesome purification.

### 4.1.3 Biological Evaluation of Compounds **164** and **170**

Compounds **164** and **170** were screened against FGFR1-3 using the FRET-based assay. The results are outlined below (Table 4.1).

**Table 4.1:** Biological results for compounds **158**, **164** and **170** when screened against FGFR1-3.

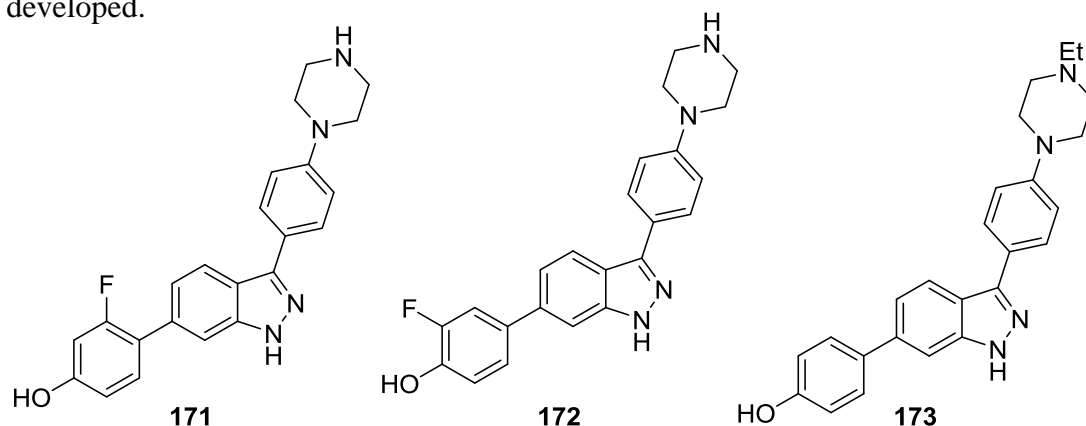
Compound No.	Structure R	IC <sub>50</sub> <sup>a</sup> (nM)			LE		
		1	2	3	1	2	3
<b>158</b>		2100 ± 30	250 ± 3	2200 ± 20	0.35	0.40	0.34
<b>164</b>		389 ± 2	28.5 ± 0.2	758 ± 3	0.32	0.38	0.31
<b>170</b>		4200 ± 40	198 ± 2	>10000	0.31	0.41	N/A

<sup>a</sup>IC<sub>50</sub> values are given as the mean ± SD of all data points, n = 2.

Compound **164** has increased in potency against FGFR1-3 when comparing to compound **158**. It exhibits a more clinically relevant potency with an IC<sub>50</sub> value of 28.5 nM against FGFR2. This shows ~14-fold selectivity over FGFR1, an increase when comparing to the ~8-fold selectivity observed for compound **158** against FGFR2 over FGFR1. Interestingly, when comparing to compound **158**, compound **170** shows ~21-fold selectivity for FGFR2 over FGFR1 which is a large increase in selectivity for such a small structural change between both compounds. Docking models of compounds **158** and **170** bound within FGFR1 show no difference in the binding modes of the compounds. It is unclear why both compounds show greater selectivity for FGFR2 over FGFR1.

## 4.2 SAR Expansion

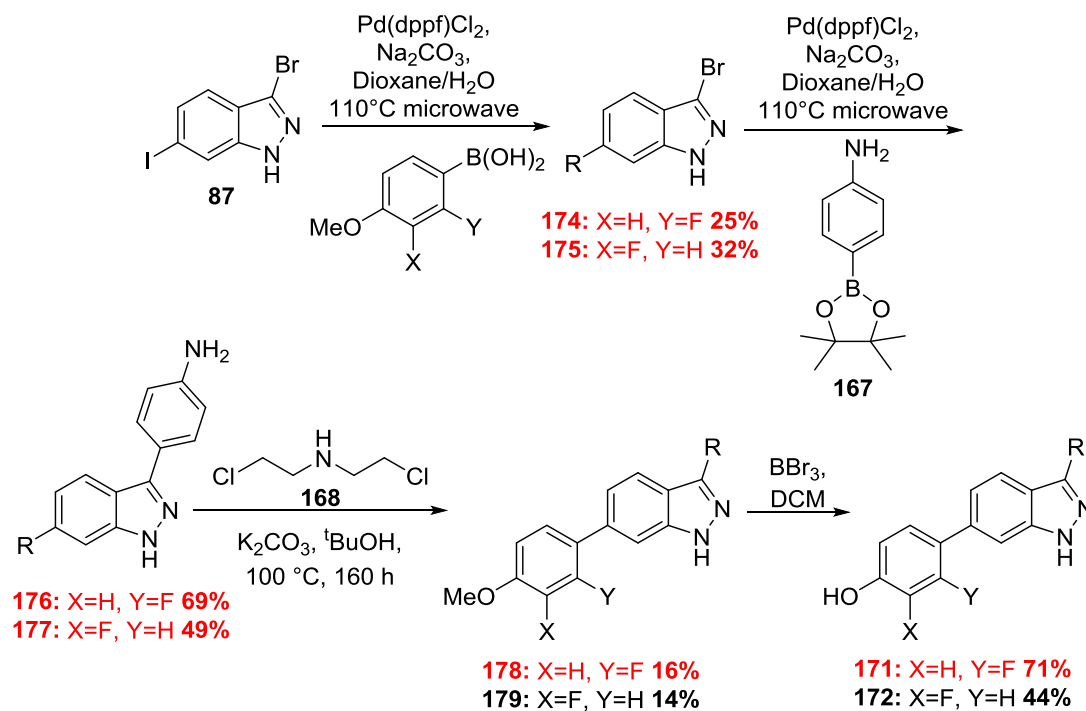
In order to expand the SAR studies for compound **164**, the following library was developed.



Compound **171** and **172** both expand upon the earlier fragment series (Section 2.5.2). Compound **173** was targeted as literature reports outline the use of this additional hydrophobic functionality to increase inhibitor binding to the FGFRs.<sup>95</sup>

### 4.2.1 Synthesis of Compounds 171 and 172

Compounds **171** and **172** were synthesised in a similar fashion to that described previously (Scheme 4.2) as summarised below (Scheme 4.5).



Scheme 4.5: Synthetic route to compounds **171** and **172**.<sup>8</sup>

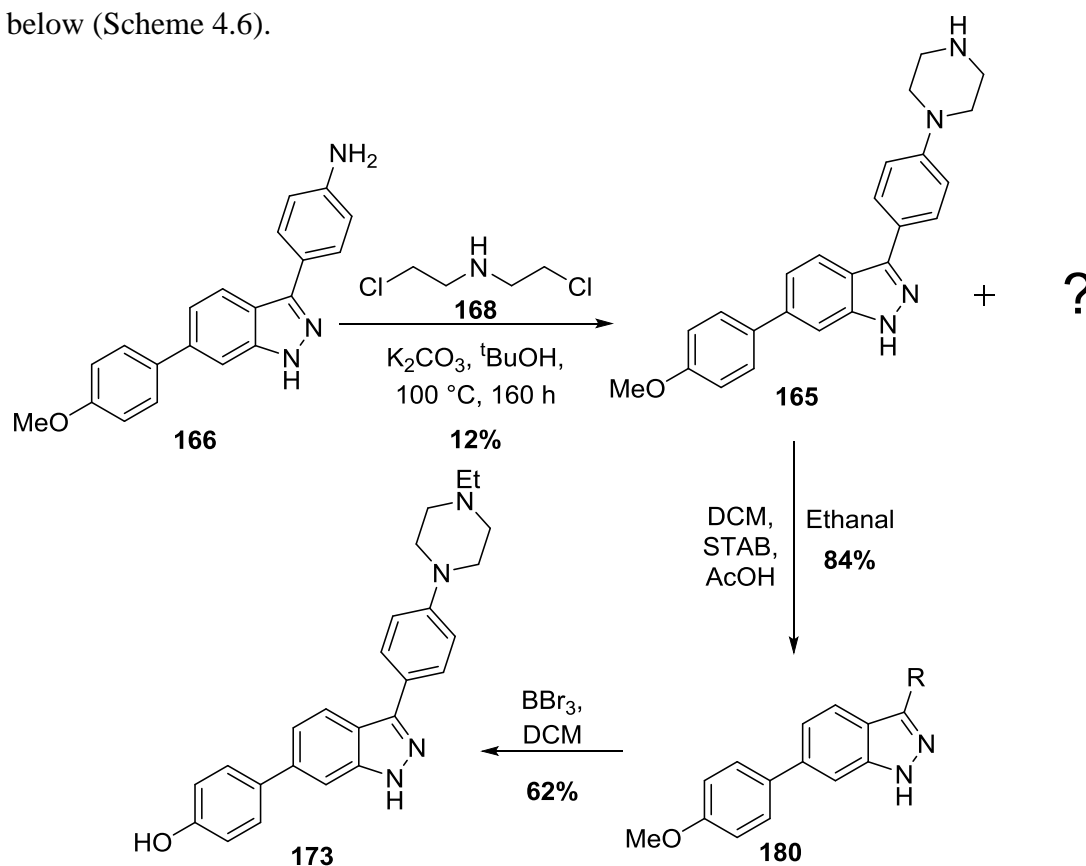
<sup>8</sup>Compounds outlined in red were synthesised by Laura Johnson (MChem) under the supervision of the Author.



Compound **87** was subjected to consecutive selective Suzuki couplings to afford compounds **176** and **177** in moderate yields. Cyclisation with compound **168** proved troublesome due to reasons outlined previously (Section 4.1.2). Compounds **178** and **179** were then deprotected to afford compounds **171** and **172** in moderate yields. Due to limited amount of material, compound **178** was not fully characterised, however, full characterisation was carried out on final compound **171**.

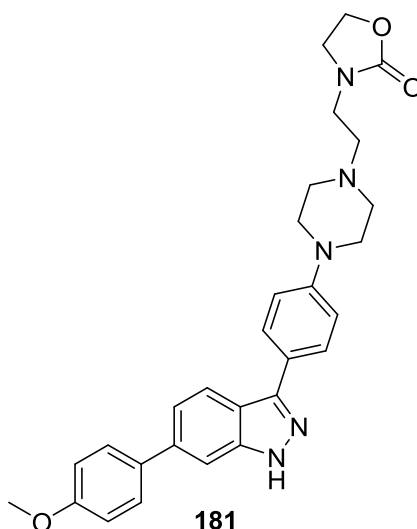
#### 4.2.2 Synthesis of Compound 173

Compound **173** was synthesised using reductive amination chemistry as summarised below (Scheme 4.6).

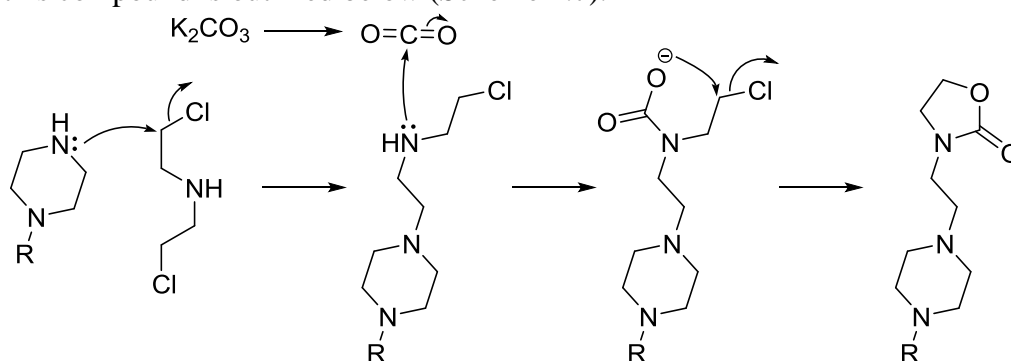


**Scheme 4.6:** Synthetic route to compound **173**. Formation of unknown side product.

Compound **166** was reacted under basic conditions with compound **168** to afford compound **165**. Upon scale up of this reaction, milligram to gram, the reaction proceeded much slower. Analysis of the reaction mixture using LC-MS indicated the presence of compound **166** and therefore additional compound **168** was added. Unexpectedly, the extra addition of compound **168** resulted in the formation of a side product. Upon purification and full characterisation, the structure of this side product was elucidated and determined to be compound **181**, obtained in a yield of 17%.

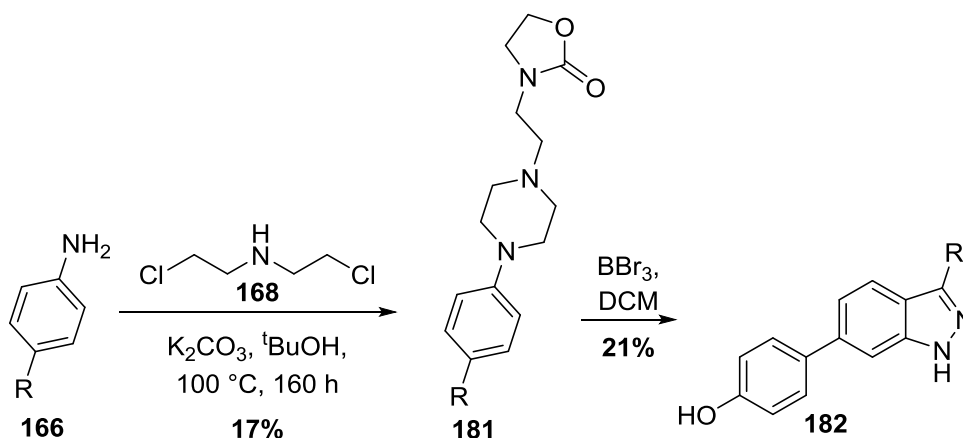


Attempts at obtaining a crystal structure were unsuccessful as compound **181** was found to be very insoluble in most solvents. A proposed mechanism for the formation of this compound is outlined below (Scheme 4.7).



**Scheme 4.7:** Proposed mechanism for the formation of compound **181**.

Presumably, the excess amount of compound **168** and the somewhat harsh basic conditions resulted in overreaction to yield compound **181**. It was desirable to obtain the additional SARs that compound **181** would provide and therefore it was subjected to deprotection as summarised below (Scheme 4.8).



**Scheme 4.8:** Synthetic route to compound **182**.

### 4.2.3 Biological Evaluation of Compounds 171-173 and 182

Compounds **171-173** and **182** were screened against FGFR1-3 using the FRET-based assay. The results are outlined below (Table 4.2).

**Table 4.2:** Biological results for compounds **164**, **171-173** and **182** when screened against FGFR1-3.

Compound No.	R	Structure R'	IC <sub>50</sub> <sup>a</sup> (nM)		
			1	2	3
<b>164</b>			389 ± 2	28.5 ± 0.2	758 ± 3
<b>171</b>			204 ± 3	77.4 ± 1	915 ± 6
<b>172</b>			268 ± 1	258 ± 2	753 ± 5
<b>173</b>			135 ± 7	77.0 ± 5	501 ± 2
<b>182</b>			449 ± 3	96.0 ± 1	NT <sup>b</sup>

<sup>a</sup> IC<sub>50</sub> values are given as the mean ± SD of all data points, n = 2. <sup>b</sup> NT = not tested.

Compound **171** and **172** show a marginal increase in potency against FGFR1 but quite a significant drop in potency against FGFR2 when compared to compound **164**. This results in a drop of ~14-fold to ~2.5-fold FGFR2 selectivity for compound **171** when compared to compound **164**. A complete loss of FGFR2 selectivity is observed for compound **172** when compared to compound **164**. Again, this trend is reflected with the results of compound **173** which shows ~2-fold selectivity preference for FGFR2. Interestingly, compound **173** exhibits an IC<sub>50</sub> value of 135 nM against FGFR1 and is the most potent compound against FGFR1. Compared to compound **164**, compound **182** shows a drop in potency against both FGFR1/2 but exhibits the second best

selectivity preference for FGFR2 over FGFR1 at ~4.5-fold. To summarise, compounds **171** and **172** show very subtle structural changes in the substituents of the 6-position phenyl ring (hydrogen for fluorine) when comparing to compound **172** and yet the selectivity profile dramatically changes. The precise reasons for this cannot be explained using docking models; crystallisation of these inhibitors within the proteins was therefore desirable in order to attempt to rationalise the observed selectivity (Section 4.4).

### 4.3 SAR Expansion of the Amide Series

In Section 3.2.4.4, it was determined that the amide series of compounds (**115**, **135**, **136**, **137** and **160**) was less selective for FGFR2 over the phenolic aryl-aryl series (**158**, **164** and **170**). In order to expand the SARs for the amide series the following target library was developed (Figure 4.1)

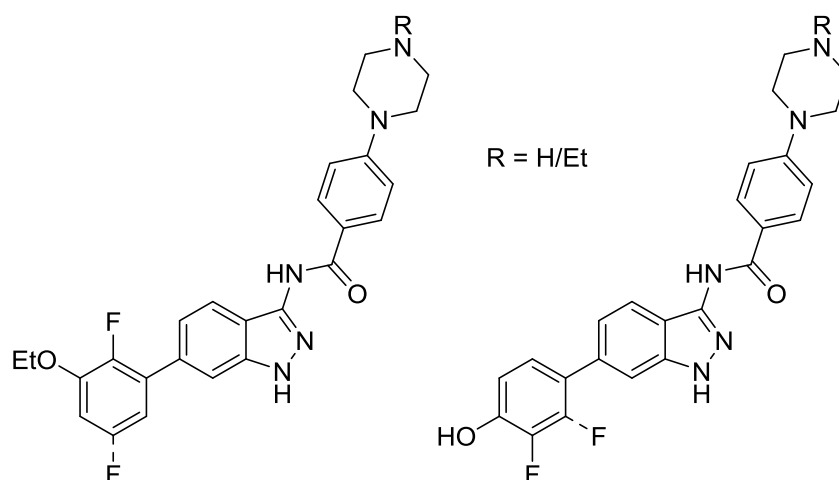


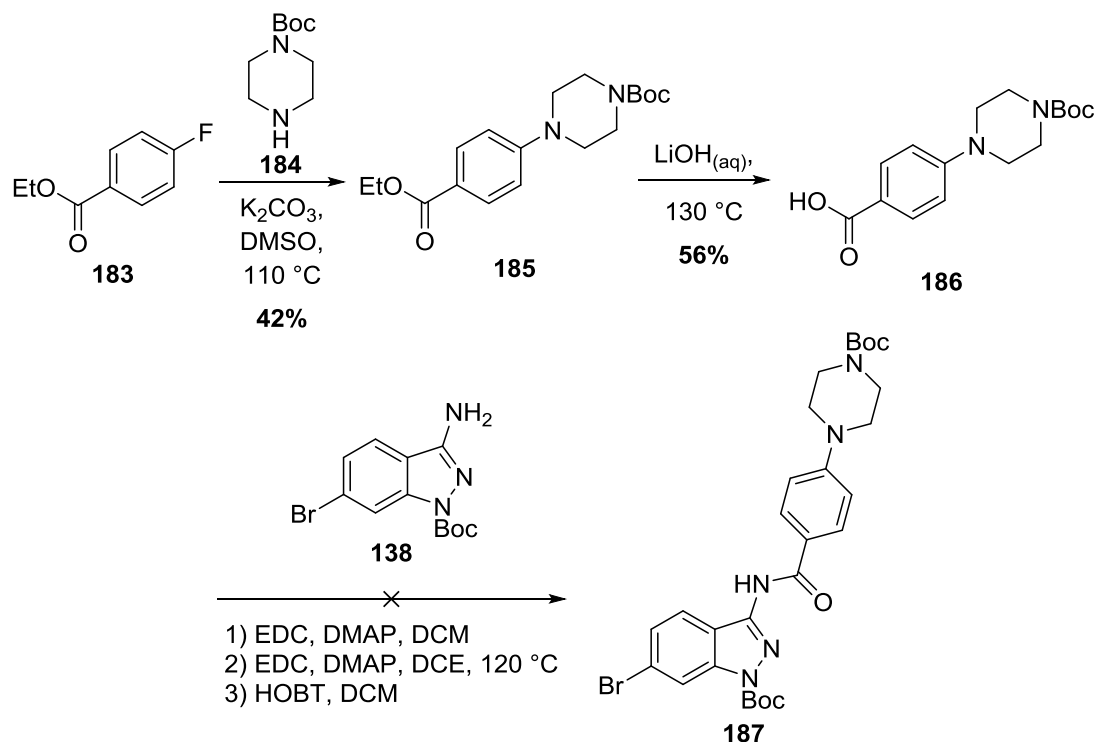
**Figure 4.1:** Target library for mono-fluorinated amide control compounds.

Thus, ‘extended’ versions of both the ethoxy- and phenol fragment series were targeted for synthesis. It was envisioned that analysis of the inhibitory behaviour of these compounds could help fully establish the selectivity impact of the aryl-aryl bond in the phenolic lead series that has been previously described (Section 3.4.3.2).

#### 4.3.1 Synthesis of the Extended Amide Series

Previously, the amide bond present in compounds **115**, **135**, **136**, **137** and **160** were synthesised *via* acyl chloride coupling conditions (Scheme 3.13), however, due to the inclusion of the piperazine ring within the target molecules, the required acyl chlorides

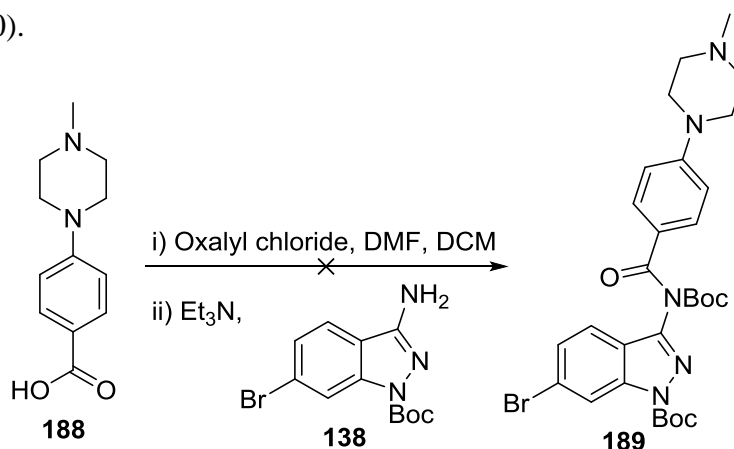
were not available in order to utilise this chemistry, and therefore an alternative synthetic approach was attempted (Scheme 4.9).



**Scheme 4.9:** Alternative synthetic routes attempted in order to obtain the desired amides.

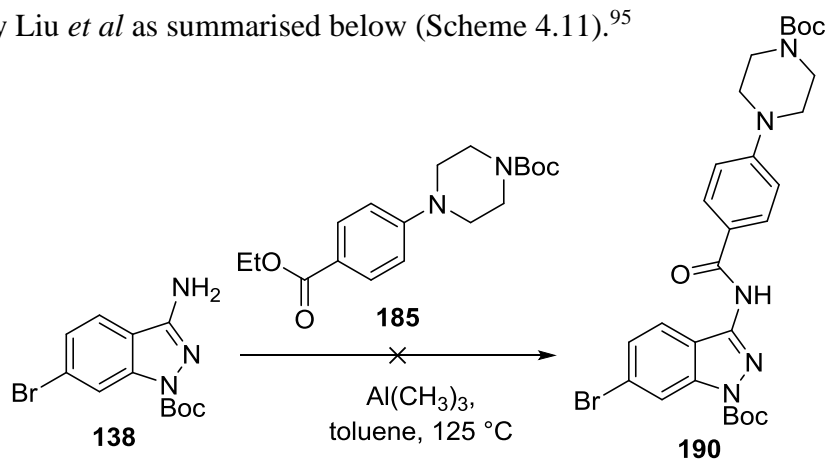
Compound **185** was synthesised from compounds **183** and **184** using  $S_NAr$  conditions outlined by Liu *et al*<sup>95</sup> in a yield of 42%. Compound **185** was then subjected to basic hydrolysis in order to afford compound **186** in a moderate yield of 56%. Attempts at using milder conditions for hydrolysis, such as 2 M NaOH at room temp, were unsuccessful. Compounds **138** and **186** were then subjected to a range of amide coupling conditions. The initial conditions using 1-ethyl-3-(3-dimethylaminopropyl)-carbodiimide (EDC), 4-dimethylaminopyridine (DMAP) and DCM were unsuccessful. A likely reason for this is due to the poor nucleophilicity of the amine in compound **138**. In order to overcome the inherently poor nucleophilicity of the amine in compound **138**, a change in solvent from DCM to 1,2-dichloroethane (DCE) was carried out, allowing higher reaction temperatures to be achieved. However, the reaction was unsuccessful. A final attempt to prepare compound **187** was carried out using an alternative amide coupling reagent; hydroxybenzotriazole (HOBT) but unfortunately the reaction was unsuccessful. It was concluded that only acyl chlorides were reactive enough in order to form the desired amide bond with compound **138**.

In order to gain access to the desired amide-containing target compounds (Figure 4.1) utilising acyl chloride chemistry, an attempt at synthesising acyl chlorides *in situ* was carried out using a method developed in-house and is summarised below (Scheme 4.10).



**Scheme 4.10:** *In situ* acyl chloride formation conditions.

Compound **188** was subjected to *in situ* acyl chloride formation conditions using DMF as an organocatalyst, forming a reactive Vilsmeier intermediate. Analysis of the reaction mixture using LC-MS indicated that formation of the acyl chloride was successful. This was elucidated by the formation of the methyl ester from MeOH, present as a solvent in LC-MS, reacting with the acyl chloride intermediate. Upon addition of compound **138**, analysis of the reaction mixture by LC-MS indicated the formation of a product with a mass that did not correspond to the desired product. Characterisation of this compound proved difficult due to the limited amount of material available. However, further work on using *in situ* acyl chloride formation was abandoned as literature outlined by Liu *et al*<sup>95</sup> indicated that the desired amide could be accessed *via* a Lewis acid catalysed coupling of an amine with a carboxylic ester. Attempts at synthesising compound **190** were carried out using an adaptation of a method by Liu *et al* as summarised below (Scheme 4.11).<sup>95</sup>

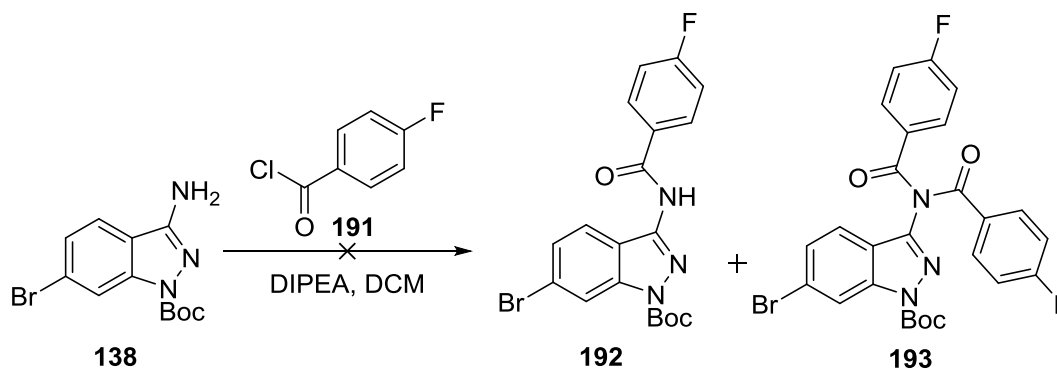


**Scheme 4.11:** Formation of the amide bond using Lewis acid assistance.

Compound **185** becomes activated when  $\text{Al}(\text{CH}_3)_3$  coordinates to the ester allowing acylation to occur with the amine in compound **138**. However, the attempted synthesis of compound **190** using this route was unsuccessful. There are two main differences between this example and the literature example; the nature of the ester and the piperazinyl protecting group. The ester in the literature example exists as the methyl variant but is present as an ethyl ester in compound **185**. This difference could influence the reaction in terms of steric interactions; the ethyl group may be too large for the nucleophilic substitution with compound **138** to take place. The literature example outlines the use of a 4-ethyl piperazinyl system whereas compound **185** shows the use of a 4-BOC-protected piperazinyl system. Analysis of the crude reaction mixture by LC-MS indicated the removal of both BOC protecting groups in starting materials **138** and **185**. This results in liberation of the 4-position piperazine amine in compound **185** allowing it to take part in the amide coupling reaction. The piperazinyl amine in compound **185** is more nucleophilic than the 3-position indazole amine in compound **138** and therefore formation of an undesired product would be expected. However, analysis of the reaction mixture by LC-MS identified only the deprotected starting materials of **138** and **185**. Several attempts at synthesising compound **190** using these conditions were carried out, varying both temperature and length of reaction time, none of which yielded the desired product. However, due to time constraints within the project further work on this area was abandoned.

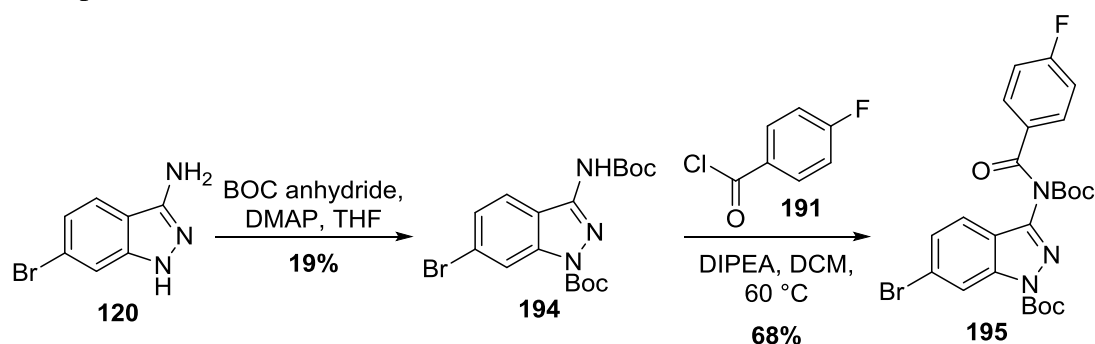
#### 4.3.1.1 Alternative Syntheses of Amide Containing Compounds

As previous work had outlined that amide containing compounds **115**, **135**, **136**, **137** and **160** were only amenable for synthesis *via* the use of acyl chlorides; it was decided to form this bond first from commercially available starting materials (Scheme 4.12).



Scheme 4.12: Acyl chloride coupling conditions.

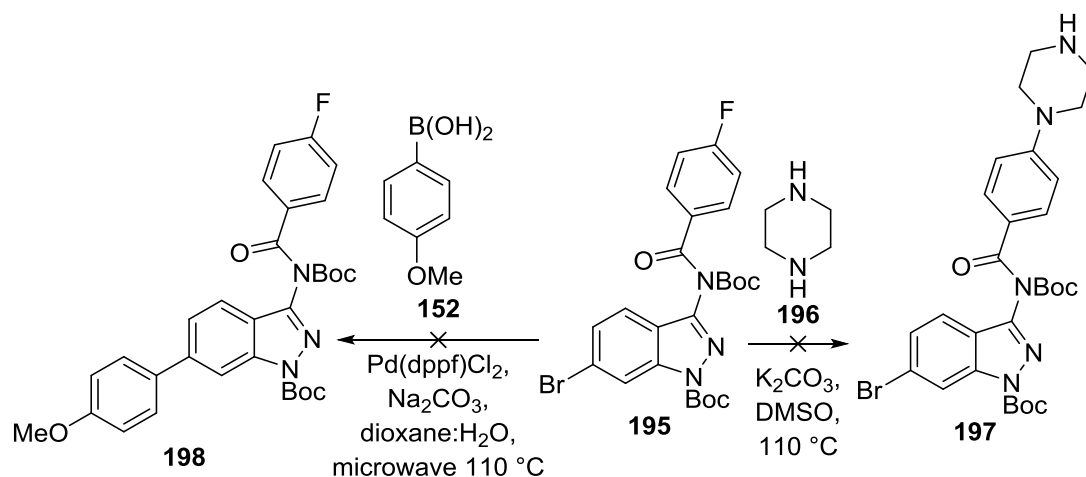
It was reasoned that synthesis of compound **192** should allow  $S_NAr$  chemistry to be carried out on the fluoro-aromatic ring and give access to compound **190**. Compound **138** was reacted with compound **191** using the conditions previously outlined (Section 3.2.4.3). However, the reaction was unsuccessful. Analysis of the reaction mixture using LC-MS indicated the presence of the desired product **192** but also the presence of the starting material **138**. Further addition of compound **191** resulted in the complete conversion of compound **192** into compound **193**, a bis-acylated compound. This phenomenon when forming amides under these conditions has been seen previously (Section 3.2.4.3), however, the formation of the bis-arylated product was usually minor. Scheme 4.12 shows the full conversion of the desired product **192** to the undesired product **193**. It is believed that the acyl chloride **191** is more reactive than the acyl chloride **130** (Section 3.2.4.3) due to the fluorine present on the aromatic ring. In order to restrict over-substitution, compound **120** was subjected to a double BOC protection as summarised below (Scheme 4.13).



**Scheme 4.13:** Use of compound **194** to improve acyl chloride coupling step.

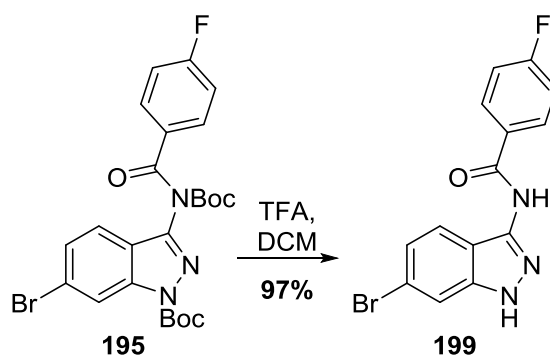
Compound **120** was reacted with 2 eq of BOC anhydride in order to obtain compound **194** in a yield of 19%. The low yield is attributed to the formation of a tri-substituted compound in whereby all free NHs present in compound **120** become protected. Compound **194** was then subjected to the same conditions as described previously (Scheme 4.12). As the 3-position amine is now secondary it can only undergo acylation once, resulting in the formation of compound **195** in a yield of 68%. Compound **195** was then subjected to  $S_NAr$  and Suzuki conditions as summarised below (Scheme 4.14).





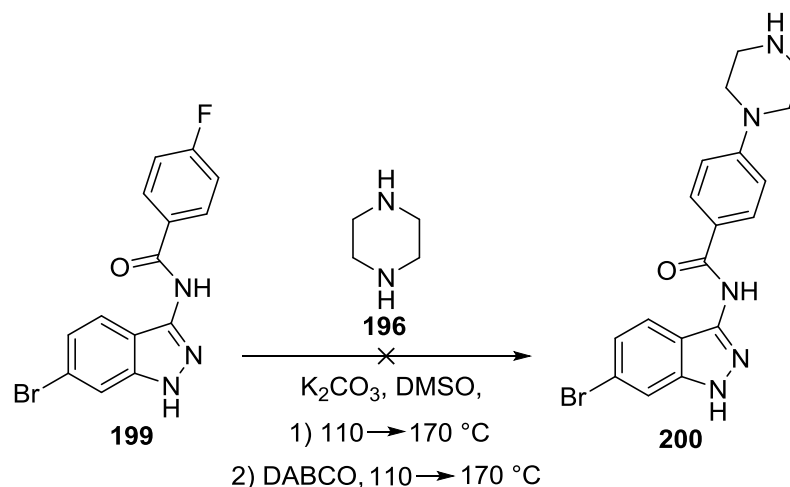
**Scheme 4.14:** Compound **195** subjected to  $S_NAr$  and Suzuki conditions.

Unfortunately, the attempted synthesis of compound **197** from compound **195** was unsuccessful. Analysis of the reaction mixture using LC-MS analysis indicated compound **196** had displaced one of the BOC protecting groups and had not interacted in the intended  $S_NAr$  fashion with the fluoro-aromatic ring. This phenomenon had been seen previously (Scheme 3.2.3). Compound **195** was also subjected to Suzuki conditions but this was also unsuccessful. Analysis of the reaction mixture using LC-MS indicated that several side-products had formed and no evidence of the desired product **198**. It was concluded that the amide bond in **195** was susceptible to hydrolysis in the harsh basic Suzuki conditions, owing to the electron withdrawing effect of the fluorine within **195**. This phenomenon was also observed earlier in the conversion of **138** into **140** (Scheme 3.15) when a pyridyl ring system was present. It was apparent that the  $S_NAr$  chemistry would need to take place prior to Suzuki coupling. Scheme 4.14 shows the interference of the BOC protecting groups present in compound **195** with compound **196** and therefore compound **195** was subjected to deprotection as summarised below (Scheme 4.15).



**Scheme 4.15:** Deprotection of compound **195**.

Compound **195** was deprotected using conditions outlined previously (Scheme 3.14) and proceeded in a yield of 97% to give compound **199**. Compound **199** was then subjected to  $S_NAr$  conditions as summarised below (Scheme 4.16).



**Scheme 4.16:** Varied  $S_NAr$  conditions.

Compound **199** was subjected to the same  $S_NAr$  conditions seen previously (Scheme 4.9). Analysis of the reaction mixture using LC-MS indicated no product mass. The reaction temperature was increased from  $110\text{ }^\circ C$  to  $170\text{ }^\circ C$  to aid the reaction, however this was unsuccessful in yielding the desired compound **200**. The reaction was repeated but with the addition of 1,4-diazabicyclo[2.2.2]octane (DABCO) as this can act as a nucleophilic catalyst for the  $S_NAr$  reaction. DABCO displaces the 4-fluorine atom in a standard  $S_NAr$  reaction forming a quaternary ammonium charged species, an effective leaving group which facilitates the substitution with compound **196**. However, analysis of the reaction mixture using LC-MS analysis indicated no product formation at  $110\text{ }^\circ C$ . The reaction temperature was increased to  $170\text{ }^\circ C$  but this was unsuccessful in yielding the desired compound **200**. It was concluded that the amide functionality was unsuitable for  $S_NAr$  chemistry. Development of this series was postponed (Section 5.2.2) and efforts focussed elsewhere.

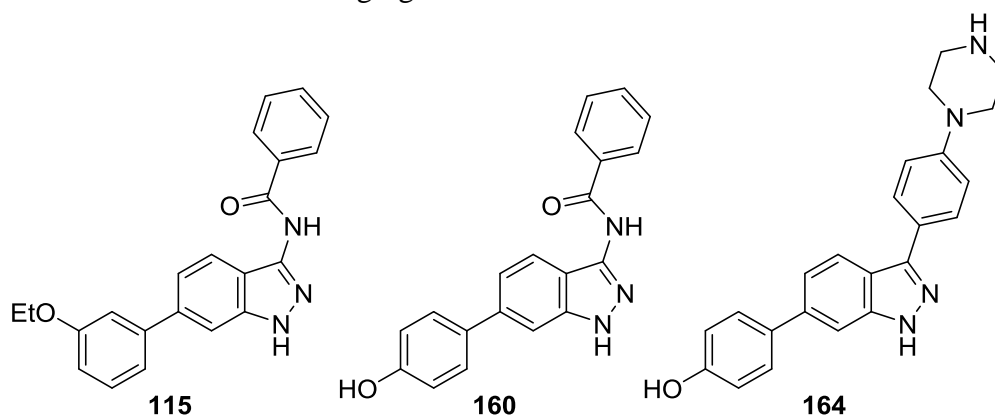
## 4.4 FGFR2 Selectivity Rationalisation

To help rationalise the observed selectivity preference of compound **164** for FGFR2 (Section 4.1.3) over FGFR1, it was decided to focus efforts on expressing and crystallising such compounds within both FGFR1 and FGFR2. All work presented throughout this Section was conducted by the Author excluding the crystallographic data processing, and structure solution and refinement which was carried out by Dr Chi Trinh.

### 4.4.1 Expression and Crystallisation of FGFR1

An FGFR1 construct of the kinase domain containing residues 458-765 with mutations C488A, C584S was provided by Prof Alexander Breeze. This particular variant has been used extensively for the determination of ligand binding conformations, with the aim to elucidate the different binding modes of type I and type II FGFR1 kinase inhibitors.<sup>135,136,137</sup> The protein consists of a His<sub>6</sub>-tag present at the C-terminus that can be removed by Tobacco Etch Virus (TEV) protease.

The FGFR1 mutant protein was crystallised according to the conditions outlined in Section 6.2.7 with the following ligands.



Crystallisation trials of the mutant protein with the His<sub>6</sub>-tag intact were unsuccessful. However, upon cleavage of the tag, crystals were obtained and the X-ray crystal structures solved. See Section 6.2.7 for specific crystallisation details.

## 4.4.2 FGFR1/Ligand Co-crystal Structures

### 4.4.2.1 FGFR1/Compound 115 Co-crystal Structure

The X-ray crystal structure of compound **115** bound within FGFR1 was solved to the resolution of 1.82 Å. The binding mode of compound **115** was analysed (Figure 4.2).

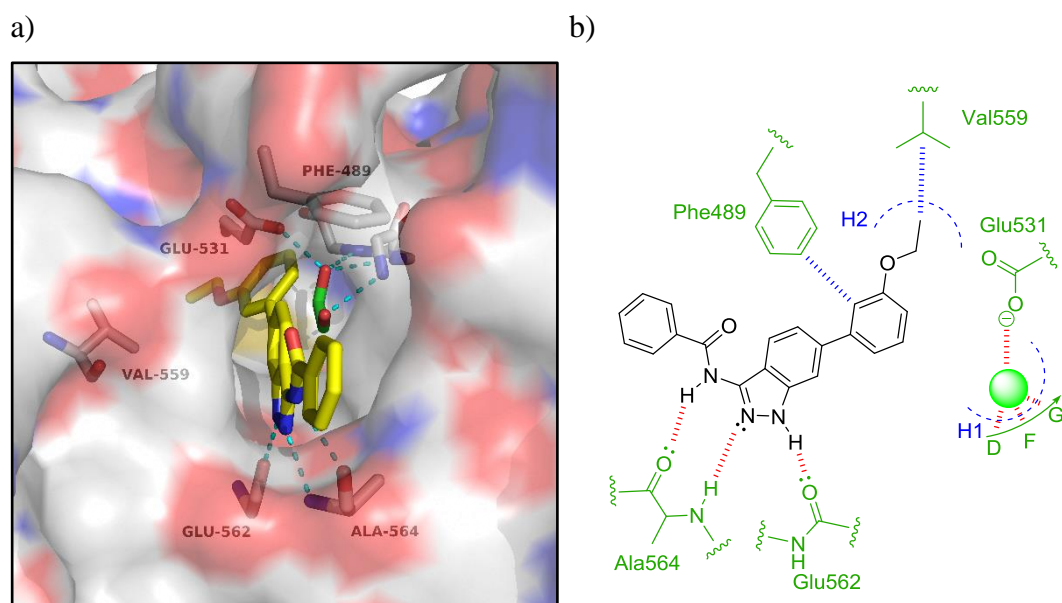


**Figure 4.2:** a) Co-crystal structure of compound **115** bound within the ATP active site of FGFR1. H-bonds are outlined in cyan. Ethylene glycol is outlined in green. b) 2D representation of binding pose of compound **115** within FGFR1. H-bonds and hydrophobic interactions are outlined in red and blue respectively. Green sphere represents ethylene glycol.

Compound **115** occupies the active site of FGFR1 forming several interactions with the enzyme. Both nitrogen atoms in the indazole ring form the crucial H-bonding donor/acceptor motif with Glu562 and Ala564 as was predicted for indazole-containing compounds outlined previously (Section 2.3.6). The amide NH also forms an H-bond with the backbone carbonyl of Ala564 as seen for compound **114** (Figure 3.3). Interestingly the ethoxy group, previously predicted to occupy the H1 pocket (Figure 2.9), now occupies the H2 pocket with the ethoxy group lying close to the residue Val559 to give a hydrophobic effect. Ethylene glycol (present in the crystallisation medium) occupies the H1 pocket, forming numerous H-bonds with close-by residues and in particular the amino acid residues within the DFG motif. Finally, the 6-position phenyl ring interacts in an edge-to-face like fashion with the phenyl ring of Phe489 resulting in a ‘closed-loop’ conformation whereby a short chain of amino acids form a ‘lid’ above compound **115** (Figure 4.2).

#### 4.4.2.2 Alternative Loop Conformation

The conditions used to crystallise FGFR1 result in crystals forming as two monomers, hereby termed ‘chain A and B’. Generally, there are minimal structural differences between these chains. However, for the FGFR1/compound **115** co-crystal structure, there are significant differences between the two chains in the morphology of the active site. Section 4.4.2.1 outlines the active site of chain A, whereby only a ‘closed-loop’ binding conformation is observed. However, for chain B, both the ‘closed-loop’ and ‘open-loop’ conformations are observed (Figure 4.3).

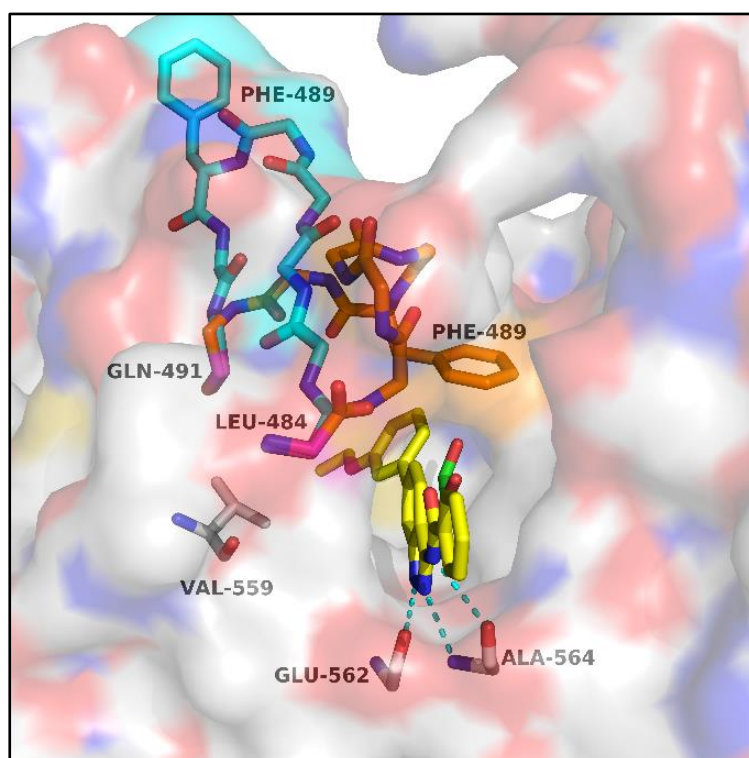


**Figure 4.3:** Active site of FGFR1, chain B, with compound **115** bound. ‘Closed-loop’ and ‘open-loop’ conformations are shown in orange and blue respectively. Loop start/end outlined in purple.

The variable loop region exists between residues 484-491. Electron density was observed for both the ‘open’ and ‘closed’ forms of the loop suggesting that ligand binding is a dynamic process. It is hypothesised that the ‘closed-loop’ form is adopted upon ligand binding and the ‘open-loop’ form is adopted in the absence of ligand binding, with both states being observed simultaneously in chain B.

#### 4.4.2.3 FGFR1/Compound 160 Co-crystal Structure

The X-ray crystal structure of compound **160** bound within FGFR1 was solved to the resolution of 1.82 Å. The binding mode of compound **160** was analysed and is outlined below (Figure 4.4).

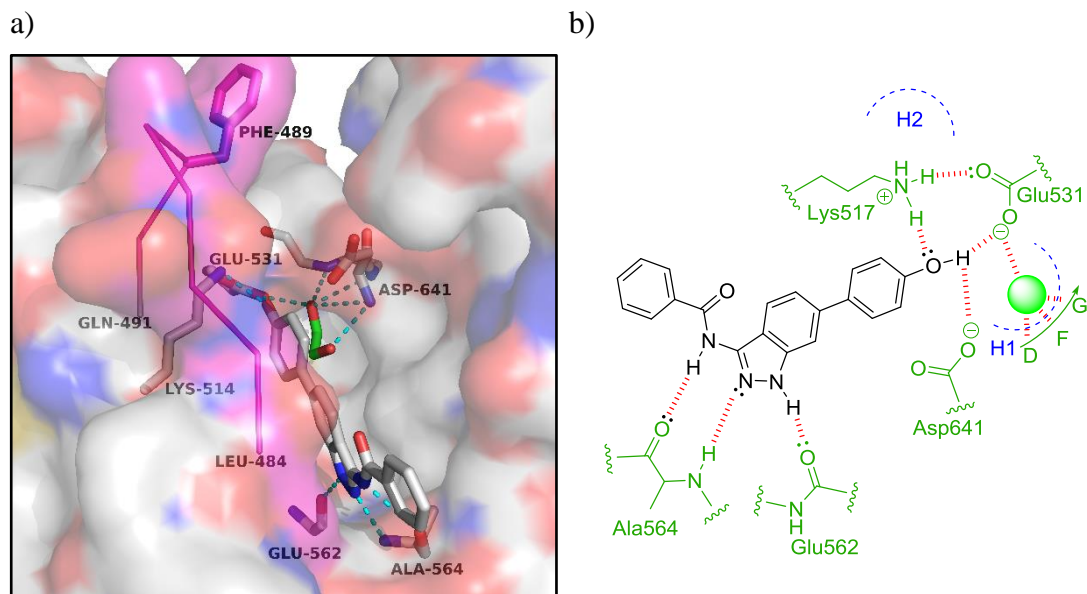


**Figure 4.4:** a) Co-crystal structure of compound **160** bound within the ATP active site of FGFR1. H-bonds are outlined in cyan. Ethylene glycol is outlined in green. The flexible loop region is outlined in purple. b) 2D representation of binding pose of compound **160** within FGFR1. H-bonds are outlined in red. Green sphere represents ethylene glycol.

Compound **160** occupies the active site of FGFR1 forming several interactions with the enzyme. The indazole nitrogens and the amide form the same H-bonds with residues Glu562 and Ala564 as was seen for compound **115** (Figure 4.2). As predicted from the docking studies of compound **34** (Figure 2.10), the phenol is involved in an H-bond donor interaction with the side chain carboxy group of Glu531. In addition to this H-bond donor interaction, an extensive H-bonding network exists between the phenol and residues Glu531, Lys514, and Asp641. As discussed previously, substitution of the hydroxy moiety to a methoxy functionality resulted in a complete loss in activity (Section 2.5.2.2) underlining the importance of this crucial H-bonding network. As outlined for compound **115** (Figure 4.2), ethylene glycol occupies the H1 pocket forming numerous H-bonds with close-by residues, particularly the amino acid backbone of the DFG motif. In contrast to the observed binding pose of compound **115**, no evidence of a ‘closed-loop’ system is observed in the case of compound **160**. Interestingly, the flexible loop region appears to be in a partial ‘open-loop’

conformation. An overlay of the variable loop conformations is outlined below (Figure 4.5).

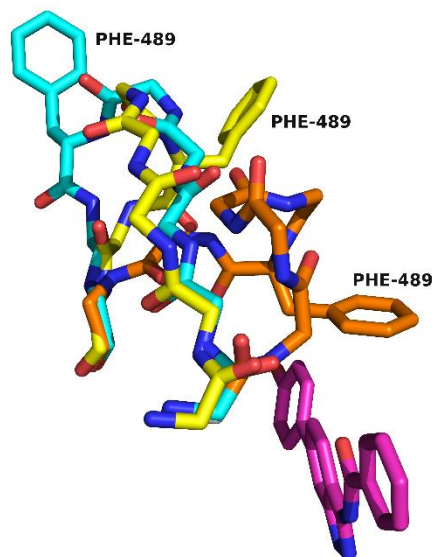


**Figure 4.5:** Overlay of FGFR1/115 and FGFR1/160 co-crystal structures. Open, partially open and closed loop conformations are outlined in cyan, yellow and orange respectively. Compound 160 is shown in purple.

The flexible loop region for the co-crystal structure of FGFR1/compound 160 appears to be in an intermediate state between the ‘open’ and ‘closed’ conformations. It is apparent that the conformation of this flexible loop region is dependent upon the ligand present within the binding site. The ethoxy group within compound 115 occupies the H2 pocket. It is thought that this has a stabilising effect on the whole system resulting in a ‘closed-loop’ conformation. Compound 160 lacks the ethoxy moiety and so, due to reduced steric crowding, the 6-position phenyl ring is relatively free to rotate. The ligand density maps for compounds 115 and 160 are shown below (Figure 4.6).

As can be seen, the ligand density for compound 160 around the 6-phenyl ring appears to be ‘spherical-like’. This suggests multiple conformations are present due to the free rotation of the 6-position phenyl ring. The ligand density for compound 115 around the 6-phenyl ring shows just one, well defined conformation in the X-ray crystal structure. This is likely due to the occupation of the H2 pocket by the ethoxy group which restricts the rotational freedom of the 6-position phenyl ring. The variable binding conformations of compound 160 suggest the flexible loop is less likely to adopt a ‘closed-loop’ conformation and can therefore offer rationale for the partially open conformation observed for compound 160.



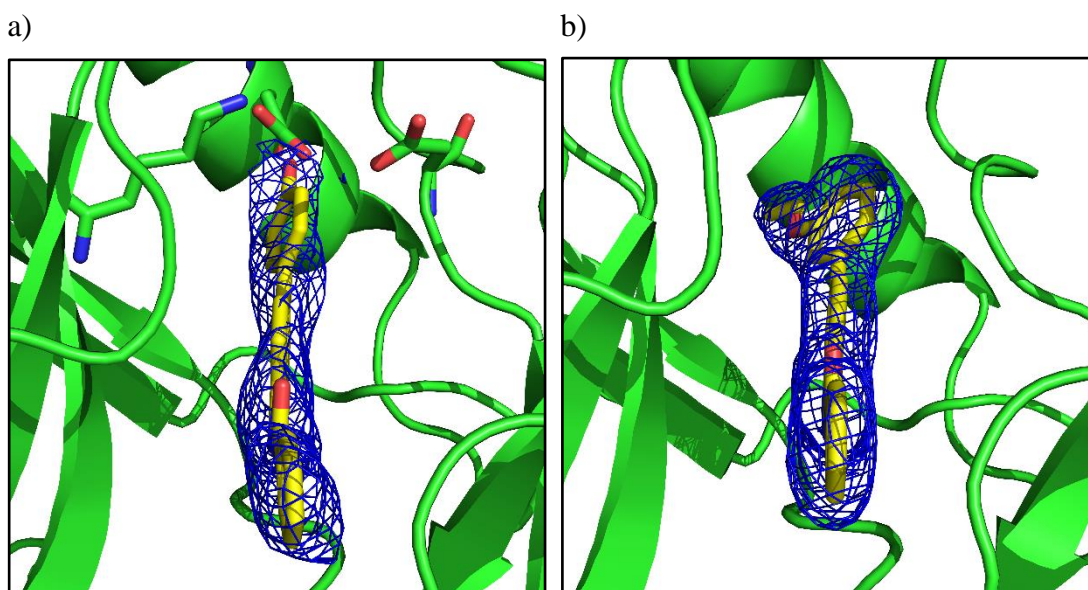


**Figure 4.6:** a) Electron density map for compound **160** bound in FGFR1. b) Electron density map for compound **115** bound in FGFR1.

#### 4.4.2.4 FGFR1/Compound 164 Co-crystal Structure

Compound **164** was also crystallised within FGFR1 and the co-crystal structure solved to the resolution of 1.80 Å. The binding mode of compound **164** was analysed (Figure 4.7).

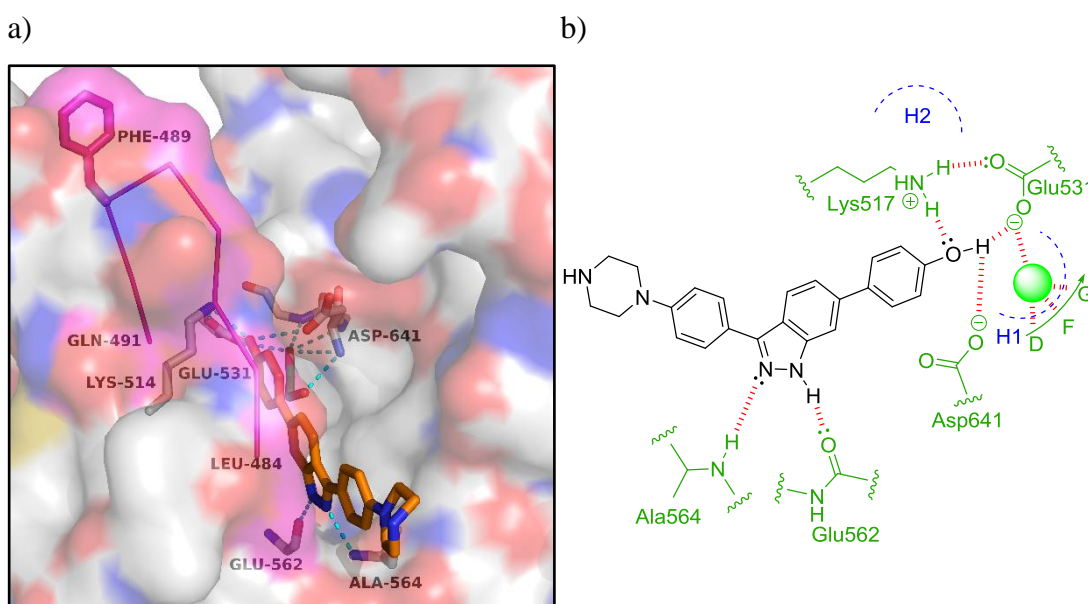


**Figure 4.7:** a) Co-crystal structure of compound **164** bound within the ATP active site of FGFR1. H-bonds are outlined in cyan. Ethylene glycol is outlined in green. The flexible loop region is outlined in purple. b) 2D representation of binding pose of compound **164** within FGFR1. H-bonds are outlined in red. Green sphere represents ethylene glycol.



Compound **164** occupies the active site of FGFR1 forming several interactions with the enzyme. Both indazole nitrogen atoms form the same H-bonds with residues Glu562 and Ala564 as was seen for compound **160** (Figure 4.4). As observed for compound **160**, the phenol is involved in the same H-bonding network with Glu531, Lys514 and Asp641. The phenyl piperazine moiety protrudes into the solvent-exposed region, forming no further interactions with the enzyme. Again, ethylene glycol occupies the H1 pocket forming numerous H-bonds with the amino acid backbone of the DFG motif. The flexible loop region now adopts an ‘open-loop’ conformation with no evidence of a partial ‘open-loop’ or ‘closed-loop’ system. The ‘spherical-like’ density for the 6-position phenyl ring was also observed for this compound (Section 4.4.5.1).

### 4.4.3 Expression and Crystallisation of FGFR2 Variants

A WT FGFR2 construct of the kinase domain consisting of residues 461-763, and a mutant FGFR2 construct of the kinase domain consisting of residues 458-763 were provided by Prof John Ladbury and Dr Chi-Chuan Lin (Section 6.2). The mutant construct involves nine mutations of tyrosine residues to phenylalanine residues (Section 8.2.6), excluding Tyr656; the first tyrosine residue to be phosphorylated upon activation of the enzyme (Section 1.3.3). This mutant was created by Dr Chi-Chuan Lin in order to study the role of autoinhibition of FGFR2, a common downregulating effect in FGFR signalling.<sup>138</sup> It was reasoned that obtaining an X-ray crystal structure on this construct would be valuable as the point-mutation Y566F is located within the hinge region of the active site (Section 1.5.1.1) and could potentially affect the binding of ligands.

With the help of Dr Trinh, the FGFR2 variants were crystallised according to the conditions outlined in Section 6.2.7 with compounds **115**, **160**, and **164**. Unfortunately, crystals were only obtained for the FGFR2 WT/compound **164** variant.

## 4.4.4 FGFR2/Ligand Co-crystal Structures

### 4.4.4.1 FGFR2/Compound 164 Co-crystal Structure

In addition to FGFR1, compound **164** was also crystallised within FGFR2 and the co-crystal structure solved to the resolution of 2.40 Å. The binding mode of compound **164** was analysed (Figure 4.8).

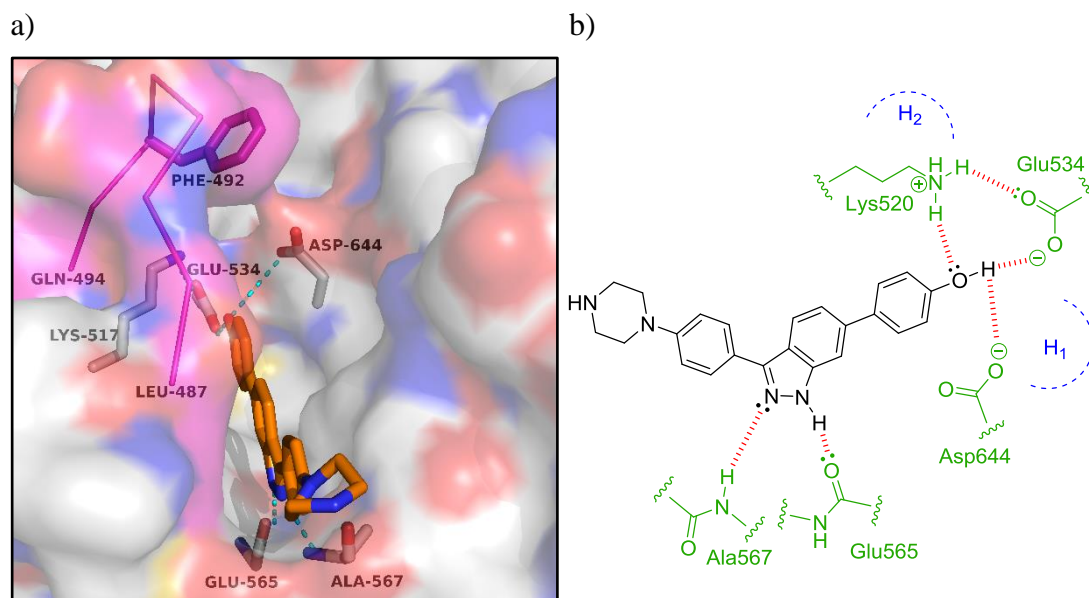


**Figure 4.8:** a) Co-crystal structure of compound **164** bound within the ATP active site of FGFR2. H-bonds are outlined in cyan. Flexible loop region outlined in purple. b) 2D representation of binding pose of compound **164** within FGFR2. H-bonds are outlined in red.

Compound **164** occupies the active site of FGFR2 in a very similar manner to that of its binding mode in FGFR1 (Figure 4.7). Both indazole nitrogen atoms form the same H-bonds with residues Glu565 and Ala567 with the phenol involved in the same H-bonding network with Glu534, Lys520 and Asp644. Again, the phenyl piperazine moiety protrudes into the solvent-exposed region forming no further interactions with the enzyme. In contrast to the FGFR1 structure, ethylene glycol is not observed within the H1 pocket. It is important to note that the lower resolution of this structure is the most likely reason for this. The flexible loop region adopts a partial ‘closed-loop’ conformation. Contrary to the situation found within the FGFR1/compound **164** co-crystal structure, the electron density for the 6-position phenyl ring was now observed to be planar and in line with the indazole ring (Section 4.4.5.1). However, accurate conclusions cannot be drawn due to the significantly lower resolution of this structure when compared to the FGFR1 structure; the rotation of the 6-position phenyl ring may not be resolved.

#### 4.4.5 Comparison of the FGFR1/FGFR2 Binding Sites

The FGFR1/compound **164** and the FGFR2/compound **164** crystal structures were superimposed onto each other and the binding sites compared (Figure 4.9).

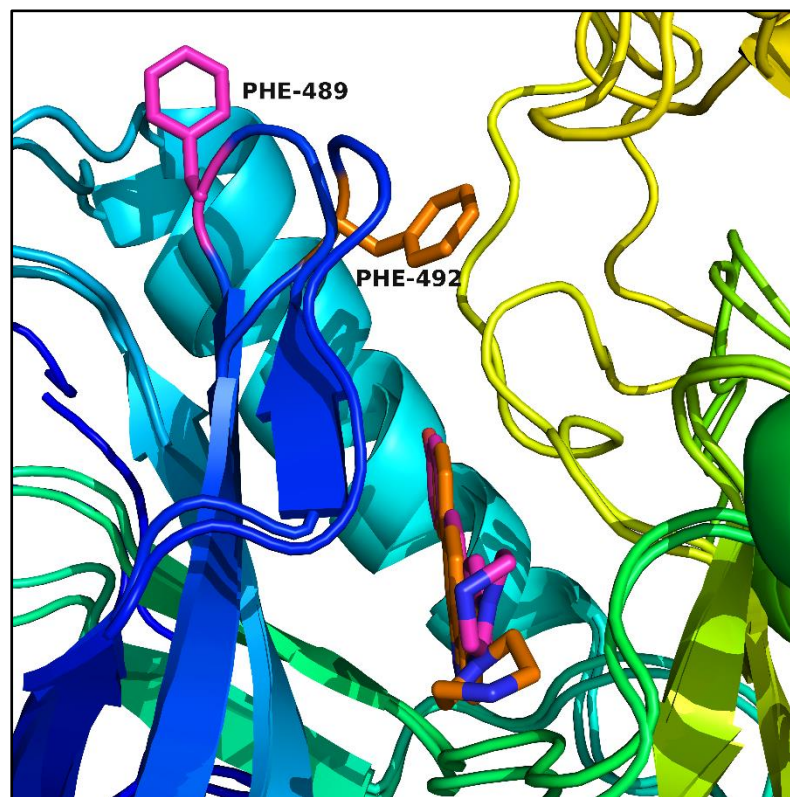


**Figure 4.9:** *Overlay of the FGFR1/164 and FGFR2/164 crystal structures. FGFR1/164 features and FGFR2/164 features are outlined in purple and orange respectively.*

There is a significant difference in the flexible loop regions for the FGFR1/compound **164** and the FGFR2/compound **164** crystal structures. The flexible loop region for the FGFR1/compound **164** structure adopts a fully ‘open-loop’ conformation whilst the loop region in the FGFR2/compound **164** structure adopts a partial ‘closed-loop’ conformation. It is possible that this difference in loop conformations could explain the observed selectivity preference of compound **164** for FGFR2 in that it is more prone to adopt a ‘closed-loop’ system for FGFR2 over FGFR1. It is hypothesised that the ‘closed-loop’ system is more stable due to additional contacts forming between the enzyme and inhibitor, most notably that of Phe492, which forms an edge-to-face interaction with the 6-position phenyl ring of compound **164**, as is observed for compound **115** when bound to FGFR1 (Figure 4.2). However, as outlined previously (Figures 4.2-4.8), this loop region has been shown to be highly flexible and so static conformations of this region of the protein may not reflect the dynamics of this region in the solution phase.

#### 4.4.5.1 Factors Affecting Sub-Type Selectivity

The ligand density maps for compound **164** bound within both FGFR1 and FGFR2 were compared and are shown below (Figure 4.10).

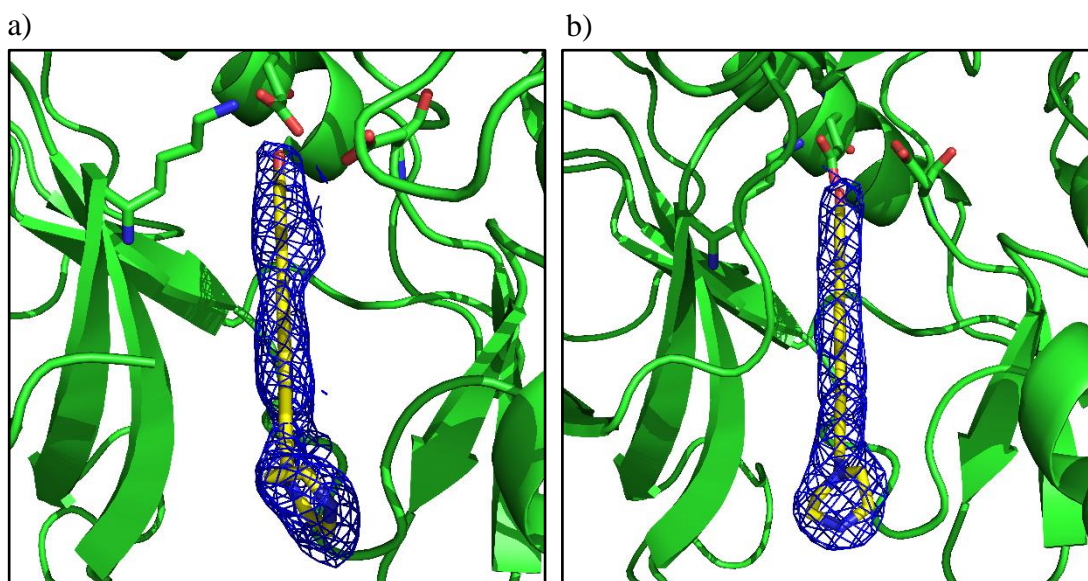


**Figure 4.10:** a) Electron density map for compound **164** bound in FGFR1. b) Electron density map for compound **164** bound in FGFR2.

The ligand electron density map for compound **164** in FGFR1 shows a slight spherical perturbation around the 6-position phenyl ring. As was seen for compound **160** (Figure 4.6), this suggests that compound **164** may adopt multiple conformations within the active site of FGFR1. In contrast, the ligand density map for compound **164** in FGFR2 appears to fit perfectly around the ligand structure in a single defined conformation. It is possible this phenomenon is due to a tighter hydrophobic packing of the ligand within the active site, resulting in restriction of the rotation of the 6-position phenyl ring. The hypothesis that compound **164** forms a tighter binding complex with FGFR2 over FGFR1 is strengthened by comparing the  $IC_{50}$  values of compound **164** (FGFR1: 389 nM and FGFR2: 29 nM) and compound **171** (FGFR1: 204 nM and FGFR2: 77 nM). Compound **171** contains an *ortho* fluorine on the 6-position phenyl ring, which will likely result in an increase in the dihedral angle between the indazole and 6-position phenyl ring. It is thought that this increase in the dihedral angle would be better accommodated in FGFR1 than FGFR2. This may result in a potency increase for FGFR1, and a potency decrease for FGFR2 (due to the increased steric clash between the inhibitor and the enzyme), and can therefore offer rationale for the different selectivity profiles of compounds **164** and **171** against FGFR1/2. However, it is important to note that the resolution of the FGFR2/compound

**164** structure was significantly lower than the FGFR1/compound **164** crystal structure, and therefore rotation of the 6-position phenyl ring may not be resolved within the FGFR2/compound **164** structure.

#### 4.4.6 Crystal Structure Summary

The binding poses for three ligands (**115**, **160** and **164**) bound within FGFR1/2 were analysed which revealed interesting points. The crystallisation of the enzymes resulted in two monomers, ‘chain A and chain B’, which were mostly similar in structure. However, identification of a flexible loop at the entrance to the active site revealed variable morphologies between the different chains. The conformations of this flexible loop region varied from the ‘open-loop’ to the ‘closed-loop’ forms with several intermediate stages outlined. It was concluded that ligand identity primarily dictated what form the flexible loop was to adopt, but other parameters such as variable chain occupancy appear to also contribute. Analysis of the ligand density maps revealed potential reasons for the observed selectivity preference of compound **164** for FGFR2, however, accurate conclusions could not be made due to substantial resolution differences between the FGFR1 and FGFR2 crystal structures.

### 4.5 Utilisation of FGFR1/2 Crystal Structures

#### 4.5.1 Docking of Compound **170**

As outlined in Section 4.1.3, compound **170** is ~21-fold selective for FGFR2 over FGFR1 (Table 4.1). It proved difficult to rationalise this selectivity preference through docking studies. Determination of the X-ray crystal structure of compound **164** bound in both FGFR1 (Figure 4.7) and FGFR2 (Figure 4.8) has opened up the opportunity to use these structures to probe the observed selectivity preference of compound **170** for FGFR2. Compound **170** was docked using the FGFR1/compound **164** crystal structure using Glide (Figure 4.11).



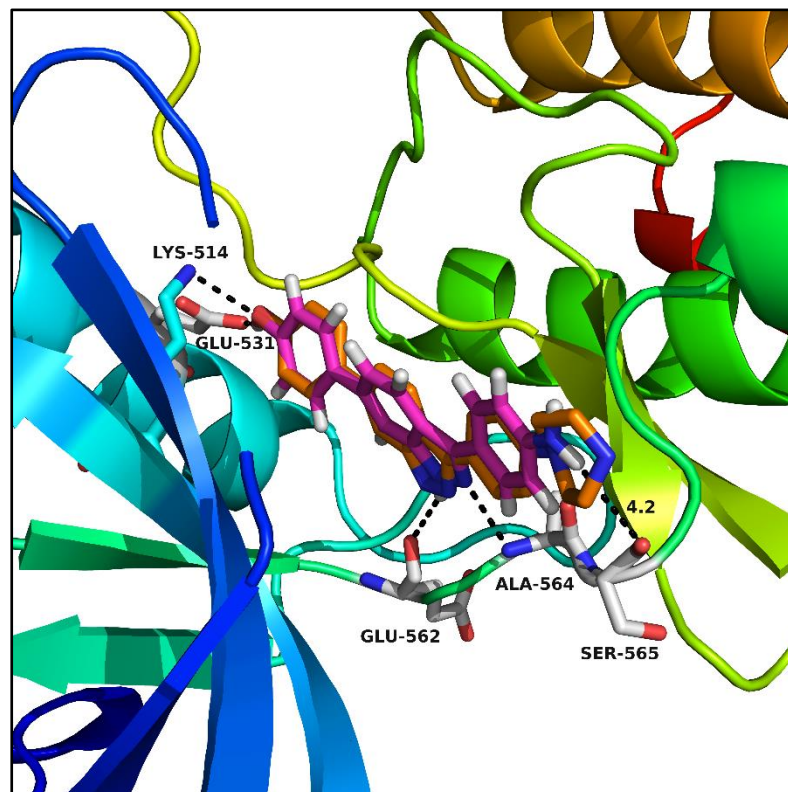


**Figure 4.11:** Compound **170** docked into the FGFR1/compound **164** crystal structure using Glide. Compounds **170** and **164** are shown in purple and orange respectively. H-bonds are outlined in black.

Compound **170** was docked into the FGFR1 crystal structure. A docking grid (Section 1.6.1) covering the active site was generated using the binding position of compound **164** as a template. The docking of compound **170** was carried out using this grid. As expected, compound **170** is predicted to occupy the ATP binding pocket in a similar way to compound **164**. The H-bonds formed between the indazole nitrogens and the hinge binding amino acids Glu562 and Ala564 are predicted to be maintained and the phenol H-bond with Glu531 is also predicted. It is important to note, the amino group for compound **170** present on the 3-position phenyl ring is not expected to H-bond with the backbone carbonyl of Ser565. At 4.2 Å, the distance between the amino group and the carbonyl of Ser565 is considered to be outside the range of an H-bond.<sup>139</sup> Compound **170** was also docked using the FGFR2/compound **164** crystal structure using Glide (Figure 4.12).

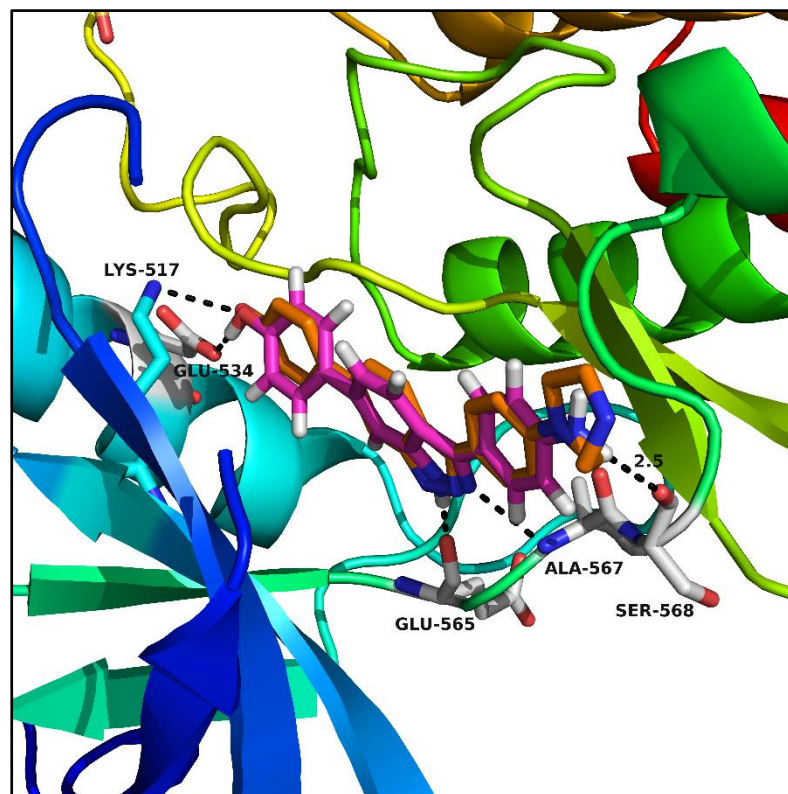


**Figure 4.12:** Compound **170** docked into the FGFR2/compound **164** crystal structure using Glide. Compound **170** and **164** are shown in purple and orange respectively. H-bonds are outlined in black.

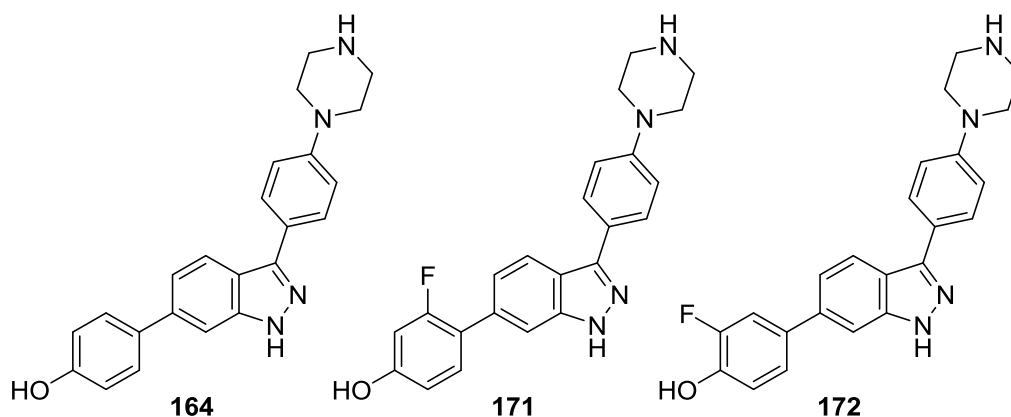
Compound **170** was docked into the FGFR2 crystal structure using the same grid generation method as was seen for the FGFR1/compound **164** co-crystal (Figure 4.12). Compound **170** is predicted to form the same H-bonding interactions with FGFR2 as was predicted in the FGFR1 crystal structure (Figure 4.11). One main difference however, is the distance between the amino group in compound **170** and the backbone carbonyl of Ser568. At 2.5 Å this is now considered a strong H-bond<sup>139</sup> and offers rationale for the observed selectivity preference of compound **170** for FGFR2. Utilisation of this H-bond to design more selective FGFR2 inhibitors is outlined (Section 5.2.1).

## 4.6 Cellular Efficacy

As discussed in Section 4.2.3, compounds **164**, **171** and **172** exhibit sub-micromolar potency against the different FGFR sub-types with compound **164** showing moderate selectivity for FGFR2. It was decided to evaluate the efficacy of these compounds against cancer cells in order to probe the role of the potency/selectivity exhibited against the enzymes within the cellular environment. Three cell lines were chosen for

these studies: JMSU1 (FGFR1-driven), SUM52 (FGFR2/FGFR1-driven) and VMCUB3 (None-FGFR driven).

JMSU1 is a cancer cell line isolated in 1988 from the malignant ascitic fluid of a 75-year-old Japanese man with bladder cancer.<sup>140</sup> It has been shown to overexpress FGFR1 with no indication of FGFR2 overexpression. SUM52 is a cancer cell line that was isolated in 1996 from a malignant pleural effusion specimen from a patient suffering from a metastatic breast carcinoma.<sup>141</sup> It has been shown to overexpress FGFR2 in addition to FGFR1.<sup>71</sup> VMCUB3 is a cancer cell line that was isolated in 1975 from a male patient suffering from a primary transition cell carcinoma present within the bladder.<sup>142</sup> It has not been shown to be FGFR-driven. It was reasoned that use of these cell lines will help establish indicative selectivity profiles of compounds **164**, **171** and **172** against the different FGFR sub-types.



#### 4.6.1 Cell Viability Assay

A reliable way to assess the efficacy of compounds **164**, **171**, and **172** against the chosen cell lines was to conduct the CellTiter-Blue® cell viability (Promega). The assay utilises a homogenous, fluorometric method for estimating the number of viable cells present in a multiwell plate and uses the indicator dye resazurin to measure metabolic capacity of cells (Figure 4.13).



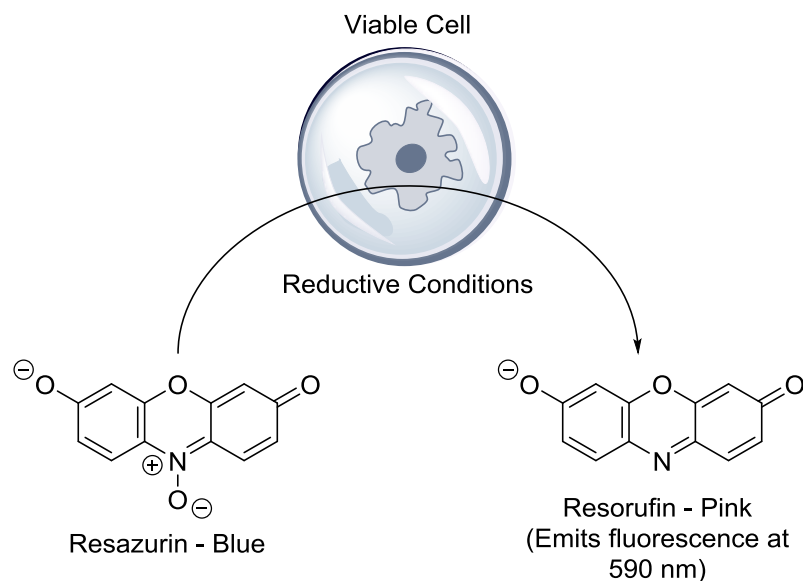
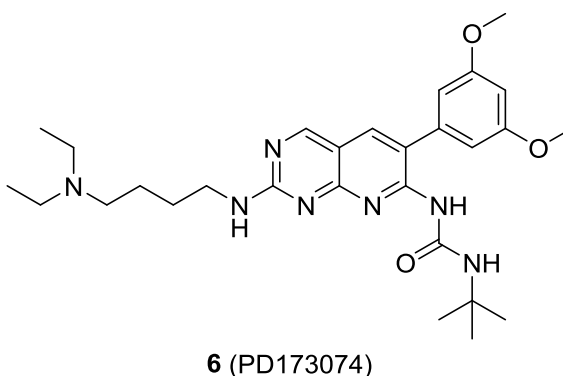


**Figure 4.13:** Basic principle of CellTiter-Blue® assay.

Viable cells, cells that have not been compromised by an inhibitor, are able to reduce resazurin to resorufin. Resazurin's colour is blue and has little intrinsic fluorescence. Once reduced to resorufin however, the colour of the solution of this substance changes to pink and the fluorescence is monitored at 590 nm. The intensity of fluorescence is proportional to the number of viable cells making it possible to obtain dose response curves. In addition to compounds **164**, **171**, and **172**, PD173074 (**6**) (Section 1.5.2.1), was also evaluated against the cell lines to act as a positive control. See Section 6.4 for experimental details.



#### 4.6.1.1 Dose Response Curves-Compound 164

Compound **164** was evaluated against each cell line. Dose response curves were plotted using non-linear curve analysis and  $IC_{50}$  values determined (Figure 4.14).

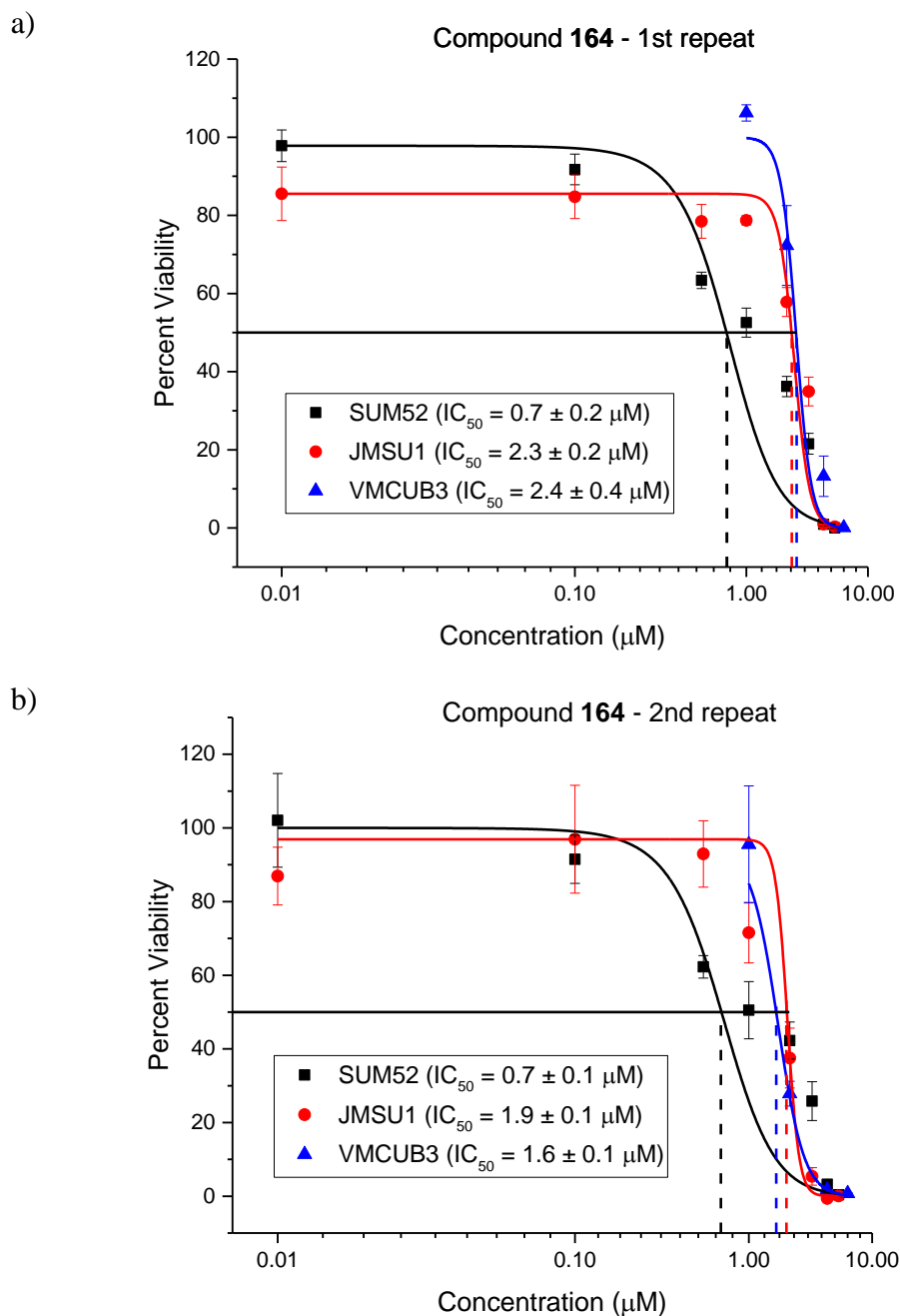


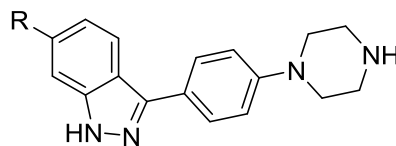
**Figure 4.14:** a) Dose response graph of three cell lines when incubated with compound **164** – 1<sup>st</sup> repeat. b) Dose response graph of three cell lines when incubated with compound **164** – 2<sup>nd</sup> repeat.

Upon analysis of these data, it is apparent that there are minimal differences between both repeated experiments.  $\text{IC}_{50}$  values for compound **164** against SUM52 are  $0.7 \mu\text{M}$  and fall within the error of each repeat. The results for compound **164** against both JMSU1 show roughly similar  $\text{IC}_{50}$  values but each repeat does not fall within the error of each other. The results for VMCUB3 show a similar trend. In order to draw accurate conclusions from the above data a further repeat would need to be carried out. Further graphical data for compounds **171**, **172**, and **6** can be found in Section 8.3.

#### 4.6.1.2 Cell Viability Results for Compounds 164, 171, 172 and 6

Compounds 171, 172 and 6 were also evaluated against each cell line. The results are outlined below (Table 4.3).

**Table 4.3:** Biological evaluation of compounds 164, 171, 172 and 6 against FGFR1-3 and various cancer cell lines.



Compound No.	Structure R	FGFR IC <sub>50</sub> <sup>a</sup> (μM)			SUM52 IC <sub>50</sub> <sup>b</sup> (μM)		JMSU1 IC <sub>50</sub> <sup>b</sup> (μM)		VMCUB3 IC <sub>50</sub> <sup>b</sup> (μM)	
		1	2	3	1 <sup>st</sup>	2 <sup>nd</sup>	1 <sup>st</sup>	2 <sup>nd</sup>	1 <sup>st</sup>	2 <sup>nd</sup>
164		0.39 ± 0.02	0.029 ± 0.02	0.76 ± 0.03	0.70 ± 0.20	0.70 ± 0.10	2.30 ± 0.20	1.90 ± 0.10	2.40 ± 0.40	1.60 ± 0.10
171		0.20 ± 0.03	0.078 ± 0.01	0.92 ± 0.06	0.50 ± 0.10	0.70 ± 0.20	2.00 ± 0.10	2.00 ± 0.20	1.20 ± 0.10	2.10 ± 0.10
172		0.27 ± 0.01	0.26 ± 0.02	0.75 ± 0.05	0.70 ± 0.10	1.50 ± 0.30	3.20 ± 0.10	3.30 ± 0.20	2.30 ± 0.10	2.90 ± 0.20
6	PD173074	0.02 ± 0.01 <sup>c</sup>	NT <sup>d</sup>	0.09 <sup>e</sup>	0.009 ± 0.001	0.007 ± 0.001	0.70 ± 0.10	1.40 ± 0.40	5.80 ± 0.50	3.90 ± 0.70

<sup>a</sup> IC<sub>50</sub> values are given as the mean ± SD of all data points, n = 2. <sup>b</sup> IC<sub>50</sub> values are given as the mean ± SD of all data points, n = 5. <sup>c</sup> Taken from reference 90. <sup>d</sup> NT = not tested. <sup>e</sup> Taken from reference 91 (no reported error).

Compound **164** shows ~14-fold preference for inhibition of FGFR2 over FGFR1 with an IC<sub>50</sub> value of 29 μM against FGFR2. Compound **164** has an IC<sub>50</sub> value of ~0.7 μM against SUM52 (FGFR2-driven). There is a significant drop in potency (~24-fold) when compound **164** is evaluated in a cellular environment. Compound **171** has an IC<sub>50</sub> value of ~0.5-0.7 μM against SUM52 and again shows a drop in potency (~9-fold) when compared to inhibition of FGFR2. Compound **172** exhibits IC<sub>50</sub> values of 0.7 and 1.5 μM for the first repeat and second repeat respectively. A further repeat is needed in order to obtain a more accurate IC<sub>50</sub> value. However, compounds **164**, **171** and **172** all show a drop in potency when compared to the IC<sub>50</sub> values of them against FGFR2. It is possible that the compounds have poor cellular penetration and do not permeate through the cell membrane. Inspection of the results for the positive control (compound **6**) show that it is an extremely potent against SUM52 exhibiting IC<sub>50</sub> values of ~7-9 nM. Interestingly, this compound has an IC<sub>50</sub> value of ~20 nM against FGFR1 and therefore compound **6** does not appear to suffer a drop in potency against SUM52. Perhaps this compound has better cell penetration.

Compounds **164**, **171**, **172** and **6** all show a drop in potency against JMSU1 and VMCUB3 when compared to SUM52. Compound **6** exhibits an IC<sub>50</sub> value of ~0.7-1.4 μM against JMSU1. Compound **6** is a known FGFR1 inhibitor and therefore the poor activity measured against JMSU1 is surprising. Perhaps, JMSU1 may not be the best cell line to evaluate FGFR1 cellular efficacy. Compound **6** exhibits an IC<sub>50</sub> value of ~3.9-5.8 μM against VMCUB3 which is substantially larger than the IC<sub>50</sub> value against SUM52 (~7-9 nM). This suggests that compound **6** has minimal off-target effects. The IC<sub>50</sub> values for **164**, **171** and **172** against both JMSU1 and VMCUB3 are similar. There appears to be a selective preference for SUM52 and may suggest some selective inhibition of FGFR2, however, due to the complexity of cellular systems, further work would need to be carried out in order to verify this.

In summary, as only two repeats were conducted care must be taken when drawing accurate conclusions. In some instances there is no overlap between the error values between repeats, this could be due to the nature of the assay e.g. cell passage – every passage increases the chance of mutations within the cell lines, equipment error – use of different pipettes etc. between different assays and human error – preparation of drug dilution series. There is a small drop in cellular potency when compared to the enzymatic IC<sub>50</sub> values for compounds **164**, **171**, and **172** which may be attributed to the poor cell permeation of the compounds.

## 4.7 Chapter Four Summary

Synthesis and biological evaluation of designed lead compound **164** has outlined ~14-fold selectivity preference for FGFR2 over FGFR1. Several derivatives (**171**, **172**, and **182**) of compound **164** were synthesised and biologically evaluated. This revealed that very subtle single atom changes between compounds **164** and **171/172** resulted in dramatically different selectivity profiles for FGFR1/2. Several of these compounds (**115**, **160**, and **164**) were crystallised within FGFR1 and FGFR2 with the binding poses analysed and potential areas of selectivity rationale identified. Compounds **164**, **171**, and **172** were then evaluated in a cellular environment for efficacy against cancer. It was found that these compounds show a slightly diminished activity in a cellular environment which may be attributed to the poor cell permeation of the compounds. In addition to the lead series, a 'control' amide series was also targeted for synthesis but unfortunately due to time constraints were not synthesised. Future work will focus on alternative syntheses to afford these compounds.

## Chapter Five – Conclusions and Future Work

---

### 5.1 Conclusion – Project Milestones

The aim of this project was to use a structure-based molecular design approach to identify a new series of inhibitors of FGFR kinases. In addition to their obvious potential use as drug leads for the treatment of cancer, it was envisioned that such molecules may also throw light on the factors governing the possible selection by inhibitors between FGFR subtypes. A summary of the project milestones is outlined below (Figure 5.1).

Hit identification using SPROUT yielded fragment **14** which was predicted to bind to the ATP binding site of FGFR1. Subsequent SBDD led to two fragment leads: **31** and **34**, known as the ethoxy and phenolic series respectively. Both these series inhibited FGFR1-3 in the single digit micromolar range. Further rounds of *de novo* design on these fragments led to the design of compound **85** but was found to be inactive upon biological evaluation. Further development of the phenolic series led to compound **158** which exhibited a preference for inhibition against FGFR2.

Further exploration into the inactivity of compound **85** revealed that potency could be regained by incorporating an amide moiety between the indazole and 3-position phenyl ring as shown by compounds **115** and **160**. However, the selectivity preference for FGFR2 was diminished. It was deduced that the governing aspect of FGFR2 selectivity observed for compound **158** was a combination of the phenolic species and the linear aryl-aryl linkage between the indazole and the 3-position phenyl ring. Further development of this core led to compound **164** which exhibited an IC<sub>50</sub> value of 28.5 nM against FGFR2, ~14-fold selectivity preference for FGFR2 over FGFR1. This selectivity preference could not be rationalised through docking studies and therefore crystallisation studies of compound **164** in both FGFR1 and FGFR2 were initiated. In addition to compound **164**, both compounds **115** and **160** were also crystallised in FGFR1. Analysis of the co-crystal structures of compounds **115**, **160**, and **164** bound within FGFR1/2 revealed key structural differences that may offer explanations for the observed selectivity preference of compound **164** for FGFR2. Docking of compound **170** within the FGFR1/2 crystal structures predicted that an H-bond may be present between compound **170** and FGFR2 that was not predicted to exist when this compound is bound to FGFR1.

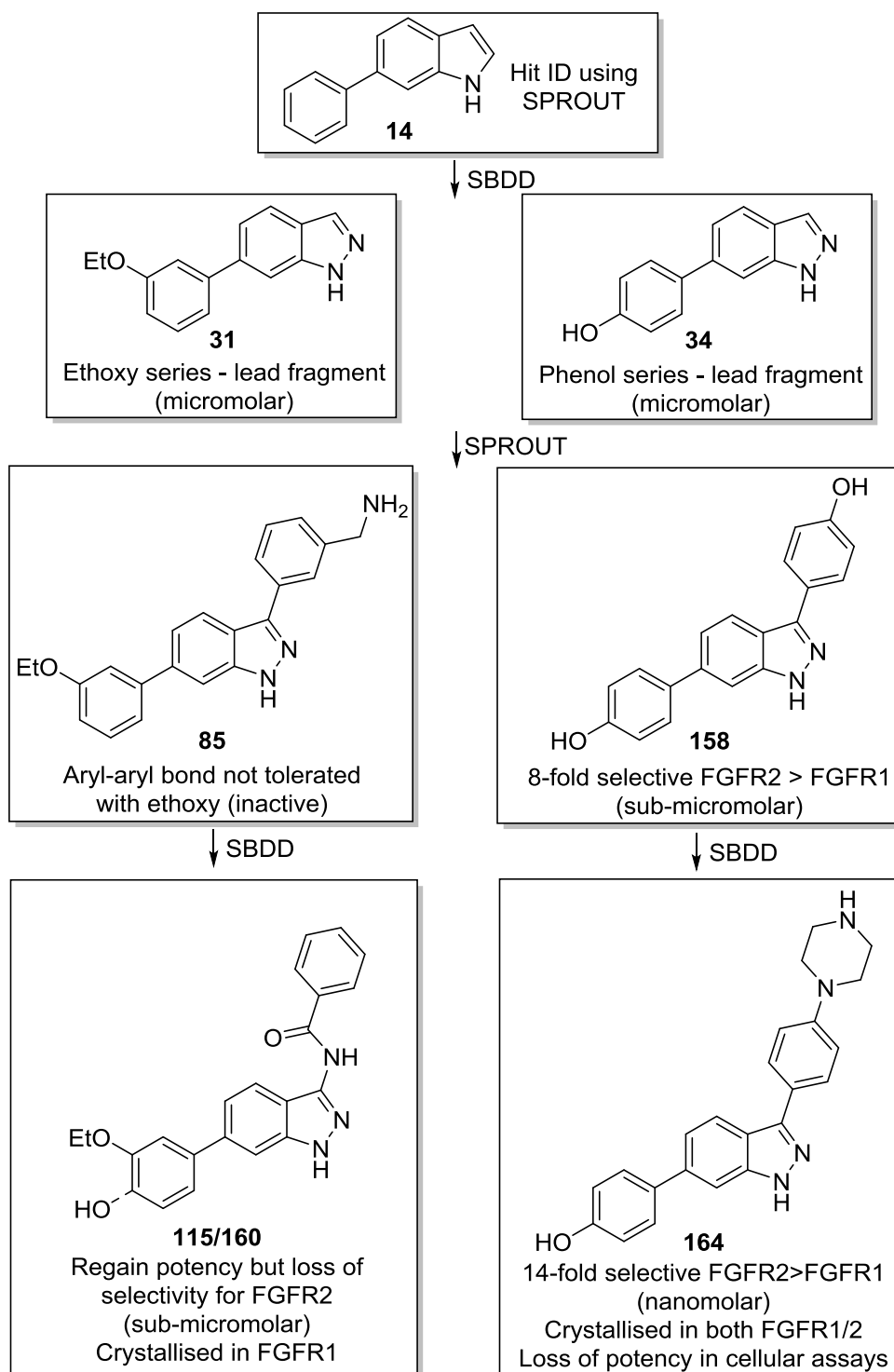


**Figure 5.1:** Project milestones from hit identification to lead compounds.

Finally, it was decided to evaluate the activity of compound **164** within a cellular environment. Compounds **164**, **171**, and **172** were subjected to cell viability assays using three cancer cell lines: SUM52 (FGFR2-driven), JMSU1 (FGFR1-driven) and VMCUB3 (none FGFR-driven). A reduction in potency of the compounds was observed compared to the measured FGFR enzyme inhibition. It was reasoned that

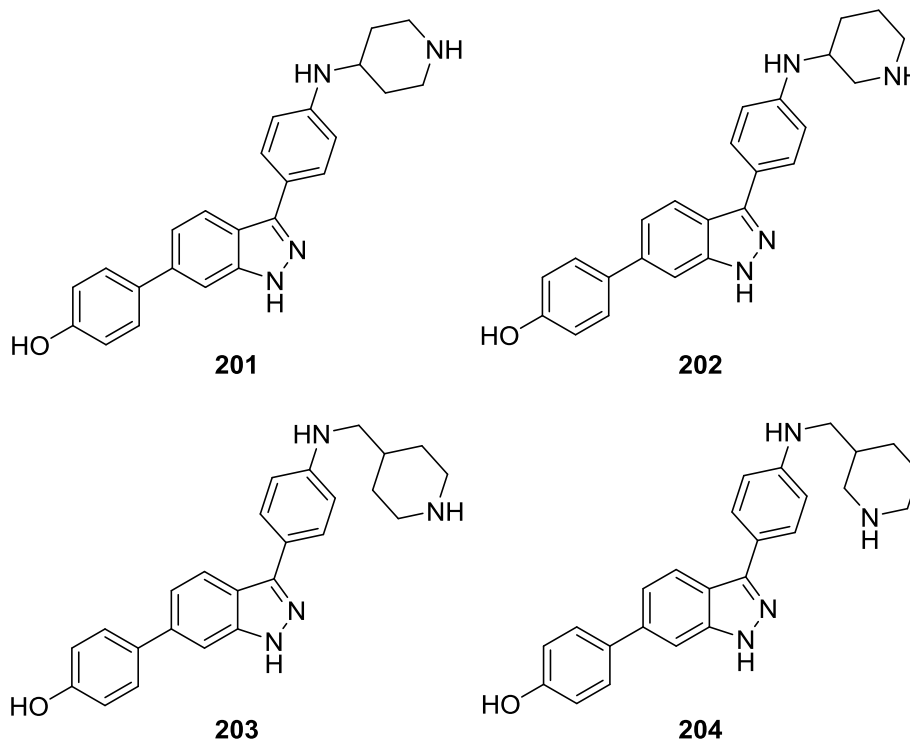
this drop in potency may be due to the poor cell membrane permeation of compounds **164**, **171** and **172**. Further structural modifications would need to be carried out with further experiments in order to address this issue.

The original project aim was to identify a new series of inhibitors for FGFR kinases, with particular focus on designing FGFR sub-type selective compounds. This conclusion outlines that the project aim has been achieved and exceeded, with future prospects of designing more selective inhibitors of FGFR2 promising.

## 5.2 Future Work

### 5.2.1 Design of Selective FGFR2 Inhibitors

Following on from the docking studies of compound **170** (Section 4.5.1), future work could involve the design of a small library of compounds containing an NH donor moiety on the 3-position phenyl ring.



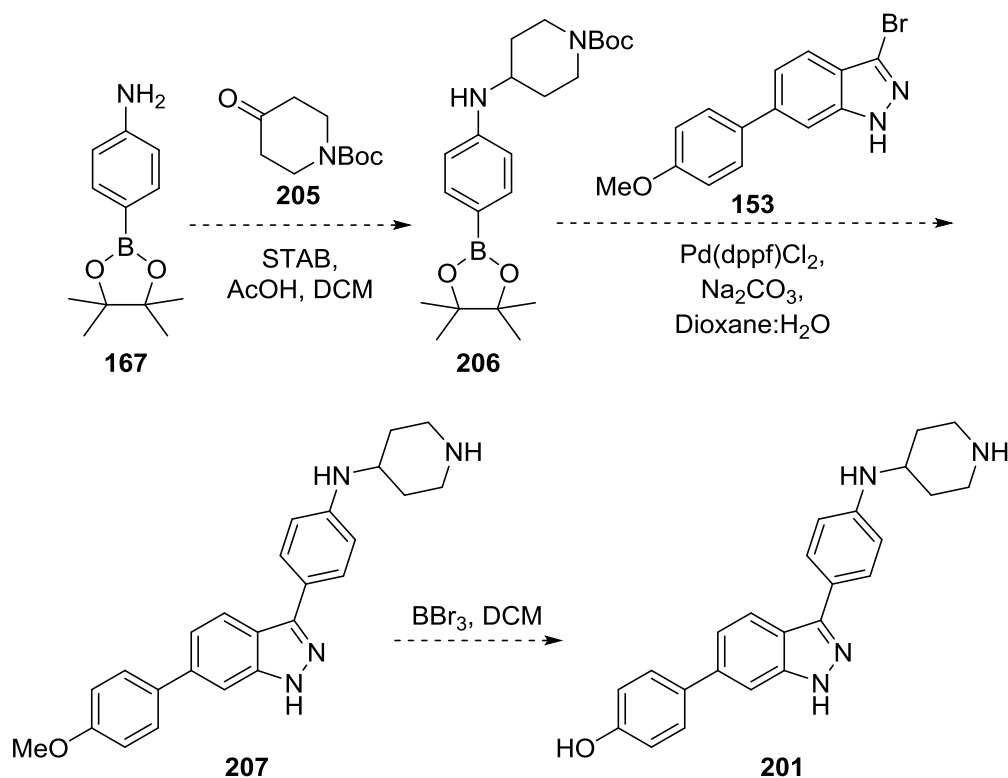
The rationale behind the design of these compounds is: the addition of the piperidine ring will increase the potency of the compound against the FGFRs, and the NH donor present on the phenyl ring would improve selectivity for FGFR2 by means of that described by the docking of compound **170** (Section 4.5.1). Compounds **201** and **202** will establish any differences between the position of the secondary amine present in



the piperidine ring. Compounds **203** and **204** introduce a methylene linker between the amine and the piperidine ring system and will provide additional SARs.

### 5.2.1.1 Proposed Synthesis of Compounds 201-204

Compounds **201-204** could be synthesised using similar chemistry to that described previously (Sections 2.4.1.2 and 4.2.1). The proposed synthesis of compound **201** is outlined below (Scheme 5.1).

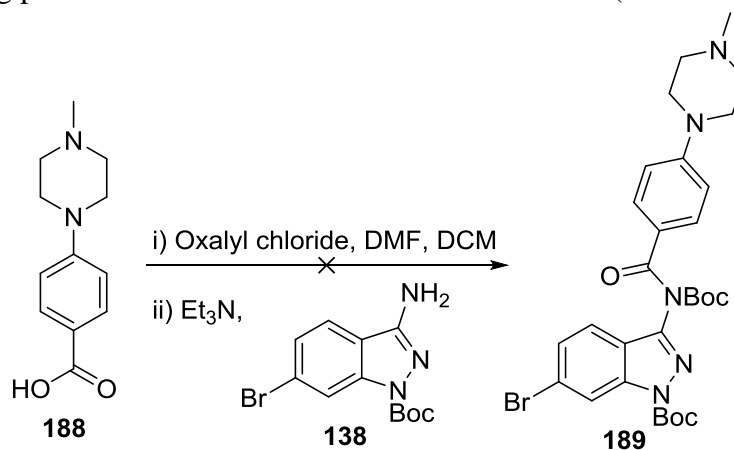


**Scheme 5.1:** Proposed synthesis of compound **201**.

Firstly, compound **206** could be synthesised from compounds **167** and **205** using reductive amination chemistry. Compound **206** could then be coupled with compound **153** using Suzuki chemistry to afford compound **207**. Subsequent deprotection would give access to the final compound **201**. This synthetic route is divergent and should allow rapid access to compounds **201-204**. These compounds could then be evaluated in the FRET-based assay (Section 8.1) to establish their potency against the FGFRs. If inhibitory activity is established, crystallisation of these compounds in both FGFR1/2 could then be carried out and an iterative process of design, synthesis and crystallisation implemented in order to design more potent and selective FGFR2 inhibitors.

### 5.2.2 Synthesis of Amide Series

Section 4.3.1 outlines the attempted synthesis of the ‘amide’ series. It was reasoned that studying the inhibitory behaviour of this series against the FGFRs could yield information as to the role of the presence of the aryl-aryl bond (in the phenolic lead series) upon selectivity (Section 4.3). Several different routes were attempted with one route showing promise. These conditions are outlined below (Scheme 5.2).



**Scheme 5.2:** *In situ acyl chloride formation conditions.*

This synthetic scheme was unsuccessful, however, analysis of the reaction mixture using LC-MS indicated successful formation of the acyl chloride. Future work could include modifications to this synthetic scheme such as: change of base, change of solvent, and/or reaction temperature, with the aim of successfully synthesising the amide bond.

### 5.2.3 Optimisation of ‘Drug-Like’ Properties

Evaluation of compounds **164**, **171**, and **172** in a cellular assay had revealed a drop in potency when compared to the biochemical assay. Structural modifications to the scaffold to improve the ‘drug-like’ properties, such as aqueous solubility and LogP/D could also be carried out while seeking to retain or increase potency/selectivity against FGFR2. A number of possibilities are outlined below (Figure 5.2).

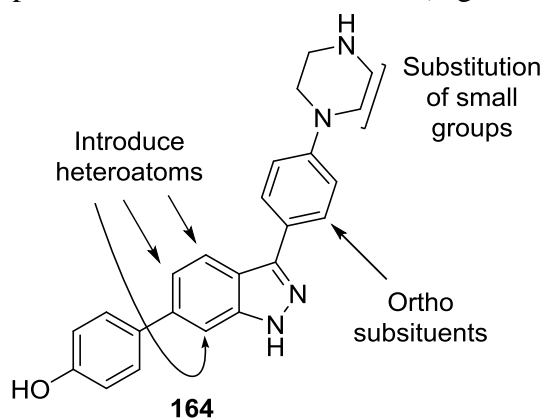


**Figure 5.2:** Potential modifications to improve ‘drug-like’ properties.

Modifications of the 6-phenyl ring have been previously shown (Section 4.2.3) to have dramatic effects upon potency and selectivity against the FGFRs and therefore modifications here are not considered. Three main modifications are presented: introduction of heteroatoms into the indazole ring, introducing a small *ortho*-substituent on the 3-position phenyl ring and introducing chirality into the piperazine ring. These modifications may improve the aqueous solubility, and increase the degree of  $sp^3$  character of atoms within the compound, characteristics which have been shown to be important to successful drug discovery.<sup>143</sup> If these modifications prove successful in improving the activity of the compounds in a cellular environment, the next step would be to evaluate these compounds *in vivo* whilst considering drug metabolism and pharmacokinetics (DMPK) parameters.

## Chapter Six – Experimental

---

### 6.1 Chemistry Experimental

#### 6.1.1 General Procedures and Instrumentation

All reagents were obtained from commercial sources and were used without further purification unless otherwise stated. All microwave reactions were carried out in a CEM Explorer 48 Autosampler using a power of 200 Watts and a pressure of 17 Bar unless otherwise stated. Thin layer chromatography (TLC) analysis was performed using aluminium pre-coated silica gel plates supplied by Merck chemicals and visualised using either ultraviolet light (254 nm), dipping in  $\text{KMnO}_4$  solution or ninhydrin solution and heated, or using an iodine tank.  $R_f$  values are recorded to two decimal places. Normal phase flash column chromatography was carried out using Geduran® silica gel 60 4063  $\mu\text{m}$ . Automated column chromatography (ACC) was performed on an Isolera Biotage® using KP- $\text{C}_{18}$ -HS SNAP 12/30/60 g cartridges using MeCN/water (0-95%) containing 0.1% TFA, at a flow rate of 12-50  $\text{mL min}^{-1}$  for reverse phase or Thomson Single Step 12/40 g pre-packed silica cartridges for normal phase chromatography. LC-MS analysis was performed on a Bruker Daltronics instrument running a gradient of increasing MeCN/water (5-95%) containing 0.1% formic acid, at 1  $\text{mL min}^{-1}$  on a 50  $\times$  20 mm  $\text{C}_{18}$  reverse phase column. Preparative high performance liquid chromatography (HPLC) was performed on an Agilent 1100 Infinity Series equipped with a UV detector and Ascentis Express  $\text{C}_{18}$  reverse phase column using MeCN/water (5-95%) containing 0.1% TFA, at a flow rate of 0.5  $\text{mL min}^{-1}$  over a period of 5-15 minutes. Analytical HPLC was performed on an Agilent 1290 Infinity Series equipped with a UV detector and a Hyperclone  $\text{C}_{18}$  reverse phase column using MeCN/water (5-95%) containing 0.1% TFA, at either 0.5  $\text{mL min}^{-1}$  over a period of five minutes or 1.0  $\text{mL min}^{-1}$  over a period of 30 minutes. Compounds are 100% pure unless otherwise stated. High resolution mass spectrometry (HRMS) was carried out using a Bruker MaXis Impact Time of Flight spectrometer using electro spray ionisation ( $\text{ES}^{+/-}$ ), giving masses correct to four decimal places.

$^1\text{H}$  and  $^{13}\text{C}$  NMR spectra were recorded at 500 MHz and 125 MHz or 100 MHz respectively on either a Bruker Advance 500 or 400 Fourier transform spectrometer. Chemical shifts are reported in ppm and are reported with reference to the residual

solvent peak. Multiplicities are reported with coupling constants and are given to the nearest 0.1 Hz. Apparent multiplicities are denoted by app. Where needed, two-dimensional correlation spectroscopy (2D-COSY), heteronuclear single quantum coherence spectroscopy (HSQC), and heteronuclear multiple bond correlation spectroscopy (HMBC) were used. Ar-q = aromatic quaternary carbon. Infrared spectra (IR) were recorded in the solid phase on a Bruker Alpha Platinum Attenuated Total Reflectance (ATR) Fourier Transform Infrared Spectroscopy (FTIR) spectrometer with vibrational frequencies given in  $\text{cm}^{-1}$ . Melting points were measured on a Stuart SMP30. Elemental analysis was carried out using a Carlo Erba 1108 Elemental Analyzer.

## 6.1.2 General Experimental Methods

### 6.1.2.1 Method A: Suzuki Reactions

A mixture of the chosen halogenated heterocycle (1.0 eq), the chosen boronic acid (1.0-2.0 eq), Pd(dppf)Cl<sub>2</sub>•DCM (0.1 eq) and Na<sub>2</sub>CO<sub>3</sub> (3.0-5.0 eq) were charged with nitrogen in a microwave vial (10 mL or 35 mL). A mixture of dioxane and water ((1:1) 5-20 mL) was degassed for ten minutes and added to the reactants under nitrogen. The reaction mixture was heated to 110 °C for 1-6 h and monitored using LC-MS. The reaction mixture was allowed to cool to 20 °C and EtOAc (5 mL or 15 mL) added and the reaction vessel sonicated, and the solution filtered through a celite pad washing thoroughly with EtOAc. Where needed a 1:1 ratio of DCM–MeOH was used to wash the celite pad. The filtrate was added to water (20 mL or 60 mL) and the organic layer separated. The aqueous layer was extracted with EtOAc (3 × 15 mL or 30 mL) and the combined organic layers washed with brine (10 mL or 30 mL), dried (MgSO<sub>4</sub>), and concentrated *in vacuo* to reveal the crude product. The crude product was purified using either ACC or column chromatography. The appropriate fractions were combined and reduced *in vacuo* to yield a solid.

### 6.1.2.2 Method B: Reductive Aminations

The chosen aldehyde (1.0-1.2 eq) was dissolved in DCM (3-15 mL) and cooled to 0 °C. The chosen secondary amine (1.0-1.2 eq) and glacial AcOH (1 drop) were added and the reaction stirred until complete, monitoring with TLC. STAB (1.6 eq) was added to the reaction and allowed to warm to 20 °C, monitoring using LC-MS. See individual compounds for work up and purification methods.

### 6.1.2.3 Method C: BOC Deprotections

The chosen BOC protected amine (1.0 eq) was dissolved in DCM (0.5-5.0 mL) and an equivalent amount of freshly distilled TFA (0.5-5.0 mL) added and the reaction stirred until complete, monitoring using LC-MS. Upon completion, the reaction mixture was reduced *in vacuo* to reveal the crude product. See individual compounds for purification methods.

### 6.1.2.4 Method D: Methoxy Deprotections

The chosen methoxy containing compound (1.0 eq) was dissolved/suspended in DCM (5-15 mL) at 0 °C. 1 M BBr<sub>3</sub> in DCM (8.0 eq) was added slowly and the reaction stirred at room temperature for 1-24 h until complete, monitoring using LC-MS. See individual compounds for work up and purification methods.

### 6.1.2.5 Method E: Acid Chloride Couplings

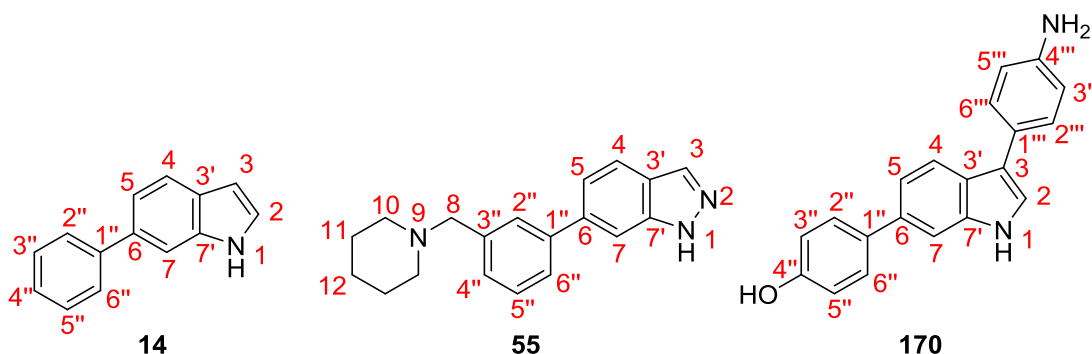
The chosen amine (1.0 eq) was dissolved in DCM (5-20 mL) and DIPEA (2.0-3.5 eq) was added and the reaction stirred for 20 minutes. The chosen acid chloride (1.2-2.0 eq) was added and the reaction stirred, monitoring using LC-MS until complete. See individual compounds for work up and purification methods.

### 6.1.2.6 Method F: Piperazine Cyclisations

The chosen aniline (1.0 eq), bis(2-chloroethyl)amine hydrochloride (1.2 eq) and K<sub>2</sub>CO<sub>3</sub> (2.4 eq) were suspended in <sup>t</sup>BuOH (5-15 mL) and the reaction was heated to 100 °C and stirred, monitoring using LC-MS until complete. See individual compounds for work up and purification methods.

## 6.1.3 Compound Numbering

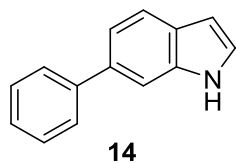
The compounds synthesised in this thesis are numbered in the following way.



## 6.1.4 Compounds

### 6.1.4.1 Chapter Two Compounds

#### Preparation of 6-phenylindole

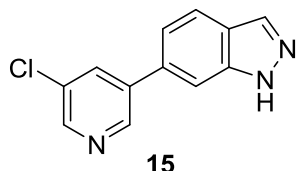


Synthesised using method A using 6-bromoindole (50 mg, 0.26 mmol, 1.0 eq), phenylboronic acid (34 mg, 0.28 mmol, 1.1 eq), Pd(dppf)Cl<sub>2</sub>•DCM (21 mg, 0.026 mmol, 0.1 eq), Na<sub>2</sub>CO<sub>3</sub> (82 mg, 0.77 mmol, 3.0 eq), dioxane 2.5 (mL) and water (2.5 mL)

and the reaction heated for 1 h. The work up proceeded using the smaller volumes of solvents and the organic solvent removed *in vacuo* to reveal a brown solid. The crude product was purified using ACC (gradient 0-40% EtOAc–hexane) and a cream solid obtained (24 mg, 0.12 mmol, 48%). The solid was crystallised from EtOH:H<sub>2</sub>O (1:1). The title compound 14 (20 mg, 0.10 mmol, 40%) was collected as colourless flakes.

**<sup>1</sup>H NMR (500 MHz, CDCl<sub>3</sub>):** 8.18 (1H, br.s, NH), 7.70 (1H, d, *J* 8.5, 4-H), 7.65 (2H, m, 2''-H and 6''-H), 7.60 (1H, s, 7-H), 7.44 (2H, app.t, *J* 7.5, 3''-H and 5''-H), 7.39 (1H, dd, *J* 8.5 and 1.5, 5-H), 7.32 (1H, app.tt, *J* 7.5 and 1.0, 4''-H), 7.23 (1H, app.t, *J* 2.5, 2-H), 6.59-6.57 (1H, m, 3-H); **<sup>13</sup>C NMR (125 MHz, CDCl<sub>3</sub>):** 142.3 (6-C), 136.4 (3'-C), 135.6 (1''-C), 128.7 (3''-C and 5''-C), 127.4 (2''-C and 6''-C), 127.2 (7'-C), 126.6 (4''-C), 124.8 (2-C), 120.9 (4-C), 119.8 (5-C), 109.6 (7-C), 102.5 (3-C); **LC-MS (ES):** RT = 2.05-2.15 min, *m/z* = 194.2 (M+H<sup>+</sup>); **R<sub>f</sub>:** 0.77 (EtOAc); **HPLC:** RT = 3.17 min; ***m/z* (ES+):** Found: 194.0965 (M+H<sup>+</sup>), C<sub>14</sub>H<sub>11</sub>N requires *MH* 194.0964; **IR:ν<sub>max</sub>/cm<sup>-1</sup> (solid):** 3379 (N-H), 3053, 3032, 2983, 2920, 2850, 1442; **M.pt:** 158.4-160.7 °C (Lit 158-161 °C)<sup>144</sup>.

#### Preparation of 6-(5-chloropyridin-3-yl)-1*H*-indazole

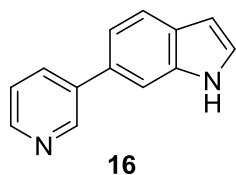


Synthesised using method A using 6-bromo-1*H*-indazole (200 mg, 1.02 mmol, 1.0 eq), 5-chloro-3-pyridineboronic acid (177 mg, 1.12 mmol, 1.1 eq), Pd(dppf)Cl<sub>2</sub>•DCM (83 mg, 0.102 mmol, 0.1 eq), Na<sub>2</sub>CO<sub>3</sub> (325 mg, 3.08 mmol,

3.0 eq), dioxane (10 mL) and water (10 mL) and the reaction heated for 1 h. The work up proceeded using the larger volumes of solvents and the organic solvent removed *in vacuo* to reveal a brown solid. The crude product was purified using column chromatography (1:1 EtOAc–hexane). The title compound 15 (14 mg, 0.06 mmol, 6%) was collected as off-brown needles.

**<sup>1</sup>H NMR (500 MHz, CDCl<sub>3</sub>):** 10.47 (1H, br.s, NH), 8.79 (1H, d, *J* 2.0, 2''-H), 8.60 (1H, d, *J* 2.0, 4''-H), 8.16 (1H, s, 3-H), 7.94 (1H, app.t, *J* 2.0, 6''-H), 7.89 (1H, d, *J* 8.0, 4-H), 7.69 (1H, d, *J* 1.5, 7-H), 7.38 (1H, dd, *J* 8.0 and 1.5, 5-H); **<sup>13</sup>C NMR (125 MHz, CDCl<sub>3</sub>):** 147.5 (4''-C), 146.4 (2''-C), 140.5 (3'-C), 138.1 (6-C), 135.3 (1''-C), 135.1 (3-C), 134.6 (6''-C), 132.3 (5''-C), 123.3 (7'-C), 121.9 (4-C), 120.8 (5-C), 108.3 (7-C); **LC-MS (ES):** RT = 1.70-1.83 min, *m/z* = 229.9 (M+H<sup>+</sup>); **R<sub>f</sub>:** 0.39 (EtOAc); **HPLC:** RT = 2.02 min; ***m/z* (ES+):** Found: 230.0473 (M+H<sup>+</sup>), C<sub>12</sub>H<sub>8</sub>ClN<sub>3</sub> requires *MH* 230.0480; **IR:ν<sub>max</sub>/cm<sup>-1</sup> (solid):** 3266 (N-H), 3091, 3053, 2958, 2851, 1628; **M.pt:** 183.8-185.0 °C.

#### Preparation of 6-pyridin-3-yl-indole

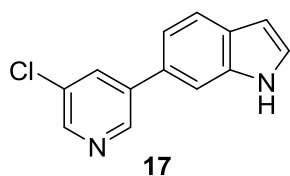


Synthesised using method A using 6-bromoindole (200 mg, 1.03 mmol, 1.0 eq), 3-pyridineboronic acid (139 mg, 1.13 mmol, 1.1 eq), Pd(dppf)Cl<sub>2</sub>•DCM (84 mg, 0.103 mmol, 0.1 eq) and Na<sub>2</sub>CO<sub>3</sub> (326 mg, 3.08 mmol, 3.0 eq), dioxane (10 mL) and water

(10 mL) and the reaction heated for 1 h. The work up proceeded using the larger volumes of solvents and the organic solvent removed *in vacuo* to reveal a purple oil. The crude product was purified using column chromatography (gradient 30-70% EtOAc–hexane) and a green semi-solid obtained. The solid was further purified using column chromatography (1:1 EtOAc–hexane). The title compound 16 (71 mg, 0.37 mmol, 36%) was collected as a cream solid.

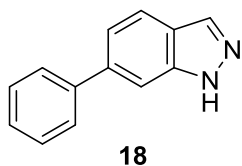
**<sup>1</sup>H NMR (500 MHz, CDCl<sub>3</sub>):** 8.95 (1H, d, *J* 1.5, 2''-H), 8.88 (1H, br.s, NH), 8.57 (1H, dd, *J* 5.0 and 1.5, 4''-H), 7.93 (1H, ddd, *J* 8.0, 2.5 and 1.5, 6''-H), 7.74 (1H, d, *J* 8.0, 4-H), 7.62 (1H, app.s, 7-H), 7.37-7.34 (2H, m, 5-H and 5''-H), 7.29 (1H, app.t, *J* 3.0, 2-H), 6.61-6.58 (1H, m, 3-H); **<sup>13</sup>C NMR (125 MHz, CDCl<sub>3</sub>):** 148.5 (2''-C), 147.7 (4''-C), 137.9 (6-C), 136.5 (3'-C), 134.6 (6''-C), 131.8 (1''-C), 127.9 (7'-C), 125.5 (2-C), 123.6 (5''-C), 121.4 (4-C), 119.4 (5-C), 109.7 (7-C), 102.6 (3-C); **LC-MS (ES):** RT = 1.31-1.52 min, *m/z* = 195.0 (M+H<sup>+</sup>); **R<sub>f</sub>:** 0.34 (EtOAc); **HPLC:** RT = 1.40 min; ***m/z* (ES+):** Found: 195.0915 (M+H<sup>+</sup>), C<sub>13</sub>H<sub>10</sub>N<sub>2</sub> requires *MH* 195.0917; **IR:ν<sub>max</sub>/cm<sup>-1</sup> (solid):** 3162 (N-H), 3125, 3087, 2918, 1575; **M.pt:** 145.4-146.4 °C (Lit 146-148 °C)<sup>145</sup>.



Preparation of 6-(5-chloropyridin-3-yl)-indole

Synthesised using method A using 6-bromoindole (200 mg, 1.03 mmol, 1.0 eq), 5-chloro-3-pyridineboronic acid (178 mg, 1.13 mmol, 1.1 eq), Pd(dppf)Cl<sub>2</sub>•DCM (84 mg, 0.103 mmol, 0.1 eq), Na<sub>2</sub>CO<sub>3</sub> (326 mg, 3.08 mmol, 3.0 eq), dioxane (10 mL) and water (10 mL) and the reaction heated for 1 h. The work up proceeded using the larger volumes of solvents and the organic solvent removed *in vacuo* to reveal a brown solid. The crude product was purified using ACC (gradient 20-50% EtOAc–hexane). The title compound 17 (51 mg, 0.22 mmol, 22%) was collected as a pale yellow solid.

**<sup>1</sup>H NMR (500 MHz, CDCl<sub>3</sub>):** 8.79 (1H, d, *J* 1.5, 2''-H), 8.57 (1H, br.s, NH), 8.52 (1H, d, *J* 2.0, 4''-H), 7.91 (1H, app.t, *J* 2.0, 6''-H), 7.74 (1H, d, *J* 8.0, 4-H), 7.58 (1H, d, *J* 1.5, 7-H), 7.32 (1H, dd, *J* 8.0 and 1.5, 5-H), 7.29 (1H, app.t, *J* 2.5, 2-H), 6.61-6.59 (1H, m, 3-H); **<sup>13</sup>C NMR (125 MHz, CDCl<sub>3</sub>):** 146.4 (4''-C), 146.2 (2''-C), 139.1 (6-C), 136.3 (3'-C), 134.2 (6''-C), 132.2 (5''-C), 130.2 (1''-C), 128.3 (7'-C), 125.8 (2-C), 121.6 (4-C), 119.3 (5-C), 109.8 (7-C), 102.8 (3-C); **LC-MS (ES):** RT = 1.89-2.14 min, *m/z* = 228.9 (M+H<sup>+</sup>); **R<sub>f</sub>:** 0.62 (EtOAc); **HPLC:** RT = 2.35 min (96%); ***m/z* (ES<sup>+</sup>):** Found: 229.0529 (M+H<sup>+</sup>), C<sub>13</sub>H<sub>8</sub>ClN<sub>2</sub> requires *MH* 229.0527; **IR:ν<sub>max</sub>/cm<sup>-1</sup> (solid):** 3381 (N-H), 3174, 3093, 2957, 2851, 1569; **M.pt:** 137.2-138.3 °C.

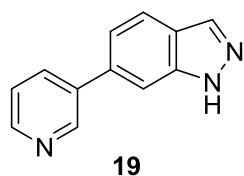
Preparation of 6-phenyl-1H-indazole

Synthesised using method A using 6-bromo-1H-indazole (50 mg, 0.26 mmol, 1.0 eq), phenylboronic acid (34 mg, 0.28 mmol, 1.1 eq), Pd(dppf)Cl<sub>2</sub>•DCM (21 mg, 0.026 mmol, 0.1 eq) Na<sub>2</sub>CO<sub>3</sub> (81 mg, 0.77 mmol, 3.0 eq), dioxane (2.5 mL) and water (2.5 mL) and the reaction heated for 1 h. The work up proceeded using the smaller volumes of solvents and the organic solvent removed *in vacuo* to reveal a brown oil. The crude product was purified using ACC (gradient 0-50% EtOAc–hexane). The title compound 18 (26 mg, 0.13 mmol, 52%) was collected as off-white needles.

**<sup>1</sup>H NMR (500 MHz, CDCl<sub>3</sub>):** 10.49 (1H, br.s, NH), 8.12 (1H, s, 3-H), 7.81 (1H, d, *J* 8.5, 4-H), 7.66-7.64 (3H, m, 7-H, 2''-H and 6''-H), 7.48-7.45 (2H, m, 3''-H and 5''-H), 7.43 (1H, dd, *J* 8.5 and 1.5, 5-H), 7.40-7.36 (1H, m, 4''H); **<sup>13</sup>C NMR (125 MHz, CDCl<sub>3</sub>):** 141.3 (1''-C), 140.8 (3'-C), 140.5 (6-C), 134.9 (3-C), 128.9

(3''-C and 5''-C), 127.6 (4''-C), 127.6 (2''-C and 6''-C), 122.5 (7'-C), 121.5 (5-C), 121.1 (4-C), 107.8 (7-C); **LC-MS (ES)**: RT = 1.82-1.99 min, m/z = 195.0 (M+H<sup>+</sup>); **R<sub>f</sub>**: 0.32 (1:1 EtOAc–petrol); **HPLC**: RT = 2.63 min; **m/z (ES<sup>+</sup>)**: Found: 195.0918 (M+H<sup>+</sup>), C<sub>13</sub>H<sub>10</sub>N<sub>2</sub> requires *MH* 195.0917; **IR**:  $\nu_{\text{max}}/\text{cm}^{-1}$  (**solid**): 3295 (N-H), 2956, 2920, 2850, 1623; **M.pt**: 152.4-154.1 °C.

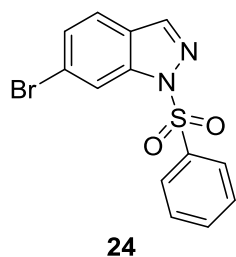
#### Preparation of 6-pyridin-3-yl-1*H*-indazole



Synthesised using method A using 6-bromo-1*H*-indazole (200 mg, 1.02 mmol, 1.0 eq), 3-pyridineboronic acid (138 mg, 1.12 mmol, 1.1 eq), Pd(dppf)Cl<sub>2</sub>•DCM (82 mg, 0.102 mmol, 0.1 eq), Na<sub>2</sub>CO<sub>3</sub> (325 mg, 3.06 mmol, 3.0 eq), dioxane (10 mL) and water (10 mL) and the reaction heated for 1 h. The work up proceeded using the larger volumes of solvents and the organic solvent removed *in vacuo* to reveal a brown solid. The crude product was purified using column chromatography (gradient 20-100% EtOAc–hexane) and a yellow solid obtained. The solid was crystallised from EtOAc. The title compound 19 (77 mg, 0.39 mmol, 39%) was collected as light brown plates.

**<sup>1</sup>H NMR (500 MHz, CDCl<sub>3</sub>)**: 11.54 (1H, br.s, NH), 8.96 (1H, d, *J* 2.0, 2''-H), 8.65 (1H, dd, *J* 4.5 and 1.5, 4''-H), 8.16 (1H, s, 3-H), 7.95 (1H, app.dt, *J* 7.5 and 2.0, 6''-H), 7.87 (1H, d, *J* 8.0, 4-H), 7.70 (1H, s, 7-H), 7.42-7.38 (2H, m, 5-H and 5''-H); **<sup>13</sup>C NMR (125 MHz, CDCl<sub>3</sub>)**: 148.5 (4''-C), 148.5 (2''-C), 140.8 (3'-C), 137.1 (1''-C), 136.6 (6-C), 135.0 (6''-C), 134.8 (3-C), 123.7 (5''-C), 123.0 (7'-C), 121.7 (4-C), 120.8 (5-C), 108.3 (7-C); **LC-MS (ES)**: RT = 1.12-1.25 min, m/z = 196.0 (M+H<sup>+</sup>); **R<sub>f</sub>**: 0.20 (EtOAc); **HPLC**: RT = 1.01 min; **m/z (ES<sup>+</sup>)**: Found: 196.0874 (M+H<sup>+</sup>), C<sub>12</sub>H<sub>9</sub>N<sub>3</sub> requires *MH* 196.0869; **IR**:  $\nu_{\text{max}}/\text{cm}^{-1}$  (**solid**): 3149 (N-H), 3037, 2909; **M.pt**: 163.5-164.3 °C.

#### Preparation of 1-(benzenesulfonyl)-6-bromo-1*H*-indazole

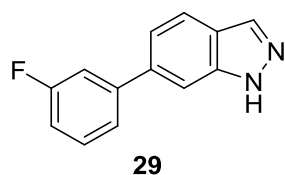


NaH (146 mg, 3.66 mmol, 1.5 eq; 60% dispersion in oil) was dissolved in DMF (2 mL) and stirred for ten minutes at 0 °C. A solution of 6-bromo-1*H*-indazole (300 mg, 2.44 mmol, 1.0 eq) in DMF (3 mL) was added dropwise and left to stir for five minutes. Benzenesulfonyl chloride (0.34 mL, 2.68 mmol, 1.1 eq) was degassed and added slowly to the reaction mixture. The reaction was allowed to warm

to 20 °C and stirred for 24 h, monitoring using LC-MS. The mixture was diluted with EtOAc (15 mL) and added to water (30 mL) and the organic layer was separated. The aqueous layer was extracted with EtOAc (2 × 15 mL) and the combined organic layers washed with brine (20 mL), dried (MgSO<sub>4</sub>), and concentrated *in vacuo* to reveal a cream solid. The crude product was crystallised from EtOH. The title compound 24 (332 mg, 0.98 mmol, 40%) as bright yellow needles.

**<sup>1</sup>H NMR (500 MHz, CDCl<sub>3</sub>):** 8.43 (1H, app.dt, *J* 1.0 and 0.5, 7-H), 8.14 (1H, d, *J* 0.5, 3-H), 8.02-7.99 (2H, m, 2''-H and 6''-H), 7.60 (1H, app.tt, *J* 7.5 and 2.0, 4''-H), 7.55 (1H, dd, *J* 8.5 and 0.5, 4-H), 7.51-7.44 (2H, m, 3''-H and 5''-H), 7.45 (1H, dd, *J* 8.5 and 1.5, 5-H); **<sup>13</sup>C NMR (125 MHz, CDCl<sub>3</sub>):** 141.1 (3-C), 140.1 (7'-C), 137.4 (1''-C), 134.5 (4''-C), 129.4 (3''-C and 5''-C), 128.0 (2''-C and 6''-C), 127.7 (5-C), 124.6 (3'-C), 124.1 (6-C), 122.3 (4-C), 116.2 (7-C); **LC-MS (ES):** RT = 2.09-2.27 min, *m/z* = 339.0 (MBr<sup>81+</sup>); **R<sub>f</sub>:** 0.48 (1:1 EtOAc–petrol); **HPLC:** RT = 2.42 min ***m/z* (ES+):** Found: 336.9652 (M+H<sup>+</sup>), C<sub>13</sub>H<sub>9</sub>BrN<sub>2</sub>O<sub>2</sub>S requires *MH* 336.9641; **IR:ν<sub>max</sub>/cm<sup>-1</sup>(solid):** 3107, 1602, 1569; **M.pt:** 161.3-163.1 °C.

#### Preparation of 6-(3-fluorophenyl)-1*H*-indazole



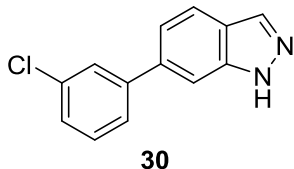
Synthesised using method A using 6-bromo-1*H*-indazole (200 mg, 1.02 mmol, 1.0 eq), 3-fluorophenylboronic acid (214 mg, 1.53 mmol, 1.5 eq), Pd(dppf)Cl<sub>2</sub>•DCM (83 mg, 0.102 mmol, 0.1 eq), Na<sub>2</sub>CO<sub>3</sub> (325 mg, 3.06 mmol, 3.0 eq),

dioxane (10 mL) and water (10 mL) and the reaction heated for 1 h. The work up proceeded using the larger volumes of solvents and the organic solvent removed *in vacuo* to reveal a brown oil. The crude product was purified using column chromatography (gradient 5-10% EtOAc–hexane). The title compound 29 (76 mg, 0.36 mmol, 35%) was collected as a colourless powder.

**<sup>1</sup>H NMR (500 MHz, CD<sub>3</sub>OD):** 7.95 (1H, d, *J* 1.0, 3-H), 7.72 (1H, dd, *J* 8.5 and 1.0, 4-H), 7.63-7.62 (1H, m, 7-H), 7.40-7.28 (4H, m, 5''-H, 6''-H, 2''-H and 5-H), 7.14-7.10 (1H, m, 4''-H), NH not observed; **<sup>13</sup>C NMR (125 MHz, CD<sub>3</sub>OD):** 164.6 (d, *J* 244.3, 3''-C), 145.1 (d, *J* 7.6, 1''-C), 142.1 (3'-C), 140.0 (d, *J* 2.3, 6-C), 134.9 (3 C), 131.5 (d, *J* 8.4, 5''-C), 124.2 (d, *J* 2.8, 6''-C), 123.8 (7'-C), 122.2 (4-C), 121.7 (5-C), 115.0 (d, *J* 22.4, 4''-C), 115.0 (d, *J* 21.4, 2''-C), 109.2 (7-C); **LC-MS (ES):** RT = 1.86-1.98 min, *m/z* = 213.0 (M+H<sup>+</sup>); **R<sub>f</sub>:** 0.48 (7:3 EtOAc–petrol); **HPLC:** RT = 2.72 min; ***m/z* (ES+):** Found: 213.0826 (M+H<sup>+</sup>), C<sub>13</sub>H<sub>9</sub>FN<sub>2</sub> requires *MH*

213.0823; **IR:**  $\nu_{\max}/\text{cm}^{-1}$  (**solid**): 3190 (N-H), 3071, 2963, 2925, 2462, 1627, 1616; **M.pt:** 114.4-116.3 °C.

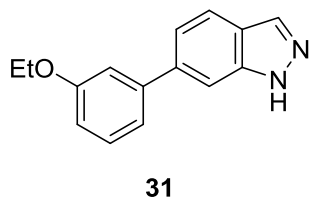
Preparation of 6-(3-chlorophenyl)-1*H*-indazole



Synthesised using method A using 6-bromo-1*H*-indazole (200 mg, 1.02 mmol, 1.0 eq), 3-chlorophenylboronic acid (175 mg, 1.12 mmol, 1.1 eq), Pd(dppf)Cl<sub>2</sub>•DCM (83 mg, 0.102 mmol, 0.1 eq), Na<sub>2</sub>CO<sub>3</sub> (325 mg, 3.06 mmol, 3.0 eq), dioxane (10 mL) and water (10 mL) and the reaction heated for 1 h. The work up proceeded using the larger volumes of solvents and the organic solvent removed *in vacuo* to reveal a brown semi-solid. The crude product was purified using column chromatography (5:95 EtOAc–hexane). The title compound 30 (42 mg, 0.18 mmol, 18%) was collected as colourless platelets.

**<sup>1</sup>H NMR (500 MHz, CD<sub>3</sub>OD):** 7.96 (1H, d, *J* 1.0, 3-H), 7.73 (1H, dd, *J* 8.5 and 1.0, 4-H), 7.62-7.61 (1H, m, 7-H), 7.57 (1H, app.t, *J* 2.0, 2''-H), 7.50 (1H, ddd, *J* 8.0, 2.0 and 1.0, 6''-H), 7.33 (1H, app.t, *J* 8.0, 5''-H), 7.29 (1H, dd, *J* 8.5 and 1.5, 5-H), 7.26 (1H, ddd, *J* 8.0, 2.0 and 1.0, 4''-H), NH not observed; **<sup>13</sup>C NMR (125 MHz, CD<sub>3</sub>OD):** 144.7 (6-C), 142.1 (3'-C), 139.8 (1''-C), 135.7 (3''-C), 134.7 (3-C), 131.3 (5''-C), 128.3 (2''-C), 126.8 (4''-C), 126.8 (6''-C), 123.9 (7'-C), 122.3 (4-C), 121.7 (5-C), 109.2 (7-C); **LC-MS (ES):** RT = 1.85-1.96 min, *m/z* = 228.9 (M+H<sup>+</sup>); **R<sub>f</sub>:** 0.51 (7:3 EtOAc–petrol); **HPLC:** RT = 2.98 min; ***m/z* (ES+):** Found: 229.0528 (M+H<sup>+</sup>), C<sub>13</sub>H<sub>9</sub>ClN<sub>2</sub> requires *MH* 229.0527; **IR:**  $\nu_{\max}/\text{cm}^{-1}$  (**solid**): 3438 (N-H), 3228, 3138, 3056, 2920, 2410, 1625, 1594, 1564; **M.pt:** 99.8-101.9 °C.

Preparation of 6-(3-ethoxyphenyl)-1*H*-indazole

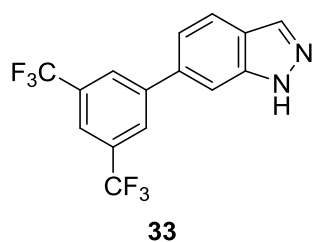


Synthesised using method B using 6-bromo-1*H*-indazole (112 mg, 0.57 mmol, 1.0 eq), 3-ethoxyphenylboronic acid (190 mg, 1.14 mmol, 2.0 eq), Pd(dppf)Cl<sub>2</sub>•DCM (46 mg, 0.057 mmol, 0.1 eq), Na<sub>2</sub>CO<sub>3</sub> (182 mg, 1.72 mmol, 3.0 eq), dioxane (10 mL) and water (10 mL) and the reaction heated for 1 h. LC-MS indicated the presence of starting material however 3-ethoxyphenylboronic acid was no longer available so 3-carboxyboronic acid (94 mg, 1.02 mmol, 1.0 eq) was added and the reaction put on for 30 minutes to consume the starting material. The work up proceeded using the larger volumes of solvents and the organic solvent removed *in vacuo* to reveal a brown solid. The crude product was purified using column

chromatography (2:3 EtOAc–hexane) and an off-white solid obtained. The solid was crystallised from toluene. The title compound 31 (52 mg, 0.218 mmol, 39%) was collected as colourless needles.

**<sup>1</sup>H NMR (500 MHz, CDCl<sub>3</sub>):** 10.54 (1H, br.s, NH), 8.16 (1H, d, *J* 1.0, 3-H), 7.84 (1H, dd, *J* 8.5 and 1.0, 4-H), 7.70-7.69 (1H, m, 7-H), 7.47 (1H, dd, *J* 8.5 and 1.5, 5-H), 7.42 (1H, app.t, *J* 8.0, 5''-H), 7.26 (1H, ddd, *J* 8.0, 1.5 and 1.0, 6''-H), 7.22 (1H, app.t, *J* 2.5, 2''-H), 6.96 (1H, ddd, *J* 8.0, 1.5 and 1.0, 4''-H), 4.15 (2H, q, *J* 7.0, CH<sub>2</sub>), 1.50 (3H, t, *J* 7.0, CH<sub>3</sub>); **<sup>13</sup>C NMR (125 MHz, CDCl<sub>3</sub>):** 159.4 (3''-C), 142.8 (1''-C), 140.7 (3'-C), 140.4 (6-C), 134.9, (3-C) 129.8 (5''-C), 122.6 (7'-C), 121.4 (5-C), 121.0 (4-C), 120.0 (6''-C), 114.1 (2''-C), 113.5 (4''-C), 107.8 (7-C), 63.6 (CH<sub>2</sub>), 14.91 (CH<sub>3</sub>); **LC-MS (ES):** RT = 1.90-2.11 min, *m/z* = 239.2 (M+H<sup>+</sup>); **R<sub>f</sub>:** 0.47 (7:3 EtOAc–petrol); **HPLC:** RT = 2.34 min; ***m/z* (ES<sup>+</sup>):** Found: 239.1191 (M+H<sup>+</sup>), C<sub>15</sub>H<sub>14</sub>N<sub>2</sub>O requires *MH* 239.1179; **IR:ν<sub>max</sub>/cm<sup>-1</sup> (solid):** 3162 (N-H), 3131, 3089, 2977, 2919, 1626, 1570, 1299; **M.pt:** 104.3-105.5 °C; **Found:** C, 75.2; H, 5.90; N, 11.6; C<sub>15</sub>H<sub>14</sub>N<sub>2</sub>O requires C, 75.6; H, 5.92; N, 11.8%.

#### Preparation of 6-(3,5-bis(trifluoromethyl)phenyl)-1*H*-indazole



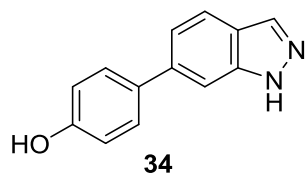
Synthesised using method A using 6-bromo-1*H*-indazole (200 mg, 1.02 mmol, 1.0 eq), 3,5-bis(trifluoromethyl)phenylboronic acid (527 mg, 2.04 mmol, 2.0 eq), Pd(dppf)Cl<sub>2</sub>•DCM (83 mg, 0.102 mmol, 0.1 eq), Na<sub>2</sub>CO<sub>3</sub> (325 mg, 3.06 mmol, 3.0 eq),

dioxane (10 mL) and water (10 mL) and the reaction heated for 1 h. The work up proceeded using the larger volumes of solvents and the organic solvent removed *in vacuo* to reveal a brown oil. The crude product was purified using column chromatography (2:3 EtOAc–hexane) and an off-white solid obtained. The solid was crystallised from toluene. The title compound 33 (144 mg, 0.436 mmol, 43%) was collected as shiny colourless plates.

**<sup>1</sup>H NMR (500 MHz, CDCl<sub>3</sub>):** 10.54 (1H, br.s, NH), 8.18 (1H, s, 3-H), 8.09 (2H, s, 2''-H and 6''-H), 7.91 (1H, dd, *J* 8.5 and 1.0, 4-H), 7.90 (1H, app.s, 4''-H), 7.74 (1H, s, 7-H), 7.43 (1H, dd, *J* 8.5 and 1.5, 5-H); **<sup>13</sup>C NMR (125 MHz, CDCl<sub>3</sub>):** 143.5 (1''-C), 140.5 (3'-C), 137.3 (6-C), 135.1 (3-C), 132.2 (q, *J* 33.3, 3''-C), 127.7 (q, *J* 7.0, 2''-C and 6''-C), 123.4 (7'-C), 123.3 (q, *J* 270.9, CF<sub>3</sub>), 122.0 (4-C), 121.2 (sept, *J* 3.8, 4''-C), 120.9 (5-C), 108.4 (7-C); **LC-MS (ES):** RT = 2.08-2.31 min,

$m/z = 331.0$  ( $M+H^+$ ); **R<sub>f</sub>**: 0.5 (1:1 EtOAc–petrol); **HPLC**: RT = 3.48 min; **m/z (ES-)**: Found: 329.0529 (M-H),  $C_{15}H_8F_6N_2$  requires *M-H* 329.0519; **IR**:  $\nu_{max}/cm^{-1}$  (solid): 3171 (N-H), 3135, 3023, 2930, 2871, 1623, 1520, 1383, 1276; **M.pt**: 169.3-170.1 °C.

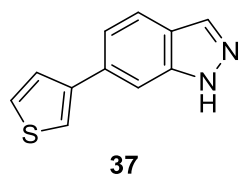
#### Preparation of 4-(1*H*-indazol-6-yl)phenol



Synthesised using method A using 6-iodo-1*H*-indazole (300 mg, 1.23 mmol, 1.0 eq), 4-hydroxyphenylboronic acid (339 mg, 2.46 mmol, 2.0 eq), Pd(dppf)Cl<sub>2</sub>•DCM (100 mg, 0.123 mmol, 0.1 eq), Na<sub>2</sub>CO<sub>3</sub> (391 mg, 3.69 mmol, 3.0 eq), dioxane (10 mL) and water (10 mL) and the reaction heated for 1 h. The work up proceeded using the larger volumes of solvents and the organic solvent removed *in vacuo* to reveal a brown solid. The crude product was purified using column chromatography (3:7 EtOAc–hexane). The title compound 34 (13 mg, 0.062 mmol, 5%) was collected as a yellow powder.

**<sup>1</sup>H NMR (500 MHz, DMSO-*d*<sub>6</sub>)**: 13.00 (1H, s, NH), 9.53 (1H, s, OH), 8.03 (1H, s, 3-H), 7.76 (1H, d, *J* 8.5, 4-H), 7.60 (1H, s, 7-H), 7.53 (2H, d, *J* 8.5, 2''-H and 6''-H), 7.33 (1H, dd, *J* 8.5 and 1.5, 5-H), 6.86 (2H, d, *J* 8.5, 3''-H and 5''-H); **<sup>13</sup>C NMR (125 MHz, DMSO-*d*<sub>6</sub>)**: 157.1 (4''-C), 140.7 (3''-C), 138.4 (6-C), 133.3 (3-C), 131.4 (1''-C), 128.2 (2''-C and 6''-C), 121.6 (7''-C), 120.7 (4-C), 119.8 (5-C), 115.7 (3''-C and 5''-C), 106.5 (7-C); **LC-MS (ES)**: RT = 1.59-1.81 min,  $m/z = 211.0$  ( $M+H^+$ ); **R<sub>f</sub>**: 0.34 (7:3 EtOAc–petrol); **HPLC**: RT = 1.88 min; **m/z (ES+)**: Found: 211.0866 ( $M+H^+$ ),  $C_{13}H_{10}N_2O$  requires *MH* 211.0866; **IR**:  $\nu_{max}/cm^{-1}$  (solid): 3264 (N-H), 2954, 2921, 2654, 1729, 1606; **M.pt**: 309.8-310.9 °C.

#### Preparation of 6-(thiophen-3-yl)-1*H*-indazole

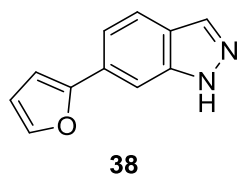


Synthesised using method A using 6-bromo-1*H*-indazole (200 mg, 1.02 mmol, 1.0 eq), 3-thienylboronic acid (224 mg, 1.75 mmol, 1.7 eq), Pd(dppf)Cl<sub>2</sub>•DCM (83 mg, 0.102 mmol, 0.1 eq), Na<sub>2</sub>CO<sub>3</sub> (325 mg, 3.06 mmol, 3.0 eq), dioxane (10 mL) and water (10 mL) and the reaction heated for 1 h. The work up proceeded using the larger volumes of solvents and the organic solvent removed *in vacuo* to reveal a brown solid. The crude product was purified using column chromatography (1:1 EtOAc–hexane) and an off-white solid obtained. The solid was crystallised from

toluene *via* hot filtration. The title compound 37 (100 mg, 0.50 mmol, 49%) was collected as off-white fluffy crystals.

**<sup>1</sup>H NMR (500 MHz, DMSO-*d*<sub>6</sub>):** 13.07 (1H, s, NH), 8.04 (1H, s, 3-H), 7.92 (1H, dd, *J* 3.0 and 1.5, 2''-H), 7.78-7.76 (2H, m, 7H and 4-H), 7.65 (1H, dd, *J* 5.0 and 3.0, 4''-H), 7.62 (1H, dd, *J* 5.0 and 1.5, 5''-H), 7.48 (1H, dd, *J* 8.5 and 1.5, 5-H); **<sup>13</sup>C NMR (125 MHz, DMSO-*d*<sub>6</sub>):** 141.8 (1''-C), 140.5 (3'-C), 133.4 (3-C), 133.1 (6-C), 127.1 (4''-C), 126.5 (5''-C), 122.0 (7'-C), 121.3 (2''-C), 120.9 (4-C), 119.7 (5-C), 106.7 (7-C); **LC-MS (ES):** RT = 1.78-2.00 min, *m/z* = 200.9 (M+H<sup>+</sup>); **R<sub>f</sub>:** 0.44 (7:3 EtOAc–petrol); **HPLC:** RT = 2.46 min; ***m/z* (ES<sup>+</sup>):** Found: 201.0482 (M+H<sup>+</sup>), C<sub>11</sub>H<sub>8</sub>N<sub>2</sub>S requires *MH* 201.0481; **IR:  $\nu_{\text{max}}$ /cm<sup>-1</sup> (solid):** 3270 (N-H), 3187, 3101, 3052, 2930, 1621, 1470, 1360; **M.pt:** 207.9-209.5 °C; **Found:** C, 65.7; H, 3.90; N, 13.7; C<sub>11</sub>H<sub>8</sub>N<sub>2</sub>S requires C, 66.0; H, 4.03; N, 14.0%.

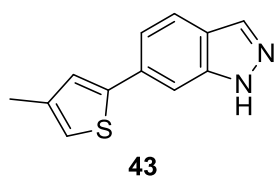
#### Preparation of 6-(furan-2-yl)-1*H*-indazole



Synthesised using method A using 6-bromo-1*H*-indazole (200 mg, 1.02 mmol, 1.0 eq), 3-furylboronic acid (229 mg, 2.04 mmol, 2.0 eq), Pd(dppf)Cl<sub>2</sub>•DCM (83 mg, 0.102 mmol, 0.1 eq), Na<sub>2</sub>CO<sub>3</sub> (325 mg, 3.06 mmol, 3.0 eq), dioxane (10 mL)

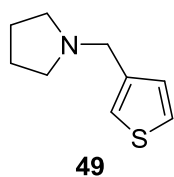
and water (10 mL) and the reaction heated for 1 h. The work up proceeded using the larger volumes of solvents and the organic solvent removed *in vacuo* to reveal a brown solid. The crude product was purified using column chromatography (2:3 EtOAc–hexane) and an off-white solid obtained. The solid was crystallised from toluene *via* hot filtration. The title compound 38 (107 mg, 0.58 mmol, 57%) was collected as a pale yellow powder.

**<sup>1</sup>H NMR (500 MHz, DMSO-*d*<sub>6</sub>):** 13.09 (1H, s, NH), 8.05 (1H, s, 3-H), 7.79-7.76 (3H, m, 3''-H, 4-H and 7-H), 7.48 (1H, dd, *J* 8.5 and 1.5, 5-H), 7.01 (1H, d, *J* 3.5, 5''-H), 6.61 (1H, dd, *J* 3.5 and 1.5, 4''-H); **<sup>13</sup>C NMR (125 MHz, DMSO-*d*<sub>6</sub>):** 153.3 (1''-C), 143.0 (3''-C), 140.2 (3'-C), 133.6 (3-C), 128.1 (6-C), 122.1 (7'-C), 121.1 (4-C), 117.0 (5-C), 112.1 (4''-C), 106.3 (5''-C), 104.0 (7-C); **LC-MS (ES):** RT = 1.74-1.98 min, *m/z* = 185.0 (M+H<sup>+</sup>); **R<sub>f</sub>:** 0.47 (7:3 EtOAc–petrol); **HPLC:** RT = 2.31 min; ***m/z* (ES<sup>+</sup>):** Found: 185.0708 (M+H<sup>+</sup>), C<sub>11</sub>H<sub>8</sub>N<sub>2</sub>O requires *MH* 185.0709; **IR:  $\nu_{\text{max}}$ /cm<sup>-1</sup> (solid):** 3173 (N-H), 3142, 3098, 2997, 2920, 2831, 1681, 1592, 1437; **M.pt:** 143.4-145.1 °C.

Preparation of 6-(4-methylthiophen-2-yl)-1H-indazole

Synthesised using method A using 6-bromo-1H-indazole (200 mg, 1.02 mmol, 1.0 eq), 4-methylthiophene-2-boronic acid (288 mg, 2.04 mmol, 2.0 eq), Pd(dppf)Cl<sub>2</sub>•DCM (83 mg, 0.102 mmol, 0.1 eq), Na<sub>2</sub>CO<sub>3</sub> (325 mg, 3.06 mmol, 3.0 eq), dioxane (10 mL) and water (10 mL) and the reaction heated for 1 h. The work up proceeded using the larger volumes of solvents and the organic solvent removed *in vacuo* to reveal a brown oil. The crude product was purified using column chromatography (1:1 EtOAc–hexane) and a yellow solid obtained. The solid was crystallised from toluene. The title compound 43 (136 mg, 0.625 mmol, 63%) was collected as off-white granules.

**<sup>1</sup>H NMR (500 MHz, CDCl<sub>3</sub>):** 8.02 (1H, d, *J* 1.0, 3-H), 7.69 (1H, dd, *J* 8.5 and 1.0, 4-H), 7.64-7.63 (1H, m, 7-H), 7.39 (1H, dd, *J* 8.5 and 1.5, 5-H), 7.15 (1H, d, *J* 1.5, 5''-H), 6.85 (1H, app.p, *J* 1.5, 3''-H), 2.26 (3H, app.d, *J* 1.0, CH<sub>3</sub>), NH not observed; **<sup>13</sup>C NMR (125 MHz, CDCl<sub>3</sub>):** 144.1 (1''-C), 140.7 (3'-C), 138.8 (4''-C), 134.9 (3-C), 133.5 (6-C), 126.2 (5''-C), 122.6 (7'-C), 121.2 (4-C), 120.6 (3''-C), 120.1 (5-C), 106.1 (7-C), 15.9 (CH<sub>3</sub>); **LC-MS (ES):** RT = 1.88-2.08 min, *m/z* = 215.1 (M+H<sup>+</sup>); **R<sub>f</sub>:** 0.51 (7:3 EtOAc–petrol); **HPLC:** RT = 2.27 min (95%); ***m/z* (ES+):** Found: 215.0633 (M+H<sup>+</sup>), C<sub>12</sub>H<sub>10</sub>N<sub>2</sub>S requires *MH* 215.0637; **IR:** ν<sub>max</sub>/cm<sup>-1</sup> (solid): 3289 (N-H), 3162, 2919, 1626, 1570, 1473; **M.pt:** 151.8-153.1 °C; **Found:** C, 67.1; H, 4.70; N, 12.9; C<sub>12</sub>H<sub>10</sub>N<sub>2</sub>S requires C, 67.3; H, 4.70; N, 13.1%.

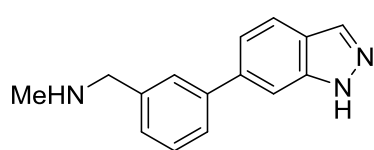
Preparation of 1-(thiophene-3-ylmethyl)pyrrolidine

Synthesised using method B using 3-thiophene-carboxaldehyde (2.0 mL, 22.8 mmol, 1.0 eq), pyrrolidine (2.29 mL, 27.4 mmol, 1.2 eq), glacial AcOH (1 drop), STAB (7.74 g, 36.5 mmol, 1.6 eq) and DCM (5 mL). The reaction was stirred for 2 h. Upon completion, 2 M NaOH<sub>(aq)</sub> (100 mL) was added to the reaction mixture and the organic layer separated. The aqueous layer was extracted with DCM (3 × 40 mL) and the combined organic layers washed with 2M NaOH<sub>(aq)</sub> (50 mL), brine (50 mL), dried (MgSO<sub>4</sub>) and reduced *in vacuo* to reveal a brown oil. The crude product was purified using Kugelrohr distillation (temp: 52 °C, pressure: 1 × 10<sup>-2</sup> Torr). The title compound 49 (3.17 g, 19.0 mmol, 83%) was collected as a colourless oil.



**<sup>1</sup>H NMR (500 MHz, CDCl<sub>3</sub>):** 7.20 (1H, dd, *J* 5.0 and 3.0, 5-H), 7.07 (1H, m, 2-H), 7.02 (1H, dd, *J* 5.0 and 1.0, 4-H), 3.56 (2H, s, CH<sub>2</sub>Ar), 2.49-2.44 (4H, m, 2-H and 5-H pyrrole), 1.76-1.71 (4H, m, 3-H and 4-H pyrrole); **<sup>13</sup>C NMR (125 MHz, CDCl<sub>3</sub>):** 140.3 (3-C), 128.4 (4-C), 125.2 (5-C), 122.3 (2-C), 55.2 (CH<sub>2</sub>Ar), 54.2 (2-C and 5-C pyrrole), 23.5 (3-C and 4-C pyrrole); **LC-MS (ES):** RT = 0.33-0.55 min, *m/z* = 168.1 (M+H<sup>+</sup>); **R<sub>f</sub>:** 0.40 (99:1 EtOAc–7.0 M NH<sub>3</sub> in MeOH); **HPLC:** RT = 0.73 min (86% - degrades overtime); ***m/z* (ES<sup>+</sup>):** Found: 168.0841 (M+H<sup>+</sup>), C<sub>9</sub>H<sub>13</sub>NS requires *MH* 168.0845; **IR: *v*<sub>max</sub>/cm<sup>-1</sup> (solid):** 2992, 2977, 2919, 2776, 1626, 1477.

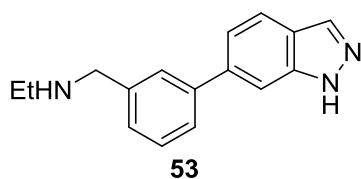
Preparation of {[3-(1*H*-indazol-6-yl)phenyl]methyl}(methyl)amine



**52**

Synthesised using method B using 3-(1*H*-indazol-6-yl)benzaldehyde (**59**) (100 mg, 0.45 mmol, 1.0 eq), 40% methylamine in water (47 μL, 0.54 mmol, 1.2 eq), AcOH (1 drop), STAB (153 mg, 0.72 mmol, 1.6 eq) and DCM (3 mL). The reaction was stirred for 24 h. 2 M NaOH<sub>(aq)</sub> (10 mL) was added to the reaction mixture and the organic layer separated. The aqueous layer was extracted with DCM (3 × 20 mL) and the combined organic layers dried (MgSO<sub>4</sub>) and reduced *in vacuo*. No further purification carried out. The title compound 52 (47 mg, 0.19 mmol, 44%) was collected as an off-white foamy solid.

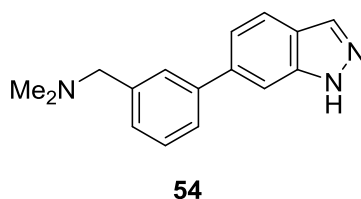
**<sup>1</sup>H NMR (500 MHz, CD<sub>3</sub>OD):** 7.95 (1H, d, *J* 1.0, 3-H), 7.73 (1H, dd, *J* 8.5 and 0.8, 4-H), 7.64 (1H, s, 7-H), 7.57 (1H, s, 2''-H), 7.50 (1H, app.dt, *J* 7.7 and 1.2, 5-H), 7.36-7.32 (2H, m, 5''-H and 6''-H), 7.24 (1H, d, *J* 7.5, 4''-H), 3.69 (2H, s, CH<sub>2</sub>), 2.32 (3H, s, CH<sub>3</sub>), NHs not observed; **<sup>13</sup>C NMR (125 MHz, CD<sub>3</sub>OD):** 142.9 (1''-C), 142.3 (7'-C), 141.4 (6-C), 140.9 (3''-C), 134.6 (3-C), 130.0 (5''-C), 128.7 (2''-C), 128.7 (4''-C), 127.4 (5-C), 123.6 (3'-C), 122.0 (4-C), 122.0 (6''-C), 109.0 (7-C), 56.3 (CH<sub>2</sub>), 35.5 (CH<sub>3</sub>); **LC-MS (ES):** RT = 1.33-1.63 min, *m/z* = 238.2 (M+H<sup>+</sup>); **R<sub>f</sub>:** 0.24 (1:2:7 7.0 M NH<sub>3</sub> in MeOH–petrol–EtOAc); **HPLC:** RT = 1.51 min; ***m/z* (ES<sup>+</sup>):** Found: 238.1339 (M+H<sup>+</sup>), C<sub>15</sub>H<sub>16</sub>N<sub>3</sub> requires *MH* 238.1344; **IR: *v*<sub>max</sub>/cm<sup>-1</sup> (solid):** 3169 (NH), 2919, 2844, 2791, 1625.

Preparation of ethyl({[3-(1*H*-indazol-6-yl)phenyl]methyl})amine

Synthesised using method B using 3-(1*H*-indazol-6-yl)benzaldehyde (**59**) (100 mg, 0.45 mmol, 1.0 eq), 70% ethylamine in water (51  $\mu$ L, 0.54 mmol, 1.2 eq), AcOH (1 drop), STAB (153 mg, 0.72 mmol, 1.6 eq) and

DCM (3 mL). The reaction was stirred for 48 h. 2 M NaOH<sub>(aq)</sub> (10 mL) was added to the reaction mixture and the organic layer separated. The aqueous layer was extracted with DCM (3  $\times$  20 mL) and the combined organic layers dried (MgSO<sub>4</sub>) and reduced *in vacuo*. No further purification carried out. The title compound 53 (66 mg, 0.26 mmol, 58%) was collected as an off-white foamy solid.

**<sup>1</sup>H NMR (500 MHz, CD<sub>3</sub>OD):** 8.03 (1H, d, *J* 1.0, 3-H), 7.77 (1H, dd, *J* 8.5 and 0.8, 4-H), 7.71 (1H, s, 7-H), 7.63 (1H, app.t, *J* 1.6, 2''-H), 7.52 (1H, app.dt, *J* 7.7 and 1.4, 5-H), 7.38-7.33 (2H, m, 5''-H and 6''-H), 7.29 (1H, d, *J* 7.6, 4''-H), 3.76 (2H, s, CH<sub>2</sub>), 2.63 (2H, q, *J* 7.1, CH<sub>2</sub>CH<sub>3</sub>), 1.12 (3H, t, *J* 7.1, CH<sub>3</sub>), NHs not observed; **<sup>13</sup>C NMR (125 MHz, CD<sub>3</sub>OD):** 142.8 (1''-C), 142.3 (7'-C), 141.3 (6-C), 141.2 (3''-C), 134.7 (3-C), 130.0 (5''-C), 128.6 (2''-C), 128.6 (4''-C), 127.3 (5-C), 123.6 (3'-C), 122.0 (4-C), 122.0 (6''-C), 109.0 (7-C), 54.3 (CH<sub>2</sub>), 44.1 (CH<sub>2</sub>CH<sub>3</sub>), 14.6 (CH<sub>3</sub>); **LC-MS (ES):** RT = 1.34-1.53 min, *m/z* = 252.2 (M+H<sup>+</sup>); **R<sub>f</sub>:** 0.36 (1:2:7 7.0 M NH<sub>3</sub> in MeOH –petrol–EtOAc); **HPLC:** RT = 1.56 min; ***m/z* (ES+):** Found: 252.1495 (M+H<sup>+</sup>), C<sub>16</sub>H<sub>18</sub>N<sub>3</sub> requires *MH* 252.1501; **IR:**  $\nu_{\max}/\text{cm}^{-1}$  (solid): 3168 (N-H), 2962, 2832, 1625.

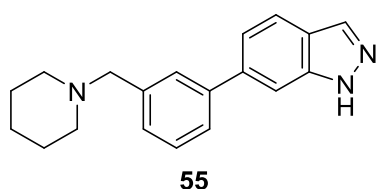
Preparation of {[3-(1*H*-indazol-6-yl)phenyl]methyl}dimethylamine

Synthesised using method B using 3-(1*H*-indazol-6-yl)benzaldehyde (**59**) (100 mg, 0.45 mmol, 1.0 eq), dimethylamine hydrochloride (44 mg, 0.54 mmol, 1.2 eq), AcOH (1 drop), STAB (153 mg, 0.72 mmol,

1.6 eq) and DCM (3 mL). The reaction was stirred for 48 h. 2 M NaOH<sub>(aq)</sub> (10 mL) was added to the reaction mixture and the organic layer separated. The aqueous layer was extracted with DCM (3  $\times$  20 mL) and the combined organic layers washed with brine (20 mL), dried (MgSO<sub>4</sub>) and reduced *in vacuo*. No further purification carried out. The title compound 54 (70 mg, 0.28 mmol, 62%) was collected as an off-white foamy solid.

**<sup>1</sup>H NMR (500 MHz, CD<sub>3</sub>OD):** 7.95 (1H, d, *J* 0.9, 3-H), 7.72 (1H, dd, *J* 8.5 and 0.8, 4-H), 7.64 (1H, s, 7-H), 7.55 (1H, s, 2''-H), 7.52-7.50 (1H, m, 5-H), 7.36-7.33 (2H, m, 5''-H and 6''-H), 7.21 (1H, d, *J* 7.6, 4''-H), 3.45 (2H, s, CH<sub>2</sub>), 2.18 (6H, s, CH<sub>3</sub>), NH not observed; **<sup>13</sup>C NMR (125 MHz, CD<sub>3</sub>OD):** 142.8 (1''-C), 142.2 (7'-C), 141.3 (6-C), 139.4 (3''-C), 134.4 (3-C), 129.9 (4''-C), 129.7 (5''-C), 129.7 (2''-C), 127.6 (5-C), 123.6 (3'-C), 122.0 (4-C), 121.9 (6''-C), 108.9 (7-C), 64.9 (CH<sub>2</sub>), 45.2 (CH<sub>3</sub>); **LC-MS (ES):** RT = 1.35-1.53 min, *m/z* = 252.2 (M+H<sup>+</sup>); **R<sub>f</sub>:** 0.48 (1:2:7 7.0 M NH<sub>3</sub> in MeOH–petrol–EtOAc); **HPLC:** RT = 1.51 min; ***m/z* (ES<sup>+</sup>):** Found: 252.1495 (M+H<sup>+</sup>), C<sub>16</sub>H<sub>18</sub>N<sub>3</sub> requires *MH* 252.1501; **IR:ν<sub>max</sub>/cm<sup>-1</sup> (solid):** 2942 (N-H), 2772, 2712, 1625; **M.pt:** 37.2-39.7 °C.

Preparation of 6-[3-(piperidin-1-ylmethyl)phenyl]-1*H*-indazole

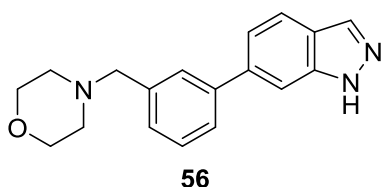


Synthesised using method B using 3-(1*H*-indazol-6-yl)benzaldehyde (100 mg, 0.45 mmol, 1.0 eq), piperidine (53 μL, 0.54 mmol, 1.2 eq), glacial AcOH (1 drop), STAB (153 mg, 0.72 mmol, 1.6 eq) and DCM (5 mL). The reaction was stirred for 2 h. Upon completion, the reaction mixture was reduced *in vacuo* and resuspended in EtOAc (10 mL) and water (10 mL) added. The aqueous layer was extracted with EtOAc (3 × 20 mL) and the combined organic layers washed with brine (40 mL), dried (MgSO<sub>4</sub>) and reduced *in vacuo* to give a yellow semi-solid. The crude product was purified using column chromatography (gradient 0.5-2% NH<sub>3(aq)</sub>(35%)–EtOAc) and a colourless semi-solid obtained. The solid was dissolved in Et<sub>2</sub>O and petrol added until precipitation was observed and then reduced *in vacuo*. The title compound 55 (106 mg, 0.36 mmol, 81%) was collected as a pale yellow foamy solid.

**<sup>1</sup>H NMR (500 MHz, CDCl<sub>3</sub>):** 10.30 (1H, br.s, NH), 8.10 (1H, s, 3-H), 7.79 (1H, dd, *J* 8.5 and 0.5, 4-H), 7.68 (1H, app.t, *J* 1.5, 2''-H), 7.64 (1H, s, 7-H), 7.55 (1H, app.dt, *J* 8.0 and 1.5, 6''-H), 7.42-7.39 (2H, m, 5-H and 5''-H), 7.32 (1H, app.dt, *J* 8.0 and 1.5, 4''-H), 3.78 (2H, s, CH<sub>2</sub>Ar), 2.65 (4H, app.s, 2-H and 6-H piperidine), 1.73-1.67 (4H, m, 3-H and 5-H piperidine), 1.52-1.46 (2H, m, 4-H piperidine); **<sup>13</sup>C NMR (125 MHz, CDCl<sub>3</sub>):** 141.6 (6-C), 140.8 (3'-C), 139.8 (1''-C), 136.0 (3''-C), 134.5 (3-C), 129.2 (5''-C), 129.0 (4''-C), 128.8 (2''-C), 127.0 (6''-C), 122.5 (7'-C), 121.1 (4-C), 121.0 (5-C), 108.1 (7-C), 62.6 (CH<sub>2</sub>Ar), 53.7 (2-C and 6-C piperidine), 24.7 (3-C and 5-C piperidine), 23.7 (4-C piperidine); **LC-MS (ES):**

RT = 1.44-1.66 min,  $m/z = 292.2$  ( $M+H^+$ ); **R<sub>f</sub>**: 0.47 (98:2 EtOAc–NH<sub>3(aq)</sub> (35%)); **HPLC**: RT = 1.75 min; **m/z (ES<sup>+</sup>)**: Found: 292.1817 ( $M+H^+$ ), C<sub>19</sub>H<sub>21</sub>N<sub>3</sub> requires *MH* 292.1808; **IR**:  $\nu_{\max}/\text{cm}^{-1}$  (**solid**): 3175 (N-H), 2997, 2859, 1599, 1487; **M.pt**: 100.4-101.9 °C.

Preparation of 6-[3-(morpholin-4-ylmethyl)phenyl]-1*H*-indazole

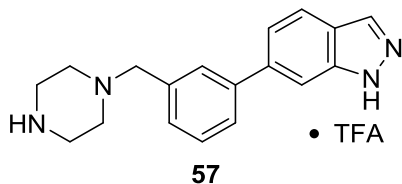


Synthesised using method B using 3-(1*H*-indazol-6-yl)benzaldehyde (100 mg, 0.45 mmol, 1.0 eq), morpholine (47  $\mu\text{L}$ , 0.54 mmol, 1.2 eq), glacial AcOH (1 drop), STAB (153 mg, 0.72 mmol, 1.6 eq) and

DCM (5 mL). The reaction was stirred for 2 h. Upon completion, the reaction mixture was reduced *in vacuo* and resuspended in EtOAc (10 mL) and water (10 mL) added. The aqueous layer was extracted with EtOAc (3  $\times$  20 mL) and the combined organic layers washed with brine (40 mL), dried (MgSO<sub>4</sub>) and reduced *in vacuo* to give a yellow semi-solid. The crude product was purified using column chromatography (1% NH<sub>3(aq)</sub>(35%)–EtOAc) and a colourless semi-solid obtained. The solid was dissolved in Et<sub>2</sub>O and petrol added until precipitation was observed and then reduced *in vacuo*. The title compound 56 (107 mg, 0.36 mmol, 81%) was collected as an off-white foamy solid.

**<sup>1</sup>H NMR (500 MHz, CDCl<sub>3</sub>)**: 8.12 (1H, d, *J* 1.0, 3-H), 7.81 (1H, d, *J* 8.5, 4-H), 7.64 (1H, s, 7-H), 7.63 (1H, app.t, *J* 2.0, 2''-H), 7.54 (1H, app.dt, *J* 7.5 and 1.5, 6''-H), 7.44-7.40 (2H, m, 5-H and 5''-H), 7.35 (1H, app.dt, *J* 7.5 and 1.5, 4''-H), 3.75 (4H, app.t, *J* 5.0, 3-H and 5-H morpholine), 3.60 (2H, s, CH<sub>2</sub>Ar), 2.52 (4H, app.t, *J* 5.0, 2-H and 6-H morpholine), NH not observed; **<sup>13</sup>C NMR (125 MHz, CDCl<sub>3</sub>)**: 141.4 (6-C), 140.8 (3'-C), 140.3 (1''-C), 138.4 (3''-C), 134.9 (3-C), 128.8 (5''-C), 128.4 (2''-C), 128.4 (4''-C), 126.5 (6''-C), 122.5 (7'-C), 121.4 (5-C), 121.1 (4-C), 107.8 (7-C), 67.0 (3-C and 5-C morpholine), 63.5 (CH<sub>2</sub>Ar), 53.7 (2-C and 6-C morpholine); **LC-MS (ES)**: RT = 1.37-1.52 min,  $m/z = 294.2$  ( $M+H^+$ ); **R<sub>f</sub>**: 0.45 (98:2 EtOAc–NH<sub>3(aq)</sub> (35%)); **HPLC**: RT = 1.67 min; **m/z (ES<sup>+</sup>)**: Found: 294.1607 ( $M+H^+$ ), C<sub>18</sub>H<sub>19</sub>N<sub>3</sub>O requires *MH* 294.1601; **IR**:  $\nu_{\max}/\text{cm}^{-1}$  (**solid**): 3162 (N-H), 3125, 3016, 2962, 2934, 1624, 1469; **M.pt**: 136.7-138.4 °C.

Preparation of 1-([3-(1*H*-indazol-6-yl)phenyl]methyl)piperazin-1-ium trifluoroacetate

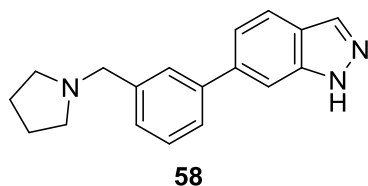


Synthesised using method C using *tert*-butyl-4-([3-(1*H*-indazole-6-yl)phenyl]methyl) piperazine-1-carboxylate (100 mg, 2.55 mmol, 1.0 eq), DCM (5 mL) and freshly distilled TFA (5 mL). The

reaction mixture was stirred for 1 h. The semi solid was suspended in Et<sub>2</sub>O and sonicated for 30 minutes and the resulting white precipitate filtered. The title compound 57 (43 mg, 0.16 mmol, 42%) was collected as an off-white powder.

**<sup>1</sup>H NMR (500 MHz, CD<sub>3</sub>OD):** 7.98 (1H, s, 3-H), 7.75 (1H, dd, *J* 8.5 and 1.0, 4-H), 7.70 (1H, app.t *J* 1.5, 2''-H), 7.67-7.64 (2H, m, 7-H and 6''-H), 7.44 (1H, app.t, *J* 8.0, 5''-H), 7.38-7.34 (2H, m, 4''-H and 5-H), 4.07 (2H, s, CH<sub>2</sub>Ar), 3.33 (4H, app.t, *J* 4.5, 3-H and 5-H piperazine), 3.12 (4H, app.t, *J* 4.5, 2-H and 6-H piperazine), NHs not observed; **<sup>13</sup>C NMR (125 MHz, CD<sub>3</sub>OD):** 143.5 (6-C), 142.2 (3'-C), 140.6 (1''-C), 134.7 (3-C), 134.1 (3''-C), 130.5 (5''-C), 130.4 (2''-C), 130.4 (4''-C), 129.2 (6''-C), 123.8 (7'-C), 122.2 (4-C), 121.9 (5-C), 109.1 (7-C), 62.4 (CH<sub>2</sub>Ar), 49.9 (2-C and 6-C piperazine), 43.3 (3-C and 5-C piperazine); **LC-MS (ES):** RT = 1.30-1.60 min, *m/z* = 293.4 (M+H<sup>+</sup>); **R<sub>f</sub>:** 0.69 (4:1 EtOAc–7.0 M NH<sub>3</sub> in MeOH); **HPLC:** RT = 0.81 min; ***m/z* (ES<sup>+</sup>):** Found: 293.1759 (M+H<sup>+</sup>), C<sub>18</sub>H<sub>20</sub>N<sub>4</sub> requires *MH* 293.1760; **IR:ν<sub>max</sub>/cm<sup>-1</sup> (solid):** 3224 (N-H), 3032, 2865, 1667 (C=O), 1626; **M.pt:** 193.5-195.9 °C.

Preparation of 6-[3-(pyrrolidin-1-ylmethyl)phenyl]-1*H*-indazole



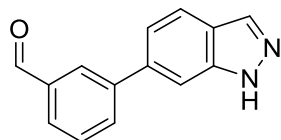
Synthesised using method B using 3-(1*H*-indazol-6-yl)benzaldehyde (200 mg, 0.90 mmol, 1.0 eq), pyrrolidine (90 μL, 1.08 mmol, 1.2 eq), AcOH (1 drop), STAB (306 mg, 1.44 mmol, 1.6 eq) and DCM

(10 mL). The reaction was stirred for 2 h. The reaction mixture was reduced to ~ 3 mL and the crude product purified using column chromatography (gradient 1-6% 7.0 M NH<sub>3</sub> in MeOH–EtOAc). The title compound 58 (213 mg, 0.77 mmol, 85%) was collected as an off-white powder.

**<sup>1</sup>H NMR (500 MHz, CDCl<sub>3</sub>):** 7.95 (1H, d, *J* 1.0, 3-H), 7.72 (1H, dd, *J* 8.5 and 1.0, 4-H), 7.64-7.63 (1H, m, 7-H), 7.58 (1H, app.t, *J* 1.5, 2''-H), 7.50 (1H, ddd, *J* 7.5, 2.0 and 1.0, 6''-H), 7.34 (1H, dd, *J* 8.5 and 1.5, 5-H), 7.32 (1H, app.t, *J* 7.5, 5''-H), 7.24

(1H, app.dt, *J* 7.5 and 2.0, 4''-H), 3.63 (2H, s, CH<sub>2</sub>Ar), 2.54-2.49 (4H, m, 2-H and 5-H pyrrole), 1.75-1.70 (4H, m, 3-H and 4-H pyrrole); <sup>13</sup>C NMR (125 MHz, CDCl<sub>3</sub>): 142.8 (6-C), 142.3 (3'-C), 141.3 (1''-C), 139.7 (3''-C), 134.7 (3-C), 129.9 (5''-C), 129.5 (2''-C), 129.5 (4''-C), 127.5 (6''-C), 123.6 (7'-C), 122.0 (5-C), 122.0 (4-C), 109.0 (7-C), 61.4 (CH<sub>2</sub>Ar), 54.9 (2-C and 5-C pyrrole), 24.1 (3-C and 4-C pyrrole); **LC-MS (ES)**: RT = 1.39-1.58 min, *m/z* = 278.2 (M+H<sup>+</sup>); **R<sub>f</sub>**: 0.25 (98:2 EtOAc–7.0 M NH<sub>3</sub> in MeOH); **HPLC**: RT = 1.71 min; **m/z (ES+)**: Found: 555.3232 (2M+H<sup>+</sup>), C<sub>18</sub>H<sub>19</sub>N<sub>3</sub> requires *MH* 555.3231; **IR:ν<sub>max</sub>/cm<sup>-1</sup> (solid)**: 3067, 3014, 2951, 2914, 2768, 1624, 1604, 1399; **M.pt**: 139.7-141.2 °C.

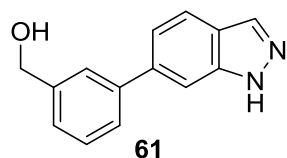
#### Preparation of 3-(1*H*-indazol-6-yl)benzaldehyde



**59**

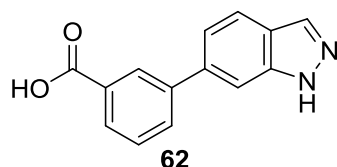
Synthesised using method A using 6-iodo-1*H*-indazole (200 mg, 0.82 mmol, 1.0 eq), 3-formylphenylboronic acid (246 mg, 1.64 mmol, 2.0 eq), Pd(dppf)Cl<sub>2</sub>•DCM (67 mg, 0.082 mmol, 0.1 eq), Na<sub>2</sub>CO<sub>3</sub> (261 mg, 2.46 mmol, 3.0 eq), dioxane (10 mL) and water (10 mL) and the reaction heated for 3 h. The work up proceeded using the larger volumes of solvents and the organic solvent removed *in vacuo* to reveal a brown oil. The crude product was purified using column chromatography (2:3 EtOAc–hexane) and a colourless semi-solid obtained. The semi-solid was dissolved in Et<sub>2</sub>O and petrol added until precipitation was observed and then reduced *in vacuo*. The title compound 59 (115 mg, 0.52 mmol, 63%) was collected as an off-white powder.

<sup>1</sup>H NMR (500 MHz, CDCl<sub>3</sub>): 10.12 (1H, s, formyl-H), 8.17 (1H, app.t, *J* 1.5, 2''-H), 8.16 (1H, s, 3-H), 7.92 (1H, ddd, *J* 7.5, 2.0 and 1.0, 6''-H), 7.90 (1H, app.dt, *J* 8.0 and 1.5, 4''-H), 7.86 (1H, dd, *J* 8.5 and 0.5, 4-H), 7.73 (1H, s, 7-H), 7.65 (1H, app.t, *J* 8.0, 5''-H), 7.46 (1H, dd, *J* 8.5 and 1.5, 5-H), NH not observed; <sup>13</sup>C NMR (125 MHz, CDCl<sub>3</sub>): 191.9 (C=O), 142.4 (6-C), 140.8 (3'-C), 138.9 (1''-C), 137.2 (3''-C), 135.0 (3-C), 133.3 (6''-C), 129.5 (5''-C), 128.8 (4''-C), 128.4 (2''-C), 123.0 (7'-C), 121.4 (5-C), 121.1 (4-C), 108.0 (7-C); **LC-MS (ES)**: RT = 1.65-1.88 min, *m/z* = 223.0 (M+H<sup>+</sup>); **R<sub>f</sub>**: 0.49 (7:3 EtOAc–petrol); **HPLC**: RT = 2.07 min; **m/z (ES+)**: Found: 223.0863 (M+H<sup>+</sup>), C<sub>14</sub>H<sub>10</sub>N<sub>2</sub>O requires *MH* 223.0866; **IR:ν<sub>max</sub>/cm<sup>-1</sup> (solid)**: 3175 (N-H), 3133, 2953, 2923, 1687 (C=O), 1624, 1487; **M.pt**: 61.2-63.4 °C.

Preparation of [3-(1*H*-indazol-6-yl)phenyl]methanol**61**

3-(1*H*-indazol-6-yl)benzaldehyde (100 mg, 0.45 mmol, 1.0 eq) was dissolved in MeOH (5 mL) and cooled to 0 °C. DIBAL (0.90 mL, 0.90 mmol, 2.0 eq) was added and the reaction left to stir at 20 °C for 16 h. The reaction mixture was concentrated *in vacuo* and water (30 mL) added. The aqueous layer was extracted with EtOAc (4 × 20 mL) and the combined organic layers washed with brine (30 mL), dried (MgSO<sub>4</sub>) and concentrated *in vacuo* to yield a white solid. The crude product was purified using column chromatography (7:3 EtOAc–hexane). The title compound 61 (66 mg, 0.29 mmol, 65%) was collected as a colourless powder.

**<sup>1</sup>H NMR (500 MHz, CD<sub>3</sub>OD):** 7.95 (1H, d, *J* 0.5, 3-H), 7.72 (1H, dd, *J* 8.5 and 1.0, 4-H), 7.63 (1H, s, 7-H), 7.58 (1H, app.s, 2''-H), 7.48 (1H, app.d, *J* 7.5, 6''-H), 7.33 (1H, app.t, *J* 7.5, 5''-H), 7.33 (1H, dd, *J* 8.5 and 1.5, 5-H), 7.25 (1H, app.d, *J* 7.5, 4''-H), 4.59 (2H, s, CH<sub>2</sub>), OH and NH not observed; **<sup>13</sup>C NMR (125 MHz, CD<sub>3</sub>OD):** 143.3 (3''-C), 142.8 (6-C), 142.2 (3'-C), 141.5 (1''-C), 134.7 (3-C), 129.8 (5''-C), 127.3 (6''-C), 127.0 (4''-C), 127.0 (2''-C), 123.5 (7'-C), 122.0 (5-C), 122.0 (4-C), 108.9 (7-C), 65.1 (CH<sub>2</sub>); **LC-MS (ES):** RT = 1.42-1.50 min, *m/z* = 278.3 (M+H<sup>+</sup>); **R<sub>f</sub>:** 0.57 (EtOAc); **HPLC:** RT = 1.89 min (92%); ***m/z* (ES<sup>+</sup>):** Found: 225.1018 (M+H<sup>+</sup>), C<sub>14</sub>H<sub>12</sub>N<sub>2</sub>O requires *MH* 225.1022; **IR:ν<sub>max</sub>/cm<sup>-1</sup> (solid):** 3172 (br. O-H), 3125, 3082, 2924, 2752, 1624; **M.pt:** 144.4-146.3 °C

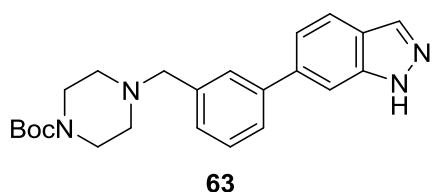
Preparation of 3-(1*H*-indazol-6-yl)benzoic acid**62**

3-(1*H*-indazol-6-yl)benzaldehyde (150 mg, 0.68 mmol, 1.0 eq) was dissolved in acetone (10 mL) and a solution of KMnO<sub>4</sub> (213 mg, 1.35 mmol, 2.0 eq) in water (7 mL) was added and the reaction stirred for 30 minutes at 25 °C. The reaction was concentrated *in vacuo* and re-dissolved in MeOH, filtering the resulting suspension. The filtrate was concentrated *in vacuo* to yield an orange solid. The crude product was purified by column chromatography (80:19:1 hexane–EtOAc–AcOH). The title compound 62 (17 mg, 0.07 mmol, 10%) was collected as a pale purple powder.

**<sup>1</sup>H NMR (500 MHz, DMSO-*d*<sub>6</sub>):** 8.23 (1H, s, 2''-H), 8.10 (1H, s, 3-H), 7.96-7.93 (2H, m, 4''-H and 6''-H), 7.86 (1H, d, *J* 8.0, 4-H), 7.77 (1H, s, 7-H), 7.59 (1H, app.t, *J* 7.5, 5''-H), 7.43 (1H, dd, *J* 8.0 and 1.0, 5-H), OH and NH not observed;

**<sup>13</sup>C NMR (125 MHz, DMSO-d<sub>6</sub>):** 167.5 (C=O), 140.8 (3'-C), 140.6 (3''-C), 137.5 (1''-C), 133.3 (3-C), 131.1 (6''-C), 129.2 (5''-C), 128.2 (4''-C), 127.8 (2''-C), 122.4 (7'-C), 121.1 (4-C), 119.9 (5-C), 107.9 (7-C), 6-C not observed; **LC-MS (ES):** RT = 1.63-1.82 min, m/z = 239.2 (M+H<sup>+</sup>); **R<sub>r</sub>:** 0.45 (50:49:1 EtOAc–petrol–AcOH); **HPLC:** RT = 1.93 min (95%); **m/z (ES<sup>+</sup>):** Found: 239.0810 (M+H<sup>+</sup>), C<sub>14</sub>H<sub>10</sub>N<sub>2</sub>O<sub>2</sub> requires *MH* 239.0815; **IR:ν<sub>max</sub>/cm<sup>-1</sup> (solid):** 3342 (br. O-H), 2954, 2803, 1693, 1628; **M.pt:** 270.3-271.4 °C.

Preparation of *tert*-butyl-4-{{3-(1*H*-indazole-6-yl)phenyl}methyl}piperazine-1-carboxylate

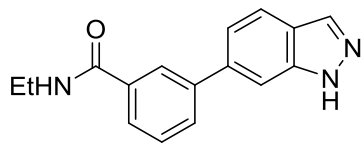


Synthesised using method B using 3-(1*H*-indazol-6-yl)benzaldehyde (132 mg, 0.59 mmol, 1.0 eq), 1-BOC-piperazine (133 mg, 0.71 mmol, 1.2 eq), glacial AcOH (1 drop), STAB (201 mg,

0.95 mmol, 1.6 eq) and DCM (10 mL). The reaction was stirred for 2 h. The reaction mixture was reduced *in vacuo* to give a yellow semi-solid. The crude product was purified using column chromatography (1:1 EtOAc–hexane, followed by 100% EtOAc) and a colourless semi-solid obtained. The solid was dissolved in Et<sub>2</sub>O and petrol added until precipitation was observed and then reduced *in vacuo*. The title compound 63 (177 mg, 0.45 mmol, 76%) was collected as off-white granules.

**<sup>1</sup>H NMR (500 MHz, CDCl<sub>3</sub>):** 8.11 (1H, d, *J* 1.0, 3-H), 7.81 (1H, dd, *J* 8.5 and 1.0, 4-H), 7.65 (1H, s, 7-H), 7.61 (1H, s, 2''-H), 7.55 (1H, app.dt, *J* 8.0 and 1.0, 6''-H), 7.44-7.40 (2H, m, 5-H and 5''-H), 7.33 (1H, app.dt, *J* 7.5 and 1.5, 4''-H), 3.61 (2H, s, CH<sub>2</sub>Ar), 3.45 (4H, app.t, *J* 4.5, 3-H and 5-H piperazine), 2.46 (4H, app.t, *J* 4.5, 2-H and 6-H piperazine), 1.46 (9H, s, <sup>t</sup>Bu-CH<sub>3</sub>); **<sup>13</sup>C NMR (125 MHz, CDCl<sub>3</sub>):** 154.8 (C=O), 141.4 (6-C), 140.7 (3'-C), 140.3 (1''-C), 138.4 (3''-C), 134.7 (3-C), 128.8 (5''-C), 128.4 (4''-C), 128.4 (2''-C), 126.5 (6''-C), 122.5 (7'-C), 121.4 (5-C), 121.1 (4-C), 107.9 (7-C), 79.7 (<sup>t</sup>Bu-C), 63.0 (CH<sub>2</sub>Ar), 52.9 (2-C and 6-C piperazine), 43.5 (3-C and 5-C piperazine), 28.5 (<sup>t</sup>Bu-CH<sub>3</sub>); **LC-MS (ES):** RT = 1.60-1.81 min, m/z = 393.8 (M+H<sup>+</sup>); **R<sub>r</sub>:** 0.44 (EtOAc); **HPLC:** RT = 2.02 min; **m/z (ES<sup>+</sup>):** Found: 393.2294 (M+H<sup>+</sup>), C<sub>23</sub>H<sub>28</sub>N<sub>4</sub>O<sub>2</sub> requires *MH* 393.2286; **IR:ν<sub>max</sub>/cm<sup>-1</sup> (solid):** 3245 (N-H), 3186, 2972, 2926, 2865, 1666; **M.pt:** 57.9-60.4 °C.

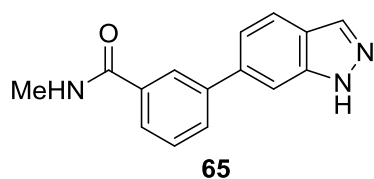


Preparation of N-ethyl-3-(1H-indazol-6-yl)benzamide**64**

3-(1H-indazol-6-yl)benzoic acid (400 mg, 1.68 mmol, 1.0 eq) was suspended in freshly distilled SOCl<sub>2</sub> (3.67 mL, 50.4 mmol, 30 eq) and refluxed for 2 h. The reaction mixture was reduced *in vacuo* and residual SOCl<sub>2</sub> removed *via* azeotrope with toluene (3 × 10 mL).

The resulting solid was dissolved in DCM (30 mL) at 0 °C and Et<sub>3</sub>N (470 μL, 3.36 mmol, 2.0 eq) was added slowly. EtNH<sub>2</sub> ((70% in H<sub>2</sub>O) 220 μL, 3.36 mmol, 2.0 eq) was added and the reaction stirred at 20 °C for 16 h. 2 M HCl (10 mL) was added to the reaction mixture and the organic layer separated washing the organic layer with 2 M HCl (10 mL). The combined aqueous layers were extracted with DCM (2 × 15 mL) and the combined organic layers washed with saturated NaHCO<sub>3(aq)</sub> (20 mL), brine (30 mL) and dried (MgSO<sub>4</sub>). The filtrate was reduced *in vacuo* and a pale orange semi-solid obtained. The crude product was purified using column chromatography (1:1 EtOAc–hexane, followed by 4:1 EtOAc–hexane) and a colourless semi-solid obtained. The solid was dissolved in Et<sub>2</sub>O and petrol added until precipitation was observed and then reduced *in vacuo*. The title compound 64 (56 mg, 0.21 mmol, 14%) was collected as a fluffy beige powder.

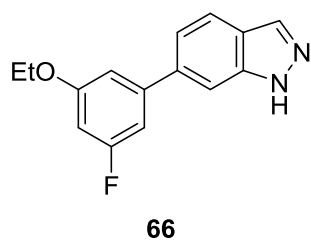
**<sup>1</sup>H NMR (500 MHz, CDCl<sub>3</sub>):** 8.05-8.01 (2H, m, 3-H and 2''-H), 7.71-7.66 (2H, m, 4-H and 4''-H), 7.58 (1H, d, *J* 7.5, 6''-H), 7.48 (1H, s, 7-H), 7.34 (1H, app.t, *J* 7.5, 5''-H), 7.26 (1H, d, *J* 8.5, 5-H), 6.88 (1H, app.s, amide NH), 3.52-3.45 (2H, m, CH<sub>2</sub>), 1.21 (3H, t, *J* 7.5, CH<sub>3</sub>), indazole NH not observed; **<sup>13</sup>C NMR (125 MHz, CDCl<sub>3</sub>):** 167.9 (C=O), 141.7 (1''-C), 140.8 (3'-C), 139.0 (6-C), 135.2 (3-C), 134.3 (3''-C), 130.6 (6''-C), 128.9 (5''-C), 126.3 (2''-C), 125.7 (4''-C), 122.6 (7'-C), 121.1 (4-C), 120.9 (5-C), 108.3 (7-C), 35.2 (CH<sub>2</sub>), 14.8 (CH<sub>3</sub>); **LC-MS (ES):** RT = 1.62-1.80 min, *m/z* = 266.5 (M+H<sup>+</sup>); **R<sub>f</sub>:** 0.39 (EtOAc); **HPLC:** RT = 12.79 min; ***m/z* (ES+):** Found: 266.1288 (M+H<sup>+</sup>), C<sub>16</sub>H<sub>15</sub>N<sub>3</sub>O requires *MH* 266.1288; **IR:ν<sub>max</sub>/cm<sup>-1</sup> (solid):** 3284 (N-H), 3227 (N-H), 3097, 3057, 2970, 1726, 1625 (C=O); **M.pt:** 127.8-130.5 °C.

Preparation of 3-(1*H*-indazol-6-yl)-*N*-methylbenzamide

3-(1*H*-indazol-6-yl)benzoic acid (500 mg, 2.10 mmol, 1.0 eq) was suspended in freshly distilled SOCl<sub>2</sub> (4.60 mL, 63.0 mmol, 30.0 eq) and refluxed for 4 h.

The reaction mixture was reduced *in vacuo* and residual SOCl<sub>2</sub> removed *via* azeotrope with toluene (3 × 10 mL). The resulting solid was dissolved in DCM (30 mL) at 0 °C and Et<sub>3</sub>N (0.59 mL, 4.20 mmol, 2.0 eq) was added slowly. MeNH<sub>2</sub> ((33% in EtOH) 0.56 mL, 4.20 mmol, 2.0 eq) was added and the reaction stirred at 20 °C for 16 h. 2 M HCl (10 mL) was added to the reaction mixture and the organic layer separated washing the organic layer with 2 M HCl (10 mL). The combined aqueous layers were extracted with DCM (2 × 15 mL) and the combined organic layers washed with saturated NaHCO<sub>3(aq)</sub> (20 mL), brine (30 mL) and dried (MgSO<sub>4</sub>). The filtrate was reduced *in vacuo* and a pale yellow semi-solid obtained. The crude product was purified using column chromatography (7:3 EtOAc–hexane followed by 9:1 EtOAc–hexane). The title compound 65 (55 mg, 0.22 mmol, 14%) was collected as a fluffy cream powder.

**<sup>1</sup>H NMR (500 MHz, CD<sub>3</sub>OD):** 8.58 (1H, br.s, amide NH), 8.16 (1H, app.t, *J* 2.0, 2''-H), 8.09 (1H, app.s, 3-H), 7.88-7.81 (3H, m, 4-H, 4''-H and 6''-H), 7.78 (1H, app.s, 7-H), 7.56 (1H, app.t, *J* 7.5, 5''-H), 7.48 (1H, dd, *J* 7.5 and 1.5, 5-H), 2.99 (3H, d, *J* 4.5, CH<sub>3</sub>), indazole NH not observed; **<sup>13</sup>C NMR (125 MHz, CD<sub>3</sub>OD):** 169.3 (C=O), 141.8 (1''-C), 141.0 (3'-C), 139.2 (6-C), 134.9 (3''-C), 133.5 (3-C), 130.2 (6''-C), 128.2 (5''-C), 126.0 (2''-C), 125.8 (4''-C), 122.5 (7'-C), 121.0 (4-C), 120.6 (5-C), 108.0 (7-C), 25.7 (CH<sub>3</sub>); **LC-MS (ES):** RT = 1.55-1.66 min, *m/z* = 252.5 (M+H<sup>+</sup>); **R<sub>f</sub>:** 0.27 (EtOAc); **HPLC:** RT = 12.34 min (97%); ***m/z* (ES<sup>+</sup>):** Found: 252.1129 (M+H<sup>+</sup>), C<sub>15</sub>H<sub>13</sub>N<sub>3</sub>O requires *MH* 252.1131; **IR:** ν<sub>max</sub>/cm<sup>-1</sup> (solid): 3270 (N-H), 3088, 2926, 2870, 1721, 1625 (C=O); **M.pt:** 86.5-90.5 °C.

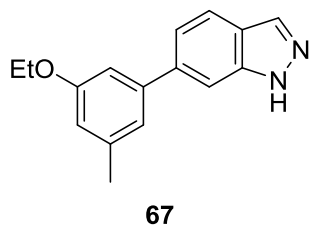
Preparation of 6-(3-ethoxy-5-fluorophenyl)-1*H*-indazole

Synthesised using method A using 6-iodo-1*H*-indazole (200 mg, 0.82 mmol, 1.0 eq), 3-ethoxy-5-fluorophenylboronic acid (226 mg, 1.23 mmol, 1.5 eq), Pd(dppf)Cl<sub>2</sub>•DCM (67 mg, 0.082 mmol, 0.1 eq), Na<sub>2</sub>CO<sub>3</sub> (261 mg, 2.46 mmol, 3.0 eq), dioxane (10 mL) and water (10 mL) and the reaction heated for 1.5 h. The work up proceeded using the larger

volumes of solvents and the organic solvent removed *in vacuo* to reveal a brown solid. The crude product was purified using column chromatography (1:4 EtOAc–hexane) and a glassy solid obtained. The solid was dissolved in Et<sub>2</sub>O and petrol added until precipitation was observed and then reduced *in vacuo*. The title compound 66 (89 mg, 0.35 mmol, 42%) was collected as a cream solid.

**<sup>1</sup>H NMR (500 MHz, DMSO-*d*<sub>6</sub>):** 13.15 (1H, br.s, NH), 8.09 (1H, s, 3-H), 7.82 (1H, d, *J* 8.0, 4-H), 7.76 (1H, s, 7-H), 7.41 (1H, dd, *J* 8.5 and 1.5, 5-H), 7.11 (1H, app.dt, *J* 10.0 and 1.5, 2''-H), 7.08 (1H, app.t, *J* 1.5, 6''-H), 6.81 (1H, app.dt, *J* 11.0 and 2.0, 4''-H), 4.13 (2H, q, *J* 7.0, CH<sub>2</sub>), 1.35 (3H, t, *J* 7.0, CH<sub>3</sub>); **<sup>13</sup>C NMR (125 MHz, DMSO-*d*<sub>6</sub>):** 163.3 (d, *J* 242.3, 3''-C), 160.2 (d, *J* 12.0, 5''-C), 143.6 (d, *J* 10.1, 1''-C), 140.3 (3''-C), 137.0 (d, *J* 2.7, 6-C), 133.4 (3-C), 122.6 (7'-C), 120.9 (4-C), 120.0 (5-C), 109.5 (d, *J* 2.4, 6''-C), 108.1 (7-C), 106.0 (d, *J* 22.7, 2''-C), 100.9 (d, *J* 25.2, 4''-C), 63.7 (CH<sub>2</sub>), 14.5 (CH<sub>3</sub>); **LC-MS (ES):** RT = 1.97-2.16 min, *m/z* = 257.4 (M+H<sup>+</sup>); **R<sub>f</sub>:** 0.33 (1:1 EtOAc–petrol); **HPLC:** RT = 15.82 min; ***m/z* (ES<sup>+</sup>):** Found: 257.1092 (M+H<sup>+</sup>), C<sub>15</sub>H<sub>13</sub>FN<sub>2</sub>O requires *MH* 257.1085; **IR:** *v*<sub>max</sub>/cm<sup>-1</sup> (solid): 3161 (N-H), 3124, 2978, 2919, 1602, 1450; **M.pt:** 90.4-91.1 °C; **Found:** C, 69.9; H, 5.30; N, 10.6; C<sub>15</sub>H<sub>13</sub>FN<sub>2</sub>O requires C, 70.3; H, 5.11; N, 10.9%.

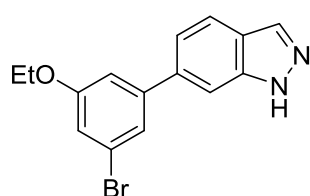
#### Preparation of 6-(3-ethoxy-5-methylphenyl)-1*H*-indazole



Synthesised using method A using 6-iodo-1*H*-indazole (200 mg, 0.82 mmol, 1.0 eq), 3-ethoxy-5-methylphenylboronic acid (221 mg, 1.23 mmol, 1.5 eq), Pd(dppf)Cl<sub>2</sub>•DCM (67 mg, 0.082 mmol, 0.1 eq), Na<sub>2</sub>CO<sub>3</sub> (261 mg, 2.46 mmol, 3.0 eq), dioxane (10 mL) and water (10 mL) and the reaction heated for 1 h. LC-MS analysis showed the reaction to be incomplete and therefore 3-ethoxy-5-methylphenylboronic acid (111 mg, 0.62 mmol, 0.75 eq) and Pd(dppf)Cl<sub>2</sub>•DCM (34 mg, 0.041 mmol, 0.05 eq) were added and the reaction heated for a further 30 minutes. The work up proceeded using the larger volumes of solvents and the organic solvent removed *in vacuo* to reveal a brown oil. The crude product was purified using column chromatography (2:3 EtOAc–hexane) and a glassy solid obtained. The glassy solid was dissolved in Et<sub>2</sub>O and reduced *in vacuo*. The title compound 67 (76 mg, 0.30 mmol, 37%) as an off-white foamy solid. **<sup>1</sup>H NMR (500 MHz, CDCl<sub>3</sub>):** 8.14 (1H, s, 3-H), 7.80 (1H, d, *J* 8.5, 4-H), 7.66 (1H, s, 7-H), 7.43 (1H, dd, *J* 8.5 and 1.4, 5-H), 7.06 (1H, s, 6''-H), 7.01 (1H, s, 2''-H), 6.77

(1H, s, 4''-H), 4.11 (2H, q, *J* 7.0, CH<sub>2</sub>), 2.42 (3H, s, CH<sub>3</sub>), 1.46 (3H, t, *J* 7.0, CH<sub>2</sub>CH<sub>3</sub>), NH not observed; <sup>13</sup>C NMR (125 MHz, CDCl<sub>3</sub>): 159.4 (3''-C), 142.6 (6-C), 140.8 (3'-C), 140.5 (1''-C), 139.9 (5''-C), 134.8 (3-C), 122.6 (7'-C), 121.5 (5-C), 121.0 (6''-C), 114.4 (4''-C), 111.1 (2''-C), 107.9 (7-C), 63.5 (CH<sub>2</sub>), 21.7 (CH<sub>3</sub>), 14.9 (CH<sub>2</sub>CH<sub>3</sub>), 4-C not observed; LC-MS (ES): RT = 1.97-2.17 min, *m/z* = 253.5 (M+H<sup>+</sup>); *R<sub>f</sub>*: 0.47 (1:1 EtOAc–petrol); HPLC: RT = 3.64 min; *m/z* (ES<sup>+</sup>): Found: 253.1335 (M+H<sup>+</sup>), C<sub>16</sub>H<sub>17</sub>N<sub>2</sub>O requires *MH* 253.1341; IR: *v*<sub>max</sub>/cm<sup>-1</sup> (solid): 3130 (N-H), 3086, 2872, 1579; *M.pt*: 95.6-98.7 °C.

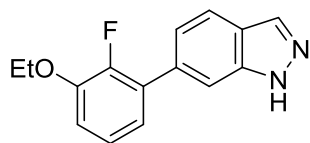
#### Preparation of 6-(3-bromo-5-ethoxyphenyl)-1*H*-indazole



**68**

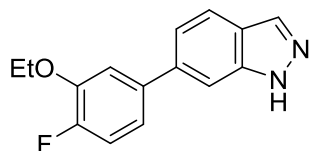
Synthesised using method A using 6-iodo-1*H*-indazole (168 mg, 0.69 mmol, 1.0 eq), 3-ethoxy-5-bromophenylboronic acid (254 mg, 1.04 mmol, 1.5 eq), Pd(dppf)Cl<sub>2</sub>•DCM (56 mg, 0.069 mmol, 0.1 eq), Na<sub>2</sub>CO<sub>3</sub> (219 mg, 2.07 mmol, 3.0 eq), dioxane (10 mL) and water (10 mL) and the reaction heated for 1 h. LC-MS analysis showed the reaction to be incomplete but the reaction was stopped due to no more boronic acid being available. The work up proceeded using the larger volumes of solvents and the organic solvent removed *in vacuo* to reveal a green semi-solid. The crude product was purified using column chromatography (1:4 EtOAc–hexane) and a colourless glassy solid obtained. The solid was dissolved in Et<sub>2</sub>O and reduced *in vacuo*. The title compound 68 (40 mg, 0.126 mmol, 18%) as an off-white solid.

<sup>1</sup>H NMR (500 MHz, CDCl<sub>3</sub>): 8.12 (1H, s, 3-H), 7.81 (1H, d, *J* 8.5, 4-H), 7.64 (1H, s, 7-H), 7.39-7.36 (2H, m, 5-H and 2''-H), 7.10 (1H, app.t, *J* 1.5, 4''-H), 7.06 (1H, app.t, *J* 2.0, 6''-H), 4.09 (2H, q, *J* 7.0, CH<sub>2</sub>), 1.45 (3H, t, *J* 7.0, CH<sub>3</sub>), NH not observed; <sup>13</sup>C NMR (125 MHz, CDCl<sub>3</sub>): 160.0 (5''-C), 144.2 (1''-C), 140.6 (3'-C), 138.9 (6-C), 135.0 (3-C), 123.2 (3''-C), 123.0 (2''-C), 122.9 (7'-C), 121.3 (5-C), 121.2 (4-C), 116.5 (6''-C), 113.3 (4''-C), 107.9 (7-C), 64.0 (CH<sub>2</sub>), 14.8 (CH<sub>3</sub>); LC-MS (ES): RT = 2.08-2.21 min, *m/z* = 319.5 (MBr<sup>81</sup>); *R<sub>f</sub>*: 0.51 (1:1 EtOAc–petrol); HPLC: RT = 3.49 min (94%); *m/z* (ES<sup>+</sup>): Found: 317.0284 (M+H<sup>+</sup>), C<sub>15</sub>H<sub>13</sub>BrN<sub>2</sub>O requires *MH* 317.0284; IR: *v*<sub>max</sub>/cm<sup>-1</sup> (solid): 3172 (N-H), 3131, 2962, 2922, 2867, 1591; *M.pt*: 90.4-96.1 °C.

Preparation of 6-(3-ethoxy-2-fluorophenyl)-1*H*-indazole**69**

Synthesised using method A using 6-iodo-1*H*-indazole (200 mg, 0.82 mmol, 1.0 eq), 3-ethoxy-2-fluorophenylboronic acid (226 mg, 1.23 mmol, 1.5 eq), Pd(dppf)Cl<sub>2</sub>•DCM (67 mg, 0.082 mmol, 0.1 eq), Na<sub>2</sub>CO<sub>3</sub> (261 mg, 2.46 mmol, 3.0 eq), dioxane (10 mL) and water (10 mL) and the reaction heated for 1 h. LC-MS indicated the reaction to be incomplete and therefore 6-iodo-1*H*-indazole (120 mg, 0.49 mmol, 0.6 eq) and Pd(dppf)Cl<sub>2</sub>•DCM (34 mg, 0.04 mmol, 0.05 eq) were added and the reaction heated for a further 30 minutes. The work up proceeded using the larger volumes of solvents and the organic solvent removed *in vacuo* to reveal a brown oil. The crude product was purified using column chromatography (3:7 EtOAc–hexane) and an off-white solid obtained. The resulting solid was crystallised from EtOH. The title compound 69 (57 mg, 0.22 mmol, 18%) was collected as off-white crystals.

**<sup>1</sup>H NMR (500 MHz, CDCl<sub>3</sub>):** 10.42 (1H, br.s, NH), 8.13 (1H, d, *J* 0.5, 3-H), 7.82 (1H, dd, *J* 8.5 and 1.0, 4-H), 7.69 (1H, s, 7-H), 7.37 (1H, app.dt, *J* 8.5 and 1.5, 5-H), 7.13 (1H, app.td, *J* 8.0 and 1.5, 5''-H), 7.07-7.04 (1H, m, 6''-H), 6.99 (1H, app.td, *J* 8.0 and 1.5, 4''-H), 4.18 (2H, q, *J* 7.0, CH<sub>2</sub>), 1.50 (3H, t, *J* 7.0, CH<sub>3</sub>); **<sup>13</sup>C NMR (125 MHz, CDCl<sub>3</sub>):** 150.0 (d, *J* 247.4, 2''-C), 147.6 (d, *J* 11.3, 3''-C), 140.3 (3'-C), 134.9 (3-C), 134.6 (6-C), 130.0 (d, *J* 11.3, 1'' C), 123.9 (d, *J* 4.9, 5''-C), 122.8 (d, *J* 2.4, 5-C), 122.7 (7'-C), 122.4 (d, *J* 2.3, 6''-C), 120.7 (4-C), 113.9 (d, *J* 2.0, 4''-C), 110.1 (d, *J* 3.6, 7-C), 65.2 (CH<sub>2</sub>), 14.9 (CH<sub>3</sub>); **LC-MS (ES):** RT = 1.90-2.05 min, *m/z* = 257.8 (M+H<sup>+</sup>); **R<sub>f</sub>:** 0.43 (1:1 EtOAc–petrol); **HPLC:** RT = 3.44 min; ***m/z* (ES<sup>+</sup>):** Found: 257.1093 (M+H<sup>+</sup>), C<sub>15</sub>H<sub>13</sub>FN<sub>2</sub>O requires *MH* 257.1090; **IR:ν<sub>max</sub>/cm<sup>-1</sup> (solid):** 3163 (N-H), 3129, 2914, 2866, 1625; **M.pt:** 132.2-132.7 °C; **Found:** C, 70.0; H, 5.10; N, 10.7; C<sub>15</sub>H<sub>13</sub>FN<sub>2</sub>O requires C, 70.3; H, 5.11; N, 10.9.

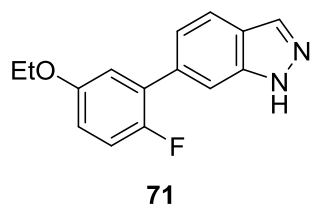
Preparation of 6-(3-ethoxy-4-fluorophenyl)-1*H*-indazole**70**

Synthesised using method A using 6-iodo-1*H*-indazole (200 mg, 0.82 mmol, 1.0 eq), 3-ethoxy-4-fluorophenylboronic acid (226 mg, 1.23 mmol, 1.5 eq), Pd(dppf)Cl<sub>2</sub>•DCM (67 mg, 0.082 mmol, 0.1 eq), Na<sub>2</sub>CO<sub>3</sub> (261 mg, 2.46 mmol, 3.0 eq), dioxane (10 mL) and water (10 mL) and the reaction heated for 1 h. The work up proceeded using the larger volumes of solvents and the

organic solvent removed *in vacuo* to reveal a brown oil. The crude product was purified using column chromatography (3:7 EtOAc–hexane) and a colourless solid obtained. The solid was crystallised from cyclohexane. The title compound 70 (67 mg, 0.26 mmol, 32%) was collected as off-white needles.

**<sup>1</sup>H NMR (500 MHz, CDCl<sub>3</sub>):** 10.32 (1H, br.s, NH), 8.12 (1H, s, 3-H), 7.81 (1H, d, *J* 8.5, 4-H), 7.61 (1H, s, 7-H), 7.38 (1H, dd, *J* 8.5 and 1.5, 5-H), 7.24-7.21 (1H, m, 2''-H), 7.19-7.14 (2H, m, 5''-H and 6''-H), 4.21 (2H, q, *J* 7.0, CH<sub>2</sub>), 1.50 (3H, t, *J* 7.0, CH<sub>3</sub>); **<sup>13</sup>C NMR (125 MHz, CDCl<sub>3</sub>):** 152.6 (d, *J* 246.6, 4''-C), 147.1 (d, *J* 10.8, 3''-C), 140.7 (3'-C), 139.8 (6-C), 137.9 (d, *J* 3.7, 1''-C), 135.0 (3-C), 122.5 (7'-C), 121.3 (5-C), 121.2 (4-C), 120.1 (d, *J* 6.9, 6''-C), 116.4 (d, *J* 18.7, 5''-C), 114.5 (d, *J* 2.3, 2''-C), 107.7 (7-C), 65.2 (CH<sub>2</sub>), 14.9 (CH<sub>3</sub>); **LC-MS (ES):** RT = 1.90-2.05 min, *m/z* = 257.1 (M+H<sup>+</sup>); **R<sub>f</sub>:** 0.27 (1:1 EtOAc–petrol); **HPLC:** RT = 2.70 min; ***m/z* (ES<sup>+</sup>):** Found: 257.1083 (M+H<sup>+</sup>), C<sub>15</sub>H<sub>14</sub>FN<sub>2</sub>O requires *MH* 257.1090; **IR:ν<sub>max</sub>/cm<sup>-1</sup> (solid):** 3299 (N-H), 2984, 1624; **M.pt:** 116.5-116.8 °C.

#### Preparation of 6-(5-ethoxy-2-fluorophenyl)-1*H*-indazole

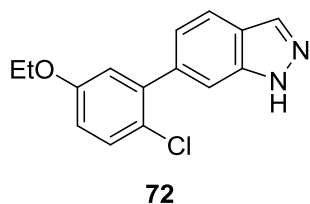


Synthesised using method A using 6-iodo-1*H*-indazole (200 mg, 0.82 mmol, 1.0 eq), 5-ethoxy-2-fluorophenylboronic acid (226 mg, 1.23 mmol, 1.5 eq), Pd(dppf)Cl<sub>2</sub>•DCM (67 mg, 0.082 mmol, 0.1 eq), Na<sub>2</sub>CO<sub>3</sub> (261 mg, 2.46 mmol, 3.0 eq), dioxane (10 mL) and water (10 mL) and the reaction heated for 1 h. The work up proceeded using the larger volumes of solvents and the organic solvent removed *in vacuo* to reveal a brown oil. The crude product was purified using column chromatography (2:3 EtOAc–hexane) and an orange semi-solid obtained. The resulting semi-solid was dissolved in CDCl<sub>3</sub> and concentrated *in vacuo* to reveal a pale orange solid. The orange solid was crystallised from cyclohexane. The title compound 71 (90 mg, 0.35 mmol, 43%) was collected as pale orange microcrystals.

**<sup>1</sup>H NMR (500 MHz, CDCl<sub>3</sub>):** 10.50 (1H, br.s, NH), 8.13 (1H, s, 3-H), 7.82 (1H, dd, *J* 8.4 and 0.6, 4-H), 7.68 (1H, s, 7-H), 7.37 (1H, app.dt, *J* 8.5 and 1.4, 5-H), 7.10 (1H, dd, *J* 10.0 and 9.0, 3''-H), 7.02 (1H, dd, *J* 6.3 and 3.1, 6''-H), 6.86 (1H, app.dt, *J* 8.9 and 3.5, 4''-H), 4.06 (2H, q, *J* 7.1, CH<sub>2</sub>), 1.44 (3H, t, *J* 7.1, CH<sub>3</sub>); **<sup>13</sup>C NMR (125 MHz, CDCl<sub>3</sub>):** 155.2 (d, *J* 2.1, 5''-C), 154.2 (d, *J* 240.3, 2''-C), 140.3 (3'-C), 134.9 (3-C), 134.7 (d, *J* 1.0, 6-C), 129.7 (d, *J* 15.1, 1''-C), 122.6 (d, *J* 2.5, 5-C),

120.8 (4-C), 116.7 (d,  $J$  22.8, 3''-C), 116.6 (d,  $J$  2.2, 6''-C), 116.6 (7''-C), 114.7 (d,  $J$  8.0, 4''-C), 110.1 (d,  $J$  3.6, 7-C), 64.2 ( $\underline{\text{CH}_2}$ ), 14.9 ( $\underline{\text{CH}_3}$ ); **LC-MS (ES)**: RT = 1.75-2.05 min,  $m/z$  = 257.0 ( $\text{M}+\text{H}^+$ ); **R<sub>f</sub>**: 0.51 (1:1 EtOAc–petrol); **HPLC**: RT = 2.99 min; **m/z (ES+)**: Found: 257.1085 ( $\text{M}+\text{H}^+$ ),  $\text{C}_{15}\text{H}_{14}\text{FN}_2\text{O}$  requires *MH* 257.1090; **IR**:  $\nu_{\text{max}}/\text{cm}^{-1}$  (solid): 3284 (N-H), 2981, 2934; **M.pt**: 114.9-115.3 °C.

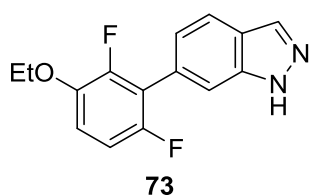
#### Preparation of 6-(2-chloro-5-ethoxyphenyl)-1*H*-indazole



Synthesised using method A using 6-iodo-1*H*-indazole (200 mg, 0.82 mmol, 1.0 eq), 5-ethoxy-2-chlorophenylboronic acid (247 mg, 1.23 mmol, 1.5 eq), Pd(dppf)Cl<sub>2</sub>•DCM (67 mg, 0.082 mmol, 0.1 eq), Na<sub>2</sub>CO<sub>3</sub> (261 mg, 2.46 mmol, 3.0 eq), dioxane (10 mL) and water (10 mL) and the reaction heated for 1 h. The work up proceeded using the larger volumes of solvents and the organic solvent removed *in vacuo* to reveal a brown oil. The crude product was purified using column chromatography (2:3 EtOAc–hexane) and an orange glassy solid obtained. The glassy solid was dissolved in Et<sub>2</sub>O and reduced *in vacuo*. The title compound **72** (178 mg, 0.65 mmol, 80%) as a pale orange foamy solid.

**<sup>1</sup>H NMR (500 MHz, CDCl<sub>3</sub>)**: 10.27 (1H, br.s, NH), 8.31 (1H, s, 3-H), 7.81 (1H, dd,  $J$  8.4 and 0.8, 4-H), 7.56 (1H, d,  $J$  1.4, 7-H), 7.38 (1H, d,  $J$  8.7, 3''-H), 7.26 (1H, dd,  $J$  8.4 and 1.4, 5-H), 6.94 (1H, d,  $J$  3.1, 6''-H), 6.87 (1H, dd,  $J$  8.7 and 3.1, 4''-H), 4.05 (2H, q,  $J$  7.0,  $\underline{\text{CH}_2}$ ), 1.43 (3H, t,  $J$  7.0,  $\underline{\text{CH}_3}$ ); **<sup>13</sup>C NMR (125 MHz, CDCl<sub>3</sub>)**: 157.6 (3''-C), 141.2 (6-C), 140.0 (3'-C), 138.4 (1''-C), 135.0 (3-C), 130.7 (5''-C), 123.9 (6''-C), 123.2 (5-C), 122.6 (7''-C), 120.4 (4-C), 117.5 (2''-C), 115.1 (4''-C), 110.3 (7-C), 63.9 ( $\underline{\text{CH}_2}$ ), 14.8 ( $\underline{\text{CH}_3}$ ); **LC-MS (ES)**: RT = 1.98-2.16 min,  $m/z$  = 273.5 ( $\text{M}+\text{H}^+$ ); **R<sub>f</sub>**: 0.50 (1:1 EtOAc–petrol); **HPLC**: RT = 2.93 min; **m/z (ES+)**: Found: 273.0793 ( $\text{M}+\text{H}^+$ ),  $\text{C}_{15}\text{H}_{14}\text{ClN}_2\text{O}$  requires *MH* 273.0795; **IR**:  $\nu_{\text{max}}/\text{cm}^{-1}$  (solid): 3175 (N-H), 3134, 2978; **M.pt**: 73.7-76.5 °C.

#### Preparation of 6-(3-ethoxy-2,6-difluorophenyl)-1*H*-indazole

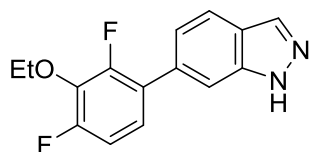


Synthesised using method A using 6-iodo-1*H*-indazole (200 mg, 0.82 mmol, 1.0 eq), 2,6-difluoro-3-ethoxyphenylboronic acid (231 mg, 1.23 mmol, 1.5 eq), Pd(dppf)Cl<sub>2</sub>•DCM (67 mg, 0.082 mmol, 0.1 eq), Na<sub>2</sub>CO<sub>3</sub> (261 mg, 2.46 mmol, 3.0 eq), dioxane (10 mL) and water (10 mL) and the reaction

heated for 1 h. LC-MS analysis showed the reaction to be incomplete and therefore 2,6-difluoro-3-ethoxyphenylboronic acid (231 mg, 1.23 mmol, 1.5 eq) was added and the reaction heated for 1 h. LC-MS showed small conversion to the product but still starting material and therefore 2,6-difluoro-3-ethoxyphenylboronic acid (231 mg, 1.23 mmol, 1.5 eq) was added and the reaction heated for 1 h. LC-MS showed no change and therefore the reaction was stopped. The work up proceeded using the larger volumes of solvents and the organic solvent removed *in vacuo* to reveal a black semi-solid. The crude product was purified using column chromatography (1:4 EtOAc–hexane). The title compound 73 (4 mg, 0.014 mmol, 2%) was collected as an off-white solid.

**<sup>1</sup>H NMR (500 MHz, CDCl<sub>3</sub>):** 8.14 (1H, s, 3-H), 7.84 (1H, d, *J* 8.5, 4-H), 7.61 (1H, s, 7-H), 7.29-7.26 (1H, m, 5-H), 6.98-6.90 (2H, m, 4''-H and 5''-H), 4.14 (2H, q, *J* 7.0, CH<sub>2</sub>), 1.47 (3H, t, *J* 7.0, CH<sub>3</sub>), NH not observed; **<sup>13</sup>C NMR (125 MHz, CDCl<sub>3</sub>):** 153.8 (dd, *J* 241.5 and 5.2, 6''-C), 150.0 (dd, *J* 248.6 and 6.7, 2''-C), 143.9 (dd, *J* 11.8 and 3.1, 3''-C), 140.0 (3''-C), 135.0 (3-C), 128.0 (7'-C), 123.6 (5-C), 123.0 (app.t, *J* 7.9, 6-C), 120.6 (4-C), 119.4 (app.t, *J* 16.0, 1''-C), 114.3 (dd, *J* 9.7 and 3.1, 4''-C), 111.6 (7-C), 110.3 (dd, *J* 24.1 and 4.2, 5''-C), 65.9 (CH<sub>2</sub>), 14.9 (CH<sub>3</sub>); **LC-MS (ES):** RT = 1.85-2.07 min, *m/z* = 275.6 (M+H<sup>+</sup>); **R<sub>f</sub>:** 0.49 (1:1 EtOAc–petrol); **HPLC:** RT = 3.08 min; ***m/z* (ES+):** Found: 275.0990 (M+H<sup>+</sup>), C<sub>15</sub>H<sub>12</sub>F<sub>2</sub>N<sub>2</sub>O requires *MH* 275.0990; **IR:ν<sub>max</sub>/cm<sup>-1</sup> (solid):** 3172 (N-H), 3132, 2921, 2878, 1630, 1579, 1490; **M.pt:** 131.0-132.7 °C.

#### Preparation of 6-(3-ethoxy-2,4-difluorophenyl)-1*H*-indazole



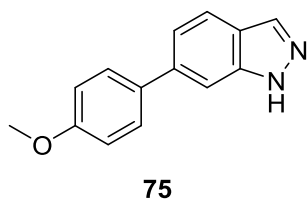
74

Synthesised using method A using 6-iodo-1*H*-indazole (200 mg, 0.82 mmol, 1.0 eq), 3-ethoxy-2,4-difluorophenylboronic acid (248 mg, 1.23 mmol, 1.5 eq), Pd(dppf)Cl<sub>2</sub>•DCM (67 mg, 0.082 mmol, 0.1 eq), Na<sub>2</sub>CO<sub>3</sub> (261 mg, 2.46 mmol, 3.0 eq), dioxane (10 mL) and water (10 mL) and the reaction heated for 1 h. LC-MS analysis showed the reaction to be incomplete and therefore 3-ethoxy-2,4-difluorophenylboronic acid (124 mg, 0.61 mmol, 0.75 eq) and Pd(dppf)Cl<sub>2</sub>•DCM (34 mg, 0.041 mmol, 0.05 eq) were added and the reaction heated for a further 30 minutes. The work up proceeded using the larger volumes of solvents and the organic solvent removed *in vacuo* to reveal a brown oil. The crude product



was purified using column chromatography (2:3 EtOAc–hexane). The title compound 74 (72 mg, 0.26 mmol, 32%) was collected as an off-white solid. **<sup>1</sup>H NMR (500 MHz, CDCl<sub>3</sub>):** 10.52 (1H, br.s, NH), 8.14 (1H, s, 3-H), 7.82 (1H, d, *J* 8.5, 4-H), 7.63 (1H, s, 7-H), 7.31 (1H, app.dt, *J* 8.5 and 1.2, 5-H), 7.15-7.10 (1H, m, 6''-H), 7.01-6.97 (1H, m, 5''-H), 4.27 (2H, q, *J* 7.0, CH<sub>2</sub>), 1.44 (3H, t, *J* 7.0, CH<sub>3</sub>); **<sup>13</sup>C NMR (125 MHz, CDCl<sub>3</sub>):** 155.7 (dd, *J* 247.9 and 4.9, 4''-C), 153.6 (dd, *J* 250.0 and 5.5, 2''-C), 140.3 (3'-C), 135.8 (app.t, *J* 14.8, 3''-C), 134.9 (3-C), 133.8 (6-C), 126.2 (dd, *J* 12.7 and 3.6, 1''-C), 123.9 (dd, *J* 8.7 and 4.1, 6''-C), 122.7 (7'-C), 122.6 (d, *J* 2.4, 5-C), 120.9 (4-C), 111.9 (dd, *J* 19.5 and 3.9, 5''-C), 110.0 (d, *J* 3.4, 7-C), 70.5 (app.t, *J* 3.1, CH<sub>2</sub>), 15.5 (CH<sub>3</sub>); **LC-MS (ES):** RT = 1.95-2.06 min, *m/z* = 275.8 (M+H<sup>+</sup>); **R<sub>f</sub>:** 0.49 (1:1 EtOAc–petrol); **HPLC:** RT = 3.60 min; ***m/z* (ES+):** Found: 275.0990 (M+H<sup>+</sup>), C<sub>15</sub>H<sub>13</sub>F<sub>2</sub>N<sub>2</sub>O requires *MH* 275.0996; **IR:ν<sub>max</sub>/cm<sup>-1</sup> (solid):** 3132 (N-H), 3089, 2924, 1495; **M.pt:** 65.7-68.2°C.

#### Preparation of 6-(4-methoxyphenyl)-1*H*-indazole

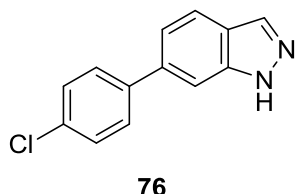


Synthesised using method A using 6-iodo-1*H*-indazole (300 mg, 1.23 mmol, 1.0 eq), 4-methoxyphenylboronic acid (280 mg, 1.84 mmol, 1.5 eq), Pd(dppf)Cl<sub>2</sub>•DCM (100 mg, 0.123 mmol, 0.1 eq), Na<sub>2</sub>CO<sub>3</sub> (391 mg, 3.69 mmol, 3.0 eq), dioxane (10 mL) and water (10 mL) and the reaction heated for 3 h. It was observed that the product and boronic acid had similar *R<sub>f</sub>* values and therefore 6-iodo-1*H*-indazole (300 mg, 1.23 mmol, 1.0 eq) was added and the reaction heated for 1 h to consume all the boronic acid. The work up proceeded using the larger volumes of solvents and the organic solvent removed *in vacuo* to reveal a brown solid. The crude product was purified using column chromatography (3:7 EtOAc–hexane) and an off-white solid obtained. The solid was crystallised from toluene. The title compound 75 (179 mg, 0.80 mmol, 43%) was collected as colourless fluffy microneedles.

**<sup>1</sup>H NMR (500 MHz, CDCl<sub>3</sub>):** 10.32 (1H, br.s, NH), 8.11 (1H, d, *J* 1.0, 3-H), 7.80 (1H, dd, *J* 8.0 and 1.0, 4-H), 7.62-7.57 (3H, m, 7-H, 2''-H and 6''-H), 7.41 (1H, dd, *J* 8.0 and 1.5, 5-H), 7.02 (2H, m, 3''-H and 5''-H), 3.88 (3H, s, CH<sub>3</sub>); **<sup>13</sup>C NMR (125 MHz, CDCl<sub>3</sub>):** 159.4 (4''-C), 140.9 (3'-C), 140.1 (6-C), 134.9 (3-C), 133.8 (1''-C), 128.6 (2''-C and 6''-C), 122.2 (7'-C), 121.2 (5-C), 121.0 (4-C), 114.3 (3''-C and 5''-C), 107.1 (7-C), 55.4 (CH<sub>3</sub>); **LC-MS (ES):** RT = 1.81-2.12 min,

$m/z = 225.4$  ( $M+H^+$ ); **R<sub>f</sub>**: 0.61 (EtOAc); **HPLC**: RT = 2.74 min; **m/z (ES<sup>+</sup>)**: Found: 225.1022 ( $M+H^+$ ),  $C_{14}H_{12}N_2O$  requires *MH* 225.1022; **IR**:  $\nu_{\max}/\text{cm}^{-1}$  (**solid**): 3264 (N-H), 2991, 2962, 2835, 1624, 1522; **M.pt**: 183.2-183.5 °C; **Found**: C, 75.1; H, 5.40; N, 12.6;  $C_{14}H_{12}N_2O$  requires C, 75.0; H, 5.39; N, 12.5%.

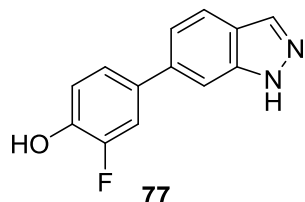
#### Preparation of 6-(4-chlorophenyl)-1*H*-indazole



Synthesised using method A using 6-iodo-1*H*-indazole (162 mg, 0.67 mmol, 1.0 eq), 4-chlorophenylboronic acid (208 mg, 1.33 mmol, 2.0 eq), Pd(dppf)Cl<sub>2</sub>•DCM (54 mg, 0.067 mmol, 0.1 eq), Na<sub>2</sub>CO<sub>3</sub> (211 mg, 2.00 mmol, 3.0 eq), dioxane (10 mL) and water (10 mL) and the reaction heated for 1 h. The work up proceeded using the larger volumes of solvents and the organic solvent removed *in vacuo* to reveal a brown oil. The crude product was purified using column chromatography (3:7 EtOAc–hexane) and a colourless solid obtained. The solid was crystallised from toluene. The **title compound 76** (77 mg, 0.338 mmol, 51%) was collected as shiny colourless plates.

**<sup>1</sup>H NMR (500 MHz, CDCl<sub>3</sub>)**: 10.42 (1H, br.s, NH), 8.13 (1H, d, *J* 0.5, 3-H), 7.83 (1H, dd, *J* 8.5 and 0.5, 4-H), 7.65-7.63 (1H, m, 7-H), 7.58 (2H, app.d, *J* 8.5, 3''-H and 5''-H), 7.45 (2H, app.d, *J* 8.5, 2'-H and 6''-H), 7.39 (1H, dd, *J* 8.5 and 1.5, 5-H); **<sup>13</sup>C NMR (125 MHz, CDCl<sub>3</sub>)**: 140.8 (3'-C), 139.8 (6-C), 139.2 (1'-C), 135.0 (3-C), 133.8 (4'-C), 129.0 (3''-C and 5''-C), 128.8 (2''-C and 6''-C), 122.8 (7'-C), 121.2 (4-C), 121.1 (5-C), 107.6 (7-C); **LC-MS (ES)**: RT = 1.84-2.01 min,  $m/z = 229.3$  ( $M+H^+$ ); **R<sub>f</sub>**: 0.69 (7:3 EtOAc–petrol); **HPLC**: RT = 2.32 min; **m/z (ES<sup>+</sup>)**: Found: 229.0524 ( $M+H^+$ ),  $C_{13}H_9ClN_2$  requires *MH* 229.0527; **IR**:  $\nu_{\max}/\text{cm}^{-1}$  (**solid**): 3169 (N-H), 3049, 2953, 2859, 1910, 1622, 1487; **M.pt**: 179.6-180.7 °C.

#### Preparation of 6-(3-fluoro-4-hydroxyphenyl)-1*H*-indazole

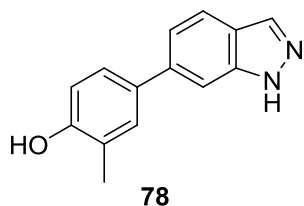


Synthesised using method D using 6-(3-fluoro-4-methoxyphenyl)-1*H*-indazole (50 mg, 0.21 mmol, 1.0 eq), 1M BBr<sub>3</sub> in DCM (1.65 mL, 1.65 mmol, 8.0 eq) and DCM (5 mL). Water (10 mL) was added but minimal precipitate was observed, therefore MeOH (10 mL) was added to aid dissolution and the organic layer separated. The aqueous layer was extracted with DCM (3 × 15 mL) and the combined organic layers dried (MgSO<sub>4</sub>) and concentrated *in vacuo* to reveal the crude product as a yellow solid. The crude product was purified using reverse-phase ACC

(0-40% MeCN–H<sub>2</sub>O–0.1% formic acid). The title compound **77** (18 mg, 0.08 mmol, 39%) was collected as a pale brown powder.

**<sup>1</sup>H NMR (500 MHz, DMSO-d<sub>6</sub>):** 13.06 (1H, br.s, NH), 9.99 (1H, br.s OH), 8.05 (1H, s, 3-H), 7.78 (1H, d, *J* 8.4, 4-H), 7.65 (1H, s, 7-H), 7.51 (1H, dd, *J* 12.8 and 2.2, 2''-H), 7.38-7.33 (2H, m, 5-H and 5''-H), 7.04 (1H, app.t, *J* 8.9, 6''-H); **<sup>13</sup>C NMR (125 MHz, DMSO-d<sub>6</sub>):** 151.3 (d, *J* 240.6, 3''-C), 144.5 (d, *J* 12.2, 4''-C), 140.5 (7'-C), 137.1 (d, *J* 1.2, 6-C), 133.3 (3-C), 132.2 (d, *J* 6.1, 1''-C), 123.1 (d, *J* 2.8, 5''-C), 121.9 (3'-C), 120.8 (4-C), 119.7 (5-C), 118.1 (d, *J* 3.3, 6''-C), 114.6 (d, *J* 19.0, 2''-C), 106.9 (7-C); **LC-MS (ES+):** RT = 0.5-0.6 min, *m/z* = 229.33 (M+H<sup>+</sup>); **R<sub>r</sub>:** 0.30 (1:1 Petrol–EtOAc); **HPLC:** RT = 2.26 min; ***m/z* (ES+):** Found: 229.0769 (M+H<sup>+</sup>), C<sub>13</sub>H<sub>9</sub>FN<sub>2</sub>O requires *MH* 229.0772; **IR:ν<sub>max</sub>/cm<sup>-1</sup> (solid):** 3277 (br.O-H), 2444, 1614, 1591; **M.pt:** >250 °C.

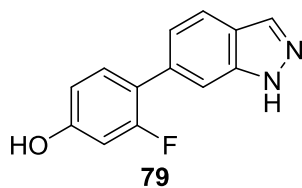
#### Preparation of 6-(3-methyl-4-hydroxyphenyl)-1*H*-indazole



Synthesised using method D using 6-(3-methyl-4-methoxyphenyl)-1*H*-indazole (50 mg, 0.21 mmol, 1.0 eq), 1M BBr<sub>3</sub> in DCM (1.68 mL, 1.68 mmol, 8.0 eq) and DCM (5 mL). Water (10 mL) was added and the resulting precipitate filtered and washed with water. The title

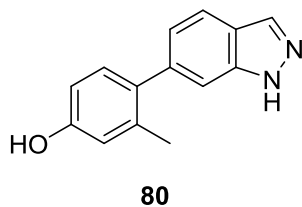
compound **78** (32 mg, 0.14 mmol, 70%) was collected as a colourless powder.

**<sup>1</sup>H NMR (500 MHz, DMSO-d<sub>6</sub>):** 8.03 (1H, d, *J* 0.7, 3-H), 7.75 (1H, d, *J* 8.4, 4-H), 7.59 (1H, br.s, 7-H), 7.43 (1H, d, *J* 1.8, 2''-H), 7.36-7.31 (2H, m, 5-H and 5''-H), 6.86 (1H, d, *J* 8.3, 6''-H), 2.19 (3H, s, CH<sub>3</sub>), NH and OH not observed; **<sup>13</sup>C NMR (125 MHz, DMSO-d<sub>6</sub>):** 155.2 (4''-C), 140.7 (7'-C), 138.6 (Ar-q), 133.2 (3-C), 131.2 (Ar-q), 129.4 (2''-C), 125.4 (5''-C), 124.3 (3''-C), 121.5 (3'-C), 120.6 (4-C), 119.8 (5-C), 115.0 (6''-C), 106.5 (7-C), 16.1 (CH<sub>3</sub>); **LC-MS (ES+):** RT = 0.5-0.6 min, *m/z* = 225.37 (M+H<sup>+</sup>); **R<sub>r</sub>:** 0.32 (1:1 Petrol–EtOAc); **HPLC:** RT = 2.43 min; ***m/z* (ES+):** Found: 225.1018 (M+H<sup>+</sup>), C<sub>14</sub>H<sub>12</sub>N<sub>2</sub>O requires *MH* 225.1022; **IR:ν<sub>max</sub>/cm<sup>-1</sup> (solid):** 3246 (br.O-H), 3203 (N-H), 2694, 2260, 1629, 1605; **M.pt:** >250 °C.

Preparation of 6-(2-fluoro-4-hydroxyphenyl)-1H-indazole

Synthesised using method D using 6-(2-fluoro-4-methoxyphenyl)-1H-indazole (50 mg, 0.21 mmol, 1.0 eq), 1M BBr<sub>3</sub> in DCM (1.65 mL, 1.65 mmol, 8.0 eq) and DCM (5 mL). Water (10 mL) was added and the resulting precipitate filtered and washed with water. The title compound **79** (37 mg, 0.16 mmol, 81%) was collected as colourless microcrystals.

**<sup>1</sup>H NMR (500 MHz, DMSO-d<sub>6</sub>):** 8.07 (1H, d, *J* 0.8, 3-H), 7.78 (1H, dd, *J* 8.4 and 0.8, 4-H), 7.56 (1H, s, 7-H), 7.39 (1H, app.t, *J* 8.5, 6''-H), 7.21 (1H, app.dt, *J* 8.4 and 1.5, 5-H), 6.73 (1H, dd, *J* 8.5 and 2.4, 5''-H), 6.68 (1H, dd, *J* 12.8 and 2.4, 3''-H), NH and OH not observed; **<sup>13</sup>C NMR (125 MHz, DMSO-d<sub>6</sub>):** 159.7 (d, *J* 245.1, 2''-C), 158.4 (d, *J* 11.8, 4''-C), 140.2 (7'-C), 133.2 (d, *J* 5.0, 6-C), 133.2 (3-C), 131.5 (d, *J* 5.4, 6''-C), 121.7 (7'-C), 121.6 (d, *J* 2.3, 5-C), 120.4 (4-C), 119.1 (d, *J* 13.2, 1''-C), 112.2 (d, *J* 2.7, 5''-C), 109.5 (d, *J* 3.1, 7-C), 103.1 (d, *J* 25.2, 3''-C); **LC-MS (ES<sup>+</sup>):** RT = 0.5-0.6 min, *m/z* = 229.33 (M+H<sup>+</sup>); **R<sub>f</sub>:** 0.32 (1:1 Petrol–EtOAc); **HPLC:** RT = 2.31 min; ***m/z* (ES<sup>+</sup>):** Found: 229.0770 (M+H<sup>+</sup>), C<sub>13</sub>H<sub>9</sub>FN<sub>2</sub>O requires *MH* 229.0772; **IR:**  $\nu_{\max}/\text{cm}^{-1}$  (solid): 3270 (br.O-H), 3002, 2804, 1624, 1596; **M.pt:** >250 °C.

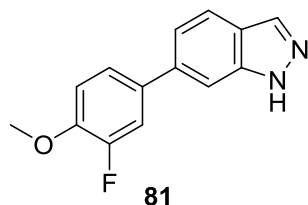
Preparation of 6-(2-methyl-4-hydroxyphenyl)-1H-indazole

Synthesised using method D using 6-(2-methyl-4-methoxyphenyl)-1H-indazole (75 mg, 0.31 mmol, 1.0 eq), 1M BBr<sub>3</sub> in DCM (2.52 mL, 2.52 mmol, 8.0 eq) and DCM (5 mL). Water (10 mL) was added and the resulting precipitate filtered and washed with water. The title compound **80** (50 mg, 0.22 mmol, 72%) was collected as a colourless powder.

**<sup>1</sup>H NMR (500 MHz, DMSO-d<sub>6</sub>):** 8.05 (1H, d, *J* 0.9, 3-H), 7.73 (1H, dd, *J* 8.3 and 0.9, 4-H), 7.33 (1H, s, 7-H), 7.05 (1H, d, *J* 8.2, 6''-H), 7.02 (1H, dd, *J* 8.3 and 1.3, 5-H), 6.70 (1H, d, *J* 2.4, 3''-H), 6.66 (1H, dd, *J* 8.2 and 2.4, 5''-H), 2.16 (3H, s, CH<sub>3</sub>), NH and OH not observed; **<sup>13</sup>C NMR (125 MHz, DMSO-d<sub>6</sub>):** 156.5 (4''-C), 140.0 (7'-C), 139.4 (Ar-q), 136.0 (Ar-q), 133.2 (3-C), 132.5 (Ar-q), 130.8 (6''-C), 122.6 (5-C), 121.4 (3'-C), 119.8 (4-C), 116.8 (3''-C), 112.8 (5''-C), 109.8 (7-C), 20.4 (CH<sub>3</sub>); **LC-MS (ES<sup>+</sup>):** RT = 0.5-0.6 min, *m/z* = 225.38 (M+H<sup>+</sup>); **R<sub>f</sub>:** 0.35 (1:1 Petrol–EtOAc); **HPLC:** RT = 2.30 min; ***m/z* (ES<sup>+</sup>):** Found: 225.1020 (M+H<sup>+</sup>), C<sub>14</sub>H<sub>12</sub>N<sub>2</sub>O requires

*MH* 225.1022; **IR**:  $\nu_{\max}/\text{cm}^{-1}$  (solid): 3184 (br.O-H), 2255, 1438; **M.pt**: 222.8-223.2 °C.

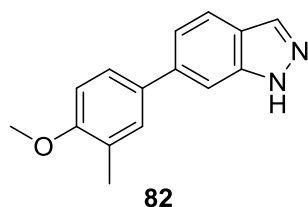
Preparation of 6-(3-fluoro-4-methoxyphenyl)-1*H*-indazole



Synthesised using method A using 6-iodo-1*H*-indazole (250 mg, 1.02 mmol, 1.0 eq), 3-fluoro-4-methoxyphenyl boronic acid (261 mg, 1.54 mmol, 1.5 eq), Pd(dppf)Cl<sub>2</sub>•DCM (84 mg, 0.102 mmol, 0.1 eq), Na<sub>2</sub>CO<sub>3</sub> (325 mg, 3.07 mmol, 3.0 eq), dioxane (2.5 mL) and water (2.5 mL) and the reaction heated for 3 h. The work up proceeded using the smaller volumes of solvents and the organic solvent removed *in vacuo* to reveal a brown solid. The crude product was purified using column chromatography (gradient 20-30% EtOAc–hexane) and an off-white solid obtained. The solid was crystallised from toluene. The title compound **81** (174 mg, 0.72 mmol, 72%) was collected as off-white needles.

**<sup>1</sup>H NMR (500 MHz, CDCl<sub>3</sub>)**: 10.15 (1H, br.s, NH), 8.10 (1H, br.s, *J* 1.1, 3-H), 7.80 (1H, d, *J* 8.4, 4-H), 7.60 (1H, s, 7-H), 7.41 (1H, d, *J* 2.2, 2''-H), 7.39-7.35 (2H, m, 5-H and 5''-H), 7.06 (1H, app.t, *J* 8.8, 6''-H), 3.95 (3H, s, CH<sub>3</sub>); **<sup>13</sup>C NMR (125 MHz, CDCl<sub>3</sub>)**: 152.6 (d, *J* 245.8, 3''-C), 147.3 (d, *J* 10.7, 4''-C), 140.8 (7'-C), 138.9 (d, *J* 1.2, 6-C), 135.1 (3-C), 134.5 (d, *J* 6.5, 1''-C), 123.1 (d, *J* 3.3, 5''-C), 122.5 (3'-C), 121.2 (5-C), 121.0 (4-C), 115.3 (d, *J* 19.0, 2''-C), 113.8 (d, *J* 2.3, 6''-C), 107.3 (7-C), 56.4 (CH<sub>3</sub>); **LC-MS (ES<sup>+</sup>)**: RT = 0.6-0.6 min, *m/z* = 243.34 (M+H<sup>+</sup>); **R<sub>f</sub>**: 0.17 (3:7 EtOAc–petrol); **HPLC**: RT = 3.00 min; ***m/z* (ES<sup>+</sup>)**: Found: 243.0926 (M+H<sup>+</sup>), C<sub>14</sub>H<sub>11</sub>FN<sub>2</sub>O requires *MH* 243.0928; **IR**:  $\nu_{\max}/\text{cm}^{-1}$  (solid): 3257 (N-H), 2965, 2937, 2840, 1618, 1517; **M.pt**: 141.1-141.8 °C.

Preparation of 6-(3-methyl-4-methoxyphenyl)-1*H*-indazole

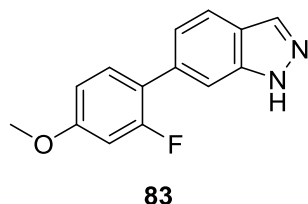


Synthesised using method A using 6-iodo-1*H*-indazole (250 mg, 1.02 mmol, 1.0 eq), 4-methoxy-3-methylphenyl boronic acid (255 mg, 1.54 mmol, 1.5 eq), Pd(dppf)Cl<sub>2</sub>•DCM (84 mg, 0.102 mmol, 0.1 eq), Na<sub>2</sub>CO<sub>3</sub> (325 mg, 3.07 mmol, 3.0 eq), dioxane (2.5 mL) and water (2.5 mL) and the reaction heated for 3 h. LC-MS analysis indicated the reaction to be incomplete and therefore 6-iodo-1*H*-indazole (125 mg, 0.51 mmol, 0.5 eq), Pd(dppf)Cl<sub>2</sub>•DCM (42 mg, 0.051 mmol, 0.05 eq) and Na<sub>2</sub>CO<sub>3</sub> (163 mg, 1.53 mmol, 1.5 eq) were added and the

reaction heated for a further 1 h. The work up proceeded using the smaller volumes of solvents and the organic solvent removed *in vacuo* to reveal a brown solid. The crude product was purified using column chromatography (7:3 Petrol–EtOAc) and an off-white solid obtained. The solid was crystallised using a mixed solvent crystallisation using EtOH and cyclohexane as the antisolvent. The title compound **82** (66 mg, 0.28 mmol, 21%) was collected as colourless needles.

**<sup>1</sup>H NMR (500 MHz, CDCl<sub>3</sub>):** 10.17 (1H, br.s, NH), 8.09 (1H, d, *J* 1.1, 3-H), 7.78 (1H, dd, *J* 8.4 and 1.1, 4-H), 7.61 (1H, s, 7-H), 7.47-7.44 (2H, m, 2''-H and 5''-H), 7.41 (1H, dd, *J* 8.4 and 1.4, 5-H), 6.94-6.90 (1H, m, 6''-H), 3.89 (3H, s, OCH<sub>3</sub>), 2.31 (3H, s, CH<sub>3</sub>); **<sup>13</sup>C NMR (125 MHz, CDCl<sub>3</sub>):** 157.6 (4''-C), 140.9 (7'-C), 140.3 (6-C), 135.0 (3-C), 133.3 (1''-C), 129.9 (2''-C), 127.1 (3''-C), 125.9 (5''-C), 122.1 (3'-C), 121.3 (5-C), 120.9 (4-C), 110.3 (6''-C), 107.0 (7-C), 55.5 (OCH<sub>3</sub>), 16.4 (CH<sub>3</sub>); **LC-MS (ES+):** RT = 0.6-0.7 min, *m/z* = 239.36 (M+H<sup>+</sup>); **R<sub>f</sub>:** 0.16 (7:3 Petrol–EtOAc); **HPLC:** RT = 3.31 min; ***m/z* (ES+):** Found: 239.1177 (M+H<sup>+</sup>), C<sub>15</sub>H<sub>14</sub>N<sub>2</sub>O requires *MH* 239.1179; **IR:**  $\nu_{\max}/\text{cm}^{-1}$  (solid): 3229 (N-H), 2921, 2837, 1625, 1518; **M.pt:** 152.8-153.7 °C.

#### Preparation of 6-(2-fluoro-4-methoxyphenyl)-1*H*-indazole



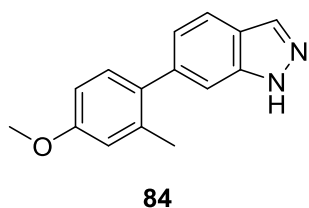
Synthesised using method A using 6-iodo-1*H*-indazole (250 mg, 1.02 mmol, 1.0 eq), 2-fluoro-4-methoxyphenylboronic acid (261 mg, 1.54 mmol, 1.5 eq), Pd(dppf)Cl<sub>2</sub>•DCM (84 mg, 0.102 mmol, 0.1 eq), Na<sub>2</sub>CO<sub>3</sub>

(325 mg, 3.07 mmol, 3.0 eq), dioxane (2.5 mL) and water (2.5 mL) and the reaction heated for 3 h. The work up proceeded using the smaller volumes of solvents and the organic solvent removed *in vacuo* to reveal a brown solid. The crude product was purified using column chromatography (1:4 EtOAc–petrol) and an off-white solid obtained. The solid was crystallised from EtOH. The title compound **83** (55 mg, 0.23 mmol, 23%) was collected as colourless needles.

**<sup>1</sup>H NMR (500 MHz, CDCl<sub>3</sub>):** 10.20 (1H, br.s, NH), 8.10 (1H, s, 3-H), 7.79 (1H, d, *J* 8.4, 4-H), 7.63 (1H, s, 7-H), 7.41 (1H, app.t, *J* 8.5, 6''-H), 7.33 (1H, app.dt, *J* 8.5 and 2.5, 5-H), 6.82-6.79 (1H, m, 5''-H), 6.75 (1H, app. dd, *J* 12.5 and 2.5, 3''-H), 3.86 (3H, s, CH<sub>3</sub>); **<sup>13</sup>C NMR (125 MHz, CDCl<sub>3</sub>):** 160.7 (d, *J* 11.0, 4''-C), 160.6 (d, *J* 246.2, 2''-C), 140.6 (7'-C), 135.2 (6-C), 134.8 (3-C), 131.6 (d, *J* 5.2, 6''-C), 122.9 (d, *J* 2.3, 5-C) 122.5 (3'-C), 121.6 (d, *J* 13.7, 1''-C), 120.9 (4-C), 110.6 (d, *J* 3.1, 5''-C), 109.8

(d,  $J$  3.3, 7-C), 102.4 (d,  $J$  26.6, 3''-C) 55.9 ( $\underline{\text{C}}\text{H}_3$ ); **LC-MS (ES+)**: RT = 0.6-0.6 min,  $m/z = 243.33$  ( $\text{M}+\text{H}^+$ ); **R<sub>f</sub>**: 0.05 (4:1 Petrol–EtOAc); **HPLC**: RT = 3.10 min; **m/z (ES+)**: Found: 243.0925 ( $\text{M}+\text{H}^+$ ),  $\text{C}_{14}\text{H}_{11}\text{FN}_2\text{O}$  requires  $MH$  243.0928; **IR:  $\nu_{\text{max}}/\text{cm}^{-1}$  (solid)**: 3220 (N-H), 3052, 2987, 1620, 1580; **M.pt**: 148.8-149.9 °C.

Preparation of 6-(2-methyl-4-methoxyphenyl)-1H-indazole

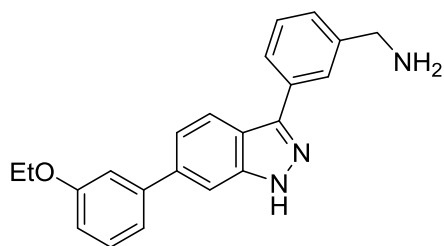


Synthesised using method A using 6-iodo-1H-indazole (250 mg, 1.02 mmol, 1.0 eq), 4-methoxy-2-methylphenylboronic acid (255 mg, 1.54 mmol, 1.5 eq), Pd(dppf)Cl<sub>2</sub>•DCM (84 mg, 0.102 mmol, 0.1 eq), Na<sub>2</sub>CO<sub>3</sub> (325 mg, 3.07 mmol, 3.0 eq), dioxane (2.5 mL) and water

(2.5 mL) and the reaction heated for 3 h. The work up proceeded using the smaller volumes of solvents and the organic solvent removed *in vacuo* to reveal a brown solid. The crude product was purified using column chromatography (7:3 hexane–EtOAc) and an off-white solid obtained. The solid was crystallised from cyclohexane. The title compound 84 (99 mg, 0.42 mmol, 41%) was collected as colourless fluffy microcrystals.

**<sup>1</sup>H NMR (500 MHz, CDCl<sub>3</sub>)**: 10.26 (1H, br.s,  $\underline{\text{N}}\text{H}$ ), 8.11 (1H, s, 3-H), 7.75 (1H, d,  $J$  8.3, 4-H), 7.38 (1H, s, 7-H), 7.20 (1H, d,  $J$  8.3, 6''-H), 7.12 (1H, dd,  $J$  8.3 and 1.2, 5-H), 6.84 (1H, d,  $J$  2.6, 3''-H), 6.81 (1H, dd,  $J$  8.3 and 2.6, 5''-H), 3.85 (3H, s,  $\underline{\text{O}}\underline{\text{C}}\underline{\text{H}}_3$ ), 2.27 (3H, s,  $\underline{\text{C}}\underline{\text{H}}_3$ ); **<sup>13</sup>C NMR (125 MHz, CDCl<sub>3</sub>)**: 159.0 (4''-C), 140.8 (7'-C), 137.5 (Ar-q), 136.9 (Ar-q), 135.0, (Ar-q), 134.6 (3-C), 131.0 (6''-C), 123.6 (5-C), 120.2 (4-C), 115.8 (3''-C), 111.2 (5''-C), 109.9 (7-C), 55.3 ( $\underline{\text{O}}\underline{\text{C}}\underline{\text{H}}_3$ ), 20.8 ( $\underline{\text{C}}\underline{\text{H}}_3$ ), one quaternary carbon not observed; **LC-MS (ES+)**: RT = 0.6-0.7 min,  $m/z = 239.38$  ( $\text{M}+\text{H}^+$ ); **R<sub>f</sub>**: 0.20 (7:3 Petrol–EtOAc); **HPLC**: RT = 3.18 min; **m/z (ES+)**: Found: 239.1178 ( $\text{M}+\text{H}^+$ ),  $\text{C}_{15}\text{H}_{14}\text{N}_2\text{O}$  requires  $MH$  239.1179; **IR:  $\nu_{\text{max}}/\text{cm}^{-1}$  (solid)**: 3250 (N-H), 2997, 2830, 1624, 1606, 1566; **M.pt**: 115.1-115.9 °C.

## 6.1.4.2 Chapter Three Compounds

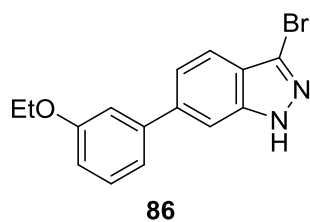
Preparation of {3-[6-(3-ethoxyphenyl)-1*H*-indazol-3-yl]phenyl}methanamine**85**

Synthesised using method A using 3-bromo-6-(3-ethoxyphenyl)-1*H*-indazole (150 mg, 0.47 mmol, 1.0 eq), 3-(aminomethyl)phenylboronic acid•HCl (133 mg, 0.71 mmol, 1.5 eq), Pd(dppf)Cl<sub>2</sub>•DCM (39 mg, 0.047 mmol, 0.1 eq), Na<sub>2</sub>CO<sub>3</sub> (250 mg,

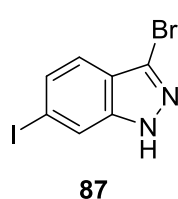
2.36 mmol, 5.0 eq), dioxane (5 mL) and water (5 mL) and the reaction heated for 2 h. LC-MS analysis showed the reaction to be incomplete therefore Pd(dppf)Cl<sub>2</sub>•DCM (39 mg, 0.047 mmol, 0.1 eq) and Na<sub>2</sub>CO<sub>3</sub> (75 mg, 0.71 mmol, 1.5 eq) were added and the reaction heated for 2 h. LC-MS analysis showed no change and therefore the reaction was stopped. The work up proceeded using the larger volumes of solvents and the organic solvent removed *in vacuo* to reveal a brown solid. The crude product was purified using column chromatography (3:10:87 7.0 M NH<sub>3</sub> in MeOH–MeOH–EtOAc) and a brown semi-solid obtained. The semi-solid was triturated with DCM. The title compound 85 (10 mg, 0.029 mmol, 6%) was collected as colourless granules.

**<sup>1</sup>H NMR (500 MHz, DMSO-*d*<sub>6</sub>):** 8.15 (1H, d, *J* 8.5, 4-H), 7.98 (1H, s, 2'''-H), 7.83 (1H, d, *J* 8.0, 6'''-H), 7.76 (1H, s, 7-H), 7.49 (1H, dd, *J* 8.5 and 1.5, 5-H), 7.45 (1H, app.t, *J* 7.5, 5'''-H), 7.39 (1H, app.t, *J* 8.0, 5''-H), 7.35 (1H, d, *J* 7.5, 4'''-H), 7.29 (1H, d, *J* 7.5, 6''-H), 7.25 (1H, app.t *J* 2.0, 2''-H), 6.95 (1H, ddd, *J* 8.0, 2.5 and 1.0, 4''-H), 4.12 (2H, q, *J* 7.0, CH<sub>2</sub>CH<sub>3</sub>), 3.83 (2H, s, CH<sub>2</sub>), 1.97 (2H, br.s, CH<sub>2</sub>NH<sub>2</sub>), 1.36 (3H, t, *J* 7.0, CH<sub>3</sub>), indazole NH not observed; **<sup>13</sup>C NMR (125 MHz, DMSO-*d*<sub>6</sub>):** 159.0 (3''-C), 144.9 (3'''-C), 143.3 (1'''-C), 142.3 (3'-C), 141.9 (1''-C), 138.3 (6-C), 133.5 (3-C), 130.0 (5''-C), 128.6 (5'''-C), 126.5 (4'''-C), 125.4 (2'''-C), 124.6 (6''-C), 121.2 (4-C), 120.8 (5-C), 119.5 (7'-C), 119.4 (6''-C), 113.6 (4''-C), 113.1 (2''-C), 108.2 (7-C), 63.1 (CH<sub>2</sub>), 45.7 (CH<sub>2</sub>NH<sub>2</sub>), 14.7 (CH<sub>3</sub>); **LC-MS (ES):** RT = 1.73-2.07 min, *m/z* = 344.2 (M+H<sup>+</sup>); **R<sub>r</sub>**: 0.17 (1:1:8 7.0 M NH<sub>3</sub> in MeOH–MeOH–EtOAc); **HPLC:** RT = 2.27 min; ***m/z* (ES+):** Found: 366.1581 (M+Na<sup>+</sup>), C<sub>22</sub>H<sub>21</sub>N<sub>3</sub>NaO requires *MH* 366.1577; **IR:ν<sub>max</sub>/cm<sup>-1</sup> (solid):** 3328 (N-H), 3263 (N-H), 3173, 2983, 2915, 2839, 1594; **M.pt:** 151.4-151.7 °C.



Preparation of 3-bromo-6-(3-ethoxyphenyl)-1H-indazole

Synthesised using method A using 3-bromo-6-iodo-1H-indazole (500 mg, 1.55 mmol, 1.0 eq), 3-ethoxyphenylboronic acid (385 mg, 2.32 mmol, 1.5 eq), Pd(dppf)Cl<sub>2</sub>•DCM (126 mg, 0.155 mmol, 0.1 eq), Na<sub>2</sub>CO<sub>3</sub> (492 mg, 4.64 mmol, 3.0 eq), dioxane (10 mL) and water (10 mL) and the reaction heated for 3 h. The work up proceeded using the larger volumes of solvents and the organic solvent removed *in vacuo* to reveal a brown oil. The crude product was purified using column chromatography (1:4 EtOAc–hexane) and a colourless solid obtained. The resulting solid was crystallised from cyclohexane. The title compound 86 (207 mg, 0.65 mmol, 42%) was collected as colourless flakes. **<sup>1</sup>H NMR (500 MHz, CDCl<sub>3</sub>):** 10.58 (1H, br.s, NH), 7.69 (1H, d, *J* 8.5, 4-H), 7.67 (1H, s, 7-H), 7.49 (1H, dd, *J* 8.5 and 1.5, 5-H), 7.39 (1H, app.t, *J* 8.0, 5''-H), 7.23-7.21 (1H, m, 6''-H), 7.18 (1H, app.t, *J* 2.0, 2''-H), 6.94 (1H, ddd, *J* 8.0, 2.5 and 1.0, 4''-H), 4.12 (2H, q, *J* 7.0, CH<sub>2</sub>), 1.47 (3H, t, *J* 7.0, CH<sub>3</sub>); **<sup>13</sup>C NMR (125 MHz, CDCl<sub>3</sub>):** 159.4 (3''-C), 142.3 (1''-C), 141.8 (6-C), 141.7 (3'-C), 129.9 (5''-C), 123.0 (7'-C), 122.5 (3-C), 122.3 (5-C), 120.4 (4-C), 120.0 (6''-C), 114.1 (2''-C), 113.7 (4''-C), 108.2 (7-C), 63.6 (CH<sub>2</sub>), 14.9 (CH<sub>3</sub>); **LC-MS (ES):** RT = 1.95-2.01 min, *m/z* = 317.1 (M+H<sup>+</sup>); **R<sub>f</sub>:** 0.46 (2:3 EtOAc–petrol); **HPLC:** RT = 3.02 min; ***m/z* (ES<sup>+</sup>):** Found: 317.0287 (M+H<sup>+</sup>), C<sub>15</sub>H<sub>13</sub>BrN<sub>2</sub>O requires *MH* 317.0284; **IR:ν<sub>max</sub>/cm<sup>-1</sup> (solid):** 3172 (N-H), 3135, 2975, 2869, 1631; **M.pt:** 132.9-133.4 °C; **Found:** C, 56.7; H, 4.10; N, 8.8; C<sub>15</sub>H<sub>13</sub>BrN<sub>2</sub>O requires C, 56.8; H, 4.13; N, 8.8%.

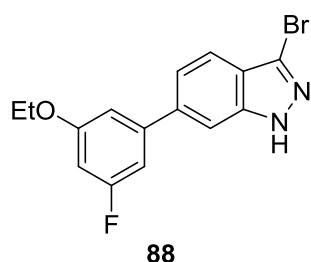
Preparation of 3-bromo-6-iodo-1H-indazole

6-Iodo-1H-indazole (3.00 g, 12.3 mmol, 1.0 eq) was dissolved in DMF (30 mL) and NBS (2.01 g, 13.5 mmol, 1.1 eq) was added to the reaction mixture and stirred for 3 h. LC-MS analysis confirmed the reaction to be complete. Water (60 mL) was added and the resulting precipitate filtered. The crude product was crystallised from EtOH. The title compound 87 (3.72 g, 11.5 mmol, 94%) was collected as yellow microcrystals.

**<sup>1</sup>H NMR (500 MHz, DMSO-d<sub>6</sub>):** 7.99 (1H, dd, *J* 1.5 and 0.5, 7-H), 7.49 (1H, dd, *J* 8.0 and 1.5, 5-H), 7.38 (1H, d, *J* 8.0, 4-H), NH not observed; **<sup>13</sup>C NMR (125 MHz, DMSO-d<sub>6</sub>):** 142.2 (3'-C), 130.0 (5-C), 121.4 (7'-C), 121.0 (4-C), 120.8 (3-C), 119.4 (7-C), 93.9 (6-C); **LC-MS (ES):** RT = 1.95-2.10 min, *m/z* = 323.0 (M+H<sup>+</sup>); **R<sub>f</sub>:** 0.61

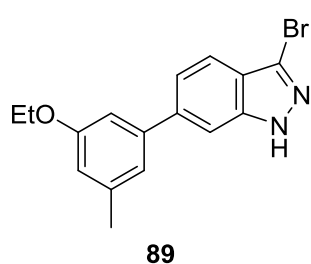
(1:1 EtOAc–petrol); **HPLC**: RT = 15.27 min; **m/z (ES-)**: Found: 320.8522 (M-H), C<sub>7</sub>H<sub>4</sub>BrIN<sub>2</sub> requires *M-H* 320.8530; **IR**: $\nu_{\max}/\text{cm}^{-1}$  (**solid**): 3188 (N-H), 3100, 2965, 2910, 1612; **M.pt**: 230.4-231.7 °C; **Found**: C,26.3; H, 1.20; N, 8.7; C<sub>7</sub>H<sub>4</sub>BrIN<sub>2</sub> requires C, 26.4; H, 1.20; N, 8.7%.

Preparation of 3-bromo-6-(3-ethoxy-5-fluorophenyl)-1*H*-indazole



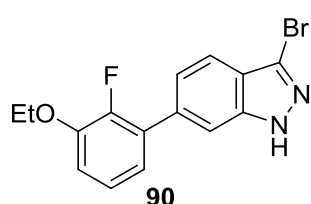
Synthesised using method A using 3-bromo-6-iodo-1*H*-indazole (500 mg, 1.55 mmol, 1.0 eq), 3-ethoxy-5-fluorophenylboronic acid (427 mg, 2.32 mmol, 1.5 eq), Pd(dppf)Cl<sub>2</sub>•DCM (126 mg, 0.155 mmol, 0.1 eq), Na<sub>2</sub>CO<sub>3</sub> (492 mg, 4.64 mmol, 3.0 eq), dioxane (10 mL) and water (10 mL) and the reaction heated for 3 h. LC-MS showed the reaction to be incomplete but was stopped to minimise formation of the bis-substituted product. The work up proceeded using the larger volumes of solvents and the organic solvent removed *in vacuo* to reveal a brown oil. The crude product was purified using column chromatography (1:9 EtOAc–hexane) and a colourless solid obtained. The resulting solid was crystallised from cyclohexane. The title compound 88 (166 mg, 0.50 mmol, 32%) was collected as a colourless flakes.

**<sup>1</sup>H NMR (500 MHz, CDCl<sub>3</sub>)**: 10.65 (1H, br.s, NH), 7.70 (1H, d, *J* 8.5, 4-H), 7.66 (1H, s, 7-H), 7.45 (1H, dd, *J* 8.5 and 1.5, 5-H), 6.96 (1H, app.t, *J* 1.5, 6''-H), 6.93 (1H, app.dt, *J* 9.5 and 1.5, 2''-H), 6.65 (1H, app.dt, *J* 10.5 and 2.0, 4''-H), 4.10 (2H, q, *J* 7.0, CH<sub>2</sub>), 1.45 (3H, t, *J* 7.0, CH<sub>3</sub>); **<sup>13</sup>C NMR (125 MHz, CDCl<sub>3</sub>)**: 163.9 (d, *J* 244.9, 3''-C), 160.6 (d, *J* 11.5, 5''-C), 143.4 (d, *J* 9.9, 1''-C), 141.7 (3'-C), 140.7 (d, *J* 2.7, 6-C), 123.1 (7'-C), 122.8 (3-C), 122.0 (5-C), 120.6 (4-C), 110.1 (d, *J* 2.6, 6''-C), 108.3 (7-C), 106.8 (d, *J* 22.7, 2''-H), 101.2 (d, *J* 25.2, 4''-C), 64.0 (CH<sub>2</sub>), 14.7 (CH<sub>3</sub>); **LC-MS (ES)**: RT = 2.11-2.25 min, *m/z* = 335.0 (M+H<sup>+</sup>); **R<sub>f</sub>**: 0.44 (3:7 EtOAc–hexane); **HPLC**: RT = 3.65 min; **m/z (ES+)**: Found: 335.0196 (M+H<sup>+</sup>), C<sub>15</sub>H<sub>12</sub>BrFN<sub>2</sub>O requires *MH* 335.0190; **IR**: $\nu_{\max}/\text{cm}^{-1}$  (**solid**): 3175 (N-H), 3137, 2984, 2875, 1601; **M.pt**: 166.4-167.6 °C; **Found**: C,53.8; H, 3.60; N, 8.4; C<sub>15</sub>H<sub>12</sub>BrFN<sub>2</sub>O requires C, 53.8; H, 3.61; N, 8.4%.

Preparation of 3-bromo-6-(3-ethoxy-5-methylphenyl)-1*H*-indazole

Synthesised using method A using 3-bromo-6-iodo-1*H*-indazole (500 mg, 1.55 mmol, 1.0 eq), 3-ethoxy-5-methylphenylboronic acid (279 mg, 1.55 mmol, 1.0 eq), Pd(dppf)Cl<sub>2</sub>•DCM (126 mg, 0.155 mmol, 0.1 eq), Na<sub>2</sub>CO<sub>3</sub> (492 mg, 4.64 mmol, 3.0 eq), dioxane (10 mL) and water (10 mL) and the reaction heated for 2 h. LC-MS analysis showed the reaction to be incomplete and therefore 3-ethoxy-5-methylphenylboronic acid (84 mg, 0.47 mmol, 0.30 eq), Pd(dppf)Cl<sub>2</sub>•DCM (126 mg, 0.155 mmol, 0.1 eq) and Na<sub>2</sub>CO<sub>3</sub> (246 mg, 2.32 mmol, 1.5 eq) were added and the reaction heated for a further 1 h. The work up proceeded using the larger volumes of solvents and the organic solvent removed *in vacuo* to reveal a brown oil. The crude product was purified using column chromatography (gradient 10-30% EtOAc–hexane) and a colourless solid obtained. The solid was crystallised from cyclohexane. The title compound 89 (100 mg, 0.30 mmol, 19%) was collected as a colourless solid.

**<sup>1</sup>H NMR (500 MHz, CDCl<sub>3</sub>):** 10.41 (1H, br.s, NH), 7.68 (1H, d, *J* 8.3, 4-H), 7.64 (1H, s, 7-H), 7.48 (1H, dd, *J* 8.4 and 1.4, 5-H), 7.04 (1H, s, 6''-H), 6.98 (1H, s, 2''-H), 6.77 (1H, s, 4''-H), 4.11 (2H, q, *J* 7.0, CH<sub>2</sub>), 2.42 (3H, s, CH<sub>3</sub>), 1.45 (3H, t, *J* 7.0, CH<sub>2</sub>CH<sub>3</sub>); **<sup>13</sup>C NMR (125 MHz, CDCl<sub>3</sub>):** 159.4 (3''-C), 142.0 (1''-C), 141.9 (3'-C), 141.8 (6-C), 140.0 (5''-C), 123.1 (3-C), 122.5 (7'-C), 122.3 (5-C), 120.9 (6''-C), 120.3 (4-C), 114.7 (4''-C), 111.2 (2''-C), 108.1 (7-C), 63.6 (CH<sub>2</sub>), 21.7 (CH<sub>3</sub>), 14.9 (CH<sub>2</sub>CH<sub>3</sub>); **LC-MS (ES):** RT = 2.18-2.38 min, *m/z* = 331.8 (M+H<sup>+</sup>); **R<sub>f</sub>:** 0.64 (1:1 EtOAc–petrol); **HPLC:** RT = 2.13 min; ***m/z* (ES+):** Found: 331.0442 (M+H<sup>+</sup>), C<sub>16</sub>H<sub>16</sub>BrN<sub>2</sub>O requires *MH* 331.0446; **IR:ν<sub>max</sub>/cm<sup>-1</sup> (solid):** 3174 (N-H), 3132, 2963, 2871, 1726; **M.pt:** 144.8-145.4 °C.

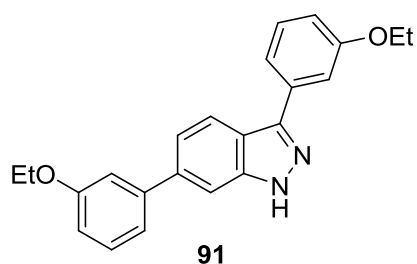
Preparation of 3-bromo-6-(3-ethoxy-2-fluorophenyl)-1*H*-indazole

Synthesised using method A using 3-bromo-6-iodo-1*H*-indazole (500 mg, 1.55 mmol, 1.0 eq), 3-ethoxy-2-fluorophenylboronic acid (429 mg, 2.33 mmol, 1.5 eq), Pd(dppf)Cl<sub>2</sub>•DCM (126 mg, 0.155 mmol, 0.1 eq), Na<sub>2</sub>CO<sub>3</sub> (492 mg, 4.65 mmol, 3.0 eq), dioxane (10 mL) and water (10 mL) and the reaction heated for 2 h. LC-MS showed the reaction to be incomplete and therefore 3-ethoxy-2-fluorophenylboronic acid (143 mg, 0.78 mmol, 0.5 eq), Pd(dppf)Cl<sub>2</sub>•DCM (126 mg,

0.155 mmol, 0.1 eq) and Na<sub>2</sub>CO<sub>3</sub> (246 mg, 2.32 mmol, 1.5 eq) were added and the reaction heated for 1 h. The work up proceeded using the larger volumes of solvents and the organic solvent removed *in vacuo* to reveal a brown solid. The crude product was purified using column chromatography (3:7 EtOAc–hexane) and a colourless solid obtained. The solid was crystallised from cyclohexane. The title compound 90 (239 mg, 0.72 mmol, 46%) was collected as colourless plates.

**<sup>1</sup>H NMR (500 MHz, CDCl<sub>3</sub>):** 10.39 (1H, br.s, NH), 7.70 (1H, d, *J* 8.5, 4-H), 7.66 (1H, s, 7-H), 7.43 (1H, app.dt, *J* 8.5 and 1.2, 5-H), 7.15 (1H, app.td, *J* 8.0 and 1.2, 5''-H), 7.04 (1H, app.td, *J* 7.6 and 1.5, 6''-H), 7.00 (1H, app.td, *J* 7.8 and 1.5, 4''-H), 4.18 (2H, q, *J* 7.0, CH<sub>2</sub>), 1.50 (3H, t, *J* 7.0, CH<sub>3</sub>); **<sup>13</sup>C NMR (125 MHz, CDCl<sub>3</sub>):** 149.9 (d, *J* 246.5, 2''-C), 147.6 (d, *J* 11.0, 3''-C), 141.4 (3'-C), 135.9 (3-C), 129.5 (d, *J* 11.0, 1''-C), 124.1 (d, *J* 4.5, 5''-C), 123.6 (d, *J* 3.5, 5-C), 123.1 (7'-C), 122.6 (6-C), 122.2 (d, *J* 1.9, 6''-C), 120.1 (4-C), 114.2 (d, *J* 2.0, 4''-C), 110.4 (d, *J* 3.7, 7-C), 65.2 (CH<sub>2</sub>), 14.8 (CH<sub>3</sub>); **LC-MS (ES):** RT = 1.88-2.16 min, *m/z* = 337.5 (M+H<sup>+</sup>); **R<sub>f</sub>:** 0.61 (1:1 EtOAc-petrol); **HPLC:** RT = 2.58 min; ***m/z* (ES+):** Found: 335.0206 (M+H<sup>+</sup>), C<sub>15</sub>H<sub>13</sub>BrFN<sub>2</sub>O requires *MH* 335.0195 **IR:ν<sub>max</sub>/cm<sup>-1</sup> (solid):** 3131 (N-H), 3029, 2877; **M.pt:** 148.6-150.3 °C; **Found:** C, 53.6; H, 3.50; N, 8.3; C<sub>15</sub>H<sub>12</sub>BrFN<sub>2</sub>O requires C, 53.8; H, 3.61; N, 8.4.

#### Preparation of 3,6-bis(3-ethoxyphenyl)-1*H*-indazole

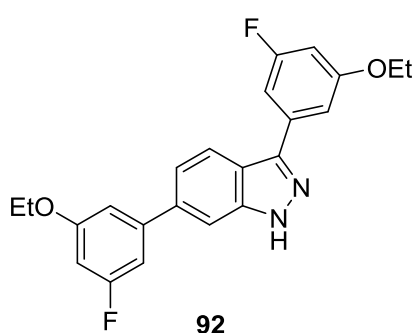


Synthesised as a side product using the same conditions as seen in the preparation of 3-bromo-6-(3-ethoxyphenyl)-1*H*-indazole (**86**). A second compound was isolated from the column and a glassy solid obtained. The solid was dissolved in Et<sub>2</sub>O and reduced *in vacuo*. The title compound 91 (107 mg, 0.30 mmol, 19%) was collected as a fluffy beige powder.

**<sup>1</sup>H NMR (500 MHz, CDCl<sub>3</sub>):** 8.06 (1H, d, *J* 8.5, 4-H), 7.66 (1H, d, *J* 8.0, 4''-H), 7.63 (1H, s, 7-H), 7.47-7.44 (2H, m, 5-H and 5''-H), 7.39-7.34 (2H, m, 4'''-H and 5'''-H), 7.16-7.14 (2H, m, 2''-H and 2'''-H), 7.00-6.97 (1H, m, 6''-H), 6.95-6.92 (1H, m, 6'''-H), 4.13 (2H, q, *J* 7.0, CH<sub>2</sub>'''), 4.07-4.01 (2H, m, CH<sub>2</sub>), 1.49 (3H, td, *J* 7.0 and 1.1, CH<sub>3</sub>'''), 1.39 (3H, td, *J* 7.0 and 1.1, CH<sub>3</sub>), NH not observed; **<sup>13</sup>C NMR (125 MHz, CDCl<sub>3</sub>):** 159.5 (3''-C), 159.3 (3'''-C), 145.5 (6-C), 142.6 (1''-C), 142.4 (1'''-C), 140.2 (3'-C), 134.8 (3-C), 130.1 (5''-C), 129.7 (5'''-C), 121.6 (5-C), 121.2 (4-C),

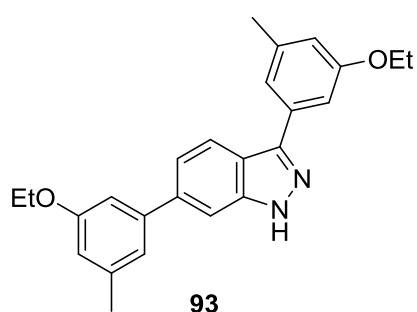
120.3 (7'-C), 120.1 (4'''-C), 120.0 (2'''-C), 114.8 (6''-C), 114.1 (2''-C), 113.6 (7-C), 113.4 (6'''-C), 108.6 (4'''-C), 63.6 ( $\underline{\text{C}}\text{H}_2$ '''), 63.5 ( $\underline{\text{C}}\text{H}_2$ ), 15.0 ( $\underline{\text{C}}\text{H}_3$ '''), 14.8 ( $\underline{\text{C}}\text{H}_3$ ); **LC-MS (ES)**: RT = 2.25-2.42 min, m/z = 359.4 (M+H<sup>+</sup>); **R<sub>f</sub>**: 0.35 (2:3 EtOAc–petrol); **HPLC**: RT = 3.14 min; **m/z (ES+)**: Found: 359.1764 (M+H<sup>+</sup>), C<sub>23</sub>H<sub>22</sub>N<sub>2</sub>O<sub>2</sub> requires *MH* 359.1754; **IR**:  $\nu_{\text{max}}/\text{cm}^{-1}$  (solid): 3165 (N-H), 2976, 2927, 1599; **M.pt**: 53.4-55.6°C.

Preparation of 3,6-bis(3-ethoxy-5-fluorophenyl)-1*H*-indazole



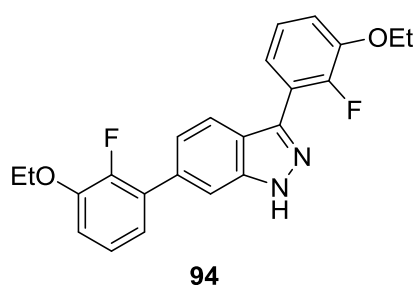
Synthesised as a side product using the same conditions as seen in the preparation of 3-bromo-6-(3-ethoxy-5-fluorophenyl)-1*H*-indazole (**88**). A second compound was isolated from the column. The title compound 92 (87 mg, 0.22 mmol, 14%) was collected as a fluffy colourless solid.

**<sup>1</sup>H NMR (500 MHz, CDCl<sub>3</sub>)**: 11.16 (1H, br.s, NH), 8.05 (1H, d, *J* 8.5, 4-H), 7.51 (1H, s, 7-H), 7.45 (1H, dd, *J* 8.5 and 1.5, 5-H), 7.36 (1H, app.s, 6'''-H), 7.32 (1H, ddd, *J* 9.3, 2.4 and 1.3, 2'''-H), 6.95 (1H, app.s, 6''-H), 6.91 (1H, app.dt, *J* 9.5 and 1.5, 2''-H), 6.69 (1H, app.dt, *J* 10.5 and 2.0, 4'''-H), 6.65 (1H, app.dt, *J* 11.0 and 2.0, 4''-H), 4.09 (4H, app.sextet, *J* 7.0,  $\underline{\text{C}}\text{H}_2$  and  $\underline{\text{C}}\text{H}_2$ '''), 1.47 (3H, t, *J* 7.0,  $\underline{\text{C}}\text{H}_3$ '''), 1.43 (3H, t, *J* 7.0,  $\underline{\text{C}}\text{H}_3$ ); **<sup>13</sup>C NMR (125 MHz, CDCl<sub>3</sub>)**: 163.9 (d, *J* 244.5, 3'''-C), 163.9 (d, *J* 244.6, 3''-C), 160.7 (d, *J* 11.6, 5'''-C), 160.5 (d, *J* 11.6, 5''-C), 144.7 (d, *J* 3.3, 3-C), 143.6 (d, *J* 9.9, 1''-C), 142.2 (3'-C), 139.4 (d, *J* 2.6, 6-C), 135.6 (d, *J* 10.7, 1'''-C), 121.7 (5-C), 121.3 (4-C), 120.4 (7'-C), 110.0 (d, *J* 2.6, 6''-C), 109.5 (d, *J* 2.6, 6'''-C), 108.4 (7-C), 106.8 (2'''-C), 106.6 (2''-C), 102.1 (d, *J* 24.9, 4'''-C), 101.0 (d, *J* 24.9, 4''-C), 64.0 ( $\underline{\text{C}}\text{H}_2$  and  $\underline{\text{C}}\text{H}_2$ '''), 14.7 ( $\underline{\text{C}}\text{H}_3$ ), 14.7 ( $\underline{\text{C}}\text{H}_3$ '''); **LC-MS (ES)**: RT = 2.37-2.50 min, m/z = 395.2 (M+H<sup>+</sup>); **R<sub>f</sub>**: 0.36 (3:7 EtOAc–hexane); **HPLC**: RT = 3.87 min; **m/z (ES+)**: Found: 395.1577 (M+H<sup>+</sup>), C<sub>23</sub>H<sub>20</sub>F<sub>2</sub>N<sub>2</sub>O<sub>2</sub> requires *MH* 395.1566; **IR**:  $\nu_{\text{max}}/\text{cm}^{-1}$  (solid): 3170 (N-H), 2978, 1608, 1587; **M.pt**: 68.4-74.0 °C.

Preparation of 3,6-bis(3-ethoxy-5-methylphenyl)-1H-indazole

Synthesised as a side product using the same conditions as seen in the preparation of 3-bromo-6-(3-ethoxy-5-methylphenyl)-1H-indazole (**89**). A second compound was isolated from the column and a glassy solid obtained. The glassy solid was dissolved in Et<sub>2</sub>O and reduced *in vacuo*.

The title compound **93** (192 mg, 0.50 mmol, 32%) was collected as an off-white solid. **<sup>1</sup>H NMR (500 MHz, CDCl<sub>3</sub>):** 11.45 (1H, br.s, NH), 8.06 (1H, d, *J* 8.5, 4-H), 7.47 (1H, s, 7-H), 7.47-7.44 (2H, m, 5-H and 6'''-H), 7.39 (1H, s, 2'''-H), 7.02 (1H, s, 6''-H), 6.97 (1H, s, 2''-H), 6.80 (1H, s, 4'''-H), 6.77 (1H, s, 4''-H), 4.11 (2H, q, *J* 7.0, CH<sub>2</sub>''), 4.07 (2H, q, *J* 7.0, CH<sub>2</sub>), 2.43 (3H, s, CH<sub>3</sub>''), 2.40 (3H, s, CH<sub>3</sub>), 1.46 (3H, t, *J* 7.0, CH<sub>2</sub>CH<sub>3</sub>''), 1.41 (3H, t, *J* 7.0, CH<sub>2</sub>CH<sub>3</sub>''); **<sup>13</sup>C NMR (125 MHz, CDCl<sub>3</sub>):** 159.5 (3'''-C), 159.4 (3''-C), 145.8 (3-C), 142.5 (1''-C), 142.4 (1'''-C), 140.4 (5''-C), 140.0 (5'''-C), 139.8 (3'-C), 134.5 (6-C), 121.7 (5-C), 121.3 (4-C), 120.9 (6'''-C), 120.9 (6''-C), 120.3 (7'-C), 115.7 (4'''-C), 114.3 (4''-C), 111.1 (2''-C), 110.6 (2'''-C), 108.3 (7-C), 63.5 (CH<sub>2</sub>''), 63.5 (CH<sub>2</sub>), 21.7 (CH<sub>3</sub>''), 21.7 (CH<sub>3</sub>), 15.0 (CH<sub>2</sub>CH<sub>3</sub>''), 14.9 (CH<sub>2</sub>CH<sub>3</sub>); **LC-MS (ES):** RT = 2.39-2.58 min, *m/z* = 287.6 (M+H<sup>+</sup>); **R<sub>f</sub>:** 0.28 (1:1 EtOAc–petrol); **HPLC:** RT = 2.81 min; ***m/z* (ES<sup>+</sup>):** Found: 387.2078 (M+H<sup>+</sup>), C<sub>25</sub>H<sub>27</sub>N<sub>2</sub>O<sub>2</sub> requires *MH* 387.2073; **IR:ν<sub>max</sub>/cm<sup>-1</sup> (solid):** 3198 (N-H), 3123, 2975, 1589.

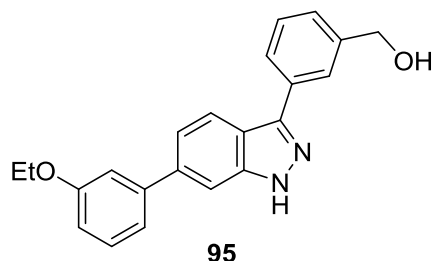
Preparation of 3,6-bis(3-ethoxy-2-fluorophenyl)-1H-indazole

Synthesised as a side product using the same conditions as seen in the preparation of 3-bromo-6-(3-ethoxy-2-fluorophenyl)-1H-indazole (**90**). A second compound was isolated from the column and a glassy solid obtained. The glassy solid was dissolved in Et<sub>2</sub>O and reduced *in vacuo*.

The title compound **94** (9 mg, 0.02 mmol, 2%) was collected as a pale purple powder. **<sup>1</sup>H NMR (500 MHz, CDCl<sub>3</sub>):** 10.52 (1H, br.s, NH), 7.94 (1H, dd, *J* 8.5 and 3.5, 4-H), 7.66 (1H, s, 7-H), 7.40 (2H, m, 5-H and 5''-H), 7.19 (1H, app.td, *J* 8.0 and 1.2, 6''-H), 7.14 (1H, app.td, *J* 8.0 and 1.2, 4''-H), 7.09-7.04 (2H, m, 5'''-H and 6'''-H), 7.00 (1H, app.td, *J* 8.0 and 1.6, 4'''-H), 4.22-4.17 (4H, m, 2 × CH<sub>2</sub>CH<sub>3</sub>), 1.52-1.48 (6H, m,

$2 \times \text{CH}_2\text{CH}_3$ );  $^{13}\text{C}$  NMR (125 MHz,  $\text{CDCl}_3$ ): 150.5 (d,  $J$  250.2,  $2''''\text{-C}$ ), 150.0 (d,  $J$  248.3,  $2''\text{-C}$ ), 147.8-147.6 (m,  $3''\text{-C}$  and  $3'''\text{-C}$ ), 141.5 (3-C), 134.7 (3'-C), 129.9 (d,  $J$  10.3,  $1''\text{-C}$ ), 124.2 (d,  $J$  4.9,  $6''\text{-C}$ ), 123.9 (d,  $J$  4.9,  $4''\text{-C}$ ), 123.0 (5-C), 122.4 (d,  $J$  2.0,  $6'''\text{-C}$ ), 122.2 (d,  $J$  3.0,  $5''\text{-C}$ ), 121.9 ( $1'''\text{-C}$ ), 121.8 ( $7'\text{-C}$ ), 121.7 (4-C), 121.4 (6-C), 114.9 (d,  $J$  1.5,  $5'''\text{-C}$ ), 113.9 (d,  $J$  1.8,  $4'''\text{-C}$ ), 110.2 (d,  $J$  3.4, 7-C), 65.2 ( $\text{CH}_2\text{CH}_3$ ), 65.1 ( $\text{CH}_2\text{CH}_3$ ), 14.9 ( $2 \times \text{CH}_2\text{CH}_3$ ); LC-MS (ES): RT = 2.19-2.29 min,  $m/z = 395.6$  ( $\text{M}+\text{H}^+$ ); Rf: 0.46 (1:1 EtOAc–petrol); HPLC: RT = 2.99 min;  $m/z$  (ES+): Found: 395.1575 ( $\text{M}+\text{H}^+$ ),  $\text{C}_{23}\text{H}_{21}\text{F}_2\text{N}_2\text{O}_2$  requires  $MH$  395.1571; IR:  $\nu_{\text{max}}/\text{cm}^{-1}$  (solid): 3169 (N-H), 2979, 2929, 1618; M.pt: 59.0–60.1 °C.

#### Preparation of {3-[6-(3-ethoxyphenyl)-1H-indazol-3-yl]phenyl}methanol



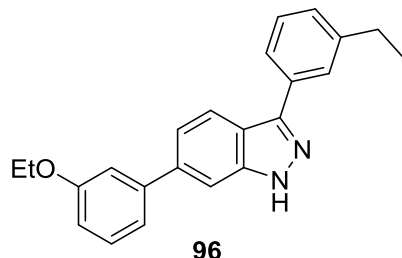
Synthesised using method A using 3-bromo-6-(3-ethoxyphenyl)-1H-indazole (150 mg, 0.47 mmol, 1.0 eq), 3-(hydroxymethyl)phenylboronic acid (108 mg, 0.71 mmol, 1.5 eq), Pd(dppf)Cl<sub>2</sub>•DCM (39 mg, 0.047 mmol, 0.1 eq), Na<sub>2</sub>CO<sub>3</sub> (150 mg,

1.42 mmol, 3.0 eq), dioxane (10 mL) and water (10 mL) and the reaction heated for 1 h. LC-MS analysis showed the reaction to be incomplete and therefore the reaction was heated for a further 2 h. The work up proceeded using the larger volumes of solvents and the organic solvent removed *in vacuo* to reveal a brown solid. The crude product was purified using column chromatography (1:4 EtOAc–hexane) and a yellow solid obtained. The solid was triturated with DCM. The title compound 95 (71 mg, 0.21 mmol, 44%) collected as a colourless solid.

$^1\text{H}$  NMR (500 MHz, DMSO- $d_6$ ): 8.13 (1H, d,  $J$  8.5, 4-H), 7.99 (1H, s,  $2'''\text{-H}$ ), 7.88 (1H, d,  $J$  7.5,  $6'''\text{-H}$ ), 7.77 (1H, s, 7-H), 7.51 (1H, dd,  $J$  8.5 and 1.5, 5-H), 7.47 (1H, app.t,  $J$  7.5,  $5'''\text{-H}$ ), 7.39 (1H, app.t  $J$  7.5,  $5''\text{-H}$ ), 7.34 (1H, d,  $J$  7.5,  $4'''\text{-H}$ ) 7.30 (1H, d,  $J$  8.0,  $6''\text{-H}$ ), 7.25 (1H, app.t,  $J$  1.5,  $2''\text{-H}$ ), 6.95 (1H, dd,  $J$  8.0 and 2.0,  $4''\text{-H}$ ), 5.28 (1H, t,  $J$  6.0, OH), 4.62 (2H, d,  $J$  6.0,  $\text{CH}_2\text{OH}$ ), 4.12 (2H, q,  $J$  7.0,  $\text{CH}_2$ ), 1.36 (3H, t,  $J$  7.0,  $\text{CH}_3$ ), NH not observed;  $^{13}\text{C}$  NMR (125 MHz, DMSO- $d_6$ ): 159.0 ( $3''\text{-C}$ ), 143.2 ( $3'''\text{-C}$ ), 143.2 ( $1'''\text{-C}$ ), 142.2 (3'-C), 141.9 ( $1''\text{-C}$ ), 138.3 (6-C), 133.5 (3-C), 130.0 ( $5''\text{-C}$ ), 128.6 ( $5'''\text{-C}$ ), 125.8 ( $4'''\text{-C}$ ), 125.0 ( $6'''\text{-C}$ ), 124.7 ( $2'''\text{-C}$ ), 121.1 (4-C), 120.8 (5-C), 119.5 ( $7'\text{-C}$ ), 119.4 ( $6''\text{-C}$ ), 113.6 ( $4''\text{-C}$ ), 113.2 ( $2''\text{-C}$ ), 108.2 (7-C), 63.1 ( $\text{CH}_2$ ), 62.9 ( $\text{CH}_2\text{OH}$ ), 14.9 ( $\text{CH}_3$ ); LC-MS (ES): RT = 1.82-2.02 min,  $m/z = 345.5$  ( $\text{M}+\text{H}^+$ ); Rf: 0.30 (4:1 EtOAc–petrol); HPLC: RT = 2.88 min;

**m/z (ES<sup>+</sup>):** Found: 345.1610 (M+H<sup>+</sup>), C<sub>22</sub>H<sub>20</sub>N<sub>2</sub>O<sub>2</sub> requires *MH* 345.1598;  
**IR:**  $\nu_{\max}/\text{cm}^{-1}$  (solid): 3196 (N-H), 3173, 2983, 2940, 1594; **M.pt:** 156.4-157.4 °C.

Preparation of 6-(3-ethoxyphenyl)-3-(3-ethylphenyl)-1H-indazole



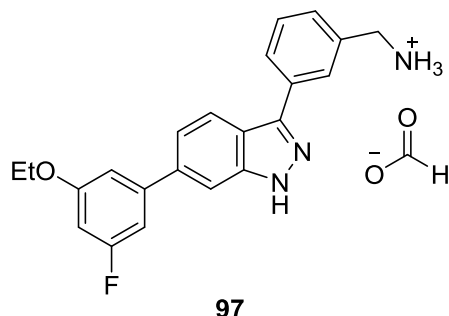
Synthesised using method A using 3-bromo-6-(3-ethoxyphenyl)-1H-indazole (150 mg, 0.47 mmol, 1.0 eq), 3-ethylphenylboronic acid (106 mg, 0.71 mmol, 1.5 eq), Pd(dppf)Cl<sub>2</sub>•DCM (39 mg, 0.047 mmol, 0.1 eq), Na<sub>2</sub>CO<sub>3</sub> (150 mg, 1.42 mmol,

3.0 eq), dioxane (5 mL) and water (5 mL) and the reaction heated for 1 h. LC-MS analysis showed the reaction to be incomplete therefore Pd(dppf)Cl<sub>2</sub>•DCM (39 mg, 0.047 mmol, 0.1 eq) and Na<sub>2</sub>CO<sub>3</sub> (75 mg, 0.71 mmol, 1.5 eq) were added and the reaction heated for 1.5 h. The work up proceeded using the larger volumes of solvents and the organic solvent removed *in vacuo* to reveal a brown oil. The crude product was purified using column chromatography (1:4 EtOAc–hexane) and a colourless glassy solid obtained. The solid was dissolved in Et<sub>2</sub>O and reduced *in vacuo*. The title compound **96** (73 mg, 0.21 mmol, 45%) as a foamy off-white solid.

**<sup>1</sup>H NMR (500 MHz, CDCl<sub>3</sub>):** 8.06 (1H, d, *J* 8.5, 4-H), 7.92 (1H, app.s, 2'''-H), 7.89 (1H, d, *J* 7.5, 6'''-H), 7.51-7.46 (2H, m, 5-H and 5'''-H), 7.40-7.35 (2H, m, 7-H and 5''-H), 7.29 (1H, d, *J* 7.5, 4'''-H), 7.17-7.14 (2H, m, 2''-H and 6''-H), 6.96-6.93 (1H, m, 4''-H), 4.14 (2H, q, *J* 7.0, OCH<sub>2</sub>), 2.73 (2H, q, *J* 7.5, CH<sub>2</sub>), 1.50 (3H, t, *J* 7.0, OCH<sub>2</sub>CH<sub>3</sub>), 1.27 (3H, t, *J* 7.5, CH<sub>3</sub>), NH not observed; **<sup>13</sup>C NMR (125 MHz, CDCl<sub>3</sub>):** 159.3 (3''-C), 145.9 (1'''-C), 145.1 (3'''-C), 142.6 (6-C), 142.4 (3'-C), 140.1 (1''-C), 133.5 (3-C), 129.7 (5''-C), 129.0 (5'''-C), 128.0 (4'''-C), 127.3 (2'''-C), 125.2 (6'''-C), 121.5 (5-C), 121.3 (4-C), 120.4 (7'-C), 120.0 (6''-C), 114.2 (2''-C), 113.3 (4''-C), 108.5 (7-C), 63.6 (OCH<sub>2</sub>), 29.0 (CH<sub>2</sub>), 15.5 (CH<sub>3</sub>), 15.0 (OCH<sub>2</sub>CH<sub>3</sub>); **LC-MS (ES):** RT = 2.30-2.47 min, m/z = 343.3 (M+H<sup>+</sup>); **R<sub>f</sub>:** 0.23 (3:7 EtOAc–petrol); **HPLC:** RT = 3.95 min; **m/z (ES<sup>+</sup>):** Found: 365.1628 (M+Na<sup>+</sup>), C<sub>23</sub>H<sub>22</sub>N<sub>2</sub>NaO requires *MH* 365.1624; **IR:**  $\nu_{\max}/\text{cm}^{-1}$  (solid): 3165 (N-H), 2963, 2927, 1603, 1581; **M.pt:** 61.0-64.0 °C.

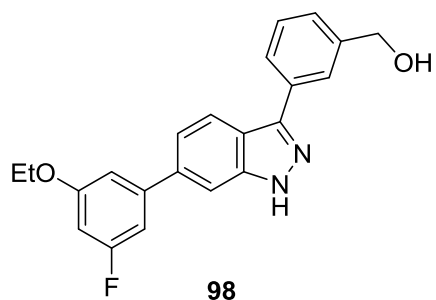


Preparation of {3-[6-(3-ethoxy-5-methylphenyl)-1*H*-indazol-3-yl]phenyl}methanaminium formate



Synthesised using method A using 3-bromo-6-(3-ethoxy-5-fluorophenyl)-1*H*-indazole (100 mg, 0.30 mmol, 1.0 eq), 3-(aminomethyl)phenylboronic acid•HCl (112 mg, 0.60 mmol, 2.0 eq), Pd(dppf)Cl<sub>2</sub>•DCM (24 mg, 0.03 mmol, 0.1 eq), Na<sub>2</sub>CO<sub>3</sub> (158 mg, 1.50 mmol, 5.0 eq), dioxane (5 mL) and water (5 mL) and the reaction heated for 3 h. LC-MS analysis showed the reaction to be incomplete and therefore Pd(dppf)Cl<sub>2</sub>•DCM (24 mg, 0.03 mmol, 0.1 eq) was added and the reaction heated for a further 3 h. The work up proceeded using the larger volumes of solvents and the organic solvent removed *in vacuo* to reveal a brown oil. The crude product was purified using column chromatography (1:10:89 7.0 M NH<sub>3</sub> in MeOH–MeOH–EtOAc) and a brown solid obtained. The solid was impure and attempts using DCM, toluene and EtOH to crystallise the solid were unsuccessful. The solid was purified using preparative HPLC (50-80% MeOH–H<sub>2</sub>O with 0.1% formic acid). Appropriate fractions were reduced *in vacuo* to ~3 mL and the compound left to precipitate overnight. The title compound 97 (4 mg, 0.011 mmol, 4%) was collected as a colourless solid.

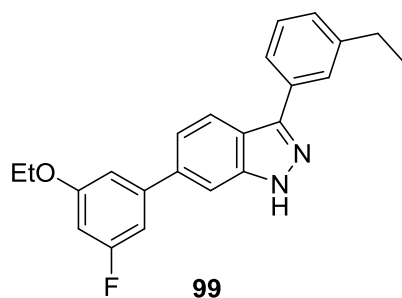
**<sup>1</sup>H NMR (500 MHz, DMSO-*d*<sub>6</sub>):** 8.35 (1H, s, formate-H), 8.21 (1H, d, *J* 8.5, 4-H), 8.06 (1H, s, 2'''-H), 7.94 (1H, d, *J* 8.0, 6'''-H), 7.82 (1H, s, 7-H), 7.53-7.49 (2H, m, 5-H and 5'''-H), 7.42 (1H, d, *J* 8.0, 4'''-H), 7.16 (1H, app.d, *J* 10.0, 2''-H), 7.12 (1H, app.s, 6''-H), 6.84 (1H, app.dt, *J* 10.5 and 2.5, 4''-H), 4.14 (2H, q, *J* 7.0, OCH<sub>2</sub>), 4.00 (2H, s, CH<sub>2</sub>), 1.36 (3H, t, *J* 7.0, CH<sub>2</sub>NH<sub>2</sub>), NHs not observed; **<sup>13</sup>C NMR (125 MHz, DMSO-*d*<sub>6</sub>):** 164.7 (formate C=O), 163.4 (d, *J* 242.1, 3''-C), 160.3 (d, *J* 12.3, 5''-C), 143.3 (d, *J* 10.1, 1''-C), 143.0 (1'''-C), 142.2 (3'-C), 139.6 (3'''-C), 137.1 (d, *J* 2.6, 6-C), 133.7 (3-C), 128.9 (5'''-C), 127.5 (4'''-C), 126.3 (2'''-C), 125.6 (6'''-C), 121.3 (4-C), 120.7 (5-C), 119.8 (7'-C), 109.6 (d, *J* 2.1, 6''-C), 108.6 (7-C), 106.0 (d, *J* 22.8, 2''-C), 100.9 (d, *J* 25.8, 4''-C), 63.7 (OCH<sub>2</sub>), 43.8 (CH<sub>2</sub>), 14.5 (CH<sub>3</sub>); **LC-MS (ES):** RT = 1.85-2.02 min, m/z = 362.8 (M-formate<sup>+</sup>); **R<sub>f</sub>:** 0.12 (5:10:85 7.0 M NH<sub>3</sub> in MeOH–MeOH–EtOAc); **HPLC:** RT = 0.60 min; **m/z (ES<sup>+</sup>):** Found: 384.1486 (M-formate<sup>+</sup>), C<sub>22</sub>H<sub>20</sub>FN<sub>3</sub>NaO requires *MH* 384.1483; **IR:** ν<sub>max</sub>/cm<sup>-1</sup> (solid): 3166 (N-H), 2982, 2633, 1659, 1566; **M.pt:** 175.0-176.3 °C.

Preparation of {3-[6-(3-ethoxy-5-fluorophenyl)-1H-indazol-3-yl]phenyl}methanol

Synthesised using method A using 3-bromo-6-(3-ethoxy-5-fluorophenyl)-1H-indazole (100 mg, 0.30 mmol, 1.0 eq), 3-(hydroxymethyl)phenylboronic acid (68 mg, 0.45 mmol, 1.5 eq), Pd(dppf)Cl<sub>2</sub>•DCM (24 mg, 0.03 mmol, 0.1 eq), Na<sub>2</sub>CO<sub>3</sub> (95 mg, 0.90 mmol,

3.0 eq), dioxane (5 mL) and water (5 mL) and the reaction heated for 2 h. LC-MS analysis showed the reaction to be incomplete and therefore Pd(dppf)Cl<sub>2</sub>•DCM (24 mg, 0.03 mmol, 0.1 eq) and Na<sub>2</sub>CO<sub>3</sub> (95 mg, 0.90 mmol, 3.0 eq) were added and the reaction heated for a further 4 h. The work up proceeded using the larger volumes of solvents and the organic solvent removed *in vacuo* to reveal a brown oil. The crude product was purified using column chromatography (3:2 EtOAc–hexane) and a yellow solid obtained. The solid was crystallised from toluene. The title compound 98 (34 mg, 0.094 mmol, 31%) collected as colourless fluffy microneedles.

**<sup>1</sup>H NMR (500 MHz, DMSO-*d*<sub>6</sub>):** 8.13 (1H, d, *J* 8.5, 4-H), 7.98 (1H, s, 2'''-H), 7.87 (1H, app.d, *J* 8.0, 6'''-H), 7.81 (1H, s, 7-H), 7.52 (1H, dd, *J* 8.5 and 1.5, 5-H), 7.47 (1H, app.t, *J* 8.0, 5'''-H), 7.34 (1H, app.d, *J* 7.5, 4'''-H), 7.16 (1H, app.dt, *J* 10.0 and 1.5, 2''-H), 7.12 (1H, app.t, *J* 1.5, 6''-H), 6.84 (1H, app.dt, *J* 11.0 and 2.0, 4''-H), 5.28 (1H, br.t, *J* 4.0, OH), 4.61 (2H, d, *J* 4.0, CH<sub>2</sub>OH), 4.14 (2H, q, *J* 7.0, CH<sub>2</sub>), 1.36 (3H, t, *J* 7.0, CH<sub>3</sub>), indazole NH not observed; **<sup>13</sup>C NMR (125 MHz, DMSO-*d*<sub>6</sub>):** 163.4 (d, *J* 241.9, 3''-C), 160.3 (d, *J* 12.0, 5''-C), 143.3 (d, *J* 10.1, 1''-C), 143.3 (Ar-q), 143.2 (Ar-q), 142.1 (3'-C), 137.1 (d, *J* 2.4, 6-C), 133.4 (3-C), 128.6 (5'''-C), 125.8 (4'''-C), 125.0 (6'''-C), 124.7 (2'''-C), 121.2 (4-C), 120.7 (5-C), 119.8 (7'-C), 109.6 (d, *J* 1.9, 6''-C), 108.5 (7-C), 106.0 (d, *J* 22.6, 2''-C), 100.9 (d, *J* 25.2, 4''-C), 63.7 (CH<sub>2</sub>), 62.9 (CH<sub>2</sub>OH), 14.5 (CH<sub>3</sub>); **LC-MS (ES):** RT = 1.98-2.15 min, *m/z* = 362.8 (M+H<sup>+</sup>); **R<sub>f</sub>:** 0.29 (7:3 EtOAc–hexane); **HPLC:** RT = 1.77 min; ***m/z* (ES+):** Found: 363.1515 (M+H<sup>+</sup>), C<sub>22</sub>H<sub>19</sub>FN<sub>2</sub>O<sub>2</sub> requires *MH* 363.1503; **IR:ν<sub>max</sub>/cm<sup>-1</sup> (solid):** 3166 (N-H), 2985, 2873, 1588; **M.pt:** 171.2-171.8 °C; **Found:** C, 73.1; H, 5.30; N, 7.8; C<sub>22</sub>H<sub>19</sub>FN<sub>2</sub>O<sub>2</sub> requires C, 72.9; H, 5.28; N, 7.7%.

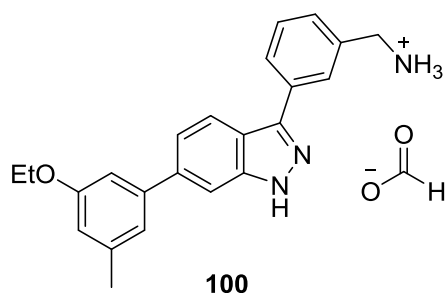
Preparation of 6-(3-ethoxy-5-fluorophenyl)-3-(3-ethylphenyl)-1H-indazole

Synthesised using method A using 3-bromo-6-(3-ethoxy-5-fluorophenyl)-1H-indazole (100 mg, 0.30 mmol, 1.0 eq), 3-ethylphenylboronic acid (67 mg, 0.45 mmol, 1.5 eq), Pd(dppf)Cl<sub>2</sub>•DCM (24 mg, 0.03 mmol, 0.1 eq), Na<sub>2</sub>CO<sub>3</sub> (95 mg, 0.90 mmol, 3.0 eq), dioxane (5 mL) and water

(5 mL) and the reaction heated for 2 h. LC-MS analysis showed the reaction to be incomplete and therefore Pd(dppf)Cl<sub>2</sub>•DCM (24 mg, 0.03 mmol, 0.1 eq) and Na<sub>2</sub>CO<sub>3</sub> (95 mg, 0.90 mmol, 3.0 eq) were added and the reaction heated for a further 2 h. LC-MS analysis showed the reaction to be incomplete and therefore Pd(dppf)Cl<sub>2</sub>•DCM (24 mg, 0.03 mmol, 0.1 eq) was added and the reaction heated for a further 1.5 h. The work up proceeded using the larger volumes of solvents and the organic solvent removed *in vacuo* to reveal a brown oil. The crude product was purified using column chromatography (1:9 EtOAc–hexane) and a colourless glassy solid obtained. The glassy solid was dissolved in Et<sub>2</sub>O and reduced *in vacuo*. The title compound 99 (28 mg, 0.078 mmol, 25%) as an off-white hygroscopic foamy solid.

**<sup>1</sup>H NMR (500 MHz, CDCl<sub>3</sub>):** 8.06 (1H, d, *J* 8.5, 4-H), 7.89 (1H, s, 2'''-H), 7.87 (1H, d, *J* 8.0, 6'''-H), 7.49 (1H, app.t, *J* 7.5, 5'''-H), 7.42 (1H, dd, *J* 8.5 and 1.5, 5-H), 7.33-7.29 (2H, m, 7-H and 4''-H), 6.93 (1H, app.t, *J* 1.5, 6''-H), 6.85 (1H, app.dt, *J* 9.5 and 1.5, 4''-H), 6.64 (1H, app.dt, *J* 10.5 and 2.0, 2''-H), 4.10 (2H, q, *J* 7.0, OCH<sub>2</sub>), 2.73 (2H, q, *J* 7.5, CH<sub>2</sub>), 1.48 (3H, t, *J* 7.0, OCH<sub>2</sub>CH<sub>3</sub>), 1.26 (3H, t, *J* 7.5, CH<sub>3</sub>), NH not observed; **<sup>13</sup>C NMR (125 MHz, CDCl<sub>3</sub>):** 163.8 (d, *J* 244.4, 3''-C), 160.5 (d, *J* 11.5, 5''-C), 146.0 (1'''-C), 145.1 (3'''-C), 143.7 (d, *J* 9.9, 1''-C), 142.2 (3'-C), 139.1 (d, *J* 2.6, 6-C), 133.3 (3-C), 129.0 (5'''-C), 128.2 (4'''-C), 127.3 (2'''-C), 125.2 (6'''-C), 121.5 (5-C), 121.3 (4-C), 120.7 (7'-C), 110.0 (d, *J* 2.5, 6''-C), 108.5 (7-C), 106.7 (d, *J* 22.6, 4''-C), 100.8 (d, *J* 25.1, 2''-C), 64.0 (OCH<sub>2</sub>), 28.9 (CH<sub>2</sub>), 15.5 (CH<sub>3</sub>), 14.8 (OCH<sub>2</sub>CH<sub>3</sub>); **LC-MS (ES):** RT = 2.40-2.56 min, *m/z* = 360.6 (M+H<sup>+</sup>); **R<sub>f</sub>:** 0.53 (1:1 EtOAc–hexane); **HPLC:** RT = 3.35 min (97%); ***m/z* (ES<sup>+</sup>):** Found: 383.1529 (M+Na<sup>+</sup>), C<sub>23</sub>H<sub>21</sub>FN<sub>2</sub>NaO requires *MH* 383.1530; **IR:ν<sub>max</sub>/cm<sup>-1</sup> (solid):** 3166 (N-H), 2965, 2928, 1585.

Preparation of {3-[6-(3-ethoxy-5-methylphenyl)-1*H*-indazol-3-yl]phenyl}methanamine

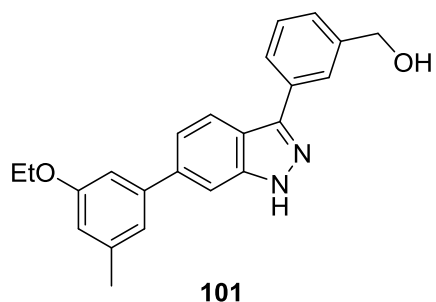


Synthesised using method A using 3-bromo-6-(3-ethoxy-5-methylphenyl)-1*H*-indazole (86 mg, 0.26 mmol, 1.0 eq), 3-(aminomethyl)phenylboronic acid•HCl (97 mg, 0.52 mmol, 2.0 eq), Pd(dppf)Cl<sub>2</sub>•DCM (64 mg, 0.078 mmol, 0.3 eq), Na<sub>2</sub>CO<sub>3</sub> (124 mg, 1.17

mmol, 4.5 eq), dioxane (5 mL) and water (5 mL) and the reaction heated for 6 h. The work up proceeded using the larger volumes of solvents and the organic solvent removed *in vacuo* to reveal a brown oil. The crude product was purified using column chromatography (3:10:87 7.0 M NH<sub>3</sub> in MeOH–MeOH–EtOAc) and a brown solid obtained. The solid was further purified using preparative HPLC (50-95% MeOH–H<sub>2</sub>O–0.1% formic acid) and a brown solid obtained. The solid was triturated in Et<sub>2</sub>O and the solid then filtered washing with DCM. The title compound 100 (22 mg, 0.06 mmol, 24%) was collected as an off-white solid.

**<sup>1</sup>H NMR (500 MHz, CD<sub>3</sub>OD):** 8.53 (1H, br.s, formate-H), 8.13 (1H, d, *J* 8.8, 4-H), 8.08 (1H, s, 2'''-H), 8.06 (1H, d, *J* 7.7, 6'''-H), 7.74 (1H, s, 7-H), 7.63 (1H, t, *J* 7.7, 5'''-H), 7.51 (2H, m, 4'''-H and 5-H), 7.10 (1H, s, 6''-H), 7.02 (1H, s, 2''-H), 6.78 (1H, s, 4''-H), 4.24 (2H, s, CH<sub>2</sub>NH<sub>2</sub>)\*, 4.11 (2H, q, *J* 7.0, CH<sub>2</sub>CH<sub>3</sub>), 2.41 (3H, s, CH<sub>3</sub>), 1.42 (3H, t, *J* 7.0, CH<sub>2</sub>CH<sub>3</sub>), indazole NH not observed; **<sup>13</sup>C NMR (125 MHz, DMSO-d<sub>6</sub>):** 159.0 (3''-C), 142.9 (3-C), 142.3 (3'''-C), 141.7 (7'-C), 139.5 (5''-C), 138.5 (1''-C), 133.8 (1'''-C), 128.9 (5'''-C), 127.6 (4'''-C), 126.4 (2'''-C), 125.8 (6'''-C), 121.2 (4-C), 120.8 (5-C), 120.2 (6''-C), 119.5 (3'-C), 114.2 (4''-C), 110.4 (2''-C), 108.2 (7-C), 63.0 (CH<sub>2</sub>CH<sub>3</sub>), 21.3 (CH<sub>3</sub>), 14.7 (CH<sub>2</sub>CH<sub>3</sub>), three Ar-qs not observed; **LC-MS (ES):** RT = 1.81-2.20 min, *m/z* = 358.7 (M+H<sup>+</sup>); **R<sub>f</sub>:** 0.14 (5:10:85 7.0 M NH<sub>3</sub> in MeOH–MeOH–EtOAc); **HPLC:** RT = 3.28 min; ***m/z* (ES+):** Found: 358.1915 (M+H<sup>+</sup>), C<sub>23</sub>H<sub>24</sub>N<sub>3</sub>O requires *MH* 358.1919; **IR: ν<sub>max</sub>/cm<sup>-1</sup> (solid):** 2974, 2872, 1591; **M.pt:** 176.4-177.9 °C.

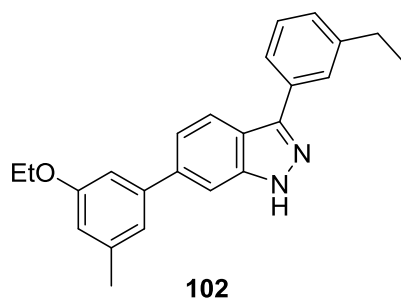
\* CH<sub>2</sub>NH<sub>2</sub> peak not observed in the <sup>1</sup>H NMR when ran in DMSO-d<sub>6</sub> but present when ran in CD<sub>3</sub>OD. Compound had poor solubility in CD<sub>3</sub>OD and therefore <sup>13</sup>C NMR was ran in DMSO-d<sub>6</sub>.

Preparation of {3-[6-(3-ethoxy-5-methylphenyl)-1*H*-indazol-3-yl]phenyl}methanol

Synthesised using method A using 3-bromo-6-(3-ethoxy-5-methylphenyl)-1*H*-indazole (97 mg, 0.29 mmol, 1.0 eq), 3-hydroxymethylphenylboronic acid (67 mg, 0.44 mmol, 1.5 eq), Pd(dppf)Cl<sub>2</sub>•DCM (48 mg, 0.058 mmol, 0.2 eq), Na<sub>2</sub>CO<sub>3</sub> (93 mg, 0.88 mmol,

3.0 eq), dioxane (5 mL) and water (5 mL) and the reaction heated for 3 h. LC-MS analysis showed the reaction to be incomplete and therefore Pd(dppf)Cl<sub>2</sub>•DCM (24 mg, 0.029 mmol, 0.1 eq) and Na<sub>2</sub>CO<sub>3</sub> (47 mg, 0.44 mmol, 1.5 eq) were added and the reaction heated for a further 1 h. The work up proceeded using the larger volumes of solvents and the organic solvent removed *in vacuo* to reveal a brown oil. The crude product was purified using column chromatography (3:1 EtOAc–hexane) and a pale yellow solid obtained. The solid was triturated with DCM and the solid filtered. The solid was crystallised from toluene. The title compound 101 (18 mg, 0.06 mmol, 18%) was collected as colourless crystals.

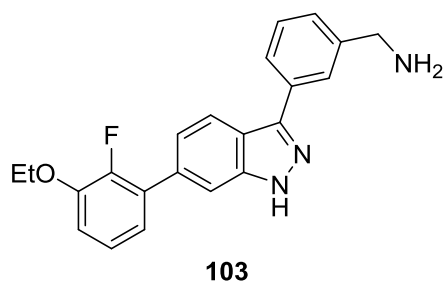
**<sup>1</sup>H NMR (500 MHz, DMSO-*d*<sub>6</sub>):** 8.12 (1H, d, *J* 8.6, 4-H), 7.99 (1H, s, 2'''-H), 7.88 (1H, d, *J* 7.5, 6'''-H), 7.76 (1H, s, 7-H), 7.50-7.45 (2H, m, 5-H and 5'''-H), 7.35 (1H, d, *J* 7.8, 4''-H), 7.13 (1H, s, 6''-H), 7.05 (1H, s, 2''-H), 6.79 (1H, s, 4''-H), 5.30 (1H, t, *J* 5.8, OH), 4.62 (2H, d, *J* 5.8, CH<sub>2</sub>OH), 4.11 (2H, q, *J* 7.0, CH<sub>2</sub>CH<sub>3</sub>), 2.37 (3H, s, CH<sub>3</sub>), 1.36 (3H, t, *J* 7.0, CH<sub>2</sub>CH<sub>3</sub>), NH peak not observed; **<sup>13</sup>C NMR (125 MHz, DMSO-*d*<sub>6</sub>):** 159.0 (3''-C), 143.3 (3-C), 143.2 (3'''-C), 142.2 (1'''-C), 141.7 (7'-C), 139.5 (5''-C), 138.5 (1''-C), 133.5 (6-C), 128.6 (5'''-C), 125.8 (4'''-C), 125.0 (6'''-C), 124.7 (2'''-C), 121.0 (4-C), 120.9 (5-C), 120.2 (6''-C), 119.5 (3'-C), 114.3 (4''-C), 110.4 (2''-C), 108.1 (7-C), 63.0 (CH<sub>2</sub>CH<sub>3</sub>), 62.9 (CH<sub>2</sub>OH), 21.3 (CH<sub>3</sub>), 14.7 (CH<sub>2</sub>CH<sub>3</sub>); **LC-MS (ES):** RT = 2.01-2.11 min, *m/z* = 359.6 (M+H<sup>+</sup>); **R<sub>f</sub>:** 0.36 (4:1 EtOAc–petrol); **HPLC:** RT = 1.64 min; ***m/z* (ES+):** Found: 359.1772 (M+H<sup>+</sup>), C<sub>23</sub>H<sub>23</sub>N<sub>2</sub>O<sub>2</sub> requires *MH* 359.1760; **IR:ν<sub>max</sub>/cm<sup>-1</sup> (solid):** 3122 (br.OH), 2978, 2918, 1589; **M.pt:** 157.8-158.1 °C.

Preparation of 6-(3-ethoxy-5-methylphenyl)-3-(3-ethylphenyl)-1H-indazole

Synthesised using method A using 3-bromo-6-(3-ethoxy-5-methylphenyl)-1H-indazole (100 mg, 0.03 mmol, 1.0 eq), 3-ethylphenylboronic acid (68 mg, 0.45 mmol, 1.5 eq), Pd(dppf)Cl<sub>2</sub>•DCM (50 mg, 0.06 mmol, 0.2 eq), Na<sub>2</sub>CO<sub>3</sub> (96 mg, 0.91 mmol, 3.0 eq), dioxane (5 mL) and water

(5 mL) and the reaction heated for 3 h. The work up proceeded using the larger volumes of solvents and the organic solvent removed *in vacuo* to reveal a brown oil. The crude product was purified using column chromatography (1:4 EtOAc–hexane). The title compound 102 (37 mg, 0.10 mmol, 23%) was collected as an off-white foamy solid.

**<sup>1</sup>H NMR (500 MHz, CDCl<sub>3</sub>):** 10.97 (1H, br.s, NH), 8.06 (1H, d, *J* 8.6, 4-H), 7.88 (1H, s, 2'''-H), 7.86 (1H, d, *J* 7.8, 6'''-H), 7.53 (1H, s, 7-H), 7.49-7.46 (2H, m, 5-H and 5'''-H), 7.29 (1H, d, *J* 7.6, 4'''-H), 7.04 (1H, s, 6''-H), 6.99 (1H, s, 2''-H), 6.77 (1H, s, 4''-H), 4.12 (2H, q, *J* 7.0, OCH<sub>2</sub>), 2.76 (2H, q, *J* 7.7, CH<sub>2</sub>), 2.43 (3H, s, CH<sub>3</sub>), 1.47 (3H, t, *J* 7.0, OCH<sub>2</sub>CH<sub>3</sub>), 1.30 (3H, t, *J* 7.7, CH<sub>2</sub>CH<sub>3</sub>); **<sup>13</sup>C NMR (125 MHz, CDCl<sub>3</sub>):** 159.4 (3''-C), 146.0 (3-C), 145.0 (3'''-C), 142.4 (1'''-C), 142.4 (7'-C), 140.4 (1''-C), 139.8 (5''-C), 133.5 (6-C), 128.9 (5-C), 127.9 (4'''-C), 127.2 (2'''-C), 125.0 (6'''-C), 121.7 (5'''-C), 121.3 (4-C), 120.9 (6''-C), 120.4 (3'-C), 114.4 (4''-C), 111.2 (2''-C), 108.2 (7-C), 63.5 (OCH<sub>2</sub>), 29.0 (CH<sub>2</sub>CH<sub>3</sub>), 21.7 (CH<sub>3</sub>), 15.6 (CH<sub>2</sub>CH<sub>3</sub>), 15.0 (OCH<sub>2</sub>CH<sub>3</sub>); **LC-MS (ES):** RT = 2.40-2.63 min, *m/z* = 358.1 (M+H<sup>+</sup>); **R<sub>f</sub>:** 0.58 (1:1 EtOAc–petrol); **HPLC:** RT = 3.21 min; ***m/z* (ES<sup>+</sup>):** Found: 357.1970 (M+H<sup>+</sup>), C<sub>24</sub>H<sub>25</sub>N<sub>2</sub>O requires *MH* 357.1967; **IR:** *v*<sub>max</sub>/cm<sup>-1</sup> (solid): 3164 (N-H), 3083, 2964, 2923, 1590; **M.pt:** 47.0-49.5 °C.

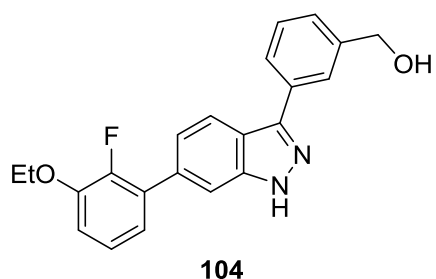
Preparation of {3-[6-(3-ethoxy-2-fluorophenyl)-1H-indazol-3-yl]phenyl}methanamine

Synthesised using method A using 3-bromo-6-(3-ethoxy-2-fluorophenyl)-1H-indazole (150 mg, 0.45 mmol, 1.0 eq), 3-(aminomethyl)phenylboronic acid•HCl (126 mg, 0.67 mmol, 1.5 eq), Pd(dppf)Cl<sub>2</sub>•DCM (37 mg, 0.045 mmol, 0.1 eq), Na<sub>2</sub>CO<sub>3</sub> (237 mg, 2.24

mmol, 5.0 eq), dioxane (5 mL) and water (5 mL) and the reaction heated for 2 h. LC-MS analysis showed the reaction to be incomplete and therefore 3-(aminomethyl)phenylboronic acid•HCl (42 mg, 0.22 mmol, 0.5 eq), Pd(dppf)Cl<sub>2</sub>•DCM (37 mg, 0.045 mmol, 0.1 eq) and Na<sub>2</sub>CO<sub>3</sub> (71 mg, 0.67 mmol, 1.5 eq) were added and the reaction heated for a further 2 h. The work up proceeded using the larger volumes of solvents and the organic solvent removed *in vacuo* to reveal a brown oil. The crude product was purified using column chromatography (3:10:87 7.0 M NH<sub>3</sub> in MeOH–MeOH–EtOAc) and a brown solid obtained. The solid was crystallised from propan-2-ol and these crystals further recrystallised from toluene. The title compound 103 (37 mg, 0.10 mmol, 23%) was collected as pale brown crystals.

**<sup>1</sup>H NMR (500 MHz, DMSO-d<sub>6</sub>):** 8.17 (1H, d, *J* 8.5, 4-H), 8.00 (1H, s, 2'''-H), 7.85 (1H, d, *J* 7.8, 6'''-H), 7.69 (1H, s, 7-H), 7.46 (1H, app.t, *J* 7.6, 5'''-H), 7.37-7.33 (2H, m, 4'''-H and 5-H), 7.24-7.16 (2H, m, 5''-H and 6''-H), 7.13 (1H, app.td, *J* 7.1 and 1.7, 4''-H), 4.17 (2H, q, *J* 7.0, CH<sub>2</sub>CH<sub>3</sub>), 3.84 (2H, s, CH<sub>2</sub>NH<sub>2</sub>), 3.31 (2H, br.s, NH<sub>2</sub>), 1.39 (3H, t, *J* 7.0, CH<sub>2</sub>CH<sub>3</sub>); **<sup>13</sup>C NMR (125 MHz, DMSO-d<sub>6</sub>):** 149.0 (d, *J* 245.4, 2''-C), 147.0 (d, *J* 111.1, 3''-C), 145.0 (3-C), 143.4 (3'''-C), 141.8 (3'-C), 133.4 (1'''-C), 132.9 (6-C), 129.2 (d, *J* 10.6, 1''-C), 128.6 (5'''-C), 126.5 (4'''-C), 125.4 (2'''-C), 124.6 (6'''-C), 124.5 (d, *J* 4.8, 5''-C), 122.3 (d, *J* 2.3, 5-C), 121.9 (d, *J* 2.1, 4''-C), 120.9 (4-C), 119.5 (7'-C), 114.0 (6''-C), 110.6 (d, *J* 3.3, 7-C), 64.4 (CH<sub>2</sub>CH<sub>3</sub>), 45.7 (CH<sub>2</sub>NH<sub>2</sub>), 14.6 (CH<sub>2</sub>CH<sub>3</sub>); **LC-MS (ES):** RT = 1.95-2.05 min, *m/z* = 362.1 (M+H<sup>+</sup>); **R<sub>f</sub>:** 0.34 (1:1:8 7.0 M NH<sub>3</sub> in MeOH–MeOH–EtOAc); **HPLC:** RT = 3.39 min; ***m/z* (ES+):** Found: 362.1675 (M+H<sup>+</sup>), C<sub>22</sub>H<sub>21</sub>FN<sub>3</sub>O requires *MH* 362.1669; **IR:ν<sub>max</sub>/cm<sup>-1</sup> (solid):** 3327 (N-H), 3260 (N-H), 3075, 2980, 1607; **M.pt:** 164.9-165.3 °C.

Preparation of {3-[6-(3-ethoxy-2-fluorophenyl)-1*H*-indazol-3-yl]phenyl}methanol



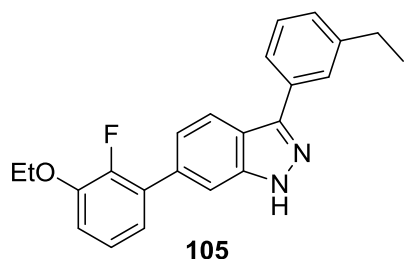
Synthesised using method A using 3-bromo-6-(3-ethoxy-2-fluorophenyl)-1*H*-indazole (150 mg, 0.45 mmol, 1.0 eq), 3-hydroxymethylphenylboronic acid (102 mg, 0.68 mmol, 1.5 eq), Pd(dppf)Cl<sub>2</sub>•DCM (37 mg, 0.045 mmol, 0.1 eq), Na<sub>2</sub>CO<sub>3</sub> (142 mg,

1.34 mmol, 3.0 eq), dioxane (5 mL) and water (5 mL) and the reaction heated for 1 h.

The work up proceeded using the larger volumes of solvents and the organic solvent removed *in vacuo* to reveal a brown oil. The crude product was purified using column chromatography (gradient 50-60% EtOAc–hexane) and an off-white solid obtained. The solid was triturated with DCM and the solid filtered. The solid was crystallised from propan-2-ol. The title compound 104 (26 mg, 0.07 mmol, 16%) was collected as colourless crystals.

**<sup>1</sup>H NMR (500 MHz, DMSO-*d*<sub>6</sub>):** 8.16 (1H, d, *J* 8.4, 4-H), 8.00 (1H, s, 2'''-H), 7.89 (1H, d, *J* 7.8, 6'''-H), 7.69 (1H, s, 7-H), 7.48 (1H, app.t, *J* 7.8, 5'''-H), 7.37-7.34 (2H, m, 4'''-H and 5-H), 7.24-7.16 (2H, m, 5''-H and 6''-H), 7.14 (1H, app.td, *J* 7.0 and 2.0, 4''-H), 5.29 (1H, t, *J* 5.8, OH), 4.62 (2H, d, *J* 5.8, CH<sub>2</sub>OH), 4.17 (2H, q, *J* 7.0, CH<sub>2</sub>CH<sub>3</sub>), 1.39 (3H, t, *J* 7.0, CH<sub>2</sub>CH<sub>3</sub>), NH peak not observed; **<sup>13</sup>C NMR (125 MHz, DMSO-*d*<sub>6</sub>):** 149.0 (d, *J* 246.4, 2''-C), 147.0 (d, *J* 12.2, 3''-C), 143.3 (3-C), 143.2 (3'''-C), 141.7 (3'-C), 133.4 (1'''-C), 133.0 (6-C), 129.3 (1''-C), 128.6 (5'''-C), 125.8 (4'''-C), 125.1 (6'''-C), 124.7 (2'''-C), 124.5 (d, *J* 4.8, 5''-C), 122.3 (d, *J* 2.3, 5-C), 121.9 (d, *J* 1.7, 4''-C), 120.8 (4-C), 119.5 (7'-C), 114.0 (6''-C), 110.6 (d, *J* 3.2, 7-C), 64.4 (CH<sub>2</sub>CH<sub>3</sub>), 62.9 (CH<sub>2</sub>OH), 14.6 (CH<sub>2</sub>CH<sub>3</sub>); **LC-MS (ES):** RT = 1.91-2.12 min, *m/z* = 362.8 (M+H<sup>+</sup>); **R<sub>r</sub>:** 0.41 (4:1 EtOAc–petrol); **HPLC:** RT = 3.81 min; ***m/z* (ES<sup>+</sup>):** Found: 363.1513 (M+H<sup>+</sup>), C<sub>22</sub>H<sub>20</sub>FN<sub>2</sub>O<sub>2</sub> requires *MH* 363.1509; **IR:ν<sub>max</sub>/cm<sup>-1</sup> (solid):** 3120 (br.OH), 3032, 2924, 2881, 1610; **M.pt:** 190.3-192.5 °C.

#### Preparation of 6-(3-ethoxy-2-fluorophenyl)-3-(3-ethylphenyl)-1*H*-indazole



Synthesised using method A using 3-bromo-6-(3-ethoxy-2-fluorophenyl)-1*H*-indazole (110 mg, 0.33 mmol, 1.0 eq), 3-ethylphenylboronic acid (74 mg, 0.49 mmol, 1.5 eq), Pd(dppf)Cl<sub>2</sub>•DCM (27 mg, 0.033 mmol, 0.1 eq), Na<sub>2</sub>CO<sub>3</sub> (104 mg,

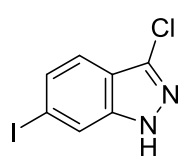
0.98 mmol, 3.0 eq), dioxane (5 mL) and water (5 mL) and the reaction heated for 2 h. LC-MS analysis showed the reaction to be incomplete and therefore Pd(dppf)Cl<sub>2</sub>•DCM (27 mg, 0.033 mmol, 0.1 eq) and Na<sub>2</sub>CO<sub>3</sub> (52 mg, 0.49 mmol, 1.5 eq) were added and the reaction heated for a further 2 h. The work up proceeded using the larger volumes of solvents and the organic solvent removed *in vacuo* to reveal a brown oil. The crude product was purified using column chromatography (1:4 EtOAc–hexane) and a glassy solid obtained. The glassy solid was dissolved in



Et<sub>2</sub>O and reduced *in vacuo*. The title compound 105 (37 mg, 0.10 mmol, 31%) was collected as a colourless foamy solid.

**<sup>1</sup>H NMR (500 MHz, CDCl<sub>3</sub>):** 10.60 (1H, br.s, NH), 8.08 (1H, d, *J* 8.5, 4-H), 7.86 (1H, s, 2'''-H), 7.83 (1H, d, *J* 7.8, 6'''-H), 7.61 (1H, s, 7-H), 7.45 (1H, app.t, *J* 7.6, 5'''-H), 7.42 (1H, app.dt, *J* 8.5 and 1.5, 5-H), 7.27 (1H, d, *J* 7.4, 4'''-H), 7.14 (1H, app.td, 8.0 and 1.3, 5''-H), 7.07-7.04 (1H, m, 6''-H), 7.00 (1H, app.td, *J* 8.0 and 1.5, 4''-H), 4.19 (2H, q, *J* 7.0, OCH<sub>2</sub>CH<sub>3</sub>), 2.77 (2H, q, *J* 7.5, CH<sub>2</sub>CH<sub>3</sub>), 1.51 (3H, t, *J* 7.0, OCH<sub>2</sub>CH<sub>3</sub>), 1.32 (3H, t, *J* 7.5, CH<sub>2</sub>CH<sub>3</sub>); **<sup>13</sup>C NMR (125 MHz, CDCl<sub>3</sub>):** 150.0 (d, *J* 248.9, 2''-C), 147.6 (d, *J* 11.8, 3''-C), 146.1 (3-C), 144.9 (3'''-C), 141.9 (3'-C), 134.5 (6-C), 133.4 (1'''-C), 129.9 (d, *J* 11.8, 1''-C), 128.9 (5'''-C), 127.9 (4'''-C), 127.1 (2'''-C), 125.0 (6'''-C), 123.9 (d, *J* 5.2, 5''-C), 123.0 (d, *J* 2.1, 5-C), 122.3 (d, *J* 2.0, 6''-C), 121.1 (4-C), 120.5 (6''-C), 113.9 (d, *J* 1.6, 4''-C), 110.4 (d, *J* 3.2, 7-C), 65.2 (OCH<sub>2</sub>CH<sub>3</sub>), 29.0 (CH<sub>2</sub>CH<sub>3</sub>), 15.6 (CH<sub>2</sub>CH<sub>3</sub>), 14.9 (OCH<sub>2</sub>CH<sub>3</sub>); **LC-MS (ES):** RT = 2.32-2.42 min, *m/z* = 361.1 (M+H<sup>+</sup>); **R<sub>f</sub>:** 0.47 (1:1 EtOAc–petrol); **HPLC:** RT = 1.49 min; ***m/z* (ES<sup>+</sup>):** Found: 361.1710 (M+H<sup>+</sup>), C<sub>23</sub>H<sub>22</sub>FN<sub>2</sub>O requires *MH* 361.1716; **IR:** *v*<sub>max</sub>/cm<sup>-1</sup> (solid): 3168 (N-H), 2965, 2930, 1609; **M.pt:** 43.6-49.6 °C.

#### Preparation of 3-chloro-6-iodo-1*H*-indazole



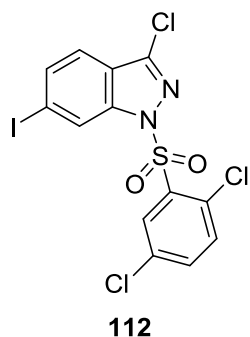
**109**

6-Iodo-1*H*-indazole (1.0 g, 4.10 mmol, 1.0 eq) was dissolved in DMF (10 mL) and cooled to 0 °C. NCS (657 mg, 4.92 mmol, 1.2 eq) was added and the reaction mixture warmed to 20 °C and stirred for 24 h. LC-MS analysis showed the reaction to be incomplete and therefore NCS (164 mg, 1.23 mmol, 0.3 eq) was added and the reaction stirred for 68 h. Water (10 mL) was added and the resulting solid was filtered and washed with water. The crude solid was purified by column chromatography (5:95 EtOAc–hexane). The title compound 109 (285 mg, 1.02 mmol, 25%) was collected as off-white microneedles.

**<sup>1</sup>H NMR (500 MHz, DMSO-*d*<sub>6</sub>):** 7.98 (1H, dd, *J* 1.2 and 0.8, 7-H), 7.49 (1H, dd, *J* 8.5 and 1.2, 5-H), 7.46 (1H, dd, *J* 8.5 and 0.8, 4-H), NH not observed; **<sup>13</sup>C NMR (125 MHz, DMSO-*d*<sub>6</sub>):** 142.3 (3'-C), 132.6 (3-C), 130.0 (4-C), 120.4 (5-C), 119.6 (7-C), 118.7 (7'-C), 93.9 (6-C); **LC-MS (ES):** RT = 1.93-2.05 min, *m/z* = 279.0 (M+H<sup>+</sup>); **R<sub>f</sub>:** 0.30 (1:4 EtOAc–hexane); **HPLC:** RT = 3.21 min; ***m/z* (ES<sup>-</sup>):** Found: 276.9036 (M-H), C<sub>7</sub>H<sub>3</sub>ClIN<sub>2</sub> requires *M-H* 276.9035;

**IR:**  $\nu_{\max}/\text{cm}^{-1}$  (solid): 3195 (N-H), 3134, 3077, 2971, 2916, 1615; **M.pt:** 211.7-215.3 °C; **Found:** C,30.4; H, 1.40; N, 10.1;  $\text{C}_7\text{H}_4\text{ClIN}_2$  requires C, 30.2; H, 1.45; N, 10.1%.

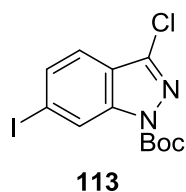
Preparation of 3-chloro-1-(2,5-dichlorobenzenesulfonyl)-6-iodo-1*H*-indazole



NaH 60% dispersion in oil (16 mg, 0.40 mmol, 1.1 eq) was charged with nitrogen in a RB flask at 0 °C. 3-Chloro-6-iodo-1*H*-indazole (100 mg, 0.36 mmol, 1.0 eq) was dissolved in DMF (1 mL) and added dropwise to the NaH and left to stir for two minutes. The reaction was allowed to warm to room temperature and stirred for a further 20 minutes. 2,5-Dichlorobenzenesulfonyl chloride (132 mg, 0.54 mmol, 1.5 eq) was dissolved in DMF (1 mL) and added in one portion to the reaction mixture and stirred for 1 h. Once complete, water (10 mL) was added and the resulting precipitate filtered and washed with water. The crude product was purified using column chromatography (1:9 EtOAc–hexane). The title compound 112 (46 mg, 0.094 mmol, 26%) was collected as colourless flakes.

**<sup>1</sup>H NMR (500 MHz, DMSO-*d*<sub>6</sub>):** 8.47 (1H, dd, *J* 1.3 and 0.6, 7-H), 8.31 (1H, d, *J* 2.5, 6''-H), 7.93 (1H, dd, *J* 8.6 and 2.5, 4''-H), 7.89 (1H, dd, *J* 8.4 and 1.3, 5-H), 7.77 (1H, d, *J* 8.6, 3''-H), 7.66 (1H, dd, *J* 8.4 and 0.6, 4-H); **<sup>13</sup>C NMR (125 MHz, DMSO-*d*<sub>6</sub>):** 142.4 (3'-C), 142.2 (Ar-q), 136.8 (4''-C), 135.0 (7'-C), 134.5 (3''-C), 134.3 (5-C), 133.0 (Ar-q), 131.5 (6''-C), 130.8 (Ar-q), 122.1 (4-C), 121.9 (7-C), 121.5 (Ar-q), 99.2 (Ar-q); **LC-MS (ES):** RT = 2.46-2.54 min, *m/z* = 510.7 ( $\text{MCl}^{37} + \text{Na}^+$ ); **R<sub>f</sub>:** 0.46 (1:4 EtOAc–hexane); **HPLC:** RT = 3.28 min; ***m/z* (ES+):** Found: 508.8156 (M+Na),  $\text{C}_{13}\text{H}_6\text{Cl}_3\text{IN}_2\text{NaO}_2\text{S}$  requires *MNa* 508.8153; **IR:**  $\nu_{\max}/\text{cm}^{-1}$  (solid): 3112, 3092, 2922, 2853, 1595; **M.pt:** 204.8-206.6 °C; **Found:** C,32.5; H, 1.30; N, 5.6;  $\text{C}_{13}\text{H}_6\text{Cl}_3\text{IN}_2\text{O}_2\text{S}$  requires C, 32.0; H, 1.20; N, 5.8%.

Preparation of *tert*-butyl 3-chloro-6-iodo-1*H*-indazole-1-carboxylate

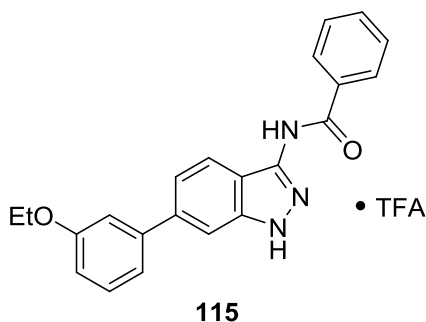


3-Chloro-6-iodo-1*H*-indazole (100 mg, 0.36 mmol, 1.0 eq) was suspended in DCM (2 mL) at 0 °C. Di-*tert*-butyl dicarbonate (137  $\mu\text{L}$ , 0.60 mmol, 1.7 eq) and  $\text{Et}_3\text{N}$  (55  $\mu\text{L}$ , 0.395 mmol, 1.1 eq) were added and the reaction stirred at room temperature for 66 h. Once complete, water (5 mL) was added and the organic layer separated. The aqueous layer was extracted with DCM (2  $\times$  10 mL) and the combined organic layers washed with brine

(20 mL), dried (MgSO<sub>4</sub>) and the filtrate concentrated *in vacuo* to reveal an orange solid. The crude product was dissolved in DCM (10 mL) and purified by silica plug (DCM). The **title compound 113** (120 mg, 0.32 mmol, 88%) was collected as a colourless oil which solidified upon standing to a yield pearlescent white solid.

**<sup>1</sup>H NMR (500 MHz, CDCl<sub>3</sub>):** 8.65 (1H, s, 7-H), 7.69 (1H, dd, *J* 8.5 and 1.5, 5-H), 7.43 (1H, d, *J* 8.5, 4-H), 1.72 (9H, s, <sup>t</sup>Bu CH<sub>3</sub>); **<sup>13</sup>C NMR (125 MHz, CDCl<sub>3</sub>):** 148.2 (C=O), 141.5 (3-C), 140.9 (3'-C), 133.4 (5-C), 124.2 (7-C), 122.9 (6-C), 121.0 (4-C), 96.7 (7'-C), 86.1 (C(CH<sub>3</sub>)<sub>3</sub>), 28.1 (<sup>t</sup>Bu CH<sub>3</sub>); **LC-MS (ES):** RT = 2.34-2.61 min, *m/z* = 401.1 (M+Na<sup>+</sup>); **R<sub>f</sub>:** 0.55 (1:4 EtOAc–hexane); **HPLC:** RT = 2.94 min; ***m/z* (ES<sup>+</sup>):** Found: 400.9524 (M+Na), C<sub>12</sub>H<sub>12</sub>ClIN<sub>2</sub>NaO<sub>2</sub> requires *MNa* 400.9524; **IR:ν<sub>max</sub>/cm<sup>-1</sup> (solid):** 3103, 2996, 2930, 1769, 1744 (C=O); **M.pt:** 113.8-115.8 °C; **Found:** C, 38.3; H, 3.20; N, 7.2; C<sub>12</sub>H<sub>12</sub>ClIN<sub>2</sub>O<sub>2</sub> requires C, 38.1; H, 3.19; N, 7.4%.

Preparation of 3-benzamido-6-(3-ethoxyphenyl)-1*H*-indazol-2-ium trifluoroacetate



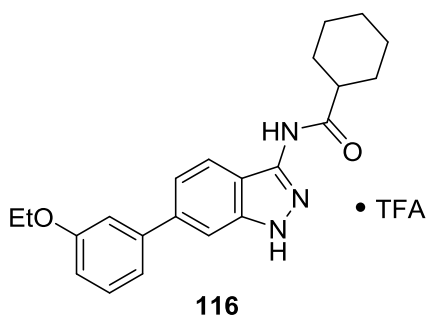
Synthesised using method C using *tert*-butyl 3-benzamido-6-(3-ethoxyphenyl)-1*H*-indazole-1-carboxylate (176 mg, 0.38 mmol, 1.0 eq), TFA (1 mL) and DCM (1 mL) and the reaction stirred for 1.5 h. The crude brown solid was triturated with MeOH and the solid filtered.

The **title compound 115** was collected as an off-white solid (45 mg, 0.10 mmol, 25%).

**<sup>1</sup>H NMR (500 MHz, DMSO-*d*<sub>6</sub>):** 10.82 (1H, br.s, amide NH), 8.10 (2H, m, 2'''-H and 6'''-H), 7.79 (1H, dd, *J* 8.5 and 1.0, 4-H), 7.67 (1H, dd, *J* 1.5 and 1.0, 7-H), 7.61 (1H, app.tt, *J* 7.5 and 1.5, 4'''-H), 7.56-7.52 (2H, m, 3'''-H and 5'''-H), 7.40-7.36 (2H, m, 5-H and 5''-H), 7.28 (1H, ddd, *J* 7.5, 1.5 and 1.0, 6''-H), 7.23 (1H, app.t, *J* 1.5, 2''-H), 6.94 (1H, ddd, *J* 8.0, 2.5 and 0.5, 4''-H), 4.12 (2H, q, *J* 7.0, CH<sub>2</sub>CH<sub>3</sub>), 1.36 (3H, t, *J* 7.0, CH<sub>3</sub>), indazole NH not observed; **<sup>13</sup>C NMR (125 MHz, DMSO-*d*<sub>6</sub>):** 165.5 (amide C=O), 159.0 (3''-C), 142.0 (1''-C), 141.7 (Ar-q), 140.1 (Ar-q), 138.6 (6-C), 133.8 (1'''-C), 131.8 (4'''-C), 130.0 (5''-C), 128.4 (3'''-C and 5'''-C), 127.9 (2'''-C and 6'''-C), 122.4 (4-C), 119.5 (5-C), 119.4 (6''-C), 116.3 (3-C), 113.5 (4''-C), 113.1 (2''-C), 107.8 (7-C), 63.1 (CH<sub>3</sub>CH<sub>2</sub>), 14.7 (CH<sub>3</sub>); **LC-MS (ES):** RT = 0.6-0.7 min, *m/z* = 358.23 (M+H<sup>+</sup>); **R<sub>f</sub>:** 0.29 (1:1 EtOAc–petrol); **HPLC:** RT = 3.21 min; ***m/z* (ES<sup>+</sup>):** Found: 380.1365 (M+Na<sup>+</sup>), C<sub>22</sub>H<sub>19</sub>N<sub>3</sub>NaO<sub>2</sub> requires *MNa* 380.1369;

**IR:**  $\nu_{\max}/\text{cm}^{-1}$  (solid): 3343 (N-H), 3250 (N-H), 3054, 2969, 2876, 1637 (C=O), 1574;  
**M.pt:** 189.8-191.1 °C.

Preparation of 3-cyclohexaneamido-6-(3-ethoxyphenyl)-1H-indazol-2-ium trifluoroacetate

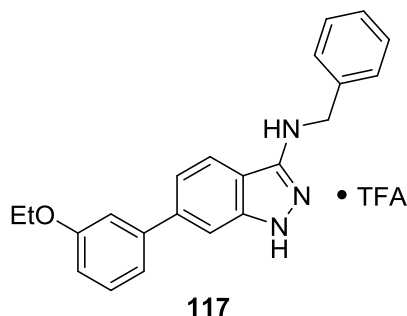


Synthesised using method C using *tert*-butyl 3-cyclohexaneamido-6-(3-ethoxyphenyl)-1H-indazole-1-carboxylate (110 mg, 0.24 mmol, 1.0 eq), TFA (1 mL) and DCM (1 mL) and the reaction stirred for 1.5 h. The crude brown solid was triturated with MeOH and the solid filtered.

The title compound 116 was collected as a pink solid (43 mg, 0.09 mmol, 38%).

**<sup>1</sup>H NMR (500 MHz, DMSO-*d*<sub>6</sub>):** 12.64 (1H, br.s, indazole NH), 10.20 (1H, br.s, amide NH), 7.78 (1H, d, *J* 8.5, 4-H), 7.60 (1H, s, 7-H), 7.37 (1H, app.t, *J* 7.5, 5''-H), 7.33 (1H, br.d, *J* 8.5, 5-H), 7.25 (1H, br.d, *J* 7.5, 6''-H), 7.20 (1H, app.t, *J* 2.0, 2''-H), 6.93 (1H, ddd, *J* 8.0, 2.5 and 0.5, 4''-H), 4.11 (2H, q, *J* 7.0, CH<sub>2</sub>CH<sub>3</sub>), 2.51-2.47 (1H, m, cyclohexyl-CH<sub>2</sub>), 1.90-1.84 (2H, m, cyclohexyl-CH<sub>2</sub>), 1.80-1.74 (2H, m, cyclohexyl-CH<sub>2</sub>), 1.68-1.63 (1H, m, cyclohexyl-CH), 1.52-1.43 (2H, m, cyclohexyl-CH<sub>2</sub>), 1.35 (3H, t, *J* 7.0, CH<sub>3</sub>), 1.31-1.15 (3H, m, cyclohexyl-CH<sub>2</sub>); **<sup>13</sup>C NMR (125 MHz, DMSO-*d*<sub>6</sub>):** 174.4 (amide C=O), 159.0 (3''-C), 142.1 (1''-C), 141.6 (Ar-q), 140.4 (Ar-q), 138.5 (6-C), 130.0 (5''-C), 122.7 (4-C), 119.4 (6''-C), 119.1 (5''-C), 115.7 (3-C), 113.5 (4''-C), 113.1 (2''-C), 107.6 (7-C), 63.0 (CH<sub>2</sub>CH<sub>3</sub>), 43.8 (cyclohexyl-C), 29.2 (cyclohexyl-C), 25.4 (cyclohexyl-C), 25.2 (cyclohexyl-C), 14.7 (CH<sub>3</sub>); **LC-MS (ES):** RT = 0.6-0.7 min, *m/z* = 364.30 (M+H<sup>+</sup>); **R<sub>f</sub>:** 0.25 (1:1 EtOAc-petrol); **HPLC:** RT = 3.39 min; ***m/z* (ES<sup>+</sup>):** Found: 386.1835 (M+Na<sup>+</sup>), C<sub>22</sub>H<sub>25</sub>N<sub>3</sub>NaO<sub>2</sub> requires *MNa* 386.1839; **IR:**  $\nu_{\max}/\text{cm}^{-1}$  (solid): 3264 (N-H), 3233 (N-H), 2928, 2853, 1668 (C=O); **M.pt:** 232.8-234.6 °C.

Preparation of 3-(benzylamino)-6-(3-ethoxyphenyl)-1*H*-indazol-2-ium trifluoroacetate

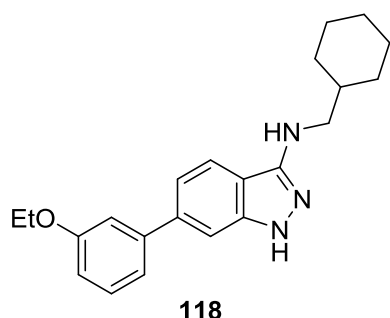


Synthesised using method C using tert-butyl 3-(benzylamino)-6-(3-ethoxyphenyl)-1*H*-indazole-1-carboxylate (80 mg, 0.18 mmol, 1.0 eq), TFA (0.5 mL) and DCM (0.5 mL) and stirred for 2.5 h. The crude product was purified by column chromatography (gradient 10-20%

EtOAc–hexane). The title compound 117 was collected as a red glassy solid (18 mg, 0.04 mmol, 22%).

**<sup>1</sup>H NMR (500 MHz, CDCl<sub>3</sub>):** 7.58 (1H, d, *J* 8.5, 4-H), 7.49-7.46 (3H, m, 7-H, 2'''-H and 6'''-H), 7.40-7.34 (3H, m, 5''-H, 3'''-H and 5'''-H), 7.33-7.27 (2H, m, 5-H and 4'''-H), 7.21 (1H, dd, *J* 7.5 and 1.0, 6''-H), 7.17 (1H, app.t, *J* 2.0, 2''-H), 6.91 (1H, ddd, *J* 8.5, 2.5 and 1.0, 4''-H), 4.67 (2H, s, NHCH<sub>2</sub>), 4.11 (2H, q, *J* 7.0, CH<sub>2</sub>CH<sub>3</sub>), 1.46 (3H, t, *J* 7.0, CH<sub>3</sub>), NHs not observed; **<sup>13</sup>C NMR (125 MHz, CDCl<sub>3</sub>):** 159.3 (3''-C), 150.6 (3-C), 143.2 (Ar-q), 142.8 (Ar-q), 141.0 (6-C), 139.6 (1'''-C), 129.8 (5''-C), 128.6 (3'''-C and 5'''-C), 127.9 (2'''-C and 6'''-C), 127.4 (4'''-C), 119.9 (6''-C), 119.4 (4-C), 119.3 (5-C), 113.9 (2''-C), 113.5 (4''-C), 108.0 (7-C), 105.0 (Ar-q), 63.5 (CH<sub>2</sub>CH<sub>3</sub>), 48.3 (NHCH<sub>2</sub>), 14.9 (CH<sub>3</sub>); **LC-MS (ES):** RT = 0.6-0.7 min, *m/z* = 344.28 (M+H<sup>+</sup>); **R<sub>f</sub>:** 0.60 (7:3 EtOAc–petrol); **HPLC:** RT = 2.92 min (71% - degrades overtime); ***m/z* (ES<sup>+</sup>):** Found: 344.1757 (M+H<sup>+</sup>), C<sub>22</sub>H<sub>22</sub>N<sub>3</sub>O requires *MH* 344.1757; **IR:ν<sub>max</sub>/cm<sup>-1</sup> (solid):** 3350 (N-H), 3061, 2976, 2926, 1599.

Preparation of N-(cyclohexylmethyl)-6-(3-ethoxyphenyl)-1*H*-indazol-3-amine



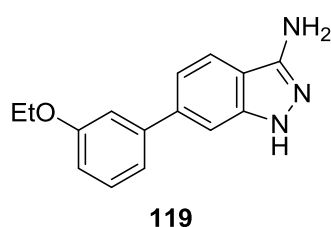
Synthesised using method B using 3-amino-6-(3-ethoxyphenyl)-1*H*-indazole (100 mg, 0.39 mmol, 1.0 eq), cyclohexane carboxaldehyde (57 μL, 0.47 mmol, 1.2 eq), glacial AcOH (1 drop), STAB (134 mg, 0.63 mmol, 1.6 eq) and DCM (3 mL). Imine formation took ten minutes monitoring by TLC. The

reaction was left to stir for 18 h. Water (5 mL) was added and the organic layer separated. The aqueous layer was extracted with DCM (3 × 10 mL) and the combined organics washed with brine (20 mL), dried (MgSO<sub>4</sub>) and reduced *in vacuo* to reveal a colourless oil (140 mg). The crude product was purified using column chromatography

(0.25% 7.0 M NH<sub>3</sub> in MeOH–DCM) and a colourless oil obtained which solidified upon standing. The title compound 118 (30 mg, 0.086 mmol, 22%) was collected as a colourless solid.

**<sup>1</sup>H NMR (500 MHz, DMSO-*d*<sub>6</sub>):** 11.34 (1H, br.s, indazole NH), 7.78 (1H, d, *J* 8.5, 4-H), 7.40 (1H, s, 7-H), 7.35 (1H, app.t, *J* 8.0, 5''-H), 7.21 (1H, ddd, *J* 7.5, 1.5 and 1.0, 6''-H), 7.18-7.15 (2H, m, 5-H and 2''-H), 6.90 (1H, ddd, *J* 8.5, 3.0 and 1.0, 4''-H), 5.92 (1H, t, *J* 5.5, NH), 4.10 (2H, q, *J* 7.0, CH<sub>2</sub>CH<sub>3</sub>), 3.10 (2H, app.t, *J* 6.5, CH<sub>2</sub>NH), 1.84-1.79 (2H, m, cyclohexyl-CH<sub>2</sub>), 1.79-1.60 (4H, m, cyclohexyl-CH<sub>2</sub>), 1.35 (3H, t, *J* 7.0, CH<sub>3</sub>), 1.25-1.11 (3H, m, cyclohexyl-CH<sub>2</sub> + CH), 0.99-0.90 (2H, m, cyclohexyl-CH<sub>2</sub>); **<sup>13</sup>C NMR (125 MHz, DMSO-*d*<sub>6</sub>):** 158.9 (3''-C), 150.2 (3-C), 142.5 (3'-C), 142.3 (1''-C), 138.5 (6-C), 129.9 (5''-C), 120.6 (4-C), 119.3 (6''-C), 117.0 (5-C), 113.3 (2''-C), 113.2 (7'-C), 112.9 (4''-C), 107.0 (7-C), 63.0 (CH<sub>2</sub>CH<sub>3</sub>), 49.8 (CH<sub>2</sub>NH), 37.0 (1'''-C), 30.9 (2'''-C and 6'''-C), 26.3 (cyclohexyl-CH<sub>2</sub>), 25.6 (cyclohexyl-CH<sub>2</sub>), 14.7 (CH<sub>3</sub>); **LC-MS (ES):** RT = 39.7-42.3 sec, *m/z* = 350.32 (M+H<sup>+</sup>); **R<sub>f</sub>:** 0.30 (69:30:1 petrol–EtOAc–7.0 M NH<sub>3</sub> in MeOH); **HPLC:** RT = 3.08 min; ***m/z* (ES<sup>+</sup>):** Found: 350.2240 (M+H<sup>+</sup>), C<sub>22</sub>H<sub>27</sub>N<sub>3</sub>O requires *MH* 350.2232; **IR:  $\nu_{\max}/\text{cm}^{-1}$  (solid):** 3402 (N-H), 3182, 2978, 2919, 2847, 1600.

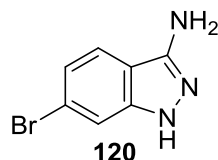
#### Preparation of 3-amino-6-(3-ethoxyphenyl)-1*H*-indazole



Synthesised using method A using 3-amino-6-bromo-1*H*-indazole (500 mg, 2.36 mmol, 1.0 eq), 3-ethoxyphenyl boronic acid (587 mg, 3.54 mmol, 1.5 eq), Pd(dppf)Cl<sub>2</sub>•DCM (193 mg, 0.236 mmol, 0.1 eq), Na<sub>2</sub>CO<sub>3</sub> (750 mg, 7.07 mmol, 3.0 eq), dioxane (10 mL) and water (10 mL) and the reaction heated for 4 h. LC-MS showed the reaction to be incomplete and therefore 3-ethoxyphenyl boronic acid (117 mg, 0.70 mmol, 0.3 eq), Pd(dppf)Cl<sub>2</sub>•DCM (39 mg, 0.048 mmol, 0.02 eq), Na<sub>2</sub>CO<sub>3</sub> (150 mg, 1.42 mmol, 0.6 eq) were added and the reaction heated for 1 h. LC-MS showed no change and therefore the reaction was stopped. The work up proceeded using the larger volumes of solvents and the organic solvent removed *in vacuo* to reveal a brown solid. The crude product was purified using column chromatography (50:49:1 EtOAc–hexane–7.0 M NH<sub>3</sub> in MeOH) and an off-white solid obtained. The resulting solid was crystallised from EtOAc. The title compound 119 (519 mg, 2.05 mmol, 43%) was collected as shiny off-white crystals.

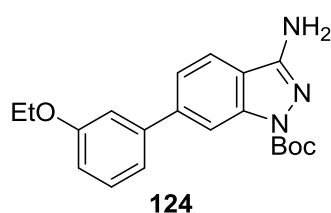
**<sup>1</sup>H NMR (500 MHz, DMSO-*d*<sub>6</sub>):** 11.41 (1H, br.s, NH), 7.73 (1H, d, *J* 8.0, 4-H), 7.41 (1H, s, 7-H), 7.35 (1H, app.t, *J* 8.0, 5'-H), 7.22 (1H, ddd, *J* 7.5, 1.5 and 1.0, 6'-H), 7.19 (1H, dd, *J* 8.5 and 1.5, 5-H), 7.17 (1H, app.t, *J* 1.5, 2'-H), 6.90 (1H, ddd, *J* 8.0, 2.5 and 0.5, 4'-H), 5.34 (2H, br.s, NH<sub>2</sub>), 4.10 (2H, q, *J* 7.0, CH<sub>2</sub>), 1.35 (3H, t, *J* 7.0, CH<sub>3</sub>); **<sup>13</sup>C NMR (125 MHz, DMSO-*d*<sub>6</sub>):** 158.9 (3''-C), 149.1 (3'-C), 142.5 (1''-C), 142.0 (7'-C), 138.3 (6-C), 129.9 (5''-C), 120.6 (4-C), 119.3 (6''-C), 117.2 (5-C), 113.5 (3-C), 113.3 (4''-C), 113.0 (2''-C), 107.1 (7-C), 63.0 (CH<sub>2</sub>), 14.7 (CH<sub>3</sub>); **LC-MS (ES):** RT = 31.3-34.2 sec, *m/z* = 254.15 (M+H<sup>+</sup>); **R<sub>f</sub>:** 0.13 (50:49:1 EtOAc–petrol–7.0 M NH<sub>3</sub> in MeOH); **HPLC:** RT = 2.20 min; ***m/z* (ES+):** Found: 254.1287 (M+H<sup>+</sup>), C<sub>15</sub>H<sub>15</sub>N<sub>3</sub>O requires *MH* 254.1289; **IR:ν<sub>max</sub>/cm<sup>-1</sup> (solid):** 3381 (N-H), 3127, 3077, 2973, 2929, 2830, 1625; **M.pt:** 185.4-186.0 °C.

#### Preparation of 3-amino-6-bromo-1*H*-indazole



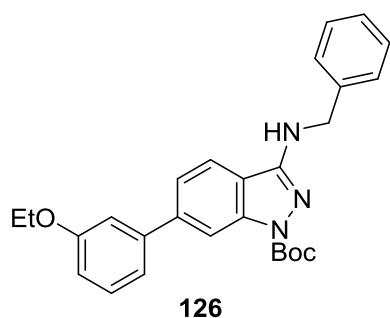
4-Bromo-2-fluorobenzonitrile (5.0 g, 25.0 mmol, 1.0 eq) was dissolved in <sup>n</sup>BuOH (25 mL) and 50-60% N<sub>2</sub>H<sub>2</sub> in water (5.20 mL, 100.0 mmol, 4.0 eq) was added and the reaction heated to 100 °C for 2 h. The reaction mixture was allowed to cool slowly and the resulting precipitate was filtered and washed with MeOH. The title compound 120 (4.17 g, 19.7 mmol, 79%) was collected as colourless microneedles. A second batch crystallised in the filtrate overnight and was collected as off-white microneedles (505 mg, 2.38 mmol, 10%).

**<sup>1</sup>H NMR (500 MHz, DMSO-*d*<sub>6</sub>):** 11.48 (1H, br.s, NH), 7.62 (1H, d, *J* 8.5, 4-H), 7.41 (1H, dd, *J* 1.5 and 0.5, 7-H), 7.01 (1H, dd, *J* 8.5 and 1.5, 5-H), 5.43 (2H, br.s, NH<sub>2</sub>); **<sup>13</sup>C NMR (125 MHz, DMSO-*d*<sub>6</sub>):** 149.3 (3'-C), 142.0 (7'-C), 122.1 (4-C), 120.3 (5-C), 119.8 (6-C), 113.1 (3-C), 111.8 (7-C); **LC-MS (ES):** RT = 27.7-30.2 sec, *m/z* = 213.96 (M+H<sup>+</sup>); **R<sub>f</sub>:** 0.17 (50:49:1 EtOAc–petrol–7.0 M NH<sub>3</sub> in MeOH); **HPLC:** RT = 1.45 min; ***m/z* (ES+):** Found: 211.9809 (M+H<sup>+</sup>), C<sub>7</sub>H<sub>6</sub>BrN<sub>3</sub> requires *MH* 211.9823; **IR:ν<sub>max</sub>/cm<sup>-1</sup> (solid):** 3401 (N-H), 3290, 3213, 3153, 2930, 1604; **M.pt:** 235.5-236.7 °C.

Preparation of *tert*-butyl 3-amino-6-(3-ethoxyphenyl)-1*H*-indazole-1-carboxylate

3-Amino-6-(3-ethoxyphenyl)-1*H*-indazole (700 mg, 2.76 mmol, 1.0 eq) was dissolved in THF (20 mL) and DMAP (101 mg, 0.83 mmol, 0.3 eq) was added and the reaction stirred for two minutes. Di-*tert*-butyl dicarbonate (698  $\mu$ L, 3.04 mmol, 1.1 eq) was added and the reaction stirred for 2 h. LC-MS showed the reaction to be incomplete and therefore di-*tert*-butyl dicarbonate (127  $\mu$ L, 0.55 mmol, 0.2 eq) was added and the reaction stirred for 15 h. LC-MS showed a small amount of starting material remaining but the reaction was stopped here to prevent over protection. The reaction mixture was reduced *in vacuo* to reveal the crude product as a brown foamy solid. The crude product was purified using column chromatography (gradient 25-40% EtOAc–hexane). The title compound 124 (667 mg, 1.89 mmol, 57%) was collected as a yellow foamy solid.

**<sup>1</sup>H NMR (500 MHz, CDCl<sub>3</sub>):** 8.31 (1H, br.s, 7-H), 7.57 (1H, dd, *J* 8.0 and 0.5, 4-H), 7.47 (1H, dd, *J* 8.5 and 1.5, 5-H), 7.36 (1H, app.t, *J* 8.0, 5''-H), 7.23 (1H, ddd, *J* 8.0, 1.5 and 1.0, 4''-H), 7.20 (1H, app.t, *J* 2.0, 2''-H), 6.92 (1H, ddd, *J* 8.5, 2.5 and 1.0, 6''-H), 4.82 (2H, br.s, NH<sub>2</sub>), 4.10 (2H, q, *J* 7.0, CH<sub>2</sub>), 1.71 (9H, s, <sup>t</sup>Bu CH<sub>3</sub>), 1.44 (3H, t, *J* 7.0, CH<sub>3</sub>); **<sup>13</sup>C NMR (125 MHz, CDCl<sub>3</sub>):** 159.4 (3''-C), 151.5 (7'-C), 149.6 (C=O), 142.8 (1''-C), 142.4 (3'-C), 141.2 (6-C), 129.9 (5''-C), 122.5 (5-C), 120.0 (6''-C), 119.4 (4-C), 117.9 (3-C), 114.0 (4''-C), 113.8 (2''-C), 113.5 (7-C), 83.8 (C(CH<sub>3</sub>)<sub>3</sub>), 64.0 (CH<sub>2</sub>), 28.3 (<sup>t</sup>Bu CH<sub>3</sub>), 14.9 (CH<sub>3</sub>); **LC-MS (ES):** RT = 39.3-43.3 sec, *m/z* = 296.20 (M-<sup>t</sup>Bu); **R<sub>f</sub>:** 0.13 (69:30:1 EtOAc–petrol–7.0 M NH<sub>3</sub> in MeOH); **HPLC:** RT = 3.51 min; ***m/z* (ES<sup>+</sup>):** Found: 354.1808 (M+H<sup>+</sup>), C<sub>20</sub>H<sub>23</sub>N<sub>3</sub>O<sub>3</sub> requires *MH* 354.1812; **IR:**  $\nu_{\max}/\text{cm}^{-1}$  (solid): 3362 (N-H), 2976, 2925, 1719, 1620.

Preparation of *tert*-butyl 3-(benzylamino)-6-(3-ethoxyphenyl)-1*H*-indazole-1-carboxylate

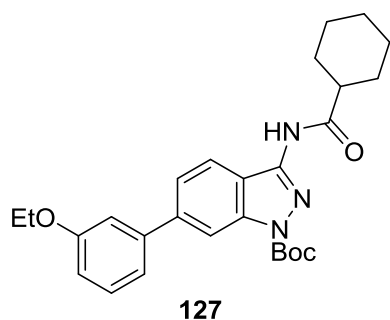
Synthesised using method B using *tert*-butyl 3-amino-6-(3-ethoxyphenyl)-1*H*-indazole-1-carboxylate (150 mg, 0.42 mmol, 1.0 eq), freshly distilled benzaldehyde (52  $\mu$ L, 0.51 mmol, 1.2 eq), STAB (144 mg, 0.68 mmol, 1.6 eq), AcOH (2  $\mu$ L, 0.036 mmol, 0.09 eq) and DCM (3 mL) and the reaction stirred for 40 minutes. TLC indicated no formation of the imine and therefore



the reaction was heated to 40 °C for 30 minutes. TLC showed no change and therefore the reaction was cooled to 0 °C and STAB (144 mg, 0.68 mmol, 1.6 eq) added. LC-MS showed small conversion to the product but majority starting material. 4 Å Molecular sieves (MS) (1 g) and benzaldehyde (22 µL, 0.21 mmol, 0.5 eq) were added and heated to 40 °C for 20 minutes. LC-MS indicated more conversion and therefore benzaldehyde (22 µL, 0.21 mmol, 0.5 eq), STAB (77 mg, 0.34 mmol, 0.8 eq) and 4 Å MS (1 g) were added and the reaction heated to 40 °C for 16 h. LC-MS indicated mainly product and therefore the reaction mixture was reduced *in vacuo* to reveal a yellow solid. The yellow solid was triturated with EtOAc and the solids removed. The filtrate was reduced *in vacuo* to give a yellow oil. The crude product was purified by column chromatography (9:1 hexane–EtOAc). The title compound 126 was collected as a colourless glassy solid (80 mg, 0.18 mmol, 42%).

**<sup>1</sup>H NMR (500 MHz, CDCl<sub>3</sub>):** 8.36 (1H, br.s, 7-H), 7.53 (1H, d, *J* 8.5, 4-H), 7.48-7.45 (3H, m, 5-H, 2'''-H and 6'''-H), 7.39-7.35 (3H, m, 5''-H, 3'''-H and 5'''-H), 7.33-7.30 (1H, m, 4'''-H), 7.24 (1H, d, *J* 7.5, 6''-H), 7.20 (1H, app.t, *J* 2.5, 2''-H), 6.93 (1H, dd, *J* 8.5 and 2.0, 4''-H), 4.74 (2H, s, NHCH<sub>2</sub>), 4.11 (2H, q, *J* 7.0, CH<sub>2</sub>CH<sub>3</sub>), 1.73 (9H, s, <sup>t</sup>Bu CH<sub>3</sub>), 1.46 (3H, t, *J* 7.0, CH<sub>3</sub>), NH not observed; **<sup>13</sup>C NMR (125 MHz, CDCl<sub>3</sub>):** 159.4 (3''-C), 152.2 (3-C), 142.7 (Ar-q), 142.4 (Ar-q), 138.9 (1'''-C), 129.9 (5''-C), 128.7 (3'''-C and 5'''-C), 128.3 (2'''-C and 6'''-C), 127.6 (4'''-C), 122.3 (5-C), 119.9 (6''-C), 119.1 (4-C), 117.8 (7'-C), 113.9 (4''-C), 113.9 (2''-C), 113.6 (7-C), 83.7 (C(CH<sub>3</sub>)<sub>3</sub>), 63.6 (CH<sub>2</sub>CH<sub>3</sub>), 47.8 (NHCH<sub>2</sub>), 28.3 (<sup>t</sup>Bu CH<sub>3</sub>), 14.9 (CH<sub>3</sub>), two Ar-qs not observed; **LC-MS (ES):** RT = 0.8-0.9 min, *m/z* = 444.31 (M+H<sup>+</sup>); **R<sub>f</sub>:** 0.65 (1:1 EtOAc–petrol); **HPLC:** RT = 2.68 min (91%); ***m/z* (ES<sup>+</sup>):** Found: 466.2100 (M+Na<sup>+</sup>), C<sub>27</sub>H<sub>29</sub>N<sub>3</sub>NaO<sub>3</sub> requires *MNa* 466.2101; **IR:ν<sub>max</sub>/cm<sup>-1</sup> (solid):** 3361 (N-H), 2978, 1716 (C=O), 1598.

Preparation of *tert*-butyl 3-cyclohexanecarboxamido-6-(3-ethoxyphenyl)-1*H*-indazole-1-carboxylate

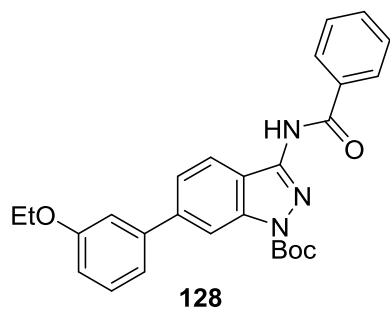


Synthesised using method E using *tert*-butyl 3-amino-6-(3-ethoxyphenyl)-1*H*-indazole-1-carboxylate (152 mg, 0.43 mmol, 1.0 eq), freshly distilled cyclohexanecarbonyl chloride (69 µL, 0.52 mmol, 1.2 eq), DIPEA (150 µL, 0.86 mmol, 2.0 eq) and DCM (5 mL) and the reaction stirred for

15 h. LC-MS analysis showed the reaction to be incomplete and therefore cyclohexanecarbonyl chloride (15  $\mu\text{L}$ , 0.11 mmol, 0.26 eq) was added and the reaction stirred for 2.5 h. A total further amount of cyclohexanecarbonyl chloride (45  $\mu\text{L}$ , 0.34 mmol, 0.8 eq) was needed over a combined time of 6 h for completion. The reaction mixture was reduced *in vacuo* to reveal the crude product as a yellow oil. The crude product was purified using column chromatography (gradient 10-20% EtOAc–hexane). The title compound 127 (150 mg, 0.33 mmol, 75%) was collected as shiny off-white crystals.

**$^1\text{H}$  NMR (500 MHz,  $\text{CDCl}_3$ ):** 8.34 (1H, br.s, 7-H), 8.27-8.17 (2H, m, NH and 4-H), 7.54 (1H, dd,  $J$  8.5 and 1.5, 5-H), 7.38 (1H, app.t,  $J$  7.5, 5''-H), 7.25 (1H, ddd,  $J$  7.5, 1.5 and 1.0, 6''-H), 7.21 (1H, app.t,  $J$  2.0, 2''-H), 6.93 (1H, ddd,  $J$  8.0, 1.5 and 1.0, 4''-H), 4.12 (2H, q,  $J$  7.0,  $\text{CH}_2\text{CH}_3$ ), 2.40 (1H, br.s, 1'''-H), 2.08-2.02 (2H, m, cyclohexyl-H), 1.90-1.84 (2H, m, cyclohexyl-H), 1.76-1.70 (10H, m,  $^t\text{Bu}$   $\text{CH}_3$  and cyclohexyl-H), 1.64-1.55 (2H, m, cyclohexyl-H), 1.46 (3H, t,  $J$  7.0,  $\text{CH}_3$ ), 1.40-1.25 (3H, m, cyclohexyl-H);  **$^{13}\text{C}$  NMR (125 MHz,  $\text{CDCl}_3$ ):** 174.5 (amide C=O), 159.4 (3''-C), 149.0 (BOC C=O), 145.3 (Ar-q), 142.9 (1''-C), 142.3 (6-C), 141.8 (Ar-q), 129.9 (5''-C), 124.7 (4-C), 123.2 (5-C), 120.0 (6''-C), 118.5 (3-C), 114.0 (2''-C), 113.9 (4''-C), 112.7 (7-C), 84.9 ( $\text{C}(\text{CH}_3)_3$ ), 63.6 ( $\text{CH}_2\text{CH}_3$ ), 45.7 (1'''-C), 29.6 (cyclohexyl- $\text{CH}_2$ ), 28.2 ( $^t\text{Bu}$   $\text{CH}_3$ ), 25.7 (cyclohexyl- $\text{CH}_2$ ), 25.6 (cyclohexyl- $\text{CH}_2$ ), 14.9 ( $\text{CH}_3$ ); **LC-MS (ES):** RT = 47.3-50.9 sec,  $m/z$  = 464.35 ( $\text{M}+\text{H}^+$ ); **R<sub>f</sub>:** 0.61 (1:1 EtOAc–petrol); **HPLC:** RT = 2.72 min (90%); **m/z (ES+):** Found: 464.2540 ( $\text{M}+\text{H}^+$ ),  $\text{C}_{27}\text{H}_{33}\text{N}_3\text{O}_4$  requires  $MH$  464.2544; **IR:**  $\nu_{\text{max}}/\text{cm}^{-1}$  (solid): 3251 (N-H), 2979, 2926, 2853, 1731 (C=O), 1701 (C=O), 1579.

Preparation of *tert*-butyl 3-benzamido-6-(3-ethoxyphenyl)-1*H*-indazole-1-carboxylate



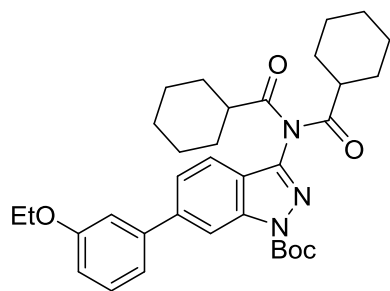
Synthesised using method E using *tert*-butyl 3-amino-6-(3-ethoxyphenyl)-1*H*-indazole-1-carboxylate (152 mg, 0.43 mmol, 1.0 eq), freshly distilled benzoyl chloride (60  $\mu\text{L}$ , 0.52 mmol, 1.2 eq), DIPEA (150  $\mu\text{L}$ , 0.86 mmol, 2.0 eq) and DCM (5 mL) the reaction stirred for 16 h. LC-MS analysis

showed the reaction to be incomplete and therefore benzoyl chloride (10  $\mu\text{L}$ , 0.09 mmol, 0.1 eq) was added and the reaction stirred for 2 h. A total further amount

of benzoyl chloride (30  $\mu\text{L}$ , 0.26 mmol, 0.6 eq) was needed over a combined time of 4 h. LC-MS showed no change in conversion of starting material to product and therefore DMAP (16 mg, 0.13 mmol, 0.3 eq) was added and the reaction heated to 35  $^{\circ}\text{C}$  and stirred for 1 h. LC-MS indicated formation of the undesired bis-product and therefore the reaction was stopped. The reaction mixture was reduced *in vacuo* to reveal the crude product as a yellow oil. The crude product was purified using column chromatography (gradient 10-20% EtOAc–hexane). The title compound 128 (37 mg, 0.081 mmol, 19%) was collected as a colourless oil.

**$^1\text{H}$  NMR (500 MHz,  $\text{CDCl}_3$ ):** 9.28 (1H, br.s, NH), 8.40 (1H, br.s, 7-H), 8.30 (1H, d,  $J$  8.5, 4-H), 8.04-8.01 (2H, m, 2'''-H and 6'''-H), 7.62-7.58 (2H, m, 5-H and 4'''-H), 7.54-7.50 (2H, m, 3'''-H and 5'''-H), 7.39 (1H, app.t,  $J$  8.0, 5''-H), 7.28 (1H, app.d,  $J$  7.5, 6''-H), 7.24 (1H, app.t,  $J$  2.0, 2''-H), 6.95 (1H, ddd,  $J$  8.0, 2.5 and 0.5, 4''-H), 4.13 (2H, q,  $J$  7.0,  $\text{CH}_2\text{CH}_3$ ), 1.69 (9H, s,  $^t\text{Bu}$   $\text{CH}_3$ ), 1.47 (3H, t,  $J$  7.0,  $\text{CH}_2\text{CH}_3$ );  **$^{13}\text{C}$  NMR (125 MHz,  $\text{CDCl}_3$ ):** 165.6 (amide C=O), 159.4 (3''-C), 149.0 (BOC C=O), 145.4 (3'-C), 143.0 (1''-C), 142.2 (6-C), 141.9 (3-C), 133.2 (1'''-C), 132.6 (5-C), 129.9 (5''-C), 128.9 (3'''-C and 5'''-C), 127.7 (2'''-C and 6'''-C), 124.6 (4-C), 123.4 (4'''-C), 120.0 (6''-C), 118.7 (7'-C), 114.0 (2''-C), 113.9 (4''-C), 112.8 (7-C), 85.1 ( $\text{C}(\text{CH}_3)_3$ ), 63.6 ( $\text{CH}_2$ ), 28.2 ( $^t\text{Bu}$   $\text{CH}_3$ ), 14.9 ( $\text{CH}_3$ ); **LC-MS (ES):** RT = 45.3-50.1 sec,  $m/z$  = 458.27 ( $\text{M}+\text{H}^+$ ); **R<sub>f</sub>:** 0.55 (1:1 EtOAc–petrol); **HPLC:** RT = 2.27 min (95%);  **$m/z$  (ES<sup>+</sup>):** Found: 480.1896 ( $\text{M}+\text{Na}^+$ ),  $\text{C}_{27}\text{H}_{27}\text{N}_3\text{NaO}_4$  requires  $M\text{Na}$  480.1894; **IR:**  $\nu_{\text{max}}/\text{cm}^{-1}$  (solid): 3252 (N-H), 3064, 2978, 1731 (C=O), 1680 (C=O).

Preparation of *tert*-butyl 3-(*N*-cyclohexanecarbonylcyclohexaneamido)-6-(3-ethoxyphenyl)-1*H*-indazole-1-carboxylate



**131**

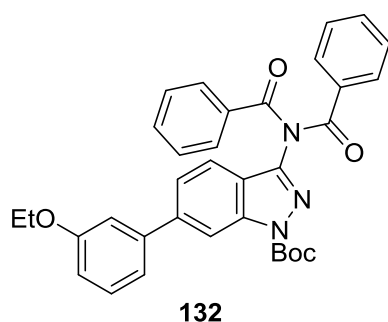
Synthesised as a side product using the same conditions as seen in the preparation of *tert*-butyl 3-cyclohexaneamido-6-(3-ethoxyphenyl)-1*H*-indazole-1-carboxylate (**127**). A second compound was isolated from the column. The title compound 131 (26 mg, 0.05 mmol, 10%)

was collected as a colourless oil.

**$^1\text{H}$  NMR (500 MHz,  $\text{CDCl}_3$ ):** 8.43 (1H, s, 7-H), 7.57 (1H, dd,  $J$  8.5 and 1.5, 5-H), 7.43 (1H, dd,  $J$  8.5 and 0.5, 4-H), 7.39 (1H, app.t  $J$  8.0, 5''-H), 7.24 (1H, ddd,  $J$  7.5, 1.5 and 1.0, 6''-H), 7.20 (1H, app.t,  $J$  2.0, 2''-H), 6.95 (1H, ddd,  $J$  8.0, 2.0 and 1.0,

4''-H), 4.12 (2H, q,  $J$  7.0,  $\underline{\text{CH}}_2\text{CH}_3$ ), 2.80 (2H, tt,  $J$  11.5 and 3.0, 1''''-H), 2.04-1.98 (4H, m, cyclohexyl-H), 1.79-1.74 (2H, m, cyclohexyl-H), 1.72 (3H, s,  $^t\text{Bu}$   $\underline{\text{CH}}_3$ ), 1.67-1.63 (2H, m, cyclohexyl-H), 1.58-1.51 (4H, m, cyclohexyl-H), 1.46 (3H, t,  $J$  7.0,  $\underline{\text{CH}}_2\text{CH}_3$ ), 1.28-1.14 (8H, m, cyclohexyl-H);  $^{13}\text{C}$  NMR (125 MHz,  $\text{CDCl}_3$ ): 179.1 (amide C=O), 159.4 (3''-C), 148.8 (BOC C=O), 145.5 (3-C), 143.1 (1''-C), 142.1 (6-C), 141.7 (3'-C), 130.0 (5''-C), 124.4 (5-C), 121.1 (7'-C), 120.0 (6''-C), 119.6 (4-C), 114.1 (2''-C), 114.0 (4''-C), 113.7 (7-C), 85.3 ( $\underline{\text{C}}(\text{CH}_3)_3$ ), 63.6 ( $\underline{\text{CH}}_2\text{CH}_3$ ), 45.4 (1''''-C), 29.7 (cyclohexyl- $\underline{\text{CH}}_2$ ), 28.2 ( $^t\text{Bu}$   $\underline{\text{CH}}_3$ ), 25.7 (cyclohexyl- $\underline{\text{CH}}_2$ ), 25.5 (cyclohexyl- $\underline{\text{CH}}_2$ ), 14.9 ( $\underline{\text{CH}}_3$ ); **LC-MS (ES)**: RT = 60.5-64.6 sec,  $m/z$  = 596.48 ( $\text{M}+\text{Na}^+$ ); **R<sub>f</sub>**: 0.73 (1:1 EtOAc–petrol); **HPLC**: RT = 4.07 min (78%); **m/z (ES<sup>+</sup>)**: Found: 596.3095 ( $\text{M}+\text{Na}^+$ ),  $\text{C}_{34}\text{H}_{43}\text{N}_3\text{NaO}_5$  requires  $MNa$  596.3095; **IR**:  $\nu_{\text{max}}/\text{cm}^{-1}$  (solid): 2977, 2928, 2853, 1737 (C=O), 1719 (C=O), 1605.

Preparation of *tert*-butyl 3-(*N*-benzoylbenzamido)-6-(3-ethoxyphenyl)-1*H*-indazole-1-carboxylate



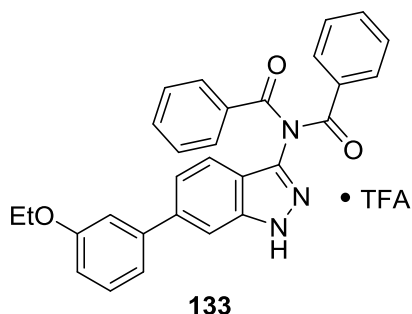
Synthesised as a side product using the same conditions as seen in the preparation of *tert*-butyl 3-benzamido-6-(3-ethoxyphenyl)-1*H*-indazole-1-carboxylate (**128**). A second compound was isolated from the column. The colourless oil was dissolved in MeOH and reduced *in vacuo*.

The title compound **132** (45 mg, 0.08 mmol, 19%) was collected as a white solid.

$^1\text{H}$  NMR (500 MHz,  $\text{CDCl}_3$ ): 8.35 (1H, br.s, 7-H), 7.88-7.85 (4H, m, 2''''-H and 6''''-H) 7.58 (1H, dd,  $J$  8.5 and 1.0, 4-H), 7.55 (1H, dd,  $J$  8.5 and 1.5, 5-H), 7.51-7.47 (2H, m, 4''''-H), 7.40-7.36 (5H, m, 5''-H, 3''''-H and 5''''-H), 7.21 (1H, ddd,  $J$  7.5, 1.5 and 1.0, 6''-H), 7.17 (1H, app.t,  $J$  2.5, 2''-H), 6.94 (1H, ddd,  $J$  8.5, 2.5 and 1.0, 4''-H), 4.11 (2H, q,  $J$  7.0,  $\underline{\text{CH}}_2\text{CH}_3$ ), 1.65 (9H, s,  $^t\text{Bu}$   $\underline{\text{CH}}_3$ ), 1.46 (3H, t,  $J$  7.0,  $\underline{\text{CH}}_3$ );  $^{13}\text{C}$  NMR (125 MHz,  $\text{CDCl}_3$ ): 172.1 (amide C=O), 159.4 (3''-C), 148.7 (BOC C=O), 146.0 (3'-C), 143.0 (1''-C), 142.1 (6-C), 141.7 (3-C), 134.0 (1''''-C), 132.8 (4''''-C), 130.0 (5''-C), 129.3 (2''''-C and 6''''-C), 128.7 (3''''-C and 5''''-C), 124.3 (4-C), 120.3 (7'-C), 120.0 (6''-C), 119.7 (5-C), 114.0 (4''-C), 114.0 (2''-C), 113.7 (7-C), 85.2 ( $\underline{\text{C}}(\text{CH}_3)_3$ ), 63.6 ( $\underline{\text{CH}}_2\text{CH}_3$ ), 28.1 ( $^t\text{Bu}$   $\underline{\text{CH}}_3$ ), 14.9 ( $\underline{\text{CH}}_3$ ); **LC-MS (ES)**: RT = 48.3-54.3 sec,  $m/z$  = 562.32 ( $\text{M}+\text{H}^+$ ); **R<sub>f</sub>**: 0.61 (1:1 EtOAc–petrol); **HPLC**: RT = 3.10 min (95%); **m/z (ES<sup>+</sup>)**: Found: 584.2156 ( $\text{M}+\text{Na}^+$ ),  $\text{C}_{34}\text{H}_{31}\text{N}_3\text{NaO}_5$  requires  $MNa$

584.2156; **IR:** $\nu_{\max}/\text{cm}^{-1}$  (**solid**): 2972, 2928, 1767 (C=O), 1743 (C=O), 1699 (C=O);  
**M.pt:** 162.9-163.5 °C.

Preparation of 3-(N-benzoylbenzamido)-6-(3-ethoxyphenyl)-1H-indazol-2-ium trifluoroacetate

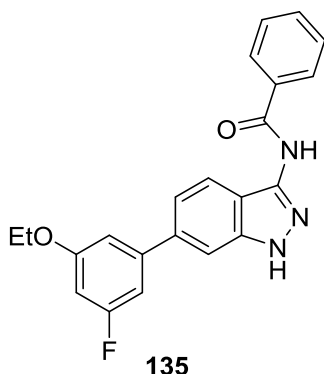


Synthesised using method C using *tert*-butyl 3-(N-benzoylbenzamido)-6-(3-ethoxyphenyl)-1H-indazole-1-carboxylate (95 mg, 0.17 mmol, 1.0 eq), TFA (1 mL) and DCM (1 mL) and stirred for 45 minutes. The crude product was purified by column chromatography (1:1 EtOAc–hexane).

The title compound **133** was collected as a colourless gummy solid (45 mg, 0.08 mmol, 46%).

**<sup>1</sup>H NMR (500 MHz, CDCl<sub>3</sub>):** 10.23 (1H, br.s, NH), 7.87-7.84 (4H, m, 2'''-H and 6'''-H), 7.58 (1H, dd, *J* 8.5 and 0.5, 4-H), 7.46 (2H, app.tt, *J* 7.5 and 1.5, 4''-H), 7.40 (1H, app.t, *J* 1.0, 7-H), 7.37-7.31 (6H, m, 5-H, 5''-H, 3'''-H and 5'''-H), 7.10-7.08 (1H, m, 6''-H), 7.05 (1H, app.t, *J* 2.5, 2''-H), 6.90 (1H, ddd, *J* 8.5, 2.5 and 1.0, 4''-H), 4.07 (2H, q, *J* 7.0, CH<sub>2</sub>CH<sub>3</sub>), 1.44 (3H, t, *J* 7.0, CH<sub>3</sub>); **<sup>13</sup>C NMR (100 MHz, CDCl<sub>3</sub>):** 172.5 (amide C=O), 159.3 (3''-C), 142.3 (Ar-q), 142.1 (Ar-q), 141.0 (1''-C), 134.1 (1'''-C), 132.6 (4'''-C), 129.2 (2'''-C and 6'''-C), 129.0 (Ar-q), 128.6 (3'''-C and 5'''-C), 122.5 (5-H), 119.9 (6''-H), 119.1 (4-H), 117.3 (3-C), 114.0 (2''-C), 113.6 (4''-C), 108.6 (7-C), 63.5 (CH<sub>3</sub>), 14.9 (CH<sub>3</sub>), one Ar-q not observed; **LC-MS (ES):** RT = 0.7-0.8 min, *m/z* = 462.23 (M+H<sup>+</sup>); **R<sub>f</sub>:** 0.66 (7:3 EtOAc–petrol); **HPLC:** RT = 3.89 min (84%-degrades overtime); ***m/z* (ES<sup>+</sup>):** Found: 484.1630 (M+Na<sup>+</sup>), C<sub>29</sub>H<sub>23</sub>N<sub>3</sub>NaO<sub>3</sub> requires *MNa* 484.1632; **IR:** $\nu_{\max}/\text{cm}^{-1}$  (**solid**): 3313 (N-H), 3063, 2980, 1692 (C=O).

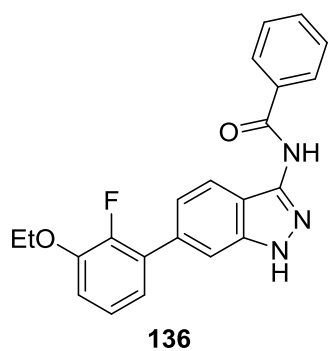
## Preparation of N-[6-(3-ethoxy-5-fluorophenyl)-1H-indazol-3-yl]benzamide



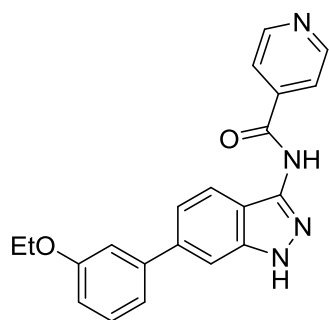
Synthesised using method A using *tert*-butyl 3-benzamido-6-bromo-1H-indazole-1-carboxylate (150 mg, 0.36 mmol, 1.0 eq), 3-ethoxy-5-fluorophenylboronic acid (99 mg, 0.54 mmol, 1.5 eq), Pd(dppf)Cl<sub>2</sub>•DCM (29 mg, 0.036 mmol, 0.1 eq), Na<sub>2</sub>CO<sub>3</sub> (115 mg, 1.08 mmol, 3.0 eq), dioxane (2 mL) and water (2 mL) and the reaction heated 3 h. The work up proceeded using the smaller

volumes of solvents and the organic solvent removed *in vacuo* to reveal a brown oil. The crude product was purified by column chromatography (gradient 40-50% EtOAc–hexane) and an off-white solid obtained. The solid was crystallised from EtOH. The title compound 135 (73 mg, 0.19 mmol, 54%) was collected as colourless microneedles.

**<sup>1</sup>H NMR (500 MHz, DMSO-*d*<sub>6</sub>):** 12.89 (1H, br.s, indazole NH), 10.83 (1H, br.s, amide NH), 8.09 (2H, d, *J* 7.0, 2''-H and 6''-H), 7.81 (1H, d, *J* 8.5, 4-H), 7.72 (1H, s, 7-H), 7.63-7.59 (1H, m, 4'''-H), 7.54 (2H, app.t, *J* 7.5, 3'''-H and 5'''-H), 7.40 (1H, dd, *J* 8.5 and 1.5, 5-H), 7.14 (1H, app.dt, *J* 10.0 and 1.5, 6''-H), 7.10 (1H, app.t, *J* 1.5, 2''-H), 6.83 (1H, app.dt, *J* 11.0 and 2.5, 4''-H), 4.14 (2H, q, *J* 7.0, CH<sub>2</sub>CH<sub>3</sub>), 1.36 (3H, t, *J* 7.0, CH<sub>3</sub>); **<sup>13</sup>C NMR (125 MHz, DMSO-*d*<sub>6</sub>):** 165.5 (amide C=O), 163.4 (d, *J* 241.9, 5''-C), 160.3 (d, *J* 12.0, 3''-C), 143.4 (d, *J* 10.1, 1''-C), 141.5 (Ar-q), 140.2 (Ar-q), 137.3 (6-C), 133.7 (1'''-C), 131.8 (4'''-C), 128.4 (3'''-C and 5'''-C), 127.9 (2'''-C and 6'''-C), 122.5 (4-C), 119.4 (5-C), 116.6 (3'-C), 109.6 (d, *J* 2.0, 2''-C), 108.2 (7-C), 106.0 (d, *J* 22.9, 6''-C), 100.9 (d, *J* 25.4, 4''-C), 63.7 (CH<sub>2</sub>CH<sub>3</sub>), 14.5 (CH<sub>3</sub>); **LC-MS (ES):** RT = 0.6-0.7 min, *m/z* = 376.24 (M+H<sup>+</sup>); **R<sub>f</sub>:** 0.19 (1:1 EtOAc–petrol); **HPLC:** RT = 3.37 min; ***m/z* (ES<sup>+</sup>):** Found: 398.1274 (M+Na<sup>+</sup>), C<sub>22</sub>H<sub>18</sub>FN<sub>3</sub>NaO<sub>2</sub> requires *MNa* 398.1275; **IR:  $\nu_{\max}$ /cm<sup>-1</sup> (solid):** 3322 (N-H), 3253 (N-H), 3049, 2969, 2879, 1639 (C=O); **M.pt:** 213.3-213.8 °C.

Preparation of N-[6-(3-ethoxy-2-fluorophenyl)-1H-indazol-3-yl]benzamide**136**

Synthesised using method A using *tert*-butyl 3-benzamido-6-bromo-1*H*-indazole-1-carboxylate (150 mg, 0.36 mmol, 1.0 eq), 2-fluoro-3-ethoxyphenylboronic acid (99 mg, 0.54 mmol, 1.5 eq), Pd(dppf)Cl<sub>2</sub>•DCM (29 mg, 0.036 mmol, 0.1 eq), Na<sub>2</sub>CO<sub>3</sub> (115 mg, 1.08 mmol, 3.0 eq), dioxane (2 mL) and water (2 mL) and the reaction heated 3 h. The work up proceeded using the smaller volumes of solvents and the organic solvent removed *in vacuo* to reveal a brown solid. The crude product was purified by column chromatography (3:2 EtOAc–hexane) and a yellow solid obtained. The solid was crystallised from EtOH. The title compound 136 (73 mg, 0.19 mmol, 54%) was collected as fluffy colourless platelets. **<sup>1</sup>H NMR (500 MHz, DMSO-*d*<sub>6</sub>):** 12.89 (1H, br.s, indazole NH), 10.84 (1H, br.s, amide NH), 8.10-8.07 (2H, m, 2'''-H and 6'''-H), 7.80 (1H, d, *J* 8.5, 4-H), 7.61 (1H, app.tt, *J* 7.5 and 1.5, 4'''-H), 7.58 (1H, s, 7-H), 7.56-7.52 (2H, m, 3'''-H and 5'''-H), 7.24-7.16 (3H, m, 5-H, 5''-H and 4''-H), 7.13-7.09 (1H, m, 6''-H), 4.15 (2H, q, *J* 7.0, CH<sub>2</sub>CH<sub>3</sub>), 1.38 (3H, t, *J* 7.0, CH<sub>3</sub>); **<sup>13</sup>C NMR (125 MHz, DMSO-*d*<sub>6</sub>):** 165.6 (amide C=O), 148.9 (d, *J* 245.3, 2''-C), 147.0 (d, *J* 11.0, 3''-C), 141.2 (Ar-q), 140.2 (Ar-q), 133.7 (1'''-C), 133.2 (6-C), 131.8 (4'''-C), 129.3 (d, *J* 10.7, 1''-C), 128.4 (3'''-C and 5'''-C), 127.9 (2'''-C and 6'''-C), 124.5 (d, *J* 4.6, 5''-C), 122.0 (d, *J* 23.6, 6''-C), 121.9 (4-C), 121.0 (4''-C), 116.3 (3'-C), 114.0 (5-C), 110.2 (7-C), 64.4 (CH<sub>2</sub>CH<sub>3</sub>), 14.6 (CH<sub>3</sub>); **LC-MS (ES):** RT = 0.6-0.7 min, *m/z* = 376.26 (M+H<sup>+</sup>); **R<sub>r</sub>:** 0.17 (1:1 EtOAc–petrol); **HPLC:** RT = 3.18 min; ***m/z* (ES<sup>+</sup>):** Found: 398.1272 (M+Na<sup>+</sup>), C<sub>22</sub>H<sub>18</sub>FN<sub>3</sub>NaO<sub>2</sub> requires *MNa* 398.1275; **IR:** ν<sub>max</sub>/cm<sup>-1</sup> (solid): 3263 (N-H), 3066, 2984, 1649 (C=O); **M.pt:** 235.1-236.7 °C.

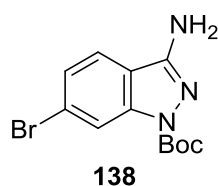
Preparation of N-[6-(3-ethoxyphenyl)-1H-indazol-3-yl]pyridine-4-carboxamide**137**

*Tert*-butyl 6-(3-ethoxyphenyl)-3-(pyridine-4-amido)-1*H*-indazole-1-carboxylate (88 mg, 0.19 mmol, 1.0 eq) was suspended in 2 M NaOH and stirred at 70 °C for 30 minutes. LC-MS analysis showed the reaction to be incomplete and therefore MeOH (10 mL) was added, to aid dissolution, and the reaction heated at 60 °C for 1 h. The MeOH was removed *in vacuo* and the remaining

aqueous layer acidified to pH 7 using 2 M HCl. The aqueous layer was extracted with DCM (3× 20 mL) and the organic layers separated. The combined organic layers were washed with brine (30 mL), dried (MgSO<sub>4</sub>) and reduced *in vacuo* to reveal the crude product as a purple glassy solid. The crude product was purified using reverse-phase ACC (gradient 0-30% MeCN–H<sub>2</sub>O in 0.1% formic acid). Appropriate fractions were collected and reduced *in vacuo* to a volume of ~3 mL until precipitation was observed. The precipitate was filtered and crystallised from EtOH. The title compound 137 (35 mg, 0.09 mmol, 48 %) was collected as light brown microneedles.

**<sup>1</sup>H NMR (500 MHz, DMSO-*d*<sub>6</sub>):** 12.96 (1H, br.s, indazole NH), 11.19 (1H, br.s, amide NH), 8.83 (2H, d, *J* 5.5, 3''-H and 5''-H), 8.00 (2H, d, *J* 5.5, 2''-H and 6''-H), 7.85 (1H, d, *J* 8.5, 4-H), 7.71 (1H, s, 7-H), 7.44-7.39 (2H, m, 5-H and 5''-H), 7.31 (1H, d, *J* 8.0, 4''-H), 7.26-7.25 (1H, m, 2''-H), 6.97 (1H, dd, *J* 8.0 and 2.5, 6''-H), 4.14 (2H, q, *J* 7.0, CH<sub>2</sub>), 1.38 (3H, t, *J* 7.0 CH<sub>3</sub>); **<sup>13</sup>C NMR (125 MHz, DMSO-*d*<sub>6</sub>):** 164.0 (amide C=O), 159.0 (3''-C), 150.3 (3'''-C and 5'''-C), 142.0 (Ar-q), 141.7 (Ar-q), 140.8 (1'''-C), 139.5 (Ar-q), 138.7 (Ar-q), 130.0 (5''-C), 122.3 (4-C), 121.7 (2'''-C and 6'''-C), 119.7 (5-C), 119.4 (4''-C), 116.1 (7'-C), 113.6 (6''-C), 113.2 (2''-C), 107.9 (7-C), 63.1 (CH<sub>2</sub>), 14.7 (CH<sub>3</sub>); **LC-MS (ES):** RT = 0.5-0.6 min, *m/z* = 359.21 (M+H<sup>+</sup>); **R<sub>f</sub>:** 0.15 (95:5 DCM–7.0 M NH<sub>3</sub> in MeOH); **HPLC:** RT = 2.32 min (97%); ***m/z* (ES<sup>+</sup>):** Found: 359.1502 (M+H<sup>+</sup>), C<sub>21</sub>H<sub>18</sub>N<sub>4</sub>O<sub>2</sub> requires *MH* 359.1503; **IR:ν<sub>max</sub>/cm<sup>-1</sup> (solid):** 3219 (N-H), 2977, 2930, 2799, 1647 (C=O); **M.pt:** 225.5-225.9 °C.

#### Preparation of *tert*-butyl 3-amino-6-bromo-1*H*-indazole-1-carboxylate



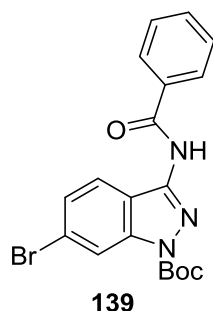
3-Amino-6-bromo-1*H*-indazole (2.28 g, 10.8 mmol, 1.0 eq) was suspended in THF (40 mL) and DMAP (395 mg, 3.23 mmol, 0.3 eq) was added and the reaction stirred for five minutes. BOC anhydride (2.97 mL, 12.9 mmol, 1.2 eq) was added dropwise over 15 minutes and the reaction stirred for 1 h monitoring for completion by LC-MS. Dissolution and a yellow hue were observed. The reaction mixture was reduced *in vacuo* to reveal the crude product as a pale brown oil. The crude solid was re-dissolved in MeOH and reduced *in vacuo* to reveal a yellow solid. The crude product was purified by column chromatography (gradient 20-50% EtOAc–hexane). The title compound 138 was collected as an off-white solid (2.66 g, 8.52 mmol, 79%). The solid was further purified by crystallisation from iso-propanol. The title compound 138



(1.36 g, 4.36 mmol, 40%) was collected as colourless granules. The filtrate was reduced *in vacuo* to reveal a beige solid (1.20 g, 3.84 mmol, 36%) which was used without further purification.

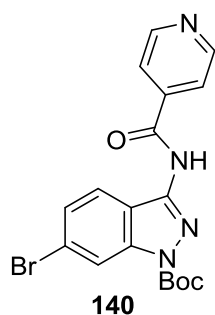
**<sup>1</sup>H NMR (500 MHz, DMSO-*d*<sub>6</sub>):** 8.11 (1H, br.s, 7-H), 7.79 1H, dd, *J* 8.0 and 0.5, 4-H), 7.45 (1H, dd, *J* 8.0 and 1.5, 5-H), 6.40 (2H, br.s NH<sub>2</sub>), 1.57 (9H, s, <sup>t</sup>Bu CH<sub>3</sub>); **<sup>13</sup>C NMR (125 MHz, DMSO-*d*<sub>6</sub>):** 152.1 (7'-C), 140.6 (3'-C), 125.5 (5-C), 122.6 (6-C), 122.5 (4-C), 118.4 (3-C), 116.7 (7-C), 82.9 (C(CH<sub>3</sub>)<sub>3</sub>), 27.8 (<sup>t</sup>Bu CH<sub>3</sub>), BOC C=O not observed; **LC-MS (ES):** RT = 0.6-0.7 min, *m/z* = 257.97 (M-<sup>t</sup>Bu+H<sup>+</sup>); **R<sub>f</sub>:** 0.42 (7:3 EtOAc–petrol); **HPLC:** RT = 3.05 min; ***m/z* (ES<sup>+</sup>):** Found: 334.0156 (M+Na<sup>+</sup>), C<sub>12</sub>H<sub>14</sub>BrN<sub>3</sub>NaO<sub>2</sub> requires *MNa* 334.0162; **IR:ν<sub>max</sub>/cm<sup>-1</sup> (solid):** 3433 (N-H), 3372 (N-H), 3182, 2976, 1731 (C=O), 1702; **M.pt:** 167.5-168.3 °C.

#### Preparation of *tert*-butyl 3-benzamido-6-bromo-1*H*-indazole-1-carboxylate



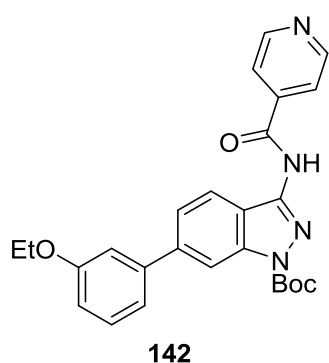
Synthesised using method E using *tert*-butyl 3-amino-6-bromo-1*H*-indazole-1-carboxylate (1.0 g, 3.20 mmol, 1.0 eq), freshly distilled benzoyl chloride (446 μL, 3.84 mmol, 1.2 eq), DIPEA (1.12 mL, 6.41 mmol, 2.0 eq) and DCM (20 mL) and the reaction stirred for 20 h. LC-MS showed the reaction to be incomplete and therefore benzoyl chloride (74 μL, 0.64 mmol, 0.2 eq) was added to the reaction and stirred for 3 h. LC-MS showed no change and therefore the reaction was stopped. The crude product was purified by column chromatography (gradient 5-10% EtOAc–hexane then flush with 1:1 EtOAc–hexane). The title compound 139 (592 mg, 1.42 mmol, 44%) was collected as an off-white glassy solid.

**<sup>1</sup>H NMR (500 MHz, CDCl<sub>3</sub>):** 8.90 (1H, br.s, NH), 8.38 (1H, br.s, 7-H), 8.18 (1H, d, *J* 9.0, 4-H), 7.98-7.95 (2H, m, 2'''-H and 6'''-H), 7.61 (1H, app.tt, *J* 7.5 and 1.0, 4'''-H), 7.54-7.50 (2H, m, 3'''-H and 5'''-H), 7.46 (1H, dd, *J* 9.0 and 2.0, 5-H), 1.71 (9H, s, <sup>t</sup>Bu CH<sub>3</sub>); **<sup>13</sup>C NMR (125 MHz, CDCl<sub>3</sub>):** 165.4 (amide C=O), 148.6 (BOC C=O), 145.3 (Ar-q), 141.8 (Ar-q), 132.9 (Ar-q), 132.8 (4'''-C), 129.0 (3'''-C and 5'''-C), 127.5 (2'''-C and 6'''-C), 127.0 (5-C), 125.7 (4-C), 124.5 (Ar-q), 118.2 (6-C), 117.5 (7-C), 85.7 (C(CH<sub>3</sub>)<sub>3</sub>), 28.1 (<sup>t</sup>Bu CH<sub>3</sub>); **LC-MS (ES):** RT = 0.7-0.8 min, *m/z* = 362.07 (M-<sup>t</sup>Bu+Br<sup>81+</sup>); **R<sub>f</sub>:** 0.62 (1:1 EtOAc–petrol); **HPLC:** RT = 3.88 min (93%); ***m/z* (ES<sup>+</sup>):** Found: 438.0423 (M+Na<sup>+</sup>), C<sub>19</sub>H<sub>18</sub>BrN<sub>3</sub>NaO<sub>3</sub> requires *MNa* 438.0424; **IR:ν<sub>max</sub>/cm<sup>-1</sup> (solid):** 3250 (N-H), 3065, 2979, 2871, 1735 (C=O), 1662; **M.pt:** 97.5-99.3 °C.

Preparation of *tert*-butyl 6-bromo-3-(pyridine-4-amido)-1*H*-indazole-1-carboxylate

Synthesised using method E using *tert*-butyl 3-amino-6-bromo-1*H*-indazole-1-carboxylate (100 mg, 0.32 mmol, 1.0 eq), isonicotinoyl chloride hydrochloride (86 mg, 0.48 mmol, 1.5 eq), DIPEA (195  $\mu$ L, 1.12 mmol, 3.5 eq) and DCM (7 mL) and the reaction stirred for 18 h. LC-MS showed no conversion and therefore the reaction was refluxed for 30 minutes. LC-MS still showed no conversion and therefore isonicotinoyl chloride hydrochloride (86 mg, 0.48 mmol, 1.5 eq) was added and the reaction refluxed for 2 h. TLC showed the reaction to be incomplete and therefore isonicotinoyl chloride hydrochloride (43 mg, 0.24 mmol, 0.75 eq) was added and the reaction heated for 30 minutes. TLC confirmed the reaction to be complete. The crude product was purified by column chromatography (gradient 50-70% EtOAc–hexane). The title compound 140 (101 mg, 0.24 mmol, 76%) was collected as a colourless solid.

**<sup>1</sup>H NMR (500 MHz, DMSO-*d*<sub>6</sub>):** 11.76 (1H, br.s, amide NH), 8.83 (2H, d, *J* 5.5, 3''-H and 5''-H), 8.33 (1H, s, 7-H), 7.99 (2H, d, *J* 5.5, 2''-H and 6''-H), 7.90 (1H, d, *J* 8.5, 4-H), 7.58 (1H, d, *J* 8.5, 5-H), 1.66 (9H, s, <sup>t</sup>Bu CH<sub>3</sub>); **<sup>13</sup>C NMR (100 MHz, DMSO-*d*<sub>6</sub>):** 165.2 (amide C=O), 150.9 (3''-C and 5''-C), 148.6 (BOC C=O), 145.3 (3-C), 141.3 (7'-C), 140.5 (1''-C), 127.0 (5-C), 125.7 (4-C), 123.7 (3'-C), 122.3 (2''-C and 6''-C), 119.6 (6-C), 117.3 (7-C), 85.7 (C(CH<sub>3</sub>)<sub>3</sub>), 28.1 (<sup>t</sup>Bu CH<sub>3</sub>); **LC-MS (ES):** RT = 0.6-0.7 min, *m/z* = 419.09 (MBr<sup>81+</sup>); **R<sub>f</sub>:** 0.30 (7:3 EtOAc–petrol); **HPLC:** RT = 2.79 min; ***m/z* (ES+):** Found: 417.0554 (M+H<sup>+</sup>), C<sub>18</sub>H<sub>17</sub>BrN<sub>4</sub>O<sub>3</sub> requires *MH* 417.0557; **IR:**  $\nu_{\max}/\text{cm}^{-1}$  (solid): 3528 (N-H), 3054, 2978, 1744 (C=O), 1722 (C=O); **M.pt:** 172.4-176.8 °C.

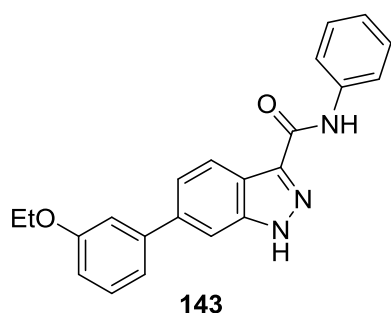
Preparation of *tert*-butyl 6-(3-ethoxyphenyl)-3-(pyridine-4-amido)-1*H*-indazole-1-carboxylate

Synthesised using method E without DIPEA using *tert*-butyl 3-amino-6-(3-ethoxyphenyl)-1*H*-indazole-1-carboxylate (438 mg, 1.24 mmol, 1.0 eq), isonicotinoyl chloride hydrochloride (331 mg, 1.86 mmol, 1.5 eq) and DCM (5 mL) and the reaction stirred for 19 h. LC-MS showed the reaction to be incomplete and therefore isonicotinoyl chloride hydrochloride (66 mg, 0.37 mmol,

0.3 eq) was added and the reaction refluxed for 2.5 h. LC-MS showed no change and therefore the reaction was stopped. The crude product was purified by column chromatography (7:3 EtOAc–hexane). Due to the high polarity of the compound the majority of the product stayed on the baseline. The column was flushed with MeOH and the crude product reduced *in vacuo*. The crude product was purified by column chromatography (50:48:2 hexane–EtOAc–7.0 M NH<sub>3</sub> in MeOH). The title compound 142 (76 mg, 0.17 mmol, 13 %) was collected as a colourless glassy solid.

**<sup>1</sup>H NMR (500 MHz, CDCl<sub>3</sub>):** 10.07 (1H, br.s, amide NH), 8.82 (2H, dd, *J* 4.5 and 1.5, 3'''-H and 5'''-H), 8.38 (1H, br.s, 7-H), 8.23 (1H, d, *J* 8.5, 4-H), 7.90 (2H, dd, *J* 4.5 and 1.5, 2'''-H and 6'''-H), 7.61 (1H, dd, *J* 8.5 and 1.5, 5-H), 7.40 (1H, app.t, *J* 8.0, 5''-H), 7.29-7.26 (1H, m, 4''-H), 7.24-7.22 (1H, m, 2''-H), 6.95 (1H, dd, *J* 8.0 and 2.0, 6''-H), 4.13 (2H, q, *J* 7.0, CH<sub>2</sub>), 1.66 (9H, s, <sup>t</sup>Bu CH<sub>3</sub>), 1.47 (3H, t, *J* 7.0, CH<sub>3</sub>); **<sup>13</sup>C NMR (100 MHz, CDCl<sub>3</sub>):** 164.1 (amide C=O), 159.4 (3''-C), 150.8 (3'''-C and 5'''-C), 148.8 (BOC C=O), 145.0 (3-C), 143.3 (6-C), 142.1 (1''-C), 141.7 (3'-C), 140.3 (1'''-C), 130.0 (5''-C), 124.3 (4-C), 123.6 (5-C), 121.4 (2'''-C and 6'''-C), 120.0 (4''-C), 118.7 (7'-C), 114.0 (6''-C), 114.0 (2''-C), 112.9 (7-C), 85.5 (C(CH<sub>3</sub>)<sub>3</sub>), 63.6 (CH<sub>2</sub>), 28.1 (<sup>t</sup>Bu CH<sub>3</sub>), 14.9 (CH<sub>2</sub>CH<sub>3</sub>); **LC-MS (ES):** RT = 0.7-0.7 min, *m/z* = 459.27 (M+H<sup>+</sup>); **R<sub>f</sub>:** 0.26 (95:5 DCM–7.0 M NH<sub>3</sub> in MeOH); **HPLC:** RT = 3.18 min; ***m/z* (ES<sup>+</sup>):** Found: 459.2025 (M+H<sup>+</sup>), C<sub>26</sub>H<sub>26</sub>N<sub>4</sub>O<sub>4</sub> requires *MH* 459.2027; **IR:ν<sub>max</sub>/cm<sup>-1</sup> (solid):** 3225 (N-H), 2977, 2930, 1732 (C=O), 1687 (C=O).

#### Preparation of 6-(3-ethoxyphenyl)-1*H*-indazole-3-phenylcarboxamide



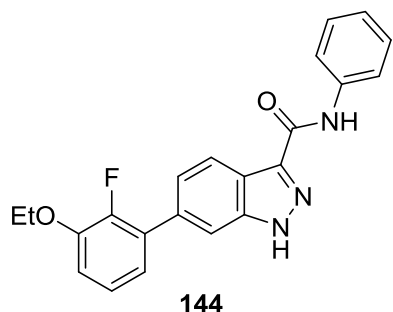
Synthesised using method A using 6-bromo-1*H*-indazole-3-phenylcarboxamide (120 mg, 0.38 mmol, 1.0 eq), 3-ethoxyphenylboronic acid (95 mg, 0.57 mmol, 1.5 eq), Pd(dppf)Cl<sub>2</sub>•DCM (31 mg, 0.038 mmol, 0.1 eq), Na<sub>2</sub>CO<sub>3</sub> (121 mg, 1.14 mmol, 3.0 eq), dioxane (2 mL) and water (2 mL) and the

reaction heated for 45 minutes. LC-MS analysis showed the reaction to be incomplete and therefore 3-ethoxyphenylboronic acid (95 mg, 0.57 mmol, 1.5 eq) was added and the reaction heated for 30 minutes. LC-MS analysis showed the reaction to be complete. The work up proceeded using the smaller volumes of solvents and the organic solvent removed *in vacuo* to reveal a brown oil. The crude product was purified using column chromatography (4:1 petrol–EtOAc) and a brown solid

obtained. The solid was crystallised from EtOH and brown needles obtained. The needles were further recrystallised from CHCl<sub>3</sub>. The title compound 143 (11 mg, 0.03 mmol, 9%) was collected as pearlescent white platelets.

**<sup>1</sup>H NMR (500 MHz, DMSO-d<sub>6</sub>):** 10.31 (1H, br.s, amide NH), 8.26 (1H, d, *J* 8.6, 4-H), 7.92-7.89 (2H, m, 2'''-H and 6'''-H), 7.83 (1H, s, 7-H), 7.60 (1H, dd, *J* 8.6 and 1.5, 5-H), 7.40 (1H, app.t, *J* 8.2, 5''-H), 7.35 (2H, app.td, *J* 7.5 and 1.8, 3'''-H and 5'''-H), 7.31-7.29 (1H, m, 4''-H), 7.26-7.25 (1H, m, 2''-H), 7.09 (1H, app.t, *J* 7.5, 4'''-H), 6.96 (1H, dd, *J* 8.2 and 2.5, 6''-H), 4.13 (2H, q, *J* 7.0, CH<sub>2</sub>), 1.36 (3H, t, *J* 7.0, CH<sub>3</sub>), indazole NH not observed; **<sup>13</sup>C NMR (125 MHz, DMSO-d<sub>6</sub>):** 160.8 (C=O), 159.0 (3''-C), 142.0 (3-C), 141.7 (6-C), 139.0 (1''-C), 138.8 (Ar-q), 138.3 (Ar-q), 130.1 (5'''-C), 128.6 (3'''-C and 5'''-C), 123.4 (4'''-C), 122.3 (5-C), 121.9 (4-C), 121.2 (3'-C), 120.2 (2'''-C and 6'''-C), 119.5 (4''-C), 113.8 (6''-C), 113.2 (2''-C), 108.4 (7-C), 63.1 (CH<sub>2</sub>), 14.7 (CH<sub>3</sub>); **LC-MS (ES):** RT = 0.7-0.8 min, *m/z* = 356.22 (M+H<sup>+</sup>); **R<sub>f</sub>:** 0.73 (2% MeOH-DCM); **HPLC:** RT = 3.77 min; ***m/z* (ES<sup>+</sup>):** Found: 356.1395 (M+H<sup>+</sup>), C<sub>22</sub>H<sub>19</sub>N<sub>3</sub>O<sub>2</sub> requires *MH* 356.1404; **IR:ν<sub>max</sub>/cm<sup>-1</sup> (solid):** 3385 (N-H), 3210, 2976, 1651 (C=O); **M.pt:** >250 °C.

#### Preparation of 6-(3-ethoxy-2-fluorophenyl)-1*H*-indazole-3-phenylcarboxamide

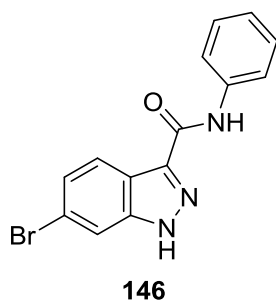


Synthesised using method A using 6-bromo-1*H*-indazole-3-phenylcarboxamide (200 mg, 0.63 mmol, 1.0 eq), 2-fluoro-3-ethoxyphenylboronic acid (175 mg, 0.95 mmol, 1.5 eq), Pd(dppf)Cl<sub>2</sub>•DCM (51 mg, 0.063 mmol, 0.1 eq), Na<sub>2</sub>CO<sub>3</sub> (200 mg, 1.89 mmol, 3.0 eq), dioxane (2 mL) and water (2 mL)

and the reaction heated for 2 h. LC-MS analysis showed the reaction to be incomplete and therefore 2-fluoro-3-ethoxyphenylboronic acid (58 mg, 0.32 mmol, 0.5 eq), Pd(dppf)Cl<sub>2</sub>•DCM (51 mg, 0.063 mmol, 0.1 eq) and Na<sub>2</sub>CO<sub>3</sub> (67 mg, 0.63 mmol, 1.0 eq) were added and the reaction heated for 1 h. LC-MS showed the reaction to be incomplete however the reaction was stopped. The work up proceeded using the smaller volumes of solvents and the organic solvent removed *in vacuo* to reveal a brown oil. The crude product was purified using column chromatography (0.5% 7.0 M NH<sub>3</sub> in MeOH-DCM) and an off-white solid obtained. The solid was triturated with EtOAc. The title compound 144 (23 mg, 0.07 mmol, 10%) was collected as off-white microcrystals.

**<sup>1</sup>H NMR (500 MHz, DMSO-*d*<sub>6</sub>):** 8.05 (1H, d, *J* 8.3, 4-H), 7.87 (2H, dd, *J* 8.5 and 0.9, 2'''-H and 6'''-H), 7.72 (1H, s, 7-H), 7.34-7.38 (2H, m, 3'''-H and 5'''-H), 7.17 (1H, app.t, *J* 7.5, 4''-H), 7.12-7.06 (3H, m, 5-H, 5''-H and 6''-H), 7.00 (1H, app.t, *J* 7.5, 4'''-H), 4.14 (2H, q, *J* 7.0, CH<sub>2</sub>), 1.38 (3H, t, *J* 7.5, CH<sub>3</sub>), NHs not observed; **<sup>13</sup>C NMR (125 MHz, DMSO-*d*<sub>6</sub>):** 162.4 (C=O), 151.1 (3-C), 149.0, (d, *J* 244.4, 2''-C), 146.9 (d, *J* 11.3, 3''-C), 139.9 (1'''-C), 136.2 (Ar-q), 130.9 (d, *J* 11.0, 1''-C), 128.5 (3'''-C and 5'''-C), 127.6 (Ar-q), 124.1 (d, *J* 4.6, 4''-C), 123.0 (Ar-q), 122.0 (d, *J* 2.4, 5-C), 121.9 (4'''-C), 120.5 (d, *J* 2.5, 6''-C), 119.8 (4-C), 118.8 (2'''-C and 6'''-C), 115.8 (d, *J* 2.5, 7-C), 112.8 (5''-C), 64.3 (CH<sub>2</sub>) 14.6 (CH<sub>3</sub>); **LC-MS (ES):** RT = 0.6-0.6 min, *m/z* = 376.24 (M+H<sup>+</sup>); **R<sub>f</sub>:** 0.28 (0.5% 7.0 M NH<sub>3</sub> in MeOH-DCM); **HPLC:** RT = 3.77 min (96%); ***m/z* (ES<sup>+</sup>):** Found: 376.1456 (M+H<sup>+</sup>), C<sub>22</sub>H<sub>18</sub>FN<sub>3</sub>O<sub>2</sub> requires *MH* 376.1455; **IR: *v*<sub>max</sub>/cm<sup>-1</sup> (solid):** 3368 (N-H), 3181, 2979, 1659 (C=O); **M.pt:** >250 °C.

#### Preparation of 6-bromo-1*H*-indazole-3-phenylcarboxamide

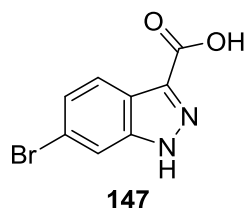


6-Bromo-1*H*-indazole-3-carboxylic acid (750 mg, 3.0 mmol, 1.0 eq) was dissolved in freshly distilled SOCl<sub>2</sub> (3.0 mL, 41.4 mmol, 13.8 eq) and refluxed for 1.5 h. LC-MS analysis indicated the reaction to be complete. The reaction mixture was reduced *in vacuo* and the resulting solid dissolved in DCM (9 mL) and Et<sub>3</sub>N (360 μL, 3.6 mmol, 1.2 eq) added and the reaction stirred for five minutes. Aniline (720 μL, 7.5 mmol, 2.5 eq) was added and the reaction heated to 45 °C for 4 h. The reaction mixture was allowed to cool to 20 °C and added to DCM (15 mL). Water (15 mL) and 2M HCl (5 mL) were added and the organic layer separated. The aqueous layers were extracted with DCM (3 × 15 mL) and the combined organic layers washed with 2M NaOH (15 mL), brine (20 mL) and dried (MgSO<sub>4</sub>) and concentrated *in vacuo* to reveal a red solid. The crude product was purified by column chromatography (0.5% MeOH-DCM) and a brown solid obtained. The solid was crystallised from EtOAc. The title compound 146 (94 mg, 0.30 mmol, 13%) was collected as brown needles.

**<sup>1</sup>H NMR (500 MHz, DMSO-*d*<sub>6</sub>):** 10.35 (1H, br.s, amide NH), 8.15 (1H, d, *J* 8.6, 4-H), 7.90 (1H, br.s, 7-H), 7.88 (2H, d, *J* 7.6, 2''-H and 6''-H), 7.43 (1H, dd, *J* 8.6 and 1.6, 5-H), 7.36 (2H, app.t, *J* 7.9, 3''-H and 5''-H), 7.12-7.08 (1H, m, 4''-H), indazole NH not observed; **<sup>13</sup>C NMR (125 MHz, DMSO-*d*<sub>6</sub>):** 160.5 (C=O), 142.1 (3-C), 138.6 (Ar-

q), 138.7 (Ar-q), 128.5 (3''-C and 5''-C), 125.6 (5-C), 123.5 (4-C), 123.3 (4''-C), 120.7 (Ar-q), 120.3 (2''-C and 6''-C), 120.2 (Ar-q), 113.5 (7-C); **LC-MS (ES)**: RT = 0.6-0.6 min, m/z = 316.05 (M+H<sup>+</sup>); **R<sub>f</sub>**: 0.68 (2% MeOH-DCM); **HPLC**: RT = 3.33 min; **m/z (ES+)**: Found: 316.0078 (M+H<sup>+</sup>), C<sub>14</sub>H<sub>10</sub>BrN<sub>3</sub>O requires *MH* 316.0077; **IR:ν<sub>max</sub>/cm<sup>-1</sup> (solid)**: 3363 (N-H), 3159, 1653, 1613, 1595; **M.pt**: >250 °C.

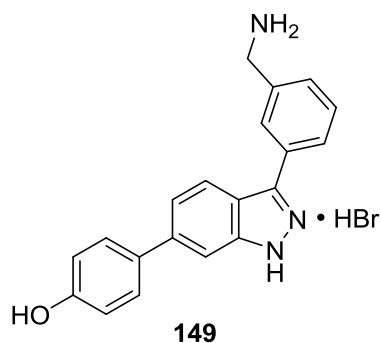
#### Preparation of 6-bromo-1*H*-indazole-3-carboxylic acid



6-Bromoisatin (100 mg, 0.44 mmol, 1.0 eq) was suspended in water (0.5 mL) and 2 M NaOH (0.5 mL) was added and the suspension heated at 55 °C for 30 minutes. The reaction mixture was cooled to 20 °C and stirred for 30 minutes. A solution of NaNO<sub>2</sub> (31 mg, 0.44 mmol, 1.0 eq) in water (0.5 mL) was cooled to 0 °C and added to the reaction mixture and stirred for five minutes. This solution was then added slowly over five minutes to a solution of H<sub>2</sub>SO<sub>4</sub> (0.1 mL) in water (0.9 mL) *via* a pipette submerged beneath the liquid surface and maintained at 0 °C for 20 minutes. SnCl<sub>2</sub>•2H<sub>2</sub>O (240 mg, 1.06 mmol, 2.4 eq) was dissolved in HCl (1 mL) and added in one portion to the reaction and the mixture warmed to 20 °C and stirred for 1 h. The resulting orange precipitate was filtered and washed with water. The crude solid was triturated with hot AcOH and the insoluble impurities removed *via* filtration and the filtrate reduced *in vacuo*. The title compound 147 (81 mg, 0.34 mmol, 76%) was collected as an orange powder.

**<sup>1</sup>H NMR (500 MHz, DMSO-*d*<sub>6</sub>)**: 8.03 (1H, d, *J* 10.5, 4-H), 7.89 (1H, s, 7-H), 7.40 (1H, d, *J* 10.5, 5-H), NH or OH not observed; **<sup>13</sup>C NMR (100 MHz, DMSO-*d*<sub>6</sub>)**: 164.0 (carboxyl C=O), 143.2 (Ar-q), 141.7 (Ar-q), 126.0 (5-C), 123.7 (4-C), 121.7 (6-C), 120.2 (3'-C), 114.3 (7-C), ; **LC-MS (ES)**: RT = 0.5-0.5 min, m/z = 483.11 (2M+H<sup>+</sup>); **R<sub>f</sub>**: 0.44 (97:2:1 DCM-MeOH-AcOH); **HPLC**: RT = 2.02 min; **m/z (ES-)**: Found: 238.9450 (M-H<sup>+</sup>), C<sub>8</sub>H<sub>5</sub>BrN<sub>2</sub>O<sub>2</sub> requires *M-H* 238.9462; **IR:ν<sub>max</sub>/cm<sup>-1</sup> (solid)**: 3116 (br.O-H), 2919, 2850, 1701 (C=O); **M.pt**: >250 °C.

Preparation of {3-[6-(4-hydroxyphenyl)-1*H*-indazol-3-yl]phenyl}methanaminium bromide



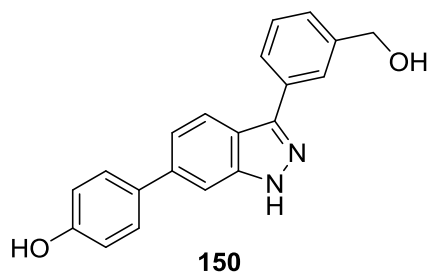
Synthesised

using method D using {3-[6-(4-methoxyphenyl)-1*H*-indazol-3-yl]phenyl}methanaminium formate (50 mg, 0.15 mmol, 1.0 eq), 1 M BBr<sub>3</sub> in DCM (1.21 mL, 1.21 mmol, 8.0 eq) and DCM (5 mL) and the reaction stirred for 2 h. Upon completion a precipitate had formed. Water (10 mL) was added resulting in the

dissolution of the precipitate and the biphasic mixture was left for 16 h. It was observed that colourless needles had precipitated in the aqueous layer. The needles were filtered and dissolved in MeOH and reduced *in vacuo* to reveal to crude solid as an off-white solid. The crude solid was purified by a mixed solvent crystallisation from water using iso-propanol as an antisolvent. The title compound 149 (8 mg, 0.03 mmol, 17%) was collected as a colourless powder.

**<sup>1</sup>H NMR (500 MHz, DMSO-*d*<sub>6</sub>):** 13.29 (1H, br.s, indazole NH), 9.58 (1H, br.s, OH), 8.24 (3H, br.s, CH<sub>2</sub>NH<sub>3</sub>), 8.20 (1H, d, *J* 8.5, 4-H), 8.14 (1H, s, 2'''-H), 8.04 (1H, app.dt, *J* 8.0 and 1.5, 6'''-H), 7.68 (1H, s, 7-H), 7.60-7.55 (3H, m, 2''-H, 6''-H and 5'''-H), 7.48 (1H, d, *J* 8.0, 4''-H), 7.46 (1H, dd, *J* 8.5, 5-H), 6.91-6.87 (2H, m, 3''-H and 5''-H), 4.13 (2H, q, *J* 5.5, CH<sub>2</sub>); **<sup>13</sup>C NMR (125 MHz, DMSO-*d*<sub>6</sub>):** 157.3 (4''-C), 142.5 (Ar-q), 142.5 (Ar-q), 138.6 (6-C), 134.6 (3'''-C), 134.2 (1'''-C), 130.9 (1''-C), 129.2 (4'''-C), 128.2 (2''-C and 6''-C), 127.0 (2'''-C), 126.6 (6'''-C), 121.1 (4-C), 120.5 (5-C), 118.8 (7'-C), 115.8 (3''-C and 5''-C), 107.0 (7-C), 42.3 (CH<sub>2</sub>), one Ar-q not observed; **LC-MS (ES):** RT = 0.4-0.5 min, *m/z* = 316.18 (M+H<sup>+</sup>); **R<sub>f</sub>:** 0.40 (15% 7.0 M NH<sub>3</sub> in DCM); **HPLC:** RT = 1.95 min; ***m/z* (ES+):** Found: 316.1444 (M+H<sup>+</sup>), C<sub>20</sub>H<sub>17</sub>N<sub>3</sub>O requires *MH* 316.1444; **IR:ν<sub>max</sub>/cm<sup>-1</sup> (solid):** 3342 (br.O-H), 1605; **M.pt:** 191.2-195.8 °C.

Preparation of 4-{3-[3-(hydroxymethyl)phenyl]-1*H*-indazol-6-yl}phenol

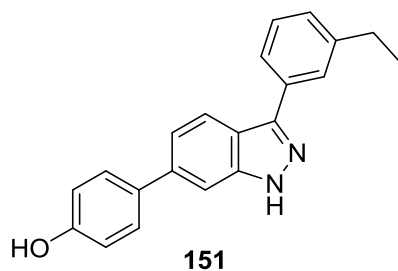


4-{3-[3-(bromomethyl)phenyl]-1*H*-indazol-6-yl}phenol\* (83 mg, 0.22 mmol, 1.0 eq) was suspended in saturated NaHCO<sub>3</sub> (3 mL) and the reaction refluxed for 18 h. A colour change of yellow to orange was observed. TLC analysis showed the reaction to be incomplete, however the reaction was stopped. The reaction mixture was reduced *in vacuo* and resuspended in water (5 mL) and sonicated for 15 minutes. The orange precipitate was filtered and washed with water. Attempts at purifying the crude solid using reverse phase ACC under acidic conditions failed due to precipitation of the compound on the column. The column was flushed with MeOH and all fractions reduced *in vacuo*. The crude solid was suspended in DCM (10 mL) and 2 M NaOH (20 mL) added and the organic layer separated. The aqueous layer was acidified to pH 1.0 (2 M HCl) and the solution extracted with DCM (20 mL) and the organic layer separated. The aqueous layer was neutralised to pH 7.0 and the solution extracted with DCM (20 mL) and the organic layer separated. The combined organic layers were reduced *in vacuo* and the crude product purified by reverse phase ACC (gradient 0-30% MeCN–H<sub>2</sub>O). The title compound 150 (2 mg,  $6 \times 10^{-3}$  mmol, 3%) was collected as an off-white solid.

\*Compound isolated as an undesired product (section 3.4.1) from reacting 3-[6-(4-methoxyphenyl)-1*H*-indazol-3-yl]phenyl}methanol (**156**) under the conditions outlined in method D.

**<sup>1</sup>H NMR (500 MHz, DMSO-*d*<sub>6</sub>):** 13.19 (1H, br.s, indazole NH), 9.59 (1H, br.s, OH), 8.08 (1H, d, *J* 8.5, 4-H), 7.97 (1H, s, 2'''-H), 7.86 (1H, d, *J* 7.5, 6'''-H), 7.65 (1H, s, 7-H), 7.59-7.56 (2H, m, 2''-H and 6''-H), 7.48-7.43 (2H, m, 5-H and 5'''-H), 7.33 (1H, d, *J* 8.0, 4'''-H), 6.90-6.87 (2H, m, 3''-H and 5''-H), 5.27 (1H, t, *J* 6.0, OH), 4.61 (2H, d, *J* 6.0, CH<sub>2</sub>); **<sup>13</sup>C NMR (125 MHz, DMSO-*d*<sub>6</sub>):** 157.3 (4''-C), 143.2 (3'''-C), 142.5 (Ar-q), 131.0 (1''-C), 128.6 (5'''-C), 128.2 (2''-C and 6''-C), 125.7 (4'''-C), 125.0 (6'''-C), 124.6 (2'''-C), 121.0 (4-C), 120.4 (5-C), 118.9 (7'-C), 115.8 (3''-C and 5''-C), 106.9 (7-C), 62.9 (CH<sub>2</sub>), three Ar-qs not observed; **LC-MS (ES):** RT = 0.5-0.6 min, *m/z* = 317.15 (M+H<sup>+</sup>); **R<sub>f</sub>:** 0.59 (EtOAc); **HPLC:** RT = 2.41 min; ***m/z* (ES<sup>+</sup>):** Found: 317.1283 (M+H<sup>+</sup>), C<sub>20</sub>H<sub>16</sub>N<sub>2</sub>O<sub>2</sub> requires *MH* 317.1285; **IR:ν<sub>max</sub>/cm<sup>-1</sup> (solid):** 3205 (br.O-H), 2922, 1670.

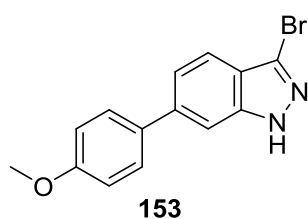


Preparation of 4-[3-(3-ethylphenyl)-1*H*-indazol-6-yl]phenol

Synthesised using method D using 3-(3-ethylphenyl)-6-(4-methoxyphenyl)-1*H*-indazole (100 mg, 0.30 mmol, 1.0 eq), 1 M BBr<sub>3</sub> in DCM (2.44 mL, 2.44 mmol, 8.0 eq) and DCM (5 mL) and the reaction stirred for 2 h. Water (10 mL) was added

and the resulting precipitate filtered and washed with water. The solid was dissolved in MeOH and reduced *in vacuo* to reveal the crude solid as an off-white solid. The crude solid was triturated in hot EtOAc. The title compound 151 (13 mg, 0.04 mmol, 14%) was collected as a colourless powder.

**<sup>1</sup>H NMR (500 MHz, DMSO-*d*<sub>6</sub>):** 8.06 (1H, d, *J* 8.5, 4-H), 7.82 (1H, s, 2'''-H), 7.80 (1H, d, *J* 7.5, 6'''-H), 7.65 (1H, s, 7-H), 7.57 (2H, d, *J* 8.5, 2''-H and 6''-H), 7.44-7.41 (2H, m, 5-H and 5'''-H), 7.24 (1H, d, *J* 7.5, 4'''-H), 6.88 (2H, d, *J* 8.5, 3''-H and 5''-H), 2.71 (2H, q, *J* 7.5, CH<sub>2</sub>), 1.25 (3H, t, *J* 7.5, CH<sub>3</sub>), heteroatoms not observed; **<sup>13</sup>C NMR (125 MHz, DMSO-*d*<sub>6</sub>):** 157.2 (4''-C), 144.3 (3'''-C), 143.2 (Ar-q), 142.5 (Ar-q), 138.5 (6-C), 133.7 (1'''-C), 131.0 (Ar-q), 128.8 (5'''-C), 128.2 (2''-C and 6''-C), 127.2 (4'''-C), 126.0 (2'''-C), 124.1 (6'''-C), 121.0 (4-C), 120.5 (5-C), 118.9 (7'-C), 115.8 (3''-C and 5''-C), 106.9 (7-C), 28.2 (CH<sub>2</sub>), 15.7 (CH<sub>3</sub>); **LC-MS (ES):** RT = 0.6-0.7 min, *m/z* = 315.77 (M+H<sup>+</sup>); **R<sub>f</sub>:** 0.64 (4:1 EtOAc–hexane); **HPLC:** RT = 3.00 min (97%); ***m/z* (ES<sup>+</sup>):** Found: 315.1490 (M+H<sup>+</sup>), C<sub>21</sub>H<sub>18</sub>N<sub>2</sub>O requires *MH* 315.1492; **IR:ν<sub>max</sub>/cm<sup>-1</sup> (solid):** 3251 (br.O-H), 2916, 1607.

Preparation of 3-bromo-6-(4-methoxyphenyl)-1*H*-indazole

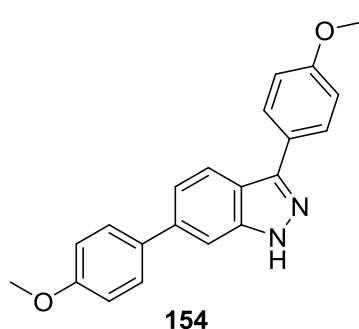
Synthesised using method A using 3-bromo-6-iodo-1*H*-indazole (500 mg, 1.55 mmol, 1.0 eq), 4-methoxyphenylboronic acid (353 mg, 2.32 mmol, 1.5 eq), Pd(dppf)Cl<sub>2</sub>•DCM (126 mg, 0.155 mmol, 0.1 eq), Na<sub>2</sub>CO<sub>3</sub> (492 mg, 4.64 mmol, 3.0 eq), dioxane (10 mL) and water

(10 mL) and the reaction heated for 5 h. The boronic acid was found to have the same *R<sub>f</sub>* as the product, therefore 3-bromo-6-iodo-1*H*-indazole (250 mg, 0.77 mmol, 0.5 eq) and Pd(dppf)Cl<sub>2</sub>•DCM (63 mg, 0.077 mmol, 0.05 eq) were added and the reaction heated for 1 h. The work up proceeded using the larger volumes of solvents and the organic solvent removed *in vacuo* to reveal a brown solid. The crude product was purified using column chromatography (20-50% EtOAc–hexane) and an off-white

solid obtained. The resulting solid was crystallised from toluene. The title compound 153 (135 mg, 0.48 mmol, 31%) was collected as off-white shiny flakes.

**<sup>1</sup>H NMR (500 MHz, DMSO-d<sub>6</sub>):** 7.69-7.66 (3H, m, 7-H, 2''-H and 6''-H), 7.60 (1H, dd, *J* 8.5 and 1.0, 4-H), 7.48 (1H, dd, *J* 8.5 and 1.5, 5-H), 7.06-7.03 (2H, m, 3''-H and 5''-H), 3.80 (3H, s, CH<sub>3</sub>), NH not observed; **<sup>13</sup>C NMR (125 MHz, DMSO-d<sub>6</sub>):** 159.2 (4''-C), 141.8 (3'-C), 139.5 (6-C), 132.3 (1''-C), 128.4 (2''-C and 6''-C), 121.1 (5-C), 121.0 (3'-C), 120.2 (3-C), 119.5 (4-C), 114.5 (3''-C and 5''-C), 107.5 (7-C), 55.2 (CH<sub>3</sub>); **LC-MS (ES):** RT = 2.01-2.09 min, *m/z* = 303.1 (M+H<sup>+</sup>); **R<sub>f</sub>:** 0.46 (1:1 EtOAc–hexane); **HPLC:** RT = 0.88 min; ***m/z* (ES+):** Found: 303.0132 (M+H<sup>+</sup>), C<sub>14</sub>H<sub>11</sub>BrN<sub>2</sub>O requires *MH* 303.0128; **IR:ν<sub>max</sub>/cm<sup>-1</sup> (solid):** 3287 (N-H), 2991, 2932, 2833, 1618; **M.pt:** 213.2-214.1 °C; **Found:** C, 55.7; H, 3.70; N, 9.2; C<sub>14</sub>H<sub>11</sub>BrN<sub>2</sub>O requires C, 55.5; H, 3.66; N, 9.2%.

#### Preparation of 3,6-bis(4-methoxyphenyl)-1*H*-indazole

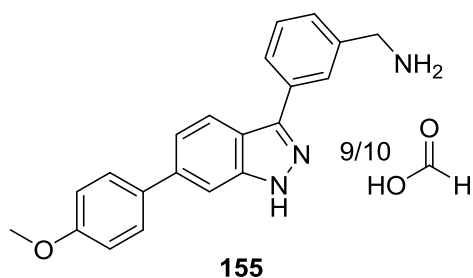


Synthesised as a side product using the same conditions as seen in the preparation of 6-(4-methoxyphenyl)-1*H*-indazole (**153**). A second compound was isolated from the column and a yellow solid obtained. The solid was triturated in hot EtOH decanting off the yellow solution and the remaining solid crystallised from EtOH.

The title compound 154 (32 mg, 0.10 mmol, 3%) was collected as off-white microneedles.

**<sup>1</sup>H NMR (500 MHz, DMSO-d<sub>6</sub>):** 13.09 (1H, br.s NH), 8.05 (1H, d, *J* 8.5, 4-H), 7.95-7.91 (2H, m, 2''' and 6'''-H), 7.70-7.67 (3H, m, 7-H, 2''-H and 6''-H), 7.44 (1H, dd, *J* 8.5 and 1.5, 5-H), 7.10-7.03 (4H, m, 3''-H, 5''-H, 3'''-H and 5'''-H), 3.82 (3H, s, CH<sub>3</sub>), 3.81 (3H, s, CH<sub>3</sub>); **<sup>13</sup>C NMR (125 MHz, DMSO-d<sub>6</sub>):** 159.0 (4''-C), 158.9 (4'''-C), 143.0 (3-C), 142.4 (3'-C), 138.0 (6-C), 132.7 (1''-C), 128.2 (2''-C and 6''-C), 127.9 (2'''-C and 6'''-C), 126.3 (1'''-C), 121.0 (4-C), 120.3 (5-C), 118.9 (7'-C), 114.4 (3''-C and 5''-C), 114.3 (3'''-C and 5'''-C), 107.2 (7-C), 55.2 (CH<sub>3</sub>), 55.2 (CH<sub>3</sub>); **LC-MS (ES):** RT = 2.05-2.19 min, *m/z* = 331.2 (M+H<sup>+</sup>); **R<sub>f</sub>:** 0.50 (7:3 EtOAc–hexane); **HPLC:** RT = 0.84 min; ***m/z* (ES+):** Found: 331.1454 (M+H<sup>+</sup>), C<sub>21</sub>H<sub>19</sub>N<sub>2</sub>O<sub>2</sub> requires *MH* 331.1441; **IR:ν<sub>max</sub>/cm<sup>-1</sup> (solid):** 3352 (N-H), 3070, 2954, 2831, 1607; **M.pt:** 197.0-198.0 °C.

Preparation of {3-[6-(4-methoxyphenyl)-1*H*-indazol-3-yl]phenyl}methanaminium formate

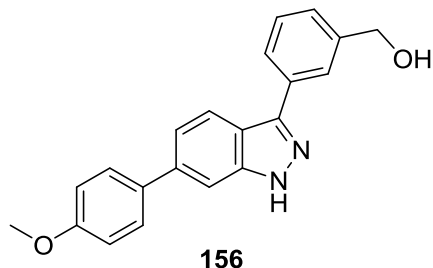


Synthesised using method A using 3-bromo-6-(4-methoxyphenyl)-1*H*-indazole (250 mg, 0.82 mmol, 1.0 eq), 3-(aminomethyl)phenylboronic acid•HCl (232 mg, 1.24 mmol, 1.5 eq), Pd(dppf)Cl<sub>2</sub>•DCM (67 mg, 0.082 mmol, 0.1 eq), Na<sub>2</sub>CO<sub>3</sub> (437 mg, 4.12 mmol, 5.0 eq), dioxane (2.5 mL) and water (2.5 mL) and the reaction heated for 3 h. LC-MS showed the reaction to be incomplete and therefore 3-(aminomethyl)phenylboronic acid•HCl (116 mg, 0.62 mmol, 0.75 eq), Pd(dppf)Cl<sub>2</sub>•DCM (34 mg, 0.041 mmol, 0.05 eq) and Na<sub>2</sub>CO<sub>3</sub> (218 mg, 2.56 mmol, 2.5 eq) were added and the reaction heated for 2 h. The celite pad was washed with DCM:MeOH (1:1) and the work up carried out using DCM instead of EtOAc. The work up proceeded using the smaller volumes of solvents and the organic solvent removed *in vacuo* to reveal a brown semi-solid. The crude product was purified using column chromatography (12% 7.0 M NH<sub>3</sub> in MeOH–EtOAc) and a brown semi-solid obtained. The semi-solid was further purified using reverse phase ACC (gradient 0-40% MeCN–H<sub>2</sub>O in 0.1% formic acid). Appropriate fractions were collected and reduced *in vacuo* to a volume of ~20 mL until precipitation was observed. The precipitate was filtered and triturated in hot MeOH removing the insoluble impurities *via* filtration. The filtrate was reduced *in vacuo* and the resulting solid triturated in hot EtOAc. The title compound 155 (67 mg, 0.20 mmol, 25%) was collected as a colourless powder.

**<sup>1</sup>H NMR (500 MHz, DMSO-*d*<sub>6</sub>):** 8.43 (1H, s, formate-H), 8.22 (1H, d, *J* 8.5, 4-H), 8.10 (1H, s, 2'''-H), 7.97 (1H, d, *J* 7.5, 6'''-H), 7.74 (1H, s, 7-H), 7.74-7.71 (2H, m, 2''-H and 6''-H), 7.53 (1H, app.t, *J* 7.5, 5'''-H), 7.49 (1H, dd, *J* 8.5 and 1.5, 5-H), 7.46 (1H, d, *J* 8.0, 4'''-H), 7.10-7.07 (2H, m, 3''-H and 5''-H), 4.05 (2H, s, CH<sub>2</sub>), 3.84 (3H, s, CH<sub>3</sub>), heteroatoms not observed; **<sup>13</sup>C NMR (125 MHz, DMSO-*d*<sub>6</sub>):** 165.2 (formate C=O), 159.0 (4''-C), 142.8 (1'''-C), 142.5 (Ar-q), 138.9 (3'''-C), 138.1 (6-C), 133.9 (Ar-q), 132.7 (3-C), 128.9 (5'''-C), 128.2 (2''-C and 6''-C), 127.5 (4'''-C), 126.4 (2''-C), 125.7 (6'''-C), 121.2 (4-C), 120.5 (5-C), 119.0 (7'-C), 114.4 (3''-C and 5''-C), 107.3 (7-C), 55.2 (CH<sub>3</sub>), 43.5 (CH<sub>2</sub>); **LC-MS (ES):** RT = 0.5-0.5 min, *m/z* = 330.23 (M+H<sup>+</sup>); **R<sub>r</sub>:** 0.57 (15% 7.0 M NH<sub>3</sub> in DCM); **HPLC:** RT = 3.00

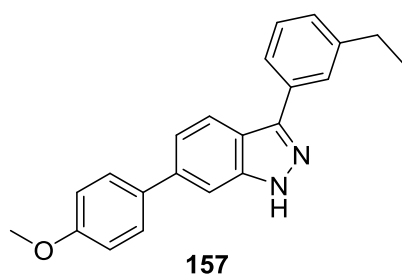
min (94%); **m/z** (**ES+**): Found: 330.1598 ( $M+H^+$ ),  $C_{21}H_{19}N_3O$  requires *MH* 330.1601; **IR**:  $\nu_{\max}/\text{cm}^{-1}$  (**solid**): 3291 (N-H), 2955, 2799, 1648; **M.pt**: 188.0-189.5 °C.

Preparation of {3-[6-(4-methoxyphenyl)-1*H*-indazol-3-yl]phenyl}methanol



Synthesised using method A using 3-bromo-6-(4-methoxyphenyl)-1*H*-indazole (250 mg, 0.82 mmol, 1.0 eq), 3-(hydroxymethyl)phenylboronic acid (188 mg, 1.24 mmol, 1.5 eq), Pd(dppf)Cl<sub>2</sub>•DCM (67 mg, 0.082 mmol, 0.1 eq), Na<sub>2</sub>CO<sub>3</sub> (262 mg, 2.47 mmol, 3.0 eq), dioxane (2.5 mL) and water (2.5 mL) and the reaction heated for 3.5 h. LC-MS showed the reaction to be incomplete and therefore 3-(hydroxymethyl)phenylboronic acid (94 mg, 0.62 mmol, 0.75 eq), Pd(dppf)Cl<sub>2</sub>•DCM (34 mg, 0.041 mmol, 0.05 eq) and Na<sub>2</sub>CO<sub>3</sub> (131 mg, 1.24 mmol, 1.5 eq) were added and the reaction heated for 1 h. The work up proceeded using the smaller volumes of solvents and the organic solvent removed *in vacuo* to reveal a brown solid. The crude product was purified using column chromatography (gradient 60-70% EtOAc–hexane) and a yellow solid obtained. The solid was crystallised from EtOH. The title compound 156 (118 mg, 0.36 mmol, 43%) was collected as yellow micro-granules.

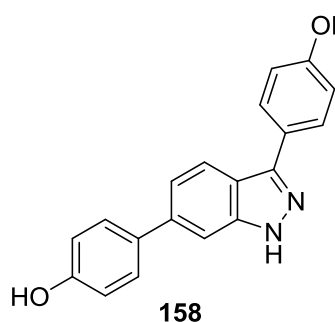
**<sup>1</sup>H NMR (500 MHz, DMSO-*d*<sub>6</sub>)**: 13.22 (1H, br.s, NH), 8.11 (1H, d, *J* 8.5, 4-H), 7.98 (1H, s, 2'''-H), 7.87 (1H, d, *J* 7.5, 6'''-H), 7.71-7.67 (3H, m, 7-H, 2''-H and 6''-H), 7.49-7.45 (2H, m, 5-H and 5'''-H), 7.34 (1H, d, *J* 8.0, 4'''-H), 7.07-7.04 (2H, m, 3''-H and 5''-H), 5.28 (1H, t, *J* 6.0, OH), 4.61 (2H, d, *J* 6.0, CH<sub>2</sub>), 3.81 (3H, s, CH<sub>3</sub>); **<sup>13</sup>C NMR (125 MHz, DMSO-*d*<sub>6</sub>)**: 159.0 (4''-C), 143.2 (Ar-q), 143.2 (Ar-q), 142.4 (Ar-q), 138.1 (6-C), 133.5 (Ar-q), 132.7 (Ar-q), 128.6 (5'''-C), 128.2 (2''-C and 6''-C), 125.7 (4'''-C), 125.0 (6'''-C), 124.7 (2'''-C), 121.1 (4-C), 120.5 (5-C), 119.0 (7'-C), 114.4 (3''-C and 5''-C), 107.3 (7-C), 62.9 (CH<sub>2</sub>), 55.2 (CH<sub>3</sub>); **LC-MS (ES)**: RT = 0.6-0.6 min, **m/z** = 331.20 ( $M+H^+$ ); **R<sub>r</sub>**: 0.59 (EtOAc); **HPLC**: RT = 3.00 min; **m/z** (**ES+**): Found: 331.1441 ( $M+H^+$ ),  $C_{21}H_{18}N_2O_2$  requires *MH* 331.1441; **IR**:  $\nu_{\max}/\text{cm}^{-1}$  (**solid**): 3172 (br.O-H), 2972, 1604; **M.pt**: 191.7-193.1 °C.

Preparation of 3-(3-ethylphenyl)-6-(4-methoxyphenyl)-1H-indazole

Synthesised using method A using 3-bromo-6-(4-methoxyphenyl)-1H-indazole (250 mg, 0.82 mmol, 1.0 eq), 3-ethylphenylboronic acid (186 mg, 1.24 mmol, 1.5 eq), Pd(dppf)Cl<sub>2</sub>•DCM (67 mg, 0.082 mmol, 0.1 eq), Na<sub>2</sub>CO<sub>3</sub> (262 mg, 2.47 mmol, 3.0 eq), dioxane (2.5 mL) and water (2.5 mL) and

the reaction heated for 3.5 h. The work up proceeded using the smaller volumes of solvents and the organic solvent removed *in vacuo* to reveal a brown semi-solid. The crude product was purified using column chromatography (7:3 hexane–EtOAc). The title compound 157 (26 mg, 0.07 mmol, 16%) was collected as colourless waxy platelets.

**<sup>1</sup>H NMR (500 MHz, DMSO-d<sub>6</sub>):** 13.20 (1H, br.s, NH), 8.08 (1H, d, *J* 8.5, 4-H), 7.83 (1H, s, 2'''-H), 7.81 (1H, d, *J* 8.0, 6'''-H), 7.71-7.76 (3H, m, 7-H, 3''H and 5''-H), 7.46 (1H, dd, *J* 8.5 and 1.5, 5-H), 7.43 (1H, app.t, *J* 7.5, 5'''-H), 7.25 (1H, d, *J* 8.0, 4'''-H), 7.07-7.04 (2H, m, 2''-H and 6''-H), 3.81 (3H, s, OCH<sub>3</sub>), 2.71 (2H, q, *J* 7.5, CH<sub>2</sub>), 1.26 (3H, t, *J* 7.5, CH<sub>2</sub>CH<sub>3</sub>); **<sup>13</sup>C NMR (125 MHz, DMSO-d<sub>6</sub>):** 159.0 (4''-C), 144.3 (3'''-C), 143.3 (Ar-q), 142.4 (Ar-q), 138.1 (6-C), 133.7 (1'''-C), 132.7 (3-C), 128.8 (5'''-C), 128.2 (3''-C and 5''-C), 127.2 (4'''-C), 126.1 (2'''-C), 124.1 (6'''-C), 121.1 (4-C), 120.5 (5-C), 119.1 (7'-C), 114.4 (2''-C and 6''-C), 107.3 (7-C), 55.2 (OCH<sub>3</sub>), 28.2 (CH<sub>2</sub>), 15.7 (CH<sub>2</sub>CH<sub>3</sub>); **LC-MS (ES):** RT = 0.7-0.8 min, *m/z* = 329.23 (M+H<sup>+</sup>); **R<sub>f</sub>:** 0.72 (4:1 EtOAc–hexane); **HPLC:** RT = 4.14 min; ***m/z* (ES+):** Found: 329.1650 (M+H<sup>+</sup>), C<sub>22</sub>H<sub>20</sub>N<sub>2</sub>O requires *MH* 329.1648; **IR:ν<sub>max</sub>/cm<sup>-1</sup> (solid):** 3235 (N-H), 2962, 2926, 1626; **M.pt:** 139.0-140.1 °C.

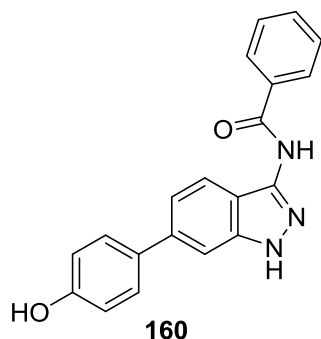
Preparation of 3,6-bis(4-hydroxyphenyl)-1H-indazole

Synthesised using method D using 3,6-bis(4-methoxyphenyl)-1H-indazole (194 mg, 0.59 mmol, 1.0 eq), 1 M BBr<sub>3</sub> in DCM (4.70 mL, 4.70 mmol, 8.0 eq) and DCM (15 mL) and the reaction stirred for 23 h. TLC analysis showed the reaction to be incomplete and therefore 1 M BBr<sub>3</sub> in DCM (588 μL, 0.588 mmol, 1.0 eq) was added and the reaction stirred for 1 h. Water (20 mL) was added and the resulting precipitate filtered and washed with DCM. The solid was dissolved in MeOH

and reduced *in vacuo* to yield the crude product as a brown solid. Purification attempts using trituration with DCM and MeOH failed as well as attempts at normal phase chromatography, possibly due to the compounds solubility issues. The crude product was triturated with small amounts of cold MeOH and filtered. The title compound 158 (73 mg, 0.24 mmol, 41%) collected as an off-white solid.

**<sup>1</sup>H NMR (500 MHz, DMSO-*d*<sub>6</sub>):** 12.97 (1H, br.s, NH), 9.57 (1H, br.s, OH), 9.55 (1H, br.s, OH), 8.00 (1H, d, *J* 8.5, 4-H), 7.82-7.79 (2H, m, 2'''-H and 6'''-H), 7.61 (1H, s, 7-H), 7.58-7.54 (2H, m, 2''-H and 6''-H), 7.39 (1H, dd, *J* 8.5 and 1.5, 5-H), 6.92-6.86 (4H, m, 3''-H, 5''-H, 3'''-H and 5'''-H); **<sup>13</sup>C NMR (125 MHz, DMSO-*d*<sub>6</sub>):** 157.2 (4''-C), 157.2 (4'''-C), 143.3 (3-C), 142.4 (3'-C), 138.3 (6-C), 131.1 (1''-C), 128.1 (2''-C and 6''-C), 128.0 (2'''-C and 6'''-C), 124.8 (1'''-C), 121.0 (4-C), 120.0 (5-C), 118.7 (7'-C), 115.8 (3''-C and 5''-C), 115.6 (3'''-C and 5'''-C), 106.7 (7-C); **LC-MS (ES):** RT = 1.67-1.81 min, *m/z* = 303.1 (M+H<sup>+</sup>); **R<sub>f</sub>:** 0.52 (EtOAc); **HPLC:** RT = 2.41 min; ***m/z* (ES<sup>+</sup>):** Found: 303.1138 (M+H<sup>+</sup>), C<sub>19</sub>H<sub>15</sub>N<sub>2</sub>O<sub>2</sub> requires *MH* 303.1128; **IR:ν<sub>max</sub>/cm<sup>-1</sup> (solid):** 3583 (O-H), 3333 (O-H), 3142, 1609, 1522; **M.pt:** 260.4-265.1 °C.

#### Preparation of N-[6-(4-hydroxyphenyl)-1*H*-indazol-3-yl]benzamide



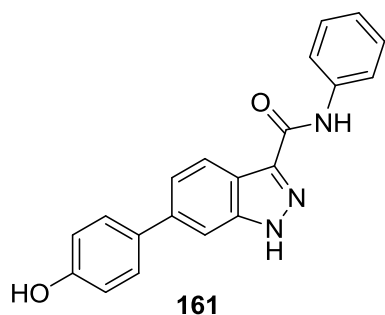
Synthesised using method D using N-[6-(4-methoxyphenyl)-1*H*-indazol-3-yl]benzamide (100 mg, 0.29 mmol, 1.0 eq), 1 M BBr<sub>3</sub> in DCM (2.33 mL, 2.33 mmol, 8.0 eq) and DCM (7 mL) and the reaction stirred for 20 h. Water (10 mL) was added and the resulting yellow precipitate collected by filtration and washed with water. The crude solid was dissolved in MeOH and

reduced *in vacuo* to reveal an off-white solid. The solid was crystallised from EtOH. The title compound 160 (36 mg, 0.11 mmol, 38%) was collected as a fluffy colourless solid.

**<sup>1</sup>H NMR (500 MHz, DMSO-*d*<sub>6</sub>):** 12.78 (1H, br.s, indazole NH), 10.81 (1H, br.s, amide NH), 9.58 (1H, s, OH), 8.12-8.09 (2H, m, 2'''-H and 6'''-H), 7.77 (1H, d, *J* 8.5, 4-H), 7.65-7.61 (1H, m, 4'''-H), 7.60-7.54 (5H, m, 7-H, 2''-H, 6''-H, 3'''-H and 5'''-H), 7.34 (1H, dd, *J* 8.5 and 1.5, 5-H), 6.91-6.88 (2H, m, 3''-H and 5''-H); **<sup>13</sup>C NMR (100 MHz, DMSO-*d*<sub>6</sub>):** 166.0 (amide C=O), 157.7 (4''-C), 142.4 (7'-C), 140.6 (6-C), 139.3 (3-C), 134.3 (1'''-C), 132.3 (4'''-C), 131.7 (1''-C), 128.9 (Ar-q),

128.7 (Ar-q), 128.4 (2'''-C and 6'''-C), 122.7 (4-C), 119.7 (5-C), 116.2 (3'-C), 116.2 (3''-C and 5''-C), 107.0 (7-C); **LC-MS (ES)**: RT = 0.5-0.6 min, m/z = 330.18 (M+H<sup>+</sup>); **R<sub>f</sub>**: 0.18 (7:3 EtOAc–petrol); **HPLC**: RT = 2.46 min; **m/z (ES+)**: Found: 330.1236 (M+H<sup>+</sup>), C<sub>20</sub>H<sub>15</sub>N<sub>3</sub>O<sub>2</sub> requires *MH* 330.1237; **IR:ν<sub>max</sub>/cm<sup>-1</sup> (solid)**: 3246 (N-H), 3100 (br.O-H), 3000, 1649 (C=O); **M.pt**: >250 °C.

Preparation of 6-(4-hydroxyphenyl)-1*H*-indazole-3-phenylcarboxamide

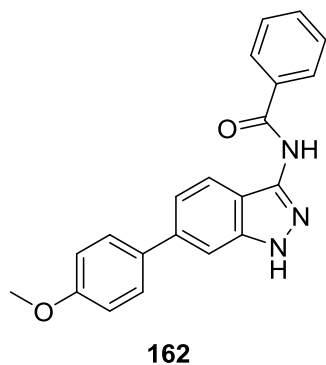


Synthesised using method D using 6-(4-methoxyphenyl)-1*H*-indazole-3-phenylcarboxamide (28 mg, 0.08 mmol, 1.0 eq), 1M BBr<sub>3</sub> in DCM (0.65 mL, 0.65 mmol, 8.0 eq) and DCM (2 mL). The crude product was purified using reverse-phase ACC (50-72% MeCN–H<sub>2</sub>O in 0.1% formic acid). The title

compound 161 (7 mg, 0.03 mmol, 27%) was collected as an off-white pearlescent powder.

**<sup>1</sup>H NMR (400 MHz, CD<sub>3</sub>OD)**: 8.28 (1H, d, *J* 8.5, 4-H), 7.79-7.76 (2H, m, 2'''-H and 6'''-H), 7.71 (1H, s, 7-H), 7.58-7.51 (3H, m, 5-H, 3''-H and 5''-H), 7.41-7.35 (2H, m, 3'''-H and 5'''-H), 7.15 (1H, app.t, *J* 7.4, 4'''-H), 6.93-6.87 (2H, m, 2''-H and 6''-H), OH and NHs not observed; **<sup>13</sup>C NMR (100 MHz, CD<sub>3</sub>OD)**: 163.0 (C=O), 158.3 (4''-C), 143.7 (Ar-q), 141.6 (Ar-q), 139.3 (Ar-q), 133.2 (Ar-q), 131.1 (Ar-q), 129.6 (3'''-C and 5'''-C), 129.3 (5-C), 123.4 (4'''-C), 122.6 (3''-C and 5''-C), 121.5 (4-C), 120.3 (2'''-C and 6'''-C), 116.5 (2''-C and 6''-C), 108.1 (7-C), one quaternary carbon not observed; **LC–MS (ES)**: RT = 0.6-0.6 min, m/z = 330.22 (M+H<sup>+</sup>); **R<sub>f</sub>**: 0.31 (5% MeOH–DCM); **HPLC**: RT = 3.04 min (97%); **m/z (ES+)**: Found: 330.1233 (M+H<sup>+</sup>), C<sub>20</sub>H<sub>15</sub>N<sub>3</sub>O<sub>2</sub> requires *MH* 330.1237; **IR:ν<sub>max</sub>/cm<sup>-1</sup> (solid)**: 3366 (N-H), 3180, 1651 (C=O); **M.pt**: >250 °C.

Preparation of N-[6-(4-methoxyphenyl)-1*H*-indazol-3-yl]benzamide

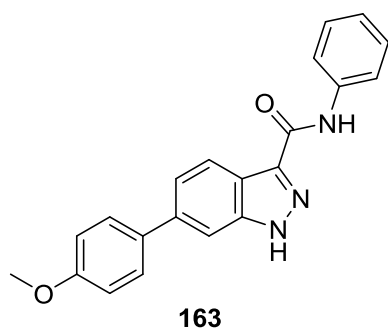


Synthesised using method A using *tert*-butyl 3-benzamido-6-bromo-1*H*-indazole-1-carboxylate (229 mg, 0.55 mmol, 1.0 eq), 4-methoxyphenylboronic acid (125 mg, 0.82 mmol, 1.5 eq), Pd(dppf)Cl<sub>2</sub>•DCM (45 mg, 0.055 mmol, 0.1 eq), Na<sub>2</sub>CO<sub>3</sub> (175 mg, 1.65 mmol, 3.0 eq), dioxane (2 mL) and water (2 mL) and the reaction heated for 3 h. The work up proceeded using the smaller

volumes of solvents and the organic solvent removed *in vacuo* to reveal a brown oil. The crude product was purified by column chromatography (gradient 50-60% EtOAc–hexane) and a cream solid obtained. The solid was crystallised from propan-2-ol. The title compound 162 (94 mg, 0.27 mmol, 50%) was collected as colourless microneedles. The filtrate was reduced *in vacuo* to reveal an off-white solid (55 mg, 0.16 mmol, 29%) which was used without further purification.

**<sup>1</sup>H NMR (500 MHz, DMSO-*d*<sub>6</sub>)**: 12.78 (1H, br.s, indazole NH), 10.80 (1H, br.s amide NH), 8.10-8.07 (2H, m, 2'''-H and 6'''-H), 7.78 (1H, d, *J* 8.5, 4-H), 7.69-7.66 (2H, m, 2''-H and 6''-H), 7.63-7.59 (2H, m, 7-H and 4'''-H), 7.56-7.52 (2H, m, 3''' H and 5'''-H), 7.35 (1H, dd, *J* 8.5 and 1.5, 5-H), 7.06-7.03 (2H, m, 3''-H and 5''-H), 3.81 (3H, s, CH<sub>3</sub>); **<sup>13</sup>C NMR (100 MHz, DMSO-*d*<sub>6</sub>)**: 165.5 (amide C=O), 159.0 (4'' C), 141.9 (7' C), 140.1 (6-C), 138.2 (3-C), 133.8 (1'''-C), 132.8 (1''-C), 131.8 (4'''-C), 128.4 (3'''-C and 5'''-C), 128.2 (2''-C and 6''-C), 127.9 (2'''-C and 6'''-C), 122.4 (4-C), 119.9 (5-C), 115.9 (3'-C), 114.4 (3''-C and 5''-C), 106.9 (7-C), 55.2 (CH<sub>3</sub>); **LC-MS (ES)**: RT = 0.6-0.6 min, *m/z* = 344.20 (M+H<sup>+</sup>); **R<sub>f</sub>**: 0.30 (7:3 EtOAc–petrol); **HPLC**: RT = 3.01 min; ***m/z* (ES<sup>+</sup>)**: Found: 344.1392 (M+H<sup>+</sup>), C<sub>21</sub>H<sub>17</sub>N<sub>3</sub>O<sub>2</sub> requires *MH* 344.1394; **IR:  $\nu_{\max}/\text{cm}^{-1}$  (solid)**: 3298 (N-H), 3250 (N-H), 3056, 3000, 2834, 1637 (C=O); **M.pt**: 213.5-215.0 °C.

#### Preparation of 6-(4-methoxyphenyl)-1*H*-indazole-3-phenylcarboxamide



Synthesised using method A using 6-bromo-1*H*-indazole-3-phenylcarboxamide (250 mg, 0.79 mmol, 1.0 eq), 4-methoxyphenylboronic acid (178 mg, 1.18 mmol, 1.5 eq), Pd(dppf)Cl<sub>2</sub>•DCM (64 mg, 0.079 mmol, 0.1 eq), Na<sub>2</sub>CO<sub>3</sub> (250 mg, 2.36 mmol, 3.0 eq), dioxane (7 mL) and water (7 mL) and the reaction heated for 3 h. The work up proceeded using the

smaller volumes of solvents and the organic solvent removed *in vacuo* to reveal a brown oil. The crude product was purified using column chromatography (0.5% 7.0 M NH<sub>3</sub> in MeOH–DCM) and an orange solid obtained. The solid was triturated with EtOAc and filtered. The title compound 163 (28 mg, 0.08 mmol, 10%) was collected as an off-white powder.

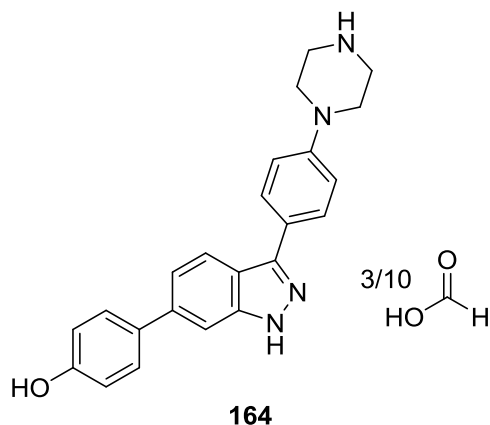
**<sup>1</sup>H NMR (500 MHz, DMSO-*d*<sub>6</sub>)**: 13.79 (1H, br.s, indazole NH), 10.33 (1H, br.s, amide NH), 8.26 (1H, d, *J* 8.5, 4-H), 7.92 (2H, d, *J* 7.9, 2'''-H and 6'''-H), 7.80 (1H,



s, 7-H), 7.74 (2H, d, 3''-H and 5''-H), 7.59 (1H, dd,  $J$  8.5 and 1.5, 5-H); 7.37 (2H, app.t,  $J$  7.9, 3'''-H and 5'''-H), 7.13-7.07 (3H, m, 2''-H, 6''-H and 4'''-H), 3.84 (3H, s,  $\underline{\text{CH}}_3$ );  $^{13}\text{C}$  NMR (100 MHz, DMSO- $d_6$ ): 161.4 (C=O), 159.6 (4''-C), 142.6 (3-C), 139.3 (Ar-q), 139.2 (Ar-q), 138.8 (Ar-q), 133.0 (Ar-q), 129.0 (3'''-C and 5'''-C), 128.8 (3''-C and 5''-C), 123.9 (4'''-C), 122.5 (5-C), 122.3 (4-C), 121.2 (3'-C), 120.7 (2'''-C and 6'''-C), 114.9 (2''-C and 6''-C), 108.0 (7-C), 55.7 ( $\underline{\text{CH}}_3$ ); LC-MS (ES): RT= 0.7-0.8 min,  $m/z$  = 344.23 ( $\text{M}+\text{H}^+$ );  $R_f$ : 0.43 (0.5% 7.0 M  $\text{NH}_3$  in MeOH-DCM); HPLC: RT = 3.52 min;  $m/z$  (ES+): Found: 344.1388 ( $\text{M}+\text{H}^+$ ),  $\text{C}_{21}\text{H}_{17}\text{N}_3\text{O}_2$  requires  $MH$  344.1394; IR: $\nu_{\text{max}}/\text{cm}^{-1}$  (solid): 3374 (N-H), 3192, 2955, 2836, 1666 (C=O); M.pt: >250 °C.

### 6.1.4.3 Chapter Four Compounds

#### Preparation of 4-{4-[6-(4-hydroxyphenyl)-1H-indazol-3-yl]phenyl}piperazin-1-ium formate



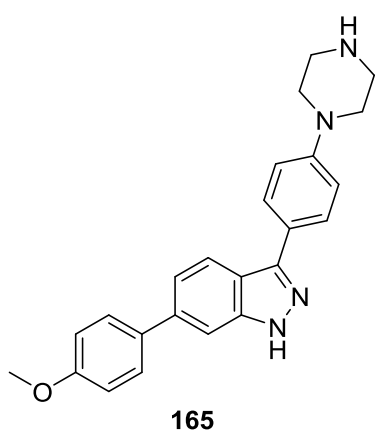
Synthesised using method D using 6-(4-methoxyphenyl)-3-[4-(piperazin-1-yl)phenyl]-1H-indazole (49 mg, 0.13 mmol, 1.0 eq), 1 M  $\text{BBr}_3$  in DCM (1.02 mL, 1.02 mmol, 8.0 eq) and DCM (5 mL) and the reaction stirred for 1 h. Water (10 mL) was added and the resulting suspension added to MeOH (10 mL) to aid dissolution. The

reaction mixture was extracted with DCM ( $3 \times 10$  mL) and the combined organic layers extracted with water ( $3 \times 10$  mL) adding MeOH (5 mL) each extraction to aid dissolution. The aqueous layer was reduced *in vacuo* to reveal a brown solid (150 mg). The crude product was purified by reverse phase ACC (gradient 0-40% MeCN- $\text{H}_2\text{O}$  in 0.1% formic acid). The title compound **164** (36 mg, 0.1 mmol, 76%) was collected as a colourless solid.

$^1\text{H}$  NMR (500 MHz, DMSO- $d_6$ ): 13.01 (1H, br.s, formate  $\underline{\text{OH}}$ ), 8.19 (1H, br.s, formate  $\underline{\text{H}}$ ), 8.02 (1H, d,  $J$  8.5, 4-H), 7.90-7.86 (2H, m, 2'''-H and 6'''-H), 7.62 (1H, s, 7-C), 7.58-7.54 (2H, m, 2''-H and 6''-H), 7.40 (1H, dd,  $J$  8.5 and 1.5, 5-H), 7.12-7.08 (2H, m, 3'''-H and 5'''-H), 6.90-6.86 (2H, m, 3''-H and 5''-H), 3.36-3.33 (4H, m, piperazine  $\underline{\text{CH}}_2$ ), 3.17-3.13 (4H, m, piperazine  $\underline{\text{CH}}_2$ ), heteroatoms not

observed;  $^{13}\text{C}$  NMR (125 MHz, DMSO- $d_6$ ): 163.6 (formate C=O), 157.2 (4''-C), 149.8 (1'''-C), 143.0 (3-C), 142.5 (3'-C), 138.3 (6-C), 131.1 (1''-C), 128.1 (2''-C and 6''-C), 127.4 (2'''-C and 6'''-C), 125.1 (4'''-C), 121.0 (4-C), 120.1 (5-C), 118.7 (7'-C), 115.9 (3'''-C and 5'''-C), 115.8 (2'''-C and 6'''-C), 106.8 (7-C), 46.4 (piperazine  $\underline{\text{C}}\text{H}_2$ ), 43.5 (piperazine  $\underline{\text{C}}\text{H}_2$ ); LC-MS (ES): RT = 0.5-0.5 min,  $m/z$  = 371.47 (M+H<sup>+</sup>); Rr: 0.31 (10% 7.0 M NH<sub>3</sub> in MeOH-DCM); HPLC: RT = 1.82 min;  $m/z$  (ES<sup>+</sup>): Found: 371.1869 (M+H<sup>+</sup>), C<sub>23</sub>H<sub>22</sub>N<sub>4</sub>O requires MH 371.1866; IR:  $\nu_{\text{max}}/\text{cm}^{-1}$  (solid): 3243 (N-H), 3232 (br.O-H), 2949, 2834, 1609; M.pt: >250 °C.

Preparation of 6-(4-methoxyphenyl)-3-[4-(piperazin-1-yl)phenyl]-1H-indazole



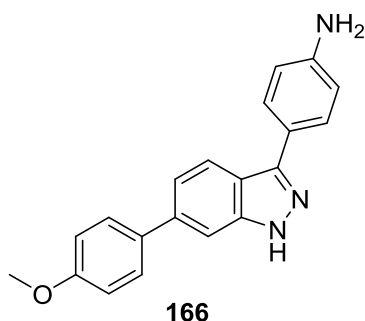
Synthesised using method F using 4-[6-(4-methoxyphenyl)-1H-indazol-3-yl]aniline (715 mg, 2.27 mmol, 1.0 eq), bis(2-chloroethyl)amine hydrochloride (486 mg, 2.72 mmol, 1.2 eq), K<sub>2</sub>CO<sub>3</sub> (752 mg, 5.44 mmol, 2.4 eq) and <sup>t</sup>BuOH (15 mL) and the reaction heated for 111 h. TLC analysis indicated the reaction to be incomplete and therefore bis(2-chloroethyl)amine hydrochloride (81 mg,

0.45 mmol, 0.2 eq) was added and stirred at 100 °C for 3 h. LC-MS analysis indicated formation of several other products and therefore the reaction was stopped. The reaction mixture was concentrated *in vacuo* to reveal a green/yellow solid. The solid was dissolved in DMSO and the solution decanted from the insoluble impurities. The crude product was purified by reverse-phase ACC (gradient 0-30% MeCN-H<sub>2</sub>O in 0.1% formic acid) and a brown/orange solid (432 mg) obtained. The product was further purified by suspending the solid in 2M NaOH (20 mL) and DCM (40 mL) added with small additions of MeOH until dissolution was observed. The aqueous layer was extracted with DCM (2 × 15 mL) and the combined organic layers washed with brine (50 mL), dried (MgSO<sub>4</sub>) and reduced *in vacuo* to reveal a yellow solid. The crude solid was purified by column chromatography (7% 7.0 M NH<sub>3</sub> in MeOH-DCM). The title compound 165 (120 mg, 0.27 mmol, 12%) was collected as an off-white powder.

$^1\text{H}$  NMR (500 MHz, DMSO- $d_6$ ): 13.01 (1H, br.s, indazole NH), 8.04 (1H, d, *J* 8.5, 4-H), 7.86-7.83 (2H, m, 2'''-H and 6'''-H), 7.70-7.67 (2H, m, 2''-H and 6''-H), 7.66 (1H, s, 7-H), 7.42 (1H, dd, *J* 8.5 and 1.0, 5-H), 7.07-7.03 (4H, m, 3''-H, 5''-H, 3'''-H

and 5''-H), 3.81 (3H, s, CH<sub>3</sub>), 3.14-3.11 (4H, m, piperazine CH<sub>2</sub>), 2.87-2.85 (4H, m, piperazine CH<sub>2</sub>), piperazine NH not observed; <sup>13</sup>C NMR (125 MHz, DMSO-d<sub>6</sub>): 158.9 (4''-C), 151.1 (1''-C), 146.3 (Ar-q), 142.4 (Ar-q), 137.9 (6-C), 132.8 (1''-C), 128.2 (2''-C and 6''-C), 127.3 (3''-C and 5''-C), 124.0 (Ar-q), 121.1 (4-C), 120.1 (5-C), 118.9 (7'-C), 115.2 (Ar-C), 114.4 (Ar-C), 107.2 (7-C), 55.2 (CH<sub>3</sub>), 49.1 (piperazine CH<sub>2</sub>), 45.6 (piperazine CH<sub>2</sub>); LC-MS (ES): RT = 0.5-0.5 min, m/z = 385.48 (M+H<sup>+</sup>); R<sub>f</sub>: 0.49 (5% 7.0 M NH<sub>3</sub> in MeOH-DCM); HPLC: RT = 2.47 min; m/z (ES<sup>+</sup>): Found: 385.2030 (M+H<sup>+</sup>), C<sub>24</sub>H<sub>24</sub>N<sub>4</sub>O requires MH 385.2023; IR: ν<sub>max</sub>/cm<sup>-1</sup> (solid): 3288 (N-H), 2920, 2830, 1607; M.pt: 226.3-227.8 °C.

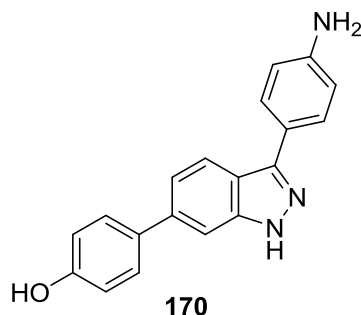
#### Preparation of 4-[6-(4-methoxyphenyl)-1H-indazol-3-yl]aniline



Synthesised using method A using 3-bromo-6-(4-methoxyphenyl)-1H-indazole (500 mg, 1.65 mmol, 1.0 eq), 4-aminophenylboronic acid•HCl (723 mg, 3.30 mmol, 2.0 eq), Pd(dppf)Cl<sub>2</sub>•DCM (135 mg, 0.165 mmol, 0.1 eq), Na<sub>2</sub>CO<sub>3</sub> (524 mg, 4.95 mmol, 3.0 eq), dioxane (10 mL) and water (10 mL) and the reaction heated for 6 h. LC-MS showed the reaction to be incomplete and therefore 4 aminophenylboronic acid•HCl (141 mg, 0.83 mmol, 0.5 eq), Pd(dppf)Cl<sub>2</sub>•DCM (68 mg, 0.083 mmol, 0.05 eq), Na<sub>2</sub>CO<sub>3</sub> (175 mg, 1.65 mmol, 1.0 eq) were added and the reaction heated for 1 h. The work up proceeded using the larger volumes of solvents and the organic solvent removed *in vacuo* to reveal a brown semi-solid. The crude product was purified using column chromatography (2 % 7.0 M NH<sub>3</sub> in MeOH-DCM) and an orange solid obtained. The product was further purified using reverse phase ACC (gradient 0-50% MeCN-H<sub>2</sub>O) and an off-white solid obtained. The solid was crystallised from EtOH and the pure compound (33 mg, 0.10 mmol, 4%) collected as shiny brown needles. The co-eluted fractions from the column were reduced *in vacuo* and the resulting solid dissolved in MeOH-DCM (1:1) and washed with 2 M NaOH (10 mL). The organic layer was reduced *in vacuo* and the resulting black solid triturated in hot EtOH and the solid filtered. The title compound 166 (277 mg, 0.87 mmol, 33%) was collected as a brown solid and used without further purification.

**<sup>1</sup>H NMR (500 MHz, DMSO-*d*<sub>6</sub>):** 12.87 (1H, br.s, indazole NH), 8.01 (1H, d, *J* 8.5, 4-H), 7.69-7.66 (4H, m, 2''-H, 6''-H, 2'''-H and 6'''-H), 7.63 (1H, s, 7-H), 7.39 (1H, dd, *J* 8.5 and 1.5, 5-H), 7.06-7.03 (2H, m, 3''-H and 5''-H), 6.71-6.68 (2H, m, 3'''-H and 5'''-H), 5.25 (2H, br.s, NH<sub>2</sub>), 3.80 (3H, s, CH<sub>3</sub>); **<sup>13</sup>C NMR (125 MHz, DMSO-*d*<sub>6</sub>):** 158.9 (4''-C), 148.5 (1'''-C), 144.0 (3-C), 142.3 (3'-C), 137.8 (6-C), 132.8 (1''-C), 128.1 (2'''-C and 6'''-C), 127.6 (2''-C and 6''-C), 121.4 (4'''-C), 121.3 (4-C), 119.8 (5-C), 118.9 (7'-C), 114.4 (3''-C and 6''-C), 114.0 (3'''-C and 5'''-C), 107.0 (7-C), 55.2 (CH<sub>3</sub>); **LC-MS (ES):** RT = 0.5-0.6 min, *m/z* = 316.39 (M+H<sup>+</sup>); **R<sub>f</sub>:** 0.35 (5% 7.0 M NH<sub>3</sub> in MeOH-DCM); **HPLC:** RT = 2.38 min; ***m/z* (ES+):** Found: 316.1447 (M+H<sup>+</sup>), C<sub>20</sub>H<sub>18</sub>N<sub>3</sub>O requires *MH* 316.1444; **IR: *v*<sub>max</sub>/cm<sup>-1</sup> (solid):** 3390 (N-H), 3088, 2920, 2830, 1607; **M.pt:** 224.7-225.2 °C.

Preparation of 4-[3-(4-aminophenyl)-1*H*-indazol-6-yl]phenol

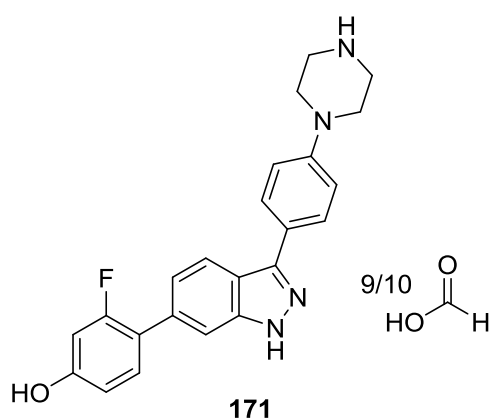


Synthesised using method D using 4-[6-(4-methoxyphenyl)-1*H*-indazol-3-yl]aniline (50 mg, 0.16 mmol, 1.0 eq), 1 M BBr<sub>3</sub> in DCM (1.27 mL, 1.27 mmol, 8.0 eq) and DCM (5 mL) and the reaction stirred for 1 h. Water (10 mL) was added and the resulting suspension added to MeOH (10 mL) to aid dissolution. The reaction mixture was extracted with DCM (3 × 10 mL) and the combined organic layers extracted with water (3 × 10 mL) adding MeOH (5 mL) each extraction to aid dissolution. The aqueous layer was reduced *in vacuo* to reveal a brown solid (149 mg). The combined organic layers were dried (MgSO<sub>4</sub>) and reduced *in vacuo* to reveal an off-white solid (6 mg). LC-MS analysis confirmed product mass in both aqueous and organic layers, therefore, both were combined and purified by reverse phase ACC (gradient 0-40% MeCN-H<sub>2</sub>O in 0.1% formic acid). Appropriate fractions were combined and reduced *in vacuo* to a volume of ~5 mL until precipitation was observed. The resulting solid was filtered under vacuum. The title compound 170 (11 mg, 0.04 mmol, 23%) was collected as a fluffy colourless solid.

**<sup>1</sup>H NMR (500 MHz, DMSO-*d*<sub>6</sub>):** 12.83 (1H, br.s, indazole NH), 9.53 (1H, br.s, OH), 7.98 (1H, d, *J* 8.5, 4-H), 7.68-7.65 (2H, m, 2'''-H and 6'''-H), 7.58 (1H, s, 7-H), 7.57-7.53 (2H, m, 2''-H and 6''-H), 7.36 (1H, dd, *J* 8.5 and 1.0, 5-H), 6.89-6.85 (2H, m, 3''-H and 5''-H), 6.71-6.67 (2H, m, 3'''-H and 5'''-H), 5.24 (2H, s, NH<sub>2</sub>); **<sup>13</sup>C NMR (125 MHz, DMSO-*d*<sub>6</sub>):** 157.1 (4''-C), 148.5 (1'''-C), 144.0 (3'-C), 142.4

(3-C), 138.2 (6-C), 131.2 (1''-C), 128.1 (2''-C and 6''-C), 127.5 (2'''-C and 6'''-C), 121.5 (4'''-C), 121.2 (4-C), 119.7 (5-C), 118.7 (7'-C), 115.8 (3''-C and 5''-C), 114.0 (3'''-C and 5'''-C), 106.6 (7-C); **LC-MS (ES)**: RT = 0.5-0.5 min, m/z = 302.37 (M+H<sup>+</sup>); **R<sub>f</sub>**: 0.42 (10% 7.0 M NH<sub>3</sub> in MeOH–DCM); **HPLC**: RT = 1.66 min; **m/z (ES<sup>+</sup>)**: Found: 302.1283 (M+H<sup>+</sup>), C<sub>19</sub>H<sub>15</sub>N<sub>3</sub>O requires *MH* 302.1288; **IR:ν<sub>max</sub>/cm<sup>-1</sup> (solid)**: 3448 (N-H), 3362 (N-H), 3252 (br.O-H), 2996, 1618; **M.pt**: >250 °C.

Preparation of 4-{4-[6-(2-fluoro-4-hydroxyphenyl)-1*H*-indazol-3-yl]phenyl}piperazin-1-ium formate



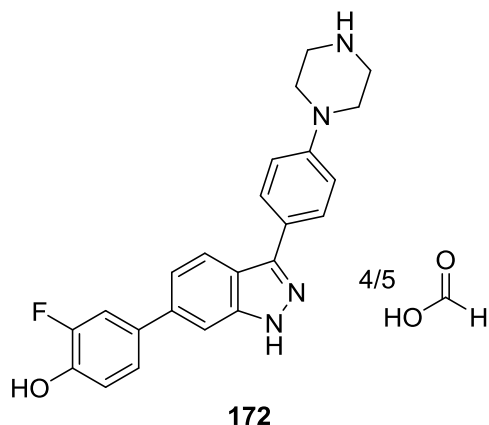
Synthesised using method D using 6-(2-fluoro-4-methoxyphenyl)-3-[4-(piperazin-1-yl)phenyl]-1*H*-indazole (16 mg, 0.04 mmol, 1.0 eq), 1M BBr<sub>3</sub> in DCM (0.32 mL, 0.32 mmol, 8.0 eq) and DCM (1 mL) and the reaction stirred for 1 h. LC-MS analysis showed no conversion and therefore 1M BBr<sub>3</sub> in DCM (0.32 mL, 0.32 mmol, 8.0 eq) was

added and the reaction stirred for 17 h. LC-MS analysis showed the reaction to be complete. The reaction mixture was concentrated *in vacuo* and the resulting solid purified by reverse-phase ACC (20-28% MeCN–H<sub>2</sub>O–0.1% formic acid). Appropriate fractions were combined and concentrated *in vacuo* to a volume of ~3 mL until a white precipitate had formed which was then filtered. The title compound **171** (15 mg, 0.04 mmol, 96%) was collected as a white powder.

**<sup>1</sup>H NMR (500 MHz, DMSO-*d*<sub>6</sub>)**: 8.29 (1H, s, formate H), 8.04 (1H, d, *J* 8.5, 4-H), 7.87 (2H, d, *J* 8.8, 3'''-H and 5'''-H), 7.58 (1H, br.s, 7-H), 7.44-7.39 (1H, m, 5''-H), 7.27 (1H, d, *J* 8.5, 5-H), 7.08 (2H, d, *J* 8.8, 2'''-H and 6'''-H) 6.74 (1H, dd, *J* 8.4 and 2.3, 6''-H), 6.70 (1H, dd, *J* 12.8 and 2.3, 3''-H), 3.28-3.21 (4H, m, piperazine CH<sub>2</sub>), 3.04-2.97 (4H, m, piperazine CH<sub>2</sub>), OH and NHs not observed; **<sup>13</sup>C NMR (125 MHz, DMSO-*d*<sub>6</sub>)**: 164.3 (formate C=O), 159.6 (d, *J* 245.1, 2''-C), 158.5 (d, *J* 11.8, 4''-C), 150.3 (4'''-C), 143.1 (Ar-q), 141.9 (Ar-q), 133.1 (6-C), 131.3 (d, *J* 5.3, 5''-C), 127.3 (3'''-C and 5'''-C), 124.4 (Ar-q), 121.8 (d, *J* 2.3, 5-C), 120.6 (4-C), 118.7 (Ar-q), 118.7 (d, *J* 12.5, 1''-C), 115.5 (2'''-C and 6'''-C), 112.1 (d, *J* 2.7, 6''-C), 109.7 (d, *J* 3.1, 7-C), 103.0 (d, *J* 25.0, 3''-C), 47.5 (piperazine CH<sub>2</sub>), 44.1 (piperazine CH<sub>2</sub>);

**LC-MS (ES):** RT = 0.5-0.6 min, m/z = 389.44 (M+H<sup>+</sup>); **R<sub>f</sub>:** 0.06 (1% 7.0 M NH<sub>3</sub> in MeOH-DCM); **HPLC:** RT = 1.95 min; **m/z (ES+):** Found: 389.1775 (M+H<sup>+</sup>), C<sub>23</sub>H<sub>21</sub>FN<sub>4</sub>O requires *MH* 389.1772; **IR:**  $\nu_{\text{max}}/\text{cm}^{-1}$  (solid): 3267 (N-H), 2808, 2737, 2670, 2490, 1582; **M.pt:** >250 °C.

Preparation of 4-{4-[6-(3-fluoro-4-hydroxyphenyl)-1*H*-indazol-3-yl]phenyl}piperazin-1-ium formate

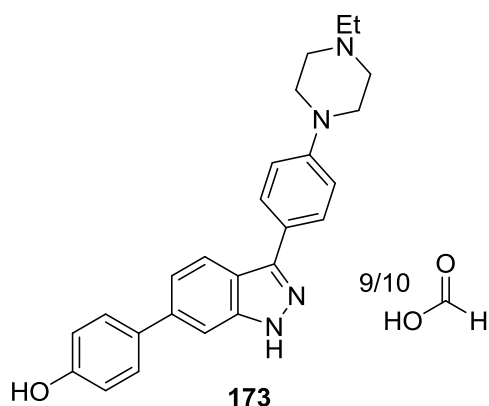


Synthesised using method D using 4-{4-[6-(3-fluoro-4-methoxyphenyl)-1*H*-indazol-3-yl]phenyl}piperazin-1-ium formate (33 mg, 0.082 mmol, 1.0 eq), 1M BBr<sub>3</sub> in DCM (0.65 mL, 0.65 mmol, 8.0 eq) and DCM (5 mL) and the reaction stirred for 16 h. The reaction mixture was reduced *in vacuo* and the crude product purified by reverse-phase

ACC (gradient 0-40% MeCN-H<sub>2</sub>O in 0.1% formic acid). The title compound 172 (9 mg, 0.022 mmol, 25%) was collected as an off-white solid.

**<sup>1</sup>H NMR (500 MHz, DMSO-*d*<sub>6</sub>):** 8.28 (1H, br.s, formate H), 8.02 (1H, d, *J* 8.5, 4-H), 7.88-7.84 (2H, m, 2''-H and 6'''-H), 7.67 (1H, s, 7-H), 7.54 (1H, dd, *J* 12.5 and 2.0, 2''-H), 7.42 (1H, dd, *J* 8.5 and 1.5, 5-H), 7.39 (1H, dd, *J* 8.5 and 1.5, 6''-H), 7.09-7.04 (3H, m, 3'''-H, 5'''-H and 5''-H), 3.24 (4H, app.t, *J* 4.5, piperazine CH<sub>2</sub>), 3.00 (4H, br.s, piperazine CH<sub>2</sub>), heteroatoms not observed; **<sup>13</sup>C NMR (100 MHz, DMSO-*d*<sub>6</sub>):** 164.2 (formate C=O), 151.8 (d, *J* 240.6, 3''-C), 150.1 (1'''-C), 145.1 (d, *J* 12.1, 4''-C), 143.5 (3-C), 142.8 (3'-C), 137.6 (6-C), 132.3 (d, *J* 6.3, 1''-C), 128.0 (2'''-C and 6'''-C), 125.7 (4'''-C), 123.6 (d, *J* 2.7, 6''-C), 121.6 (4-C), 120.6 (5-C), 119.5 (7'-C), 118.7 (d, *J* 3.2, 5''-C), 116.5 (3'''-C and 5'''-C), 115.1 (d, *J* 19.0, 2''-C), 107.8 (7-C), 46.1 (piperazine CH<sub>2</sub>), 43.4 (piperazine CH<sub>2</sub>); **LC-MS (ES):** RT = 0.5-0.6 min, m/z = 389.40 (M+H<sup>+</sup>); **R<sub>f</sub>:** 0.44 (20% 7.0 M NH<sub>3</sub> in MeOH-DCM); **HPLC:** RT = 1.94 min (99%); **m/z (ES+):** Found: 389.1789 (M+H<sup>+</sup>), C<sub>23</sub>H<sub>21</sub>FN<sub>4</sub>O requires *MH* 389.1772; **IR:**  $\nu_{\text{max}}/\text{cm}^{-1}$  (solid): 3288 (br.O-H), 2925, 1610; **M.pt:** 219.2-223.4 °C.

Preparation of 1-ethyl-4-{4-[6-(4-hydroxyphenyl)-1*H*-indazol-3-yl]phenyl}piperazin-1-ium formate

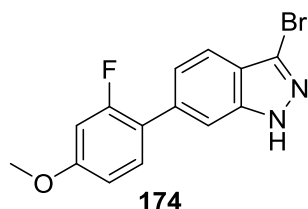


Synthesised using method D using 3-[4-(4-ethylpiperazin-1-yl)phenyl]-6-(4-methoxyphenyl)-1*H*-indazole (68 mg, 0.16 mmol, 1.0 eq), 1M BBr<sub>3</sub> in DCM (1.32 mL, 1.32 mmol, 8.0 eq) and DCM (3 mL) and the reaction stirred for 1 h. LC-MS analysis showed the reaction to be incomplete and therefore 1M BBr<sub>3</sub> in DCM (0.16 mL, 0.16 mmol, 1.0 eq) and the reaction stirred for five minutes. LC-MS analysis showed the reaction to be complete. Water (15 mL) was added and the reaction mixture transferred to a separating funnel. MeOH–DCM (1:1, 20 mL) was added to aid dissolution and the organic layer separated. The aqueous layer was extracted with DCM (2 × 15 mL) with addition of MeOH to aid dissolution of precipitate in aqueous layer. The combined organic layers were dried (MgSO<sub>4</sub>) and reduced *in vacuo* to reveal the crude product as a yellow solid. LC-MS analysis of the aqueous layer showed product and therefore the aqueous layer was reduced *in vacuo* and combined with the yellow solid. The crude product was purified by reverse-phase ACC (gradient 0-40% MeCN–H<sub>2</sub>O in 0.1% formic acid). The title compound 173 (41 mg, 0.10 mmol, 62%) was collected as an off-white solid.

**<sup>1</sup>H NMR (500 MHz, DMSO-*d*<sub>6</sub>):** 8.14 (1H, br.s, formate H), 8.01 (1H, d, *J* 8.5, 4-H), 7.85 (2H, d, *J* 8.5, 2'''-H and 6'''-H), 7.62 (1H, s, 7-H), 7.56 (2H, d, *J* 8.5, 2''-H and 6''-H), 7.39 (1H, d, *J* 8.5, 5-H), 7.07 (2H, d, *J* 8.5, 3'''-H and 5'''-H), 6.87 (2H, d, *J* 8.5, 3''-H and 5''-H), 3.23 (4H, app.t, *J* 4.5, piperazine CH<sub>2</sub>), 2.58 (4H, app.t, *J* 4.5, piperazine CH<sub>2</sub>), 2.44 (2H, q, *J* 7.0, CH<sub>2</sub>CH<sub>3</sub>), 1.06 (3H, t, *J* 7.0, CH<sub>2</sub>CH<sub>3</sub>), heteroatoms not observed; **<sup>13</sup>C NMR (100 MHz, DMSO-*d*<sub>6</sub>):** 163.7 (formate C=O), 157.7 (4''-C), 150.8 (1'''-C), 143.7 (3-C), 142.9 (3'-C), 138.8 (6-C), 131.6 (1''-C), 128.6 (2''-C and 6''-C), 127.9 (2'''-C and 6'''-C), 124.8 (4'''-C), 121.5 (4-C), 120.5 (5-C), 119.2 (7'-C), 116.3 (3''-C and 5''-C), 115.8 (3'''-C and 5'''-C), 107.3 (7-C), 52.6 (piperazine CH<sub>2</sub>), 52.0 (CH<sub>2</sub>CH<sub>3</sub>), 48.2 (piperazine CH<sub>2</sub>), 12.2 (CH<sub>2</sub>CH<sub>3</sub>); **LC-MS (ES):** RT = 0.5-0.5 min, *m/z* = 399.51 (M+H<sup>+</sup>); **R<sub>f</sub>:** 0.42 (12% MeOH–DCM); **HPLC:** RT = 1.92 min; ***m/z* (ES<sup>+</sup>):** Found: 399.2174 (M+H<sup>+</sup>), C<sub>25</sub>H<sub>26</sub>N<sub>4</sub>O requires

*MH* 399.2179; **IR**:  $\nu_{\max}/\text{cm}^{-1}$  (solid): 3173 (br.O-H), 2840, 2773, 2694, 1604; **M.pt**: >250 °C.

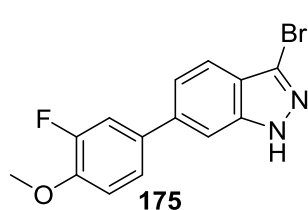
Preparation of 3-bromo-6-(2-fluoro-4-methoxyphenyl)-1*H*-indazole



Synthesised using method A using 3-bromo-6-iodo-1*H*-indazole (750 mg, 2.3 mmol, 1.0 eq), 2-fluoro-4-methoxyphenylboronic acid (395 mg, 2.32 mmol, 1.0 eq), Pd(dppf)Cl<sub>2</sub>•DCM (190 mg, 0.23 mmol, 0.1 eq), Na<sub>2</sub>CO<sub>3</sub> (738 mg, 7.0 mmol, 6.0 eq), dioxane (10 mL) and water (10 mL) and the reaction heated for 6 h. LC-MS analysis showed the reaction to be incomplete and therefore 2-fluoro-4-methoxyphenylboronic acid (79 mg, 0.47 mmol, 0.2 eq) and Pd(dppf)Cl<sub>2</sub>•DCM (190 mg, 0.23 mmol, 0.1 eq) were added and the reaction heated for a further 3 h. LC-MS analysis showed the reaction to be complete. The work up proceeded using the larger volumes of solvents and the organic solvent removed *in vacuo* to reveal a brown oil. The crude product was purified using column chromatography (gradient 20-30% EtOAc–petrol). The title compound 174 (182 mg, 0.57 mmol, 25%) was collected as colourless microcrystals.

**<sup>1</sup>H NMR (500 MHz, DMSO-*d*<sub>6</sub>)**: 13.46 (1H, br.s, NH), 7.66-7.62 (2H, m, 4-H and 7-H), 7.54 (1H, app.t, *J* 9.0, 6''-H), 7.36 (1H, dd, *J* 8.6 and 1.3, 5-H), 6.98 (1H, dd, *J* 13.0 and 2.5, 3''-H), 6.92 (1H, dd, *J* 8.6 and 2.5, 5''-H), 3.83 (3H, s, CH<sub>3</sub>), **<sup>13</sup>C NMR (125 MHz, DMSO-*d*<sub>6</sub>)**: 160.3 (d, *J* 11.1, 4''-C), 159.7 (d, *J* 245.0, 2''-C), 141.2 (7'-C), 134.4 (d, *J* 1.1, 6-C), 131.5 (d, *J* 5.0, 6''-C), 122.8 (d, *J* 2.6, 5-C), 121.1 (Ar-q), 120.2 (Ar-q), 120.1 (d, *J* 13.3, 1''-C), 119.2 (4-C), 111.0 (d, *J* 2.9, 5''-C), 110.2 (d, *J* 3.4, 7-C), 102.1 (d, *J* 26.6, 3''-C), 55.7 (CH<sub>3</sub>); **LC-MS (ES)**: RT = 0.6-0.7 min, *m/z* = 321.27 (M+H<sup>+</sup>); **R<sub>r</sub>**: 0.38 (4:1 petrol–EtOAc); **HPLC**: RT = 3.66 min; ***m/z* (ES-)**: Found: 318.9887 (M–H<sup>+</sup>), C<sub>14</sub>H<sub>9</sub>BrFN<sub>2</sub>O requires *M-H* 318.9887; **IR**:  $\nu_{\max}/\text{cm}^{-1}$  (solid): 3172 (N-H), 2938, 2883, 1624; **M.pt**: 194.1-196.0°C.

Preparation of 3-bromo-6-(3-fluoro-4-methoxyphenyl)-1*H*-indazole



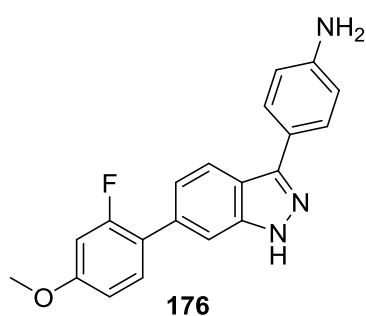
Synthesised using method A using 3-bromo-6-iodo-1*H*-indazole (750 mg, 2.32 mmol, 1.0 eq), 3-fluoro-4-methoxyphenylboronic acid (395 mg, 2.32 mmol, 1.0 eq), Pd(dppf)Cl<sub>2</sub>•DCM (190 mg, 0.23 mmol, 0.1 eq), Na<sub>2</sub>CO<sub>3</sub> (738 mg, 6.96 mmol, 3.0 eq), dioxane (10 mL) and water (10 mL) and the reaction heated for 6 h. LC-MS analysis showed the reaction to be incomplete and therefore



3-fluoro-4-methoxyphenylboronic acid (79 mg, 0.47 mmol, 0.2 eq) and Pd(dppf)Cl<sub>2</sub>•DCM (95 mg, 0.12 mmol, 0.05 eq) were added and the reaction heated for a further 9 h. LC-MS analysis showed the reaction to be complete. The work up proceeded using the larger volumes of solvents and the organic solvent removed *in vacuo* to reveal a brown oil. The crude product was purified using column chromatography (gradient 20-30% EtOAc–petrol). The title compound **175** (237 mg, 0.74 mmol, 32%) was collected as an off-white powder.

**<sup>1</sup>H NMR (500 MHz, DMSO-d<sub>6</sub>):** 13.47 (1H, br.s, NH), 7.75 (1H, s, 7-H), 7.65 (1H, dd, *J* 13.0 and 2.2, 2''-H), 7.62 (1H, d, *J* 8.5, 4-H), 7.57-7.54 (1H, m, 5''-H), 7.52 (1H, dd, *J* 8.5 and 1.4, 5-H), 7.28 (1H, app.t, *J* 8.9, 6''-H), 3.90 (3H, s, CH<sub>3</sub>), **<sup>13</sup>C NMR (125 MHz, DMSO-d<sub>6</sub>):** 151.7 (d, *J* 243.8, 3''-C), 146.9 (d, *J* 10.8, 4''-C), 141.6 (7'-C), 138.3 (d, *J* 1.8, 6-C), 132.9 (d, *J* 6.4, 1''-C), 123.4 (d, *J* 3.1, 5''-C), 121.3 (Ar-q), 121.0 (5-C), 120.2 (Ar-q), 119.6 (4-C), 114.6 (d, *J* 18.8, 2''-C), 114.2 (d, *J* 2.0, 6''-C), 107.9 (7-C), 56.1 (CH<sub>3</sub>); **LC-MS (ES):** RT = 0.6-0.7 min, *m/z* = 321.24 (M+H<sup>+</sup>); **R<sub>f</sub>:** 0.24 (7:3 petrol–EtOAc); **HPLC:** RT = 3.58 min; ***m/z* (ES<sup>+</sup>):** Found: 321.0042 (M+H<sup>+</sup>), C<sub>14</sub>H<sub>10</sub>BrFN<sub>2</sub>O requires *MH* 321.0033; **IR:ν<sub>max</sub>/cm<sup>-1</sup> (solid):** 3176, 3134, 2955, 2904, 1622; **M.pt:** 211.9-212.9 °C.

#### Preparation of 4-[6-(2-fluoro-4-methoxyphenyl)-1*H*-indazol-3-yl]aniline



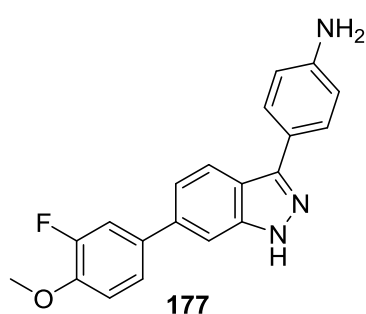
Synthesised using method A using 3-bromo-6-(2-fluoro-4-methoxyphenyl)-1*H*-indazole (170 mg, 0.53 mmol, 1.0 eq), 4-aminophenylboronic acid pinacol ester (232 mg, 1.06 mmol, 2.0 eq), Pd(dppf)Cl<sub>2</sub>•DCM (43 mg, 0.053 mmol, 0.1 eq), Na<sub>2</sub>CO<sub>3</sub> (168 mg, 1.59 mmol, 3.0 eq), dioxane (2.5 mL)

and water (2.5 mL) and the reaction heated for 3 h. The work up proceeded using the smaller volumes of solvents and the organic solvent removed *in vacuo* to reveal a yellow solid. The solid was purified using column chromatography (2% 7.0 M NH<sub>3</sub> in MeOH–DCM). The title compound **176** (115 mg, 0.36 mmol, 69%) was collected as a yellow powder.

**<sup>1</sup>H NMR (500 MHz, DMSO-d<sub>6</sub>):** 12.92 (1H, br.s, NH), 8.04 (1H, d, *J* 8.5, 4-H), 7.68 (2H, d, *J* 8.5, 3'''-H and 5'''-H), 7.59 (1H, s, 7-H), 7.54 (1H, app.t, *J* 9.0, 6''-H), 7.27 (1H, d, *J* 8.5, 5-H), 6.97 (1H, dd, *J* 12.9 and 2.5, 3''-H), 6.92 (1H, dd, *J* 8.5 and 2.5, 5''-H), 6.71 (2H, d, *J* 8.5, 2''' and 6'''-H), 5.27 (2H, br.s, NH<sub>2</sub>), 3.83 (3H, s, CH<sub>3</sub>);

**<sup>13</sup>C NMR (125 MHz, DMSO-*d*<sub>6</sub>):** 160.1 (d, *J* 11.3, 4''-C), 159.8 (d, *J* 243.8, 2''-C), 148.6 (Ar-q), 144.1 (3-C), 141.8 (7'-C), 132.6 (d, *J* 1.3, 6-C), 131.4 (d, *J* 5.3, 6''-C), 127.6 (3'''-C and 5'''-C), 121.5 (d, *J* 1.9, 5-C), 121.3 (Ar-q), 121.0 (4-C), 120.6 (d, *J* 13.5, 1''-C), 119.0 (3'-C), 114.0 (2'''-C and 6'''-C), 111.0 (d, *J* 2.9, 5''-C), 109.8 (d, *J* 3.3, 7-C), 102.1 (d, *J* 26.5, 3''-C), 55.7 (CH<sub>3</sub>); **LC-MS (ES):** RT = 0.5-0.6 min, *m/z* = 334.36 (M+H<sup>+</sup>); **R<sub>r</sub>:** 0.21 (2% 7.0 M NH<sub>3</sub> in MeOH-DCM); **HPLC:** RT = 2.31 min; ***m/z* (ES<sup>+</sup>):** Found: 356.1167 (M+Na<sup>+</sup>), C<sub>20</sub>H<sub>16</sub>BrN<sub>3</sub>NaO requires *MNa* 356.1170; **IR:ν<sub>max</sub>/cm<sup>-1</sup> (solid):** 3449 (N-H), 3386 (N-H), 2974, 1616; **M.pt:** 182.8-185.1 °C.

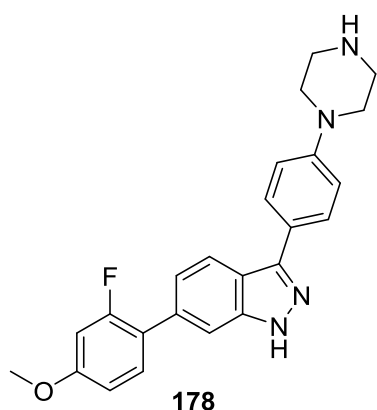
Preparation of 4-[6-(3-fluoro-4-methoxyphenyl)-1*H*-indazol-3-yl]aniline



Synthesised using method A using 3-bromo-6-(3-fluoro-4-methoxyphenyl)-1*H*-indazole (214 mg, 0.67 mmol, 1.0 eq), 4-aminophenylboronic acid pinacol ester (292 mg, 1.33 mmol, 2.0 eq), Pd(dppf)Cl<sub>2</sub>•DCM (54 mg, 0.067 mmol, 0.1 eq), Na<sub>2</sub>CO<sub>3</sub> (212 mg, 2.00 mmol, 3.0 eq), dioxane (2.5 mL) and water (2.5 mL) and the reaction heated for 3 h. LC-MS analysis showed the reaction to be incomplete and therefore 4-aminophenylboronic acid pinacol ester (73 mg, 0.33 mmol, 0.5 eq) and Pd(dppf)Cl<sub>2</sub>•DCM (27 mg, 0.033 mmol, 0.05 eq) were added and the reaction heated for 2 h. LC-MS analysis showed the reaction to be complete. The work up proceeded using the smaller volumes of solvents and the organic solvent removed *in vacuo* to reveal a brown oil. The crude oil was purified using column chromatography (2% MeOH-DCM) and a brown solid obtained. The brown solid was further purified by reverse-phase ACC (20-49% MeCN-H<sub>2</sub>O-0.1% formic acid). Appropriate fractions were combined and concentrated *in vacuo* to a volume of ~3 mL until a white precipitate had formed which was then filtered. The title compound 177 (108 mg, 0.32 mmol, 49%) was collected as an off-white powder. **<sup>1</sup>H NMR (500 MHz, DMSO-*d*<sub>6</sub>):** 12.93 (1H, br.s, indazole NH), 8.03 (1H, d, *J* 8.5, 4-H), 7.69-7.65 (3H, m, 7-H, 3'''-H and 5'''-H), 7.64 (1H, dd, *J* 12.9 and 2.2, 2''-H), 7.55 (1H, dd, *J* 8.6 and 1.4, 5''-H), 7.42 (1H, dd, *J* 8.5 and 1.4, 5-H), 7.28 (1H, app.t, *J* 8.9, 6''-H) 6.71 (2H, d, *J* 8.5, 2''' and 6'''-H), 5.27 (2H, br.s, NH<sub>2</sub>), 3.90 (3H, s, CH<sub>3</sub>), **<sup>13</sup>C NMR (125 MHz, DMSO-*d*<sub>6</sub>):** 151.8 (d, *J* 243.7, 3''-C), 148.5 (Ar-q), 146.6 (d, *J* 10.6, 4''-C), 144.0 (Ar-q), 142.2 (Ar-q), 136.5 (d, *J* 1.2, 6-C), 133.5 (d, *J* 6.4,

1''-C), 127.6 (3'''-C and 5'''-C), 123.1 (d,  $J$  3.2, 5''-C), 121.4 (4-C), 121.3 (Ar-q), 119.7 (5-C), 119.1 (Ar-q), 114.4 (d,  $J$  18.7, 2''-C), 114.2 (d,  $J$  2.1, 6''-C), 114.0 (2'''-C and 6'''-C), 107.4 (7-C), 56.1 ( $\underline{\text{C}}\text{H}_3$ ); **LC-MS (ES)**: RT = 0.6-0.6 min,  $m/z$  = 334.38 ( $\text{M}+\text{H}^+$ ); **R<sub>f</sub>**: 0.14 (2% 7.0 M  $\text{NH}_3$  in MeOH-DCM); **HPLC**: RT = 2.25 min; **m/z (ES+)**: Found: 334.1416 ( $\text{M}+\text{H}^+$ ),  $\text{C}_{20}\text{H}_{16}\text{FN}_3\text{O}$  requires *MH* 334.1356; **IR**:  $\nu_{\text{max}}/\text{cm}^{-1}$  (solid): 3380 (N-H), 3144, 3100, 2894, 1613; **M.pt**: 239.4-239.9 °C.

Preparation of 6-(2-fluoro-4-methoxyphenyl)-3-[4-(piperazin-1-yl)phenyl]-1H-indazole

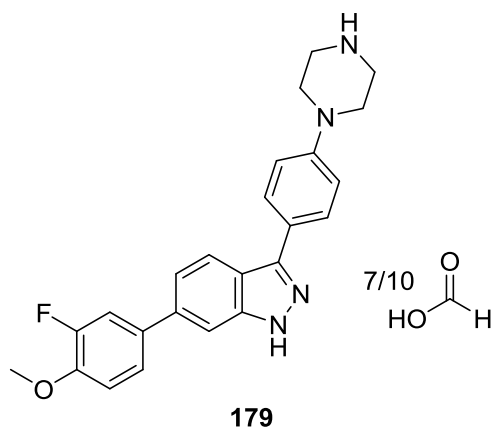


Synthesised using method F using 4-[6-(2-fluoro-4-methoxyphenyl)-1H-indazol-3-yl]aniline (106 mg, 0.34 mmol, 1.0 eq), bis-(2-chloroethyl)-amine hydrochloride (73 mg, 0.40 mmol, 1.2 eq) and  $\text{K}_2\text{CO}_3$  (112 mg, 0.81 mmol, 2.4 eq) and  $^t\text{BuOH}$  (5 mL) and the reaction heated for 159 h, monitoring using LC-MS. The reaction mixture was concentrated *in vacuo* and the solid was purified by column

chromatography (4% 7.0 M  $\text{NH}_3$  in MeOH-DCM). The title compound 178 (16 mg, 0.04 mmol, 12%) was collected as a brown solid. Due to the insufficient amount of material obtained only partial characterisation was carried out.

**LC-MS (ES)**: RT = 1.4-1.5 min,  $m/z$  = 334.18 ( $\text{M}+\text{H}^+$ ).

Preparation of 4-{4-[6-(3-fluoro-4-methoxyphenyl)-1H-indazol-3-yl]phenyl}piperazin-1-ium formate



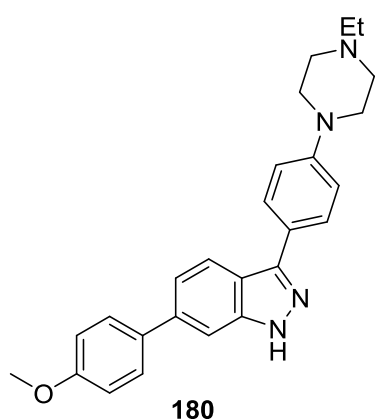
Synthesised using method F using 4-[6-(3-fluoro-4-methoxyphenyl)-1H-indazol-3-yl]aniline (98 mg, 0.29 mmol, 1.0 eq), bis(2-chloroethyl)amine hydrochloride (63 mg, 0.35 mmol, 1.2 eq),  $\text{K}_2\text{CO}_3$  (98 mg, 0.71 mmol, 2.4 eq) and  $^t\text{BuOH}$  (5 mL) and the reaction heated for 152 h. TLC analysis indicated the reaction to be incomplete and

therefore bis(2-chloroethyl)amine hydrochloride (10 mg, 0.056 mmol, 0.2 eq) was added and stirred at 100 °C for 3 h. LC-MS analysis indicated formation of several

other products and therefore the reaction was stopped. The reaction mixture was concentrated *in vacuo* to reveal a yellow solid. The solid was suspended in DCM–MeOH (1:1) and 2 M NaOH (30 mL) added and the organic layer separated. The aqueous layer was extracted with DCM–MeOH (1:1, 3 × 20 mL) and the combined organic layers washed with 2 M HCl (50 mL) and the organic layer separated. The aqueous layer was re-basified using 2 M NaOH and then extracted with DCM–MeOH (1:1, 3 × 20 mL) and the organic layers separated. LC-MS indicated the product in both organic layers and therefore were combined and reduced *in vacuo* to reveal an orange solid. The crude solid was dissolved in DMSO and the solution decanted from the insoluble impurities. The crude product was purified by reverse-phase ACC (gradient 5-50% MeCN–H<sub>2</sub>O in 0.1% formic acid) and an orange solid obtained. The orange solid was triturated with MeOH. The title compound 179 (17 mg, 0.042 mmol, 14%) was collected as a pink solid. The filtrate from the trituration was reduced *in vacuo* and collected as an orange solid (59 mg) and used without further purification.

**<sup>1</sup>H NMR (500 MHz, DMSO-*d*<sub>6</sub>):** 8.30 (1H, br.s, formate H), 8.07 (1H, d, *J* 8.5, 4-H), 7.89 (2H, d, *J* 8.5, 2''-H and 6''-H), 7.74 (1H, s, 7-H), 7.66 (1H, dd, *J* 7.5 and 1.5, 5''-H), 7.57 (1H, d, *J* 8.5, 6''-H), 7.48 (1H, d, *J* 8.5, 5-H), 7.29 (1H, app.t, *J* 8.5, 2''-H), 7.10 (2H, d, *J* 8.5, 3''-H and 5''-H), 3.91 (3H, s, CH<sub>3</sub>), 3.26 (4H, s, piperazine CH<sub>2</sub>), 3.02 (4H, s, piperazine CH<sub>2</sub>), NHs not observed; **<sup>13</sup>C NMR (100 MHz, DMSO-*d*<sub>6</sub>):** 152.3 (d, *J* 243.6, 3''-C), 151.0 (1''-C), 147.2 (d, *J* 10.6, 4''-C), 143.7 (3'-C), 142.8 (3-C), 137.2 (6-C), 133.9 (d, *J* 6.5, 1''-C), 127.9 (2''-C and 6''-C), 124.9 (4''-C), 123.7 (d, *J* 3.1, 6''-C), 121.7 (4-C), 120.6 (5-C), 119.7 (7'-C), 116.0 (3''-C and 5''-C), 115.0 (d, *J* 18.9, 2''-C), 114.8 (d, *J* 1.8, 5''-C), 108.1 (7-C), 56.6 (CH<sub>3</sub>), 48.2 (piperazine CH<sub>2</sub>), 44.8 (piperazine CH<sub>2</sub>), formate C=O not observed; **LC-MS (ES):** RT = 0.5-0.6 min, *m/z* = 403.47 (M+H<sup>+</sup>); **R<sub>f</sub>:** 0.13 (4:1, EtOAc–7.0 M NH<sub>3</sub> in MeOH); **HPLC:** RT = 2.39 min; ***m/z* (ES<sup>+</sup>):** Found: 403.1927 (M+H<sup>+</sup>), C<sub>24</sub>H<sub>23</sub>FN<sub>4</sub>O requires *MH* 403.1929; **IR: *v*<sub>max</sub>/cm<sup>-1</sup> (solid):** 3168 (N-H), 2822, 1611; **M.pt:** 191.3-193.4 °C.

Preparation of 3-[4-(4-ethylpiperazin-1-yl)phenyl]-6-(4-methoxyphenyl)-1H-indazole

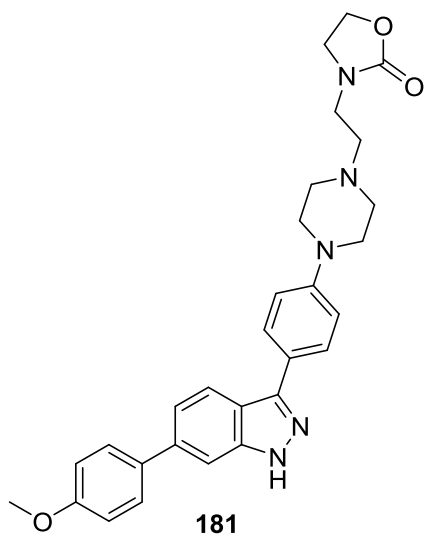


Synthesised using method B using 6-(4-methoxyphenyl)-3-[4-(piperazin-1-yl)phenyl]-1H-indazole (100 mg, 0.26 mmol, 1.0 eq), ethanal (18  $\mu$ L, 0.31 mmol, 1.2 eq), AcOH (1 drop), STAB (88 mg, 0.42 mmol, 1.6 eq) and DCM (3 mL) and the reaction stirred for 1 h. LC-MS analysis showed the reaction to be incomplete and therefore ethanal (9  $\mu$ L, 0.15 mmol, 0.6 eq) was added and the reaction stirred for

30 minutes. STAB (88 mg, 0.42 mmol, 1.6 eq) was added and the reaction stirred for 1.5 h. LC-MS analysis showed the reaction to be complete. Water (10 mL) was added and the resulting precipitate filtered. The filtrate was extracted with DCM (2  $\times$  15 mL) and the combined organic layers washed with brine (20 mL), dried (MgSO<sub>4</sub>) and reduced *in vacuo* to reveal a colourless semi-solid. The filtered solid was dissolved in MeOH–DCM (1:1) and combined with the semi-solid and purified by column chromatography (3% 7.0 M NH<sub>3</sub> in MeOH–DCM). The title compound 180 (90 mg, 0.22 mmol, 84%) was collected as a colourless semi-solid.

**<sup>1</sup>H NMR (500 MHz, CDCl<sub>3</sub>):** 11.89 (1H, br.s, indazole NH), 8.01 (1H, d, *J* 9.0, 4-H), 7.96 (2H, d, *J* 8.5, 2'''-H and 6'''-H), 7.51 (2H, d, *J* 9.0, 2''-H and 6''-H), 7.40-7.37 (2H, m, 5-H and 7-H), 7.06 (2H, d, *J* 8.5, 3'''-H and 5'''-H), 6.98 (2H, d, *J* 8.5, 3''-H and 5''-H), 3.85 (3H, s, OCH<sub>3</sub>), 3.27 (4H, app.t, *J* 5.0, piperazine CH<sub>2</sub>), 2.63 (4H, app.t, *J* 5.0, piperazine CH<sub>2</sub>), 2.50 (2H, q, *J* 7.0, CH<sub>2</sub>CH<sub>3</sub>), 1.16 (3H, t, *J* 7.0, CH<sub>2</sub>CH<sub>3</sub>); **<sup>13</sup>C NMR (100 MHz, CDCl<sub>3</sub>):** 159.2 (4''-C), 151.1 (1'''-C), 145.5 (3-C), 142.6 (3'-C), 139.6 (6-C), 133.7 (1''-C), 128.6 (2''-C and 6''-C), 128.4 (2'''-C and 6'''-C), 124.7 (4'''-C), 121.4 (4-C), 121.0 (5-C), 119.8 (7'-C), 116.0 (3'''-C and 5'''-C), 114.3 (3''-C and 5''-C), 107.7 (7-C), 55.4 (OCH<sub>3</sub>), 52.8 (piperazine CH<sub>2</sub>), 52.4 (CH<sub>2</sub>CH<sub>3</sub>), 48.7 (piperazine CH<sub>2</sub>), 12.0 (CH<sub>2</sub>CH<sub>3</sub>); **LC-MS (ES):** RT = 0.6-0.7 min, m/z = 413.49 (M+H<sup>+</sup>); **R<sub>f</sub>:** 0.43 (5% 7.0 M NH<sub>3</sub> in MeOH–DCM); **HPLC:** RT = 2.43 min; **m/z (ES<sup>+</sup>):** Found: 413.2332 (M+H<sup>+</sup>), C<sub>26</sub>H<sub>28</sub>N<sub>4</sub>O requires *MH* 413.2336; **IR:**  $\nu_{\max}/\text{cm}^{-1}$  (solid): 3168, 3012, 2819, 1608.

Preparation of 3-[2-(4-{4-[6-(4-methoxyphenyl)-1*H*-indazol-3-yl]phenyl}piperazin-1-yl)ethyl]-1,3-oxazolidin-2-one

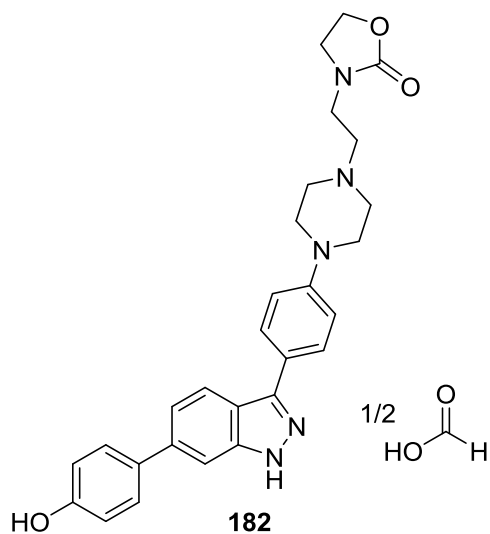


Synthesised as a side product using the same conditions as seen in the preparation of 6-(4-methoxyphenyl)-3-[4-(piperazin-1-yl)phenyl]-1*H*-indazole (**166**). A second compound was isolated from the column. The title compound 181 (193 mg, 0.39 mmol, 17%) was collected as an off-white solid.

**<sup>1</sup>H NMR (500 MHz, DMSO-*d*<sub>6</sub>):** 13.01 (1H, br.s, indazole NH), 8.06 (1H, d, *J* 8.5, 4-H), 7.85 (2H, d, *J* 8.5, 2''-H and 6''-H), 7.68 (2H, d,

*J* 8.5, 2''-H and 6''-H), 7.66 (1H, s, 7-H), 7.42 (1H, d, *J* 8.5, 5-H), 7.09-7.04 (4H, m, 3''-H, 5''-H, 3'''-H and 5'''-H), 4.24 (2H, app.t, *J* 7.0, oxazolidinone OCH<sub>2</sub>), 3.81 (3H, s, CH<sub>3</sub>), 3.61 (2H, app.t, *J* 7.0, oxazolidinone NCH<sub>2</sub>), 3.32 (2H, t, *J* 6.5, piperazine-CH<sub>2</sub>CH<sub>2</sub>-oxazolidinone), 3.20 (4H, app.t, *J* 4.0, piperazine CH<sub>2</sub>), 2.59 (4H, app.t, *J* 4.0, piperazine CH<sub>2</sub>), 2.53 (2H, t, *J* 6.5, piperazine-CH<sub>2</sub>CH<sub>2</sub>-oxazolidinone); **<sup>13</sup>C NMR (100 MHz, DMSO-*d*<sub>6</sub>):** 159.4 (4''-C), 158.4 (oxazolidinone C=O), 150.9 (1'''-C), 143.8 (3-C), 142.8 (3'-C), 138.8 (6-C), 133.2 (1''-C), 128.7 (2''-C and 6''-C), 127.9 (3'''-C and 5'''-C), 124.7 (4'''-C), 121.6 (4-C), 120.6 (5-C), 119.4 (7'-C), 115.8 (2'''-C and 6'''-C), 114.9 (3''-C and 5''-C), 107.6 (7-C), 62.1 (oxazolidinone OCH<sub>2</sub>), 55.7 (OCH<sub>3</sub>), 55.4 (piperazine-CH<sub>2</sub>CH<sub>2</sub>-oxazolidinone), 53.0 (piperazine CH<sub>2</sub>), 48.5 (piperazine CH<sub>2</sub>), 44.8 (oxazolidinone NCH<sub>2</sub>), 41.1 (piperazine-CH<sub>2</sub>CH<sub>2</sub>-oxazolidinone); **LC-MS (ES):** RT = 0.6-0.6 min, *m/z* = 498.61 (M+H<sup>+</sup>); **R<sub>f</sub>:** 0.37 (5% 7.0 M NH<sub>3</sub> in MeOH-DCM); **HPLC:** RT = 1.94 min; ***m/z* (ES<sup>+</sup>):** Found: 498.2498 (M+H<sup>+</sup>), C<sub>29</sub>H<sub>33</sub>N<sub>5</sub>O<sub>4</sub> requires *MH* 498.2498; **IR:** *v*<sub>max</sub>/cm<sup>-1</sup> (solid): 3234 (N-H), 2939, 2833, 1723 (C=O), 1608; **M.pt:** >250 °C.

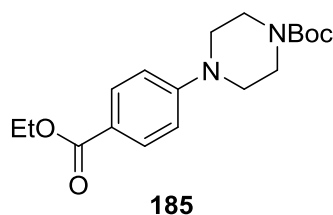
Preparation of 4-{4-[6-(4-hydroxyphenyl)-1H-indazol-3-yl]phenyl}-1-[2-(2-oxo-1,3-oxazolidin-3-yl)ethyl]piperazin-1-ium formate



Synthesised using method D using 3-[2-(4-[4-[6-(4-methoxyphenyl)-1H-indazol-3-yl]phenyl]piperazin-1-yl)ethyl]-1,3-oxazolidin-2-one (70 mg, 0.14 mmol, 1.0 eq), 1 M BBr<sub>3</sub> in DCM (1.13 mL, 1.13 mmol, 8.0 eq) and DCM (3 mL) and the reaction stirred for 45 minutes. MeOH (10 mL) was added and the reaction mixture reduced *in vacuo* to reveal the crude product as an orange solid. The crude product was purified by

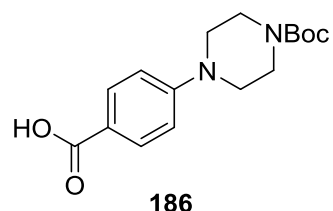
reverse phase ACC (gradient 0-40% MeCN–H<sub>2</sub>O in 0.1% formic acid) and an orange glassy solid obtained. The product was further purified by column chromatography (gradient 2-5% MeOH–DCM). The title compound 182 (14 mg, 0.029 mmol, 21%) was collected as a colourless solid.

**<sup>1</sup>H NMR (500 MHz, DMSO-*d*<sub>6</sub>):** 12.98 (1H, br.s, indazole NH), 8.17 (1H, br.s, formate H), 8.01 (1H, d, *J* 8.5, 4-H), 7.84 (2H, d, *J* 8.5, 2'''-H and 6'''-H), 7.61 (1H, s, 7-H), 7.58-7.54 (2H, m, 2''-H and 6''-H), 7.39 (1H, dd, *J* 8.5 and 1.5, 5-H), 7.07 (2H, d, *J* 8.5, 3'''-H and 5'''-H), 6.89-6.86 (2H, m, 3''-H and 5''-H), 4.26-4.22 (2H, m, oxazolidinone OCH<sub>2</sub>), 3.62-3.59 (2H, m, oxazolidinone NCH<sub>2</sub>), 3.32 (2H, app.t, *J* 6.0, piperazine-CH<sub>2</sub>CH<sub>2</sub>-oxazolidinone), 3.20 (4H, app.t, *J* 5.0, piperazine CH<sub>2</sub>), 2.58 (4H, app.t, *J* 5.0, piperazine CH<sub>2</sub>), 2.54-2.50 (2H, m, piperazine-CH<sub>2</sub>CH<sub>2</sub>-oxazolidinone); **<sup>13</sup>C NMR (125 MHz, DMSO-*d*<sub>6</sub>):** 163.8 (formate C=O), 158.4 (oxazolidinone C=O), 157.7 (4''-C), 150.9 (1'''-C), 143.7 (3-C), 142.9 (3'-C), 138.8 (6-C), 131.6 (1''-C), 128.6 (2''-C and 6''-C), 127.8 (2'''-C and 6'''-C), 124.7 (4'''-C), 121.5 (4-C), 120.5 (5-C), 119.2 (7'-C), 116.3 (3''-C and 5''-C), 115.8 (3'''-C and 5'''-C), 107.3 (7-C), 62.1 (oxazolidinone OCH<sub>2</sub>), 55.4 (piperazine-CH<sub>2</sub>CH<sub>2</sub>-oxazolidinone), 53.0 (piperazine CH<sub>2</sub>), 48.5 (piperazine CH<sub>2</sub>), 44.8 (oxazolidinone NCH<sub>2</sub>), 41.1 (piperazine-CH<sub>2</sub>CH<sub>2</sub>-oxazolidinone); **LC-MS (ES):** RT = 0.5-0.6 min, *m/z* = 484.56 (M+H<sup>+</sup>); **R<sub>r</sub>:** 0.38 (12% MeOH–DCM); **HPLC:** RT = 1.94 min (96%); ***m/z* (ES<sup>+</sup>):** Found: 484.2345 (M+H<sup>+</sup>), C<sub>28</sub>H<sub>29</sub>N<sub>5</sub>O<sub>3</sub> requires *MH* 484.2343; **IR:  $\nu_{\max}$ /cm<sup>-1</sup> (solid):** 3270 (br. O-H), 2824, 1705 (C=O); **M.pt:** >250 °C.

Preparation of *tert*-butyl 4-[4-(ethoxycarbonyl)phenyl]piperazine-1-carboxylate

Ethyl-4-fluorobenzoate (4.36 mL, 29.7 mmol, 1.0 eq) was dissolved in DMSO (40 mL) and  $K_2CO_3$  (12.3 g, 89.2 mmol, 3.0 eq) and 1-BOC-piperazine (6.92 g, 37.1 mmol, 1.25 eq) were added and the reaction stirred at 120 °C for 21 h. TLC analysis showed the reaction to be incomplete and therefore 1-BOC-piperazine (1.11 g, 5.94 mmol, 0.2 eq) was added and the reaction stirred for 2 h. TLC showed no change and therefore the reaction was stopped. The reaction mixture was cooled to 20 °C and water (100 mL) added. The solution was extracted with EtOAc (3 × 100 mL) and the combined organic layers washed with brine (100 mL), dried ( $MgSO_4$ ) and reduced *in vacuo* to reveal an off-white semi-solid. The crude product was purified using column chromatography (4:1 hexane–EtOAc). The title compound 185 (4.21 g, 12.6 mmol, 42%) was collected as a fluffy colourless solid.

**$^1H$  NMR (500 MHz,  $CDCl_3$ ):** 7.95-7.92 (2H, m, 3-H and 5-H), 6.88-6.85 (2H, m, 2-H and 6-H), 4.33 (2H, q,  $J$  7.0,  $CH_2CH_3$ ), 3.58 (4H, app.t,  $J$  5.5, piperazine 2-H and 6-H), 3.30 (4H, app.t,  $J$  5.5, piperazine 3-H and 5-H), 1.49 (9H, s,  $^tBu$   $CH_3$ ) 1.37 (3H, t,  $J$  7.0,  $CH_2CH_3$ );  **$^{13}C$  NMR (100 MHz,  $CDCl_3$ ):** 166.6 (ester C=O), 154.7 (carbamate C=O), 154.0 (1-C), 131.2 (3-C and 5-C), 120.7 (4-C), 114.0 (2-C and 6-C), 80.1 ( $C(CH_3)_3$ ), 60.4 ( $CH_2CH_3$ ), 47.7 (piperazine 3-C and 5-C), 43.2 (piperazine 2-H and 6-H), 28.4 ( $^tBu$   $CH_3$ ), 14.4 ( $CH_2CH_3$ ); **LC-MS (ES):** RT = 0.7-1.0 min,  $m/z$  = 279.36 ( $M-^tBu+H^+$ ); **R<sub>f</sub>:** 0.34 (4:1 petrol–EtOAc); **HPLC:** RT = 3.08 min;  **$m/z$  (ES+):** Found: 357.1785 ( $M+Na^+$ ),  $C_{18}H_{26}N_2NaO_4$  requires  $MH$  257.1785; **IR:**  $\nu_{max}/cm^{-1}$  (solid): 2977, 2931, 1689 (C=O), 1609 (C=O); **M.pt:** 123.6-124.9 °C.

Preparation of 4-[4-[(*tert*-butoxy)carbonyl]piperazin-1-yl]benzoic acid

*Tert*-butyl 4-[4-(ethoxycarbonyl)phenyl]piperazine-1-carboxylate (2.09g, 6.26 mmol, 1.0 eq) was suspended in 2M NaOH (30 mL) and  $LiOH \cdot H_2O$  (1.57g, 37.5 mmol, 6.0 eq) was added. THF (10 mL) was added to aid dissolution and the reaction stirred at 130 °C for 16 h. LC-MS analysis indicated the reaction to be complete. The reaction mixture was cooled to 20 °C and acidified to pH 4.0 (2 M HCl). EtOAc (60 mL) was added and the organic layer separated and the aqueous layer extracted with EtOAc (3 × 40 mL). The combined organic layers were

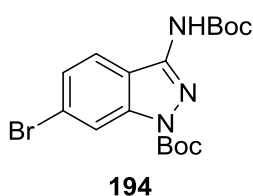


dried (MgSO<sub>4</sub>) and reduced *in vacuo* to reveal an off-white solid. The crude solid was triturated with EtOAc and filtered. The title compound 186 (1.08 g, 3.53 mmol, 56%) was collected as shiny colourless flakes.

**<sup>1</sup>H NMR (500 MHz, DMSO-d<sub>6</sub>):** 12.27 (1H, br.s, OH), 7.78-7.75 (2H, m, 3-H and 5-H), 6.96-6.93 (2H, m, 2-H and 6-H), 3.46-3.43 (4H, m, 2'-H and 6'-H), 3.30-3.27 (4H, m, 3'-H and 5'-H), 1.41 (9H, s, <sup>t</sup>Bu CH<sub>3</sub>); **<sup>13</sup>C NMR (125 MHz, DMSO-d<sub>6</sub>):** 167.2 (Ar C=O), 153.8 (1-C), 153.5 (BOC C=O), 130.8 (3-C and 5-C), 119.6 (4-C), 113.6 (2-C and 6-C), 79.0 (C(CH<sub>3</sub>)<sub>3</sub>), 46.6 (2'-C and 6'-C), 43.5 (3'-C and 5'-C)\*, 28.0 (<sup>t</sup>Bu CH<sub>3</sub>); **LC-MS (ES):** RT = 0.5-0.6 min, m/z = 305.42 (M-H<sup>+</sup>); **R<sub>f</sub>:** 0.32 (1:1 EtOAc–hexane in 2% AcOH); **HPLC:** RT = 2.83 min; **m/z (ES+):** Found: 305.1516 (M-H<sup>+</sup>), C<sub>16</sub>H<sub>22</sub>N<sub>2</sub>O<sub>4</sub> requires *MH* 305.1507; **IR:** ν<sub>max</sub>/cm<sup>-1</sup> (solid): 2973, 2872, 1670 (C=O); **M.pt:** >250 °C.

\*Carbon peak not visible on <sup>13</sup>C NMR but present on HSQC – peak broadening due to the deshielding effect of the BOC group carbonyl.

Preparation of *tert*-butyl 6-bromo-3-[[*tert*-butoxy]carbonyl]amino}-1*H*-indazole-1-carboxylate

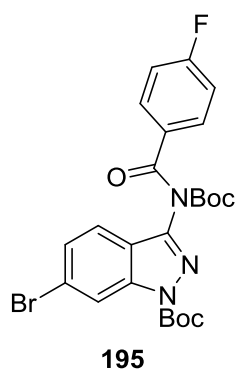


3-Amino-6-bromo-1*H*-indazole (1.59 g, 7.47 mmol, 1.0 eq) and DMAP (320 mg, 2.61 mmol, 0.35 eq) were suspended in dry THF (20 mL) at 0 °C and stirred for five minutes. BOC anhydride (1.80 mL, 7.85 mmol, 1.05 eq) was added dropwise over ten minutes and the reaction allowed to warm to 20 °C and stirred for 2.5 h. LC-MS analysis showed majority product to be mono-protected with small amounts of the starting material, the bis-protected and the tri-protected compounds. The reaction was cooled to 0 °C and BOC anhydride (1.80 mL, 7.85 mmol, 1.05 eq) added dropwise over ten minutes and the reaction allowed to warm to 20 °C and stirred for 15 h. LC-MS analysis showed no starting material or mono-protected compound however, showed a 1:1 ratio of the bis-protected and tri-protected compound. The reaction mixture was reduced *in vacuo* and suspended in EtOAc (200 mL) and the organic layer washed with 1 M HCl (2 × 20 mL), saturated NaHCO<sub>3</sub> (40 mL) and brine (40 mL). The solution was dried (MgSO<sub>4</sub>) and reduced *in vacuo* to reveal a yellow oil. The crude product was purified by column chromatography (95:5 Hexane–EtOAc) and a colourless oil obtained. The oil was dissolved in DCM and reduced *in vacuo*. The title

compound **194** (589 mg, 1.43 mmol, 19%) was collected as a glassy fluffy colourless solid.

**<sup>1</sup>H NMR (500 MHz, CDCl<sub>3</sub>):** 8.36 (1H, br.s, 7-H), 8.02 (1H, d, *J* 9.0, 4-H), 7.41 (1H, dd, *J* 9.0 and 1.5, 5-H), 7.20 (1H, br.s, NH), 1.71 (9H, s, <sup>t</sup>Bu CH<sub>3</sub>), 1.54 (9H, s, <sup>t</sup>Bu CH<sub>3</sub>); **<sup>13</sup>C NMR (125 MHz, CDCl<sub>3</sub>):** 152.5 (C=O), 148.8 (C=O), 145.0 (Ar-q), 141.8 (Ar-q), 126.8 (5-C), 124.8 (4-C), 124.3 (Ar-q), 118.0 (Ar-q), 117.6 (7-C), 85.3 (C(CH<sub>3</sub>)<sub>3</sub>), 82.0 (C(CH<sub>3</sub>)<sub>3</sub>), 28.2 (<sup>t</sup>Bu CH<sub>3</sub>), 28.2 (<sup>t</sup>Bu CH<sub>3</sub>); **LC-MS (ES):** RT = 0.8-0.8 min, *m/z* = 412.32 (M+H<sup>+</sup>); **R<sub>r</sub>:** 0.28 (4:1 EtOAc–hexane); **HPLC:** RT = 2.61 min; ***m/z* (ES+):** Found: 434.0699 (M+Na<sup>+</sup>), C<sub>17</sub>H<sub>22</sub>BrN<sub>3</sub>O<sub>4</sub> requires *MH* 434.0686; **IR: ν<sub>max</sub>/cm<sup>-1</sup> (solid):** 3236 (N-H), 2978, 2933, 1731 (C=O); **M.pt:** 95.0-102.7 °C.

Preparation of *tert*-butyl 6-bromo-3-{N-[(*tert*-butoxy)carbonyl]4-fluorobenzamido}-1*H*-indazole-1-carboxylate

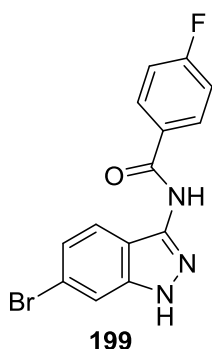


Synthesised using method E using *tert*-butyl 6-bromo-3-[(*tert*-butoxy)carbonyl]amino}-1*H*-indazole-1-carboxylate (560 mg, 1.36 mmol, 1.0 eq), freshly distilled 4-fluorobenzoyl chloride (193 μL, 1.63 mmol, 1.2 eq), DIPEA (473 μL, 2.72 mmol, 2.0 eq) and DCM (30 mL) and the reaction heated at 60 °C for 70 h. LC-MS analysis showed the reaction to be complete. The reaction mixture was cooled to 20 °C and 1.0 M HCl (20 mL) was added and the organic layer separated. The aqueous layer was extracted with DCM (2 × 20 mL) and the combined organic layers combined and washed with 1.0 M NaOH (20 mL), brine (40 mL) and dried (MgSO<sub>4</sub>). The filtrate was reduced *in vacuo* to reveal the crude product as a fluffy off-white solid (705 mg). The crude product was purified by column chromatography (95:5 hexane–EtOAc) and a colourless glassy solid obtained. The solid was dissolved in DCM and reduced *in vacuo*. The title compound **195** (496 mg, 0.93 mmol, 68%) was collected as a colourless fluffy solid.

**<sup>1</sup>H NMR (500 MHz, CDCl<sub>3</sub>):** 8.41 (1H, br.s, 7-H), 7.87-7.84 (2H, m, 2''-H and 6''-H), 7.47 (1H, dd, *J* 8.5 and 1.5, 5-H), 7.40 (1H, d, *J* 8.5, 4-H), 7.16-7.12 (2H, m, 3''-H and 5''-H), 1.70 (9H, s, <sup>t</sup>Bu CH<sub>3</sub>), 1.33 (9H, s, <sup>t</sup>Bu CH<sub>3</sub>); **<sup>13</sup>C NMR (125 MHz, CDCl<sub>3</sub>):** 170.2 (amide C=O), 165.3 (d, *J* 254.4, 4''-C), 151.5 (BOC C=O), 148.5 (BOC C=O), 145.1 (3-C), 141.5 (3'-C), 131.3 (d, *J* 9.3, 2''-C and 6''-C), 131.3 (Ar-q), 127.7 (5-C), 124.0 (Ar-q), 120.7 (Ar-q), 120.6 (4-C), 118.4 (7-C), 115.6 (d, *J* 22.3,

3''-C and 5''-C), 85.9 (C(CH<sub>3</sub>)<sub>3</sub>), 84.8 (C(CH<sub>3</sub>)<sub>3</sub>), 28.1 (<sup>t</sup>Bu CH<sub>3</sub>), 27.6 (<sup>t</sup>Bu CH<sub>3</sub>); **LC-MS (ES)**: RT = 0.8-0.9 min, m/z = 536.40 (MBr<sup>81+</sup>); **R<sub>f</sub>**: 0.47 (4:1 petrol–EtOAc); **HPLC**: RT = 2.79 min (88%-degrades overtime); **m/z (ES+)**: Found: 534.1014 (M+H<sup>+</sup>), C<sub>24</sub>H<sub>25</sub>BrFN<sub>3</sub>O<sub>5</sub> requires *MH* 534.1034; **IR:ν<sub>max</sub>/cm<sup>-1</sup> (solid)**: 2979, 1738 (C=O), 1699 (C=O); **M.pt**: 103.3-109.6 °C.

Preparation of N-(6-bromo-1*H*-indazol-3-yl)-4-fluorobenzamide



Synthesised using method C using *tert*-butyl 6-bromo-3-{N-[(*tert*-butoxy)carbonyl]4-fluorobenzamido}-1*H*-indazole-1-carboxylate (300 mg, 0.56 mmol, 1.0 eq), TFA (5 mL) and DCM (5 mL) and the reaction stirred for 30 minutes. The crude product was used without purification. The title compound 199 was collected as a colourless solid (181 mg, 0.54 mmol, 97%).

**<sup>1</sup>H NMR (500 MHz, DMSO-*d*<sub>6</sub>)**: 12.92 (1H, br.s, indazole NH), 10.89 (1H, br.s, amide NH), 8.16-8.12 (2H, m, 2''-H and 6''-H), 7.72-7.69 (2H, m, 4-H and 7-H), 7.39-7.34 (2H, m, 3''-H and 5''-H), 7.21 (1H, dd, *J* 9.0 and 1.5, 5-H); **<sup>13</sup>C NMR (125 MHz, DMSO-*d*<sub>6</sub>)**: 164.5 (amide C=O), 164.3 (d, *J* 249.5, 4''-C), 141.7 (3'-C), 140.5 (3-C), 130.7 (d, *J* 9.2, 2''-C and 6''-C), 130.1 (d, *J* 2.8, 1''-C), 123.9 (4-C), 122.8 (5-C), 119.9 (7'-C), 115.8 (6-C), 115.4 (d, *J* 21.8, 3''-C and 5''-C), 112.7 (7-C); **LC-MS (ES)**: RT = 0.5-0.6 min, m/z = 335.48 (M+H<sup>+</sup>); **R<sub>f</sub>**: 0.13 (4:1 petrol–EtOAc); **HPLC**: RT = 2.94 min; **m/z (ES+)**: Found: 333.9987 (M+H<sup>+</sup>), C<sub>14</sub>H<sub>9</sub>BrFN<sub>3</sub>O requires *MH* 333.9958; **IR:ν<sub>max</sub>/cm<sup>-1</sup> (solid)**: 3337 (N-H), 3230 (N-H), 2053, 1673 (C=O); **M.pt**: >250 °C

## 6.2 Biochemical Experimental

### 6.2.1 General Methods and Equipment

Media and appropriate equipment were sterilised using either a Classic Prestige Medical bench-top autoclave or an LTE Touchclave Ecotech autoclave. Sterile conditions were maintained using a bench-top Bunsen burner. Bacterial cultures were incubated in a MaxQ 6000 or MaxQ 8000 Thermo Scientific incubator or an Infors HT orbital shaker. Lysogeny Broth (LB)-agar plates were incubated in a Gallenkamp economy size 1 incubator.

Centrifugation was performed using either: an Eppendorf 5424R bench-top centrifuge, an Eppendorf 5810R bench-top centrifuge, or a Sorvall Lynx 6000 centrifuge. Sonication of cell mixtures was carried out using a Fischerbrand™ Model 120 Sonic Dismembrator. Purification of protein was performed on either an Äkta Pure protein purification system or an Äkta Prime. Resin/protein mixtures were rotated and mixed using a roller mixer SRT6 apparatus. Spectrophotometric readings were measured using either a Jenway 6320D spectrophotometer, a Nanodrop 2000, or Genesys 6 spectrophotometer. Sodium dodecyl sulphate-polyacrylamide gel electrophoresis (SDS-PAGE) was carried out using a Bio-Rad mini protean tetra system and polyacrylamide gels imaged using a Syngene G:Box apparatus. Concentration of protein was carried out using a 10K Daltons (Da) molecular weight cut-off (MWCO) Amicon® Ultra-4 Centrifugal Filter device. Mass spectrometry (MS) analysis of proteins was carried out using a Synapt G2S Q-IMT-Time of flight (TOF) mass spectrometer coupled to a nano ACQUITY ultra performance liquid chromatography (UPLC) LC-MS apparatus. Analytical grade reagents were supplied from commercial sources and used without further purification. Solutions were made using 18.2 MΩ H<sub>2</sub>O and pH of buffers adjusted using 2 M NaOH, concentrated NaOH, 2 M HCl and concentrated HCl.

### 6.2.2 Media and Buffers

Media and buffers were made in-house unless otherwise stated. Buffers used in purification of protein were filtered through a 0.22 µm membrane using Stericup and Steritop vacuum-driven filtration systems. Media was sterilised by autoclave at 121 °C for 45 minutes, buffers were used without sterilisation.

**6.2.2.1 Growth Media**

- Terrific broth (TB) media: 12 g/L Tryptone, 24 g/L Yeast extract, 9.4 g/L K<sub>2</sub>HPO<sub>4</sub>, 2.2 g/L KH<sub>2</sub>PO<sub>4</sub>, Glycerol 4 mL/L in H<sub>2</sub>O.
- LB media: 25 g/L LB freeze-dried powder (Fisher) in H<sub>2</sub>O.
- LB-agar media: 35 g/L LB with agar (Sigma Aldrich) in H<sub>2</sub>O.

**6.2.2.2 General Buffers for Protein Purification and Analysis****FGFR1:**

- Ni-Nitrilotriacetic acid (NTA) Buffer A: 20 mM tris-(hydroxymethyl)-aminomethane (Tris) (pH 7.8), 300 mM NaCl, 10 mM imidazole, 2 mM tris(2-carboxyethyl)phosphine (TCEP).
- Ni-NTA Buffer B: 20 mM Tris (pH 8.0), 300 mM NaCl, 300 mM imidazole, 2 mM TCEP.
- Ion exchange (IEX) Q Buffer A: 20 mM Tris (pH 8.0), 1 mM TCEP.
- IEX Q Buffer B: 20 mM Tris (pH 8.0), 1 mM TCEP, 1 M NaCl.
- Size exclusion chromatography (SEC) Buffer A: 40 mM 4-(2-hydroxyethyl)-1-piperazineethanesulfonic acid (HEPES) (pH 7.5), 200 mM NaCl, 1 mM TCEP, 10% glycerol.
- SEC Buffer B: 20 mM Tris (pH 7.8), 20 mM NaCl, 2 mM TCEP (storage buffer).

**FGFR2:**

- Cobalt Resin Buffer A: 20 mM Tris (pH 8.0), 300 mM NaCl, 10 mM Imidazole, 1 mM 2-mercaptoethanol (BME).
- Cobalt Resin Buffer B: 20 mM Tris (pH 8.0), 300 mM NaCl, 250 mM Imidazole, 1 mM BME.
- SEC Buffer C: 20 mM HEPES (pH 7.5), 100 mM NaCl, 1 mM TCEP (storage buffer).

**SDS-PAGE**

- SDS-PAGE 10 × running buffer: 0.19 M Tris, 1.92 M glycine, 1% (w/v) SDS
- SDS-PAGE 2 × loading buffer: 100 mM Tris (pH 6.8), 200 mM dithiothreitol (DTT), 4% (w/v) SDS, 0.2% bromophenol blue, 20% glycerol.
- Coomassie Stain: Coomassie G250, 30% (v/v) methanol and 10% (v/v) acetic acid.
- Coomassie Destain: 40% (v/v) methanol and 10% (v/v) acetic acid.

### 6.2.3 Standard Protocol

#### 6.2.3.1 Transformation of Competent *E.coli* Cells

20  $\mu\text{L}$  of stock BL21 (DE3) competent cells were mixed with 1.0  $\mu\text{L}$  of purified plasmid(s)\* (FGFR2 1Y alone, FGFR2 1Y and protein tyrosine phosphatase 1B (PTP-1B, FGFR2 WT and PTP-1B) in an Eppendorf tube on ice for ten minutes. The cells were then subjected to heat shock for 90 seconds at 42 °C and incubation on ice for a further five minutes to allow uptake of the plasmid. 750  $\mu\text{L}$  of LB media was added and the cells incubated at 37 °C, 200 revolutions per minute (rpm) for 1 h. The cells were then spun at 6000 rpm for two minutes and the supernatant removed. The concentrated cells containing the FGFR2 1Y plasmid alone were then used to inoculate kanamycin (50  $\mu\text{g}/\text{mL}$ ) treated LB agar plates. The concentrated cells containing FGFR2/PTP-1B plasmids were then used to inoculate kanamycin (50  $\mu\text{g}/\text{mL}$ ) and ampicillin (50  $\mu\text{g}/\text{mL}$ ) treated LB agar plates. Inoculated plates were then incubated at 37 °C overnight and kept at 4 °C to stop growth.

\* Plasmid constructs for FGFR2 1Y and FGFR2 WT were provided in-house by Dr. Chi-Chuan Lin and plasmid construct PTP-1B was obtained as a glycerol stock from Addgene.

#### 6.2.3.2 Inoculation of LB Agar Plates

A BL21 star glycerol stock containing the FGFR1 mutant construct\* was streaked onto a tetracycline (12.5  $\mu\text{g}/\text{mL}$ ) and ampicillin (100  $\mu\text{g}/\text{mL}$ ) treated LB agar plate and incubated at 37 °C overnight and kept at 4 °C to stop growth.

\*FGFR1 construct provided in-house by Dr. Simon Skinner.

#### 6.2.3.3 Mini Culture

Single colonies of the transformed *E.coli* cells grown on the appropriate LB agar plate were picked and used to inoculate 100 mL of TB media containing tetracycline (12.5  $\mu\text{g}/\text{mL}$ ) and ampicillin (100  $\mu\text{g}/\text{mL}$ ) for the FGFR1 construct, or 100 mL of LB media containing kanamycin (50  $\mu\text{g}/\text{mL}$ ) alone for the FGFR2 1Y construct, or kanamycin (50  $\mu\text{g}/\text{mL}$ ) and ampicillin (50  $\mu\text{g}/\text{mL}$ ) for the FGFR2/PTP-1B construct. Flasks were then incubated at 37 °C, 200 rpm overnight. Glycerol stocks were made by taking cells and mixing with 50% glycerol ( $\text{H}_2\text{O}$ ) in a 1:1 ratio and then stored at -80 °C for future use.

#### 6.2.3.4 Overexpression of FGFR1

6 × 600 mL of sterilised TB media in 1L flasks containing tetracycline (12.5 µg/mL) and ampicillin (100 µg/mL) were inoculated with 2.5 mL of cells from the overnight mini culture and then incubated at 37 °C, 250 rpm until the optical density at 600 nm (OD<sub>600</sub>) = 0.8-1.0. Bacterial cultures were allowed to cool to 20 °C and then induced using isopropyl β-D-1-thiogalactopyranoside (IPTG) (0.1 mM) and grown overnight. Cell cultures were then centrifuged at 4 °C, 5000 rpm for 1 h, discarding the supernatant. The cell pellet was suspended in Ni-NTA Buffer A at a ratio of 2:1 respectively and stored at -20 °C for future use.

#### 6.2.3.5 Overexpression of FGFR2 Variants

4 × 1L of sterilised LB media containing kanamycin (50 µg/mL) alone for the FGFR2 1Y construct or kanamycin (50 µg/mL) and ampicillin (50 µg/mL) for the FGFR2/PTP-1B construct in 2L flasks were inoculated with 1 mL of cells from the corresponding overnight mini culture and then incubated at 37 °C, 200 rpm until the OD<sub>60</sub> = ~0.7. Bacterial cultures were allowed to cool to 20 °C and then induced using IPTG (0.5 mM) and grown overnight. Cell cultures were then centrifuged at 4 °C, 5000 rpm for 1 h, discarding the supernatant and the cell pellet stored at -20 °C for future use.

### 6.2.4 Purification of FGFR1

#### 6.2.4.1 Ni-NTA His<sub>6</sub>-tag Chromatography

Cell pellet was defrosted and one protease tablet (cOmplete™, ethylenediaminetetraacetic acid (EDTA)-free Protease Inhibitor Cocktail-Sigma) and 5 µL of benzonase® (≥ 250 units (U)/µL-Sigma) added and the cell mixture lysed using sonication (10 seconds on/10 seconds off at 70% amplitude for 20 cycles). The cell mixture was then centrifuged at 20000 rpm for 1 h, passing the supernatant through a 0.45 µm membrane. The supernatant was loaded onto a 5 mL pre-equilibrated His-Trap™ High Performance column (GE Healthcare) connected to an Äkta Prime. The column was then flushed with Ni-NTA Buffer A (~30 column volumes (CVs)) until A<sub>280</sub> returned to baseline. The column was then washed with 9% Ni-NTA Buffer B (10 CVs) followed by elution of the desired protein with 100%

Ni-NTA Buffer B (10 CVs). Column fractions were analysed by UV trace on the Äkta Prime and pooled accordingly.

#### **6.2.4.2 Cleavage of His<sub>6</sub>-tag and IEX Chromatography**

Protein sample from the nickel column was transferred to standard grade regenerated cellulose tubing (MWCO:6-8KDa) and 5 µL TEV protease ( $\geq 3000$  U/mg-Sigma) added and the tubing dialysed in IEX Q Buffer A ( $\times 100$  dilution factor) for 4 h and then overnight with fresh IEX Q Buffer A ( $\times 100$  dilution factor). Protein sample was then loaded onto a pre-equilibrated 5 mL Q Sepharose column (GE Healthcare) and washed with IEX Q Buffer A (~45 CVs). Protein was then eluted by gradient (0-35%) of IEX Q Buffer B over ~25 CVs. The desired protein was observed to elute over the initial 10 CVs and the purity analysed by SDS-PAGE (Section 8.2.1) and pooled accordingly.

#### **6.2.4.3 SEC**

Protein sample from the ion exchange chromatography column was concentrated to ~10 mL and two 5 mL aliquots prepared. The first aliquot was loaded directly onto a pre-equilibrated superdex 75 size exclusion column and the protein eluted with SEC Buffer A (~150 mL) at 1 mL/min. Fractions were analysed by SDS-PAGE (Section 8.2.1), pooled accordingly and concentrated to ~11.7 mg/mL (2.5 mL).  $5 \times 500$  µL aliquots were snap frozen in liquid nitrogen and stored at  $-80$  °C for future use. The second aliquot was loaded directly onto a pre-equilibrated superdex 75 size exclusion column and the protein eluted with SEC Buffer B (~150 mL). Fractions were analysed by SDS-PAGE, pooled accordingly and concentrated to ~10.1 mg/mL (2 mL) and used directly in crystallisation trials (Section 6.2.7).

### **6.2.5 Purification of FGFR2 Variants**

#### **6.2.5.1 Cobalt Resin His<sub>6</sub>-tag Chromatography**

Cell pellet was defrosted and one protease tablet (cOmplete™, EDTA-free Protease Inhibitor Cocktail-Sigma) and cobalt resin buffer A added to the pellet at a ratio of 2:1 pellet to buffer and the cell mixture lysed using sonication (5 seconds on/25 seconds off at 70% amplitude for 60 cycles). The cell mixture was then centrifuged at  $4$  °C, 20000 rpm for 1 h. The supernatant was decanted and added to cobalt resin (TALON® Metal Affinity Resin, Clontech) at a ratio of 4:1 respectively and the resin rotated and



mixed at 4 °C for 30 minutes. The resin was then centrifuged at 4 °C, 3000 rpm for five minutes followed by careful removal of the liquid without disturbing the resin. The resin was then washed with cobalt resin buffer A (2 × 5 mL) to ensure all unbound protein was removed. 20 µL of calf-intestinal alkaline phosphatase (CIP) (10,000 U/mL) was added to the resin containing the construct expressing FGFR 1Y alone and left to rotate and mix overnight at 4 °C to ensure full dephosphorylation. The resin was then suspended in 5 mL of cobalt resin buffer A, washed under gravity with cobalt resin buffer A (4 × 5 mL) until all unbound protein was eluted, monitoring by Bradford blue assay. The desired protein was then eluted using cobalt resin buffer B (~15 mL) until no more protein was detected by Bradford blue assay.

#### **6.2.5.2 SEC**

Protein sample from the cobalt resin chromatography was concentrated to ~3-5 mL at 4 °C, 3000 rpm and then loaded directly onto a pre-equilibrated superdex 100 size exclusion column and the protein eluted with SEC Buffer C (~120 mL) at 1 mL/min. Fractions were analysed by SDS-PAGE (Section 8.2.3), pooled accordingly and concentrated to: ~9.8 mg/mL (400 µL) for the FGFR 1Y alone construct, ~10.0 mg/mL (1 mL) for the FGFR 1Y/PTP-1B construct and ~9.0 mg/mL (1.4 mL) for the FGFR2 WT/PTP-1B construct. The desired amounts of protein were used directly in crystal trials (Section 6.2.7) with the remainder stored at -80 °C for future use.

#### **6.2.5.3 Cleavage of His<sub>6</sub>-tag**

700 µL of FGFR2 WT (9 mg/mL) was defrosted and 7 µL of thrombin (1U/µL) added and the mixture rotated and mixed at 4 °C overnight. The protein mixture was then added to a 1 mL mixture of cobalt resin/benzamidinium beads (1:1) and rotated and mixed at 4 °C for 15 minutes to remove uncleaved protein and thrombin. The mixture was then centrifuged at 4 °C, 10000 rpm for five minutes and the supernatant carefully removed and added directly onto a pre-equilibrated superdex 100 size exclusion column and the protein eluted with SEC Buffer C (~120 mL) at 1 mL/min. Fractions were analysed by SDS-PAGE (Section 8.2.3), pooled accordingly and concentrated to ~10 mg/mL (280 µL). The protein was used directly in crystal trials (Section 6.2.7).

## 6.2.6 SDS-PAGE

### 6.2.6.1 Preparation of Gels

Acrylamide gels were prepared using the components listed in Table 6.1.

**Table 6.1:** SDS-PAGE gel components.

	<b>Stacking</b>	<b>Separating</b>
<b>2 × 1 mm gel</b>	<b>5%</b>	<b>10%</b>
1.5 M Tris (Lower)	-	2.0 mL
0.5 M Tris (Upper)	1.25 mL	-
40 % (w/v) acrylamide	0.75 mL	2.65 mL
H <sub>2</sub> O	3.0 mL	3.35 mL
10% Ammonium persulfate (APS) (w/v)	100 µL	100 µL
Tetramethylethylenediamine (TEMED)	45 µL	45 µL

All components were mixed together with the exception of APS and TEMED, these were added immediately prior to pouring the mixture into the mould. It is important to note fresh APS is needed in order to have efficient setting.

### 6.2.6.2 Running Procedure

15 µL of protein in buffer was mixed with 7 µL of loading buffer and the solutions heated at 95 °C for 5 minutes. Protein solutions were then loaded into 10 or 15 well gels made in-house or pre-cast (Bio Rad Mini Protean TGX Gels) and the gels ran at a constant current of 80 mA until the protein bands reached the bottom of the gel.

### 6.2.6.3 Visualisation and Imaging

The gels were stained using either coomassie stain or instant blue. Gels were stained with coomassie stain for ~1 h with gentle rocking or until protein bands became visible. The stain was then removed and coomassie destain added for 15 minutes with rocking. Two further rounds of fresh destain were added to ensure full destaining. Gels were stained with instant blue until protein bands became visible (~20 minutes). Gels were then imaged using a Syngene G:Box apparatus (Section 8.2).

#### 6.2.6.4 Protein Concentration Determination

The UV absorbance of protein samples was measured using either a Nanodrop 2000 or Genesys 6 spectrophotometer. For measurements using the nanodrop 2000 apparatus, 2  $\mu$ L of sample was loaded onto the aperture after the apparatus had been calibrated with a blank buffer reference measurement. For measurements using the Genesys 6 spectrophotometer protein samples were diluted in buffer and the absorption measured, with a blank buffer measurement as a reference. The absorbance was measured at 280 nm and protein concentration determined using the Beer-Lambert law.

$$A = \epsilon cl$$

**Equation 6.1:** *The Beer-Lambert law. A = absorbance,  $\epsilon$  = molar extinction coefficient ( $M^{-1} cm^{-1}$ ), c = concentration (M), l = path length (cm)*

Extinction coefficients were calculated using ProtParam (Table 6.2):<sup>146</sup>

**Table 6.2:** Extinction Coefficients for FGFR kinases.

Protein	Extinction Coefficient, $\epsilon_{280}$
FGFR1	46870 $M^{-1} cm^{-1}$
FGFR2 1Y	33460 $M^{-1} cm^{-1}$
FGFR2 WT	46870 $M^{-1} cm^{-1}$

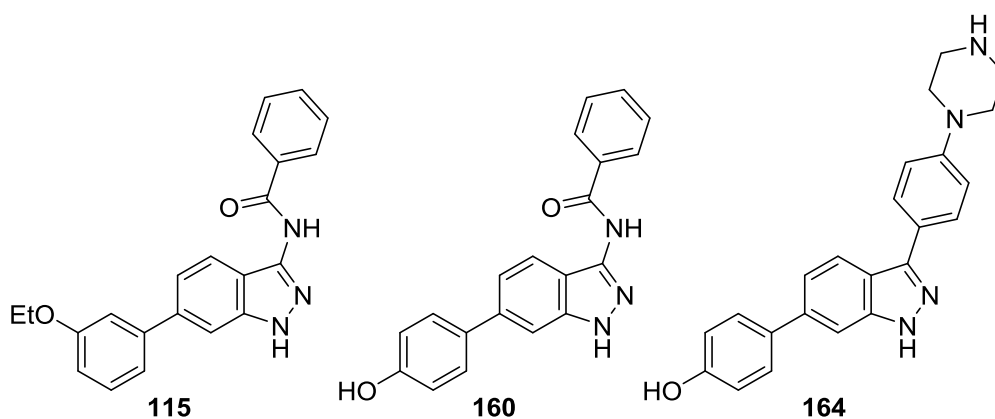
## 6.2.7 Crystallisation Trials

### 6.2.7.1 Equipment and Protocol

Crystal trials were performed using an automated robotic system (Formulatrix) available for use in the Astbury centre, University of Leeds. Crystallisation reagents were dispensed into 96-well blocks using a formulator liquid handler. Protein samples and reagents were mixed and dispensed into 3-drop 96-well crystallisation sitting-drop plates using an NT8 crystallisation system, stored in a Rockimager 1000 at either 4 °C or 20 °C, and imaged at various times to monitor crystal growth. Crystals were then picked and flash frozen in liquid nitrogen with the desired anti-freeze present and then the crystals exposed to X-ray diffraction at either the Diamond Light Source Facility (DLSF) or the European Synchrotron Radiation Facility (ESRF). Data processing was carried out by CCP4 and then the structures manipulated in WinCoot to provide the final PDB file.

### 6.2.7.2 Preparation of Ligands

Compounds **115**, **160** and **164** were dissolved in dimethyl sulphoxide (DMSO) at a concentration of 50 mM. Compounds **115** and **160** were then diluted with the same buffer as what the protein was stored in (Section 6.2.2.2) to  $\times 10$  concentration of the corresponding protein. Final DMSO concentrations for compounds **115** and **160** were 5%. Final DMSO concentration for compound **164** was 0.5% for all crystal trials excluding the FGFR2 WT cleaved trials where the final DMSO concentration was 5%.



### 6.2.7.3 Crystallisation of FGFR1

Purified FGFR1 protein at a concentration of 0.28 mM (10 mg/mL) in 20 mM Tris (pH 7.81), 20 mM NaCl, 2 mM TCEP was mixed with the diluted ligand samples at a ratio of 9:1 respectively. This gave final concentrations of protein and ligand at 0.28 mM (1:1 ratio). Protein/ligand samples (0.5  $\mu$ L) were then mixed with screening solutions (0.5  $\mu$ L) to form a final drop volume of 1  $\mu$ L. Crystals were then grown using the vapour diffusion method (Figure 6.1).

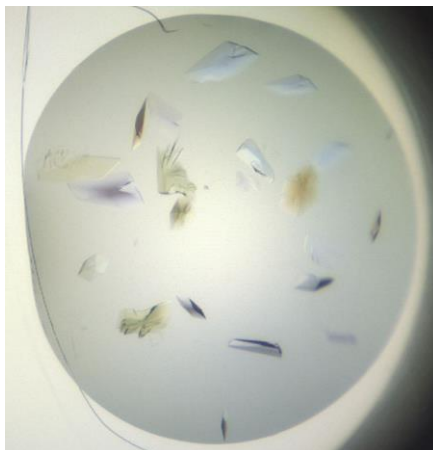


**Figure 6.1:** Crystallisation drop showing representative FGFR1/ligand co-crystals.

#### 6.2.7.3.1 Tray Setup and Screening Conditions

Protein/ligand samples containing compounds **115**, **160** and **164** were in drop 1, 2 and 3 respectively with R being the reservoir for that specific screening condition (Figure 6.2). The screening conditions for this trial were: 0.185 M ammonium sulphate, 20% ethylene glycol and then varying levels of polyethylene glycol (PEG) 8000 (16-22%) and pH (6.2-6.8). The pH was adjusted with 1 M PCTP buffers (pH 4.0 and pH 9.5-Molecular Dimensions) with a final concentration of 95 mM PCTP.

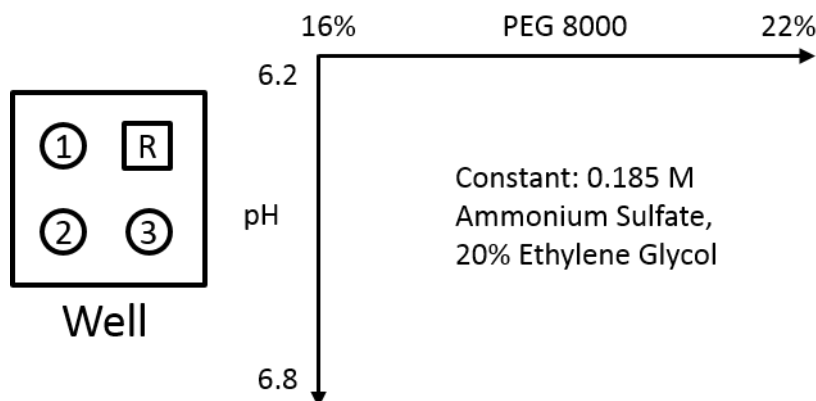


**Figure 6.2:** Well setup and screening conditions for FGFR1 crystallisation trials.

Precise conditions for crystal structures are as follows:

- Ligand **115** – 0.185 M ammonium sulphate, 20% ethylene glycol, 17.636% PEG 8000 and 0.095 M PCPT pH 6.71.
- Ligand **160** – 0.185 M ammonium sulphate, 20% ethylene glycol, 16.545% PEG 8000 and 0.095 M PCPT pH 6.71.
- Ligand **164** – 0.185 M ammonium sulphate, 20% ethylene glycol, 17.091% PEG 8000 and 0.095 M PCPT pH 6.71.

#### **6.2.7.4 Crystallisation of FGFR2 1Y**

Purified FGFR2 1Y (monophosphorylated) and FGFR2 1Y (unphosphorylated) protein at a concentration of 0.27 mM (10 mg/mL) in 20 mM HEPES (pH 7.5), 100 mM NaCl, 1 mM TCEP were mixed with the diluted ligand samples at a ratio of 9:1 respectively. This gave final concentrations of protein and ligand at 0.27 mM (1:1 ratio). Protein/ligand samples (1.0  $\mu$ L) were then mixed with screening solutions (1.0  $\mu$ L) to form a final drop volume of 2  $\mu$ L. Crystals were then grown using the vapour diffusion method.

#### **6.2.7.5 Crystallisation of FGFR2 WT**

Purified FGFR2 WT (uncleaved) at a concentration of 0.24 mM (9 mg/mL) and FGFR2 WT (cleaved) at a concentration of 0.29 mM (10 mg/mL) in 20 mM HEPES (pH 7.5), 100 mM NaCl, 1 mM TCEP were mixed with the diluted ligand samples at a ratio of 9:1 respectively. This gave final concentrations of protein and ligand at 0.24 mM and 0.29 mM (1:1 ratio) for FGFR2 WT uncleaved/cleaved respectively with a final concentration of 5% DMSO. Protein/ligand samples (1.0  $\mu$ L for uncleaved, 0.2  $\mu$ L for cleaved) were then mixed with screening solutions (1.0  $\mu$ L for uncleaved, 0.2  $\mu$ L for cleaved) to form a final drop volume of 2  $\mu$ L for uncleaved and 0.4  $\mu$ L for cleaved. Crystals were then grown using the vapour diffusion method.

##### **6.2.7.5.1 Tray Setup and Screening Conditions**

Protein/ligand samples containing compounds **115**, **160** and **164** were in drop 1, 2 and 3 respectively with R being the reservoir for that specific screening condition. Three screening conditions for FGFR2 crystallisation were used and are outlined below (Figure 6.3).

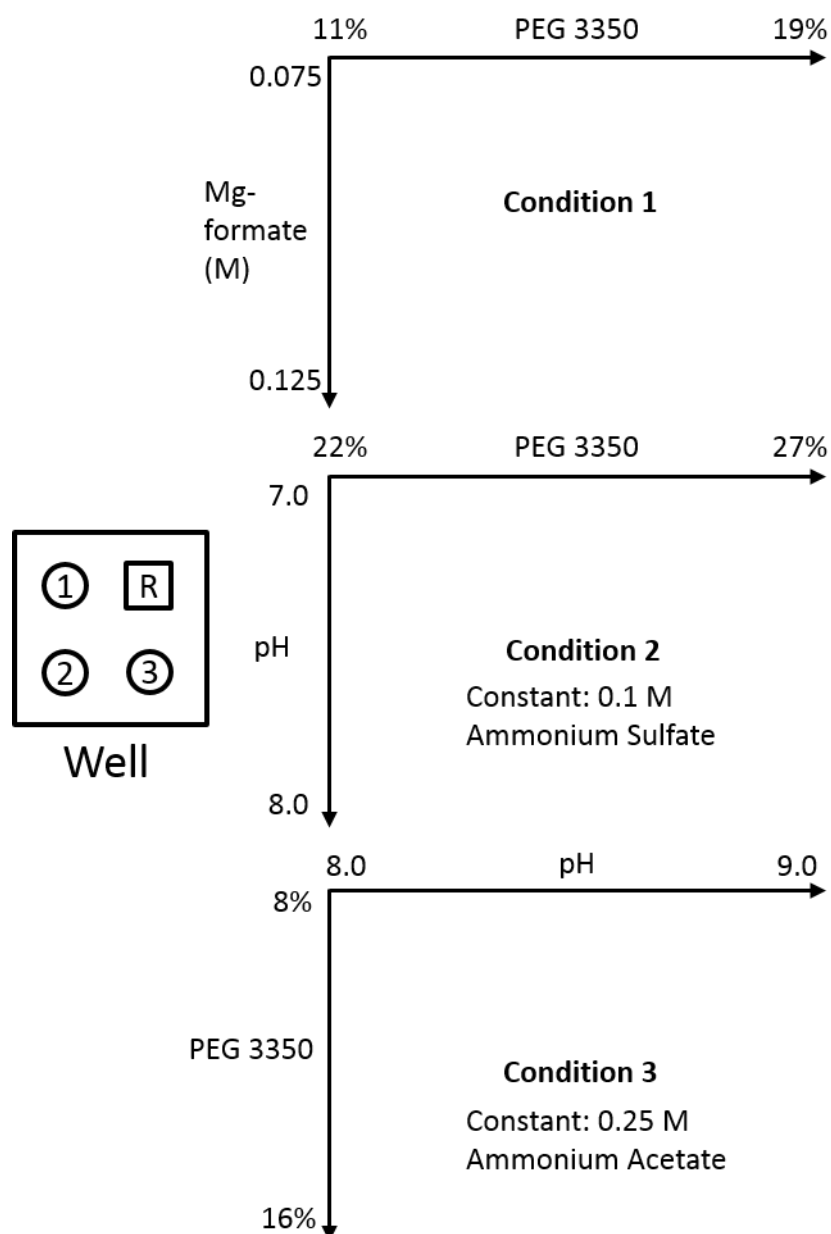


**Figure 6.3:** Well setup and screening conditions for FGFR2 crystallisation trials.

**Condition one:** Varying concentrations (11-19%) of PEG 3350 in water and varying concentrations (0.075-0.125 M) of Mg-formate and stored at 20 °C.

**Condition two:** Constant concentration of 0.1 M ammonium sulphate, varying levels (22-27%) of PEG 3350 in water and varying pH (7.0-8.0). The pH was adjusted with 1 M HEPES buffers (pH 6.0 and pH 9.0) with a final concentration of 0.1 M HEPES and stored at 20 °C.

**Condition three:** Constant concentration of 0.25 M ammonium acetate, varying levels (8-16%) of PEG 3350 in water and varying pH (8.0-9.0). The pH was adjusted with 1 M Tris buffers (pH 7.0 and pH 9.0) with a final concentration of 0.1 M Tris and stored at 20 °C.

## **6.3 Biological Experimental**

### **6.3.1 Equipment and Materials**

All reagents were obtained from commercial suppliers. Cell culture was carried out under aseptic conditions using a Biomat Class II Laminar Flow Hood. Cells were incubated using a Sanyo incubator. Cell counts were carried out using a Beckman Coulter Z2 cell and particle counter. Fluorescence measurements were carried out using a Berthold Mithras LB 940 Multimode microplate reader.

### **6.3.2 Tissue Culture**

#### **6.3.2.1 Cell Lines**

The following cell lines were used in this study: JMSU-1 – FGFR1-driven bladder cancer cell, SUM52 – FGFR2-driven breast cancer cell and VMCUB-3 – non FGFR-driven bladder cancer cell.

#### **6.3.2.2 Inhibitors**

The inhibitors used in this study were: PD173074 (10 mM in DMSO-Sigma) and compounds **115**, **160** and **164**. Stock solutions of 10 mM in DMSO were made of each compound, stored at -20 °C and thawed when needed.

#### **6.3.2.3 Cell Culture**

Stocks of each cell line were provided by Dr Julie Burns. Cells were cultured in either 25 cm<sup>2</sup> or 75 cm<sup>2</sup> vented canted-neck cell culture flasks (Corning) in a humidified incubator at 37 °C under an atmosphere of 5% CO<sub>2</sub> in air. SUM52 and JMSU-1 cells were cultured in Roswell Park Memorial Institute (RPMI)-1640 growth medium (Sigma) containing 10% foetal calf serum (FCS; Biosera) and 2 mM GlutaMAX (Life Technologies). VMCUB-3 cells were cultured in Dulbecco's modified eagle medium (MEM) growth medium (Sigma) containing 10% FCS and 2 mM GlutaMAX.

#### **6.3.2.4 Cell Passage**

Stock cells were passaged at, or near to confluence. Existing medium was aspirated and the cells rinsed with calcium/magnesium-free phosphate-buffered saline (PBS) solution followed with incubation in PBS containing 0.1% (*w/v*) EDTA for 2-5 minutes at 37 °C. JMSU-1 cells were briefly rinsed with PBS/EDTA buffer and



not incubated due to their propensity to detach easily. The PBS/EDTA buffer was aspirated and the cells contained in 25 cm<sup>2</sup> flasks and 75 cm<sup>2</sup> flasks incubated with either 0.5 or 1 mL 0.05% trypsin-0.02% EDTA (Sigma) respectively at 37 °C for approximately five minutes or until the cells detached. Growth medium (4.5 or 9 mL) was added to the cells to make a total volume of 5/10 mL and then an appropriate amount of cells (1 in 10 for confluent SUM52, 1 in 20 for confluent JMSU-1 and VMCUB-3) taken and added to a fresh 75 cm<sup>2</sup> flask and then medium added to make a final volume of 15 mL.

### 6.3.2.5 Cell Counting

Detached cell suspensions (pre-passage) were used to seed plates with a desired number of cells/well for cell viability assays. 100 µL of cells were added to 9.9 mL Isoton II Diluent (Beckman Coulter) and then the number of cells counted twice and a mean value calculated. The cell counter was flushed and the background measured with fresh Isoton between every reading to ensure accurate measurements.

### 6.3.2.6 CellTiter-Blue® Viability Assay

For each cell line a 70-80% confluent 75 cm<sup>2</sup> flask was selected and cell suspensions produced and counted as described above. Cells were then diluted with the appropriate medium to  $\sim 5 \times 10^4$  cells/mL. 100 µL of cells were then dispensed into a flat bottom 96-well plate (Corning) as shown in Figure 6.4. This would ensure a final density of  $5 \times 10^3$  cells/well.

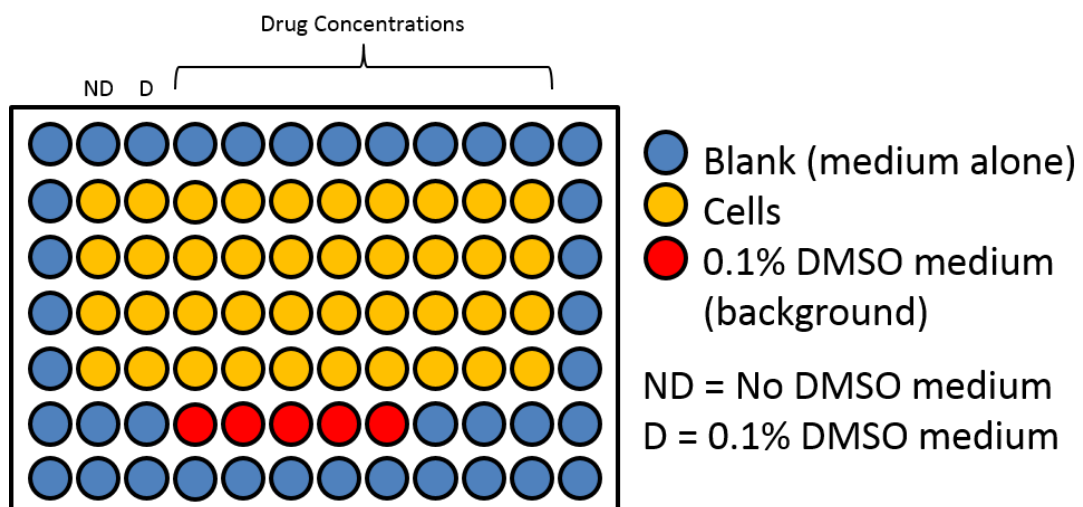


**Figure 6.4:** Plate setup for cell viability assays.

Cells were incubated for 24 h to ensure the cells had adhered and recovered from trypsinisation. The medium from the wells containing cells was aspirated and then 100 µL of medium containing the appropriate inhibitor concentrations was added. The plate was then incubated at 37 °C, 5% CO<sub>2</sub> for 72 h. CellTiter-Blue reagent was pre-warmed to 37 °C and then 20 µL added to each well, excluding the wells indicated as blanks. The plates were kept dark to ensure minimal photolysis of the reagent and incubated at 37 °C, 5 % CO<sub>2</sub> for 2 h. After incubation, 50 µL of 3% SDS was added to each well containing the CellTiter-Blue reagent to stop the reaction. The wells were then subjected to excitation at 540 nm and emission 590 nm respectively and the fluorescence measured. Results were blanked with a medium no cell control and then normalised to the DMSO control. Each experiment was carried out in duplicate. Data were plotted using Origin® 2016 and IC<sub>50</sub> values calculated (Section 8.3) using a dose response non-linear curve fit with the following equation:

$$Y = A1 + \frac{A2 - A1}{1 + 10^{(LOGx0-x)p}}$$

**Equation 6.2:** Formula for dose response non-linear curve fit. *A1 = bottom asymptote, A2 = top asymptote, p = hill slope.*

## References

---

1. Hanahan, D.; Weinberg, R. A., The hallmarks of cancer. *Cell*. **2000**, *100* (1), 57-70.
2. Ferlay, J.; Soerjomataram, I.; Ervik, M.; Dikshit, R.; Eser, S.; Mathers, C.; Rebelo, M.; Parkin, D. M.; Forman, D.; Bray, F., Cancer incidence and mortality worldwide: sources, methods and major patterns in GLOBOCAN 2012. *Int. J. Cancer* **2014**, *136* (5), E359-E386.
3. Hanahan, D.; Weinberg, R. A., Hallmarks of Cancer: The Next Generation. *Cell*. **2011**, *144* (5), 646-674.
4. Weinberg, R. A., How cancer arises. *Sci. Am.* **1996**, *275* (3), 62-70.
5. Kankanala, J. Design, Synthesis and Biological Evaluation of Inhibitors of FGFR, VEGFR-2 and Ras Proteins. University of Leeds (Department of Chemistry), 2011.
6. Bertoli, C.; Skotheim, J. M.; de Bruin, R. A. M., Control of cell cycle transcription during G1 and S phases. *Nat. Rev. Mol. Cell. Bio.* **2013**, *14* (8), 518-528.
7. Malumbres, M.; Barbacid, M., Cell cycle, CDKs and cancer: a changing paradigm. *Nat. Rev. Cancer* **2009**, *9* (3), 153-166.
8. Harper, J. W.; Elledge, S. J., The DNA damage response: Ten years after. *Mol. Cell*. **2007**, *28* (5), 739-745.
9. Chial, H., Proto-oncogenes to oncogenes to cancer. *Nat. Edu.* **2008**, *1* (1), 33.
10. Sherr, C. J., Principles of tumor suppression. *Cell*. **2004**, *116* (2), 235-246.
11. Anand, P.; Kunnumakara, A. B.; Sundaram, C.; Harikumar, K. B.; Tharakan, S. T.; Lai, O. S.; Sung, B. Y.; Aggarwal, B. B., Cancer is a Preventable Disease that Requires Major Lifestyle Changes. *Pharm. Res.* **2008**, *25* (9), 2097-2116.
12. Manning, G.; Whyte, D. B.; Martinez, R.; Hunter, T.; Sudarsanam, S., The protein kinase complement of the human genome. *Science*. **2002**, *298* (5600), 1912-1934.
13. Hunter, T.; Bartholomew, M., Sefton., *Protein Phosphorylation: Part A, Protein Kinases: Assays, Purification, Antibodies, Functional Analysis, Cloning, and Expression*. Academic Press, Inc.: 24-28 Oval Road, London NW1 7DX, 1991; Vol. 200, p 763.
14. Nelson, D. L.; Cox, M. M., *Lehninger: Principles of Biochemistry*. 5th ed.; W. H. Freeman and Co: New York, 2008.
15. Chauhan, J. S.; Mishra, N. K.; Raghava, G. P. S., Identification of ATP binding residues of a protein from its primary sequence. *Bmc. Bioinformatics*. **2009**, *10*, 9.
16. Muller, C. W.; Schulz, G. E., Structure of the complex between adenylate kinase from escherichia-coli and the inhibitor ap5a refined at 1.9 a resolution - a model for a catalytic transition-state. *J. Mol. Biol.* **1992**, *224* (1), 159-177.

17. Lipmann, F., Metabolic generation and utilization of phosphate bond energy. *Adv. Enzymol. Rel. S. Bi.* **1941**, *1*, 99-162.
18. Groth, C.; Lardelli, M., The structure and function of vertebrate Fibroblast Growth Factor Receptor 1. *Int. J. Dev. Biol.* **2002**, *46* (4), 393-400.
19. Sleeman, M.; Fraser, J.; McDonald, M.; Yuan, S. N.; White, D.; Grandison, P.; Kumble, K.; Watson, J. D.; Murison, J. G., Identification of a new fibroblast growth factor receptor, FGFR5. *Gene* **2001**, *271* (2), 171-182.
20. Eswarakumar, V. P.; Lax, I.; Schlessinger, J., Cellular signaling by fibroblast growth factor receptors. *Cytokine. Growth. F. R.* **2005**, *16* (2), 139-149.
21. Presta, M.; Dell'Era, P.; Mitola, S.; Moroni, E.; Ronca, R.; Rusnati, M., Fibroblast growth factor/fibroblast growth factor receptor system in angiogenesis. *Cytokine. Growth. F. R.* **2005**, *16* (2), 159-178.
22. Cross, M. J.; Claesson-Welsh, L., FGF and VEGF function in angiogenesis: signalling pathways, biological responses and therapeutic inhibition. *Trends Pharmacol. Sci.* **2001**, *22* (4), 201-207.
23. Plotnikov, A. N.; Schlessinger, J.; Hubbard, S. R.; Mohammadi, M., Structural basis for FGF receptor dimerization and activation. *Cell.* **1999**, *98* (5), 641-650.
24. Johnson, D. E.; Williams, L. T., Structural and functional diversity in the FGF receptor multigene family. *Adv. Cancer. Res.* **1993**, *60*, 1-41.
25. Hou, J. Z.; Kan, M.; Wang, F.; Xu, J. M.; Nakahara, M.; McBride, G.; McKeegan, K.; McKeegan, W. L., Substitution of putative half-cystine residues in heparin-binding fibroblast growth-factor receptors - loss of binding-activity in both 2-loop and 3-loop isoforms. *J. Biol. Chem.* **1992**, *267* (25), 17804-17808.
26. Shimizu, A.; Tada, K.; Shukunami, C.; Hiraki, Y.; Kurokawa, T.; Magane, N.; Kurokawa-Seo, M., A novel alternatively spliced fibroblast growth factor receptor 3 isoform lacking the acid box domain is expressed during chondrogenic differentiation of ATDC5 cells. *J. Biol. Chem.* **2001**, *276* (14), 11031-11040.
27. Xu, J. M.; Nakahara, M.; Crabb, J. W.; Shi, E. G.; Matuo, Y.; Fraser, M.; Kan, M.; Hou, J. Z.; McKeegan, W. L., Expression and immunochemical analysis of rat and human fibroblast growth-factor receptor (flg) isoforms. *J. Biol. Chem.* **1992**, *267* (25), 17792-17803.
28. Kalinina, J.; Dutta, K.; Ilghari, D.; Beenken, A.; Goetz, R.; Eliseenkova, A. V.; Cowburn, D.; Mohammadi, M., The Alternatively Spliced Acid Box Region Plays a Key Role in FGF Receptor Autoinhibition. *Structure.* **2012**, *20* (1), 77-88.
29. Mohammadi, M.; Olsen, S. K.; Ibrahimi, O. A., Structural basis for fibroblast growth factor receptor activation. *Cytokine. Growth. F. R.* **2005**, *16* (2), 107-137.
30. Li, E.; Hristova, K., Receptor tyrosine kinase transmembrane domains Function, dimer structure and dimerization energetics. *Cell. Adhes. Migr.* **2010**, *4* (2), 249-254.

31. Casteran, N.; De Sepulveda, P.; Beslu, N.; Aoubala, M.; Letard, S.; Lecocq, E.; Rottapel, R.; Dubreuil, P., Signal transduction by several KIT juxtamembrane domain mutations. *Oncogene*. **2003**, *22* (30), 4710-4722.
32. Hubbard, S. R., Juxtamembrane autoinhibition in receptor tyrosine kinases. *Nat. Rev. Mol. Cell. Bio.* **2004**, *5* (6), 464-470.
33. Ornitz, D. M.; Itoh, N., The Fibroblast Growth Factor signaling pathway. *Wires. Dev Biol.* **2015**, *4* (3), 215-266.
34. Furdui, C. M.; Lew, E. D.; Schlessinger, J.; Anderson, K. S., Autophosphorylation of FGFR1 kinase is mediated by a sequential and precisely ordered reaction. *Mol. Cell.* **2006**, *21* (5), 711-717.
35. Lew, E. D.; Furdui, C. M.; Anderson, K. S.; Schlessinger, J., The Precise Sequence of FGF Receptor Autophosphorylation Is Kinetically Driven and Is Disrupted by Oncogenic Mutations. *Sci. Signal.* **2009**, *2* (58), 10.
36. Schlessinger, J., Cell signaling by receptor tyrosine kinases. *Cell.* **2000**, *103* (2), 211-225.
37. Seo, J. H.; Suenaga, A.; Hatakeyama, M.; Taiji, M.; Imamoto, A., Structural and Functional Basis of a Role for CRKL in a Fibroblast Growth Factor 8-Induced Feed-Forward Loop. *Mol. Cell. Biol.* **2009**, *29* (11), 3076-3087.
38. Kouhara, H.; Hadari, Y. R.; SpivakKroizman, T.; Schilling, J.; BarSagi, D.; Lax, I.; Schlessinger, J., A lipid-anchored Grb2-binding protein that links FGF-receptor activation to the Ras/MAPK signaling pathway. *Cell.* **1997**, *89* (5), 693-702.
39. Lamothe, B.; Yamada, M.; Schaeper, U.; Birchmeier, W.; Lax, I.; Schlessinger, J., The docking protein Gab1 is an essential component of an indirect mechanism for fibroblast growth factor stimulation of the phosphatidylinositol 3-kinase/Akt antiapoptotic pathway. *Mol. Cell. Biol.* **2004**, *24* (13), 5657-5666.
40. Brent, A. E.; Tabin, C. J., FGF acts directly on the somitic tendon progenitors through the Ets transcription factors Pea3 and Erm to regulate scleraxis expression. *Development.* **2004**, *131* (16), 3885-3896.
41. Manning, B. D.; Cantley, L. C., AKT/PKB signaling: Navigating downstream. *Cell.* **2007**, *129* (7), 1261-1274.
42. Haberman, Y.; Alon, L. T.; Eliyahu, E.; Shalgi, R., Receptor for activated C kinase (RACK) and protein kinase C (PKC) in egg activation. *Theriogenology.* **2011**, *75* (1), 80-89.
43. Reilly, J. F.; Mickey, G.; Maher, P. A., Association of fibroblast growth factor receptor 1 with the adaptor protein Grb14 - Characterization of a new receptor binding partner. *J. Biol. Chem.* **2000**, *275* (11), 7771-7778.
44. Cross, M. J.; Lu, L. G.; Magnusson, P.; Nyqvist, D.; Holmqvist, K.; Welsh, M.; Claesson-Welsh, L., The Shb adaptor protein binds to tyrosine 766 in the FGFR-1 and regulates the Ras/MEK/MAPK pathway via FRS2 phosphorylation in endothelial cells. *Mol. Biol. Cell.* **2002**, *13* (8), 2881-2893.

45. Dudka, A. A.; Sweet, S. M. M.; Heath, J. K., Signal Transducers and Activators of Transcription-3 Binding to the Fibroblast Growth Factor Receptor Is Activated by Receptor Amplification. *Cancer. Res.* **2010**, *70* (8), 3391-3401.
46. Su, W. C. S.; Kitagawa, M.; Xue, N. R.; Xie, B.; Garofalo, S.; Cho, J.; Deng, C. X.; Horton, W. A.; Fu, X. Y., Activation of Stat1 by mutant fibroblast growth-factor receptor in thanatophoric dysplasia type II dwarfism. *Nature.* **1997**, *386* (6622), 288-292.
47. Dikic, I.; Giordano, S., Negative receptor signalling. *Curr. Opin. Cell. Biol.* **2003**, *15* (2), 128-135.
48. Guy, G. R.; Jackson, R. A.; Yusoff, P.; Chow, S. Y., Sprouty proteins: modified modulators, matchmakers or missing links? *J. Endocrinol.* **2009**, *203* (2), 191-202.
49. Torii, S.; Kusakabe, M.; Yamamoto, T.; Maekawa, M.; Nishida, E., Sef is a spatial regulator for Ras/MAP kinase signaling. *Dev. Cell.* **2004**, *7* (1), 33-44.
50. Kovalenko, D.; Yang, X. H.; Chen, P. Y.; Nadeau, R. J.; Zubanova, O.; Pigeon, K.; Friesel, R., A role for extracellular and transmembrane domains of Sef in Sef-mediated inhibition of FGF signaling. *Cell. Signal.* **2006**, *18* (11), 1958-1966.
51. Camps, M.; Nichols, A.; Gillieron, C.; Antonsson, B.; Muda, M.; Chabert, C.; Boschert, U.; Arkininstall, S., Catalytic activation of the phosphatase MKP-3 by ERK2 mitogen-activated protein kinase. *Science.* **1998**, *280* (5367), 1262-1265.
52. Wong, A.; Lamothe, B.; Li, A.; Schlessinger, J.; Lax, I., FRS2 alpha attenuates FGF receptor signaling by Grb2-mediated recruitment of the ubiquitin ligase Cbl. *P. Natl. Acad. Sci. USA.* **2002**, *99* (10), 6684-6689.
53. Ahmed, Z.; George, R.; Lin, C. C.; Suen, K. M.; Levitt, J. A.; Suhling, K.; Ladbury, J. E., Direct binding of Grb2 SH3 domain to FGFR2 regulates SHP2 function. *Cell. Signal.* **2010**, *22* (1), 23-33.
54. Vert, G.; Chory, J., Crosstalk in Cellular Signaling: Background Noise or the Real Thing? *Dev. Cell.* **2011**, *21* (6), 985-991.
55. Gong, S. G., Isoforms of Receptors of Fibroblast Growth Factors. *J. Cell. Physiol.* **2014**, *229* (12), 1887-1895.
56. Johnson, D. E.; Lu, J.; Chen, H.; Werner, S.; Williams, L. T., The human fibroblast growth-factor receptor genes - a common structural arrangement underlies the mechanisms for generating receptor forms that differ in their 3rd immunoglobulin domain. *Mol. Cell. Biol.* **1991**, *11* (9), 4627-4634.
57. Pownall, M. E.; Isaacs, H. V. In *Fgf signalling in vertebrate development*, Colloquium Series on Developmental Biology, Morgan & Claypool Life Sciences: 2010; pp 1-75.
58. Olsen, S. K.; Garbi, M.; Zampieri, N.; Eliseenkova, A. V.; Ornitz, D. M.; Goldfarb, M.; Mohammadi, M., Fibroblast Growth Factor (FGF) Homologous Factors Share Structural but Not Functional Homology with FGFs. *J. Biol. Chem.* **2003**, *278* (36), 34226-34236.

59. Beenken, A.; Mohammadi, M., The FGF family: biology, pathophysiology and therapy. *Nat. Rev. Drug. Discov.* **2009**, *8* (3), 235-253.
60. Wittekind, C., TNM system 2010. *Pathologie* **2010**, *31* (5), 331-332.
61. di Martino, E.; Tomlinson, D. C.; Knowles, M. A., A Decade of FGF Receptor Research in Bladder Cancer: Past, Present, and Future Challenges. *Adv. Urol.* **2012**, *2012*, 10.
62. May, M.; Brookman-Amisshah, S.; Roigas, J.; Hartmann, A.; Storkel, S.; Kristiansen, G.; Gilfrich, C.; Borchardt, R.; Hoschke, B.; Kaufmann, O.; Gunia, S., Prognostic Accuracy of Individual Uropathologists in Noninvasive Urinary Bladder Carcinoma: A Multicentre Study Comparing the 1973 and 2004 World Health Organisation Classifications. *Eur. Urol.* **2010**, *57* (5), 850-858.
63. van Rhijn, B. W. G.; Montironi, R.; Zwarthoff, E. C.; Jobsis, A. C.; van der Kwast, T. H., Frequent FGFR3 mutations in urothelial papilloma. *J. Pathol.* **2002**, *198* (2), 245-251.
64. Adar, R.; Monsonego-Ornan, E.; David, P.; Yayon, A., Differential activation of cysteine-substitution mutants of fibroblast growth factor receptor 3 is determined by cysteine localization. *J. Bone Miner. Res.* **2002**, *17* (5), 860-868.
65. Webster, M. K.; dAvis, P. Y.; Robertson, S. C.; Donoghue, D. J., Profound ligand-independent kinase activation of fibroblast growth factor receptor 3 by the activation loop mutation responsible for a lethal skeletal dysplasia, thanatophoric dysplasia type II. *Mol. Cell. Biol.* **1996**, *16* (8), 4081-4087.
66. Tomlinson, D. C.; Baldo, O.; Hamden, P.; Knowles, M. A., FGFR3 protein expression and its relationship to mutation status and prognostic variables in bladder cancer. *J. Pathol.* **2007**, *213* (1), 91-98.
67. Tomlinson, D. C.; L'Hote, C. G.; Kennedy, W.; Pitt, E.; Knowles, M. A., Alternative splicing of fibroblast growth factor receptor 3 produces a secreted isoform that inhibits fibroblast growth factor-induced proliferation and is repressed in urothelial carcinoma cell lines. *Cancer. Res.* **2005**, *65* (22), 10441-10449.
68. Tomlinson, D. C.; Lamont, F. R.; Shnyder, S. D.; Knowles, M. A., Fibroblast Growth Factor Receptor 1 Promotes Proliferation and Survival via Activation of the Mitogen-Activated Protein Kinase Pathway in Bladder Cancer. *Cancer. Res.* **2009**, *69* (11), 4613-4620.
69. deMedina, S. G. D.; Chopin, D.; ElMarjou, A.; Delouvee, A.; LaRoche, W. J.; Hoznek, A.; Abbou, C.; Aaronson, S. A.; Thiery, J. P.; Radvanyi, F., Decreased expression of keratinocyte growth factor receptor in a subset of human transitional cell bladder carcinomas. *Oncogene.* **1997**, *14* (3), 323-330.
70. Ricol, D.; Cappellen, D.; El Marjou, A.; Gil-Diez-de-Medina, S.; Girault, J. M.; Yoshida, T.; Ferry, G.; Tucker, G.; Poupon, M. F.; Chopin, D.; Thiery, J. P.; Radvanyi, F., Tumour suppressive properties of fibroblast growth factor receptor 2-IIIb in human bladder cancer. *Oncogene.* **1999**, *18* (51), 7234-7243.

71. Tannheimer, S. L.; Rehemtulla, A.; Ethier, S. P., Characterization of fibroblast growth factor receptor 2 overexpression in the human breast cancer cell line SUM-52PE. *Breast. Cancer. Res.* **2000**, *2* (4), 311-320.
72. Hunter, D. J.; Kraft, P.; Jacobs, K. B.; Cox, D. G.; Yeager, M.; Hankinson, S. E.; Wacholder, S.; Wang, Z. M.; Welch, R.; Hutchinson, A.; Wang, J. W.; Yu, K.; Chatterjee, N.; Orr, N.; Willett, W. C.; Colditz, G. A.; Ziegler, R. G.; Berg, C. D.; Buys, S. S.; McCarty, C. A.; Feigelson, H. S.; Calle, E. E.; Thun, M. J.; Hayes, R. B.; Tucker, M.; Gerhard, D. S.; Fraumeni, J. F.; Hoover, R. N.; Thomas, G.; Chanock, S. J., A genome-wide association study identifies alleles in FGFR2 associated with risk of sporadic postmenopausal breast cancer. *Nat. Genet.* **2007**, *39* (7), 870-874.
73. Campbell, T. M.; Castro, M. A. A.; de Santiago, I.; Fletcher, M. N. C.; Halim, S.; Prathalingam, R.; Ponder, B. A. J.; Meyer, K. B., FGFR2 risk SNPs confer breast cancer risk by augmenting oestrogen responsiveness. *Carcinogenesis.* **2016**, *37* (8), 741-750.
74. Reed, M., Principles of cancer treatment by surgery. *Surgery. (Oxford).* **2009**, *27* (4), 178-181.
75. Falk, S., Principles of cancer treatment by radiotherapy. *Surgery. (Oxford).* **2003**, *21* (11), 269-272.
76. Bhosle, J.; Hall, G., Principles of cancer treatment by chemotherapy. *Surgery. (Oxford).* **2009**, *27* (4), 173-177.
77. Bateman, A.; Martin, M. J.; O'Donovan, C.; Magrane, M.; Alpi, E.; Antunes, R.; Bely, B.; Bingley, M.; Bonilla, C.; Britto, R.; Bursteinas, B.; Bye-A-Jee, H.; Cowley, A.; Da Silva, A.; De Giorgi, M.; Dogan, T.; Fazzini, F.; Castro, L. G.; Figueira, L.; Garmiri, P.; Georghiou, G.; Gonzalez, D.; Hatton-Ellis, E.; Li, W. Z.; Liu, W. D.; Lopez, R.; Luo, J.; Lussi, Y.; MacDougall, A.; Nightingale, A.; Palka, B.; Pichler, K.; Poggioli, D.; Pundir, S.; Pureza, L.; Qi, G. Y.; Rosanoff, S.; Saidi, R.; Sawford, T.; Shypitsyna, A.; Speretta, E.; Turner, E.; Tyagi, N.; Volynkin, V.; Wardell, T.; Warner, K.; Watkins, X.; Zaru, R.; Zellner, H.; Xenarios, I.; Bougueleret, L.; Bridge, A.; Poux, S.; Redaschi, N.; Aimo, L.; Argoud-Puy, G.; Auchincloss, A.; Axelsen, K.; Bansal, P.; Baratin, D.; Blatter, M. C.; Boeckmann, B.; Bolleman, J.; Boutet, E.; Breuza, L.; Casal-Casas, C.; de Castro, E.; Coudert, E.; Cuche, B.; Doche, M.; Dornevil, D.; Duvaud, S.; Estreicher, A.; Famiglietti, L.; Feuermann, M.; Gasteiger, E.; Gehant, S.; Gerritsen, V.; Gos, A.; Gruaz-Gumowski, N.; Hinz, U.; Hulo, C.; Jungo, F.; Keller, G.; Lara, V.; Lemercier, P.; Lieberherr, D.; Lombardot, T.; Martin, X.; Masson, P.; Morgat, A.; Neto, T.; Nospikel, N.; Paesano, S.; Pedruzzi, I.; Pilbout, S.; Pozzato, M.; Pruess, M.; Rivoire, C.; Roechert, B.; Schneider, M.; Sigrist, C.; Sonesson, K.; Staehli, S.; Stutz, A.; Sundaram, S.; Tognolli, M.; Verbregue, L.; Veuthey, A. L.; Wu, C. H.; Arighi, C. N.; Arminski, L.; Chen, C. M.; Chen, Y. X.; Garavelli, J. S.; Huang, H. Z.; Laiho, K.; McGarvey, P.; Natale, D. A.; Ross, K.; Vinayaka, C. R.; Wang, Q. H.; Wang, Y. Q.; Yeh, L. S.; Zhang, J.; UniProt, C., UniProt: the universal protein knowledgebase. *Nucleic. Acids. Res.* **2017**, *45* (D1), D158-D169.
78. Altschul, S. F.; Gish, W.; Miller, W.; Myers, E. W.; Lipman, D. J., Basic local alignment search tool. *J. Mol. Biol.* **1990**, *215* (3), 403-410.



79. Goujon, M.; McWilliam, H.; Li, W. Z.; Valentin, F.; Squizzato, S.; Paern, J.; Lopez, R., A new bioinformatics analysis tools framework at EMBL-EBI. *Nucleic. Acids. Res.* **2010**, *38*, W695-W699.
80. Nakanishi, Y.; Akiyama, N.; Tsukaguchi, T.; Fujii, T.; Sakata, K.; Sase, H.; Isobe, T.; Morikami, K.; Shindoh, H.; Mio, T.; Ebiike, H.; Taka, N.; Aoki, Y.; Ishii, N., The Fibroblast Growth Factor Receptor Genetic Status as a Potential Predictor of the Sensitivity to CH5183284/Debio 1347, a Novel Selective FGFR Inhibitor. *Mol. Cancer Ther.* **2014**, *13* (11), 2547-2558.
81. Bunney, T. D.; Wan, S. Z.; Thiyagarajan, N.; Sutto, L.; Williams, S. V.; Ashford, P.; Koss, H.; Knowles, M. A.; Gervasio, F. L.; Coveney, P. V.; Katan, M., The Effect of Mutations on Drug Sensitivity and Kinase Activity of Fibroblast Growth Factor Receptors: A Combined Experimental and Theoretical Study. *Ebiomedicine.* **2015**, *2* (3), 194-204.
82. Cheng, W. Y.; Wang, M. X.; Tian, X.; Zhang, X. J., An overview of the binding models of FGFR tyrosine kinases in complex with small molecule inhibitors. *Eur. J. Med. Chem.* **2017**, *126*, 476-490.
83. Klein, T.; Vajpai, N.; Phillips, J. J.; Davies, G.; Holdgate, G. A.; Phillips, C.; Tucker, J. A.; Norman, R. A.; Scott, A. D.; Higazi, D. R.; Lowe, D.; Thompson, G. S.; Breeze, A. L., Structural and dynamic insights into the energetics of activation loop rearrangement in FGFR1 kinase. *Nat. Commun.* **2015**, *6*, 12.
84. Roth, G. J.; Binder, R.; Colbatzky, F.; Dallinger, C.; Schlenker-Herceg, R.; Hilberg, F.; Wollin, S. L.; Kaiser, R., Nintedanib: From Discovery to the Clinic. *J. Med. Chem.* **2015**, *58* (3), 1053-1063.
85. Shaw, A. T.; Hsu, P. P.; Awad, M. M.; Engelman, J. A., Tyrosine kinase gene rearrangements in epithelial malignancies. *Nat. Rev. Cancer* **2013**, *13* (11), 772-787.
86. Chase, A.; Grand, F. H.; Cross, N. C. P., Activity of TK1258 against primary cells and cell lines with FGFR1 fusion genes associated with the 8p11 myeloproliferative syndrome. *Blood* **2007**, *110* (10), 3729-3734.
87. André, F.; Bachelot, T.; Campone, M.; Dalenc, F.; Perez-Garcia, J. M.; Hurvitz, S. A.; Turner, N.; Rugo, H.; Smith, J. W.; Deudon, S., Targeting FGFR with dovitinib (TKI258): preclinical and clinical data in breast cancer. *Clin. Cancer. Res.* **2013**, *19* (13), 3693-3702.
88. Bello, E.; Colella, G.; Scarlato, V.; Oliva, P.; Berndt, A.; Valbusa, G.; Serra, S. C.; D'Incalci, M.; Cavalletti, E.; Giavazzi, R.; Damia, G.; Camboni, G., E-3810 Is a Potent Dual Inhibitor of VEGFR and FGFR that Exerts Antitumor Activity in Multiple Preclinical Models. *Cancer. Res.* **2011**, *71* (4), 1396-1405.
89. Gavine, P. R.; Mooney, L.; Kilgour, E.; Thomas, A. P.; Al-Kadhimi, K.; Beck, S.; Rooney, C.; Coleman, T.; Baker, D.; Mellor, M. J.; Brooks, A. N.; Klinowska, T., AZD4547: An Orally Bioavailable, Potent, and Selective Inhibitor of the Fibroblast Growth Factor Receptor Tyrosine Kinase Family. *Cancer. Res.* **2012**, *72* (8), 2045-2056.
90. Smyth, E. C.; Turner, N. C.; Pearson, A.; Peckitt, C.; Chau, I.; Watkins, D. J.; Starling, N.; Rao, S.; Gillbanks, A.; Kilgour, E.; Sumpter, K. A.; Smith, N. R.;

- Cutts, R.; Rooney, C.; Thomas, A. L.; Ajaz, M. A.; Chua, S.; Brown, G.; Popat, S.; Cunningham, D., Phase II study of AZD4547 in FGFR amplified tumours: Gastroesophageal cancer (GC) cohort pharmacodynamic and biomarker results. *J. Clin. Oncol.* **2016**, *34* (4), 1.
91. Mohammadi, M.; Froum, S.; Hamby, J. M.; Schroeder, M. C.; Panek, R. L.; Lu, G. H.; Eliseenkova, A. V.; Green, D.; Schlessinger, J.; Hubbard, S. R., Crystal structure of an angiogenesis inhibitor bound to the FGF receptor tyrosine kinase domain. *Embo. J.* **1998**, *17* (20), 5896-5904.
92. Miyake, M.; Ishii, M.; Koyama, N.; Kawashima, K.; Kodama, T.; Anai, S.; Fujimoto, K.; Hirao, Y.; Sugano, K., 1-tert-Butyl-3-(3,5-dimethoxyphenyl)-2-(4-diethylamino-butylamino)-pyrido [2,3-d] pyrimidin-7-yl-urea (PD173074), a Selective Tyrosine Kinase Inhibitor of Fibroblast Growth Factor Receptor-3 (FGFR3), Inhibits Cell Proliferation of Bladder Cancer Carrying the FGFR3 Gene Mutation along with Up-Regulation of p27/Kip1 and G(1)/G(0) Arrest. *J. Pharmacol. Exp. Ther.* **2010**, *332* (3), 795-802.
93. Guagnano, V.; Kauffmann, A.; Wohrle, S.; Stamm, C.; Ito, M.; Barys, L.; Pornon, A.; Yao, Y.; Li, F.; Zhang, Y.; Chen, Z.; Wilson, C. J.; Bordas, V.; Le Douget, M.; Gaither, L. A.; Borawski, J.; Monahan, J. E.; Venkatesan, K.; Brummendorf, T.; Thomas, D. M.; Garcia-Echeverria, C.; Hofmann, F.; Sellers, W. R.; Graus-Porta, D., FGFR Genetic Alterations Predict for Sensitivity to NVP-BGJ398, a Selective Pan-FGFR Inhibitor. *Cancer. Discov.* **2012**, *2* (12), 1118-1133.
94. Mohammadi, M.; McMahon, G.; Sun, L.; Tang, C.; Hirth, P.; Yeh, B. K.; Hubbard, S. R.; Schlessinger, J., Structures of the tyrosine kinase domain of fibroblast growth factor receptor in complex with inhibitors. *Science.* **1997**, *276* (5314), 955-960.
95. Liu, J.; Peng, X.; Dai, Y.; Zhang, W.; Ren, S. M.; Ai, J.; Geng, M. Y.; Li, Y. X., Design, synthesis and biological evaluation of novel FGFR inhibitors bearing an indazole scaffold. *Org. Biomol. Chem.* **2015**, *13* (28), 7643-7654.
96. Eathiraj, S.; Palma, R.; Hirschi, M.; Volckova, E.; Nakuci, E.; Castro, J.; Chen, C. R.; Chan, T. C. K.; France, D. S.; Ashwell, M. A., A novel mode of protein kinase inhibition exploiting hydrophobic motifs of autoinhibited kinases discovery of atp-independent inhibitors of fibroblast growth factor receptor. *J. Biol. Chem.* **2011**, *286* (23), 20677-20687.
97. O'Hare, T.; Shakespeare, W. C.; Zhu, X. T.; Eide, C. A.; Rivera, V. M.; Wang, F.; Adrian, L. T.; Zhou, T. J.; Huang, W. S.; Xu, Q. H.; Metcalf, C. A.; Tyner, J. W.; Loriaux, M. M.; Corbin, A. S.; Wardwell, S.; Ning, Y. Y.; Keats, J. A.; Wang, Y. H.; Sundaramoorthi, R.; Thomas, M.; Zhou, D.; Snodgrass, J.; Commodore, L.; Sawyer, T. K.; Dalgarno, D. C.; Deininger, M. W. N.; Druker, B. J.; Clackson, T., AP24534, a Pan-BCR-ABL Inhibitor for Chronic Myeloid Leukemia, Potently Inhibits the T315I Mutant and Overcomes Mutation-Based Resistance. *Cancer. Cell.* **2009**, *16* (5), 401-412.
98. Tan, L.; Wang, J.; Tanizaki, J.; Huang, Z. F.; Aref, A. R.; Rusan, M.; Zhu, S. J.; Zhang, Y. Y.; Ercan, D.; Liao, R. G.; Capelletti, M.; Zhou, W. J.; Hur, W.; Kim, N.; Sim, T.; Gaudet, S.; Barbie, D. A.; Yeh, J. R. J.; Yun, C. H.; Hammerman, P. S.; Mohammadi, M.; Janne, P. A.; Gray, N. S., Development

- of covalent inhibitors that can overcome resistance to first-generation FGFR kinase inhibitors. *P. Natl. Acad. Sci. USA*. **2014**, *111* (45), E4869-E4877.
99. Hagel, M.; Miduturu, C.; Sheets, M.; Rubin, N.; Weng, W. F.; Stransky, N.; Bifulco, N.; Kim, J. L.; Hodous, B.; Brooijmans, N.; Shutes, A.; Winter, C.; Lengauer, C.; Kohl, N. E.; Guzi, T., First Selective Small Molecule Inhibitor of FGFR4 for the Treatment of Hepatocellular Carcinomas with an Activated FGFR4 Signaling Pathway. *Cancer. Discov.* **2015**, *5* (4), 424-437.
100. Simmons, K. J.; Chopra, I.; Fishwick, C. W. G., Structure-based discovery of antibacterial drugs. *Nat. Rev. Microbiol.* **2010**, *8* (7), 501-510.
101. Anderson, A. C., The process of structure-based drug design. *Chem. Biol.* **2003**, *10* (9), 787-797.
102. Turner, L., Identification of Novel Inhibitors of FXIIa using Fragment-Led Structure Based Drug Design. The University of Leeds (Department of Chemistry), 2014.
103. Schrödinger *Maestro*, LLC: New York, 2012.
104. Friesner, R. A.; Banks, J. L.; Murphy, R. B.; Halgren, T. A.; Klicic, J. J.; Mainz, D. T.; Repasky, M. P.; Knoll, E. H.; Shelley, M.; Perry, J. K.; Shaw, D. E.; Francis, P.; Shenkin, P. S., Glide: A new approach for rapid, accurate docking and scoring. 1. Method and assessment of docking accuracy. *J. Med. Chem.* **2004**, *47* (7), 1739-1749.
105. [www.pymol.org](http://www.pymol.org), Last accessed 19/04/2017.
106. Schneider, G.; Fechner, U., Computer-based de novo design of drug-like molecules. *Nat. Rev. Drug. Discov.* **2005**, *4* (8), 649-663.
107. Cain, R., Design and Synthesis of Metallo- $\beta$ -Lactamase Inhibitors. The University of Leeds (Department of Chemistry), 2012.
108. Smith, G. B.; Dezeny, G. C.; Hughes, D. L.; King, A. O.; Verhoeven, T. R., Mechanistic studies of the suzuki cross-coupling reaction. *J. Org. Chem.* **1994**, *59* (26), 8151-8156.
109. Liu, Q.; Batt, D. G.; DeLucca, G. V.; Shi, Q.; Tebben, A. J., Carbazole carboxamide compounds useful as kinase inhibitors, US20100160303. Google Patents: 2010.
110. Bartholomew, C. H., Mechanisms of catalyst deactivation. *Appl Catal. A-Gen.* **2001**, *212* (1-2), 17-60.
111. Baldwin, I. R.; Down, K. D.; Faulder, P.; Gaines, S.; Hamblin, J. N.; Harrison, Z. A.; Jones, K. L.; Jones, P. S.; Keeling, S. E.; Le, J., Indazole derivatives for use in the treatment of influenza virus infection, WO2012032065A1. Google Patents: 2012.
112. Baldwin, I. R.; Down, K. D.; Faulder, P.; Gaines, S.; Hamblin, J. N.; Le, J.; Lunniss, C. J.; Parr, N. J.; Ritchie, T. J.; Robinson, J. E., Benzpyrazol derivatives as inhibitors of pi3 kinases, WO2009147188A1. Google Patents: 2009.
113. Kuntz, I. D.; Chen, K.; Sharp, K. A.; Kollman, P. A., The maximal affinity of ligands. *P. Natl. Acad. Sci. USA*. **1999**, *96* (18), 9997-10002.

114. Schultes, S.; de Graaf, C.; Haaksma, E. E. J.; de Esch, I. J. P.; Leurs, R.; Krämer, O., Ligand efficiency as a guide in fragment hit selection and optimization. *Drug. Discov. Today. Technol.* **2010**, *7* (3), e157-e162.
115. Lennox, A. J. J.; Lloyd-Jones, G. C., Selection of boron reagents for Suzuki-Miyaura coupling. *Chem. Soc. Rev.* **2014**, *43* (1), 412-443.
116. Lee, C. Y.; Ahn, S. J.; Cheon, C. H., Protodeboronation of ortho- and para-Phenol Boronic Acids and Application to ortho and meta Functionalization of Phenols Using Boronic Acids as Blocking and Directing Groups. *J. Org. Chem.* **2013**, *78* (23), 12154-12160.
117. Duquenne, C.; Johnson, N.; Knight, S. D.; Lafrance, L.; Miller, W. H.; Newlander, K.; Romeril, S.; Rouse, M. B.; Tian, X.; Verma, S. K., Indazoles, WO2011140325A1. Google Patents: 2011.
118. Altman, R. A.; Fors, B. P.; Buchwald, S. L., Pd-catalyzed amination reactions of aryl halides using bulky biarylmonophosphine ligands. *Nat. Protoc.* **2007**, *2* (11), 2881-2887.
119. Ngwendson, J. N.; Atemnkeng, W. N.; Schultze, C. M.; Banerjee, A., A convenient synthesis of symmetric 1,2-diarylethenes from arylmethyl phosphonium salts. *Org. Lett.* **2006**, *8* (18), 4085-4088.
120. Yan, G. B.; Yang, M. H.; Wu, X. M., Synthetic applications of arylboronic acid via an aryl radical transfer pathway. *Org. Biomol. Chem.* **2013**, *11* (46), 7999-8008.
121. Bogenstaetter, M.; Chai, W.; Kwok, A. K., Bicyclic compounds as h3 receptor ligands, WO2002012224A3. Google Patents: 2002.
122. Zeng, D.; Tahar-Djebbar, I.; Xiao, Y.; Kameche, F.; Kayunkid, N.; Brinkmann, M.; Guillon, D.; Heinrich, B.; Donnio, B.; Ivanov, D. A.; Lacaze, E.; Kreher, D.; Mathevet, F.; Attias, A.-J., Intertwined Lamello-Columnar Coassemblies in Liquid-Crystalline Side-Chain  $\Pi$ -Conjugated Polymers: Toward a New Class of Nanostructured Supramolecular Organic Semiconductors. *Macromolecules.* **2014**, *47* (5), 1715-1731.
123. Kelly, J. W.; Sekijima, Y., Compositions and methods for stabilizing transthyretin and inhibiting transthyretin misfolding, WO2004056315A3. Google Patents: 2005.
124. Brady, R. M.; Vom, A.; Roy, M. J.; Toovey, N.; Smith, B. J.; Moss, R. M.; Hatzis, E.; Huang, D. C. S.; Parisot, J. P.; Yang, H.; Street, I. P.; Colman, P. M.; Czabotar, P. E.; Baell, J. B.; Lessene, G., De-Novo Designed Library of Benzoylureas as Inhibitors of BCL-X-L: Synthesis, Structural and Biochemical Characterization. *J. Med. Chem.* **2014**, *57* (4), 1323-1343.
125. Zhao, B.; Li, Y.; Xu, P.; Dai, Y.; Luo, C.; Sun, Y.; Ai, J.; Geng, M.; Duan, W., Discovery of Substituted 1 H-Pyrazolo [3, 4-b] pyridine Derivatives as Potent and Selective FGFR Kinase Inhibitors. *ACS Med. Chem. Lett.* **2016**, *7* (6), 629-634.
126. Akatsuka, H.; Sugama, H.; Awai, N.; Kawaguchi, T.; Takahashi, Y.; Iijima, T.; Shen, J.; Xia, G.; Xie, J. Morpholine derivative, WO2008153182A1. 2008.

127. Allen, J. R.; Amegadzie, A. K.; Gardinier, K. M.; Gregory, G. S.; Hitchcock, S. A.; Hoogestraat, P. J.; Jones, W. D. J.; Smith, D. L. Cb1 modulator compounds, WO2005066126A1. 2005.
128. Wrzeciono, U.; Linkowska, E.; Felinska, W., Azoles .3. Nitroderivatives of 3-Chloroindazole and Effect of C-5-, C-6-Nitrogroups and N-Nitrogroups on Reactivity of C-3 Chlorine Atom. *Pharmazie*. **1978**, *33* (7), 419-424.
129. Blunt, R.; Eatherton, A. J.; Garzya, V.; Healy, M. P.; Myatt, J.; Porter, R. A., Benzoxazinone derivatives for the treatment of glytl mediated disorders, WO2011012622A1. Google Patents: 2011.
130. Bahmanyar, S.; Bates, R. J.; Blease, K.; Calabrese, A. A.; Daniel, T. O.; Delgado, M.; Elsner, J.; Erdman, P.; Fahr, B.; Ferguson, G., Aminotriazolopyridines and their use as kinase inhibitors, WO2010027500A1. Google Patents: 2010.
131. Gao, L.-J.; Kovackova, S.; Šála, M.; Ramadori, A. T.; De Jonghe, S.; Herdewijn, P., Discovery of Dual Death-Associated Protein Related Apoptosis Inducing Protein Kinase 1 and 2 Inhibitors by a Scaffold Hopping Approach. *J. Med. Chem.* **2014**, *57* (18), 7624-7643.
132. Gauss, C. M.; Herbert, B.; Ma, J.; Nguyen, T. M.; Schumacher, R. A.; Tehim, A.; Xie, W., Indoles, 1h-indazoles, 1,2-benzisoxazoles, and 1,2-benzisothiazoles, and preparation and uses thereof, WO2005063767A3. Google Patents: 2005.
133. Appel, R., Tertiary Phosphane-Tetrachloromethane, a Versatile Reagent for Chlorination, Dehydration, and P-N Linkage. *Angew. Chem. Int. Edit.* **1975**, *14* (12), 801-811.
134. Qu, Z.; Chen, X.; Qu, L.; Yuan, J.; Li, H.; Zhao, Y., Synthesis of Novel Piperazine Phosphoramidate Analogues of 2-Arylquinolones. *Phosphorus. Sulfur.* **2010**, *185*, 1516-1520.
135. Tucker, Julie A.; Klein, T.; Breed, J.; Breeze, Alexander L.; Overman, R.; Phillips, C.; Norman, Richard A., Structural Insights into FGFR Kinase Isoform Selectivity: Diverse Binding Modes of AZD4547 and Ponatinib in Complex with FGFR1 and FGFR4. *Structure.* **2014**, *22* (12), 1764-1774.
136. Klein, T.; Tucker, J.; Holdgate, G. A.; Norman, R. A.; Breeze, A. L., FGFR1 Kinase Inhibitors: Close Regioisomers Adopt Divergent Binding Modes and Display Distinct Biophysical Signatures. *ACS Med. Chem. Lett.* **2014**, *5* (2), 166-171.
137. Norman, R. A.; Schott, A. K.; Andrews, D. M.; Breed, J.; Foote, K. M.; Garner, A. P.; Ogg, D.; Orme, J. P.; Pink, J. H.; Roberts, K.; Rudge, D. A.; Thomas, A. P.; Leach, A. G., Protein-Ligand Crystal Structures Can Guide the Design of Selective Inhibitors of the FGFR Tyrosine Kinase. *J. Med. Chem.* **2012**, *55* (11), 5003-5012.
138. Lew, E. D.; Bae, J. H.; Rohmann, E.; Wollnik, B.; Schlessinger, J., Structural basis for reduced FGFR2 activity in LADD syndrome: Implications for FGFR autoinhibition and activation. *P. Natl. Acad. Sci. USA.* **2007**, *104* (50), 19802-19807.

139. Dannenberg, J. J., *An Introduction to Hydrogen Bonding* By George A. Jeffrey (University of Pittsburgh). Oxford University Press: New York and Oxford. 1997. ix + 303 pp. \$60.00. ISBN 0-19-509549-9. *J. Am. Chem. Soc.* **1998**, *120* (22), 5604-5604.
140. Morita, T.; Shinohara, N.; Honma, M.; Tokue, A., Establishment and characterization of a new cell-line from human bladder-cancer (JMSU1). *Urol. Res.* **1995**, *23* (3), 143-149.
141. Ethier, S. P.; Kokeny, K. E.; Ridings, J. W.; Dilts, C. A., erbB family receptor expression and growth regulation in a newly isolated human breast cancer cell line. *Cancer. Res.* **1996**, *56* (4), 899-907.
142. Williams, R. D., Human urologic cancer cell-lines. *Invest. Urol.* **1980**, *17* (5), 359-363.
143. Lovering, F.; Bikker, J.; Humblet, C., Escape from Flatland: Increasing Saturation as an Approach to Improving Clinical Success. *J. Med. Chem.* **2009**, *52* (21), 6752-6756.
144. Tischler, A. N.; Lanza, T. J., 6-substituted indoles from o-halonitrobenzenes. *Tetrahedron. Lett.* **1986**, *27* (15), 1653-1656.
145. Molander, G. A.; Canturk, B.; Kennedy, L. E., Scope of the Suzuki-Miyaura Cross-Coupling Reactions of Potassium Heteroaryltrifluoroborates. *J. Org. Chem.* **2009**, *74* (3), 973-980.
146. Gasteiger, E.; Hoogland, C.; Gattiker, A.; Duvaud, S.; Wilkins, M. R.; Appel, R. D.; Bairoch, A., Protein Identification and Analysis Tools on the ExPARy Server. In *The Proteomics Protocols Handbook*, Walker, J. M., Ed. Humana Press: 2005.

## Appendices

### 8.1 Appendix 1.0 – FRET-Based Z'-Lyte Assay®

The Z'-Lyte assay is a competitive inhibition FRET-based assay that uses a fluorescence-based, coupled-enzyme format and is based on the differential sensitivity of non-phosphorylated and phosphorylated peptides to proteolytic cleavage. The assay involves two reactions. The first reaction involves the phosphorylation of a specific tyrosine residue on a specific protein. This protein is labelled with two fluorophores; Coumarin (donor) and Fluorescein (acceptor) and these make up a FRET pair (Figure 8.1).<sup>147</sup>

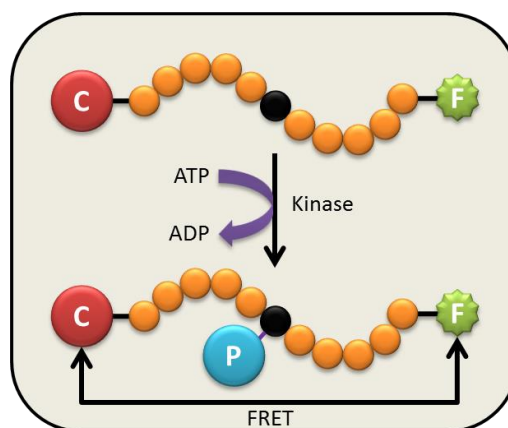


**Figure 8.1:** Kinase reaction for FRET-based Z'-lyte assay. Adapted from reference 147.

The second reaction is a development reaction in which a site-specific protease cleaves non-phosphorylated protein, leaving phosphorylated protein unaffected. The cleavage disrupts the FRET between the donor and the acceptor which is measurable (Figure 8.2).

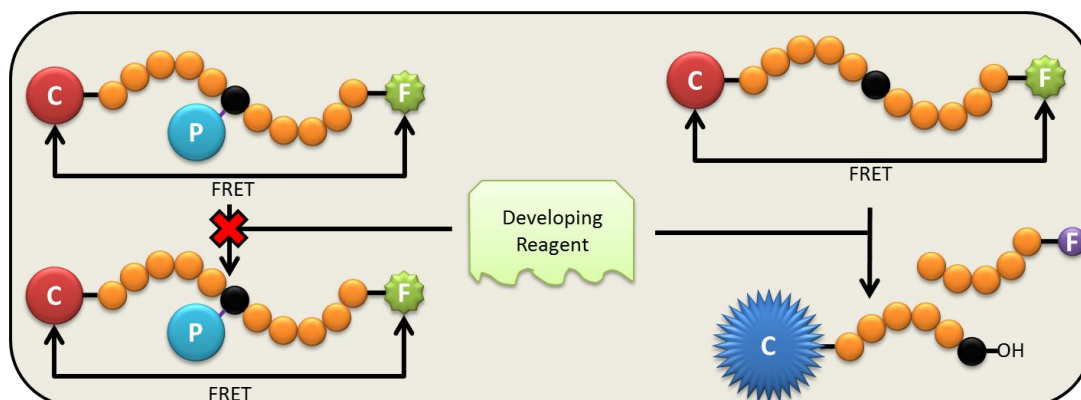


**Figure 8.2:** Development reaction for FRET-based Z'-lyte assay. Adapted from reference 147.

The ratio of donor emission to acceptor emission quantifies reaction progress and is calculated (Equation 8.1).<sup>147</sup>

$$\text{Emission Ratio} = \frac{\text{Courmarin Emission (445 nm)}}{\text{Fluorescein (520 nm)}}$$

**Equation 8.1:** Adapted from reference 147.

For each assay a Z-prime value is calculated and is a measure of assay robustness. This calculation incorporates the standard deviation observed in each control experiment and is a common measure of assay performance.

### 8.1.1 FGFR1 Assay Conditions

The 2X FGFR1/Tyr 04 mixture is prepared in 50 mM HEPES pH 7.5, 0.01% BRIJ-35, 10 mM MgCl<sub>2</sub>, 4 mM MnCl<sub>2</sub>, 1 mM ethylene glycol-bis(β-aminoethyl ether)-N,N,N',N'-tetraacetic acid (EGTA), 2 mM DTT. The final 10 μL Kinase Reaction consists of 0.44-2.45 ng FGFR1 and 2 μM Tyr 04 in 50 mM HEPES pH 7.5, 0.01% BRIJ-35, 10 mM MgCl<sub>2</sub>, 2 mM MnCl<sub>2</sub>, 1 mM EGTA, 1 mM DTT. After 1 hour Kinase Reaction incubation, 5 μL of a 1:64 dilution of Development Reagent B is added.  $K_m \text{ app} = 25 \mu\text{M}$ .

### 8.1.2 FGFR2 Assay Conditions

The 2X FGFR2/Tyr 04 mixture is prepared in 50 mM HEPES pH 7.5, 0.01% BRIJ-35, 10 mM MgCl<sub>2</sub>, 4 mM MnCl<sub>2</sub>, 1 mM EGTA, 2 mM DTT. The final 10 μL Kinase Reaction consists of 0.19-1.99 ng FGFR2 and 2 μM Tyr 04 in 50 mM HEPES pH 7.5, 0.01% BRIJ-35, 10 mM MgCl<sub>2</sub>, 2 mM MnCl<sub>2</sub>, 1 mM EGTA, 1 mM DTT. After the 1 hour Kinase Reaction incubation, 5 μL of a 1:64 dilution of Development Reagent B is added.  $K_m \text{ app} = 5 \mu\text{M}$ .

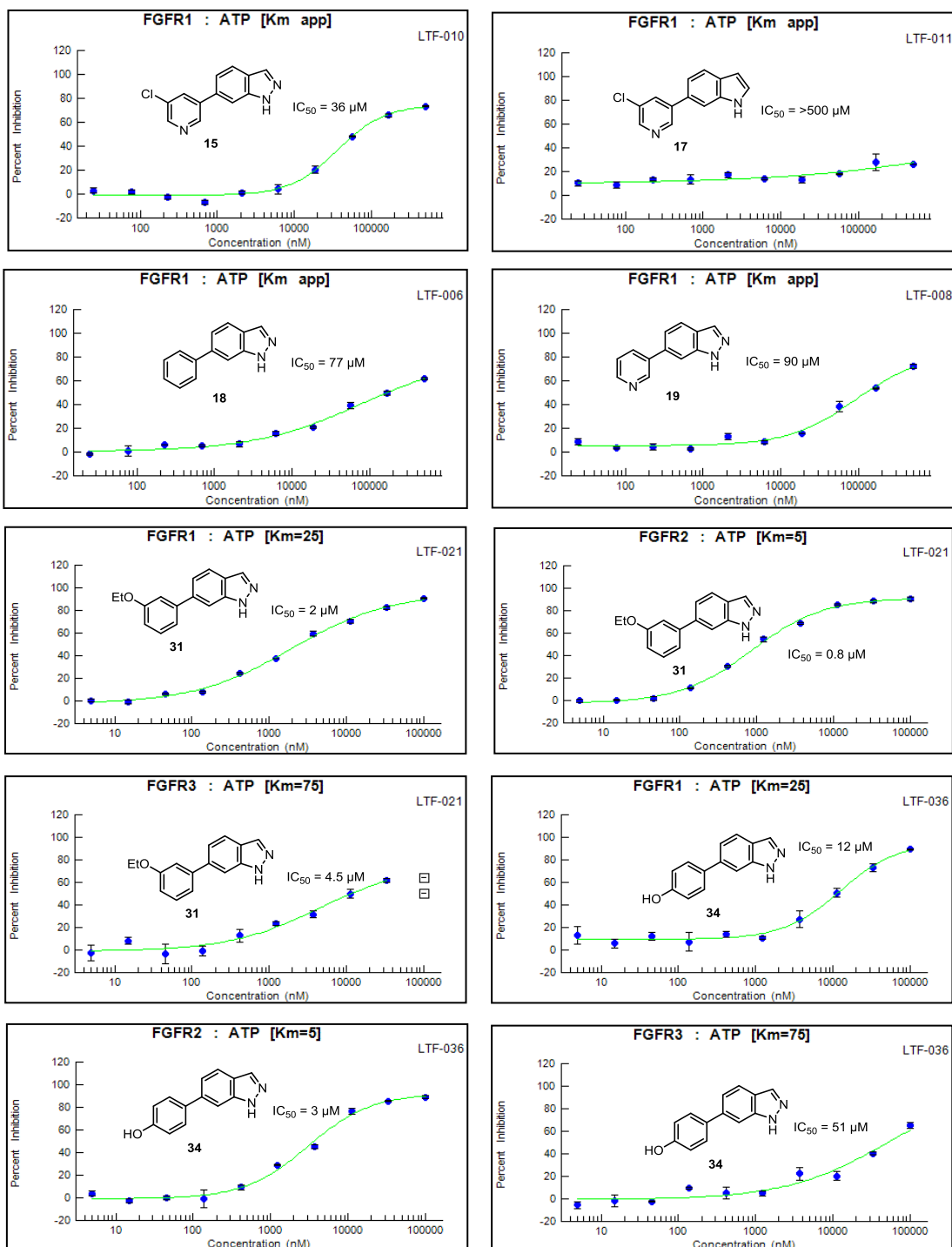
### 8.1.3 FGFR3 Assay Conditions

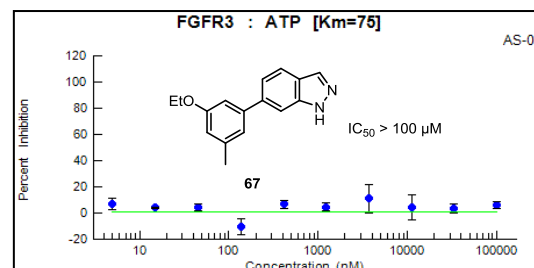
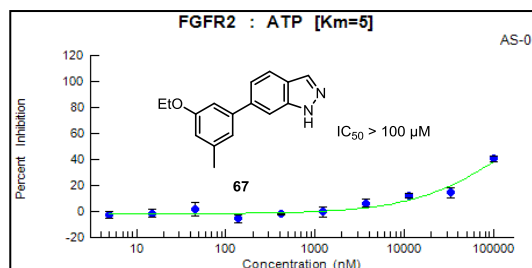
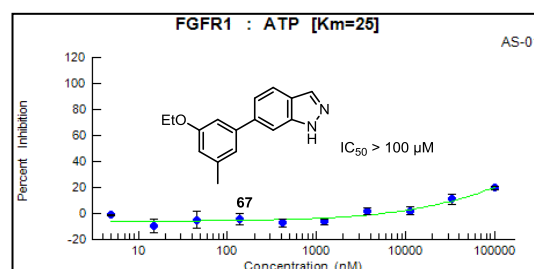
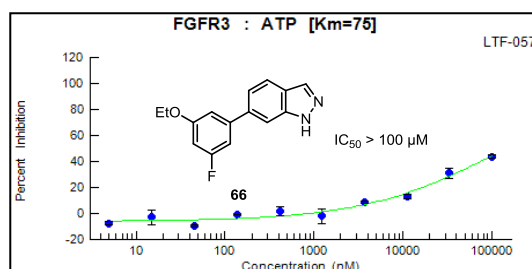
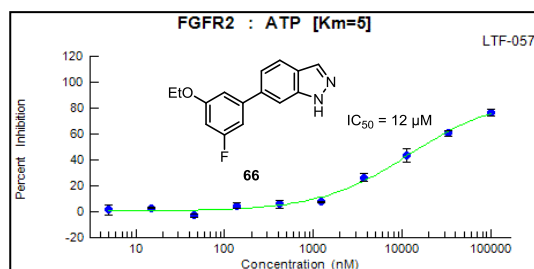
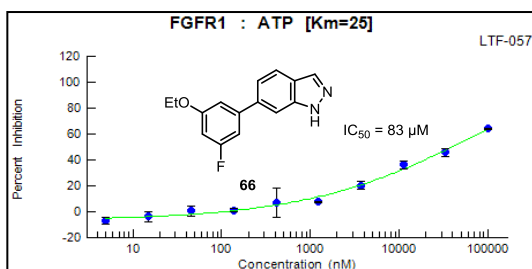
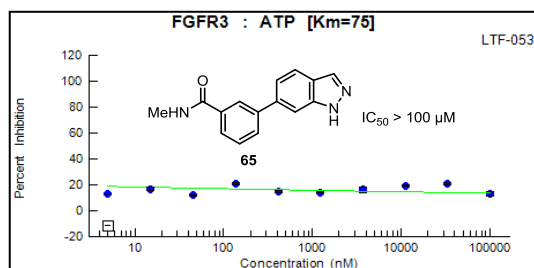
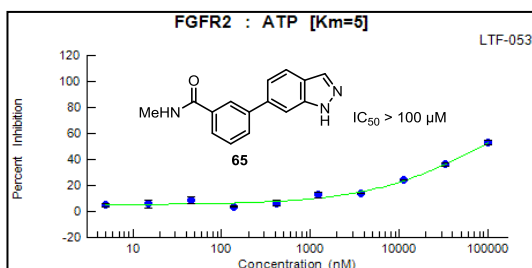
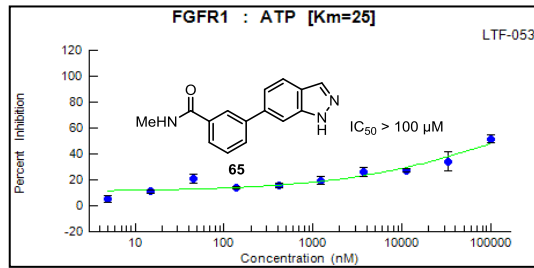
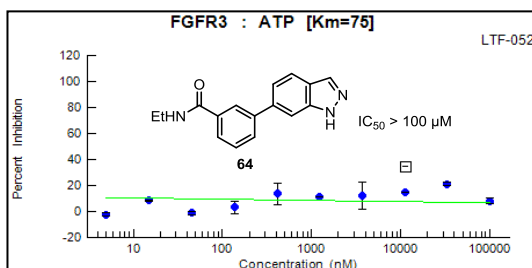
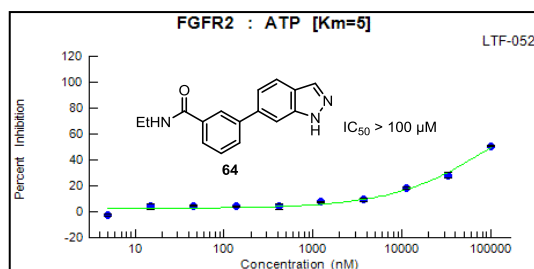
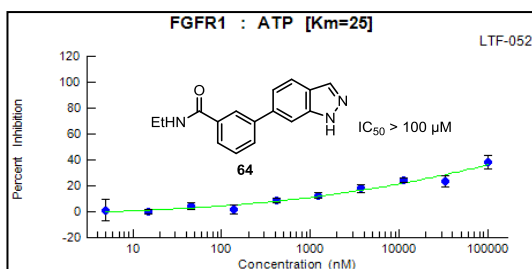
The 2X FGFR3/Tyr 04 mixture is prepared in 50 mM HEPES pH 7.5, 0.01% BRIJ-35, 10 mM MgCl<sub>2</sub>, 4 mM MnCl<sub>2</sub>, 1 mM EGTA, 2 mM DTT. The final 10 μL Kinase Reaction consists of 0.56-3.5 ng FGFR3 and 2 μM Tyr 04 in 50 mM HEPES pH 7.5, 0.01% BRIJ-35, 10 mM MgCl<sub>2</sub>, 2 mM MnCl<sub>2</sub>, 1 mM EGTA, 1 mM DTT. After the 1 hour Kinase Reaction incubation, 5 μL of a 1:64 dilution of Development Reagent B is added.  $K_m \text{ app} = 75 \mu\text{M}$ .

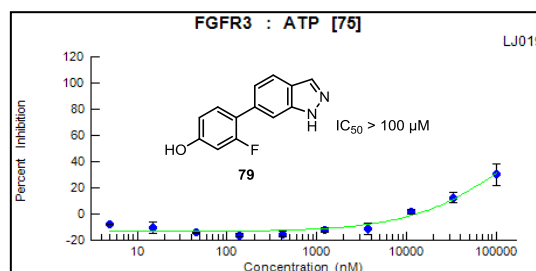
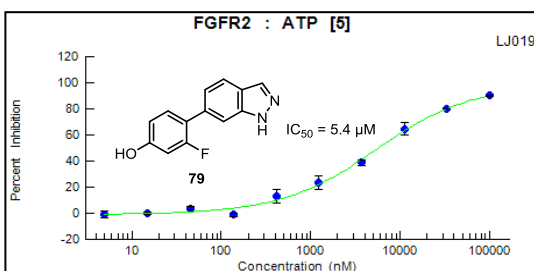
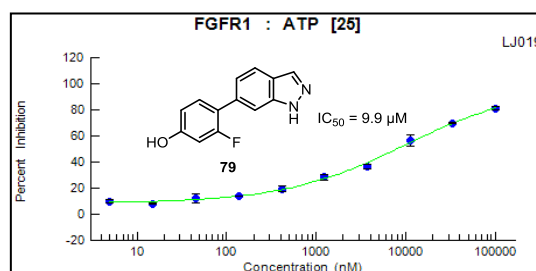
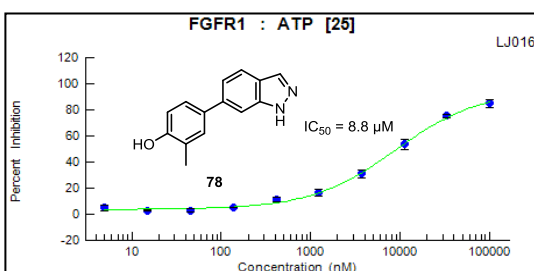
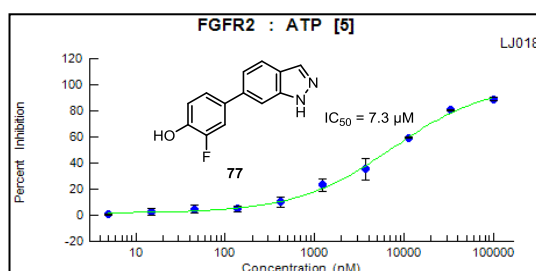
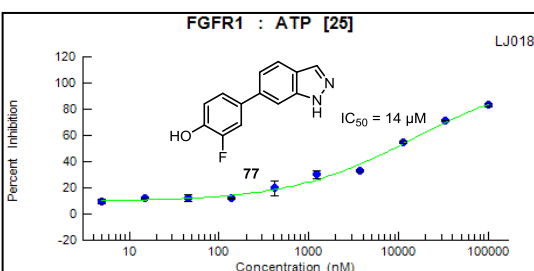
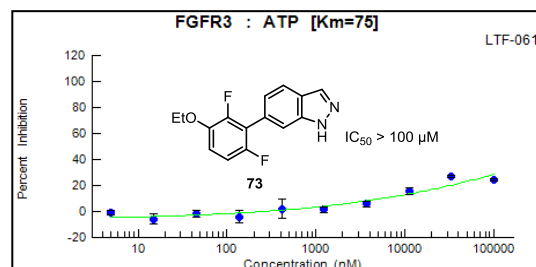
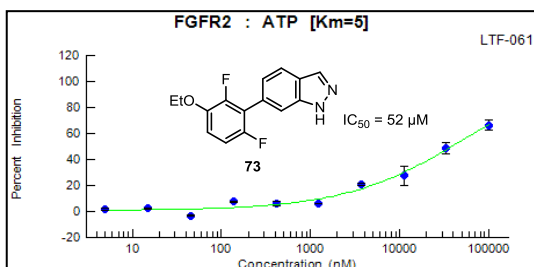
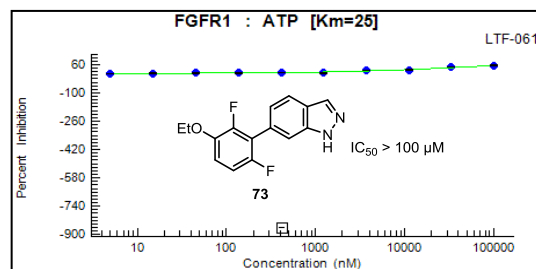
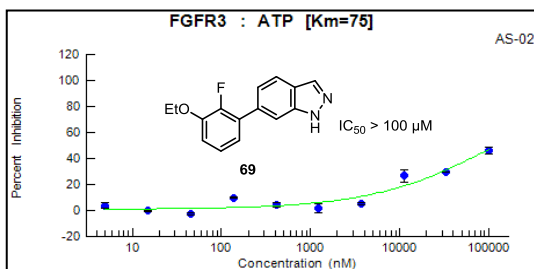
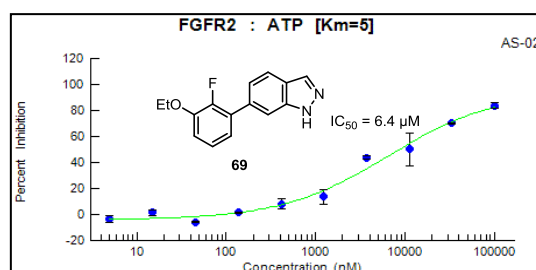
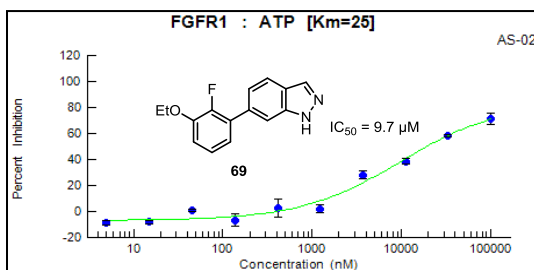


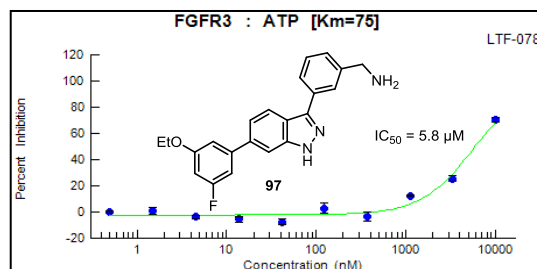
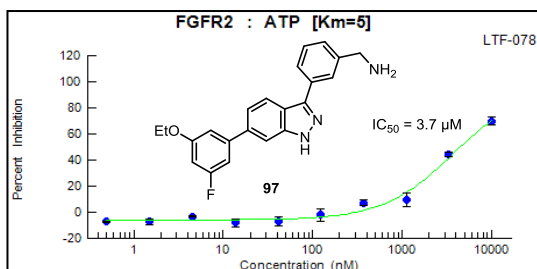
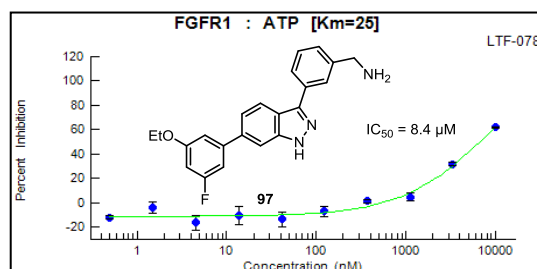
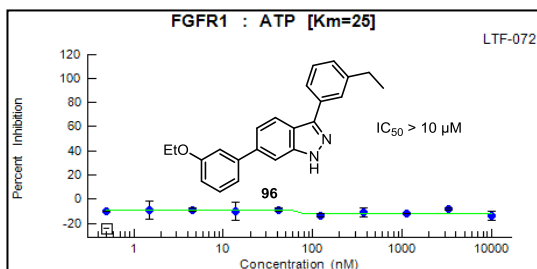
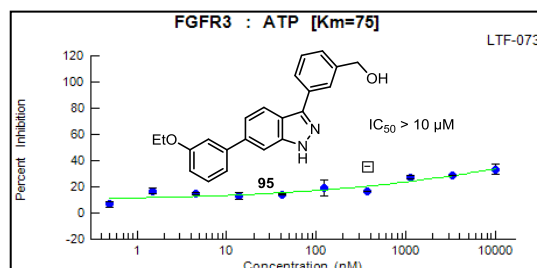
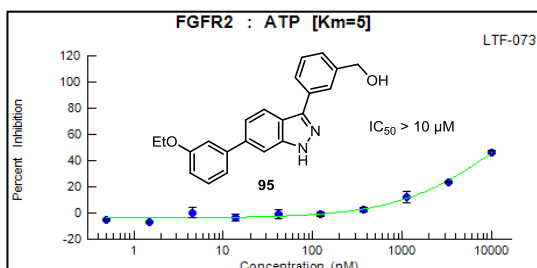
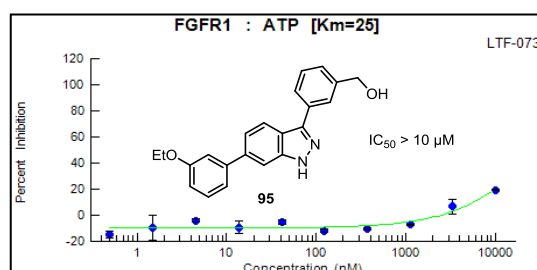
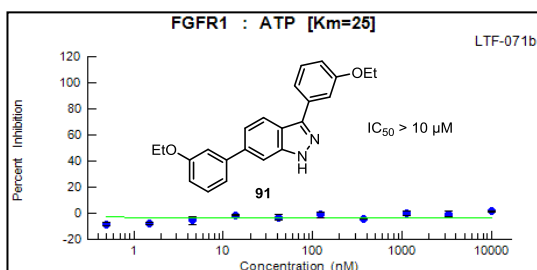
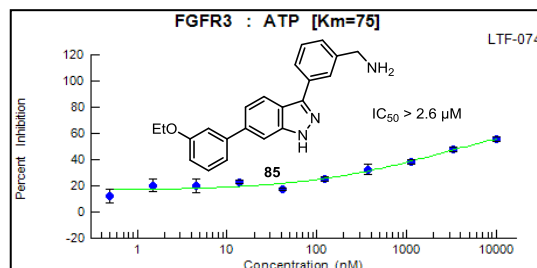
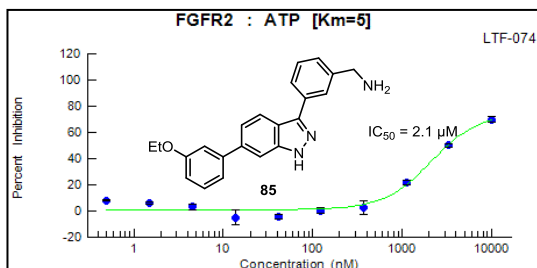
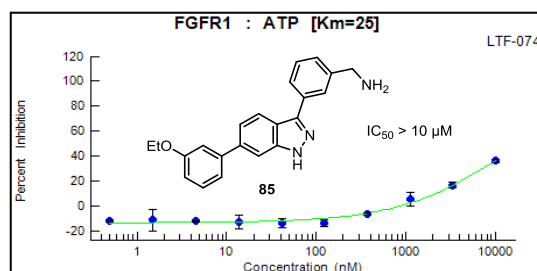
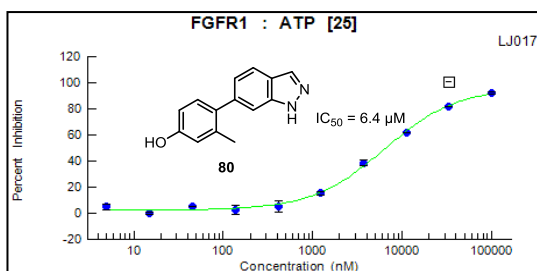
### 8.1.4 IC<sub>50</sub> Curves

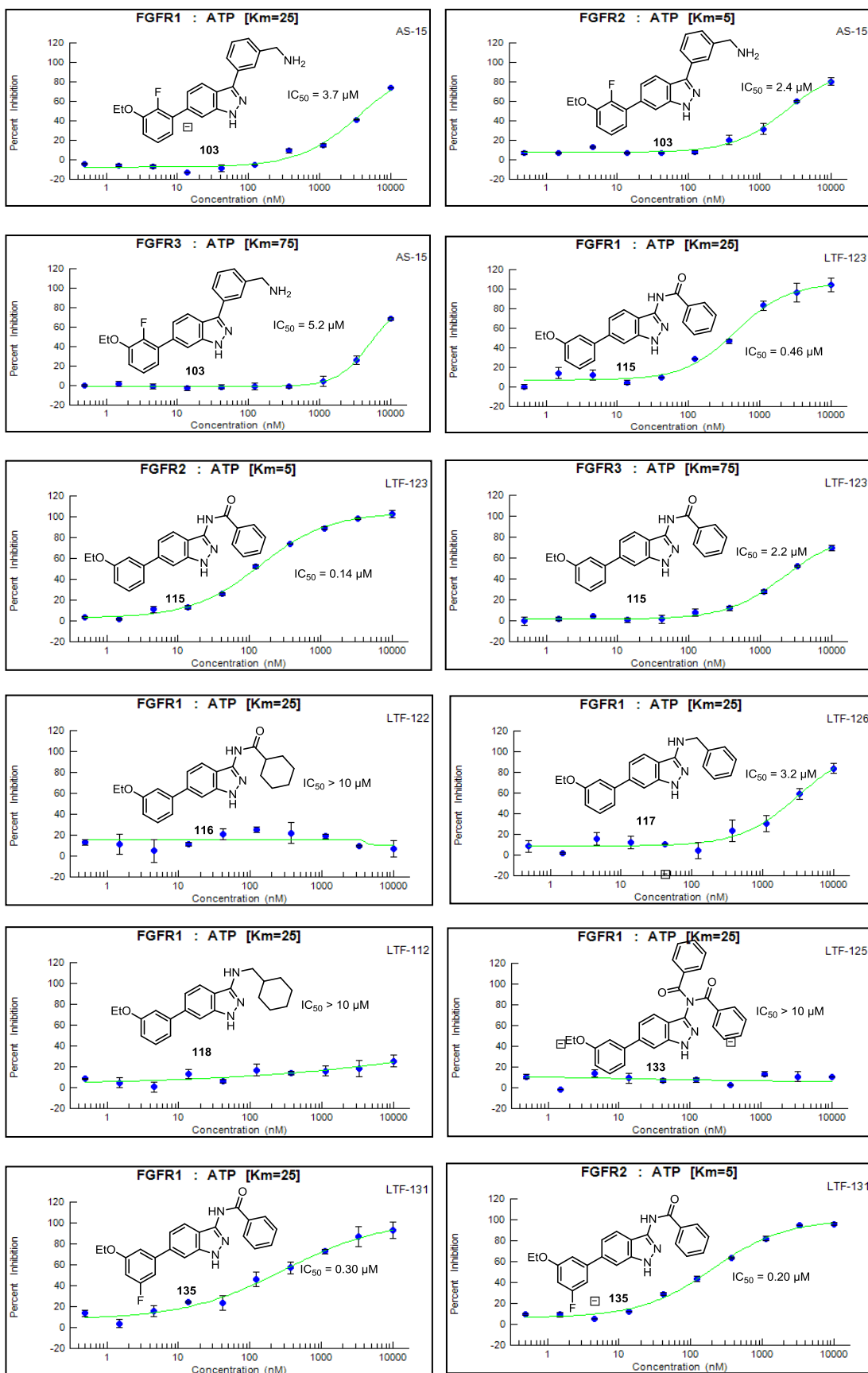
IC<sub>50</sub> values were determined using a 10-point titration experiment with 3-fold serial dilutions starting from a concentration of 500, 100 or 10 μM.

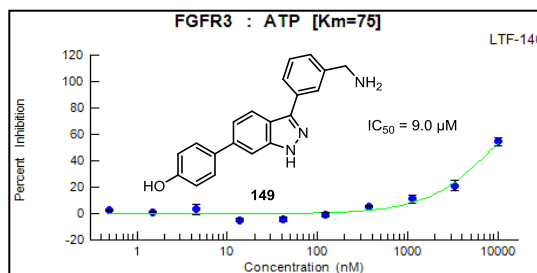
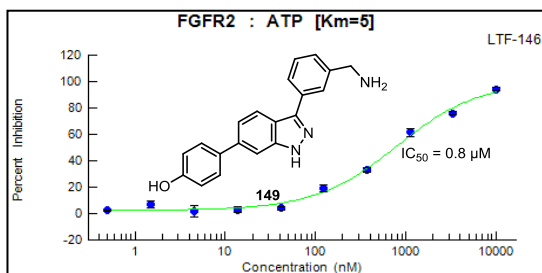
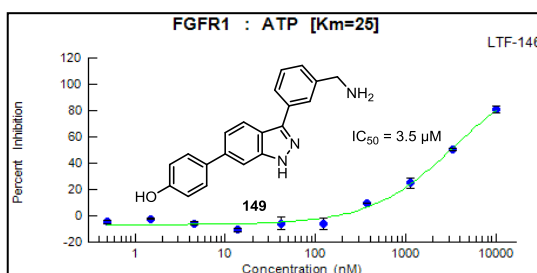
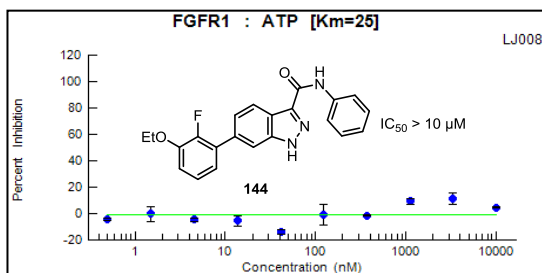
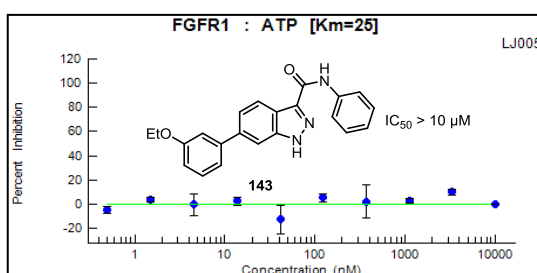
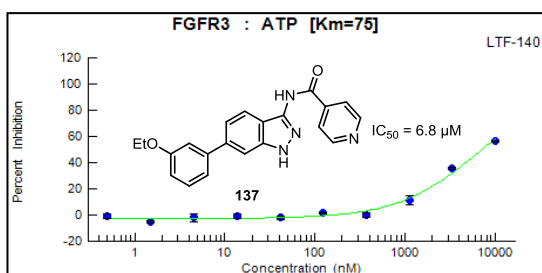
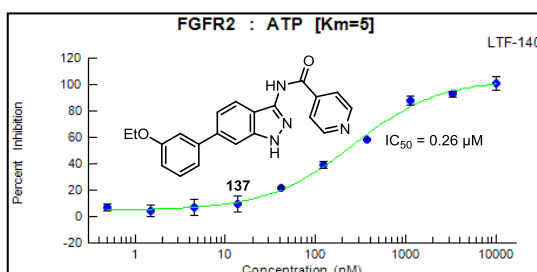
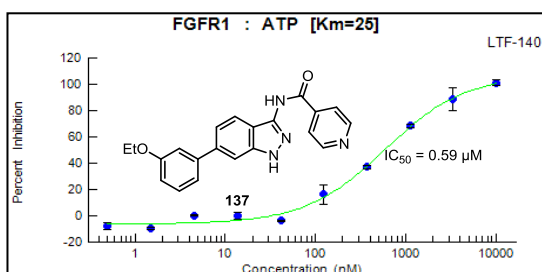
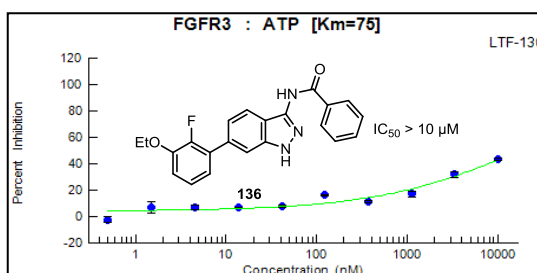
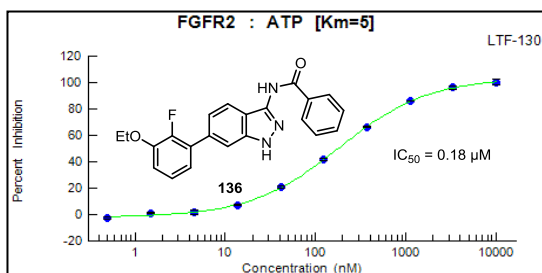
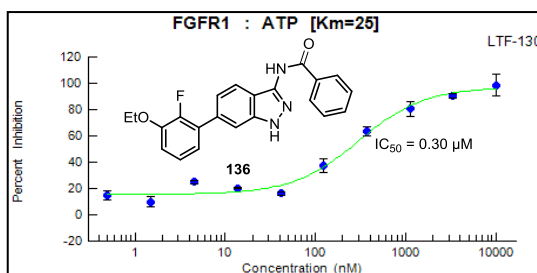
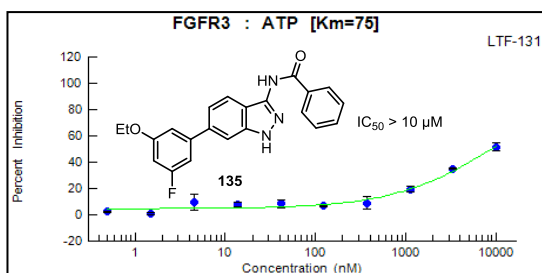


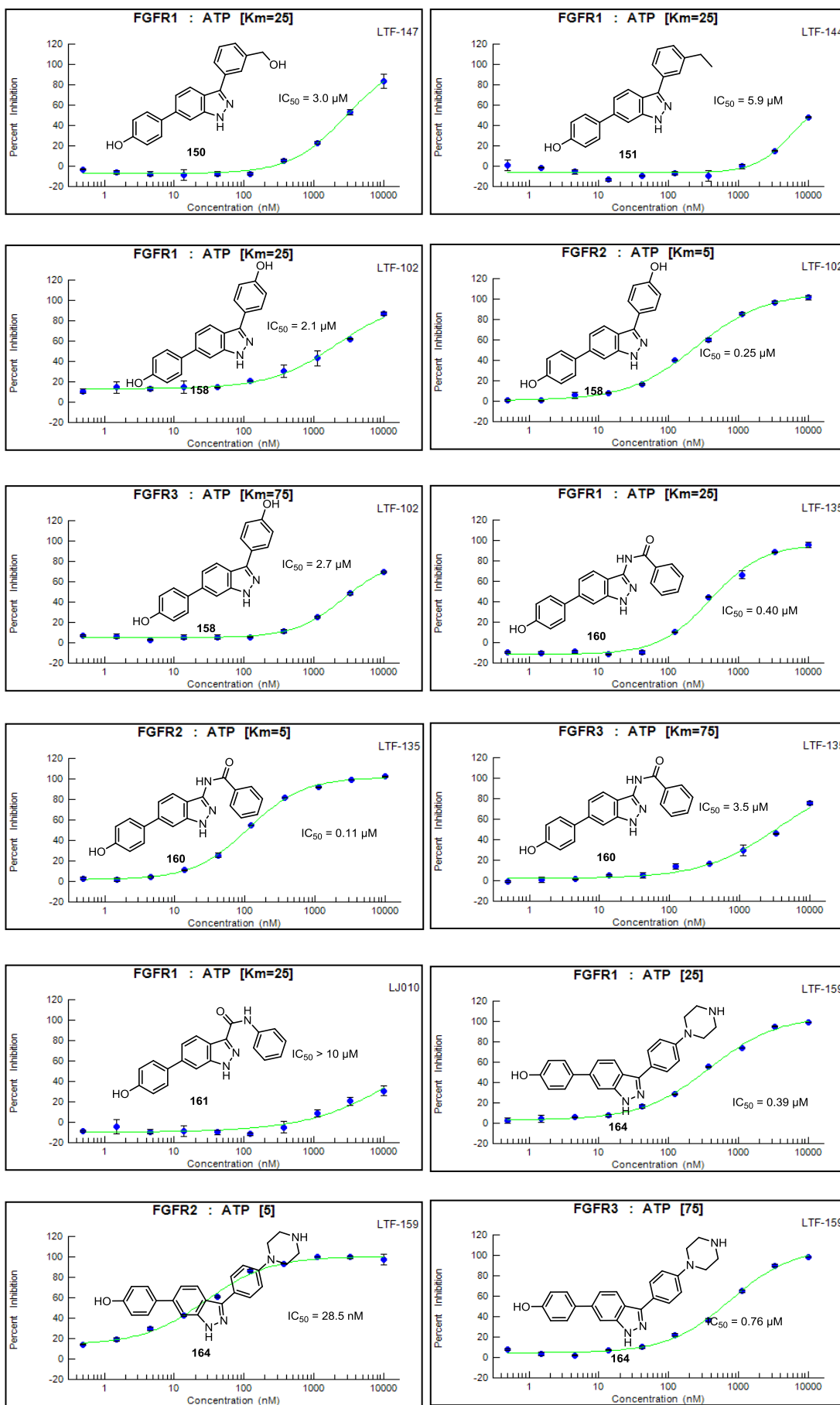


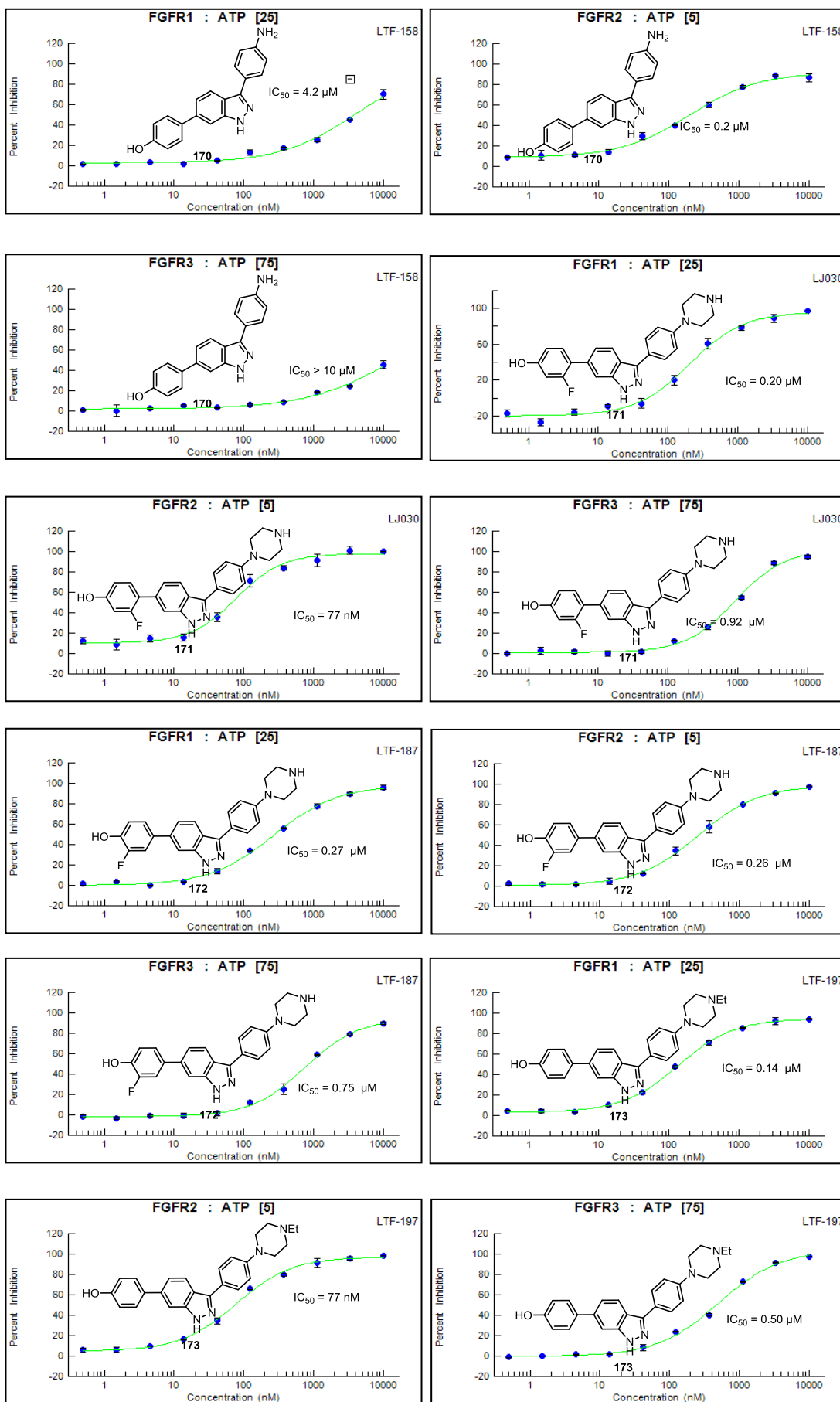




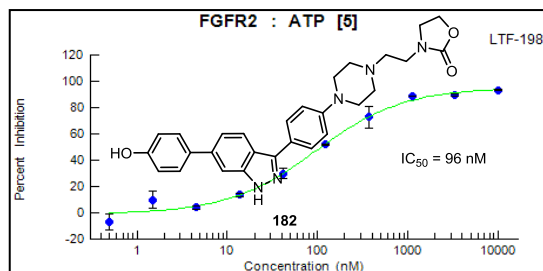
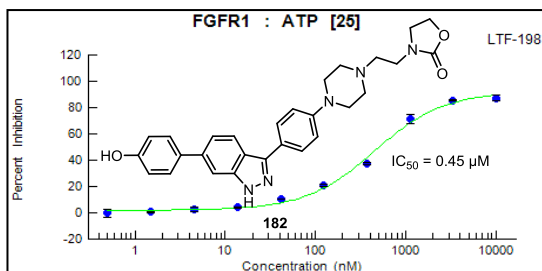






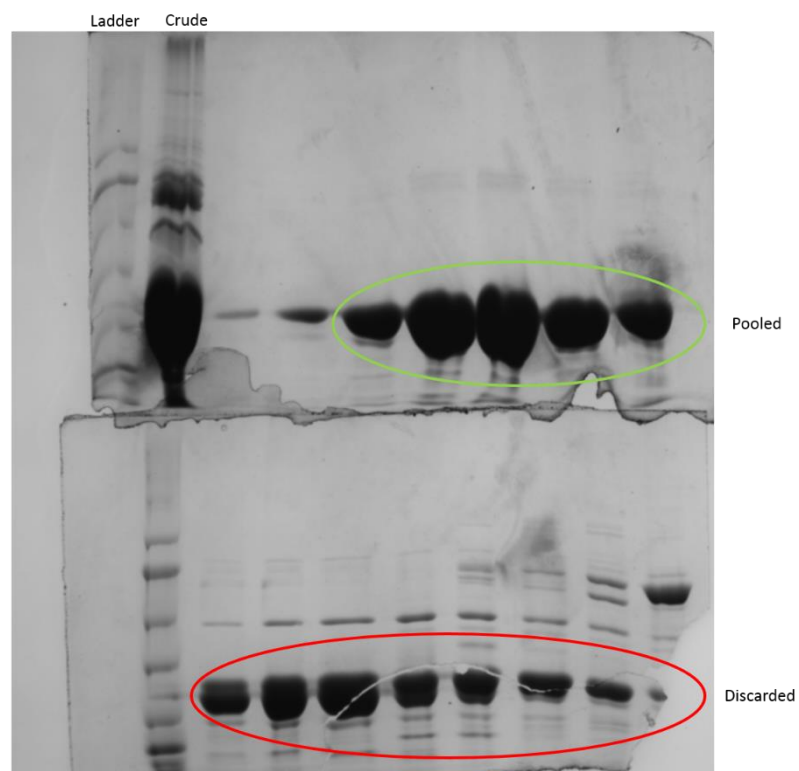




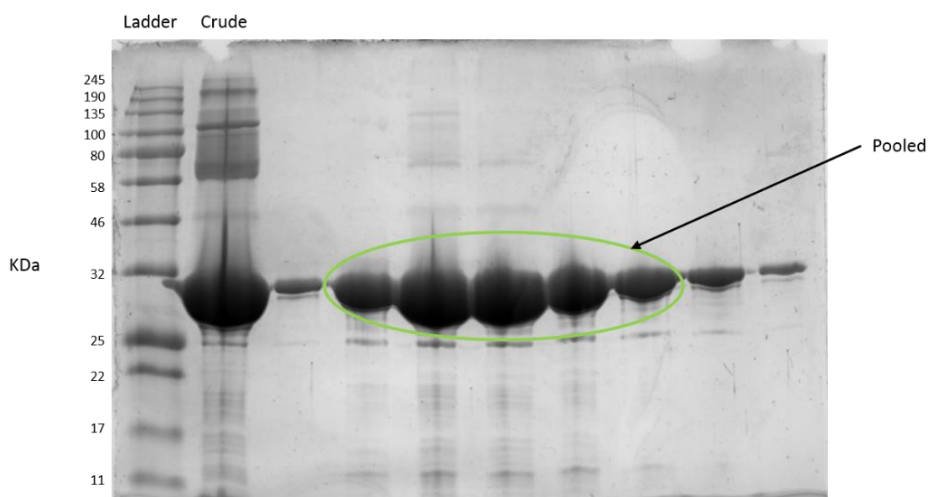


## 8.2 Appendix 2.0 – Protein Expression and Crystallisation

### 8.2.1 FGFR1-SDS-PAGE



SDS-PAGE gel after IEX column.



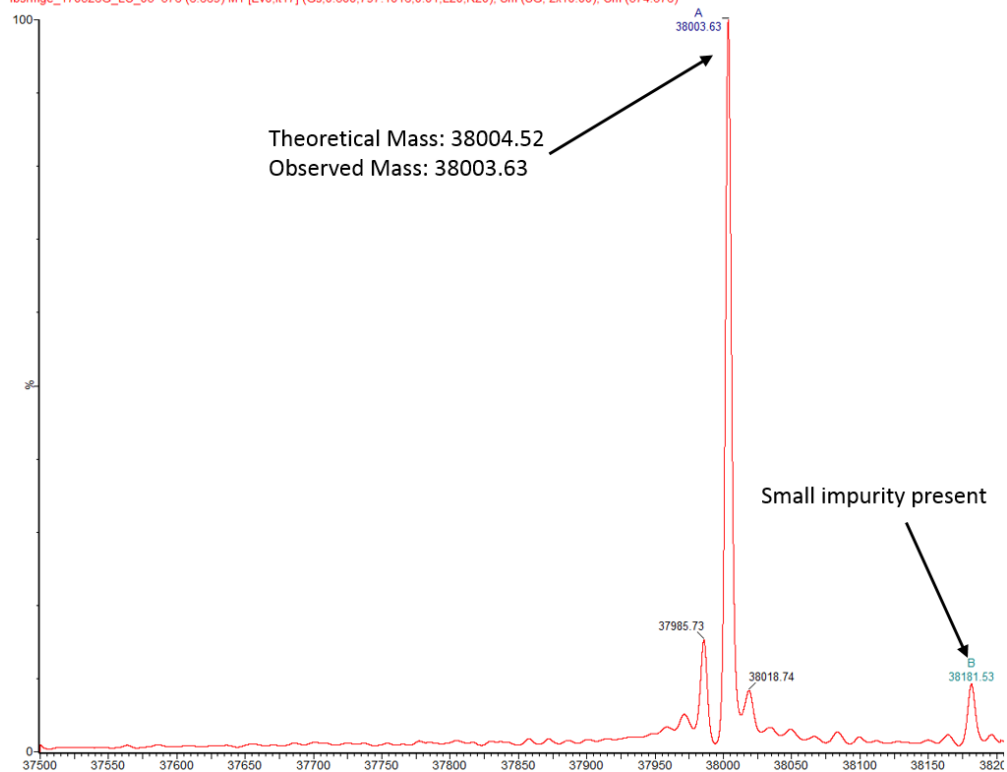
SDS-PAGE gel after SEC column.

Ladder = Color Prestained Protein Standard, Broad Range (11–245 kDa)-BioLabs

### 8.2.2 FGFR1-MS

1705-204: Chi 1

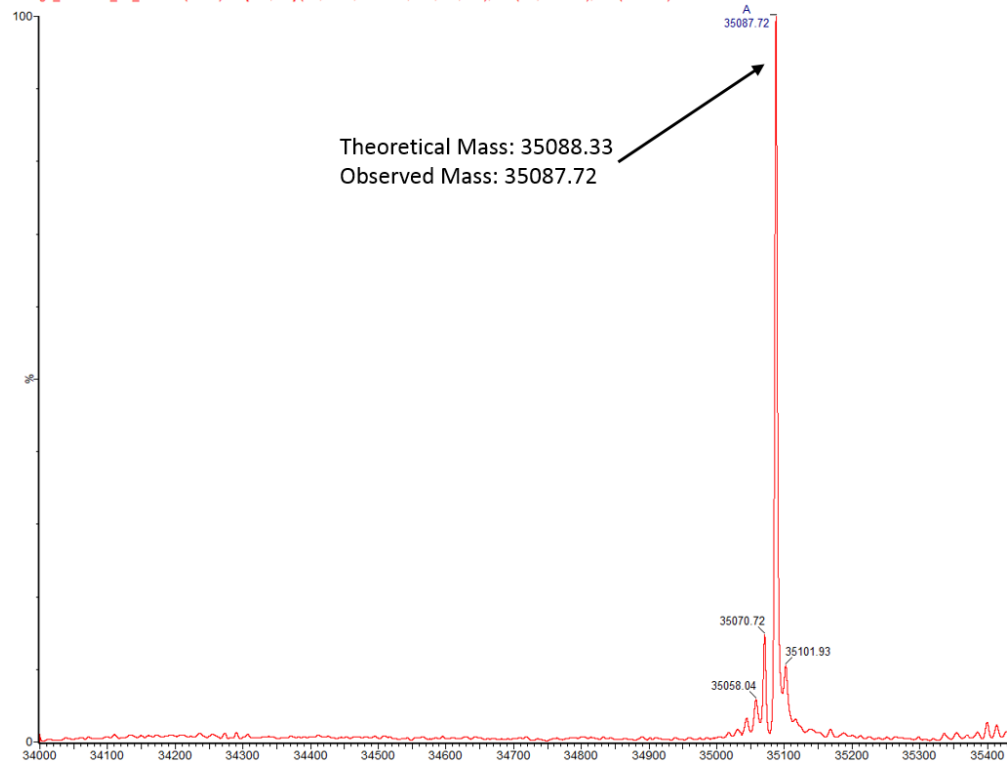
fbsmge\_170526G\_LC\_03 376 (6.669) M1 [Ev0.I17] (Gs.0.300.797.1016.0.01.L20.R20); Sm (SG, 2x10.00); Cm (374.376)



#### Pre His-Tag Cleavage/Post Ni-NTA Column

1707-271: Chi

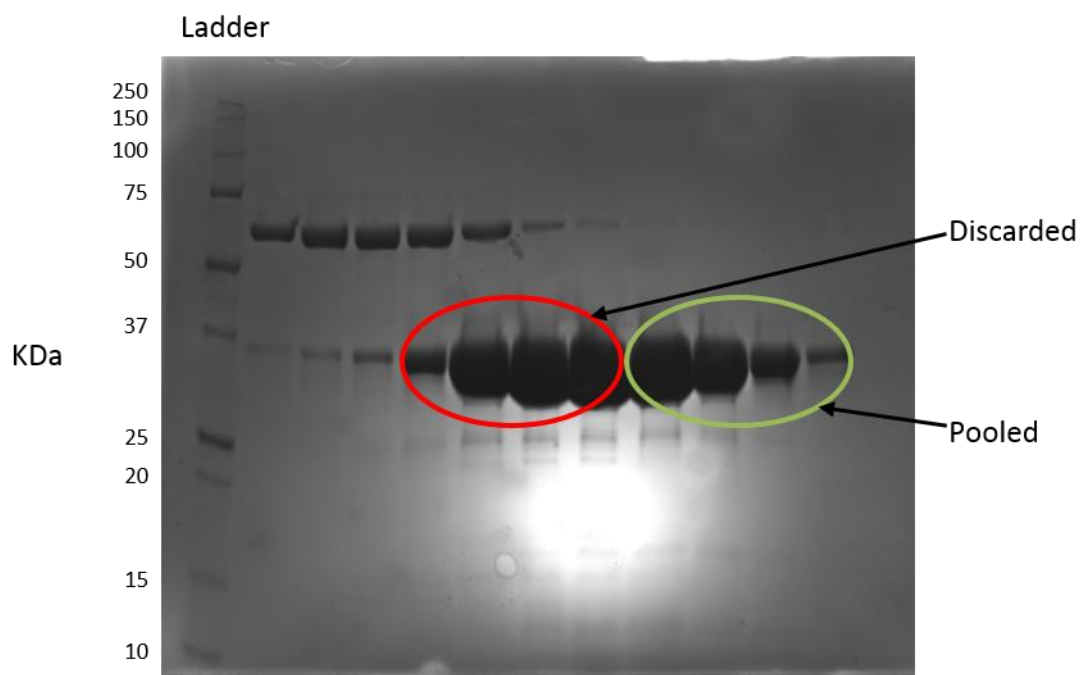
fbsmge\_170712G\_LC\_07 379 (6.721) M1 [Ev0.I19] (Gs.0.300.772.1131.0.01.L60.R60); Sm (SG, 2x10.00); Cm (379.388)



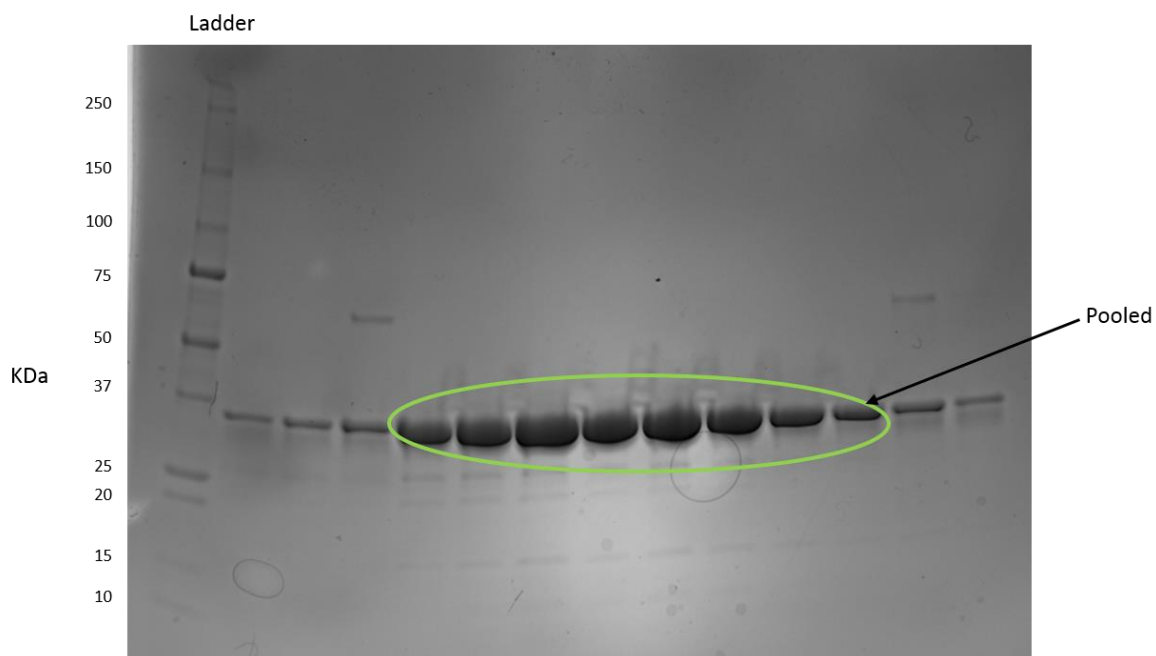
#### Post His-Tag Cleavage/Post SEC Column

## 8.2.3 FGFR2-SDS-PAGE

### 8.2.3.1 FGFR2 1Y

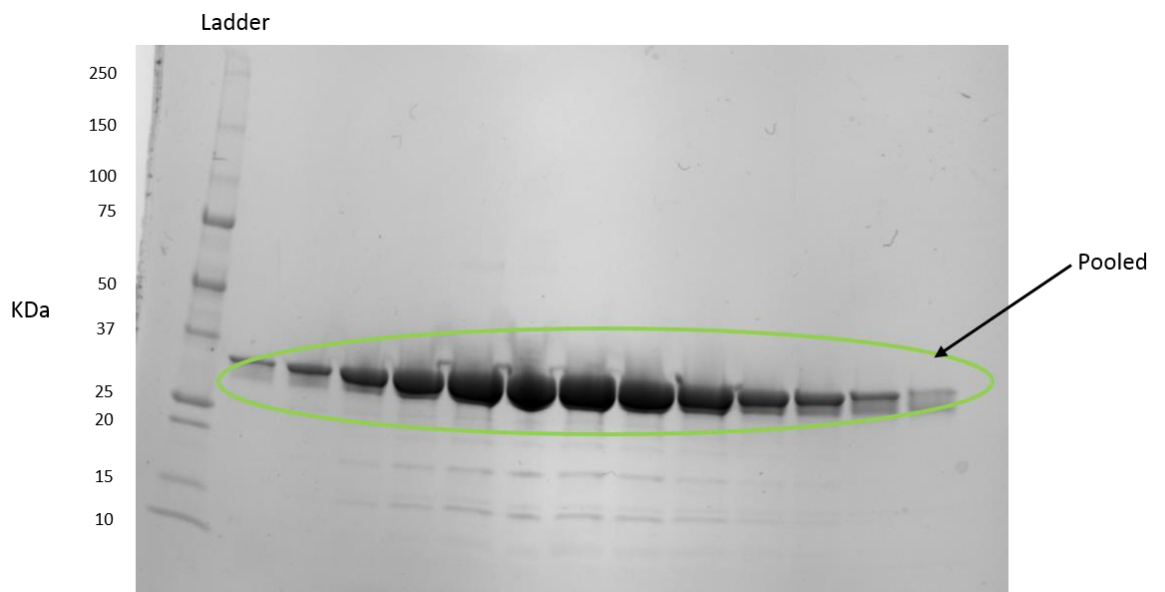


SDS-PAGE gel after SEC column with FGFR2 1Y alone construct that was treated with CIP.

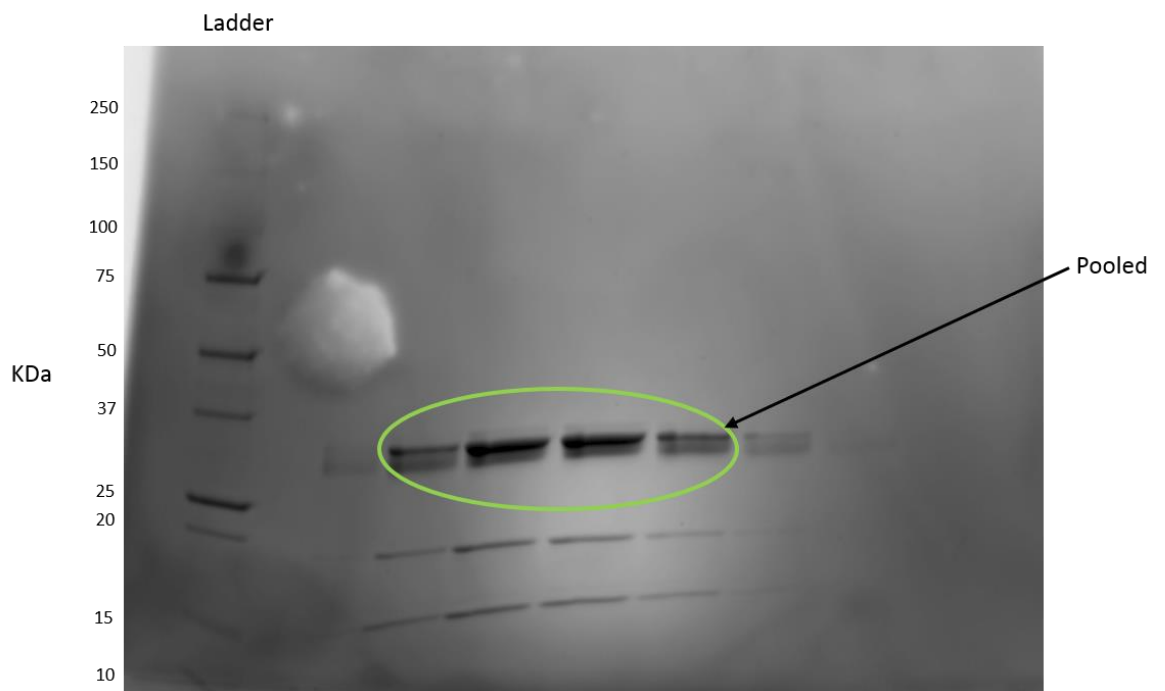


SDS-PAGE gel after SEC column with FGFR2 1Y/PTP-1B construct. Cleaner expression when using the FGFR2 1Y/PTP-1B construct.

**8.2.3.2 FGFR2 WT**



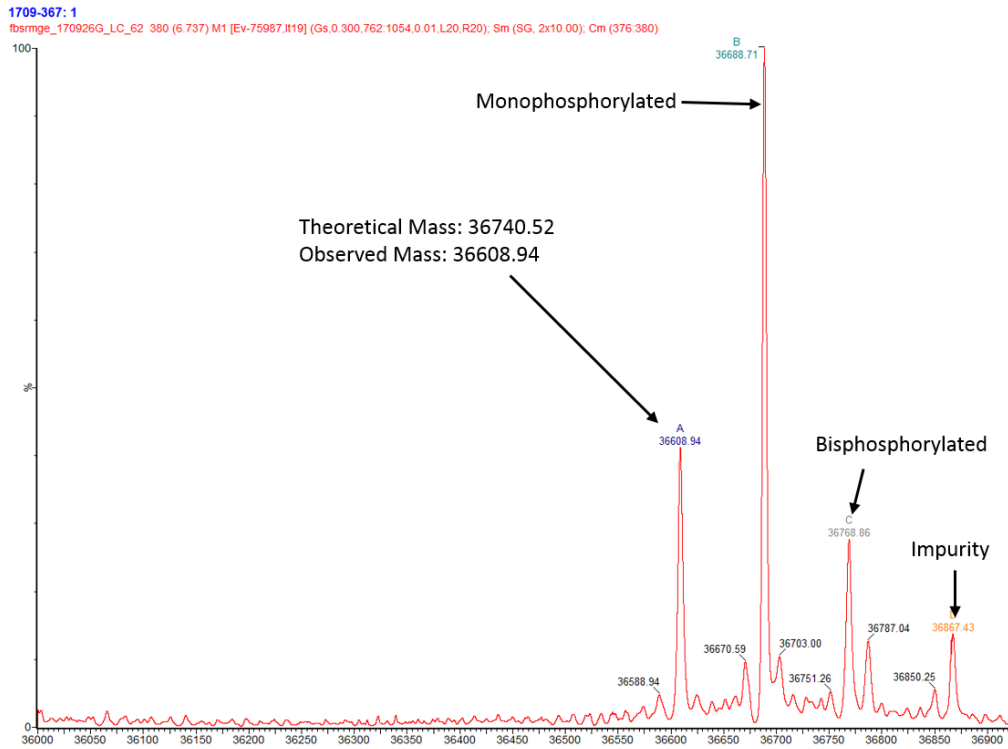
SDS-PAGE gel after SEC column with FGFR2 WT/PTP-1B construct.



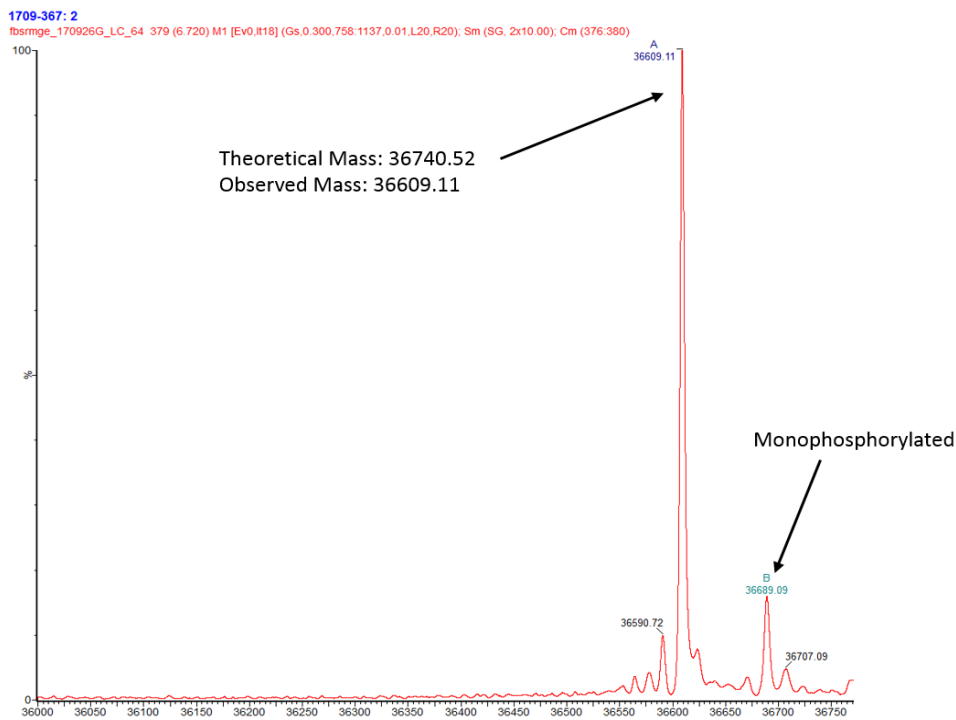
SDS-PAGE gel after HisTag cleavage and SEC column with FGFR2 WT/PTP-1B construct.

Ladder = Precision Plus Protein™ All Blue Prestained Protein Standards (10-250 kDa)-BioRad

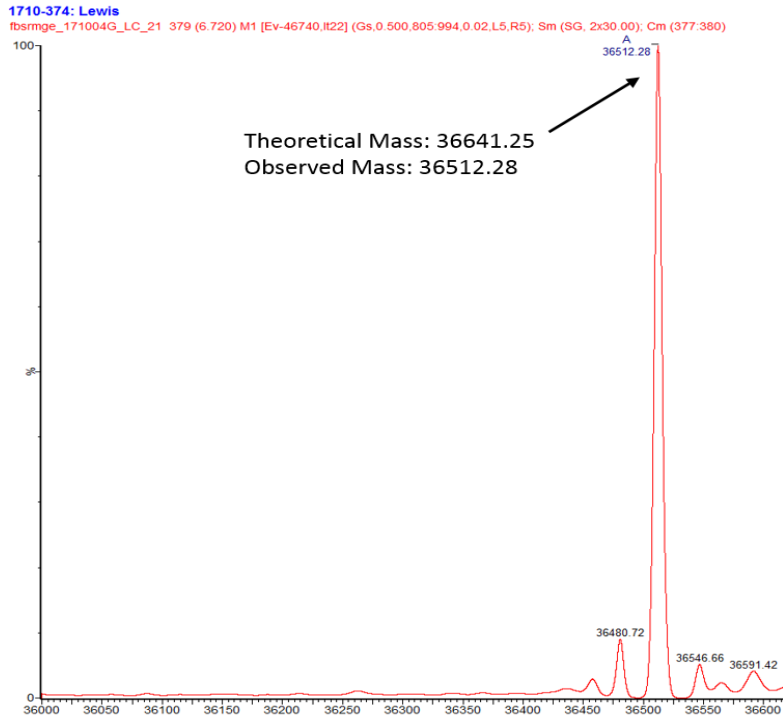
### 8.2.4 FGFR2-Mass Spectrometry



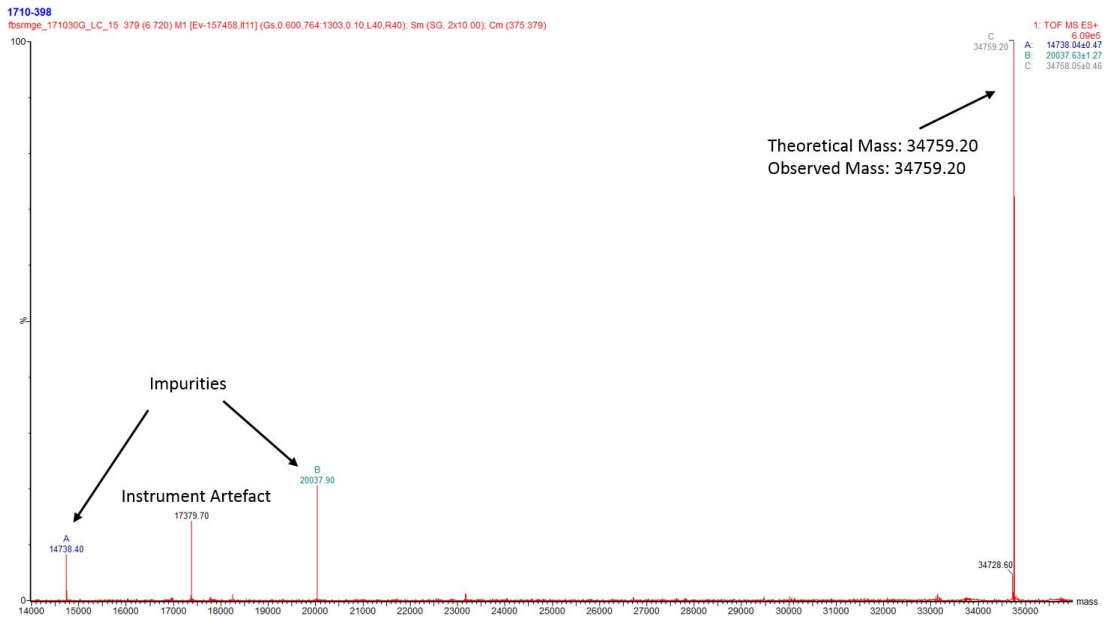
FGFR2 1Y alone construct when treated with CIP after SEC column. Observed mass is construct minus N-terminal Met amino acid.



FGFR2 1Y/PTP1-B construct after SEC column. Again observed mass is loss of initial Met residue. Co-expression with a phosphatase is more efficient at dephosphorylation than treating with a phosphatase



FGFR2 WT after SEC column. Again observed mass is loss of initial Met residue.



FGFR2 WT with the HisTag cleaved. Two impurities are present, these can also be seen on the SDS-PAGE gel.

## 8.2.5 FGFR1 Sequence

FGFR1 (C488A, C584S) MHHHHHGGSTSLYKKAGSSENLYFQ\ (TAG)

```

46      47      48      49      50      51
789012345678901234567890123456789012345678901234567890123456
GAGVSEYELPEDPRWELPRDRLVLGKPLGEGAFGQVVLAEAIGLDKDKPNRVTKVAVKML

52      53      54      55      56      57
789012345678901234567890123456789012345678901234567890123456
KSDATEKDLSDLISEMEMMMKMGKHKNIINLLGACTQDGPLYVIVEYASKGNLREYLRQAR

58      59      60      61      62      63
789012345678901234567890123456789012345678901234567890123456
RPPGLEYSSYNPSHNPEEQQLSSKDLVSCAYQVARGMEYLASKKCIHRDLAARNVLTEDNV

64      65      66      67      68      69
789012345678901234567890123456789012345678901234567890123456
MKIADFGGLARDIHHIDYYKKTTNGRLPVKWMPEALFDRIYTHQSDVWSFGVLLWEIFTL

70      71      72      73      74      75
789012345678901234567890123456789012345678901234567890123456
GGSPYPGVPVEELFKLLKEGHRMDKPSNCTNELYMMMRDCWHAVPSQRPTFKQLVEDLDR

76
789012345
IVALTSNQE

```

Mutations are outlined in red (C488A and C584S).

## 8.2.6 FGFR2 1Y Sequence

FGFR2 1Y MGSSHHHHHHSSGLVPR\ (TAG)

```

46      47      48      49      50      51
890123456789012345678901234567890123456789012345678901234567
GSHMGVSEFELPEDPKWEFPRDKLTLGKPLGEGCFGQVVMMAEAVGIDKDKPKEAVTVAVK

52      53      54      55      56      57
890123456789012345678901234567890123456789012345678901234567
MLKDDATEKDLSDLVSEMEMMMKMGKHKNIINLLGACTQDGPLYVIVEFASKGNLREFLR

58      59      60      61      62      63
890123456789012345678901234567890123456789012345678901234567
ARRPGMEFSDINRVPEEQMTFKDLVSCTFQLARGMEFLASQKCIHRDLAARNVLTENN

64      65      66      67      68      69
890123456789012345678901234567890123456789012345678901234567
PVMKIADFGGLARDINNIDYFKKTTNGRLPVKWMPEALFDREVYTHQSDVWSFGVLMWEIF

70      71      72      73      74      75
890123456789012345678901234567890123456789012345678901234567
TLGGSPYPGIPVEELFKLLKEGHRMDKPANCTNELFMMMRDCWHAVPSQRPTFKQLVEDL

76
890123
DRILTL

```



### 8.2.7 FGFR2 WT Sequence

```

FGFR2 WT      MGSSHHHHHSSGLVPR\ (TAG)
      47      48      49      50      51      52
123456789012345678901234567890123456789012345678901234567890
GSHMEYELPEDPKWEFPRDKLTLGKPLGEGCFGQVVM AEAVGIDKDKPKEAVTVAVKMLK
      53      54      55      56      57      58
123456789012345678901234567890123456789012345678901234567890
DDATEKDLSDLVSEMEMMKMIGKHKNIINLLGACTQDGPLYVIVEYASKGNLREYLRARR
      59      60      61      62      63      64
123456789012345678901234567890123456789012345678901234567890
PPGMEYSYDINRVPEEQMTFKDLVSCYQLARGMEYLA SQKCIHRDLAARNVLTENNVN
      65      66      67      68      69      70
123456789012345678901234567890123456789012345678901234567890
KIADFGLARDINNIDYYKTTNGRLPVKWM APEALFDRVYTHQSDVWSFGVLMWEIFTLG
      71      72      73      74      75      76
123456789012345678901234567890123456789012345678901234567890
GSPYPGIPVEELFKLLKEGHRMDK PANCTNELYMMMRDCWHAVPSQRPTFKQLVEDLDRI

123
LTL

```

## 8.2.8 Crystallographic Statistics

<b>Data Statistics</b>				
Dataset	FGFR1/115	FGFR1/160	FGFR1/164	FGFR2/164
Source	DLSF	DLSF	DLSF	ESRF
Beamline	I04-1	I04-1	I04-1	ID30A-1
Wavelength (Å)	0.9159	0.9159	0.9159	0.9660
Resolution range (Å)	63.00 – 1.82 (1.87 – 1.82)	22.01 – 1.82 (1.87 – 1.82)	98.51 – 1.71 (1.75 – 1.71)	80.54 – 2.28 (2.34 – 2.28)
Space Group	<i>C</i> 1 2 1	<i>C</i> 1 2 1	<i>C</i> 1 2 1	<i>P</i> 4 <sub>1</sub> 2 <sub>1</sub> 2
Unit-Cell parameters (Å)	a = 208.78 b = 57.77 c = 65.94 $\alpha$ = 90.00 $\beta$ = 107.17 $\gamma$ = 90.00	a = 207.30 b = 57.51 c = 65.97 $\alpha$ = 90.00 $\beta$ = 107.44 $\gamma$ = 90.00	a = 206.26 b = 57.56 c = 65.79 $\alpha$ = 90.00 $\beta$ = 107.22 $\gamma$ = 90.00	a = 113.84 b = 113.84 c = 117.41 $\alpha$ = 90.00 $\beta$ = 90.00 $\gamma$ = 90.00
Completeness (%)	98.7 (99.8)	99.2 (99.6)	97.4 (96.8)	99.9 (100.0)
Total reflections	225749	225056	279019	255783
Unique reflections	66492	66115	77609	35802
Redundancy	3.4 (2.9)	3.4 (2.9)	3.6 (3.7)	7.1 (7.4)
<i>I</i> / $\sigma$ ( <i>I</i> )	11.3 (1.1)	16.7 (1.3)	14.1 (1.3)	6.6 (0.9)
<i>R</i> <sub>merge</sub> (%)	3.8 (78.9)	2.6 (84.0)	3.1 (83.7)	13.6 (253.7)
<i>R</i> <sub>pim</sub> (%)	3.5 (72.7)	2.4 (76.3)	2.9 (73.7)	7.7 (138.9)
<i>CC</i> <sub>1/2</sub>	0.99 (0.63)	0.99 (0.69)	0.99 (0.71)	0.99 (0.68)
<b>Refinement Statistics</b>				
Resolution range (Å)	63.00 – 1.82	22.01 – 1.82	98.51 – 1.80	80.50 – 2.40
<i>R</i> factor (%)	19.9	19.5	20.0	22.5
<i>R</i> <sub>free</sub> (%) †	24.4	24.2	24.6	29.1
No. of protein non-H atoms	4534	4544	4521	4533
No. of ligand non-H atoms	54	25	56	56
No. of water molecules	197	231	188	98
No. of sulphate ions	6	8	5	2
No. of ethylene glycol molecules	4	5	8	1
R.m.s.d bond lengths (Å)	0.013	0.013	0.018	0.013
R.m.s.d bond angles (°)	1.594	1.601	1.870	1.621
<b>Ramachandran Plot ‡</b>				
Favoured region (%)	98.2	97.7	98.2	95.0
Outliers (%)	0	0.2	0.2	0.7

Values given in parentheses correspond to those in the outermost shell of the resolution range.

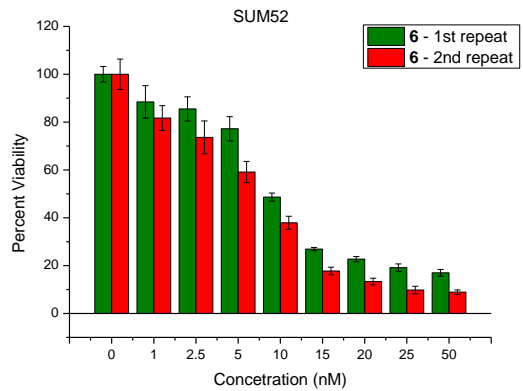
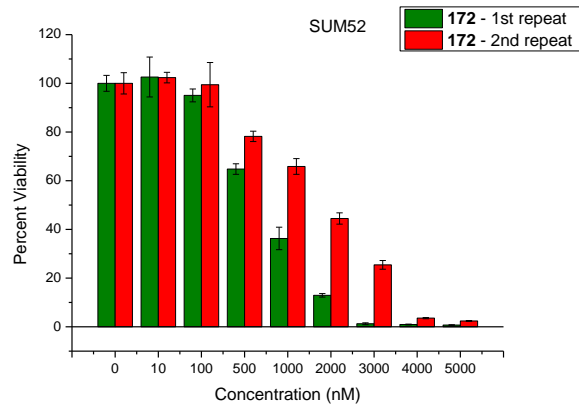
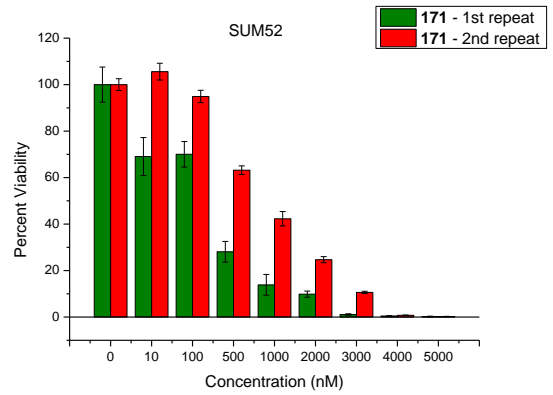
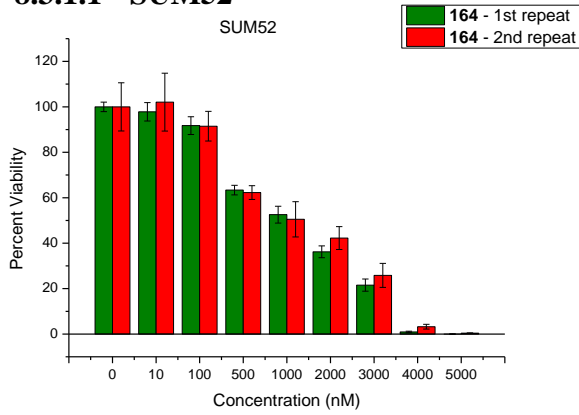
† *R*<sub>free</sub> was calculated with 5% of the reflections set aside randomly.

‡ Ramachandran analysis using the program MolProbity.<sup>148</sup>

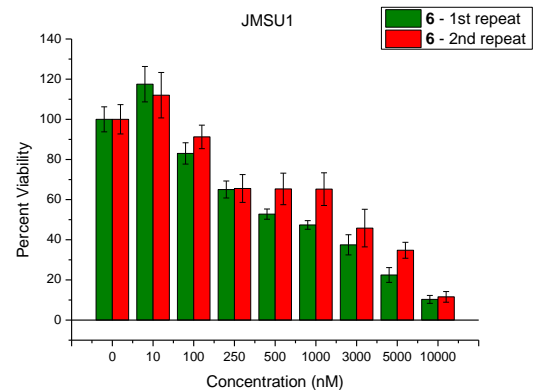
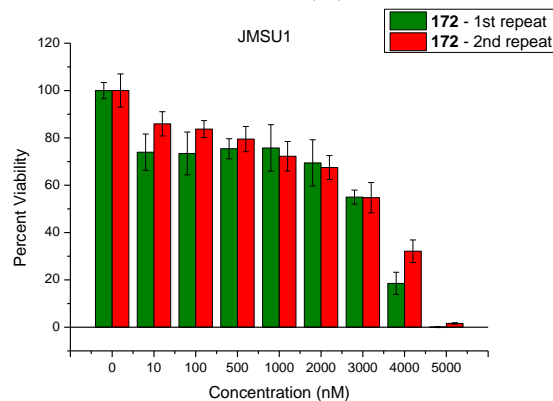
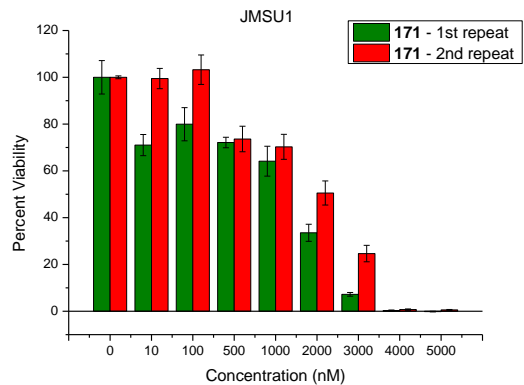
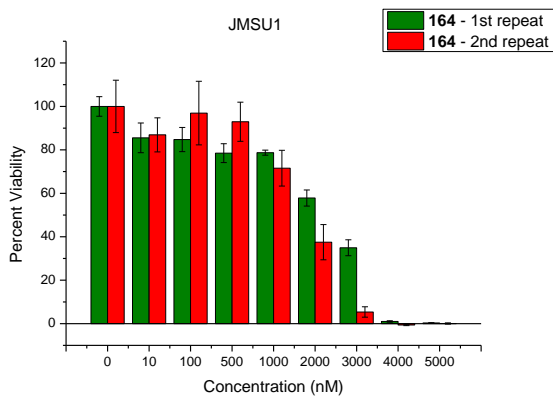
## 8.3 Appendix 3.0 – Cell Viability Graphs

### 8.3.1 Duplicate Measurement Graphs

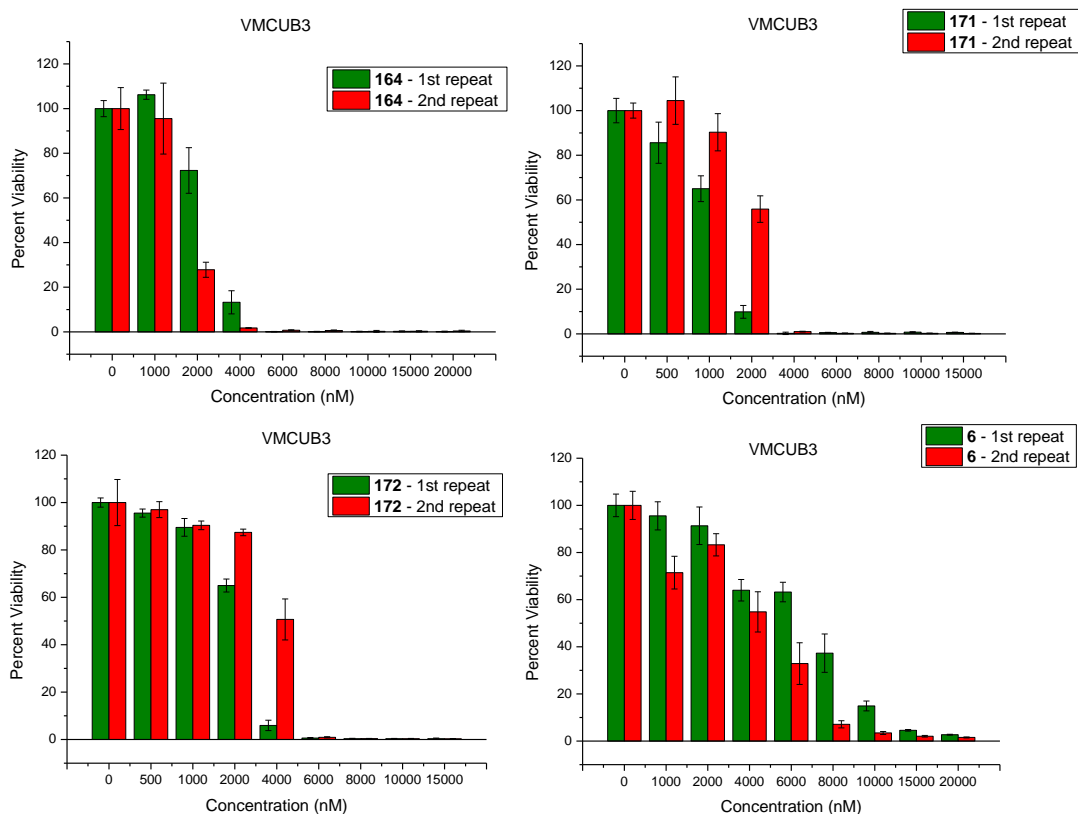
#### 8.3.1.1 SUM52



#### 8.3.1.2 JMSU1

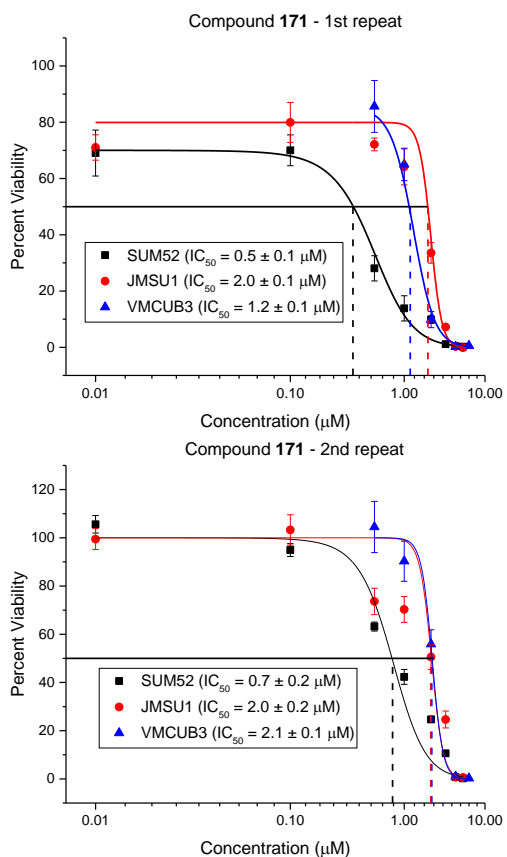


### 8.3.1.3 VMCUB3

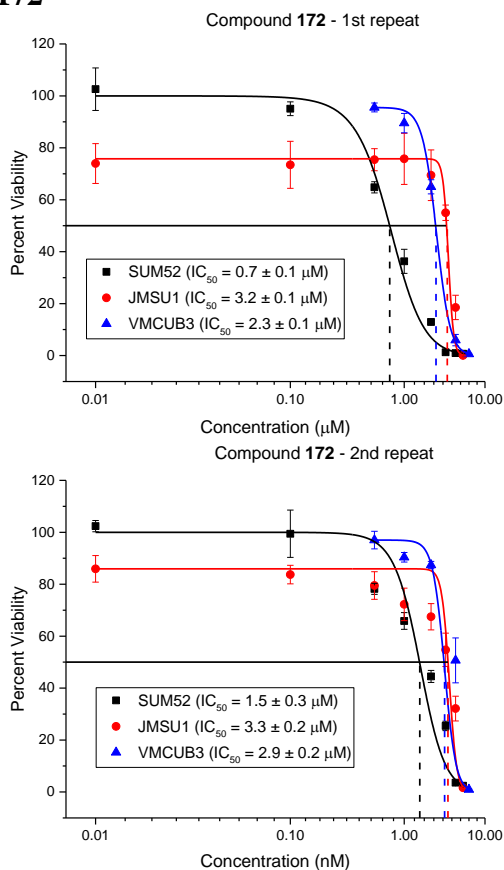


## 8.3.2 Dose Response Inhibitor Curves

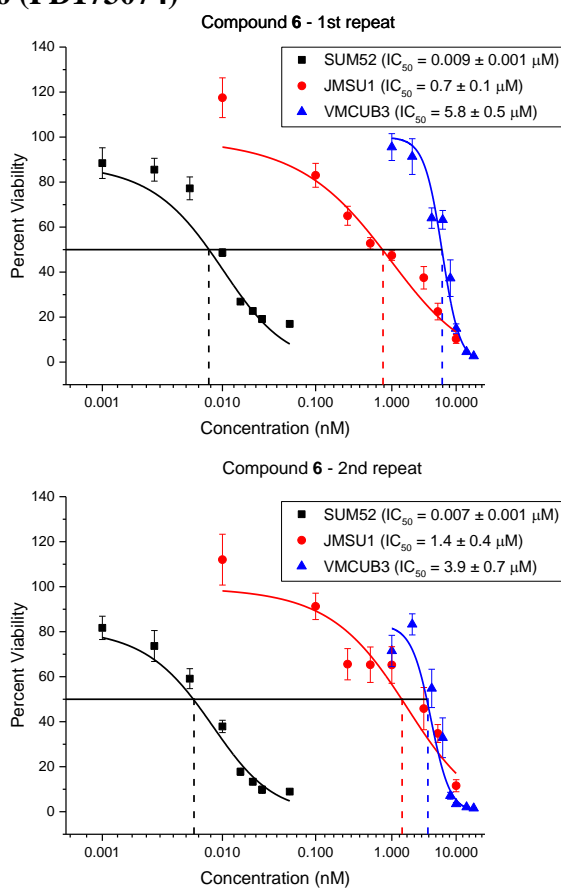
### 8.3.2.1 Compound 171



### 8.3.2.2 Compound 172



### 8.3.2.3 Compound 6 (PD173074)



## 8.4 Appendix 4.0 – Amino Acid Abbreviations

Alanine	Ala	A
Arginine	Arg	R
Asparagine	Asn	N
Aspartic acid	Asp	D
Cysteine	Cys	C
Glutamic acid	Glu	E
Glutamine	Gln	Q
Glycine	Gly	G
Histidine	His	H
Isoleucine	Ile	I
Leucine	Leu	L
Lysine	Lys	K
Methionine	Met	M
Phenylalanine	Phe	F
Proline	Pro	P
Serine	Ser	S
Threonine	Thr	T
Tryptophan	Trp	W
Tyrosine	Tyr	Y
Valine	Val	V

## 8.5 Appendices References

147. Z'-Lyte<sup>®</sup> Screening Protocol and Assay Conditions. Life Technologies, Paisley, Scotland, 2015.
148. Chen, V. B.; Arendall, W. B.; Headd, J. J.; Keedy, D. A.; Immormino, R. M.; Kapral, G. J.; Murray, L. W.; Richardson, J. S.; Richardson, D. C., MolProbity: all-atom structure validation for macromolecular crystallography. *Acta Crystallogr. D* **2010**, *66*, 12-21.